

# Green Chemistry

Cutting-edge research for a greener sustainable future

[www.rsc.org/greenchem](http://www.rsc.org/greenchem)

Volume 11 | Number 7 | July 2009 | Pages 897–1068



ISSN 1463-9262

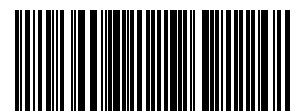
RSC Publishing

Schaak *et al.*  
Toward green metallurgy

Streit *et al.*  
Identifying ionic liquid stable cellulases

Zhang  
Fluorous techniques in green chemistry

Beckers *et al.*  
Marrying gas power and hydrogen energy



1463-9262(2009)11:7;1-7

# Green Chemistry

Cutting-edge research for a greener sustainable future

[www.rsc.org/greenchem](http://www.rsc.org/greenchem)

Volume 11 | Number 7 | July 2009 | Pages 897–1068



Downloaded on 27 November 2010  
Published on 05 July 2009 on <http://pubs.rsc.org> | doi:10.1039/B912749H

ISSN 1463-9262

Varma *et al.*  
Synthesis of silver nanoparticles

Keller *et al.*  
Photocatalytic removal of  
monoterpenes

Ondruschka *et al.*  
Chemistry driven by suction

Dewulf *et al.*  
Preparative HPLC vs. preparative SFC

RSC Publishing

# Green Chemistry

Cutting-edge research for a greener sustainable future

[www.rsc.org/greenchem](http://www.rsc.org/greenchem)

RSC Publishing is a not-for-profit publisher and a division of the Royal Society of Chemistry. Any surplus made is used to support charitable activities aimed at advancing the chemical sciences. Full details are available from [www.rsc.org](http://www.rsc.org)

## IN THIS ISSUE

ISSN 1463-9262 CODEN GRCHFJ 11(7) 897–1068 (2009)



### Cover

See Streit *et al.*, pp. 957–965. To benefit from nature's biodiversity by applying metagenomics for the identification of cellulases stable in ionic liquids.

Image reproduced with permission from Wolfgang R. Streit, from *Green Chem.*, 2009, **11**, 957.



### Inside cover

See Keller *et al.*, pp. 966–973. UV-A light driven (photo)catalysis for efficiently removing environmentally-unfriendly odorous and irritant monoterpenes from wood-derived industry effluent releases.

Image reproduced with permission from Nicolas Keller, from *Green Chem.*, 2009, **11**, 966.

## CHEMICAL TECHNOLOGY

### T49

Drawing together research highlights and news from all RSC publications, *Chemical Technology* provides a 'snapshot' of the latest applications and technological aspects of research across the chemical sciences, showcasing newsworthy articles and significant scientific advances.

## Chemical Technology

July 2009/Volume 6/Issue 7

[www.rsc.org/chemicaltechnology](http://www.rsc.org/chemicaltechnology)

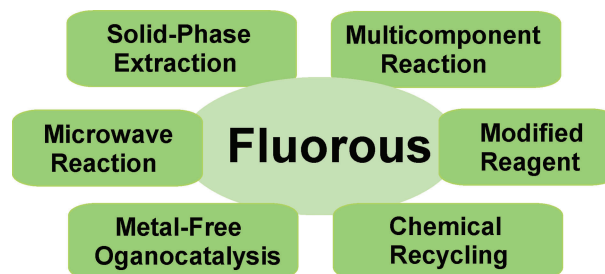
## CRITICAL REVIEW

### 911

#### Green chemistry aspects of fluororous techniques—opportunities and challenges for small-scale organic synthesis

Wei Zhang\*

Fluororous chemistry has a potential to become a combinatorial green chemistry technology. This *critical review* discusses its applications for small-scale organic synthesis in the discovery, medicinal chemistry, and academic labs.



## EDITORIAL STAFF

**Editor**

Sarah Ruthven

**Assistant editors**

Sarah Dixon, Katie Dryden-Holt

**Publishing assistant**

Jessica-Jane Doherty

**Team leader, Informatics**

Stephen Wilkes

**Technical editor**

Edward Morgan

**Production administration coordinator**

Sonya Spring

**Administration assistants**

Aliya Anwar, Jane Orchard, Julie Thompson

**Publisher**

Emma Wilson

Green Chemistry (print: ISSN 1463-9262; electronic: ISSN 1463-9270) is published 12 times a year by the Royal Society of Chemistry, Thomas Graham House, Science Park, Milton Road, Cambridge, UK CB4 0WF.

All orders, with cheques made payable to the Royal Society of Chemistry, should be sent to RSC Distribution Services, c/o Portland Customer Services, Commerce Way, Colchester, Essex, UK CO2 8HP. Tel +44 (0) 1206 226050; E-mail sales@rscdistribution.org

2009 Annual (print + electronic) subscription price: £1027; US\$2013. 2009 Annual (electronic) subscription price: £924; US\$1811. Customers in Canada will be subject to a surcharge to cover GST. Customers in the EU subscribing to the electronic version only will be charged VAT.

If you take an institutional subscription to any RSC journal you are entitled to free, site-wide web access to that journal. You can arrange access via Internet Protocol (IP) address at [www.rsc.org/ip](http://www.rsc.org/ip). Customers should make payments by cheque in sterling payable on a UK clearing bank or in US dollars payable on a US clearing bank. Periodicals postage paid at Rahway, NJ, USA and at additional mailing offices. Airfreight and mailing in the USA by Mercury Airfreight International Ltd., 365 Blair Road, Avenel, NJ 07001, USA.

US Postmaster: send address changes to Green Chemistry, c/o Mercury Airfreight International Ltd., 365 Blair Road, Avenel, NJ 07001. All despatches outside the UK by Consolidated Airfreight.

PRINTED IN THE UK

**Advertisement sales:** Tel +44 (0) 1223 432246; Fax +44 (0) 1223 426017; E-mail [advertising@rsc.org](mailto:advertising@rsc.org)

For marketing opportunities relating to this journal, contact [marketing@rsc.org](mailto:marketing@rsc.org)

# Green Chemistry

Cutting-edge research for a greener sustainable future

[www.rsc.org/greenchem](http://www.rsc.org/greenchem)

Green Chemistry focuses on cutting-edge research that attempts to reduce the environmental impact of the chemical enterprise by developing a technology base that is inherently non-toxic to living things and the environment.

## EDITORIAL BOARD

**Chair**

Professor Martyn Poliakoff  
Nottingham, UK

**Scientific Editor**

Professor Walter Leitner  
RWTH-Aachen, Germany

**Associate Editors**

Professor C. J. Li  
McGill University, Canada

**Members**

Professor Paul Anastas  
Yale University, USA  
Professor Joan Brennecke  
University of Notre Dame, USA  
Professor Mike Green  
Sasol, South Africa  
Professor Buxing Han  
Chinese Academy of Sciences,  
China

Professor Shu Kobayashi,  
University of Tokyo, Japan  
Dr Alexei Lapkin  
Bath University, UK  
Professor Steven Ley  
Cambridge, UK  
Dr Janet Scott  
Unilever, UK  
Professor Tom Welton  
Imperial College, UK

## ADVISORY BOARD

James Clark, York, UK  
Avelino Corma, Universidad  
Politécnica de Valencia, Spain  
Mark Harmer, DuPont Central  
R&D, USA  
Herbert Hugl, Lanxess Fine  
Chemicals, Germany  
Roshan Jachuck,  
Clarkson University, USA  
Makato Misono, nite,  
Japan

Colin Raston,  
University of Western Australia,  
Australia  
Robin D. Rogers, Centre for Green  
Manufacturing, USA  
Kenneth Seddon, Queen's  
University, Belfast, UK  
Roger Sheldon, Delft University of  
Technology, The Netherlands  
Gary Sheldrake, Queen's  
University, Belfast, UK

Pietro Tundo, Università ca  
Foscari di Venezia, Italy

## INFORMATION FOR AUTHORS

Full details of how to submit material for publication in Green Chemistry are given in the Instructions for Authors (available from <http://www.rsc.org/authors>). Submissions should be sent via ReSource: <http://www.rsc.org/resource>.

Authors may reproduce/republish portions of their published contribution without seeking permission from the RSC, provided that any such republication is accompanied by an acknowledgement in the form: (Original citation) – Reproduced by permission of the Royal Society of Chemistry.

© The Royal Society of Chemistry 2009. Apart from fair dealing for the purposes of research or private study for non-commercial purposes, or criticism or review, as permitted under the Copyright, Designs and Patents Act 1988 and the Copyright and Related Rights Regulations 2003, this publication may only be reproduced, stored or transmitted, in any form or by any means, with the prior permission in writing of the Publishers or in the case of reprographic reproduction in accordance with the terms of licences issued by the Copyright Licensing Agency in the UK. US copyright law is applicable to users in the USA.

The Royal Society of Chemistry takes reasonable care in the preparation of this publication but does not accept liability for the consequences of any errors or omissions.

Ⓢ The paper used in this publication meets the requirements of ANSI/NISO Z39.48-1992 (Permanence of Paper).

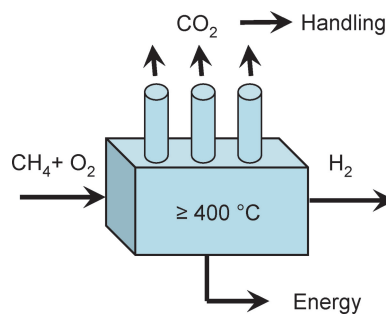
Royal Society of Chemistry: Registered Charity No. 207890

921

### Marrying gas power and hydrogen energy: A catalytic system for combining methane conversion and hydrogen generation

Jurriaan Beckers,\* Cyril Gaudillère, David Farrusseng and Gadi Rothenberg\*

Ceria-based catalysts are good candidates for combining methane combustion and hydrogen generation. They are robust crystalline materials that perform well at 400 °C–550 °C, in some cases even without precious metals. This makes them attractive for applications in the energy conversion market.

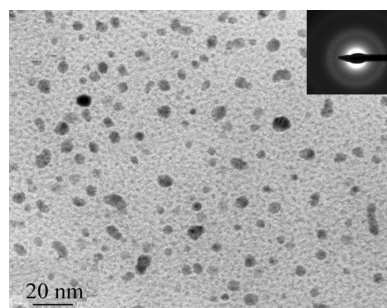


926

### Glutathione promoted expeditious green synthesis of silver nanoparticles in water using microwaves

Babita Baruwati, Vivek Polshettiwar and Rajender S. Varma\*

Silver nanoparticles ranging from 5–10 nm in size have been synthesized under microwave irradiation conditions using glutathione, an absolutely benign antioxidant that serves as the reducing as well as capping agent in aqueous medium.

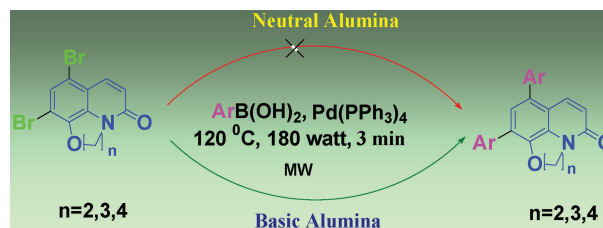


931

### Basic alumina-supported highly effective Suzuki–Miyaura cross-coupling reaction under microwave irradiation: application to fused tricyclic oxa-aza-quinolones

Pritam Saha, Subhendu Naskar, Priyanka Paira, Abhijit Hazra, Krishnendu B. Sahu, Rupankar Paira, Sukdeb Banerjee and Nirup B. Mondal\*

It has been found that basic alumina efficiently promotes a solvent free, Pd(PPh<sub>3</sub>)<sub>4</sub> catalyzed Suzuki–Miyaura cross-coupling reaction in lieu of traditional mineral bases under microwave irradiation.

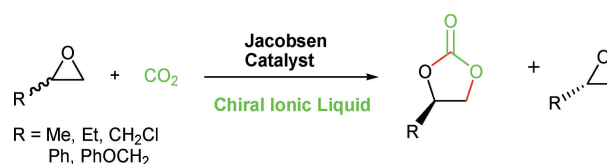


935

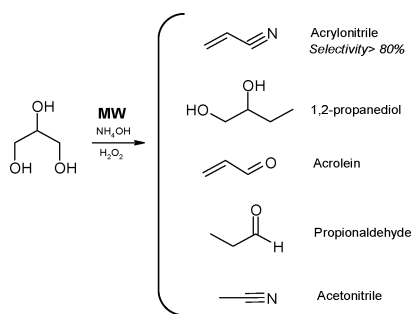
### Chiral ionic liquids improved the asymmetric cycloaddition of CO<sub>2</sub> to epoxides

Suling Zhang, Yongzhong Huang, Huanwang Jing,\* Weixuan Yao and Peng Yan

Several chiral ionic liquids were used as cocatalysts to enhanced the asymmetric cycloaddition of carbon dioxide to epoxide. The matching absolute configurations of ILs induce a higher ee of chiral propylene carbonate.



939

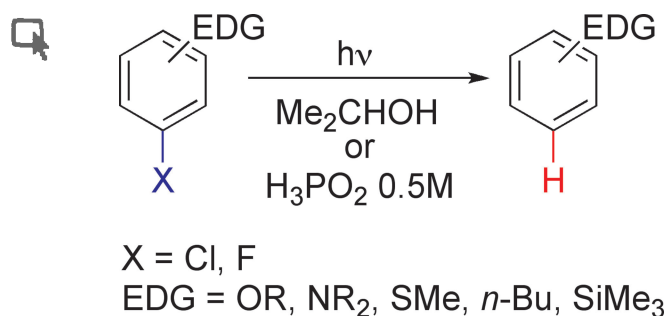


### Efficient microwave-promoted acrylonitrile sustainable synthesis from glycerol

Vanesa Calvino-Casilda,\* M. Olga Guerrero-Pérez and Miguel A. Bañares

Solvent-free microwave-activation, in the liquid phase using an alumina supported V-Sb-O catalyst, affords highly efficient conversion (47%) of glycerol into acrylonitrile under mild conditions, short reaction times and in the absence of any solvent; in addition, it increases selectivity (>80%) compared to conventional thermal activation.

942

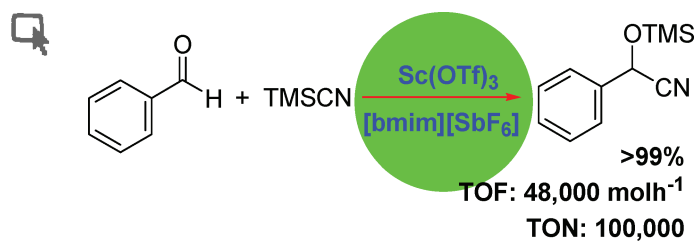


### Eco-friendly hydrodehalogenation of electron-rich aryl chlorides and fluorides by photochemical reaction

Valentina Dichiarante, Maurizio Fagnoni\* and Angelo Albini

A green protocol for the reduction of aryl chlorides and fluorides is reported. This involves irradiation in the presence of mild reducing agents such as *i*-PrOH or H<sub>3</sub>PO<sub>2</sub>.

946

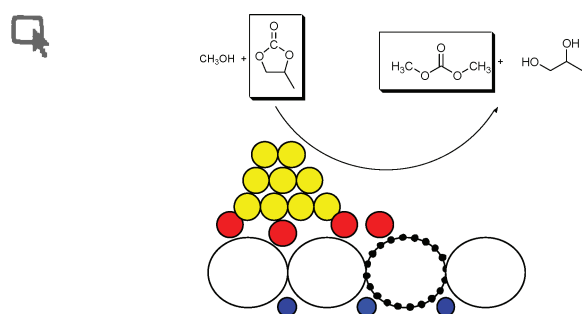


### A dream combination for catalysis: highly reactive and recyclable scandium(III) triflate-catalyzed cyanosilylations of carbonyl compounds in an ionic liquid

Boyoung Y. Park, Ka Yeon Ryu, Jung Hwan Park and Sang-gi Lee\*

Highly efficient Sc(OTf)<sub>3</sub>-catalyzed cyanosilylations of carbonyl compounds have been achieved in an ionic liquid.

949



### Gold nanoparticles promote the catalytic activity of ceria for the transalkylation of propylene carbonate to dimethyl carbonate

Raquel Juárez, Avelino Corma\* and Hermenegildo García\*

A small percentage (0.5 wt%) of gold nanoparticles (5 nm) boosts the catalytic activity and selectivity of nanoparticulated ceria for the transalkylation of propylene carbonate.

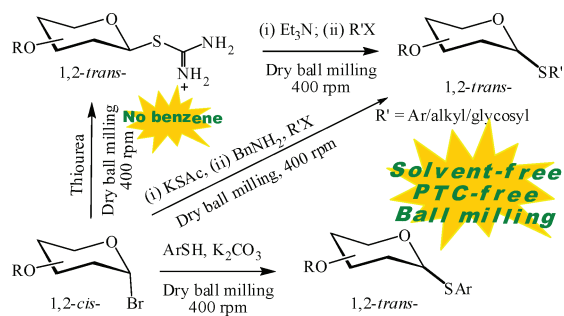
## COMMUNICATIONS

953

**Solvent-free synthesis of thioglycosides by ball milling**

Premanand Ramrao Patil and K. P. Ravindranathan Kartha\*

Thioglycosides have been prepared in excellent yields by three different routes from a range of readily available glycosyl halides by a solvent-free procedure employing a planetary ball mill.



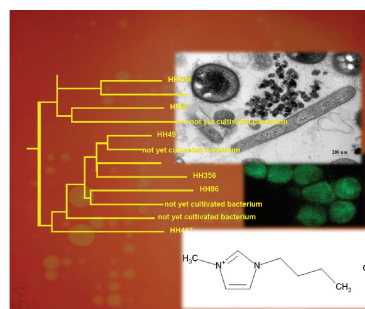
## PAPERS

957

**Applying metagenomics for the identification of bacterial cellulases that are stable in ionic liquids**

Julia Pottkämper, Peter Barthen, Nele Ilmberger, Ulrich Schwaneberg, Alexander Schenk, Michael Schulte, Nikolai Ignatiev and Wolfgang R. Streit\*

Using nature's biodiversity and the non-cultivated bacteria to find novel and robust cellulases for use in ionic liquids

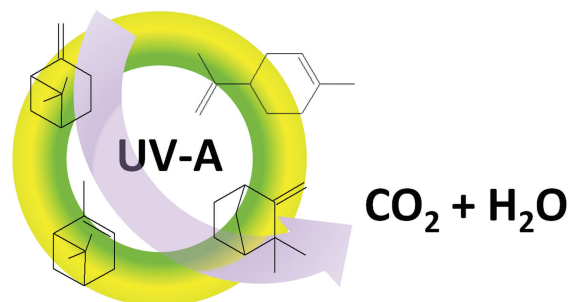


966

**Photocatalytic removal of monoterpenes in the gas phase. Activity and regeneration**

Ibtissam Salem, Nicolas Keller and Valérie Keller\*

Gas phase UV-A photocatalysis over  $\text{TiO}_2$  was used for removing various monoterpenes such as  $\beta$ - and  $\alpha$ -pinene, camphene and limonene in the 20–80 °C temperature range. Regeneration procedures were investigated for designing optimized reaction/regeneration alternative cycles.

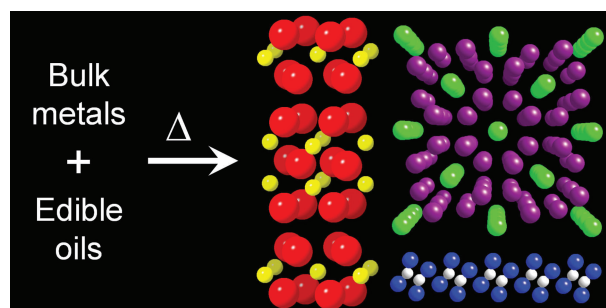


974

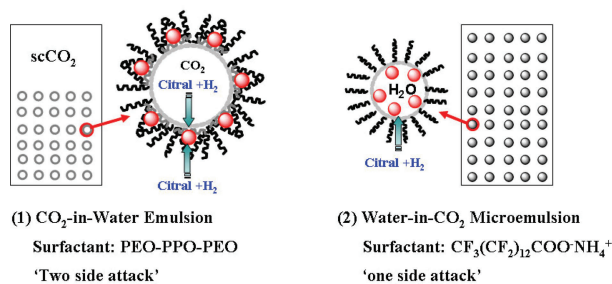
**Toward green metallurgy: low-temperature solution synthesis of bulk-scale intermetallic compounds in edible plant and seed oils**

Nathaniel L. Henderson, Matthew D. Straesser, Philip E. Sabato and Raymond E. Schaak\*

Crystalline intermetallic compounds can be formed in recyclable edible plant and seed oils through the reaction of bulk powders of late transition metals and low-melting main group metals.



979

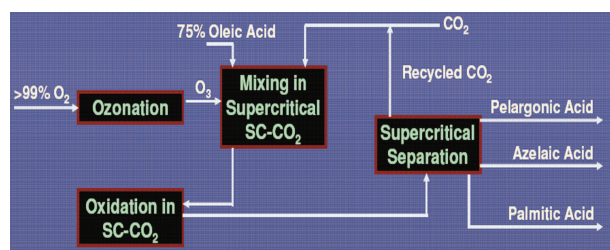


### Selective hydrogenation of citral catalyzed with palladium nanoparticles in CO<sub>2</sub>-in-water emulsion

Ruixia Liu, Chaoyong Wu, Qiang Wang, Jun Ming, Yufen Hao, Yancun Yu and Fengyu Zhao\*

The environmental benign CO<sub>2</sub>-in-water emulsion was formed by assembling poly (ethylene oxide)-poly (propylene oxide)-poly (ethylene oxide) at the water-CO<sub>2</sub> interphase. Higher TOF of 6313 h<sup>-1</sup> obtained in citral hydrogenation is benefited from the 'two sides attack' model in the present emulsion.

986

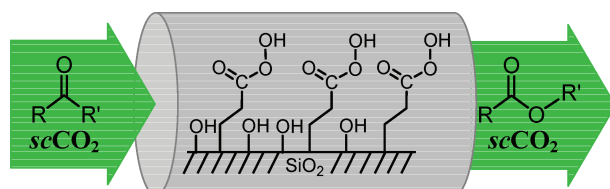


### Supercritical-fluid-assisted oxidation of oleic acid with ozone and potassium permanganate

Darrell L. Sparks, L. Antonio Estévez and Rafael Hernandez\*

The image shows the proposed process flow diagram for ozonolysis of oleic acid in supercritical carbon dioxide. This process integrates reaction with product separation, eliminating the need for energy-intensive operations such as distillation.

994

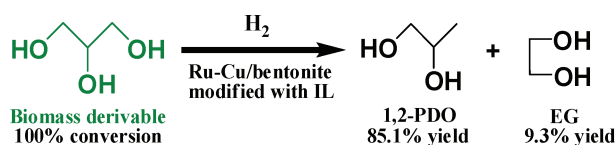


### Baeyer-Villiger oxidation of ketones with a silica-supported peracid in supercritical carbon dioxide under flow conditions

Rossella Mello, Andrea Olmos, Javier Parra-Carbonell, María Elena González-Núñez\* and Gregorio Asensio

[2-Pericarboxyethyl]-functionalized silica performs the Baeyer-Villiger oxidation of ketones in supercritical carbon dioxide at 250 bar and 40 °C under flow conditions. The reagent can be recycled by treatment with acidic 70% hydrogen peroxide at 0 °C.

1000



### Hydrogenolysis of glycerol catalyzed by Ru-Cu bimetallic catalysts supported on clay with the aid of ionic liquids

Tao Jiang,\* Yinxi Zhou, Shuguang Liang, Huizhen Liu and Buxing Han\*

Ru-Cu/clay catalysts, successfully prepared with the aid of a functional ionic liquid, are very efficient for catalyzing the hydrogenolysis of glycerol to produce 1,2-propanediol.



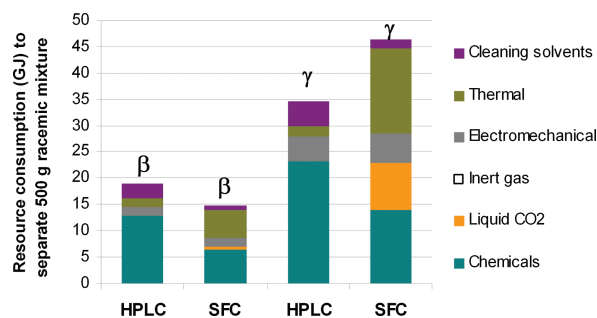
## PAPERS

1007

### Exergetic life cycle analysis for the selection of chromatographic separation processes in the pharmaceutical industry: preparative HPLC versus preparative SFC

Geert Van der Vorst, Herman Van Langenhove, Frederik De Paep, Wim Aelterman, Jules Dingenen and Jo Dewulf\*

Prep-HPLC and Prep-SFC are compared and evaluated for their integral resource consumption. The evaluation is performed on a specific enantiomeric separation using exergetic life cycle analysis within enlarging system boundaries  $\alpha$ ,  $\beta$  and  $\gamma$ .

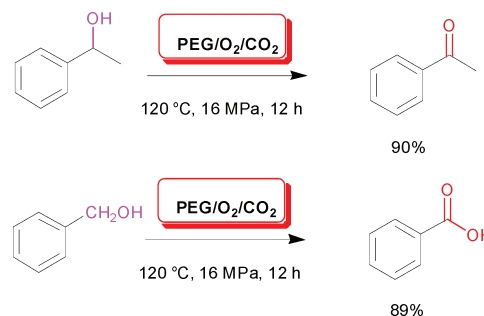


1013

### Polyethylene glycol radical-initiated oxidation of benzylic alcohols in compressed carbon dioxide

Jin-Quan Wang, Liang-Nian He\* and Cheng-Xia Miao

The PEG radical from its oxidative degradation was first used to initiate the oxidation of benzylic alcohols to carbonyl compounds without the need of a catalyst and additive in a viable synthetic, cost-effective and environmentally benign way, in which PEG/O<sub>2</sub>/CO<sub>2</sub> acts as initiator, oxidant and solvent.

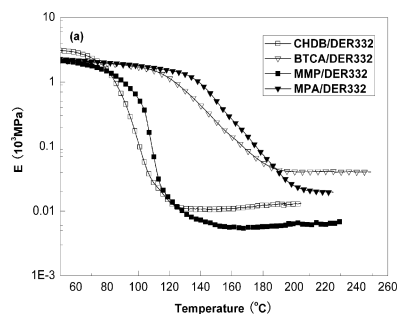


1018

### Rosin-based acid anhydrides as alternatives to petrochemical curing agents

Xiaoqing Liu, Wenbo Xin and Jinwen Zhang\*

Epoxyes cured with rosin-based curing agents exhibited similar moduli as epoxyes cured with their corresponding monocyclic curing agent analogues in the glassy state, but had a higher  $T_g$  than the latter.

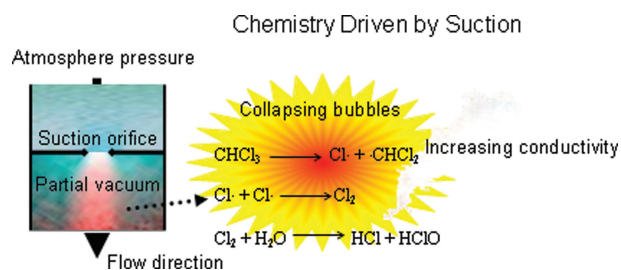


1026

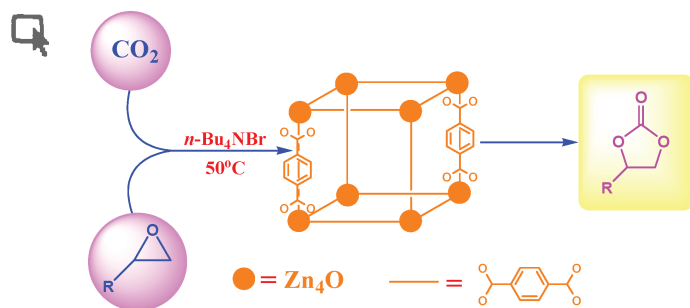
### Chemistry driven by suction

Zhilin Wu, Bernd Ondruschka,\* Yongchun Zhang, David H. Bremner, Haifeng Shen and Marcus Franke

Hydrodynamic cavitation induced by suction initiates decomposition of volatile halocarbons and facilitates two-phase mixing to promote heterogeneous reactions.



1031

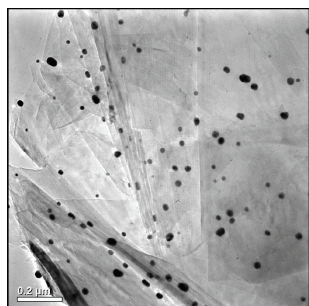


### MOF-5/*n*-Bu<sub>4</sub>NBr: an efficient catalyst system for the synthesis of cyclic carbonates from epoxides and CO<sub>2</sub> under mild conditions

Jinliang Song, Zhaofu Zhang, Suqin Hu, Tianbin Wu, Tao Jiang and Buxing Han\*

Heterogeneous catalyst metal-organic frameworks and quaternary ammonium salts have excellent synergetic effect in promoting the cycloaddition of CO<sub>2</sub> with epoxides to produce five-membered cyclic carbonates under mild reaction conditions.

1037

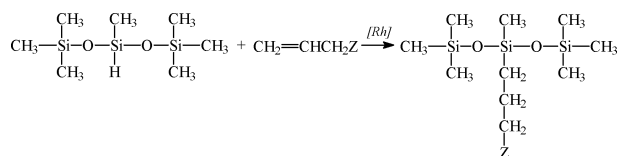


### Solvent-free selective epoxidation of cyclooctene using supported gold catalysts

Salem Bawaked, Nicholas F. Dummer, Nikolaos Dimitratos, Donald Bethell, Qian He, Christopher J. Kiely and Graham J. Hutchings\*

The epoxidation of cyclooctene under solvent-free conditions gives high activity with high epoxide selectivity using graphite-supported gold nanoparticles prepared using a sol-immobilisation method.

1045

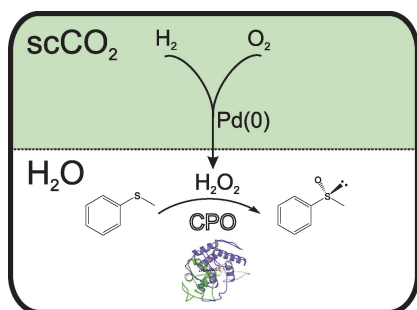


### Hydrosilylation of functionalised olefins catalysed by rhodium siloxide complexes in ionic liquids

Hieronim Maciejewski, Karol Szubert, Bogdan Marciniec\* and Juliusz Pernak

The use of ionic liquids for the immobilization of rhodium siloxide complexes has brought about highly effective catalysts for the hydrosilylation processes. Using the biphasic system enables easy separation of the product, recovery and reuse of the catalyst, which is fundamental for "green chemistry".

1052



### Chemo-enzymatic cascade oxidation in supercritical carbon dioxide/water biphasic media

Sanjib Kumar Karmee, Christoph Roosen, Christina Kohlmann, Stephan Lütz, Lasse Greiner\* and Walter Leitner\*

Enantioselective sulfoxidation by cascade reaction of Pd(0) catalysed formation of H<sub>2</sub>O<sub>2</sub> and enzymatic oxidation using chloroperoxidase from *Caldariomyces fumago*. Supercritical carbon dioxide was used as medium for *in situ* generation of H<sub>2</sub>O<sub>2</sub> directly from H<sub>2</sub> and O<sub>2</sub>.

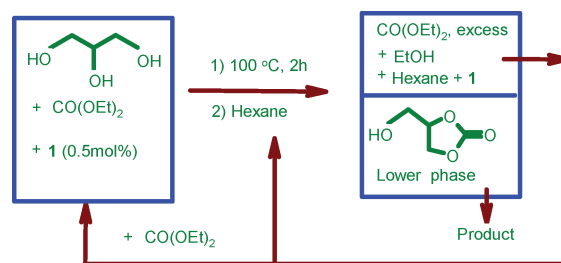
## PAPERS

1056

**Effect of liophilicity of catalyst in cyclic carbonate formation by transesterification of polyhydric alcohols**

Yogesh Patel, Jimil George, S. Muthukumar Pillai and Pradip Munshi\*

Glycerol carbonate has been made by the environmentally friendly process of using a recyclable distannoxane catalyst with a turn over frequency of 100 h<sup>-1</sup>. Liophilicity of the catalyst facilitates easy recovery of product and catalyst.



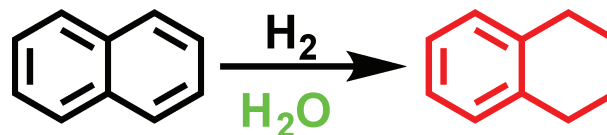
**1** = ClR<sub>2</sub>SnOSnR'<sub>2</sub>Cl. R=R'=<sup>n</sup>Bu, **1a**. Yield=100%. TOF= 100 h<sup>-1</sup>

1061

**Enhancing the selectivity of the hydrogenation of naphthalene to tetralin by high temperature water**


Yan Cheng, Honglei Fan, Suxiang Wu, Qian Wang, Jin Guo, Liang Gao, Baoning Zong and Buxing Han\*

High temperature water can enhance the selectivity and suppress the formation of coke significantly in the hydrogenation of naphthalene to produce tetralin catalyzed by a Fe–Mo based catalyst.



## FREE E-MAIL ALERTS AND RSS FEEDS


Contents lists in advance of publication are available on the web *via* [www.rsc.org/greenchem](http://www.rsc.org/greenchem) – or take advantage of our free e-mail alerting service ([www.rsc.org/ej\\_alert](http://www.rsc.org/ej_alert)) to receive notification each time a new list becomes available.

 Try our RSS feeds for up-to-the-minute news of the latest research. By setting up RSS feeds, preferably using feed reader software, you can be alerted to the latest Advance Articles published on the RSC web site. Visit [www.rsc.org/publishing/technology/rss.asp](http://www.rsc.org/publishing/technology/rss.asp) for details.

## ADVANCE ARTICLES AND ELECTRONIC JOURNAL

Free site-wide access to Advance Articles and the electronic form of this journal is provided with a full-rate institutional subscription. See [www.rsc.org/ejs](http://www.rsc.org/ejs) for more information.

\* Indicates the author for correspondence: see article for details.

 Electronic supplementary information (ESI) is available *via* the online article (see <http://www.rsc.org/esi> for general information about ESI).

## AUTHOR INDEX

- Aelterman, Wim, 1007  
 Albin, Angelo, 942  
 Antonio Estévez, L., 986  
 Asensio, Gregorio, 994  
 Bañares, Miguel A., 939  
 Banerjee, Sukdeb, 931  
 Barthen, Peter, 957  
 Baruwati, Babita, 926  
 Bawaked, Salem, 1037  
 Beckers, Jurriaan, 921  
 Bethell, Donald, 1037  
 Bremner, David H., 1026  
 Calvino-Casilda, Vanesa, 939  
 Cheng, Yan, 1061  
 Corma, Avelino, 949  
 De Paep, Frederik, 1007  
 Dewulf, Jo, 1007  
 Dichiarante, Valentina, 942  
 Dimitratos, Nikolaos, 1037  
 Dingenen, Jules, 1007  
 Dummer, Nicholas F., 1037  
 Fagnoni, Maurizio, 942  
 Fan, Honglei, 1061  
 Farrusseng, David, 921  
 Franke, Marcus, 1026  
 Gao, Liang, 1061  
 García, Hermenegildo, 949  
 Gaudillère, Cyril, 921  
 George, Jimil, 1056  
 González-Núñez, María Elena, 994  
 Greiner, Lasse, 1052  
 Guerrero-Pérez, M. Olga, 939  
 Guo, Jin, 1061  
 Han, Buxing, 1000, 1031, 1061  
 Hao, Yufen, 979  
 Hazra, Abhijit, 931  
 He, Liang-Nian, 1013  
 He, Qian, 1037  
 Henderson, Nathaniel L., 974  
 Hernandez, Rafael, 986  
 Hu, Suqin, 1031  
 Huang, Yongzhong, 935  
 Hutchings, Graham J., 1037  
 Ignatiev, Nikolai, 957  
 Ilmberger, Nele, 957  
 Jiang, Tao, 1000, 1031  
 Jing, Huanwang, 935  
 Juárez, Raquel, 949  
 Karmee, Sanjib Kumar, 1052  
 Keller, Nicolas, 966  
 Keller, Valérie, 966  
 Kiely, Christopher J., 1037  
 Kohlmann, Christina, 1052  
 Lee, Sang-gi, 946  
 Leitner, Walter, 1052  
 Liang, Shuguang, 1000  
 Liu, Huizhen, 1000  
 Liu, Ruixia, 979  
 Liu, Xiaoqing, 1018  
 Lütz, Stephan, 1052  
 Maciejewski, Hieronim, 1045  
 Marciniak, Bogdan, 1045  
 Mello, Rossella, 994  
 Miao, Cheng-Xia, 1013  
 Ming, Jun, 979  
 Mondal, Nirup B., 931  
 Munshi, Pradip, 1056  
 Naskar, Subhendu, 931  
 Olmos, Andrea, 994  
 Ondruschka, Bernd, 1026  
 Paira, Priyanka, 931  
 Paira, Rupankar, 931  
 Park, Boyoung Y., 946  
 Park, Jung Hwan, 946  
 Parra-Carbonell, Javier, 994  
 Patel, Yogesh, 1056  
 Pernak, Juliusz, 1045  
 Pillai, S. Muthukumar, 1056  
 Polshettiwar, Vivek, 926  
 Pottkämper, Julia, 957  
 Ramrao Patil, Premanand, 953  
 Ravindranathan Kartha, K. P., 953  
 Roosen, Christoph, 1052  
 Rothenberg, Gadi, 921  
 Ryu, Ka Yeon, 946  
 Sabato, Philip E., 974  
 Saha, Pritam, 931  
 Sahu, Krishnendu B., 931  
 Salem, Ibtissam, 966  
 Schaak, Raymond E., 974  
 Schenk, Alexander, 957  
 Schulte, Michael, 957  
 Schwaneberg, Ulrich, 957  
 Shen, Haifeng, 1026  
 Song, Jinliang, 1031  
 Sparks, Darrell L., 986  
 Straesser, Matthew D., 974  
 Streit, Wolfgang R., 957  
 Szubert, Karol, 1045  
 Van der Vorst, Geert, 1007  
 Van Langenhove, Herman, 1007  
 Varma, Rajender S., 926  
 Wang, Jin-Quan, 1013  
 Wang, Qian, 1061  
 Wang, Qiang, 979  
 Wu, Chaoyong, 979  
 Wu, Suixiang, 1061  
 Wu, Tianbin, 1031  
 Wu, Zhilin, 1026  
 Xin, Wenbo, 1018  
 Yan, Peng, 935  
 Yao, Weixuan, 935  
 Yu, Yancun, 979  
 Zhang, Jinwen, 1018  
 Zhang, Suling, 935  
 Zhang, Wei, 911  
 Zhang, Yongchun, 1026  
 Zhang, Zhaofu, 1031  
 Zhao, Fengyu, 979  
 Zhou, Yinxi, 1000  
 Zong, Baoning, 1061

To our referees:

**Dank u wel** kiitos takk fyrir **aitäh** děkuji *D'akujem*

**Благодаря** Спасибо **Thank you** *Tak grazie*

**Takk Tack** 唔該 **Danke** **Merci** **gracias**

**Ευχαριστώ** どうもありがとうございます。

As a result of your commitment and support, RSC journals have a reputation for the highest quality content. Your expertise as a referee is invaluable – thank you.

RSC Publishing

[www.rsc.org/publishing](http://www.rsc.org/publishing)

Registered Charity Number 207890



## Catalysis for a Sustainable World

30th August 4th September 2009  
Salamanca (Spain)

### The Main Topics Covered by the Congress are:

1. Catalysis by Design
2. Catalysis for Chemicals and Fine Chemicals
3. Selective Catalytic Oxidation using Environmentally Friendly Oxidants
4. Upgrading Oils and Improving Fuel Quality
5. Purification and Elimination of Pollutants: Chemical and Photochemical Catalysis Processes
6. Chemicals and Fuels from Biomass
7. Coal and Gas to Liquids
8. Hydrogen Production, Purification and Storage
9. Electrocatalysis and Fuel Cells
10. Synthesis of Nanostructured Catalysts
11. Catalysts at Work
12. Single and Multisite Catalysis: Homogeneous, Enzymatic and Cascade Reactions
13. Catalytic Processes, Catalyst Decay and Regeneration
14. High-Throughput Technologies

### Plenary Lecturers invited:

- M. S. Rigutto, Shell Research and Technology Centre Amsterdam, The Netherlands (Topic: Present and future challenges in refining and petrochemistry)
- P. T. Anastas, Yale University, USA (Topic: Green chemistry)
- E. Iglesia, University of California at Berkeley, USA (Topic: Kinetics, reaction mechanisms and active sites)
- J. Lercher, Technical University of Munich, Germany (Topic: Activation of alkanes)
- P. Gallezot, IRCELYON, France (Topic: Biomass to chemicals)
- A. Corma Canós, Instituto de Tecnología Química, UPV-CSIC, Spain (Boudart Award Lecture)

Organization:



<http://www.europacat2009.eu>

Please visit conference Website at:

<http://www.greenchem2009.ac.cn>



### Invitation

On behalf of the conference organizing committee, we would like to invite you to participate in the Joint Conference of the 4th International Conference on Green and Sustainable Chemistry (GSC-4) and the 2nd Asian-Oceanian Conference on Green and Sustainable Chemistry (AOC-2), which will be held in Beijing, August 20-24, 2009. The purpose of the conference is to stimulate the interaction and exchange of ideas of practitioners in green and sustainable chemistry and to promote the cleaner chemistry across the world. This conference will consist of plenary lectures, keynotes, oral and poster presentations. We sincerely hope that the scope of the conference will serve the interest of the participants. We warmly welcome all participants and sponsors of the event.

### Organized by

Institute of Chemistry, Chinese Academy of Sciences (CAS)  
Shanghai Key Laboratory of Green Chemistry and Chemical Processes, East  
China Normal University  
Peking University  
University of Science and Technology of China

### Main Topics

Benign synthesis routes  
Green catalysis  
Alternative solvents  
Renewable and green raw materials  
Green chemistry for energy  
Clean processes

# Chemical Technology

Instrument measures freezing temperatures of thousands of water droplets

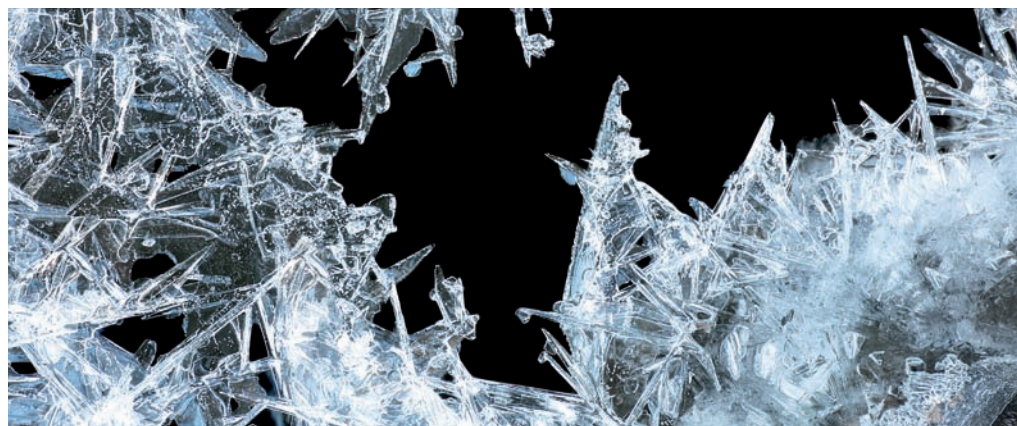
## Supercool microfluidics

Our understanding of life and technology at extreme temperatures could become clearer thanks to a microfluidic device that studies ice formation.

George Whitesides, at Harvard University, Cambridge, US, and colleagues have developed a microfluidic device that produces supercooled water drops (droplets that remain liquid below 0°C) and measures the temperature at which ice nucleates in them. The device is two orders of magnitude faster than current state-of-the-art ice nucleation instruments and very accurate, claims the team.

Ice nucleation controls water's freezing process. Studying how water behaves is important for our comprehension of a wide range of processes, including precipitation formation, icing on roads and aircraft wings and life below 0°C, explains Whitesides.

'Methods of generating fundamental information about water in all of its forms – ice, water vapour and others – are both an opportunity for science



and a societal obligation,' he says. 'This study addresses one (of many) unresolved fundamental questions – how does the nucleation of freezing of water droplets occur? The instrument generates statistically large numbers of data under very carefully controlled and very well understood conditions.'

'This is an amazing piece of microfluidic technology designed for tackling longstanding problems,' enthuses Thomas Koop, an expert

**Understanding ice nucleation is important in many fields, including snowmaking at ski resorts and reactive compound storage**

in supercooled water and ice nucleation at Bielefeld University, Germany. 'I can envisage numerous applications in various fields of metastable liquids.'

Whitesides agrees that the device is suitable for studying other metastable liquids and expects that it will become an important tool.  
*Keith Farrington*

### Reference

C A Stan et al, *Lab Chip*, 2009, DOI:10.1039/b906198c

## In this issue

Find us on...  twitter

### Chips and alcohol - a powerful combination

Microchannel-based fuel cell offers safe and high-power energy

### Drug delivery's a blast

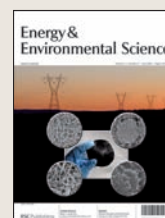
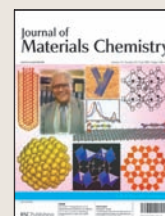
Earthquake-like wave delivers medicine mist to lungs

### Interview: Linking electronics

George Malliaras discusses the interplay between organic electronics and biology

### Instant insight: Rewriting the genetic code

Researchers' dreams of automated gene synthesis could soon become a reality, predict Jingdong Tian and colleagues



The latest applications and technological aspects of research across the chemical sciences

# Application highlights

Microchannel-based fuel cell offers safe and high-power energy

## Chips and alcohol – a powerful combination

An on-chip fuel cell that can be powered by a variety of fuels has been developed by Japanese scientists. The fuel can be chosen to suit the cell's application, from laptops to mobile phones, they say.

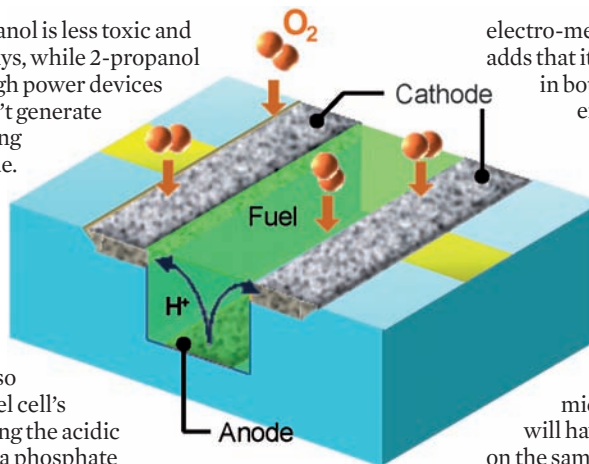
Many research groups are working on miniaturising conventional fuel cells but, as yet, they are not compatible with other microdevices. Tetsuya Osaka and colleagues from Waseda University, Tokyo, have made a microchannel-based fuel cell that is pump-free, membraneless and air-breathing (it uses oxygen from the air as its oxidant). Its simple monolithic design – its two electrodes are made in a single substrate – means it is easier to make than conventional fuel cells, says Osaka.

Osaka had previously tested the fuel cell using methanol. Methanol is suitable for long-life applications but is toxic, he explains, so he repeated the test using ethanol and

2-propanol. Ethanol is less toxic and renewable, he says, while 2-propanol is suitable for high power devices because it doesn't generate catalyst-poisoning carbon monoxide.

He found that ethanol and 2-propanol generated voltages comparable to that of methanol. He also improved the fuel cell's safety by replacing the acidic electrolyte with a phosphate buffer, which kept the pH neutral without significantly affecting the power output.

Changming Li, a fuel cell expert at Nanyang Technological University, Singapore, describes the work as 'a new approach to develop efficient micro power sources by using micro-



**Fuel oxidation at the anode generates protons, which travel to the cathode then react with oxygen from the air to become water**

electro-mechanical systems' and adds that it demonstrates advances in both microfabrication and energy systems.

Osaka says he is working towards integrating the fuel cell with other microdevices to demonstrate they work in a real system. 'This work will help contribute to the development of microdevices because they will have their own power source on the same chip,' he predicts. He adds that a possible goal would be an on-chip blood-screening sensor powered by glucose in the blood.

*Emma Shiells*

### Reference

S Tominaka *et al*, *Energy Environ. Sci.*, 2009, DOI:10.1039/b906216e

Porous scaffolds exploit wood's architectural properties

## Trees take on tissue engineering

Italian scientists have turned wood into bone mimics that could be used to repair damaged limbs.

Anna Tampieri, at the Institute of Science and Technology for Ceramics, Faenza, and colleagues were inspired by nature's highly organised hierarchal structures to make porous hydroxyapatite scaffolds with structures similar to that of real bone. The scaffolds 'pave the way for realising prosthetic devices which could get closer to the extraordinary performance of human tissues', they claim.

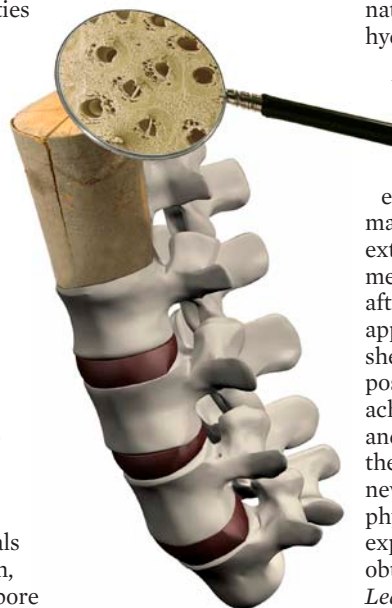
The team heated the wood to decompose the organic parts that make up most of its weight, leaving behind the carbon template. They reacted the template first with calcium, then oxygen and then carbon dioxide to form calcium carbonate. Finally, they converted it to hydroxyapatite using a phosphate donor.

The material keeps its original microstructure, exploiting the

unique architectural properties of the wood's cellular make-up, explains Tampieri. This means cells and blood vessels can grow through the structure and incorporate it into the original bone.

'Current [hydroxyapatite] production processes do not generate an organised hierarchical structure,' says Tampieri, adding that this often makes the hydroxyapatite inadequate for bearing the body's weight and managing in vivo stresses.

'This is an interesting study,' says Iain Gibson, an expert in biomedical materials at the University of Aberdeen, UK. 'Although the resulting pore structures obtained do not match those of cancellous (spongy) bone, they provide an interesting first step in proving the concept of using a



**Turning wood into bone: a new meaning to tree surgery?**

natural template to produce porous hydroxyapatite scaffolds, and as a potential route to produce biomaterial scaffolds for tissue repair and drug delivery.'

Tampieri says the method could find use beyond tissue engineering. 'Materials able to maintain adequate properties at extremely high temperatures and mechanical stress are highly sought after for use in several different applications, such as space vehicles,' she comments. 'An intriguing possibility is that of simultaneously achieving high values of strength and toughness, for which ordinarily there is a trade-off. In addition, new materials with extreme physical properties, such as thermal expansion or piezoelectricity, can be obtained.'

*Leanne Marle*

### Reference

A Tampieri *et al*, *J. Mater. Chem.*, 2009, DOI: 10.1039/b900333a



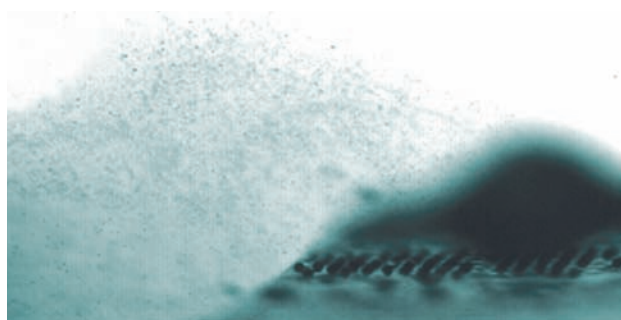
## Earthquake-like wave delivers medicine mist to lungs

# Drug delivery's a blast

A portable, miniature system for delivering steroids into asthma patients' lungs has been developed by scientists in Australia. The system is cheaper and more efficient than conventional nebulisers and could be used to administer vaccines, antibiotics and other drugs, they say.

The battery-powered device, developed by Leslie Yeo and colleagues at Monash University, Clayton, generates a surface acoustic wave, a 10-nanometre earthquake-like wave, which travels across the device's surface. When Yeo placed a liquid droplet containing salbutamol, an anti-asthmatic drug, on the surface, the wave blasted the droplet into a fine mist suitable for inhalation into the lungs.

Conventional inhalers rely on a patient's ability to breathe in a drug-containing aerosol. With



the new device, Yeo can alter the drug aerosol's production rate to account for variability in patients' breathing patterns and so deliver the maximum lung dose to the individual. This could be useful for infants, young children or people who have severe cases of asthma, he says.

The device can easily fit in the palm of your hand and is reusable,

**The drug-containing droplet is blasted into a fine mist by the surface acoustic wave**

#### Reference

A Qi *et al*, *Lab Chip*, 2009, DOI:10.1039/b903575c

explains Yeo – an insertable cartridge would provide the drug and be replaced when empty. It delivers a lung dose (percentage of drug delivered to the lower lung region) of 70 to 80 per cent, much higher than the 30 to 40 per cent doses obtained with conventional inhalers. This means less of the drug is wasted, states Yeo.

'This is a most promising aerosol generation technology that can soon be translated into commercialised devices for pulmonary drug delivery,' comments Hsueh-Chia Chang, an expert in microfluidics and medical diagnostics, at the University of Notre Dame, US.

'The delivery of asthmatic steroids is just the tip of the iceberg,' predicts Yeo. 'We hope to be able to deliver vaccines, antibiotics and other drugs in the future.'

Michael Brown

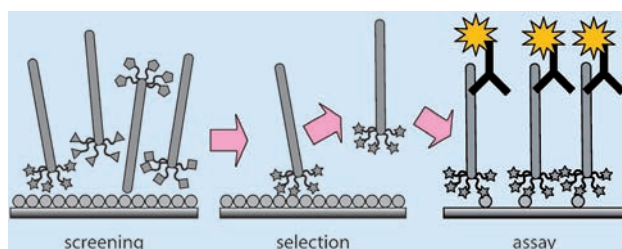
## New tool holds promise for biological studies

# Viruses count quantum dots

Measuring quantum dot (QD) concentrations using viruses could lead to improved cancer imaging, according to scientists in Canada.

Quantum dots have been used in a wide range of biological applications, from tissue imaging to drug delivery. Accurately measuring their concentration is vital for these fields to advance, say Warren Chan and Sawitri Mardiyani, at the University of Toronto. The pair used phage display – a method that uses a library of viruses called phages, each with a different peptide exposed on their surface – to measure QDs.

They coated QDs with one of three different compounds – mercaptoacetic acid (MAA), mercaptoundecanoic acid or bovine serum albumin – and attached them to gelatin-coated substrates. They exposed the QDs to a phage library and some of the surface peptides bound to the QDs. They then washed away the unbound viruses and used an enzyme-linked immunosorbent assay to analyse the bound ones.



They found one peptide sequence that bound only to MAA-coated QDs and showed that they could use it to measure the concentrations of MAA-coated QD solutions ranging from 10 to 1000 nanomoles per litre.

Absorbance and emission spectroscopy are commonly used to measure QD concentrations. However, these methods do not give accurate results in the presence of trypan blue. This stain is commonly used in cancer studies to colour an organism's dead or damaged cells blue, explains Chan, but its high absorbance renders quantum dots invisible. Chan and Mardiyani spiked a solution of MAA-coated QDs with

**QD-specific phages are isolated and used to measure QD concentrations in an enzyme-linked immunosorbent assay**

#### Reference

S Mardiyani and W C W Chan, *J. Mater. Chem.*, 2009, DOI: 10.1039/b906466d

trypan blue and demonstrated that the phage assay could still detect the QD concentration.

'It is important to develop tools that can quantify whole quantum dots in biological environments,' says Chan, 'because in order to optimise the design of these nanoparticles for diagnostic or therapeutic applications, such as cancer imaging, we need to map out their in vivo behaviour.'

'I'd like to see the specificity tested in a more complex environment, such as an actual stained cell and then it could be a valuable, useful tool,' comments Paul Barker from the University of Cambridge, UK, who studies peptides interacting with nanoparticles.

This is something they are exploring, according to Chan: 'We will determine whether immunoassay strategies can be used to measure nanoparticles in cells and tissues and check that the biological environment does not interfere with the binding interactions.' Christina Hodkinson

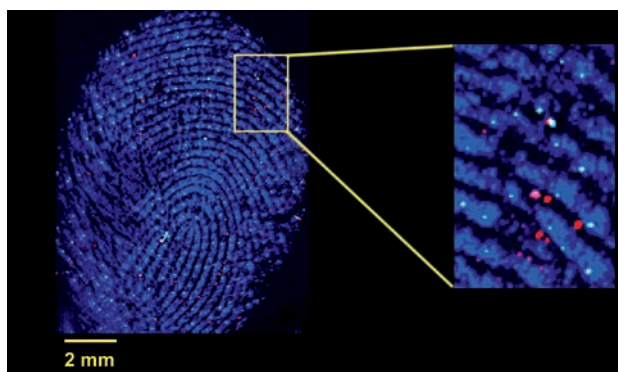
Forensic technique identifies contaminants in crime scene prints

## Exposing explosive fingerprints

US scientists have used infrared (IR) spectroscopy to distinguish between overlapping fingerprints and reveal their chemical history.

Ira Levin and colleagues, at the National Institutes of Health, Bethesda, claim the technique can identify latent (invisible) fingerprints containing contaminants, such as drugs or explosives, and filter out overlapping fingerprints originating from the natural secretions found in fingertips. Previous IR studies of fingerprints have been based only on natural secretions, says Levin, and so failed to provide this extra forensic evidence.

The group took an IR spectroscopic image of two overlapping fingerprints – one natural fingerprint and one containing an explosive. They then distinguished the contaminated fingerprint's spectral image



from the overlapping print using a mathematical method called multivariate analysis. The resulting image clearly showed the explosive in between the fingerprint's ridges. 'You can obtain a fingerprint with the associated forensic evidence which can go through MI5 or FBI databases

**Infrared imaging reveals traces of explosive (red) on a fingerprint**

#### Reference

T Chen, Z D Schultz and I W Levin, *Analyst*, 2009, DOI:10.1039/b908228j

to target an individual,' explains Levin.

Claude Roux, director of the Centre for Forensic Science at the University of Technology, Sydney, Australia, comments that although this is not the first research to be done in this area, it is 'interesting and very relevant because it combines two major aspects of forensic investigations: human identification and chemical characterisation. It shows that not only can IR spectroscopic imaging identify controlled substances, such as explosives, but it can also link these chemicals with the person who touched them.'

Levin says work needs to be done to make the technique more easily accessible but he is confident that it will be useful to forensic teams worldwide. *Jane Hordern*

# 42nd IUPAC CONGRESS

## Chemistry Solutions

2-7 August 2009 | SECC | Glasgow | Scotland | UK

Sponsored by  Schering-Plough

- Analysis & Detection
- Chemistry for Health
- Communication & Education
- Energy & Environment
- Industry & Innovation
- Materials including MC9 conference
- Synthesis & Mechanism

#### Deadlines:

Poster abstract – 5 June 2009

Early bird registration – 5 June 2009

Standard registration – 5 July 2009

Further information: [iupac2009@rsc.org](mailto:iupac2009@rsc.org)

Tel: +44 (0) 1223 432254 / 432380



# Linking electronics

*George Malliaras discusses the interplay between organic electronics and biology with Fay Riordan*



**George Malliaras**

**George Malliaras is a professor in the department of materials science and engineering at Cornell University, New York, US, where he carries out research focusing on organic electronics. He also chairs the *Journal of Materials Chemistry* editorial board.**

## What inspired you to become a scientist?

As a kid, I used to like playing with things that would explode or produce fire. What I liked most was to understand how something works rather than to prove it right, so I thought I would be a scientist rather than an engineer. But lately I have been moving more and more into engineering.

## How did you first become interested in organic electronics?

My interest started when I met my future adviser, Georges Hadziioannou, whilst in the Netherlands studying for a masters degree in silicon surfaces with second harmonic generation. Georges came to give a seminar on polymers and hinted about polymer electronics being a very emerging and exciting field. I found it fascinating and the rest is history!

## What projects are you working on at the moment?

One project I'm working on has to do with the interplay between ionic and electronic carriers in organic materials. I think this will become the biggest new direction in organic electronics. Because organic materials are soft, they can carry ions in addition to electrons and holes. The interplay between the two creates a lot of fascinating physical phenomena and can yield many novel devices. I think the most interesting area is the interface between biology and electronics. Biology works in aqueous media and involves the exchange of ions. On the other hand, solid state electronics is what we like to base our technology on. So organic electronics can link the two fields.

## What is the biggest challenge facing organic electronics?

I think the challenge, and the opportunity, is the interface of organic electronics with biology. So far, organic electronics has been copying traditional electronics. For example, there's a light emitting diode and there's also an organic light emitting diode. The same goes for thin film transistors, solar cells and so on. I think now we have to go beyond that and look at identifying the characteristics of organics. I think, as I said before, that the most promising area is the interplay between ionic and electronic carriers. Bringing biologists aboard will be the biggest challenge but would also generate the biggest opportunities. The community went through a growing phase about 15 years ago when chemists and physicists got together and

developed common objectives and that boosted the field tremendously. Now is the time to bring the biologists aboard.

## What sort of applications arise from the interplay between biology and electronics?

Bioelectronics can yield devices such as biomedical implants, biosensors, environmental monitoring systems and much more.

## What's been your favourite electronics invention or advance?

It's got to be the transistor. This gave rise to electronics as we know it today.

## How do you see the future of electronics?

I see it becoming ubiquitous. The electronics that we have today are still highly localised. For example, you have electronics that exist in gadgets such as your cell phone, but there are not yet electronics integrated into everyday things around us like clothing, the walls, the table and so on. I think that in the future we will see more and more of that.

## What's been your most exciting achievement in your research career?

Students! Seeing the students after they leave the group do really, really well, much better than I ever could. That is the crowning achievement I think.

## What do you enjoy most about your role as chair of the *Journal of Materials Chemistry* editorial board?

I really like interacting with the staff who run the journal and I think it's incredibly professional. I enjoy meeting people and potential authors and saying to them, 'Hey, what do you think of *Journal of Materials Chemistry*? Maybe you could think about submitting your next paper there.' Across the board, I've heard excellent comments and I've spoken to many authors who have been very satisfied with the way that their papers were handled. I find it a lot of fun.

## And finally, if you weren't a scientist, what would you be and why?

That's a hard one. From very early on I felt as though I liked to experiment with stuff, so I'm finding it difficult to think of something I would have done instead. Actually, the first thing I ever wanted to do was work as a litter collector. Because my mum used to throw my old toys away, I thought it would be such a great job because of all the toys you would find in the litter!

## Intelligent features, better separations and faster results

...with highest purity and yield

Isolera™, the new flash purification system from Biotage dramatically shortens purification run-times with a new higher flow rate of 200 mL/minute. Simply load your sample, choose a default method, or create a sample specific method (using the TLC-to-gradient feature), and hit Run.

New advanced features include: the ability to collect fractions on two separate wavelengths, use of up to four solvents in a single gradient and isocratically add a third co-solvent.

Available in single cartridge and 4-cartridge configurations, Isolera systems come complete with SNAP cartridges and everything needed to begin purifying samples.

Visit [www.biotage.com](http://www.biotage.com) for more information or contact your Biotage representative to schedule a demonstration.

  
**Biotage**  
[www.biotage.com](http://www.biotage.com)



### **New! Biotage® SNAP Cartridges:**

- Four different media types  
KP-SIL, KP-NH, KP-C18-HS and  
NEW HP-SIL (high-performance)
- Universal fit with Luer-Lok®  
connections
- 20% more loading capacity
- Higher peak resolution
- Five popular sizes:  
10g, 25g, 50g, 100g, and 340g

## Instant insight

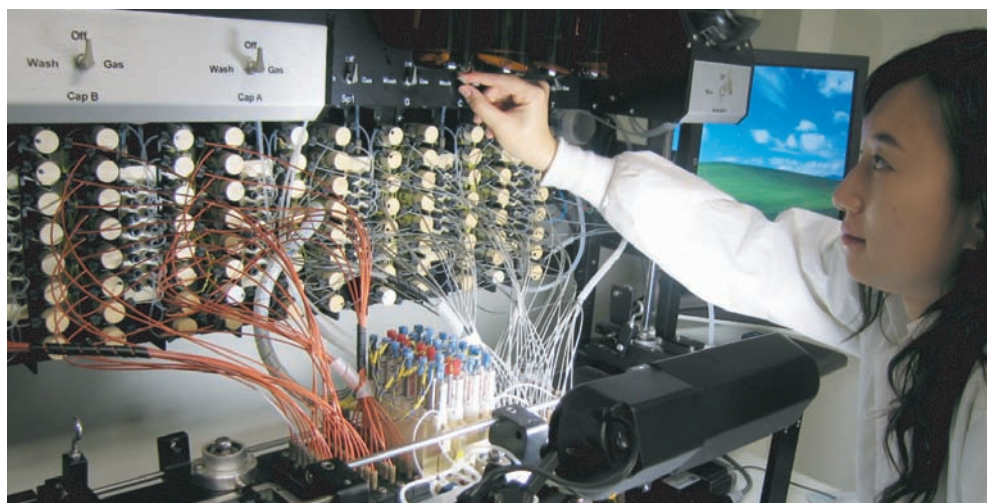
# Rewriting the genetic code

Researchers' dreams of automated gene synthesis could soon become a reality, predict Jingdong Tian and colleagues at Duke University, Durham, US

The emerging field of synthetic biology aims to re-engineer existing biological systems and create novel ones in order to achieve new functions and fashion new products, all through rewriting the genetic code, DNA. The applications are broad and significant, including biomolecular design and engineering; DNA nanotechnology and networks construction; metabolic engineering; and genome synthesis. These improved or new biological systems could help solve our food, energy, material, pharmaceutical and environmental problems in the near future.

The traditional way of modifying DNA sequences is called genetic engineering and mainly relies on various enzymatic activities to manipulate DNA. The future way of doing business would be directly through de novo gene and genome synthesis. Therefore, the ability to rapidly, accurately and economically synthesise DNA constructs of any size or sequence is crucial. Scientists believe that as soon as the technology is automatic and cheap enough, it will replace conventional genetic engineering and transform biomedical research as we know it. Imagine the degree of freedom researchers will enjoy if, at the touch of a screen, they get all the DNA sequences they can dream about synthesised for them.

Today, DNA oligonucleotide synthesis (less than 200 bases) has been automated and is based on the phosphoramidite four-step cycle process, which couples acid-activated deoxynucleoside phosphoramidites to deoxynucleosides on a solid support. Methods for synthesising longer, gene-sized DNA molecules are being improved and mainly rely on the assembly of pre-synthesised oligonucleotides. However, the



overall development of gene and genome synthesis technology has lagged far behind that of gene and genome sequencing. For instance, sequencing a small microbial genome consisting of a few megabases using today's automated genome sequencer would cost only a few thousand dollars and a couple of days. To synthesise the same genome from scratch using available commercial technology (which has yet to be accomplished) would cost tens of millions of dollars and take a whole research team several months. Even worse, the tons of chemical waste (mainly organic solvent) resulting from a small genome synthesis project would surely cause environmental concerns.

The main challenges in technology development for de novo gene synthesis include improving or inventing new DNA synthesis chemistry, reducing or eliminating synthesis errors, miniaturising the reaction apparatus, increasing the throughput of oligonucleotide synthesis and automating the gene assembly process. Synthesis errors accumulate rapidly in an elongating DNA molecule if the step-wise

**Bulky commercial DNA synthesisers are currently used to synthesise short oligonucleotides, the building blocks for gene assembly**

coupling efficiency is less than 100 per cent (it is currently 99.5 to 99.8 per cent). Identifying and correcting those errors is one of the most costly and time-consuming steps in gene synthesis and the hardest process to automate.

To increase throughput and reduce cost and chemical consumption, a current trend is to use DNA microchip and microfabrication techniques to miniaturise and massively parallelise the oligonucleotide synthesis process. Scientists are testing new technologies, such as digital photolithography, inkjet printing, electrochemical array and microfluidics. A few research groups have demonstrated the feasibility of using oligonucleotides synthesised and harvested from DNA microchips for gene assembly. Once scientists optimise the process, synthesising a whole microbial genome from a single microchip will become feasible.

Read more in 'Advancing high-throughput gene synthesis technology' in issue 7 of *MolecularBioSystems*, a synthetic biology theme issue

**Reference**  
J Tian et al, *Mol. BioSyst.*, 2009, DOI: 10.1039/b822268c

# Essential elements

## New journal: *Polymer Chemistry*

On 1 June, RSC Publishing announced that *Polymer Chemistry* – a new journal encompassing all aspects of synthetic and biological macromolecules, and related emerging areas – will be the latest title to join its journal portfolio.

Launching early in 2010, the journal will provide a showcase for the ongoing efforts driving polymer chemistry, highlighting the creativity of the field and previously inaccessible applications. Monthly issues will contain a full mix of research articles including communications, reviews and full papers. The journal will have a broad scope, covering areas of polymer chemistry of interest to materials scientists and bioscientists, as well as all traditional areas of the field.



Editor-in-chief of *Polymer Chemistry* is David Haddleton of the University of Warwick, UK. In outlining his vision for *Polymer Chemistry*, he describes how the new journal 'will report on the best polymer chemistry from

around the globe and will become a high impact factor journal that all polymer chemists will be proud to have on their CV.'

*Polymer Chemistry* joins an exclusive group of journals launched by RSC Publishing in the past 12 months. *Metallomics* and *Integrative Biology* both published their first issues in January 2009, with new journals *Nanoscale* and *Analytical Methods* due to follow later this year.

The current issue of *Polymer Chemistry* will be freely available to everyone on the website from launch until the end of 2011. Free online institutional access to previous issue content during 2010 and 2011 is also available following a simple registration process.

Visit [www.rsc.org/polymers](http://www.rsc.org/polymers) to find out more.

## Free advertising

Finding the right candidate for your vacancy can be a time-consuming, not to mention costly, process. The good news is that *Chemistry World Jobs*, the website for vacancies in chemistry and the chemical sciences, can make this experience easier for you.

Registration is free, and from 1 July to 30 September advertising your vacancy is also free! Simply register your details to create an account, and then upload your job vacancy or training course. What could be easier?

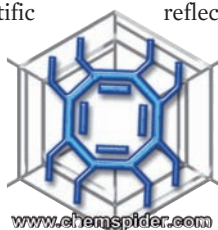
*Chemistry World Jobs* has many registered job seekers who, once new positions are uploaded, are alerted of these vacancies. Therefore, your role will be immediately seen by ideal candidates.

Contact [recruitment@rsc.org](mailto:recruitment@rsc.org) or set up your account today at [www.chemistryworldjobs.org](http://www.chemistryworldjobs.org)

## Community embraces RSC-ChemSpider

Hailed by some as 'a scientific "marriage" made in heaven,' news about RSC's recent acquisition of ChemSpider spread fast through the blogosphere and other channels.

ChemSpider, a free online service providing access to almost 21.5 million unique chemical entities sourced from over 200 different data sources and integration to a multitude of other online services, is the richest single source of structure-based chemistry information. Its acquisition



[www.chemspider.com](http://www.chemspider.com)

reflects RSC's commitment to providing access to premium resources of chemistry data and information. This complements RSC's existing leading role in online chemistry, including award-winning semantic mark-up technology and the release of the InChI resolver, recently launched in partnership with ChemSpider.

Antony Williams, the original host of ChemSpider, is excited by the new possibilities. 'What originally started as a hobby

project to give back something to the chemistry community has become one of the primary internet resources for chemistry. And this from home built computers in a basement, with no funding and a team of volunteers,' he says. 'With the resources, reputation and vision of the RSC to support ChemSpider, our long term goal is to deliver the primary online platform where chemists will resource information and collaborate with a worldwide community of scientists.'

The ChemSpider website will be re-launched later in the year. Visit [www.chemspider.com](http://www.chemspider.com)

*Chemical Technology* (ISSN: 1744-1560) is published monthly by the Royal Society of Chemistry, Thomas Graham House, Science Park, Milton Road, Cambridge UK CB4 0WF. It is distributed free with *Chemical Communications*, *Journal of Materials Chemistry*, *The Analyst*, *Lab on a Chip*, *Journal of Atomic Absorption Spectrometry*, *Green Chemistry*, *CrystEngComm*, *Physical Chemistry Chemical Physics*, *Energy & Environmental Science* and *Analytical Abstracts*. *Chemical Technology* can also be purchased separately. 2009 annual subscription rate: £199; US \$396. All orders accompanied by payment should be sent to Sales and Customer Services, RSC (address above). Tel +44 (0) 1223 432360, Fax +44 (0) 1223 426017 Email: [sales@rsc.org](mailto:sales@rsc.org)

**Editor:** Joanne Thomson  
**Deputy editor:** Sarah Dixon  
**Associate editors:** Celia Gitterman, Elinor Richards  
**Interviews editor:** Ruth Doherty  
**Web editors:** Nicola Convine, Michael Townsend, Debora Giovannelli  
**Essential elements:** Kathryn Lees, Sarah Day, Valerie Simpson  
**Publishing assistant:** Christina Ableman  
**Publisher:** Graham McCann

Apart from fair dealing for the purposes of research or private study for non-commercial purposes, or criticism or review, as permitted under the Copyright, Designs and Patents Act 1988 and the copyright and Related Rights Regulations 2003, this publication may only be reproduced, stored or transmitted, in any form or by any means, with the prior permission of the Publisher or in the case of reprographic reproduction in accordance with the terms of licences issued by the Copyright Licensing Agency in the UK. US copyright law is applicable to users in the USA.

The Royal Society of Chemistry takes reasonable care in the preparation of this publication but does not accept liability for the consequences of any errors or omissions. The RSC is not responsible for individual opinions expressed in *Chemical Technology*. Content does not necessarily express the views or recommendations of the RSC.

Royal Society of Chemistry: Registered Charity No. 207890.

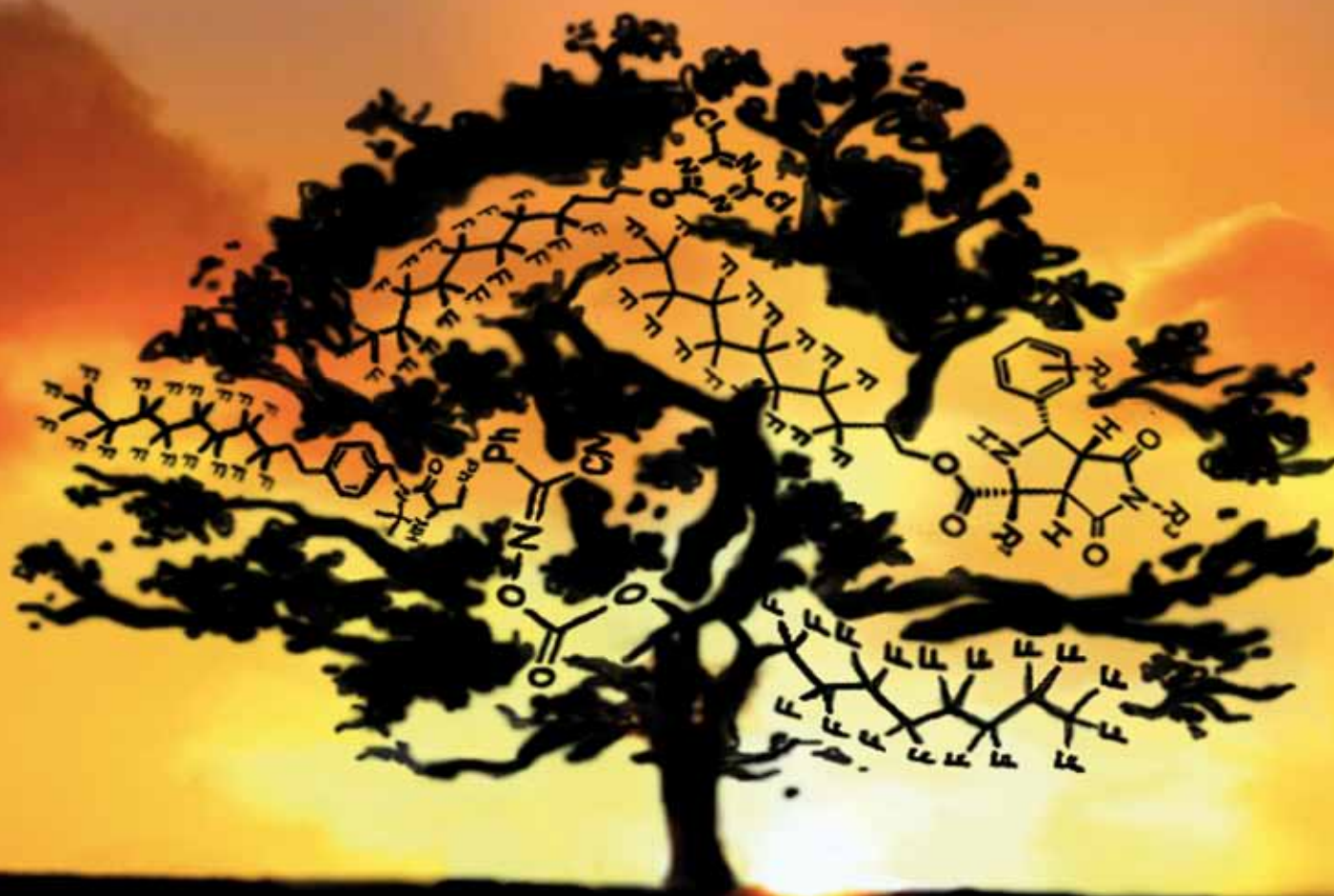
RSC Publishing

# Green Chemistry

Cutting-edge research for a greener sustainable future

[www.rsc.org/greenchem](http://www.rsc.org/greenchem)

Volume 11 | Number 8 | August 2009 | Pages 1069–1272



ISSN 1463-9262

RSC Publishing

Shao *et al.*  
Synthesis of glycols

Zhang  
Fluorous techniques in green chemistry

Aiken *et al.*  
Reactions in gas-expanded liquids

Pan *et al.*  
Hydrolysis of polycarbonate in sub-critical water



1463-9262(2009)11:8;1-6

# Green chemistry aspects of fluorous techniques—opportunities and challenges for small-scale organic synthesis

Wei Zhang\*

Received 20th November 2008, Accepted 27th April 2009

First published as an Advance Article on the web 14th May 2009

DOI: 10.1039/b820740b

Described in this paper is a personal overview of the green chemistry aspects of fluorous technologies. The unique phase separation and broad combinatorial capabilities of fluorous technologies have led to the development of fluorous chromatography-free separations, chemical recycling techniques, atom economic reactions, energy-focused microwave reactions, metal-free organocatalysis, aqueous media reactions, and modified reagents. These green chemistry techniques have been demonstrated in discovery chemistry, medicinal chemistry, and academic research labs dealing with small-scale organic synthesis. Issues such as the environmental impact of fluorous chemicals are also discussed.

## 1. Introduction

In recent years, the advancement of green chemistry has been showcased by numerous examples of large-scale process chemistry and chemical engineering.<sup>1</sup> The well-known 12 principles of green chemistry such as designing new atom economic and energy efficient routes, using environmentally friendly solvents and renewable feed stocks, and developing chemical recycling techniques have become common practices in chemical industry.<sup>2</sup> Implementation of green chemistry in discovery chemistry and academic research settings, however, is a quite different case.<sup>3</sup> The primary function of these labs is to synthesize structurally diverse but small amounts of molecules for physical, chemical, and biological property studies. In these labs, a wide range of

synthetic, analytical and separation methods has to be used. A single green chemistry technique may not generate significant impacts. A strategy which comprehensively addresses different green chemistry concerns in small-scale organic synthesis has yet to be developed.

## 2. Green chemistry techniques for small-scale organic synthesis

Many new tools with the potential for green chemistry applications have been introduced during the development of combinatorial chemistry.<sup>4</sup> Among them, solid-phase synthesis is designed to facilitate the separation process in high-throughput synthesis.<sup>5</sup> This chromatography-free technique significantly reduces the amount of solvent for product purifications. However, the heterogeneous synthesis usually has limitations on both reaction scope and sample analysis capability. The development of solid-supported chemicals and soluble-polymer support for solution-phase synthesis addresses these limitations to some extent.<sup>6</sup> Microwave heating is a powerful and controllable energy source for organic synthesis. It significantly reduces the reaction time since microwave energy can be directly applied to the reactants while generating instant super hot spots.<sup>7</sup> The heating process is so fast that the real reaction temperature could be much higher than the temperature measured by an external IR or internal fiber-optical probe.<sup>7c</sup> Microwave reactions could offer both better product selectivity and higher yield. Many reactions can be carried out using less solvent or even under solvent-free conditions. However, microwave techniques have no direct impact on the separation of reaction mixtures, which is a time-consuming step in the synthesis of compound libraries. Multicomponent reactions are an atom economic way to construct complex molecules.<sup>8</sup> The power of the multicomponent reactions has been further enhanced through integration with a phase tag-based separation technique such as solid-phase synthesis or fluorous synthesis. Reactions in aqueous media avoids the use of some toxic and flammable organic solvents,<sup>9</sup> but product purifications, in most cases, still need a significant amount of organic solvents. Alternative solvents such as supercritical fluids,

Department of Chemistry, University of Massachusetts Boston,  
100 Morrissey Boulevard, Boston, MA 02125, USA.  
E-mail: wei2.zhang@umb.edu; Fax: +1 617-287-6030



Wei Zhang

*Dr Wei Zhang is an Associate Professor in the Department of Chemistry, University of Massachusetts Boston. He received his B.Sc. degree from Nanjing University and Ph.D. from the University of Pittsburgh under the supervision of the late Professor Paul Dowd. His previous positions include Research Assistant Professor at the University of Pittsburgh, Section Chemist at DuPont Agricultural Products,*

*and Director of Discovery Chemistry at Fluorous Technologies, Inc. Dr Wei Zhang is known for his research work in the areas of synthetic free radicals, combinatorial chemistry, and fluorous technologies. He has published over 100 peer-reviewed papers including several review articles.*



ionic liquids, and perfluorinated (fluorous) solvents have been introduced for their unique phase separation capabilities and green chemistry advantages.<sup>10</sup>

With the recent diagram shift in the pharmaceutical industry, efforts for the development of combinatorial chemistry and associated techniques have been deemphasized. However, the awareness of green chemistry has dramatically increased.<sup>11</sup> Among the research labs involved in small-scale organic synthesis, many of them have managed to implement a green chemistry principle to make the existing project “greener,” or put a green chemistry sticker on the existing project if it has a green chemistry component. Many green chemistry publications are related to the modifications of well-established reactions under microwave, ball mill, solvent-free, or aqueous conditions. These kinds of practices have attracted many synthetic chemists entering the field of green chemistry. Introduction of new green chemistry is always appreciated. However, integration of existing green chemistry techniques is equally important, especially for small-scale organic synthesis. A combinatorial green chemistry approach should be developed to address issues in all three aspects of organic synthesis which include reaction, sample analysis, and product separation. The fluororous chemistry presented in this article has demonstrated good potential to become a new platform technology for green chemistry applications.

### 3. Features and challenges of fluororous technologies

Introduced as a new technique for phase-tag-based separations, fluororous chemistry has shown broad applications in homogeneous catalysis,<sup>12</sup> high-throughput synthesis of small molecules,<sup>13</sup> separation of biomolecules,<sup>14</sup> preparation of nanomaterials, non-covalent immobilization for microarray screenings, enzymatic catalysis, microfluidic devices,<sup>15</sup> and green chemistry.<sup>16</sup>

Among many special features associated with the fluororous molecules, the solvophobicity with aqueous and organic solvents are exploited in the development of new phase-tag-based separation techniques. The early development of fluororous technology was focused on biphasic catalysis.<sup>12</sup> For a mixture containing organic and fluororous phases, homogenous fluororous catalytic reaction is carried out at a high temperature, and biphasic separation of the catalyst is conducted at a low temperature. This is an innovative concept and the biphasic recycling system has a good potential for large-scale process chemistry applications. However, the biphasic technique is not suitable for small-scale organic synthesis. The “heavy fluororous” catalysts need to have more than 60% fluorine content to ensure good partition coefficient in fluororous solvents; they are not so atom economic in the synthesis of a small amount of organic molecules.

Fluorous solvents have disputable toxicological properties. Cyclic and related perfluorocarbons have been developed as blood plasma substitutes because of their nontoxic nature, good oxygen and carbon dioxide dissolving power, and high stability.<sup>17</sup> However, many perfluorocarbons are known to be environmentally persistent and the low boiling point perfluorocarbons are believed to be responsible for ozone depletion and global warming.<sup>18</sup> Toxicity concerns have been raised on perfluorooctanoic acid (PFOA) and perfluorooctane sulfonate (PFOS) type compounds.<sup>19</sup> Other than the persistent and

potential toxicity issues, the cost of perfluorinated chemicals is another concern if they are used as solvents for organic reactions and separations.

Two questions need to be answered in order to address the cost and potential toxicity issues: (1) How can fluorine content be significantly reduced but still retain the fluororous characteristics for separation? (2) Is it possible to do fluororous chemistry without using the perfluorinated solvents? The development of “light fluororous” chemistry has opened up an avenue to achieve these goals.<sup>13b,d</sup> In “light fluororous” chemistry, short perfluorocarbon chains such as C<sub>8</sub>F<sub>17</sub> or C<sub>6</sub>F<sub>13</sub> are used as tags to significantly reduce the fluorine content. Fluorous solid-phase extraction (F-SPE) using fluororous silica gel containing a C<sub>8</sub>F<sub>17</sub> stationary phase is a primary way to separate light fluororous compounds.<sup>20</sup> “Light fluororous” chemistry successfully eliminates the use of fluororous solvents in both the reaction and separation steps. In addition, because the reactions are performed in common organic solvents, they are more adaptable to conventional chemical and biochemical processes. Other than the fluororous solvent-free F-SPE, a “fluorous solvent tuning” technique has been explored. It usually applies to “medium fluororous” tags and still requires fluororous solvents such as perfluorinated ethers for liquid–liquid extractions.<sup>21</sup>

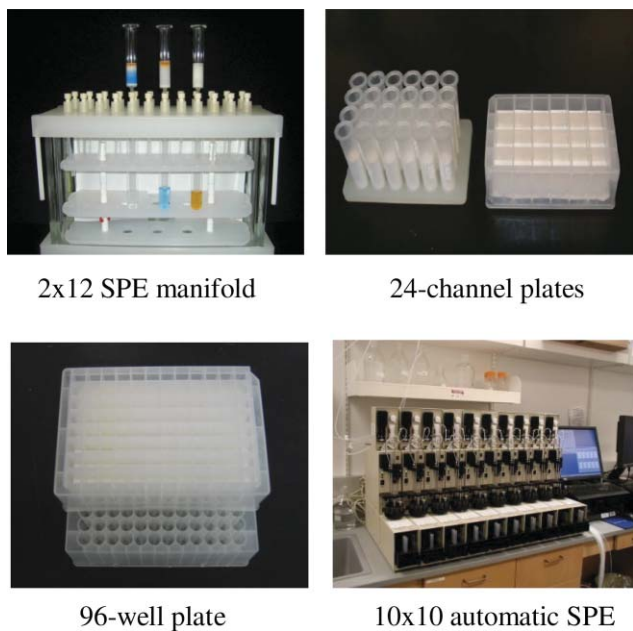
### 4. Fluorous techniques for green chemistry applications

Described in this Section are selected examples of fluororous-based green chemistry techniques for small-scale organic synthesis. The examples developed from the author’s research group were originally introduced as new combinatorial chemistry tools and have not been fully integrated for green chemistry applications. They still have room for further improvement.

#### 4.1. Fluorous solid-phase extraction (F-SPE) for chromatography-free separations

Current drug discovery programs usually require the preparation of small amounts (5–50 mg) but big numbers (50–500) of analogs for biological screenings and structure activity relationship (SAR) studies. In medicinal chemistry labs, more chemical wastes are generated from the sample purifications rather than from the reactions. Chromatography is the most popular method for compound purification; it generates large amounts of waste solvent and is a time-consuming step in compound library synthesis. The application of F-SPE technique increases the synthetic efficiency and also reduces the amount of solvent for purifications.

Because of their solvophobic and fluorophilic natures, fluororous molecules can be retained in fluororous silica gel cartridges when elute with a fluorophobic solvent such as 80 : 20 MeOH–H<sub>2</sub>O. After letting the non-fluorous molecules pass through, the fluororous component is then washed out from the cartridge with a stronger solvent such as MeOH or MeCN. In the separation of light fluororous molecules, F-SPE has much higher separation efficiency than fluororous liquid–liquid extraction. In addition to the commonly used 2 × 12 SPE vacuum manifold, 24-, 48-, and 96-well plates, and automatic F-SPE have been developed for parallel and sequential separations (Scheme 1).<sup>22</sup>



**Scheme 1** Different F-SPE devices for parallel separations.

F-SPE has found broad applications in the separation of mixtures containing fluororous catalysts, reagents, scavengers, and reactants.<sup>20c</sup>

An example of using 1-(perfluorooctyl)propyl isothiocyanate (F-IA) as an amine scavenger in combination with F-SPE for the preparation of a 96-membered urea library is shown in Scheme 2.<sup>22c</sup> Parallel reactions were conducted at 0.1 mmol scale using eight isocyanates (1.0 equiv) and twelve amines (1.2 equiv.). The unreacted amines were quenched with F-IA (0.4 equiv). The 96 reaction mixtures were loaded onto a 96-well F-SPE plate with 0.5 mL of DMSO and then washed three times with 1.25 mL of DMSO. The first two receiving plates containing the products were concentrated under a high vacuum centrifuge evaporator. A total of 500 mL of solvent (5.2 mL per compound) was used for the purification of 96 products by F-SPE. The yields and purity distributions of 96 ureas are shown in Scheme 2. Among the 96 products, 95 products have yields greater than 50% and 95 products have purities greater than 90%.

#### 4.2. Recovery and recycling techniques in fluororous synthesis

Chemical recycling is good for cost reduction and it is also an important principle of green chemistry.<sup>2</sup> Catalyst and solvent recycling has been well-developed in large-scale synthesis, but it is traditionally not a major concern in small-scale synthesis. Only limited techniques, such as solid-supported reagents and catalysts, are available for chemical recovery. Since non-fluorinated compounds are unstuck to fluororous silica gels, this so-called Teflon coated separation median can be easily cleaned up by washing with MeOH, acetone, or MeCN for reuse. The 96-well plate described in Section 4.1 can be reused a dozen times as long as insoluble particles such as metal catalysts or strong acids and bases are not loaded onto the fluororous silica gel, as this may cause irreversible absorptions.

Fluororous catalysts have been successfully recycled by using fluororous silica gel and PTFE as the non-covalent support<sup>23</sup>

or by F-SPE.<sup>24</sup> Scheme 3 shows a Suzuki reaction using a fluororous Pd catalyst which was immobilized on fluororous silica gel support through non-covalent bonding. The reaction was carried out in a common organic solvent. The fluororous catalyst absorbed on the fluororous silica gel was recovered and reused for three times without significant loss of reactivity. Information on the recovery of organocatalysts is presented in Section 4.9.

#### 4.3. Real-time analysis for monitoring of fluororous reactions

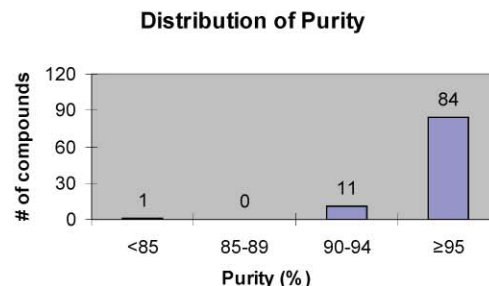
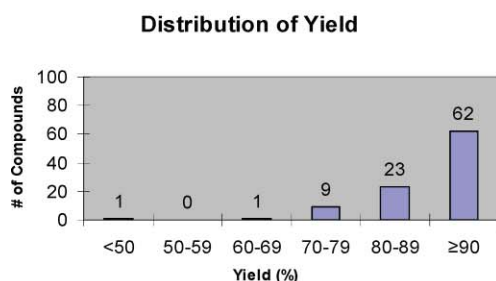
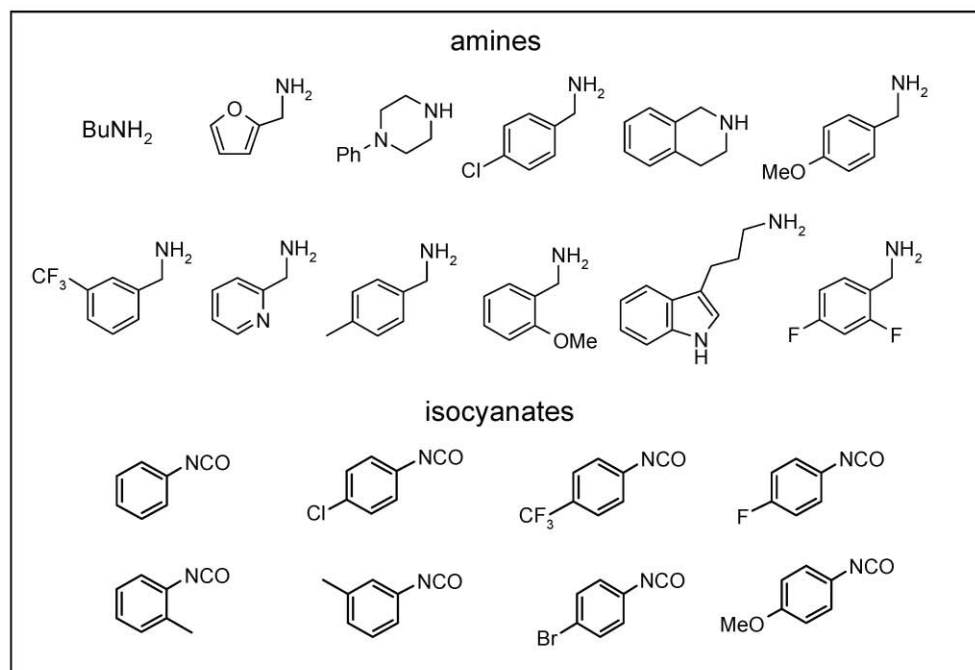
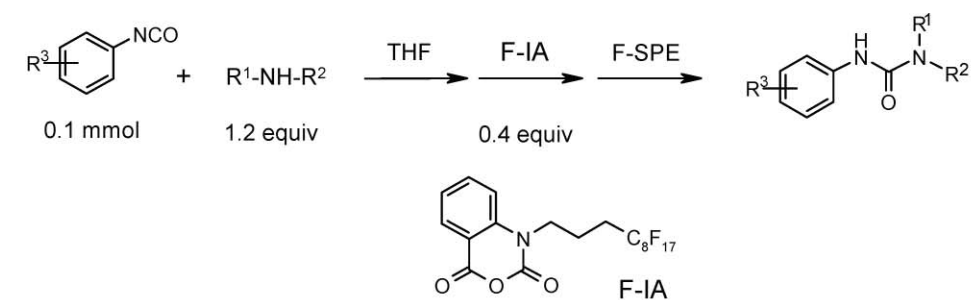
Using real-time analysis to monitor the reaction process is another green chemistry principle.<sup>2</sup> Contrary to solid-phase synthesis in which reaction intermediates attached to the solid support are difficult to be analyzed with conventional tools, fluororous reactions can be easily monitored by analytical methods such as TLC, LC-MS, IR, and NMR since the fluororous molecules have defined molecular weights and structures and they are usually soluble in common organic solvents. The reaction and analytical conditions developed for conventional solution-phase reactions can be easily adapted for fluororous synthesis.

The example shown in Scheme 4 is a fluororous dichlorotriazine (F-DCT)-promoted amide coupling reaction. Each reaction step was closely followed by <sup>1</sup>H NMR analysis.<sup>25</sup> In the first step, one equiv. of F-DCT was mixed with two equiv. of *p*-bromobenzoic acid in THF-*d*<sub>6</sub>. Analysis of the mixture showed no reaction occurred (Scheme 4, a). In the second step, after the addition of 2.1 equiv. of *N*-methylmorpholine (NMM), <sup>1</sup>H NMR analysis showed a chemical shift change of the aromatic protons indicating the formation of activated acid **1** (Scheme 4, b). In the 3rd step, after the addition of two equiv. of *p*-methylbenzylamine, <sup>1</sup>H NMR analysis indicated the formation of amide product **2** (Scheme 4, c). The reaction mixture was then purified by F-SPE to give amide product in 93% yield with a good purity (Scheme 4, d).

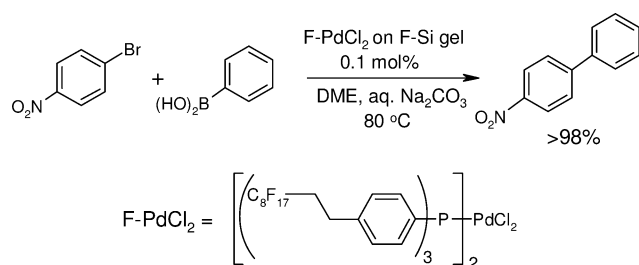
Another general way to follow fluororous reactions is by HPLC with a C<sub>18</sub> or a fluororous (C<sub>8</sub>F<sub>17</sub>) phase.<sup>26</sup> Shown in Scheme 5 is an F-HPLC chromatogram of a 5-component mixture sample generated in fluororous mixture synthesis (see Section 4.7).<sup>27</sup> Under a gradient elution with 80:20 MeOH-H<sub>2</sub>O to 100% MeOH, the mixture was nicely separated based on the fluorine content. The LC-MS gave the MS spectrum for characterization of each LC peak.

#### 4.4. Tagging and detagging strategy for fluororous linkers

One of the green chemistry principles is to avoid the use of auxiliaries and protecting groups.<sup>2</sup> It is very important in large-scale synthesis for both environmental and cost reduction considerations. However, the use of protecting groups is not always avoidable in medicinal chemistry, especially in the preparation of complex molecules. Fluororous linkers can be used to “kill two birds with one stone” and to provide benefits to both reaction and separation steps.<sup>28</sup> The protective linker is used for functional group protection and also for F-SPE. At the linker cleavage step, displacement reactions are employed to detach the fluororous linker and introduce the new groups. This two-in-one strategy maximizes the separation advantage of the fluororous tag and minimizes the effort for the tagging and detagging steps.



**Scheme 2** Synthesis of 96 ureas by fluorous scavenging and SPE techniques (ref. 22c).



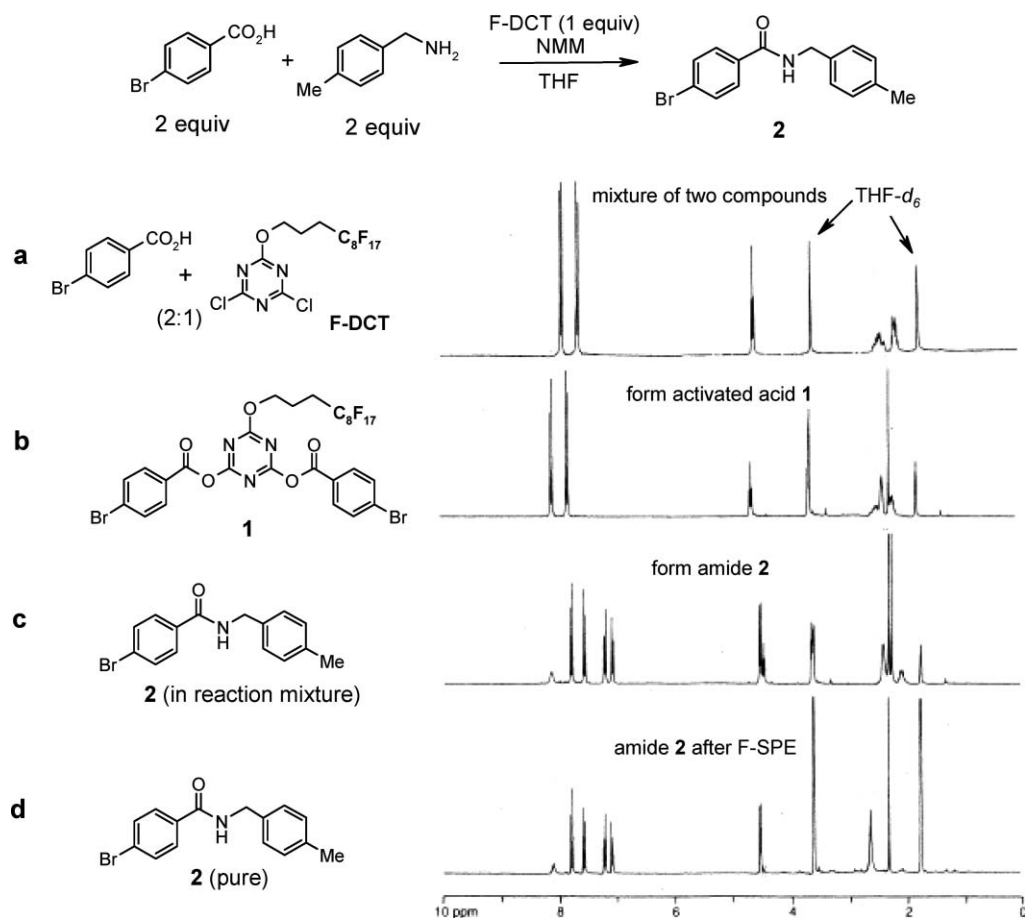
**Scheme 3** Reaction and recovery of fluorous Pd catalyst.

The example shown in Scheme 6 demonstrates the utility of perfluorooctanesulfonyl linker in the synthesis of proline-fused heterocyclic compounds.<sup>29</sup> Fluorous benzaldehydes were used

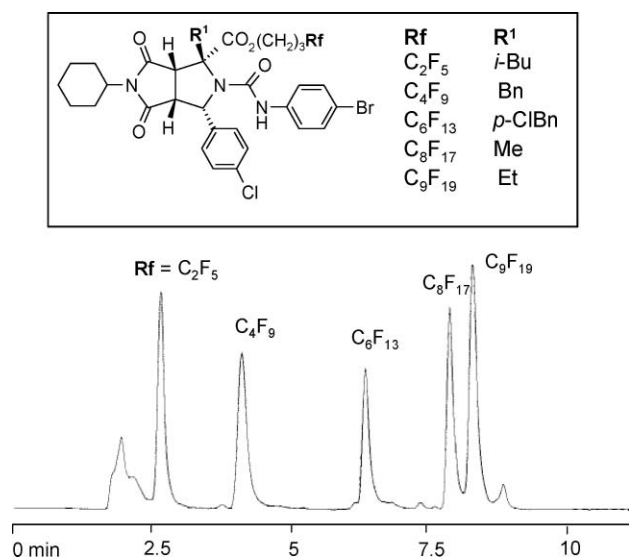
for one-pot, three-component [3 + 2] cycloaddition to form intermediates **3**. The cycloaddition products were subjected to Suzuki coupling reactions to displace the tag and generate the biaryl functional group. Four sets of building blocks were used in the two-step parallel synthesis of products **4** which have four points of diversity ( $R^1$  to  $R^4$ ). More examples of using protective linkers and displacement cleavage protocols for diversity-oriented synthesis can be found in literature.<sup>30</sup>

#### 4.5. Microwave-assisted fluorous synthesis (MAFS) for fast reactions and easy separations

As a powerful and controllable heating source, microwave irradiation has been employed in the development of numerous



**Scheme 4** Monitoring the amide coupling reaction by  $^1\text{H}$  NMR (in  $\text{THF-}d_6$ ) (ref. 25). (a) F-DCT (1.0 equiv) and *p*-bromobenzoic acid (2.0 equiv) in  $\text{THF-}d_6$ ; (b) form activated acid **1** after addition of NMM; (c) form amide **2** after addition of amine; (d) product **2** after F-SPE.



**Scheme 5** F-HPLC analysis of a mixture sample (ref. 27).

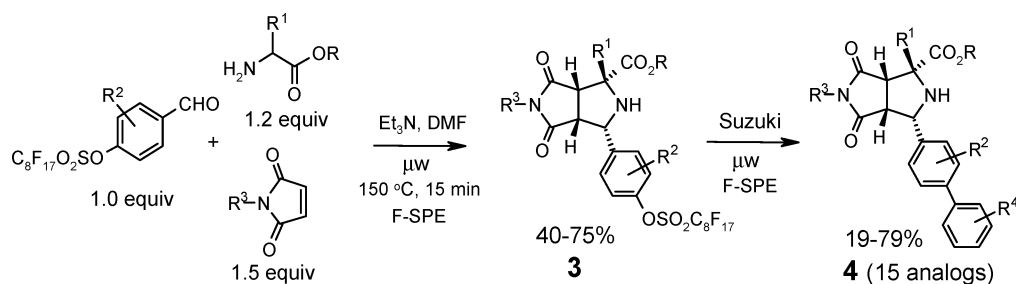
green chemistry reactions.<sup>31</sup> The microwave synthesis offers advantages of reduced reaction time, improved product yield and selectivity, and minimal amounts of reaction solvent. However, it has no direct impact on product purifications. Progress has been made in the combination of microwave heating with polymer-

supported reactions to simplify separations.<sup>7b,32</sup> However, such a technique still has limitations caused by relatively low physical and chemical stability of polymer support under microwave heating. The C–F bond of fluoros molecules has excellent chemical stability (Teflon is a fluoros polymer). Fluoros tags are stable for microwave reactions at elevated temperatures. MAFS has been demonstrated as a powerful tool for solution-phase synthesis of compound libraries.<sup>33</sup>

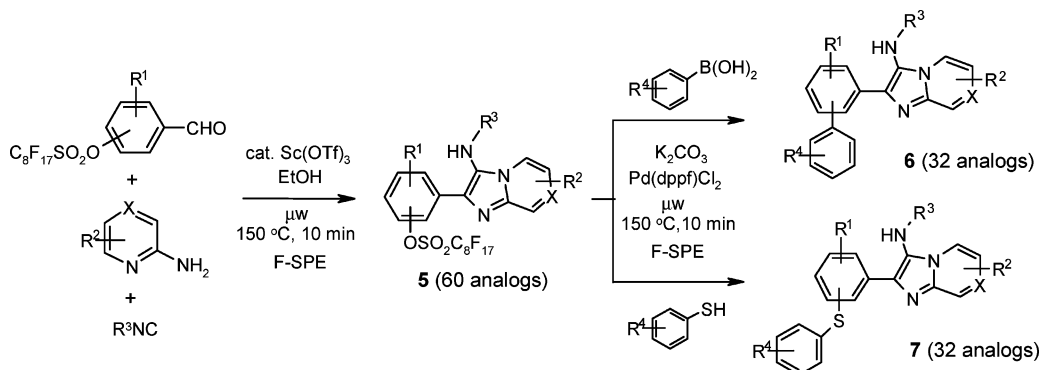
In addition to the example described in Scheme 6, another example for MAFS of heterocyclic compounds is shown in Scheme 7.<sup>34</sup> Perfluoroalkanesulfonyl-protected benzaldehydes reacted with isonitriles and 2-aminopyridines or 2-aminopyrazines to form imidazo[1,2-*a*]pyridine or imidazo[1,2-*a*]pyrazine ring systems **5**. The condensed products were then subjected to Pd-catalyzed cross-coupling reactions with boronic acids or thiols to produce compounds **6** or **7**. Both the intermediates and the final products were purified by F-SPE.

#### 4.6. Atom economic fluoros multicomponent reactions (F-MCRs)

Atom economy is another important principle of green chemistry.<sup>2</sup> A multicomponent reaction (MCR) generates multiple bonds in a single reaction process, which is a highly efficient way to construct complicated molecules.<sup>8</sup> Performing post-condensation modifications further increases the molecular



**Scheme 6** Synthesis of diaryl-substituted proline derivatives **4**.



**Scheme 7** MAFS of heterocyclic compounds.

complexity and molecular diversity. It is a green chemistry approach to make drug-like molecules for lead generation programs. F-MCR employs a fluorous input as the limiting agent.<sup>30</sup> After the MCR, the fluorous component is fished out from the reaction mixture by F-SPE and then used for post-MCR modifications. The fluorous tag can be removed by intermolecular or intramolecular displacement reactions.

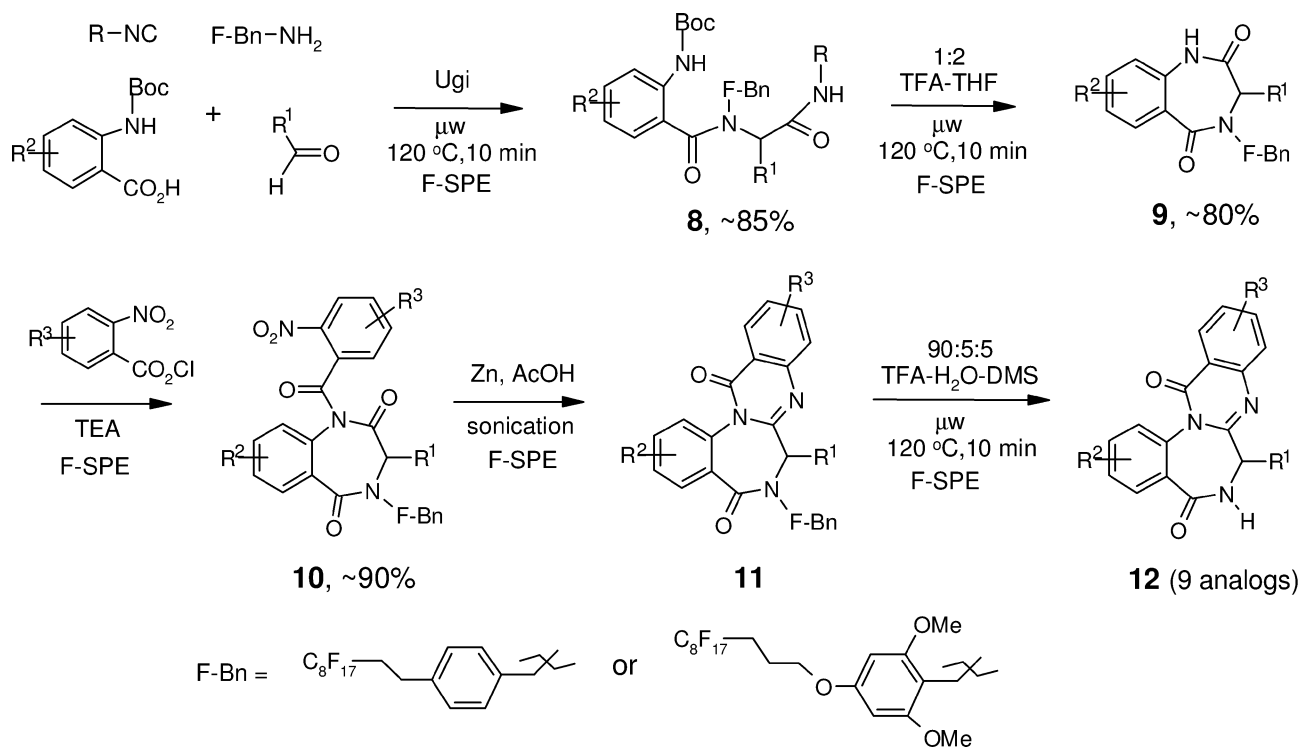
A fluorous Ugi MCR-initiated synthesis of benzodiazepine-quinazolinone alkaloids is highlighted in Scheme 8.<sup>35</sup> Fluorous benzyl amine (F-BnNH<sub>2</sub>) was used as the limiting agent for Ugi reactions to form **8**. The Boc group was selectively removed by the treatment of **1** : 2 TFA-THF under microwave conditions to form benzodiazepinedione **9**. Compounds **9** were acylated with 2-nitrobenzoyl chloride to form **10**, which then underwent nitro group reduction followed by spontaneous cyclization to form benzodiazepine-quinazolinones **11**. The F-Bn linker was removed by the treatment with 90 : 5 : 5 TFA-H<sub>2</sub>O-dimethylsulfide to give final products **12**. This is a good example that demonstrates a combinatorial approach using MCRs, fluorous linkers, and microwave reactions in the synthesis of natural product analogs. More examples can be found in the literature.<sup>30</sup>

Another highly atom economic reaction was discovered in the study of intramolecular [3 + 2] cycloaddition reactions (Scheme 9).<sup>36</sup> The one-pot reaction of fluorous aminoester with excess amounts of *O*-allyl salicylaldehyde **13** generated a novel hexacyclic compound **14** containing four new rings, six new bonds, and seven diastereocenters. The structure of the major diastereoisomer has been confirmed by X-ray crystal structure analysis.

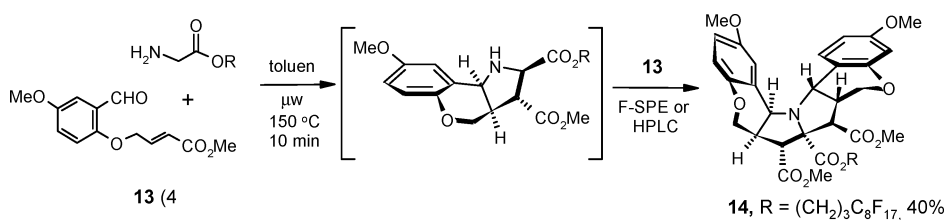
#### 4.7. Highly efficient fluorous mixture synthesis (FMS) of chemical libraries

Fluorous mixture synthesis (FMS) is a new solution-phase technique that produces individual pure compounds without the effort of deconvolution.<sup>37</sup> A set of substrates attached to a corresponding set of homologous fluorous tags is used for mixture synthesis. Fluorous HPLC separates the mixtures and gives individual pure products after the cleavage of fluorous tags. The most important feature of FMS is its high efficiency, which is directly proportional to the number of components mixed and the length of the synthesis.

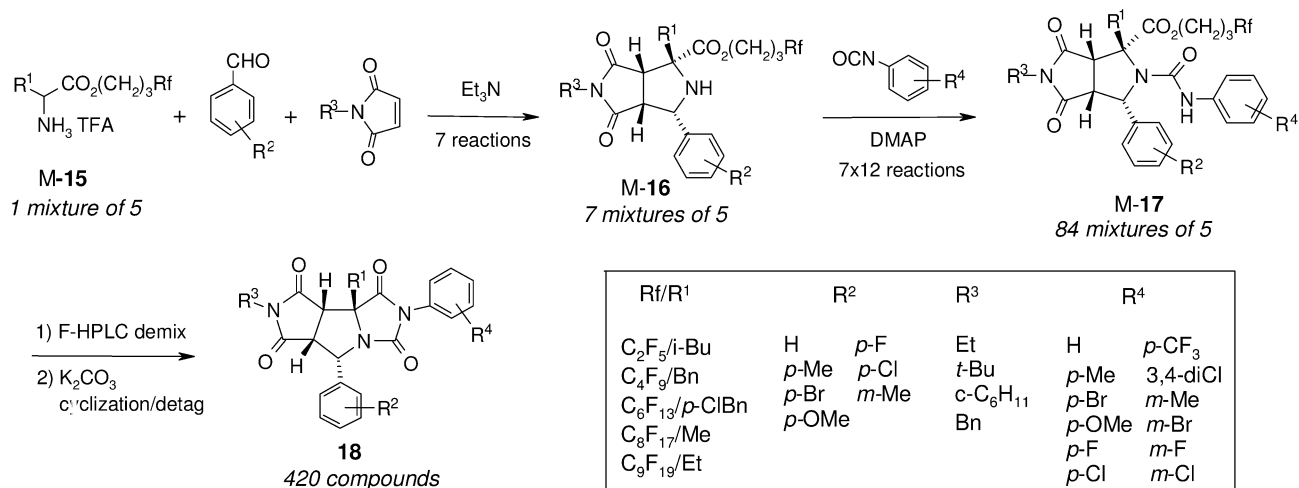
The preparation of a 420-member heterocyclic compound library by FMS is highlighted in Scheme 10.<sup>27</sup> Five  $\alpha$ -amino acids bearing different R<sup>1</sup> groups were paired with five fluorous alcohols (C<sub>2</sub>F<sub>5</sub>/*i*-Bu, C<sub>4</sub>F<sub>9</sub>/Bn, C<sub>6</sub>F<sub>13</sub>/*p*-ClBn, C<sub>8</sub>F<sub>17</sub>/Me, C<sub>9</sub>F<sub>19</sub>/Et). An equal molar mixture of five fluorous aminoesters **M-15** were split to seven portions for 1,3-dipolar cycloaddition reactions with one of the seven benzaldehydes and one of the four maleimides. The resulting seven mixtures of **M-16** were each split into twelve portions and reacted with one of the twelve phenylisocyanates to form 84 mixtures of **M-17**. F-HPLC demixing followed by parallel detagging produced a 420-member library of **18**. The following numbers show the efficiency of FMS. The 420 (84 × 5) ureas **M-17** were prepared in a total of 91 steps (7 cycloaddition + 84 isocyanate reactions) by FMS. If this library were made by parallel synthesis, it would take a total of 455 reactions (35 cycloadditions + 420 isocyanate reactions). In addition to dramatically reducing the numbers of reactions, only 84 HPLC prep-separations were performed to demix and purify 420 ureas **17**. In other words, each HPLC injection generated



**Scheme 8** Synthesis of benzodiazepine-quinazolinones.



**Scheme 9** One-pot synthesis of a novel hexacyclic ring system.



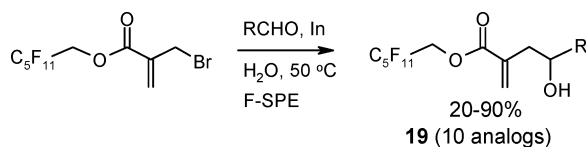
**Scheme 10** Five-component FMS of a 420-member compound library.

5 products (see Scheme 5). The effort and solvent saved by FMS is significant. The power of FMS has also been demonstrated in the synthesis of analogs, diastereomers, and enantiomers of natural products developed by the Curran group.<sup>38</sup>

#### 4.8. Fluorous reactions and separations in aqueous media

Because water is inexpensive and nontoxic, it has been considered by many people as a green solvent for large-scale synthesis.<sup>10</sup> But others have argued that waste water treatment can be a difficult task since the aqueous waste cannot be burned like organic waste and has to be discharged in to the environment after treatment.<sup>39</sup> Nevertheless, using water as a solvent for small-scale synthesis has advantages simply based on the considerations of low cost, nonflammable, and nontoxic natures of water.<sup>9</sup> However, most aqueous reactions still need a significant amount of organic solvent for purification. Fluorous chemistry has the potential to use water as the primary solvent for both reactions and separations.

The combination of aqueous reactions and F-SPE purification has been demonstrated in indium-mediated allylation of aldehydes with fluorous bromides (Scheme 11).<sup>40</sup> The reaction mixture containing compound **19** was directly loaded onto a short path of fluorous silica gel and isolated by gradient elution using acetone–water or simply just water. Using water as a major solvent for both reaction and separation increases the green chemistry aspect of the synthesis. So far this is the only example reported in the literature; more developments in this area are expected.



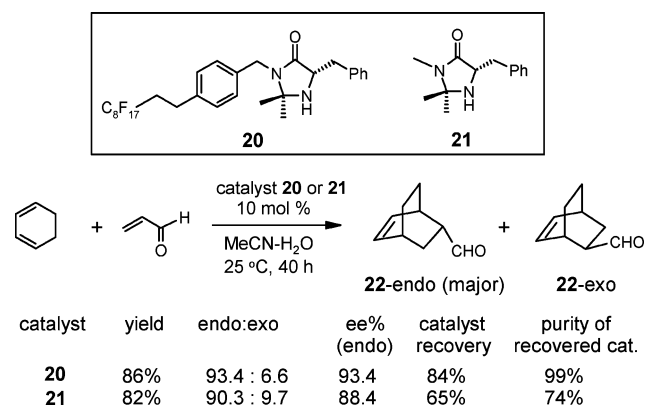
**Scheme 11** H<sub>2</sub>O-based reaction and F-SPE separation of compound **19**.

There is a new separation protocol called “just add water” that has been developed for fluorous synthesis. Because of enhanced hydrophobicity, some fluorous products such as biomolecules can be easily precipitated out from the reaction mixture when suspended in water. This protocol has been successfully applied to synthesis of oligonucleotides<sup>41</sup> and peptides.<sup>42</sup>

#### 4.9. Metal-free fluorous organocatalysis and catalyst recovery

Because of its novel activation mechanisms, mild reaction conditions, and its environmentally friendly nature, organocatalysis has attracted a high level of interest and has been applied to enantioselective Michael, aldol, Diels–Alder, Mannich, and 1,3-dipolar cycloaddition reactions.<sup>43</sup> However, organocatalysis usually requires a high catalyst loading (5–30 mol%). Without an appropriate catalyst recovery technique, organocatalysis will have a high cost concern for large-scale reactions. Fluorous organocatalysis has good potential to retain the catalyst activity while addressing the catalyst recovery issue. The fluorous versions of proline, pyrrolidine, prolinol, imidazolidinone, and cinchona-type organocatalysts have been introduced and the recovery issue has been discussed.<sup>44</sup>

The example shown in Scheme 12 demonstrates the reactivity and recovery of fluorous imidazolidinone (MacMillan) catalyst **20** for the asymmetric Diels–Alder reactions.<sup>45</sup> Compared to the normal imidazolidinone catalyst **21**,<sup>46</sup> fluorous catalyst **20** gave product **22-endo** in a slightly better yield (86%) and enantioselectivity (93.4% ee). Fluorous catalyst **20** was recovered by F-SPE in 84% yield with 99% purity. It can be directly used for the next round of reaction. On the other hand, regular imidazolidinone catalyst **21** was recovered by acid–base work up in 65% yield with only 74% purity. It cannot be used for the next round of reaction without further purification.

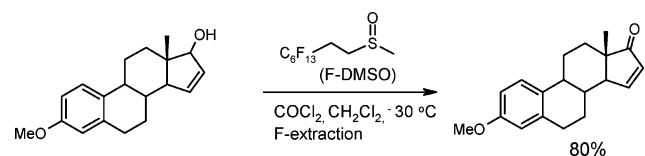


**Scheme 12** Fluorous and nonfluorous imidazolidinone-catalyzed Diels–Alder reactions.

#### 4.10. Fluorous-attached reagents for improved chemical and physical properties

Modification of a reagent to reduce its unwanted chemical and physical properties while still retaining good reactivity is another green chemistry principle.<sup>2</sup> Immobilization of reagents or catalysts on solid support is a useful strategy, but the reactivity of the solid-supported reagent is hard to anticipate because of its heterogeneous nature when reacted.<sup>47</sup> A fluorous-modified reagent usually maintains its original reactivity and also has good recovery.

Tributyltin hydride is a popular reagent for free radical reactions. However, the separation of organotin derivatives from the reaction mixture is not an easy task. The development of fluorous tributyltin hydride provided a new way to address the separation issue.<sup>48</sup> The DMSO-based Swern oxidation reaction provides another example. This reaction is notorious for the problem of releasing malodorous and volatile dimethyl sulfide. The fluorous DMSO has been developed, and has proven to be a good oxidation agent for converting alcohols to corresponding aldehydes or ketones.<sup>49</sup> Scheme 13 shows the fluorous reaction using similar procedures for the classic Swern protocol. The oxidized product was produced in a good yield, and the fluorous



**Scheme 13** Fluorous DMSO for the Swern oxidation.

sulfide was recovered by extraction with FC72 and then treated with H<sub>2</sub>O<sub>2</sub> to give regenerated fluoros DMSO in 88% yield. Since fluoros sulfide is less volatile than dimethyl sulfide, it made the reaction process almost odorless. Fluoros sulfide has also been used to make a borane complex for the hydroboration of alkenes and for asymmetric reduction of ketones with a chiral catalyst.<sup>50</sup>

The utility of odorless and recyclable fluoros reagents can be future extended. Isocyanides (or isonitriles) are an important component of Ugi multicomponent reactions, but suffer from a strong pernicious odor.<sup>51</sup> The development of fluoros isocyanides may result in odorless reactants for Ugi reactions. Since the isocyanide will be part of the product, a cleavable fluoros tag for isocyanide is required.

## 5. Conclusions and prospective view

Green chemistry introduces a new philosophy and sets a high standard for conducting chemical research and production. We are charged to maximize the benefits of chemical products we introduce to society, and to minimize any side effects that could be harmful to our environment. This is a continuous challenge that needs to be acknowledged by fellow chemists through increased environmental protection awareness and the advancement of new technologies.

Fluoros chemistry overlaps with many combinatorial techniques and has many green chemistry aspects in reaction, analysis, and separation steps. The hybridization of green chemistry and combinatorial chemistry is expected to introduce more “green tools” into the toolbox for small-scale organic synthesis. The development of light fluoros chemistry has significantly reduced the environmental impact caused by the use of persistent fluoros solvents and heavy fluoros chemicals. However, there still remains much to do in further increasing the commercial availability of fluoros reagents, the reduction of their price, the introduction of more biodegradable fluoros tags such as perfluoroethers,<sup>52</sup> and integration of fluoros techniques into automatic systems in industrial labs. To have a better understanding of fluoros separation mechanisms may result in the development of new silica gels and polymer-based sorbents with improved performance for F-SPE and F-HPLC.<sup>53</sup> Collaborative research efforts from fluoros, organofluorine, polymer, organic, and analytical chemists, combined with a good business development strategy are required to advance fluoros chemistry to be a greener and mainstream synthetic technology.

## Acknowledgements

The author thanks University of Massachusetts Boston Center for Green Chemistry and the Joseph P. Healey Grant for partial support of this work.

## References

- (a) *Green Engineering*, ed. P. T. Anastas, L. G. Heine and T. C. Williamson, Oxford University Press, Oxford, 2000; (b) *Green Chemical Syntheses and Processes*, ed. P. T. Anastas, L. G. Heine and T. C. Williamson, American Chemical Society Publication, 2001; (c) *Handbook of Green Chemistry & Technology*, ed. J. H. Clark and D. Macquarrie, Blackwell Science Ltd, Oxford, 2002; (d) *Advancing Sustainability Through Green Chemistry and Engineering*, ed. R. L. Lankey and P. T. Anastas, American Chemical Society Publication, 2005.
- For twelve principles of green chemistry, see: P. T. Anastas and J. C. Warner, *Green Chemistry: Theory and Practice*, Oxford University Press, Oxford, 1998.
- J. L. Tucker, *Org. Process Res. Dev.*, 2006, **10**, 315–319.
- Handbook of Combinatorial Chemistry*, ed. K. C. Nicolaou, R. Hanko and W. Hartwig, Wiley-VCH, Weinheim, 2002, vol. 1 and 2.
- (a) *Organic Synthesis on Solid Phase*, ed. F. Z. Dorwald, Wiley-VCH, Weinheim, 2000; (b) *Solid Phase Organic Synthesis*, ed. K. Burgess, John Wiley & Sons, New York, 2000.
- (a) T. J. Dickerson, N. N. Reed and K. D. Janda, *Chem. Rev.*, 2002, **102**, 3325–3343; (b) S. V. Ley, I. R. Baxendale, R. N. Bream, P. S. Jackson, A. G. Leach, D. A. Longbottom, M. Nesi, R. I. Storer and S. J. Taylor, *J. Chem. Soc., Perkin Trans. 1*, 2000, 3815–4195.
- (a) *Microwaves in Organic Synthesis*, ed. A. Loupy, Wiley-VCH, Weinheim, 2002; (b) C. O. Kappe and A. Stadler, *Microwaves in Organic and Medicinal Chemistry*, Wiley-VCH, Weinheim, 2005; (c) M. A. Herrero, J. M. Kremsner and C. Oliver Kappe, *J. Org. Chem.*, 2008, **73**, 36–47.
- (a) *Multicomponent Reactions*, ed. J. Zhu and H. Bienayme, Wiley, Weinheim, 2005; (b) A. Dömling, *Chem. Rev.*, 2006, **106**, 17–89.
- C. J. Li, and T.-H. Chan, *Comprehensive Organic Reactions in Aqueous Media*, 2nd edn, Wiley-VCH, Hoboken, 2007.
- (a) R. A. Sheldon, *Green Chem.*, 2005, **7**, 267–278; (b) C. Capello, U. Fischer and K. Hungerbühler, *Green Chem.*, 2007, **9**, 927–934; (c) J. H. Clark and S. J. Tavener, *Org. Process Res. Dev.*, 2007, **11**, 149–155; (d) I. T. Horváth, *Green Chem.*, 2008, **10**, 1024–1028.
- (a) H.-J. Federsel, *Drug Discovery Today*, 2006, **11**, 966–974; (b) D. J. C. Constable, P. J. Dunn, J. D. Hayler, G. R. Humphrey, J. L. Leazer, Jr., R. J. Linderman, K. Lorenz, J. Manley, B. A. Pearlman, A. Wells, A. Zaksh and T. Y. Zhang, *Green Chem.*, 2007, **9**, 411–420.
- (a) I. T. Horváth, *Acc. Chem. Res.*, 1998, **31**, 641–650; (b) E. de Wolf, G. van Koten and B.-J. Deelman, *Chem. Soc. Rev.*, 1999, **28**, 37–41; (c) L. P. Barthel Rosa and J. A. Gladysz, *Coord. Chem. Rev.*, 1999, **190–192**, 587–605; (d) G. Pozzi and I. Shepperson, *Coord. Chem. Rev.*, 2003, **242**, 115–124.
- (a) D. P. Curran, *Angew. Chem., Int. Ed.*, 1998, **37**, 1174–1196; (b) W. Zhang, *Tetrahedron*, 2003, **59**, 4475–4489; (c) W. Zhang, *Chem. Rev.*, 2004, **104**, 2531–2556; (d) D. P. Curran, *Aldrichimica Acta*, 2006, **39**, 3–9.
- (a) W. Zhang, in *Current Fluoroorganic Chemistry. New Synthetic Directions, Technologies, Materials and Biological Applications*, ed. V. A. Soloshonok, K. Mikami, T. Yamazaki, J. T. Welch and J. Honek, Oxford University Press, 2006, pp. 207–220; (b) C. Y. Nicholas, D. Yuksel, L. Dafik and K. Kumar, *Curr. Opin. Chem. Biol.*, 2006, **10**, 1–8.
- (a) D. P. Curran, *Science*, 2008, **321**, 1645–1646; (b) W. Zhang and C. Cai, *Chem. Commun.*, 2008, 5686–5694 and references cited there in.
- (a) J.-M. Vincent, A. Rabion and R. H. Fish, in *Green Chemical Syntheses and Processes*, ed. P. T. Anastas, L. G. Heine and T. C. Williamson, ACS Symposium Series 767, ACS 2000, pp. 172–181; (b) F. Montanari, G. Pozzi and S. Quici, in *Green Chemistry – Challenging Perspectives*, ed. P. Tundo and P. Anastas, Oxford University Press, 2000, pp. 145–160; (c) D. P. Curran and Z. Lu, *Green Chem.*, 2001, **3**, G3–G7; (d) S. J. Tavener and J. H. Clark, *J. Fluorine Chem.*, 2003, **123**, 31–36; (e) J. A. Gladysz, *Pure Appl. Chem.*, 2001, **73**, 1319–1324; (f) I. T. Horváth, *Green Chem.*, 2008, **10**, 1024–1028; (g) J. A. Gladysz, in *Green Catalysis, vol. 1: Homogeneous Catalysis*, ed. P. T. Anastas, Wiley-VCH, Weinheim, 2009, pp. 17–38.
- K. C. Lowe, *Tissue Eng.*, 2003, **9**, 389–399.
- M. A. K. Khalil, R. A. Rasmussen, J. A. Culbertson, J. M. Prins, E. P. Grimsrud and M. J. Shearer, *Environ. Sci. Technol.*, 2003, **37**, 4358–4361.
- G. L. Kennedy, J. L. Butenhoff, G. W. Olsen, J. C. O’Connor, A. M. Seacat, R. G. Perkins, L. B. Biegel, S. R. Murphy and D. G. Farrar, *Crit. Rev. Toxicol.*, 2004, **34**, 351–384.
- (a) D. P. Curran, *Synlett*, 2001, 1488–1496; (b) D. P. Curran, in *Handbook of Fluoros Chemistry*, ed. J. A. Gladysz, D. P. Curran and I. T. Horváth, Wiley-VCH, Weinheim, 2004, pp. 101–127; (c) W. Zhang and D. P. Curran, *Tetrahedron*, 2006, **62**, 11837–11865.
- (a) M. S. Yu, D. P. Curran and T. Nagashima, *Org. Lett.*, 2005, **7**, 3677–3680; (b) Q. Chu, M. S. Yu and D. P. Curran, *Tetrahedron*, 2007, **63**, 9890–9895.



- 22 (a) W. Zhang, Y. Lu and T. Nagashima, *J. Comb. Chem.*, 2005, **7**, 893–897; (b) W. Zhang and Y. Lu, *J. Comb. Chem.*, 2006, **8**, 890–896; (c) W. Zhang and Y. Lu, *J. Comb. Chem.*, 2007, **9**, 836–843.
- 23 (a) C. C. Tzschucke, C. Markert, H. Glatz and W. Bannwarth, *Angew. Chem., Int. Ed.*, 2002, **41**, 4500–4503; (b) B. Croxtall, E. G. Hope and A. M. Stuart, *Chem. Commun.*, 2003, 2430–2431; (c) E. G. Hope, A. M. Stuart and A. J. West, *Green Chem.*, 2004, **6**, 345–350; (d) R. Bernini, S. Cacchi, G. Fabrizi, G. Forte, S. Niembro, F. Petrucci, R. Pleixats, A. Prastaro, R. M. Sebastian, R. Soler, M. Tristany and A. Vallribera, *Org. Lett.*, 2008, **10**, 561–564.
- 24 (a) L. V. Dinh and J. A. Gladysz, *Angew. Chem., Int. Ed.*, 2005, **44**, 4095–4097; (b) F. O. Seidel and J. A. Gladysz, *Adv. Synth. Catal.*, 2008, **350**, 2443–2449.
- 25 C. H.-T. Chen and W. Zhang, *Mol. Diversity*, 2005, **9**, 353–359.
- 26 W. Zhang, *J. Fluorine Chem.*, 2008, **129**, 910–919.
- 27 W. Zhang, Y. Lu, C. H.-T. Chen, L. Zeng and D. B. Kassel, *J. Comb. Chem.*, 2006, **8**, 687–695.
- 28 (a) W. Zhang, in *Handbook of Fluorous Chemistry*, eds J. A. Gladysz, D. P. Curran, I. T. Horvath, Wiley-VCH, Weinheim, 2004, pp. 222–236; (b) W. Zhang, *Curr. Opin. Drug Discovery Dev.*, 2004, **7**, 784–797; (c) W. Zhang, *Chem. Rev.*, 2009, **109**, 749–795.
- 29 W. Zhang and C. H.-T. Chen, *Tetrahedron Lett.*, 2005, **46**, 1807–1810.
- 30 W. Zhang, *Comb. Chem. High Throughput Screening*, 2007, **10**, 19–229.
- 31 R. S. Varma, *Green Chem.*, 2008, **10**, 1129–1130.
- 32 A. Stadler and C. Oliver Kappe, *Eur. J. Org. Chem.*, 2001, 919–925.
- 33 W. Zhang, in *Microwave Methods in Organic Synthesis, Topics Curr. Chem.*, ed. M. Larhed and K. Olofsson, Springer, 2006, vol. 266, pp. 145–166.
- 34 Y. Lu and W. Zhang, *QSAR Comb. Sci.*, 2004, **23**, 827–835.
- 35 W. Zhang, J. P. Williams, Y. Lu, T. Nagashima and Q. Chu, *Tetrahedron Lett.*, 2007, **48**, 563–565.
- 36 W. Zhang, Y. Lu and S. Geib, *Org. Lett.*, 2005, **7**, 2269–2272.
- 37 (a) Z. Y. Luo, Q. S. Zhang, Y. Oderaotoshi and D. P. Curran, *Science*, 2001, **291**, 1766–1769; (b) W. Zhang, *Arkivoc*, 2004, (i), 101–109; (c) Q. Zhang and D. P. Curran, *Chem.–Eur. J.*, 2005, **11**, 4866–4880.
- 38 Selected papers on FMS: (a) W. Zhang, Z. Luo, C. H.-T. Chen and D. P. Curran, *J. Am. Chem. Soc.*, 2002, **124**, 10443–1044; (b) S. Dandapani, M. Jeske and D. P. Curran, *Proc. Natl. Acad. Sci. U. S. A.*, 2004, **101**, 12008–12012; (c) C. S. Wilcox, V. Gudipati, H. Lu, S. Turkyilmaz and D. P. Curran, *Angew. Chem., Int. Ed.*, 2005, **44**, 6938–6940; (d) D. P. Curran, Q. S. Zhang, C. Richard, H. Lu, V. Gudipati and C. S. Wilcox, *J. Am. Chem. Soc.*, 2006, **128**, 9561–9573; (e) F. Yang and D. P. Curran, *J. Am. Chem. Soc.*, 2006, **128**, 14200–14205; (f) W. H. Jung, S. Guyenne, C. Riesco-Tagundo, J. Mancuso, S. Nakamura and D. P. Curran, *Angew. Chem., Int. Ed.*, 2008, **47**, 1130–1133.
- 39 D. G. Blackmond, A. Armstrong, V. Coombe and A. Wells, *Angew. Chem., Int. Ed.*, 2007, **46**, 3798–3800.
- 40 C. S. Reid, Y. Zhang and C.-J. Li, *Org. Biomol. Chem.*, 2007, **5**, 3589–3591.
- 41 S. Tripathi, K. Misra and Y. S. Sanghvi, *Org. Prep. Proc.*, 2005, **37**, 257–263.
- 42 M. Vittorio and K. Kumar, *J. Am. Chem. Soc.*, 2004, **126**, 9528–9529.
- 43 (a) A. Berkessel and H. Groger, *Asymmetric Organocatalysis—From Biomimetic Concepts to Applications in Asymmetric Synthesis*, Wiley-VCH, Weinheim, 2005; (b) *Enantioselective Organocatalysis—Reactions and Experimental Procedures*, ed. P. I. Dalko, Wiley-VCH, Weinheim, 2007.
- 44 (a) F. Fache and O. Piva, *Tetrahedron Lett.*, 2001, **42**, 5655–5657; (b) F. Fache and O. Piva, *Tetrahedron: Asymmetry*, 2003, **14**, 139–143; (c) Z. Dalicsek, F. Pollreis, A. Gomory and T. Soos, *Org. Lett.*, 2005, **7**, 3243–3246; (d) L. Zu, J. Wang, H. Li and W. Wang, *Org. Lett.*, 2006, **8**, 3077–3079; (e) A. V. Malkov, M. Figlus, S. Stoncius and P. Kocovsky, *J. Org. Chem.*, 2007, **72**, 1315–1325; (f) H. Cui, Y. Li, C. Zheng, G. Zhao and S. Zhu, *J. Fluorine Chem.*, 2008, **129**, 45–50; (g) Q. Chu, M. S. Yu and D. P. Curran, *Org. Lett.*, 2008, **10**, 749–752; (h) L. Zu, H. Xie, H. Li, J. Wang and W. Wang, *Org. Lett.*, 2008, **10**, 1211–1214.
- 45 Q. Chu, W. Zhang and D. P. Curran, *Tetrahedron Lett.*, 2006, **47**, 9287–9290.
- 46 (a) K. A. Ahrendt, C. J. Borths and D. W. C. MacMillan, *J. Am. Chem. Soc.*, 2000, **122**, 4243–4244; (b) R. M. Wilson, W. S. Jen and D. W. C. MacMillan, *J. Am. Chem. Soc.*, 2005, **127**, 11616–118617.
- 47 (a) F. Cozzi, *Adv. Synth. Catal.*, 2006, **348**, 1367–1390; (b) M. Benaglia, *New J. Chem.*, 2006, **30**, 1525–1533; (c) M. Benaglia, A. Puglisi and F. Cozzi, *Chem. Rev.*, 2003, **103**, 3401–3429.
- 48 D. P. Curran and S. Hadida, *J. Am. Chem. Soc.*, 1996, **118**, 2531–2532.
- 49 D. Crich and S. Neelamkavil, *J. Am. Chem. Soc.*, 2001, **123**, 7449–7450.
- 50 D. Crich and S. Neelamkavil, *Org. Lett.*, 2002, **4**, 4175–4177.
- 51 A. Dömling and I. Ugi, *Angew. Chem.*, 2000, **39**, 3168–3210.
- 52 Q. L. Chu, C. Henry and D. P. Curran, *Org. Lett.*, 2008, **10**, 2453–2456.
- 53 G. Osei-Prempeh, H.-J. Lehmler, S. E. Rankin and B. L. Knutson, *Ind. Eng. Chem. Res.*, 2008, **47**, 530–538.

# Marrying gas power and hydrogen energy: A catalytic system for combining methane conversion and hydrogen generation†

Jurriaan Beckers,<sup>\*a</sup> Cyril Gaudillère,<sup>b</sup> David Farrusseng<sup>b</sup> and Gadi Rothenberg<sup>\*a</sup>

Received 9th January 2009, Accepted 31st March 2009

First published as an Advance Article on the web 14th April 2009

DOI: 10.1039/b900516a

**Ceria-based catalysts are good candidates for integrating methane combustion and hydrogen generation. These new, tuneable catalysts are easily prepared. They are robust inorganic crystalline materials, and perform well at the 400 °C–550 °C range, in some cases even without precious metals. This makes them attractive for practical applications in the energy conversion market.**

Achieving a sustainable energy economy is, without a doubt, one of the biggest challenges that we face in the 21st century. Several factors make this challenge both urgent and important. Fossil oil reserves are running out, CO<sub>2</sub> emissions are heating up our planet, and world energy demands are growing alarmingly.<sup>1,2</sup> Clearly, we must find alternative solutions. Much work is being done in several parallel fields, including harnessing solar,<sup>3,4</sup> wind,<sup>5</sup> and geothermal power,<sup>6</sup> developing safer nuclear technologies,<sup>7</sup> and refining biomass.<sup>8–11</sup> Indeed, recent surveys show that mankind must work on all these fronts to reach the goal of sustainable energy.<sup>12</sup>

The problem is that the current energy market is a conservative one, with companies looking first and foremost for pragmatic solutions. Moreover, any change from one energy source to another will be perforce a gradual one, since such changes often require new and costly infrastructure. Hydrogen, for example, may be the fuel of the future, but there is no free hydrogen available on Earth. One way of minimising this problem is by combining conventional and renewable fuels, both in end-user applications (e.g. hybrid cars) and at power stations.<sup>13</sup> In the past decade, much work has been done on the partial oxidation of methane, focussing on generating syn-gas.<sup>14–20</sup> Several groups have succeeded in finding good catalyst formulations for this purpose, optimising the CO and H<sub>2</sub> yields. In this communication, we take a different approach, presenting a catalytic route for simultaneously converting methane and generating hydrogen (Scheme 1). This protocol can be applied in existing plants, using methane from both fossil and renewable sources. We synthesise and test a variety of ceria-based catalysts,<sup>21,22</sup> and show that good results can be obtained with platinum, ruthenium, and importantly, nickel.

Ceria lends itself well for the combined combustion/coking process. It is often used as an ‘active support’ in oxidation reactions, because of the facile Ce<sup>3+</sup> ↔ Ce<sup>4+</sup> + e<sup>-</sup> redox cycle.<sup>23</sup> Moreover, the ceria lattice is easily doped with a variety of metals, allowing for tuning of both activity and selectivity.<sup>22,24–28</sup> Importantly, the ability of (doped) ceria to store carbonaceous species at its surface increases the hydrogen production in methane cracking over noble metals,<sup>29</sup> as well as in steam reforming<sup>30–32</sup> and syn-gas production.<sup>33–37</sup> Here, we combine these two advantages, screening 21 different catalysts (catalysts 1–21). We chose Pt, Ru, Ir and Ni as active metals, since they can coke and/or combust hydrocarbons.<sup>22,29,38,39</sup> Subsequently, we chose Cr, Cu, W, Sn, Bi, Fe, Zr, Pr, and Gd as dopants, based on our previous work with doped cerias.<sup>22,40</sup> All catalysts contain one of the active metals, and either plain or doped ceria. The catalysts were prepared *via* two methods. Pt, Ir and Ni were impregnated on the (doped) ceria supports. Alternatively, ceria-based mixed oxides were prepared containing either Pt or Ru. Using mixed oxides allows a more intimate mixing, decreasing particle size and increasing stability.<sup>27,40–42</sup>

Table 1 shows the catalyst composition and activity data for catalysts 1–21, and Fig. 1 shows photos of three of the catalysts, before impregnation with the active metals. Plain ceria is pale yellow, and the photos show the homogeneous mixing of the dopants and the ceria. In the case of copper (14), the black colour indicates the presence of CuO instead of Cu<sub>2</sub>O, which is yellow/red.<sup>43</sup> To achieve the simultaneous cracking and combustion reactions, we added both CH<sub>4</sub> and O<sub>2</sub> in a 2 : 3 molar ratio (see Scheme 1). After heating to 400 °C in 20%v/v O<sub>2</sub> in Ar, the testing was started by feeding the reaction mixture (CH<sub>4</sub> : O<sub>2</sub> : Ar, 2 : 3 : 5) to one of the channel reactors, while the exit gasses were analysed by GC. The reaction mixture was then switched to the next reactor, and the process repeated until all catalysts were tested. Reactions were then repeated at 450 °C, 500 °C and 550 °C.

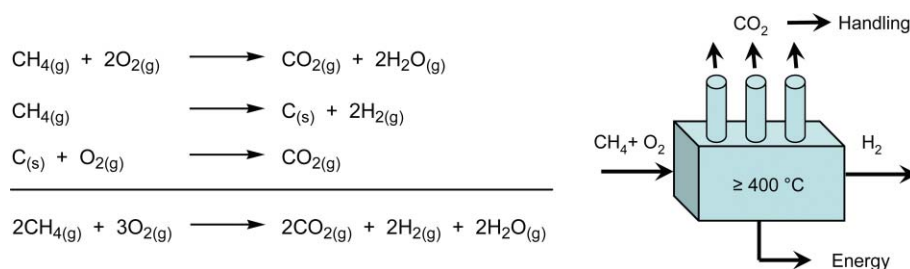
Fig. 2 shows the methane conversion and hydrogen yield obtained with catalysts 1–21 at 550 °C (the Ce–Pt mixed oxide 7 achieves the maximum hydrogen yield already at 400 °C). This hydrogen yield is defined as the hydrogen detected during the experiments, expressed as a percentage of the maximum amount of hydrogen that can be obtained from the methane feed. The maximum yield of 100%, for example, pertains to two moles of H<sub>2</sub> per mole of CH<sub>4</sub>. The catalysts are ranked by hydrogen yield, showing the active metal in each case. The data show several highly active catalysts (with up to 97% methane conversion), that also display high hydrogen yields (~ 30%). The best catalysts contain either Pt, Ru or, importantly, Ni as active

<sup>a</sup>Van't Hoff Institute for Molecular Sciences, University of Amsterdam, Nieuwe Achtergracht 166, 1018 WV, Amsterdam, The Netherlands.

E-mail: J.Beckers@uva.nl, G.Rothenberg@uva.nl; Fax: +31 20 525 5604

<sup>b</sup>University Lyon 1, IRCELYON, 2, Avenue Albert Einstein, F-69626, Villeurbanne, France

† Electronic supplementary information (ESI) available: Further details and Fig. S1 and S2. See DOI: 10.1039/b900516a



**Scheme 1** Combined methane combustion, coking and simultaneous generation of hydrogen and coke combustion using ceria-based catalysts (left), and a cartoon of the proposed combined hydrogen- and conventional power plant (right). Note that hydrogen can also form *via* the water-gas shift equilibrium if CO is present.

**Table 1** Catalysts composition and activity data

Catalyst	Composition	Methane conversion and hydrogen yield								CO <sub>x</sub> formation		
		400 °C		450 °C		500 °C		550 °C		550 °C		
		Activity (%) <sup>a</sup>	Hydrogen yield (%) <sup>b</sup>	Activity (%) <sup>a</sup>	Hydrogen yield (%) <sup>b</sup>	Activity (%) <sup>a</sup>	Hydrogen yield (%) <sup>b</sup>	Activity (%) <sup>a</sup>	Hydrogen yield (%) <sup>b</sup>	CO <sub>2</sub> (% v/v) <sup>c</sup>	CO (% v/v) <sup>c</sup>	H <sub>2</sub> : CO <sup>d</sup>
1	1% Pt/CeO <sub>2</sub>	79	15	85	21	90	27	95	31	16	1.5	7.5
2	1% Pt/Ce <sub>0.97</sub> Cu <sub>0.03</sub> O <sub>2</sub>	71	5	69	4	69	5	70	5	16	0.2	8.2
3	1% Pt/Ce <sub>0.95</sub> Cr <sub>0.05</sub> O <sub>2</sub>	1	0	1	0	0	0	3	0	0	0	
4	1% Pt/Ce <sub>0.90</sub> Zr <sub>0.02</sub> Fe <sub>0.08</sub> O <sub>2</sub>	5	0	65	0	65	0	66	0	16	0	
5	Ce <sub>0.90</sub> Pt <sub>0.02</sub> W <sub>0.02</sub> O <sub>2</sub> /Pt <sup>o</sup>	4	0	66	0	70	2	78	4	16	0.6	7.3
6	Ce <sub>0.96</sub> Pt <sub>0.02</sub> Sn <sub>0.02</sub> O <sub>2</sub> /Pt <sup>o</sup>	70	5	69	4	69	4	71	6	16	0.3	6.7
7	Ce <sub>0.98</sub> Pt <sub>0.02</sub> O <sub>2</sub>	95	32	93	30	94	31	97	32	15	1.6	7.0
8	Ce <sub>0.92</sub> Ru <sub>0.08</sub> O <sub>2</sub> /RuO <sub>2</sub>	3	0	83	20	89	25	94	30	16	1.4	7.6
9	Ce <sub>0.90</sub> Ru <sub>0.05</sub> Fe <sub>0.05</sub> O <sub>2</sub> /RuO <sub>2</sub>	2	0	74	11	69	5	56	0	14	0	
10	Ce <sub>0.95</sub> Ru <sub>0.05</sub> O <sub>2</sub>	3	0	82	19	87	24	93	29	16	1.2	8.4
11	Ce <sub>0.96</sub> Ru <sub>0.02</sub> Cu <sub>0.02</sub> O <sub>2</sub>	3	0	85	21	86	22	92	27	16	1.4	6.9
12	Ce <sub>0.87</sub> Ru <sub>0.05</sub> Cr <sub>0.08</sub> O <sub>2</sub> <sup>e</sup>	1	0	0	0	1	0	2	0	0	0	
13	1% Ir/CeO <sub>2</sub>	6	0	70	5	73	9	77	11	16	0.4	10
14	1% Ir/Ce <sub>0.92</sub> Cu <sub>0.08</sub> O <sub>2</sub>	48	0	39	0	57	0	66	0	16	0	
15	1% Ir/Ce <sub>0.92</sub> Cr <sub>0.08</sub> O <sub>2</sub>	2	0	0	0	0	0	2	0	0	0	
16	1% Ir/Ce <sub>0.87</sub> Cr <sub>0.08</sub> Bi <sub>0.05</sub> O <sub>2</sub>	1	0	0	0	1	0	1	0	0	0	
17	1% Ir/Ce <sub>0.96</sub> Zr <sub>0.02</sub> Fe <sub>0.02</sub> O <sub>2</sub>	4	0	40	0	47	0	65	0	16	0	
18	3.2% Ni/CeO <sub>2</sub>	68	4	77	15	84	24	91	31	16	1.6	6.9
19	2.2% Ni/Ce <sub>0.70</sub> Zr <sub>0.30</sub> O <sub>2</sub>	1	0	12	0	14	0	21	0	5	0	
20	3.5% Ni/Ce <sub>0.90</sub> Pr <sub>0.10</sub> O <sub>2</sub>	60	0	66	0	70	2	75	14	13	0.7	7.5
21	5.0% Ni/Ce <sub>0.90</sub> Gd <sub>0.10</sub> O <sub>2</sub>	85	24	86	0	91	29	93	28	15	1.5	6.8

<sup>a</sup> Expressed as the percentage of methane converted. <sup>b</sup> The amount of hydrogen detected during the experiments, expressed as a percentage of the maximum amount of hydrogen that can be obtained from the methane feed. For example, the maximum yield of 100% pertains to two moles of H<sub>2</sub> per mole of CH<sub>4</sub>. <sup>c</sup> These are the actual CO and CO<sub>2</sub> concentrations in volume percent, as detected by GC, and not the calculated yields, given for hydrogen (see footnote b). <sup>d</sup> Determined from the actual H<sub>2</sub> and CO concentrations, not from the "hydrogen yield". <sup>e</sup> XRD analysis shows that some Cr has segregated into a separate Cr<sub>2</sub>O<sub>3</sub> phase.

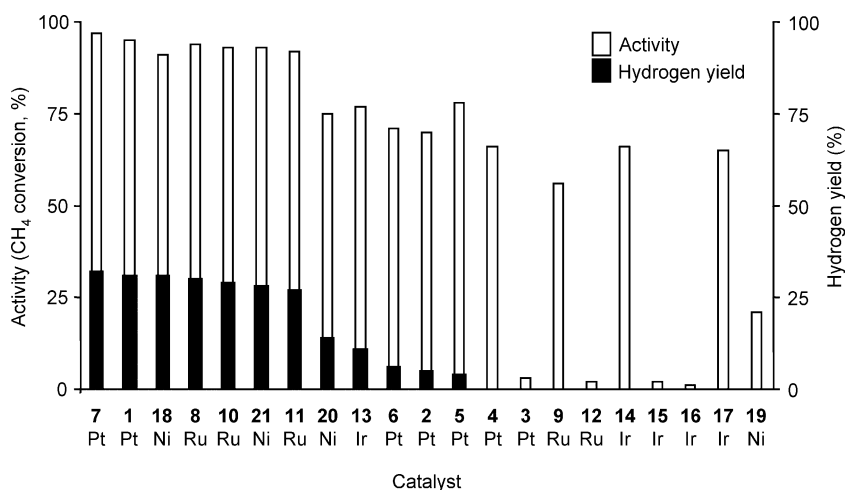


**Fig. 1** Photos of catalyst **3** Ce<sub>0.95</sub>Cr<sub>0.05</sub>O<sub>2</sub>, **17** Ce<sub>0.96</sub>Zr<sub>0.02</sub>Fe<sub>0.02</sub>O<sub>2</sub> and **14** Ce<sub>0.92</sub>Cu<sub>0.08</sub>O<sub>2</sub>, before impregnation with the active metals, showing the homogeneous mixing of the dopants and the ceria. In the case of copper (**14**), the black colour indicates the presence of CuO instead of Cu<sub>2</sub>O, which is typically yellow/red.<sup>43</sup>

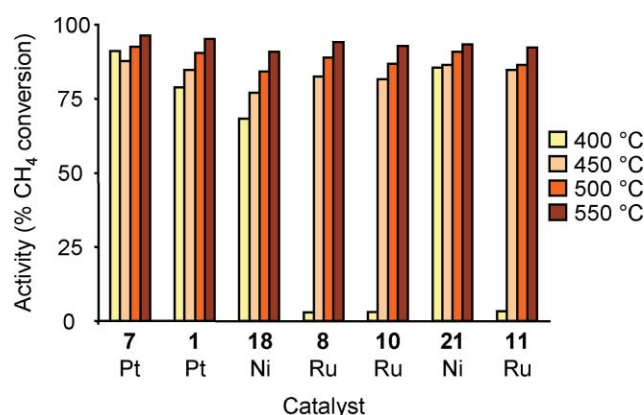
metal. Interestingly, most of the good catalysts consist of ceria and one of the active metals, without an extra dopant. Indeed, the second metal can have three effects: Firstly, it can lower

activity and hydrogen yield (compare the Pt based **2**, **5**, **6** with **1** and **7**). Secondly, it can inhibit the hydrogen generation but not the combustion (**4**, **14** and **17**).<sup>44</sup> Thirdly, it can inhibit both hydrogen generation and combustion (**3**, **12**, **15** and **16**). All of the inactive catalysts contain chromium, and the inhibition occurs for both the impregnated and mixed oxide samples (calcined at 500 °C and 700 °C, respectively). This shows that there is a strong interaction between the active metal and the poisoning chromium.

The methane conversion of the seven best catalysts at various temperatures is given in Fig. 3. The activity increases with temperature, and at 550 °C, the conversion is close to 100%. The ruthenium catalysts (**8**, **10**, **11**) show a large drop in activity at lower temperatures. Conversely, the platinum and nickel catalysts (**1**, **7**, **21**) show the smallest variation in activity, and are therefore applicable in the widest temperature range.

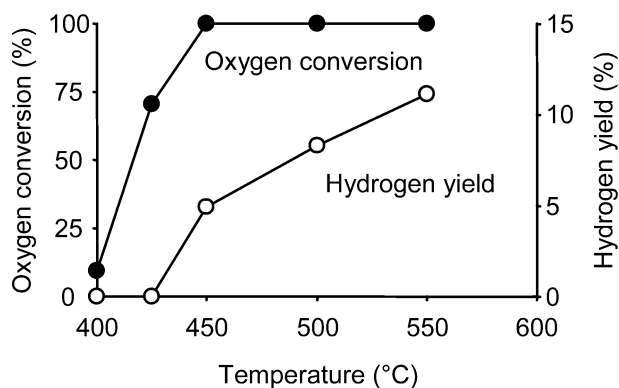


**Fig. 2** Methane conversion and hydrogen yield at 550 °C obtained with catalysts 1–21, showing also the active metal in each case (the catalysts are ranked by hydrogen yield).



**Fig. 3** Methane conversion activity at the 400 °C–550 °C range for the seven best catalysts.

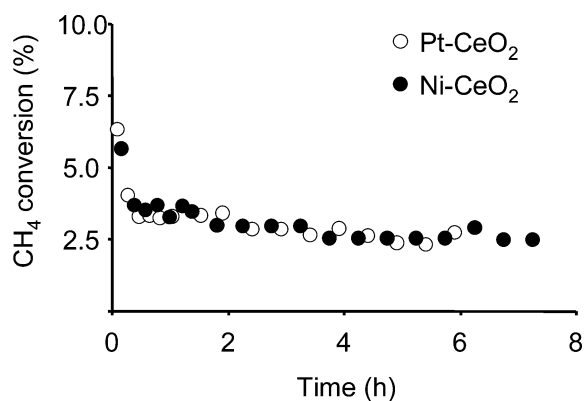
Importantly, all the catalysts that produce H<sub>2</sub> do so only at full O<sub>2</sub> conversion. That is, coking and hydrogen production start when no oxygen is left for combustion. Fig. 4 shows a typical example using catalyst 13. Note that above 450 °C more H<sub>2</sub> forms, while the amount of combustion (measured as CO<sub>2</sub> concentration) remains constant. This indicates that no *in situ*



**Fig. 4** Oxygen conversion (left) and hydrogen yield (right) for catalyst 13, 1% Ir/CeO<sub>2</sub>. Note that the CO<sub>2</sub> yield is constant from 450 °C onwards.

coke combustion occurs at higher temperatures. The carbon balance also drops, since some of it is deposited as coke on the catalyst surface (the carbon balance and hydrogen yields for all catalysts at all four reaction temperatures are given in the ESI†). Table 1 shows that all hydrogen producing catalysts also give a small amount of CO, with a H<sub>2</sub> : CO ratio of ~ 7 for the most active ones. Hydrogen yield and CO production are correlated: the higher the hydrogen yield, the more CO is produced. Indeed, control experiments showed that at higher oxygen concentration, all the methane is combusted into CO<sub>2</sub>, without formation of hydrogen. Conversely, at lower oxygen concentrations methane conversion is lower, and more H<sub>2</sub> and CO form.

The observation that the hydrogen generation only starts at full oxygen combustion, and that no *in situ* coke combustion occurs, prompted us to investigate the stability of the catalysts. For this, we fed the reaction mixture without oxygen (20% CH<sub>4</sub>/Ar) over the Ni/CeO<sub>2</sub> catalyst 18, and a Pt/CeO<sub>2</sub> catalyst with comparable metal loading (3.8% Pt/CeO<sub>2</sub> and 3.2% Ni/CeO<sub>2</sub>). The data presented in Fig. 5 show that after an initial drop, the activity remains stable for more than 7 h. Importantly, the catalyst can be easily regenerated *in situ* by temporarily closing the CH<sub>4</sub> feed. This makes all the oxygen available for the combustion of the coke. The advantage of this



**Fig. 5** Stability tests for catalyst 18, (● symbols; 3.2% Ni/CeO<sub>2</sub>), and a 3.8% Pt/CeO<sub>2</sub> catalyst (○). Reaction conditions: 500 °C, 20% CH<sub>4</sub>/Ar at a total flow rate of 50 mL/min.

*in situ* regeneration is that it allows a continuous generation of heat.

We also checked the thermodynamic feasibility of the above reactions using a simple numerical model (a full-scale simulation of the processes on the catalyst surface is out of the scope of this project). Starting from the experimental  $\text{CH}_4 : \text{O}_2 : \text{Ar}$  molar ratios of 2 : 3 : 5, the models show that the equilibrium mixtures contain both  $\text{H}_2$  and  $\text{CO}_2$ . Moreover, the hydrogen content increases with temperature, with the ratio  $\text{H}_2 : \text{CO}_2 : \text{CO}$  reaching 10 : 16 : 1.8 at 550 °C. This is very close to the experimental data of our best catalysts. For example, the  $\text{H}_2 : \text{CO}_2 : \text{CO}$  ratio of **1** is 11 : 16 : 1.5. Although the model is a very simplistic one, the results are nevertheless encouraging.

The two best catalysts regarding activity and hydrogen yield are Pt impregnated on ceria **1** and the Pt–ceria mixed oxide **7**. These catalysts contain roughly equal amounts of platinum (1 wt% and 1.5 wt%, respectively), and show comparable performance. The mixed oxide has one important practical advantage—it is easily prepared in a one-pot reaction. The cerium nitrate and dopant salt are simply weighed in a crucible, heated to 110 °C under vacuum, and calcined to 700 °C in air. Moreover, the intimate mixing of the precursors affords highly effective, very small particles, saving on costly metal ingredients. All that being said, the most interesting catalyst is in fact **18** (3.2% Ni/CeO<sub>2</sub>). This catalyst performs almost as well as the Pt-containing ones, but the relative costs (~ 20 €/g for Pt and 8 €/kg for Ni<sup>45,46</sup>) give the Ni catalyst a significant advantage.

In summary, we show here that ceria-based catalysts are good candidates for combining methane combustion and hydrogen generation. These new, tuneable catalysts are easily prepared. They are robust inorganic crystalline materials, and perform well even without precious metals. All this makes them attractive for practical applications in the energy conversion market.

## Experimental

### Materials and instrumentation

Chemicals were purchased from Sigma-Aldrich or Merck and used as received. Gasses were purchased from Air Liquide and had a purity of 99.5% or higher. Powder X-Ray diffraction measurements were performed using a Philips PW-series X-Ray diffractometer with a Cu tube radiation source ( $\lambda = 1.54 \text{ \AA}$ ), a vertical axis goniometer and a proportional detector. The  $2\theta$  detection measurement range was 10°–93° with a 0.02° step size and a 5 second dwell time. GC analysis was performed on two Agilent instruments, one equipped with a Poraplot Q column to separate  $\text{CO}_2$  and  $\text{CH}_4$  (He carrier gas), and one equipped with a 5 Å molsieve column to separate  $\text{H}_2$ , CO,  $\text{CH}_4$  and  $\text{O}_2$  (Ar carrier gas). All catalytic tests were performed using the “SWITCH 16” setup (AMTEC GmbH, developed in collaboration with CNRS), allowing for the testing of up to 16 catalysts simultaneously.<sup>47</sup> Thermodynamic calculations were performed using the Outokumpu HSC Chemistry software package (Version 4.1).<sup>48</sup>

### Procedure for catalyst synthesis

The procedure for catalyst preparation was described in detail previously.<sup>22,40</sup> The metal nitrates are weighed in a porcelain

crucible and heated to about 100 °C, so that the cerium nitrate melts. The mixture is stirred until all components are dissolved or have melted, 2–4 drops of water are added to aid the dissolution. The crucible is placed in a vacuum oven set at 140 °C and the pressure is carefully lowered to < 10 mbar (in 10–15 min), making sure no vigorous boiling occurs. After 4 h, the samples are placed in a furnace and calcined under static air at 700 °C (ramp rate 300 °C/h, 5 h hold). The resulting solid is pulverized, ground and sieved in fractions of 125–212  $\mu\text{m}$  (catalytic testing) and < 125  $\mu\text{m}$  (XRD measurements). The surface area typically ranges from 20–60  $\text{m}^2/\text{g}$ . Impregnation was performed using aqueous solutions of the appropriate metal chlorides, followed by 24 h drying at 110 °C, and finally calcining to 500 °C at 5 °C/min with a 5 h hold. The ceria based mixed oxides which were impregnated with nickel were purchased from Riedel de Haën and have surface areas typically ranging from 100–200  $\text{m}^2/\text{g}$ . The impregnation was performed using aqueous solutions of nickel nitrate hexahydrate, followed by 1 h drying step at 100 °C, and finally calcining to 500 °C at 1 °C/min with a 8 h hold.

### Procedure for testing catalytic activity

The “SWITCH 16” system enables testing of a batch of sixteen catalysts at a time. The reaction mixture is fed to one of the reactors, and the exit flow of this reactor is directed to the GC’s for analysis. Meanwhile, an oxygen/helium flow is fed to the remaining reactors to maintain the sample’s integrity. The reactors are stainless steel tubes with an inner diameter of 4.7 mm, each fitted with a thermocouple. In a typical experiment, 100–150 mg of sample (125–212  $\mu\text{m}$ , bed volume 0.1–0.15  $\text{cm}^3$ ) was placed between quartz wool plugs in the reactor, and the reactors were placed in the oven. The reaction mixture was led to an empty reference reactor, and the oven was heated to the first reaction temperature at 180 °C/h, with the other reactors under oxygen flow (20%  $\text{O}_2/\text{He}$ ). When the temperature was reached, the reaction mixture, consisting of 20% v/v  $\text{CH}_4$  and 30% v/v  $\text{O}_2$  in He, was fed to each reactor consecutively for 20 min, and two GC analyses were performed after 7 and 14 min. When this was complete, the reaction mixture was directed to the reference reactor and the oven was heated to the next set point. This way, all reactors were analysed from 400–550 °C at 50 °C intervals. The total flow rates were kept at 50 mL/min in each step.

## References

- 1 G. A. Olah, A. Goepfert, and G. K. Surya Prakash, *Beyond Oil and Gas: The Methanol Economy*, Wiley-VCH, Weinheim, 2006, p 2.
- 2 R. C. Darton, *Process Saf. Environ. Prot.*, 2003, **81**, 295.
- 3 B. B. Rath and J. Marder, *Adv. Mater. Process.*, 2007, **165**, 62.
- 4 H. Bönemann, G. Khelashvili, S. Behrens, A. Hinsch, K. Skupien and E. Dinjus, *J. Cluster Sci.*, 2007, **18**, 141.
- 5 M. Korpas and C. J. Greiner, *Renewable Energy*, 2008, **33**, 1199.
- 6 R. Bertani, *Geothermics*, 2005, **34**, 651.
- 7 S. David, *Nucl. Phys. A*, 2005, **751**, 429.
- 8 A. Demirbas, *Prog. Energy Combust. Sci.*, 2005, **31**, 171.
- 9 M. Balat, *Int. J. Green Energy*, 2008, **5**, 212.
- 10 D. A. G. Aranda, R. T. P. Santos, N. C. O. Tapanes, A. L. D. Ramos and O. A. C. Antunes, *Catal. Lett.*, 2008, **122**, 20.
- 11 S. Albertazzi, F. Basile, J. Brandin, J. Einvall, G. Fornasari, C. Hulteberg, M. Sanati, F. Trifiro and A. Vaccari, *Biomass Bioenergy*, 2008, **32**, 345.
- 12 G. Carr, *The Economist*, 2008, 3.

- 13 S. N. Ireland, B. McGrellis and N. Harper, *Fuel*, 2004, **83**, 905.
- 14 T. V. Choudhary and V. R. Choudhary, *Angew. Chem., Int. Ed.*, 2008, **47**, 1828.
- 15 S. Fukada, N. Nakamura and J. Monden, *Int. J. Hydrogen Energy*, 2004, **29**, 619.
- 16 A. C. W. Koh, L. W. Chen, W. K. Leong, B. F. G. Johnson, T. Khimyak and J. Y. Lin, *Int. J. Hydrogen Energy*, 2007, **32**, 725.
- 17 T. Shishido, M. Sukenobu, H. Morioka, M. Kondo, Y. Wang, K. Takaki and K. Takehira, *Appl. Catal., A*, 2002, **223**, 35.
- 18 A. P. E. York, T. C. Xiao, M. L. H. Green and J. B. Claridge, *Catal. Rev. - Sci. Eng.*, 2007, **49**, 511.
- 19 M. F. Mark and W. F. Maier, *Angew. Chem., Int. Ed. Engl.*, 1994, **33**, 1657.
- 20 R. Quiceno, O. Deutschmann, J. Warnatz and J. Pérez-Ramírez, *Catal. Today*, 2007, **119**, 311.
- 21 G. Rothenberg, E. A. de Graaf and A. Blik, *Angew. Chem., Int. Ed.*, 2003, **42**, 3366.
- 22 J. Beckers, F. Clerc, J. H. Blank and G. Rothenberg, *Adv. Synth. Catal.*, 2008, **350**, 2237.
- 23 A. Trovarelli, C. de Leitenburg, M. Boaro and G. Dolcetti, *Catal. Today*, 1999, **50**, 353.
- 24 M. Jobbágy, F. Mariño, B. Schöbrod, G. Baronetti and M. Laborde, *Chem. Mater.*, 2006, **18**, 1945.
- 25 P. Bera, S. T. Aruna, K. C. Patil and M. S. Hegde, *J. Catal.*, 1999, **186**, 36.
- 26 A. Tschöpe, W. Liu, M. Flytzani-Stephanopoulos and J. Y. Ying, *J. Catal.*, 1995, **157**, 42.
- 27 D. Tibiletti, E. A. de Graaf, S. P. Teh, G. Rothenberg, D. Farrusseng and C. Mirodatos, *J. Catal.*, 2004, **225**, 489.
- 28 R. T. Baker, S. Bernal, G. Blanco, A. M. Cordon, J. M. Pintado, J. M. Rodríguez-Izquierdo, F. Fally and V. Perrichon, *Chem. Commun.*, 1999, 149.
- 29 E. Odier, Y. Schuurman and C. Mirodatos, *Catal. Today*, 2007, **127**, 230.
- 30 T. J. Huang, H. J. Lin and T. C. Yu, *Catal. Lett.*, 2005, **105**, 239.
- 31 T. J. Huang and M. C. Huang, *Chem. Eng. J.*, 2008, **145**, 149.
- 32 J. H. Xu, C. M. Y. Yeung, J. Ni, F. Meunier, N. Acerbi, M. Fowles and S. C. Tsang, *Appl. Catal., A*, 2008, **345**, 119.
- 33 S. Pengpanich, V. Meeyoo and T. Rirksomboon, *Catal. Today*, 2004, **93–95**, 95.
- 34 T. L. Zhu and M. Flytzani-Stephanopoulos, *Appl. Catal., A*, 2001, **208**, 403.
- 35 P. Corbo and F. Migliardini, *Int. J. Hydrogen Energy*, 2007, **32**, 55.
- 36 S. A. Larrondo, A. Kodjaian, I. Fabregas, M. G. Zimicz, D. G. Lamas, B. E. W. de Reça and N. E. Amadeo, *Int. J. Hydrogen Energy*, 2008, **33**, 3607.
- 37 W. F. Maier, K. Stowe and S. Sieg, *Angew. Chem., Int. Ed.*, 2007, **46**, 6016.
- 38 J. R. Nielsen and D. L. Trimm, *J. Catal.*, 1977, **48**, 155.
- 39 M. M. Slinko, V. N. Korchak and N. V. Peskov, *Appl. Catal., A*, 2006, **303**, 258.
- 40 J. H. Blank, J. Beckers, P. F. Collignon, F. Clerc and G. Rothenberg, *Chem.–Eur. J.*, 2007, **13**, 5121.
- 41 J. H. Blank, J. Beckers, P. F. Collignon and G. Rothenberg, *ChemPhysChem*, 2007, **8**, 2490.
- 42 J. Beckers and G. Rothenberg, *Dalton Trans.*, 2008, 6573.
- 43 N. N. Greenwood, and A. Earnshaw, *Chemistry of the Elements*, Pergamon Press, Oxford, 1989, p 1373.
- 44 The addition of Zr/Fe to either Pt or Ir (**4**, **17**), or Cu to Ir (**14**), inhibits hydrogen generation, even at full oxygen conversion. Catalysts **9** and **19** also show no hydrogen yield, but these do not achieve full oxygen conversion under these reaction conditions.
- 45 [www.platinum.matthey.com/prices/current\\_historical.html](http://www.platinum.matthey.com/prices/current_historical.html).
- 46 [www.lme.com/nickel.asp](http://www.lme.com/nickel.asp).
- 47 G. Morra, A. Desmartin-Chomel, C. Daniel, U. Ravon, D. Farrusseng, R. Cowan, A. Krusche and C. Mirodatos, *Chem. Eng. J.*, 2008, **138**, 379.
- 48 [www.outotec.com](http://www.outotec.com).

# Glutathione promoted expeditious green synthesis of silver nanoparticles in water using microwaves

Babita Baruwati, Vivek Polshettiwar and Rajender S. Varma\*

Received 2nd February 2009, Accepted 27th April 2009

First published as an Advance Article on the web 5th May 2009

DOI: 10.1039/b902184a

Silver nanoparticles ranging from 5–10 nm in size have been synthesized under microwave irradiation conditions using glutathione, an absolutely benign antioxidant that serves as the reducing as well as capping agent in aqueous medium. This rapid protocol yields the nanoparticles within 30–60 s at a power level as low as 50 W. The effect of microwave power on the morphology of ensuing silver nanoparticles is investigated for this green and sustainable procedure which is adaptable for the synthesis of palladium, platinum and gold nanoparticles.

## Introduction

Over the past decade, the increased emphasis on developing green and sustainable chemical processes has led to numerous efforts toward the elimination or at least minimization of waste generation. Implementing sustainable methodologies in almost all areas of chemistry, including nanomaterial synthesis<sup>1</sup> entails eliminating toxic reagents and solvents. The choice of an environmentally benign solvent, the use of a multipurpose agent that serves the purpose of a reducing, capping and dispersing agent are some of the key issues that may be addressed in green synthesis of nanomaterials.<sup>1</sup>

Synthesis of silver nanoparticles is of much interest to the scientific community because of their wide range of applications in catalysis,<sup>2</sup> electronics,<sup>3</sup> photonics,<sup>4</sup> optoelectronics,<sup>5</sup> sensing,<sup>6</sup> and pharmaceuticals.<sup>7</sup> Specifically, these nanoparticles are strong candidates for Surface Enhanced Raman Spectroscopic (SERS) studies<sup>8</sup> that yet again prompts the interest of the scientific community to develop newer green synthetic methods for obtaining these nanoparticles.

Numerous pathways have been employed for the synthesis of silver nanoparticles with different morphologies as well as size distributions including NaBH<sub>4</sub> reduction,<sup>9</sup> polyol process,<sup>10–12</sup> use of plant extracts,<sup>13,14</sup> photoreduction<sup>15</sup> *etc.* Most of these proceed *via* wet chemistry methods with the use of highly reactive reducing agents such as sodium borohydride, hydrazine *etc.* that are not environmentally friendly. Some of them use noxious and highly volatile organic solvents. To eliminate the use of toxic reducing agents, the use of amino acids,<sup>16</sup> vitamins,<sup>17</sup> and other eco-friendly biological agents in the synthesis of metal nanoparticles have been reported.<sup>18–20</sup> In conjunction with the use of these

eco-friendly reducing agents and solvents, microwave irradiation (MW) is emerging as a rapid and environment friendly mode of heating for the generation of nanomaterials. It offers a rapid and volumetric heating of solvents, reagents, and intermediates, that provides uniform nucleation and growth conditions for nanomaterial synthesis.<sup>21–25</sup>

Engaged in the development of greener and sustainable pathways for organic synthesis and nanomaterials,<sup>26–33</sup> herein we report an easy and rapid synthesis of silver nanoparticles using glutathione as a reducing as well as capping agent under MW irradiation conditions in pure aqueous medium. To the best of our knowledge, glutathione has not been reported for the synthesis of silver nanoparticles.

The choice of glutathione (Fig. 1, GHS), as a reducing agent was made because of its benign nature and the presence of a highly reactive thiol group that can be used to reduce the metal salts. GHS is a tripeptide consisting of glutamic acid, cysteine and glycine units and is an ubiquitous antioxidant present in human and plant cells. Besides the thiol group, each GSH molecule also contains amine and carboxylate functionalities that provide coupling possibilities for further cross-linking to other molecules of biological or sensing interest.

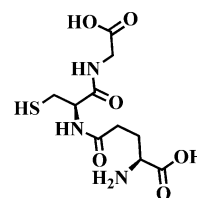


Fig. 1 Molecular structure of glutathione, GSH (reduced).

## Results and discussions

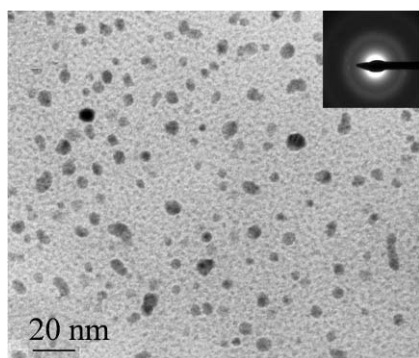
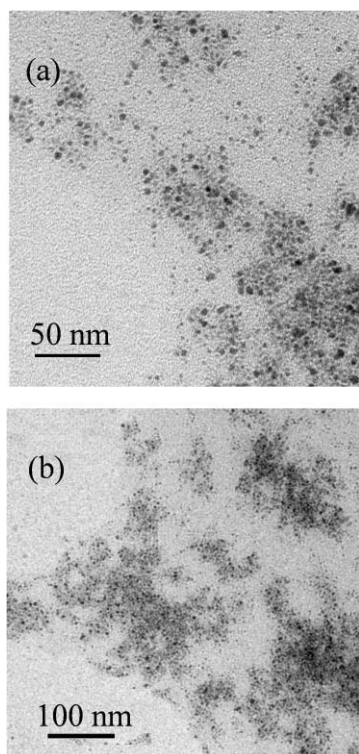
The first step in developing this protocol, was the optimization of MW power, exposure time and glutathione concentration. Reactions were conducted at three different power levels *i.e.* 50, 75 and 100 W for 30, 45 and 60 s (Table 1).

Under all of the above reaction conditions (Table 1), silver nanoparticles with spherical morphology in the size range 5–50 nm were obtained. At lower power levels (50 W) and shorter reaction times (30 s), mostly unreacted silver nitrate remained in the reaction mixture. With increase in reaction time to 60 s, nanoparticles of 5–10 nm size with spherical morphology was observed (Fig. 2). At higher power levels (75 and 100 W) with 30 s reaction times, nanoparticles of 4–10 nm were obtained (Fig. 3a, b). However, with longer reaction times (60 s), increased

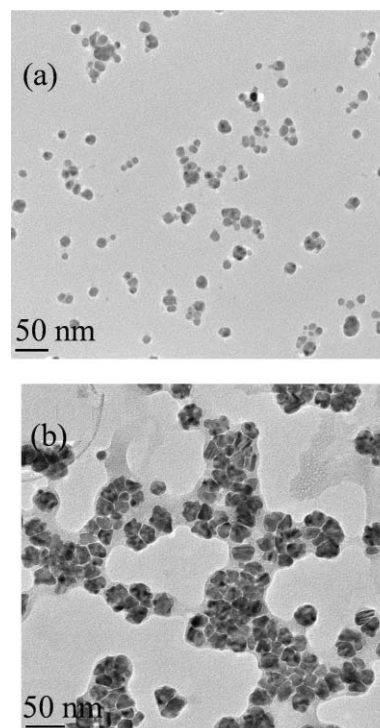
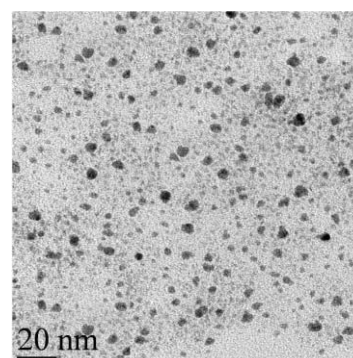
Sustainable Technology Division, National Risk Management Research Laboratory, U. S. Environmental Protection Agency, MS 443, Cincinnati, Ohio 45268, USA. E-mail: varma.rajender@epa.gov; Fax: +1 513-569-7677; Tel: +1 513-487-2701

**Table 1** Effect of MW power and glutathione concentration on Ag nanoparticle formation

Entry	MW power/W	Time/S	Temperature/°C	Pressure/Psi
1	50	30	34	28
2	50	45	41	33
3	50	60	47	54
4	75	30	39	47
5	75	45	51	56
6	75	60	62	130
7	100	30	42	60
8	100	45	56	128
9	100	60	61	148

**Fig. 2** TEM micrographs of the as-synthesized nanoparticles at 50 W for 60 s with a silver nitrate to glutathione mole ratio of 1.0 : 0.15. Inset is the electron diffraction pattern for the corresponding nanoparticles.**Fig. 3** TEM micrographs of the as synthesized nanoparticles at (a) 75 W and (b) 100 W for 30 s with a silver nitrate to glutathione mole ratio of 1.0 : 0.15.

size and agglomeration of the particles were observed (Fig. 4a, b). When the ratio of silver nitrate to glutathione was less than 1.0 : 0.15, incomplete reduction of silver nitrate occurred as seen in the UV-Visible spectrum. No particle formation was discerned in the absence of glutathione. Increasing the silver nitrate to glutathione mole ratio to 1.0 : 0.30 did not produce particles at 50 W and 60 s, but very small particles in the size range 2–6 nm were obtained when the power was increased to 75 W. Fig. 5 shows the TEM micrograph of the particles synthesized at 75 W for 60 s with a silver nitrate to glutathione mole ratio of 1 : 0.30. Reactions performed under conventional heating at 60 °C, keeping all other conditions intact, did not yield any particles even after 24 h. Thus, the optimized reaction conditions were 50 W power level, 45–60 s exposure time and 1 : 0.15 silver nitrate to glutathione mole ratio, to get uniformly distributed particles in the size range

**Fig. 4** TEM micrographs of the as-synthesized nanoparticles at (a) 75 W and (b) 100 W for 60 s with a silver nitrate to glutathione mole ratio of 1.0 : 0.15.**Fig. 5** TEM micrographs of the as synthesized nanoparticles at 75 W for 60 s with a silver nitrate to glutathione mole ratio of 1.0 : 0.30.



5–10 nm. The dispersion of the particles was quite stable and did not result in precipitation even after several weeks of storage under ambient conditions.

The formation of dendritic nanostructures (Fig. 6) on the TEM grid was observed when the reaction mixtures without complete conversion of silver nitrate were loaded on the TEM grid prior to the washing procedure. This was observed in our earlier studies related to the formation of silver trees and was attributed to the fact that the copper and carbon present in the TEM grid is responsible for catalyzing the reaction.<sup>34</sup> It was independently verified by separate reactions using copper turnings and activated carbon which generates similar dendritic structures thus raising the concern about the conclusions derived solely on the basis of TEM studies.<sup>34</sup>

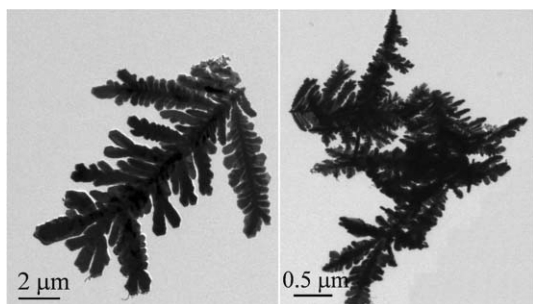


Fig. 6 TEM micrographs of the dendritic nanostructures.

It can be seen from the UV-Vis spectrum (Fig. 7) of the reaction mixtures at different reaction conditions, that heating silver nitrate alone in the MW oven have not resulted in any change in the silver nitrate absorption peak at 300 nm. However, when glutathione was added to the reaction mixture, no silver nitrate peak was observed and the silver plasmon peak appeared in the wavelength range 350–450 nm. The peak shifting towards red was observed with an increase in the amount of glutathione.

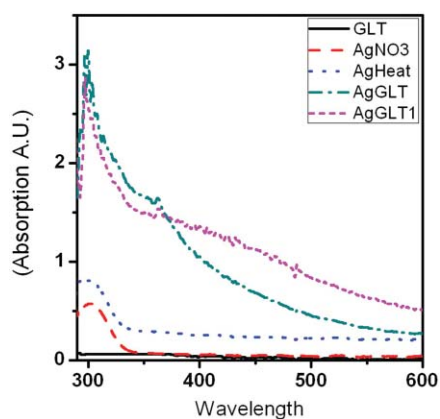


Fig. 7 UV-visible plots of silver nitrate, glutathione (GSH) and silver nanoparticles synthesized with glutathione.

X-ray diffraction pattern confirms the formation of only silver nanoparticles. Fig. 8 is the corresponding X-ray diffraction pattern for the nanoparticles synthesized at 75 W power level for 60 s. The diffraction pattern has some background noise that might be caused by the very small crystallite sizes as well as the organic coating on the as-synthesized nanoparticles. Electron

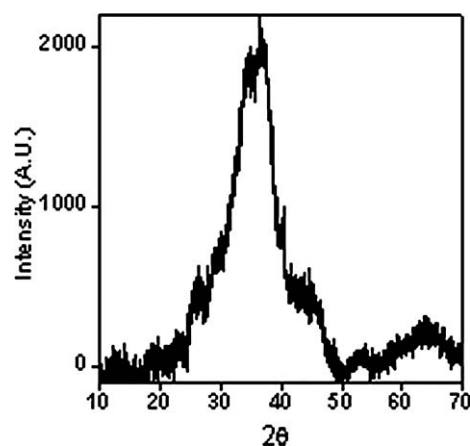


Fig. 8 X-ray diffraction pattern of the as-synthesized Ag nanoparticles at 75 W power level for 60 s.

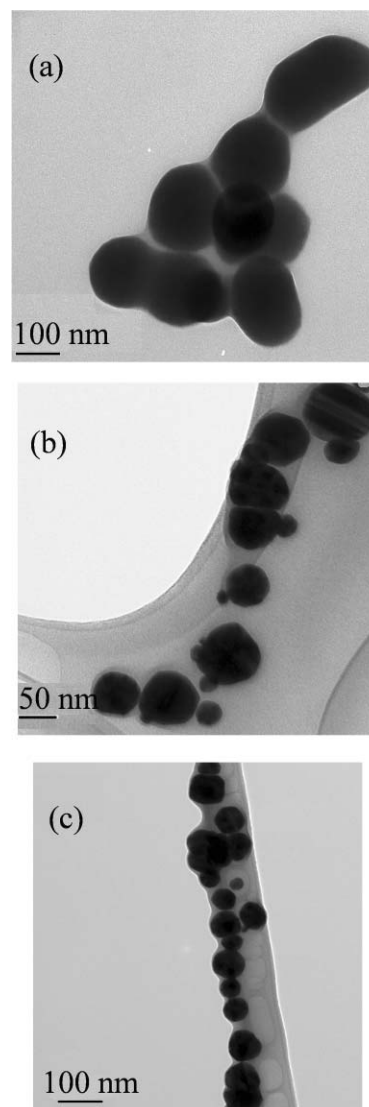


Fig. 9 TEM of the as-synthesized (a) Au, (b) Pt, and (c) Pd nanoparticles.

dispersive X-ray analysis (EDAX) studies of these nanoparticles confirmed the results of X-ray diffraction.

This developed protocol is far superior and sustainable compared to recently reported MW-protocol using amino acids.<sup>16</sup> The main difference is, their protocol needs starch as a coating agent in addition to L-lysine, however, in our protocol, glutathione is acting as both reducing as well as coating agent. In addition, reaction temperature is as high as 150 °C as compared to our protocol, which is very modest, 45–50 °C.

This green and sustainable synthesis procedure could also be adopted for the synthesis of other noble metal nanoparticles such as palladium, platinum and gold. In the case of these noble metals however, bigger particle sizes in the range 100–120 nm were observed. Fig. 9(a–c) shows the TEM micrographs for the as-synthesized gold, platinum and palladium nanoparticles, respectively.

## Conclusions

In conclusion, we have developed a rapid and green protocol for the synthesis of silver nanoparticles as well as other noble metals using glutathione, a benign antioxidant, that serves as both a reducing and capping agent. The entire process was carried out in pure water without using any toxic reagents or organic solvents. The effect of MW power on the morphology of silver nanoparticles was investigated. The method could be further exploited for the large scale and continuous synthesis of these nanoparticles.

## Experimental

### Chemicals

AgNO<sub>3</sub>, Na<sub>2</sub>PdCl<sub>4</sub>, Na<sub>2</sub>PtCl<sub>6</sub>·6H<sub>2</sub>O and Glutathione (reduced form) were purchased from Aldrich Chemicals and used as received.

### Synthesis of silver nanoparticles

In a typical synthesis procedure, 1 mmol of silver nitrate was dissolved in 5 mL of distilled water. To this 0.046 g of glutathione (reduced), dissolved in 2 mL of water was added. The mixture was then transferred to a 10 mL crimp sealed thick walled glass tube equipped with a pressure sensor and magnetic bar. The tube was then placed inside the cavity of a CEM Discover focused MW synthesis system for 30–60 s operated at a power of 50 W. The reaction was performed at different power levels to optimize the reaction conditions. Formation of the particles could be observed from the change of color of the reaction mixture. The colorless solution turns reddish brown at the end of the reaction. After completion of the reaction, the tube was rapidly cooled to room temperature, particles centrifuged, and dispersed in water. The dispersion and centrifugation process was repeated twice to remove any unreacted silver nitrate or glutathione from the final product. These nanoparticles were then used for further characterizations.

### Synthesis of Pd, Pt and Au nanoparticles

In a typical procedure, 0.05 mmol of Na<sub>2</sub>PdCl<sub>4</sub> (for Pd) was dissolved in 5 mL water in a crimp sealed thick walled glass

tube equipped with a pressure sensor and magnetic bar. 2 mL of water containing 0.046 g glutathione was added to it. The slight brownish Na<sub>2</sub>PdCl<sub>4</sub> solution instantly became bright orange as soon as glutathione was added to it. The mixture was then subjected to MW irradiation for 45–60 s at 75 W power. The color of the solution becomes dark brown at the end of the reaction. After completion of the reaction, the tube was rapidly cooled to room temperature, particles centrifuged, and dispersed in water. The dispersion and centrifugation process was repeated twice to remove any unreacted silver nitrate or glutathione from the final product. These nanoparticles were then used for further characterizations.

The same procedure was adopted for the synthesis of platinum nanoparticles using Na<sub>2</sub>PtCl<sub>6</sub>·6H<sub>2</sub>O as the source of platinum.

For the synthesis of Au nanoparticles, 5 mL of 3 mM solution of HAuCl<sub>4</sub> was used as the precursor.

## Characterizations

The phase of the as-synthesized metal nanoparticles was determined by X-ray diffraction in an MMS X-ray diffractometer with a Cu K $\alpha$  source in the 2 $\theta$  range 10 to 70. The data were collected with a step of 1° min<sup>-1</sup>. A few drops of the as-synthesized nanoparticles were added to a quartz plate and dried at room temperature before recording the X-ray pattern. TEM micrographs were recorded on a Phillips CM 20 TEM microscope at an operating voltage of 200 kV. A drop of the as-synthesized nanoparticles was loaded on a carbon coated copper grid and then allowed to dry at room temperature before recording the micrographs. The UV-Visible spectra were recorded in a Hewlett and Packard 845X UV-Visible system.

## Acknowledgements

Babita Baruwati and Vivek Polshettiwar were supported, in part, by the Postgraduate Research Program at the National Risk Management Research Laboratory administered by the Oak Ridge Institute for Science and Education through an interagency agreement between the U.S. Department of Energy and the U.S. Environmental Protection Agency.

## References

- 1 P. Raveendran, J. Fu and S. L. Wallen, *J. Am. Chem. Soc.*, 2003, **125**, 13940.
- 2 N. R. Jana, T. K. Sau and T. Pal, *J. Phys. Chem. B*, 1999, **103**, 115.
- 3 G. N. R. Tripathi, *J. Am. Chem. Soc.*, 2003, **125**, 1178.
- 4 W. Wang and S. A. Asher, *J. Am. Chem. Soc.*, 2001, **123**, 12528.
- 5 Y. Cui and C. M. Lieber, *Science*, 2001, **291**, 851.
- 6 A. D. McFarland and R. P. Van Duyne, *Nano Lett.*, 2003, **3**, 1057.
- 7 E. Ulkur, O. Oncul, H. Karagoz, E. Yeniz and B. Celikoz, *Burns*, 2005, **31**, 874.
- 8 P. J. Stepanek, P. Y. Turpin and J. Bok, *J. Phys. Chem. B*, 2002, **106**, 1543.
- 9 Y. Qu, R. Porter, F. Shan, J. D. Carter and T. Guo, *Langmuir*, 2006, **22**, 6367.
- 10 F. Gao, Q. Lu and S. Komarneni, *Chem. Mater.*, 2005, **17**, 856.
- 11 P. V. Silvert, R. H. Urbina and K. T. Elhissen, *J. Mater. Chem.*, 1997, **7**, 293.
- 12 J. H. Yang, L. H. Lu, H. S. Wang, W. D. Shi and H. J. Zhang, *Cryst. Growth Des.*, 2006, **6**, 2155.
- 13 S. S. Shankar, A. Rai, A. Ahmad and M. Shastry, *J. Colloid Interface Sci.*, 2004, **275**, 496.

- 14 S. Kundu, M. Mandal, S. K. Ghosh and T. Pal, *J. Colloid Interface Sci.*, 2004, **272**, 134.
- 15 J. L. Marignier, J. Belloni, M. O. Delcourt and J. P. Chevalier, *Nature*, 1985, **317**, 344.
- 16 B. Hu, S.-B. Wang, K. Wang, M. Zhang and S.-H. Yu, *J. Phys. Chem. C*, 2008, **112**, 11169.
- 17 M. N. Nadagouda and R. S. Varma, *Cryst. Growth Des.*, 2007, **7**, 2582.
- 18 P. Mukherjee, A. Ahmad, D. Mandal, S. Senapati, S. R. Sainkar, M. I. Khan, R. Parishcha, P. V. Ajaykumar, M. Alam, R. Kumar and M. Sastry, *Nano Lett.*, 2001, **1**, 515.
- 19 A. Panacek, L. Kvitek, R. Prucek, M. Kolar, R. Vecerova, N. Pizurova, V. K. Sharma, T. Nevecna and R. Zboril, *J. Phys. Chem. B*, 2006, **110**, 16248.
- 20 M. N. Nadagouda and R. S. Varma, *Cryst. Growth Des.*, 2007, **7**, 686.
- 21 W. J. Sommer and M. Weck, *Langmuir*, 2007, **23**, 11991.
- 22 J. A. Gerbec, D. Magana, A. Washington and G. F. Strouse, *J. Am. Chem. Soc.*, 2005, **127**, 15791.
- 23 V. Polshettiwar, M. N. Nadagouda and R. S. Varma, *Chem. Commun.*, 2008, 6318.
- 24 B. Baruwati, M. N. Nadagouda and R. S. Varma, *J. Phys. Chem. C*, 2008, **112**, 18399.
- 25 M. N. Nadagouda and R. S. Varma, *Cryst. Growth Des.*, 2008, **8**, 291.
- 26 V. Polshettiwar and R. S. Varma, *Chem. Soc. Rev.*, 2008, **37**, 1546.
- 27 V. Polshettiwar and R. S. Varma, *Acc. Chem. Res.*, 2008, **41**, 629.
- 28 V. Polshettiwar, B. Baruwati and R. S. Varma, *Green Chem.*, 2009, **11**, 127.
- 29 C. R. Strauss and R. S. Varma, *Top. Curr. Chem.*, 2006, **266**, 199.
- 30 H. Choi, Y. J. Kim, R. S. Varma and D. D. Dionysiou, *Chem. Mater.*, 2006, **18**, 5377.
- 31 V. Polshettiwar and R. S. Varma, *Chem.–Eur. J.*, 2009, **15**, 1582.
- 32 V. Polshettiwar and R. S. Varma, *Org. Biomol. Chem.*, 2009, **7**, 37.
- 33 V. Polshettiwar, B. Baruwati and R. S. Varma, *ACS Nano*, 2009, **3**, 728.
- 34 M. N. Nadagouda and R. S. Varma, *Aust. J. Chem.*, 2009, **62**, 260.

# Basic alumina-supported highly effective Suzuki–Miyaura cross-coupling reaction under microwave irradiation: application to fused tricyclic oxa-aza-quinolones†

Pritam Saha, Subhendu Naskar, Priyankar Paira, Abhijit Hazra, Krishnendu B. Sahu, Rupankar Paira, Sukdeb Banerjee and Nirup B. Mondal\*

Received 11th February 2009, Accepted 21st April 2009

First published as an Advance Article on the web 28th April 2009

DOI: 10.1039/b902916h

Basic alumina used in lieu of traditional mineral bases efficiently promotes a solvent free, Pd(PPh<sub>3</sub>)<sub>4</sub> catalyzed Suzuki–Miyaura cross-coupling reaction under microwave irradiation.

## Introduction

The Suzuki–Miyaura cross-coupling reaction of aryl halides with aryl boronic acids is one of the most versatile and widely used reactions for the selective construction of carbon–carbon bonds, in particular for the formation of biaryl derivatives.<sup>1</sup> As the biaryl motifs are found in a range of pharmaceuticals, herbicides and natural products,<sup>2</sup> the development of this versatile reaction has received much attention in recent years. A plethora of reports have appeared in the literature regarding improvements that comprise modification of the catalysts<sup>1,3</sup> (with or without palladium), variation of solvents<sup>1,3,4</sup> (organic, aqueous or none), use of bases<sup>1,3,5</sup> (with or without), and reaction tools like classical heating<sup>1,6</sup> or microwave irradiation,<sup>7</sup> with particular emphasis for cleaner and more environmentally benign ways to make target molecules. As biaryl quinolones are known to possess neuroprotective properties,<sup>8</sup> we became interested in constructing the biaryl derivatives from our recently synthesized novel fused tricyclic quinolones<sup>9</sup> using the Suzuki–Miyaura reaction. The emphasis was on the optimization of yield of the biaryl products under green reaction conditions. The microwave irradiation technique was employed in the reactions, as this tool is well known for achieving energy efficiency and enhancing the rate of reaction as well as product yields. We were particularly attracted by the possibility of using a solid-supported reaction, as it is well documented that in such cases organic compounds get adsorbed on the surface of inorganic oxides like alumina or silica which themselves do not absorb or restrict the transmission of microwave irradiation.<sup>10</sup> This is also the case with reagents immobilized on porous solid supports which have an advantage over the conventional solution phase reactions because of the good dispersion of active sites, associated selectivities and easier work up.<sup>10</sup>

A systematic study was performed for optimization of yield of the products on our model systems varying the catalysts, bases, solvents, solid supports, and the time period. Herein, we report an efficient system for the Suzuki–Miyaura reaction of fused tricyclic dihalo quinolones using basic alumina as solid support and Pd(PPh<sub>3</sub>)<sub>4</sub> as catalyst in a solvent-free medium under microwave irradiation.

## Results and discussion

At the outset, we chose 5,7-dibromo-1,4-oxazino quinolone and *p*-methoxy phenyl boronic acid as model reaction partners to evaluate the effects of various conditions under microwave irradiation. The results revealed that the reactions catalyzed by Pd(OAc)<sub>2</sub>/PPh<sub>3</sub> in toluene–H<sub>2</sub>O using bases like KF, Cs<sub>2</sub>CO<sub>3</sub> or even K<sub>3</sub>PO<sub>4</sub> were ineffective and only low yield was obtained with Na<sub>2</sub>CO<sub>3</sub>. In alternative solvents, *viz.* dioxane and CH<sub>3</sub>CN, the reaction yielded no products, though in DCE and DMF low to moderate yields were obtained. In reactions carried out in DMF using Na<sub>2</sub>CO<sub>3</sub> along with PdCl<sub>2</sub>/PPh<sub>3</sub> or PdCl<sub>2</sub>(PPh<sub>3</sub>)<sub>2</sub> as the catalyst, the yields of the products were found to be 45–50%. Similar reaction protocols with Na<sub>2</sub>CO<sub>3</sub> and Pd(PPh<sub>3</sub>)<sub>4</sub> instead of PdCl<sub>2</sub>(PPh<sub>3</sub>)<sub>2</sub> produced better results. Further studies with Pd(PPh<sub>3</sub>)<sub>4</sub> using different solvents and bases revealed that moderate yield could be obtained in DMF or H<sub>2</sub>O in the presence of Na<sub>2</sub>CO<sub>3</sub> within 5 min of the reaction. Taking into account the efficacy of the catalyst Pd(PPh<sub>3</sub>)<sub>4</sub>, the study was further extended using solid supports like silica and alumina because of the fact that organic groups can robustly anchor to their surface.<sup>11</sup> Moreover, these are excellently stable and readily available. Indeed, using 1 mol% of Pd(PPh<sub>3</sub>)<sub>4</sub>, the silica gel-supported reaction in the presence of Na<sub>2</sub>CO<sub>3</sub> yielded 75%, neutral alumina in the presence of KF yielded 80% (Table 1, entry 8, 11), whilst basic alumina afforded the most effective conversion (90%) to the biaryl product (Table 1, entry 20). However, lower yields were obtained when the reactions were performed by changing the combination of bases with solid supports with different proportions of the catalyst. It is notable that only 0.1 mol% of Pd(PPh<sub>3</sub>)<sub>4</sub> with basic alumina could afford 90% yield even in 3 min (Table 1, entry 21), whereas neutral alumina was found to be totally ineffective in absence of a base (Table 1, entry 23–25).

The good performance of basic alumina could be ascribed to the presence of ‘interfacial’ boronic esters, originating from electrostatic interaction between the electron deficient boron

Indian Institute of Chemical Biology, 4 Raja S. C. Mullick Road, Jadavpur, Kolkata, 700 032, India. E-mail: nirup@iicb.res.in; Fax: +91-33-2473-5197; Tel: +91-33-2473-3491

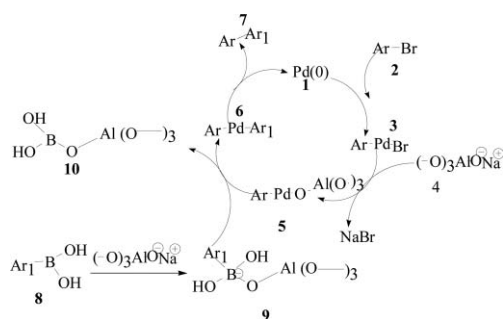
† CCDC reference number 711585. For crystallographic data in CIF or other electronic format see DOI: 10.1039/b902916h

**Table 1** Optimization of catalyst [Pd(PPh<sub>3</sub>)<sub>4</sub>] loading on different solid supports in the reaction between **1a** and *p*-methoxyphenyl boronic acid under microwave irradiation<sup>a</sup>

Entry	Solid support–base	Pd(PPh <sub>3</sub> ) <sub>4</sub> (mol%)	Temperature/°C	Time (min)	Yield <sup>b</sup> (%)
1	Silica gel–KF	0.5	90	5	40
2	Silica gel–KF	0.5	110	5	50
3	Silica gel–KF	0.5	120	5	50
4	Silica gel–KF	1.0	120	3	55
5	Silica gel–KF	2.0	120	5	55
6	Silica gel–Na <sub>2</sub> CO <sub>3</sub>	0.5	110	5	60
7	Silica gel–Na <sub>2</sub> CO <sub>3</sub>	0.5	120	3	65
8	Silica gel–Na <sub>2</sub> CO <sub>3</sub>	1.0	120	3	75
9	Silica gel–Na <sub>2</sub> CO <sub>3</sub>	2.0	120	6	80
10	Neutral alumina–KF	0.5	120	5	75
11	Neutral alumina–KF	1.0	120	4	80
12	Neutral alumina–KF	2.0	120	5	80
13	Neutral alumina–Na <sub>2</sub> CO <sub>3</sub>	0.5	120	5	55
14	Neutral alumina–Na <sub>2</sub> CO <sub>3</sub>	1.0	130	5	60
15	Neutral alumina–Na <sub>2</sub> CO <sub>3</sub>	2.0	130	5	60
16	Basic alumina	0.5	90	3	80
17	Basic alumina	0.5	110	3	85
18	Basic alumina	0.5	120	3	90
19	Basic alumina	0.5	130	3	90
20	Basic alumina	1.0	120	3	90
21	Basic alumina	0.1	120	3	90
22	Basic alumina	0.05	120	5	70
23	Neutral alumina	0.5	120	15	NR <sup>c</sup>
24	Neutral alumina	1.0	120	20	NR
25	Neutral alumina	2.0	120	20	NR

<sup>a</sup> All the studies were performed by using **1a** and *p*-methoxyphenyl boronic acid under microwave irradiation at 180 W. <sup>b</sup> Isolated yield. <sup>c</sup> No reaction.

atom of boronic acid and the oxygen atom of the solid framework, as depicted in Scheme 1, which facilitates the reaction. However, the remarkable difference of efficacy between the two forms of alumina might be due to the structural and compositional differences among various forms of alumina that are associated with differing surface reactivity and catalytic activity.

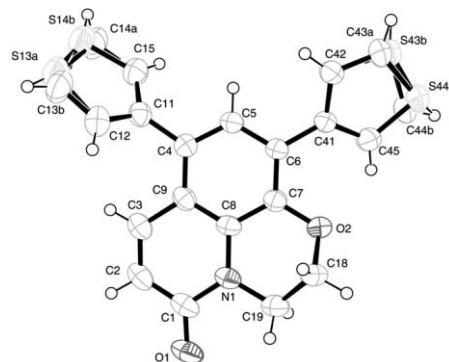
**Scheme 1** Plausible pathway for basic alumina-supported Suzuki–Miyaura cross coupling reaction.

In order to compare the advantages of the use of microwave irradiation, we performed the reaction for **2a** using an oil bath at 120 °C. It is noteworthy that only 21% of **2a** could be isolated after 23 hours of reaction. On the contrary 90% of the same was obtained in 3 min under microwave irradiation.

We then examined the optimal set of reaction conditions with a variety of oxazino (**1a**), oxazepino (**1b**), and oxazocino (**1c**) quinolones with different aryl/heteroaryl boronic acids, (Table 2). It can be seen from the table that the newly developed

reaction condition is an effective biarylation protocol with 80–90% yield.

Finally, generalization of this methodology was also established satisfactorily by performing reactions on simpler aryl bromides (*viz.* substituted bromobenzene) with different aryl and heteroaryl boronic acids. The products were characterized by MS, <sup>1</sup>H and <sup>13</sup>C NMR spectroscopy. Single crystal X-ray crystallographic analysis of a biaryl derivative (**2c**) was carried out for unambiguous determination of its structure (Fig. 1).<sup>†</sup>

**Fig. 1** ORTEP Diagram of 7,9-di-thiophen-3-yl-2,3-dihydro-1-oxa-3a-aza-phenalen-4-one (**2c**); ellipsoids are drawn at 50% probability level.

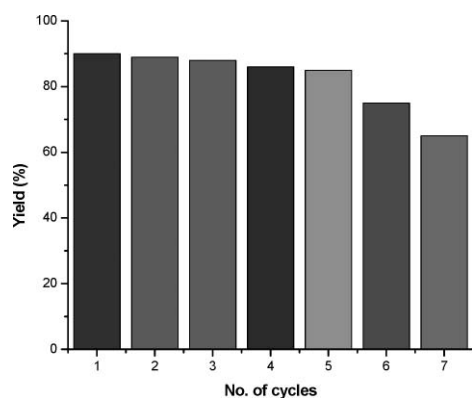
We also investigated the reusability of the solid support, as it is very important for industrial and pharmaceutical application. It was found that basic alumina, on calcination at 150 °C for 5 h (after washing with water and acetone) could be recycled 4–5 times with insignificant change in its activity (Fig. 2).

**Table 2** Suzuki cross coupling reaction of 5,7-dibromoquinolone (**1a–c**) with different boronic acids under microwave irradiation

$\text{Pd(PPh}_3)_4$  (0.1 mol%),  
 Basic alumina,  
 $\text{ArB(OH)}_2$  (2 equiv.)  
 120°C, 180 watt,  
 3 mins

Aryl bromide	Boronic acid	Time/min	Product <sup>a</sup>	$\text{Pd(PPh}_3)_4$ (mol%)	Yield <sup>b</sup> (%)
<b>1a</b>		3	<b>2a:</b> Ar = p-OMe Ph	0.1	90
<b>1a</b>		3	<b>2b:</b> Ar = furan-2-yl	0.1	86
<b>1a</b>		3	<b>2c:</b> Ar = thiophen-3-yl	0.1	88
<b>1a</b>		3	<b>2d:</b> Ar = pyridin-3-yl	0.1	88
<b>1a</b>		3	<b>2e:</b> Ar = naphthalen-2-yl	0.1	90
<b>1a</b>		3	<b>2f:</b> Ar = quinoline-8-yl	0.1	85
<b>1b</b>		3	<b>3a:</b> Ar = p-OMe Ph	0.1	90
<b>1b</b>		3	<b>3b:</b> Ar = furan-2-yl	0.1	84
<b>1b</b>		3	<b>3c:</b> Ar = thiophen-3-yl	0.1	88
<b>1b</b>		3	<b>3d:</b> Ar = pyridin-3-yl	0.1	88
<b>1c</b>		3	<b>4a:</b> Ar = p-OMe Ph	0.1	90
<b>1c</b>		3	<b>4b:</b> Ar = furan-2-yl	0.1	83
<b>1c</b>		3	<b>4c:</b> Ar = thiophen-3-yl	0.1	88
<b>1c</b>		3	<b>4d:</b> Ar = pyridin-3-yl	0.1	89

<sup>a</sup> The products were characterized by MS, <sup>1</sup>H and <sup>13</sup>C NMR spectroscopy. <sup>b</sup> Isolated Yield.

**Fig. 2** Reusability of the basic alumina.

To the best of our knowledge this is the first report of basic alumina-supported Suzuki-Miyaura cross-coupling reaction.

## Conclusion

In conclusion, we have developed an environmentally benign solid support system for Suzuki–Miyaura cross coupling reaction of heteroaryl bromides and boronic acids under microwave irradiation using basic alumina. The novelty of the system lies in its energy efficiency, low cost, easy availability of the solid support and also elimination of the use of any base or solvent. The operational simplicity and general applicability of the procedure as well as reusability of the basic alumina is expected to contribute to the development of a green technology of biaryl heteroaromatics.

## Experimental

### General procedure

The substrate, fused tricyclic-oxa-aza-quinolone (1 mol), was dissolved in a minimum amount of chloroform, added to a round-bottomed flask and basic alumina (500 mg) was added to it. The organic solvent was evaporated to dryness under reduced pressure. To the residue, boronic acid (2 mol) and Pd(PPh<sub>3</sub>)<sub>4</sub> (0.1 mol%) were added. The solid mixture was then stirred at room temperature under inert atmosphere for an additional 10–15 minutes to ensure efficient mixing. The flask was then fitted with a septum, and the mixture was subjected to irradiation in a microwave reactor (CEM, Discover, USA) at 120 °C (180 W) for 3 min (as monitored by TLC). After cooling, ethyl acetate was added and the slurry stirred at room temperature for 10 minutes. The mixture was then vacuum filtered through a sintered glass funnel. The filtrate was evaporated to dryness under reduced pressure and the residue was purified by flash chromatography to isolate the product. In the recycling experiment the residue obtained was washed with acetone and water (3–4 times) and subjected to calcination at 150 °C. The calcinated material could be further utilised in coupling reactions.

### Acknowledgements

We would like to thank the Council of Scientific and Industrial Research (CSIR), New Delhi, for financial support in the form of fellowships to P. Saha, S. Naskar, P. Paira, A. Hazra, K. B. Sahu and R. Paira. We are also thankful to Dr B. Achari, Emeritus Scientist, CSIR, for critical suggestions and encouragement. Our special thanks are due to Professor B. C. Ranu and Mr. S. Guha of IACS, Kolkata, for their generous cooperation in utilizing the MW instrument and crystallographic analysis.

### Notes and references

- 1 (a) N. Miyaura, K. Yamada and A. Suzuki, *Tetrahedron Lett.*, 1979, **20**, 3437–3440; (b) N. Miyaura and A. Suzuki, *Chem. Rev.*, 1995, **95**, 2457–2483; (c) A. Suzuki, *J. Organomet. Chem.*, 1999, **576**, 147–168; (d) A. Suzuki, *J. Organomet. Chem.*, 2002, **653**, 83–90; (e) S. Kotha, K. Lahiri and D. Kashinath, *Tetrahedron*, 2002, **58**, 9633–9695; (f) N. Miyaura, *Metal-Catalyzed Cross-Coupling Reactions*, ed. A. de Meijere and F. Diederich, Wiley-VCH, Weinheim, 2nd edn, 2004, vol. 1, pp 41–124.
- 2 (a) G. Bringmann, C. Gunther, M. Ochse, O. Schupp and S. Tasler, in *Progress in the Chemistry of Organic Natural Products*; ed. W. Herz, H. Falk, G. W. Kirby, R. E. Moore and C. Tamm, Springer, Wien, Austria, 2001, vol. 82, pp 1–249; (b) G. Bringmann and D. Feineis, *Act. Chim. Thérapeut.*, 2000, **26**, 151–171; (c) G. Bringmann, in *Guidelines and Issue for the Discovery and Drug Development Against Tropical Diseases*, ed. H. Vial, A. Fairlamb and R. Ridley, World Health Organisation, Geneva, 2003, p. 145–152.
- 3 (a) J. Yan and Z.-S. Zhou, *Tetrahedron Lett.*, 2005, **46**, 8173–8175; (b) J. Yan, W. Hu and W. Zhou, *Synth. Commun.*, 2006, **36**, 2097–2102.
- 4 (a) C. -J. Li and T. H. Chan, *Organic Reaction in Aqueous Media*, Wiley, New York, 1997; (b) P. A. Grieco, *Organic Synthesis in Water*, Academic Press, Dordrecht, The Netherlands, 1997; (c) B. Cornils and W. A. Herrmann, *Aqueous Phase Organometallic Catalysis*, 2nd edn, Wiley-VCH, Weinheim, 2004; (d) N. E. Leadbeater, *Chem. Commun.*, 2005, 2881–2902; (e) C.-J. Li, *Chem. Rev.*, 2005, **105**, 3095–3166; (f) S. Shi and Y. Zhang, *Green Chem.*, 2008, **10**, 868–872.
- 5 (a) B. R. Lipshutz, T. B. Petersen and A. R. Abela, *Org. Lett.*, 2008, **10**, 1333–1336; (b) N. Cousaert, P. Toto, N. Willand and B. Deprez, *Tetrahedron Lett.*, 2005, **46**, 6529–6532.
- 6 J. Lemo, K. Heuze and D. Astruc, *Org. Lett.*, 2005, **7**, 2253–2256.
- 7 (a) N. E. Leadbeater and M. Marco, *Org. Lett.*, 2002, **4**, 2973–2976; (b) N. E. Leadbeater and M. Marco, *Angew. Chem., Int. Ed.*, 2003, **42**, 1407–1409; (c) N. E. Leadbeater and M. Marco, *J. Org. Chem.*, 2003, **68**, 5660–5667.
- 8 Z. Wang, B. Wang and J. Wu, *J. Comb. Chem.*, 2007, **9**, 811–817.
- 9 (a) R. Dutta, D. Mandal, N. Panda, N. B. Mondal, S. Banerjee, S. Kumar, M. Weber, P. Lugar and N. P. Sahu, *Tetrahedron Lett.*, 2004, **45**, 9361–9364; (b) P. Paira, A. Hazra, K. B. Sahu, S. Banerjee, N. B. Mondal, N. P. Sahu, M. Weber and P. Lugar, *Tetrahedron*, 2008, **64**, 4026–4036.
- 10 (a) G. Bram, A. Loupy and D. Villemin, in *Solid Supports and Catalysts in Organic Synthesis*, ed. K. Smith, Ellis Horwood Prentice Hall, Chichester, 1992, ch. 12, p. 302; (b) R. S. Varma, *Green Chem.*, 1999, **1**, 43–55.
- 11 (a) S. Gronowitz and C. Roos, *Acta Chem. Scand.*, 1975, **29b**, 990–998; (b) S. Gronowitz, J. Malm and A. B. Hoernfeldt, *Collect. Czech. Chem. Commun.*, 1991, **56**, 2340–2351; (c) C. A. Fleckenstein and H. Plennio, *Green Chem.*, 2007, **9**, 1287–1291; (d) N. T. S. Phan and P. Styring, *Green Chem.*, 2008, **10**, 1055–1060; (e) F. Schneider and B. Ondruschka, *ChemSusChem*, 2008, **1**, 622–625; (f) G. W. Kabalka, R. M. Pagri, L. Wang, V. Namboodiri and C. M. Hair, *Green Chem.*, 2000, **2**, 120–122; (g) J.-H. Li, C.-L. Deng and Y.-X. Xie, *Synth. Commun.*, 2007, **37**, 2433–2448.

# Chiral ionic liquids improved the asymmetric cycloaddition of CO<sub>2</sub> to epoxides†

Suling Zhang, Yongzhong Huang, Huanwang Jing,\* Weixuan Yao and Peng Yan

Received 2nd December 2008, Accepted 3rd April 2009

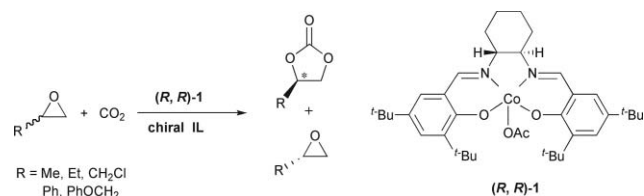
First published as an Advance Article on the web 14th April 2009

DOI: 10.1039/b821513h

The new catalyst system of chiral SalenCo(OAc)/chiral ionic liquid was developed to catalyze the asymmetric cycloaddition reaction of CO<sub>2</sub> and epoxides yielding the chiral cyclic carbonates. The synergistic effect between them is discussed.

Carbon dioxide is the most abundant waste produced by human activities and one of the greenhouse gases. The preparation of cyclic carbonates *via* cycloaddition of CO<sub>2</sub> to epoxides is one of the effective routes for CO<sub>2</sub> fixation. Over the past decade, a number of catalyst systems have been developed for the coupling reaction of carbon dioxide and epoxides to generate cyclic carbonates<sup>1–14</sup> that can be extensively used as monomers for polymer synthesis, aprotic solvents, pharmaceutical intermediates *etc.*<sup>15</sup>

Ionic liquids are well-known as catalysts and alternative solvents in organic synthesis,<sup>16–18</sup> and include amino acid-based ILs.<sup>19,20</sup> Even though some ionic liquids have been used in the coupling of CO<sub>2</sub> and epoxides,<sup>12,13,17</sup> no chiral ionic liquids (CIL) have been investigated in asymmetric cycloaddition reactions until now. In view of the fact that enantiomerically pure cyclic carbonates have been rarely reported, except for the chiral SalenCo(III)X catalysts accompanied with the salt of tetrabutylammonium halide (TBAB)<sup>13</sup> or phenyltrimethyl ammonium tribromide (PTAT)<sup>2</sup> as cocatalyst, new methodologies for the asymmetric cycloaddition of CO<sub>2</sub> to epoxides are still desired in terms of their atom economic and environmentally benign characteristics. Herein, we report a new effective catalyst system of SalenCo(OAc)/chiral ionic liquid to catalyze these attractive reactions (Scheme 1).



Scheme 1 Asymmetric cycloaddition of CO<sub>2</sub> to epoxides.

State Key Laboratory of Applied Organic Chemistry, College Chemistry and Chemical Engineering, Lanzhou University, Lanzhou, Gansu, 730000, China. E-mail: hwjing@lzu.edu.cn

† Electronic supplementary information (ESI) available: Spectra of the new ionic liquids. See DOI: 10.1039/b821513h

Pursuant to our own efforts toward the development of highly efficient catalysts for this asymmetric cycloaddition,<sup>21</sup> we decided to use CILs as co-catalysts instead of TBAB or PTAT based on a mechanistic understanding: the mechanism of the coupling reaction of epoxides and CO<sub>2</sub> must involve two catalytic centers, a Lewis acid and a Lewis base center. The Jacobsen catalyst gives a good chiral Lewis acidic center, and the chiral anion of CIL supplies, simultaneously, another chiral Lewis basic center for this coupling reaction. To examine the synergistic effect between two chiral centers, several chiral ionic liquids of TBAX (X = amino acidic anions, tartaric acidic anions, lactic acidic anion) were synthesized and tested as co-catalyst for the reaction. The results are listed in Table 1.

The chiral ionic liquids were prepared from TBAB and natural amino acids and used as cocatalysts in the asymmetric cycloaddition of CO<sub>2</sub> to propylene oxide (PO) at room temperature catalyzed by Jacobsen catalyst. The catalytic results (Table 1, entries 1, 3–9, 11, 13) revealed that the ee values of chiral propylene carbonate (PC) were evidently enhanced compared to the ee value produced by catalyst (*R,R*)-**1** combined with TBAB as cocatalyst (entry 22), and the highest ee value of (*S*)-PC was 74.6% achieved with [TBA][L-Pro] as cocatalyst (entry 9). When the reaction was carried out at 0 °C, the ee value of (*S*)-PC were augmented to over 80% (entries 2), and the selective factors (*S*) were superior to 10. When the parallel experiments were carried out using catalyst (*S,S*)-**1** (entries 28–40) instead of (*R,R*)-**1**, the interesting phenomenon of enantioselectivity cooperation was obviously demonstrated: some CILs gave the positive effect of cooperation with the catalyst (*R,R*)-**1** yielding the (*S*)-PC with a higher ee value and the negative effect of cooperation with catalyst (*S,S*)-**1** yielding the (*R*)-PC in lower ee value (entries 1–2 *vs.* 28–29; 5 *vs.* 32); and some of CILs gave the negative effect of cooperation with catalyst (*R,R*)-**1** yielding the (*S*)-PC with a lower ee value and the positive effect of cooperation with catalyst (*S,S*)-**1** yielding the (*R*)-PC with higher ee value (entries 8 *vs.* 35; 13 *vs.* 40). The same results were obtained from the CILs of lactic acid (entries 14, 15) and of tartaric acids (entries 16, 19). In contrast, when the racemic ILs of [TBA][Tar] were used as cocatalysts, both (*R*)-PC and (*S*)-PC were obtained with a lower ee value (entries 21 and 48).

When the cation of L-tartaric acid based CIL was changed from Bu<sub>4</sub>N<sup>+</sup> to the dimethylpyridinium, the catalyst of (*R,R*)-**1**/[dimethylpyridinium]<sub>2</sub>[L-Tar] generates the (*S*)-PC with a higher ee value (entries 23, 70% ee; 24, 61.4% ee) *versus* the catalyst of (*S,S*)-**1**/[dimethylpyridinium]<sub>2</sub>[L-Tar], which generates the (*R*)-PC with a lower ee value (entries 50, 44% ee; 51, 14% ee).



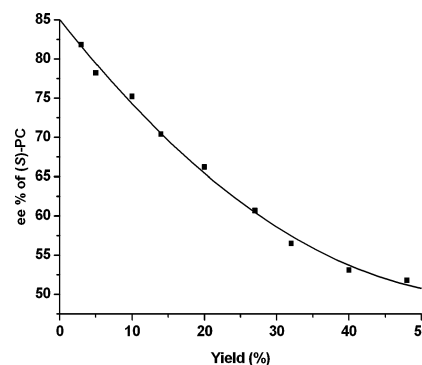
**Table 1** The effect of chiral ionic liquid in the coupling reaction of CO<sub>2</sub> and propylene oxide<sup>a</sup>

Entry	Co-catalyst	Time/h <sup>b</sup>	PC (ee%/yield%) <sup>b</sup>	S <sup>c</sup>	Entry	Time/h <sup>d</sup>	PC (ee%/yield%) <sup>d</sup>	S <sup>c</sup>
1	[TBA][L-Ala]	12	59.5(S)/32	5.3	28	12	36.1(R)/43	3.2
2	[TBA][L-Ala] <sup>e</sup>	20	85.2(S)/10	13.9	29	24	67.0(R)/12	5.7
		24	76(S)/12	8.1				
3	[TBA] <sub>2</sub> [L-Glu]	12	49.2(S)/18	3.4	30	12	45.0(R)/8	2.7
4	[TBA] <sub>2</sub> [L-Asp]	12	45.8(S)/16	3.0	31	12	47.1(R)/21	3.2
5	[TBA][L-Phe]	12	37.6(S)/26	2.6	32	12	13.9(R)/27	1.4
6	[TBA][L-Thr]	12	48.4(S)/26	2.8	33	12	45.1(R)/34	3.3
7	[TBA][L-Lys]	12	57.2(S)/36	5.0	34	12	51.6(R)/42	4.6
8	[TBA][L-His]	12	43.6(S)/8	2.6	35	12	43.3(R)/18	2.8
		24	38.6(S)/15	2.5		18	41.3(R)/26	2.8
9	[TBA][L-Pro]	4	74.6(S)/3	7.4	36	12	59.6(R)/24	4.7
		12	60.1(S)/20	4.6				
10	[TBA][L-Pro] <sup>e</sup>	24	62.5(S)/18	5.3	37	24	60.1(R)/17	4.5
11	[TBA][D-Pro]	12	46.1(S)/31	3.3	38	12	47.7(R)/36	3.4
12	[TBA][D-Pro] <sup>e</sup>	60	81(S)/3	10	39	60	64.1(R)/16	5.2
13	[TBA][L-Leu]	12	50.2(S)/36	4.0	40	12	52.2(R)/41	3.5
14	[TBA][L-Lac]	6	54.5(S)/42	5.1	41	6	53.6(R)/44	5.0
15	[TBA][L-Lac] <sup>d</sup>	6	64.2(S)/20	5.7	42	6	66.4(R)/20	5.8
16	[TBA] <sub>2</sub> [L-Tar]	1	70.4(S)/14	6.5	43	2	66.4(R)/15	5.6
		4	51.5(S)/46	4.7		4	51.1(R)/30	3.9
17	2[TBA] <sub>2</sub> [L-Tar]	12	47.7(S)/39	3.8	44	12	47.4(R)/22	3.1
	4[TBA] <sub>2</sub> [L-Tar]		45.1(S)/36	3.5			28.6(R)/18	1.9
	6[TBA] <sub>2</sub> [L-Tar]		41.6(S)/37	3.0				
	32[TBA] <sub>2</sub> [L-Tar]		38.6(S)/34	2.7				
18	[TBA] <sub>2</sub> [L-Tar] <sup>f</sup>	24	3.2(S)/30	1.1	45 <sup>g</sup>	72	1.0(S)/10	1.02
19	[TBA] <sub>2</sub> [D-Tar]	4	41.8(S)/45	3.4	46	4	43.6(R)/44	3.7
20	6[TBA] <sub>2</sub> [D-Tar]	12	44.8(S)/24	3.0	47	12	40.1(R)/48	3.4
	32[TBA] <sub>2</sub> [D-Tar]		23.4(S)/20	1.7			36.2(R)/39	2.7
21	[TBA] <sub>2</sub> [rac-Tar]	6	38(S)/36	2.7	48	6	37(R)/38	2.7
22	2TBAB	1	35.8(S)/40	2.6	49	1	35.5(R)/40	2.6
23	[1,2-Dimethylpyridinium] <sub>2</sub> [L-Tar]	72	70(S)/12	6.4	50	72	44.3(R)/14	2.8
24	[1,4-Dimethylpyridinium] <sub>2</sub> [L-Tar]	72	61.4(S)/17	4.7	51	72	14.0(R)/18	1.4
25	[1,2-Dimethylpyridinium] <sub>2</sub> [D-Tar]	72	32(S)/10	2.0	52	72	69.1(R)/12	6.4
26	[1,4-Dimethylpyridinium] <sub>2</sub> [D-Tar]	72	16(S)/12	1.4	53	72	60(R)/15	4.4
27	[1-Ethyl-2-methylpyridinium] <sub>2</sub> [L-Tar]	72	49.6(S)/23	3.5	54	72	47.5(R)/20	3.2

<sup>a</sup> Reaction conditions: propylene oxide 7 ml, 100 mmol; catalyst 60 mg, 0.1 mmol (0.1%); co-catalyst 0.1 mmol; CO<sub>2</sub> 100 psi; *T* = 25 °C. <sup>b</sup> Catalyst: (*R,R*)-**1**. <sup>c</sup>  $S = \ln[1 - c(1 + ee)] / \ln[1 - c(1 - ee)]$ , where *c* is the conversion and *ee* is the enantiomeric excess of the resulting propylene carbonate.

<sup>d</sup> Catalyst: (*S,S*)-**1**. <sup>e</sup> *T* = 0 °C. <sup>f</sup> Racemic catalyst **1**. <sup>g</sup> Catalyst: [TBA]<sub>2</sub>[L-Tar] 1.0 g.

The same phenomena were also observed using the CIL of [1,2-dimethylpyridinium]<sub>2</sub>[D-Tar] and [1,4-dimethylpyridinium]<sub>2</sub>[L-Tar] as cocatalyst (entries 25–26, 52–53). These more clear evidences can be explained by the enantioselectivity cooperation between chiral catalyst and cocatalyst: the cocatalyst with *R,R* chirality increased the *ee* values of (*S*)-PC catalyzed by (*R,R*)-**1**; it decreased the *ee* values of (*R*)-PC catalyzed by (*S,S*)-**1**. This explanation could be proved by the blank experiment, using a racemic catalyst **1** and chiral cocatalyst of [TBA]<sub>2</sub>[L-Tar] for this reaction, to give a 3.2% *ee* value of (*S*)-PC (entry 18). It can be also seen that the CIL of [TBA]<sub>2</sub>[L-Tar] only can be used as the catalyst for reaction (entry 45) showing activity with 1% *ee*. Consequently, a lower loading of cocatalyst slightly affected the selectivity of reactions, especially for the amino acid based cocatalysts. Contrarily, if more cocatalyst of [TBA]<sub>2</sub>[L-Tar] was used, it markedly decreased the *ee* value of chiral-PC (entries 17, 20, 44, 47), in which a bigger drop of *ee* value was attributed to the opposite chirality between catalyst and cocatalyst (entries 20, 44). We can also notice that when the yield was increased, the *ee* value of product was decreased (entries 2, 9, 16). For the most effective catalyst system SalenCo(OAc)/[TBA]<sub>2</sub>[L-Tar], this tendency was carefully determined and is depicted in Fig. 1.



**Fig. 1** The *ee*% of (*S*)-PC versus yield. Reaction condition: PO 7 ml, 100 mmol, (*R,R*)-**1** 0.1 mmol, [TBA]<sub>2</sub>[L-Tar] 0.1 mmol, CO<sub>2</sub> 100 psi, *T* = 25 °C.

To further extend the scope of the reaction, various epoxides were used in this asymmetric cycloaddition in the presence of the catalyst SalenCo(OAc)/[TBA]<sub>2</sub>[L-Tar] at room temperature (Table 2). The results demonstrated that this catalyst was active for the substrates with various substituted groups, in which the substrates with small substituted groups, for example, epichlorohydrin and 1,2-epoxybutane, can acquire

**Table 2** Asymmetric cycloaddition of CO<sub>2</sub> to various epoxides<sup>a</sup>

Entry	Epoxide	CC (ee%/yield%) <sup>b</sup>	Time/h	Entry	CC (ee%/yield%) <sup>c</sup>	Time/h
1	1,2-Epoxybutane	47.2(S)/12	18	5	60.8(R)/24	18
2	Epichlorohydrin	21.3(R)/16	6	6	9(S)/20	6
3	1,2-Epoxy-3-phenoxy propane	4(S)/25	18	7	3(R)/29	18
4	Styrene oxide	3(S)/27	72	8	2(R)/32	72

<sup>a</sup> Reaction condition: epoxide 100 mmol; catalyst 60 mg, 0.1 mmol [TBA]<sub>2</sub>[L-Tar] 63 mg, 0.1 mmol; CO<sub>2</sub> 100 psi; *T* = 25 °C. <sup>b</sup> Catalyst: (R,R)-1. <sup>c</sup> Catalyst: (S,S)-1.

**Table 3** Recycling of catalyst (R,R)-1/[TBA]<sub>2</sub>[L-Tar]<sup>a</sup>

Recycle time	Time/h	PC (ee%/yield%)	S
fresh	4	50.8(S)/46	4.6
1	4	47.3(S)/42	4.0
2	4	47.8(S)/41	4.0
3	4	47.0(S)/39	3.7

<sup>a</sup> Reaction condition: PO 100 mmol; catalyst (R,R)-1 60 mg, 0.1 mmol [TBA]<sub>2</sub>[L-Tar] 63 mg, 0.1 mmol; CO<sub>2</sub> 100 psi; *T* = 25 °C

corresponding cyclic carbonates with higher ee values (entries 1–2, 5–6), and the substrates with larger substituted groups, for example, styrene oxide and 1,2-epoxy-3-phenoxy propane, can acquire corresponding cyclic carbonates with lower ee values (entries 3–4, 7–8).

To test the recycling of catalyst (R,R)-1/[TBA]<sub>2</sub>[L-Tar], 5 mL methanol was added to the residue. The catalyst was precipitated quantitatively, collected by filtration and dried in vacuum. For the next run, it was necessary to reoxidize the catalyst using acetic acid, and add 0.1 mmol CIL. For three times of reuse, the activity and enantioselectivity of catalyst (R,R)-1 stayed at the same level (Table 3).

We can conclude that the new catalyst system of SalenCo(OAc)/CIL exhibits good activity for the asymmetric cycloaddition of CO<sub>2</sub> to epoxide under very mild condition. Beyond these data, the most important point must be emphasized—that the chiral catalyst SalenCo(OAc) and chiral cocatalyst of CIL work together in an additive or a synergistic manner. The same absolute configurations of it induce a higher ee of chiral PC; and the opposite absolute configurations of it induce a lower ee of chiral PC.

## Experimental

### Preparation of chiral ionic liquid

The preparation of CIL is a simple reaction carried out by mixing the precise molar ratio of amino acid and TBAB, freshly made from AgOH, or substituted pyridinium iodide in water. The reaction mixture was stirred for 24 h and then filtered. The filtrate was concentrated under reduced pressure to afford the desired CIL product as a colorless liquid or a pale yellow liquid at room temperature. Some chiral ionic liquids were prepared by referring to the literature method.<sup>22,23</sup> The Jacobsen catalyst, (t-Bu)<sub>2</sub>SalenCo(OAc), was synthesized by referring to the literature method.<sup>24–26</sup>

### Preparation of chiral cyclic carbonate

Epoxide (100 mmol), SalenCo(OAc) catalyst (0.1 mmol) and chiral ionic liquid (0.1 mmol) were added to a 100 ml stainless autoclave equipped with a magnetic stir bar and pressurized with CO<sub>2</sub> to 100 psi. After a proper reaction time, it was released to terminate the reaction. The remainder mixture was fractionally distilled under reduced pressure or recrystallized with ethanol to obtain the chiral cyclic carbonate.

## Acknowledgements

We are grateful to the financial support of the National Natural Science Foundation of China (NSFC 20773055, 20843005).

## Notes and references

- W. Yamada, Y. Kitaichi, H. Tanaka, T. Kojima, M. Sato, T. Ikeno and T. Yamada, *Bull. Chem. Soc. Jpn.*, 2007, **80**, 1391.
- T. Chang, H. W. Jing, L. L. Jin and W. Y. Qiu, *J. Mol. Catal. A: Chem.*, 2007, **264**, 241.
- R. L. Paddock and S. T. Nguyen, *J. Am. Chem. Soc.*, 2001, **123**, 11498.
- L. L. Jin, H. W. Jing, T. Chang, X. L. Bu and L. Wang, *J. Mol. Catal. A: Chem.*, 2007, **261**, 262.
- M. Aresta, A. Dibenedetto, L. Gianfrate and C. Pastore, *J. Mol. Catal. A: Chem.*, 2003, **204–205**, 245.
- W. N. Sit, S. M. Ng, K. Y. Kwong and C. P. Lau, *J. Org. Chem.*, 2005, **70**, 8583.
- R. L. Paddock and S. T. Nguyen, *Chem. Commun.*, 2004, 1622.
- A. Berkessel and M. Brandenburg, *Org. Lett.*, 2006, **8**, 4401.
- H. S. Kim, J. J. Kim, S. D. Lee, M. S. Lah, D. Moon and H. G. Jang, *Chem.–Eur. J.*, 2003, **9**, 678.
- H.-W. Jing and S. T. Nguyen, *J. Mol. Catal. A: Chem.*, 2007, **261**, 12.
- J. M. Sun, S. I. Fujita, F. Y. Zhao and M. Arai, *Green Chem.*, 2004, **6**, 613.
- H. Z. Yang, Y. L. Gu, Y. Q. Deng and F. Shi, *Chem. Commun.*, 2002, 274.
- X. B. Lu, B. Liang, Y. J. Zhang, Y. Z. Tian, Y. M. Wang, C. X. Bai, H. Wang and R. Zhang, *J. Am. Chem. Soc.*, 2004, **126**, 3732.
- Y. Xie, Z. F. Zhang, T. Jiang, J. L. He, B. X. Han, T. B. Wu and K. L. Ding, *Angew. Chem., Int. Ed.*, 2007, **46**, 7255.
- K. C. Nicolaou, Z. Yang, J. J. Liu, H. Ueno, P. G. Nantermet, R. K. Guy, C. F. Claiborne, J. Renaud, E. A. Couladouros, K. Paulvannanand and E. J. Sorensen, *Nature*, 1994, **367**, 630.
- D. B. Zhao, M. Wu, Y. Kou and E. Z. Min, *Catal. Today*, 2002, **74**, 157.
- J. M. Sun, S. I. Fujita and M. Arai, *J. Organomet. Chem.*, 2005, **690**, 3490.
- W. S. Miao and T. H. Chan, *Acc. Chem. Res.*, 2006, **39**, 897.

- 
- 19 G. H. Tao, L. He, W. S. Liu, L. Xu, W. Xiong, T. Wang and Y. Kou, *Green Chem.*, 2006, **8**, 639.
- 20 G. H. Tao, L. He, N. Sun and Y. Kou, *Chem. Commun.*, 2005, 3562.
- 21 L. L. Jin, Y. Z. Huang, H. W. Jing, T. Chang and P. Yan, *Tetrahedron: Asymmetry*, 2008, **19**, 1947.
- 22 K. Fukumoto, M. Yoshizawa and H. Ohno, *J. Am. Chem. Soc.*, 2005, **127**, 2398.
- 23 C. R. Allen, P. L. Richard, A. J. Ward, L. G. A. Water, A. F. Masters and T. Maschmeyer, *Tetrahedron Lett.*, 2006, **47**, 7367.
- 24 J. F. Larrow and E. N. Jacobsen, *J. Org. Chem.*, 1994, **59**, 1939.
- 25 W. H. Leung, E. Y. Y. Chan, E. K. F. Chow, I. D. Williams and S. M. Peng, *J. Chem. Soc., Dalton Trans.*, 1996, 1229.
- 26 Y. G. Hu, X. D. Huang, Z. J. Yao and Y. L. Wu, *J. Org. Chem.*, 1998, **63**, 2456.

# Efficient microwave-promoted acrylonitrile sustainable synthesis from glycerol

Vanesa Calvino-Casilda,<sup>\*a</sup> M. Olga Guerrero-Pérez<sup>b</sup> and Miguel A. Bañares<sup>a</sup>

Received 6th March 2009, Accepted 16th April 2009

First published as an Advance Article on the web 22nd April 2009

DOI: 10.1039/b904689e

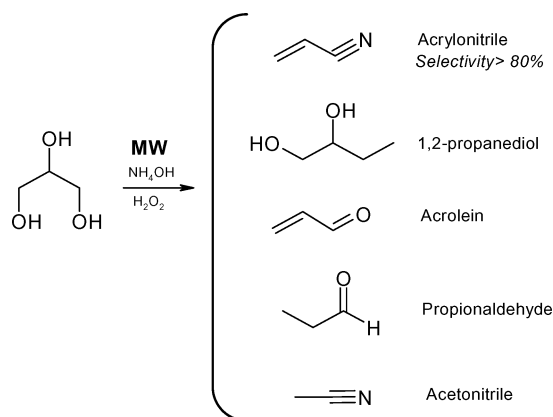
Solvent-free microwave-activation, in the liquid phase using an alumina supported V-Sb-O catalyst, affords highly efficient conversion (47%) of glycerol into acrylonitrile under mild conditions, short reaction times and in the absence of any solvent; in addition, it increases selectivity (>80%) compared to conventional thermal activation.

Commodity chemicals derived from fossil resources at present would be producible in future biorefineries from renewable resources, such as plant-derived sugar and other compounds.<sup>1</sup> Glycerol is a main by-product in biodiesel production; subsequently, its effective utilization will contribute to biodiesel promotion.<sup>2–6</sup>

Several processes to transform glycerol into valuable chemicals have been described,<sup>7–11</sup> but the reactivity of its three hydroxyl groups is quite similar, making it difficult to control selectivity. In this sense, the use of an additional reactant may narrow the product distribution. For example, the reaction of glycerol with ammonia and oxygen can yield acrylonitrile.<sup>12</sup> Acrylonitrile is nowadays produced using propylene as a starting material; with this new process, propylene, a fossil raw material, would be replaced by glycerol, a renewable source. In addition, this process can be carried out under mild conditions. The novel glycerol ammoxidation process has been run in the vapor phase; liquid-phase ammoxidation of glycerol would be a more desirable route to produce acrylonitrile, but its yield is too low. We describe, for the first time, the microwave-assisted liquid-phase reaction of glycerol with ammonia and hydrogen peroxide, which is run in the absence of any solvent (Scheme 1).

The short reaction time, and unique reactive features of microwave-assisted syntheses are ideally suited to an increasingly demanding chemical industry affording high conversions with peculiar selectivity. The use of catalysts in *dry media* (solvent-free conditions) is highly interesting because it may combine its catalytic effect with mild conditions and good selectivity.<sup>13</sup> This method thus offers a practical alternative to conventional heating in traditional catalysis.

The alumina-supported Sb-V oxide catalysts were prepared by two different methods, depending on the antimony precursor; as described elsewhere.<sup>14,15</sup> In the first preparation method (Sb<sub>1</sub>V/Al<sub>2</sub>O<sub>3</sub>\* series),<sup>14</sup> Sb<sub>2</sub>O<sub>3</sub> was added to an aqueous solution of NH<sub>4</sub>VO<sub>3</sub>, this solution was kept under stirring at 80 °C for



**Scheme 1** Possible products in the catalytic reaction of glycerol with ammonia and hydrogen peroxide under microwave activation.

50 min, then,  $\gamma$ -Al<sub>2</sub>O<sub>3</sub> was added. The resulting solution was dried in a rotatory evaporator at 80 °C at 0.3 atm. The resulting solid was dried at 115 °C for 24 h and then calcined at 400 °C for 4 h in air. For the second preparation method (Sb<sub>1</sub>V/Al<sub>2</sub>O<sub>3</sub>\*\* series), the same procedure was used but Sb was added as soluble tartrate complex.<sup>15</sup> The catalysts were prepared so that a total coverage of V + Sb would correspond to their dispersion limit loading on alumina, typically known as monolayer coverage.

The microwave equipment employed in this work is a Multi-mode MicroSYNTH Labstation provided with magnetic stirring and a PRO-6 Rotor reactor vessel. The temperature control during the reaction was carried out by an IR sensor. Milestone quartz vessels, with a capacity of 5 mL, were used to carry out the microwave activated reaction. These vessels support high pressure and are provided by a pressure relief spring in case the increasing pressure due to the ammonia vapour overcomes the spring pressure. Glycerol (0.5 mmol) and 200 mg of the catalyst were blended in the quartz vessel and hydrogen peroxide (15 mmol) and ammonia (57 mmol) were added. The mixture was introduced in the microwave equipment and irradiated with a power high enough (0–100 W) to reach 100 °C of temperature with a heating ramp of 10 °C min<sup>-1</sup>. The reactor vessel was sealed and held in the microwave for 60 min under continuous stirring while temperature and power were registered by easyCONTROL software. After cooling, the reaction products were extracted and filtered. The reaction was followed using a HP5890 gas chromatograph (GC) equipped with a 50 m long Ultra2–5% phenyl methyl siloxane capillary column and a flame ionization detector (FID).

For comparative purposes, the reaction was also run under conventional thermal activation. Similar to microwave-activated

<sup>a</sup>Catalytic Spectroscopy Laboratory Instituto de Catálisis y Petroleoquímica (CSIC) Marie Curie, 2, E-28049, Madrid, Spain. E-mail: vcalvino@icp.csic.es; Fax: +34 915 85 47 60

<sup>b</sup>Departamento de Ingeniería Química Universidad de Málaga, E-29071, Málaga, Spain

**Table 1** Characterization results obtained for the catalysts

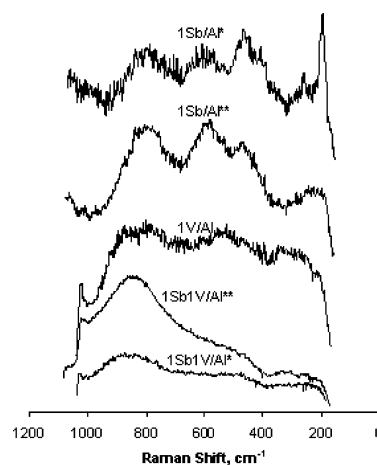
Catalyst	Wt. (%Sb)	Wt. (%V)	BET area/ m <sup>2</sup> g <sup>-1</sup>	Phases determined by Raman spectroscopy
V/Al	—	8.4	130	VO <sub>x</sub>
Sb/Al*	31.4	—	122	α-Sb <sub>2</sub> O <sub>4</sub>
Sb/Al**	29.1	—	105	Amorphous SbO <sub>x</sub> species
Sb1V/Al*	10.1	4.2	118	VO <sub>x</sub>
Sb1V/Al**	9.4	3.8	139	VO <sub>x</sub> , VSbO <sub>4</sub>

Catalyst preparation: \*Sb<sub>2</sub>O<sub>3</sub> precursor/\*\*Sb-tartrate complex precursor. Wt % obtained by ICP.

runs, a mixture of glycerol (0.5 mmol), hydrogen peroxide (15 mmol) and ammonia (57 mmol) was heated in an oil batch reactor at 100 °C while stirring and in absence of any solvent. After 5 min, the catalyst (200 mg) was added and the reaction time started. The reaction was monitored by gas chromatography, as described above.

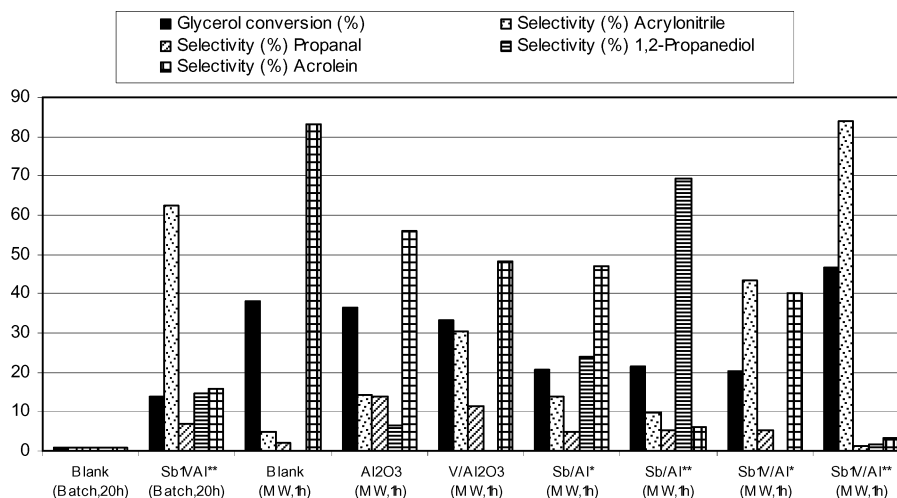
The catalysts have been characterized by XRD, *in situ* Raman spectroscopy (hydrated and dehydrated), and nitrogen physisorption at -196 °C to determine the BET area values. Table 1 summarizes the characterization data. The Raman spectrum of SbV/Al exhibits a broad Raman band near 800 and 880 cm<sup>-1</sup> owing to the formation of defective rutile VSbO<sub>4</sub> phase<sup>17</sup> (Fig. 1). The absence of diffraction peaks indicates that VSbO<sub>4</sub> crystals are nanoscaled, typically smaller than 4 nm. Vanadium-containing catalysts exhibit a Raman band near 1030 cm<sup>-1</sup>, which is sensitive to hydration and broad bands in the 800–900 cm<sup>-1</sup> region, are characteristic of bridging oxygen vibrations of surface polymeric vanadia species.<sup>18</sup> 1Sb/Al\* exhibit an intense Raman band at 190 cm<sup>-1</sup>, characteristic of segregated Sb<sub>2</sub>O<sub>3</sub> crystallites.<sup>19</sup> 1Sb/Al\*\* exhibit broad features at 780, 600, 468 and 210 cm<sup>-1</sup>, characteristic of surface amorphous antimony oxide.<sup>19</sup>

Fig. 2 shows activity/selectivity values for glycerol conversion under microwave and conventional thermal activations. Blank runs under thermal activation yield negligible conversion after 1 h (not shown), and very little conversion after 20 h. Tests

**Fig. 1** *In situ* Raman spectra of the catalysts.

under conventional thermal activation in the liquid phase at 100 °C shows low performance and only Sb<sub>1</sub>V/Al<sub>2</sub>O<sub>3</sub>\*\* catalyst affords some glycerol conversion (13.9%) and 62.5% selectivity to acrylonitrile after 20 h of reaction (Fig. 2), which is much worse than its performance after 1 h at 100 °C under microwave activation (46.8% conversion and 83.8% selectivity). The rest of catalysts are not active under conventional thermal activation.

Blank microwave-activated reaction reaches ca. 38.2% glycerol conversion in 1 h at 100 °C, and produces acrolein as the main reaction product; thus, under these reaction conditions the dehydration of glycerol to yield acrolein can occur without any catalyst. The presence of alumina moderately shifts selectivity towards acrylonitrile and propanal. Antimony doping does not have a strong effect on total conversion values, but affects catalyst structure and selectivity. Nanoscaled α-Sb<sub>2</sub>O<sub>4</sub> forms if a suspension of Sb<sub>2</sub>O<sub>3</sub> is used as an antimony precursor (Sb/Al\*); its performance is essentially like that of bare alumina. Molecularly dissolved antimony tartrate complex precursor (Sb/Al\*\*) produces dispersed amorphous SbO<sub>x</sub> species on

**Fig. 2** Glycerol conversion (%) and selectivity (%) to main products under conventional thermal activation (oil batch, 100 °C) for 20 h and under microwave (MW) activation for 1 h (Power = 0–100 W, heating ramp = 10 °C min<sup>-1</sup>) Catalyst preparation: \* Sb<sub>2</sub>O<sub>3</sub> precursor/\*\*Sb-tartrate complex precursor.

alumina and shift product distribution towards 1,2-propanediol. The presence of vanadia on alumina (V/Al) slightly promotes acrylonitrile. Neither of the single-oxide doped aluminas become significantly more efficient for acrylonitrile formation, since these samples (V/Al, Sb/Al\*\* and Sb/Al\*) are essentially selective to oxygenates. The addition of antimony modulates the selectivity of alumina-supported vanadium oxide catalysts, which is consistent with the trends for vapor-phase conversion of glycerol to acrylonitrile under thermal activation.<sup>12</sup> The antimony precursor (Sb<sub>2</sub>O<sub>3</sub> suspension *vs.* molecularly dissolved antimony tartrate complex) results in significantly different structures and catalytic behavior for the V-Sb-oxide system. Sb1V/Al\* catalyst, in which rutile VSbO<sub>4</sub> species have not been detected (Table 1), produces acrylonitrile and acrolein with similar selectivity values at a rather low glycerol conversion, lower than that afforded by V/Al. Rutile VSbO<sub>4</sub> forms on alumina when antimony is added as a dissolved tartrate complex, (Table 1); its performance for glycerol conversion to acrylonitrile is dramatically increased, reaching more than 80% selectivity to acrylonitrile at 47% conversion. This is consistent with the relevance of the rutile VSbO<sub>4</sub> phase for ammoxidation of propane to acrylonitrile,<sup>16</sup> and suggests that propane ammoxidation and glycerol conversion to acrylonitrile exhibit similar mechanistic reaction steps. Acrolein is the main reaction product obtained under microwave activation in the absence of a catalyst. Acrolein appears to be a critical intermediate in the ammoxidation of C<sub>3</sub> hydrocarbons (propane and propylene) to produce acrylonitrile.<sup>16</sup> Thus, the microwave activation would transform glycerol into acrolein and the rutile VSbO<sub>4</sub> phase would be efficient to form carbon–nitrogen bonds transforming acrolein into acrylonitrile with a very high selectivity. This reactive system is significantly more efficient than conventional gas-phase thermal activation, which demands much higher temperatures (400 °C) to afford 58.3% selectivity to acrylonitrile at 82.6% glycerol conversion.<sup>12</sup>

In summary, microwave activation dramatically enhances selectivity and activity values to acrylonitrile drastically reducing reaction time. These results underline the advantage of using microwave activation for a selective and energetically efficient valorization of glycerol and the relevance of the rutile VSbO<sub>4</sub> phase to transform glycerol into acrylonitrile. These results present a selective new process for valorization of glycerol—a renewable raw material—to acrylonitrile under mild conditions.

This microwave-assisted process is a novel cost-effective and solvent-free route to produce acrylonitrile.

## Acknowledgements

This research was funded by Spanish Ministry of Education and Science (CTQ2008–04261/PPQ) and ESF COST Action D36–006–06. The authors thank also Prof. Martín-Aranda from Department of Inorganic Chemistry and Technical Chemistry (UNED, Madrid) for her help with the Microwave equipment. Alumina was provided by Girdler-Süd-Chemie.

## Notes and references

- 1 S. Fernando, S. Adhikari, C. Chandrapal and N. Murali, *Energy Fuels*, 2006, **20**, 1727.
- 2 G. W. Huber, S. Iborra and A. Corma, *Chem. Rev.*, 2006, **106**, 4044.
- 3 R. Luque, L. Herrero-Davila, J. M. Campelo, J. H. Clark, J. M. Hidalgo, D. Luna, J. M. Marinas and A. A. Romero, *Energy and Environmental Science*, 2008, **1**, 542.
- 4 J. N. Chheda, G. W. Huber and J. A. Dumesic, *Angew. Chem., Int. Ed.*, 2007, **46**, 7164.
- 5 A. Behr, J. Eilting, K. Irawadi, J. Leschinski and F. Lindner, *Green Chemistry*, 2008, **10**, 13.
- 6 M. Pagliaro and M. Rossi, “*The Future of Glycerol, New Uses of a Versatile Raw Material*”, RSC Publishing, (2008) ISBN: 9780854041244.
- 7 A. M. Ruppert, J. D. Meelkijk, B. W. Kuipers, B. H. Ern e and B. M. Weckhuysen, *Chem.–Eur. J.*, 2008, **14**, 2016.
- 8 M. O. Guerrero-P erez, J. M. Rosas, J. Bedia, J. Rodr iguez-Mirasol and T. Cordero, *Recent Pat. Chem. Eng.*, 2009, **2**(1), 11.
- 9 M. Pagliaro, M. Rossi, C. Della Pina, R. Ciriminna, H. Kimura, *European Journal of Lipid Science and Technology*, 2009, 10.1002/ejlt.200800210.
- 10 C-H. Zhou, J. N. Beltramini, Y-X. Fan and G. Q. Lu, *Chem. Soc. Rev.*, 2008, **37**, 527.
- 11 Y. Zheng, X. Chen and Y. Shen, *Chem. Rev.*, 2008, **108**, 5253.
- 12 M. O. Guerrero-P erez and M. A. Ba ares, *ChemSusChem*, 2008, **1**, 511.
- 13 A. Loupy, “*Microwaves in Organic Synthesis*” 2nd edn. Wiley-VCH, Weinheim, Germany, 2006.
- 14 M. O. Guerrero-P erez, J. L. G. Fierro, M. A. Vicente and M. A. Ba ares, *J. Catal.*, 2002, **206**, 339.
- 15 M. O. Guerrero-P erez, J. L. G. Fierro and M. A. Ba ares, *Top. Catal.*, 2006, **41**, 43.
- 16 M. O. Guerrero-P erez and M. A. Ba ares, *Chem. Commun.*, 2002, **12**, 1292.
- 17 G. Xiong, V. S. Sullivan, P. C. Stair, G. W. Zajac, S. S. Trail, J. A. Kaduk, J. T. Gobab and J. F. Brazdil, *J. Catal.*, 2005, **230**, 317.
- 18 M. A. Ba ares and I. E. Wachs, *J. Raman Spectrosc.*, 2002, **33**, 359.
- 19 M. O. Guerrero-P erez, J. L. G. Fierro and M. A. Ba ares, *Top. Catal.*, 2006, **41**, 43.

# Eco-friendly hydrodehalogenation of electron-rich aryl chlorides and fluorides by photochemical reaction†

Valentina Dichiarante, Maurizio Fagnoni\* and Angelo Albini

Received 10th March 2009, Accepted 7th April 2009

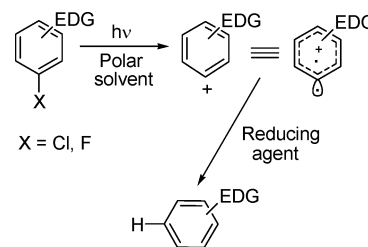
First published as an Advance Article on the web 15th April 2009

DOI: 10.1039/b904897a

Aryl chlorides and fluorides are smoothly hydrodehalogenated by irradiation either in neat *i*-PrOH or in a polar solution in the presence of hypophosphorous acid or triethylsilane. The procedure gives the halogen-free products in good to excellent yields under mild eco-friendly conditions and avoids the recourse to toxic metal catalysts.

The activation of the carbon–halogen bond in aromatic compounds is an important issue. In particular, the transformation of a C–X bond into a C–H bond (hydrodehalogenation reaction) has a significant role for the remediation of environmental pollutants, where it appears a reasonable means either for the complete detoxification of diffuse contaminants or for their transformation into less noxious chemicals.<sup>1</sup> A clean reaction would also have some use in organic synthesis for the elimination of an aromatic halogen after it had acted as protecting/orientating group in aromatic electrophilic substitutions.<sup>2,3</sup> Catalytic hydrogenation, reductions by using (low-valent) metal compounds, hydrides or (complex) metal hydrides as well as reductions with some nucleophilic neutral or anionic species have been used for this purpose.<sup>1</sup> Aryl chlorides and fluorides are markedly less reactive with respect to the corresponding bromides and iodides and are rather resistant to chemical reduction, especially when substituted with electron-donating groups.<sup>1</sup> Among chlorides, some chloroanisoles and 4-chloroanilines have been reduced quantitatively by using an *N*-heterocyclic carbene-palladacycle complex in *i*-PrOH<sup>4</sup> and some success has been obtained with chlorophenols under Pd(II) catalysis at 100 °C in the presence of K<sub>2</sub>CO<sub>3</sub> and triphenylphosphine.<sup>5</sup> Ionic liquids (e.g. molten tetrabutylammonium bromide) have been used as the reaction medium in the Pd-nanoparticle catalyzed hydrodehalogenation of 4-chloroanisole that occurred in 92% yield at 90–100 °C under hydrogen atmosphere.<sup>6</sup> As for the strong aryl–fluorine bond, this often remains unchanged under reductive conditions<sup>1,5</sup> and its activation is not trivial. Positive results were reported for 4-fluoro- and 2-fluoroanisoles by using a CuCl<sub>2</sub>·2H<sub>2</sub>O/lithium sand system<sup>7</sup> and monocoordinate nickel/*N*-heterocyclic carbene complexes<sup>8</sup> as the reducing agents, respectively, and for 4-fluoroaniline by homogeneous and/or heterogeneous Rh catalyzed hydrogenation.<sup>9</sup> Photodehalogenations where light makes the Ar–X bond labile could be

an interesting alternative but, to the best of our knowledge, a general method for the *clean* photoreduction of aryl chlorides and fluorides has been not reported as yet.<sup>10</sup> It is known that irradiation stimulates/accelerates the hydrodehalogenation of haloanisoles and haloanilines mediated by LiAlH<sub>4</sub><sup>11</sup> or SmI<sub>2</sub>.<sup>12</sup> However, it recently emerged that electron-rich aryl chlorides and fluorides undergo photoheterolysis in polar solvents and yield a (triplet) phenyl cation (Scheme 1).<sup>13</sup> This species has been demonstrated to have a π<sup>5</sup>σ<sup>1</sup> structure with the charge delocalized over the ring and the divalent carbon has a carbene (radical) character.<sup>14</sup> The usefulness of phenyl cations for electrophilic arylation reactions has been demonstrated.<sup>13</sup> We surmised that this intermediate could likewise be used for a mild metal-free, hydrodehalogenation reaction. Some support to this idea came from the earlier finding that 4-chloroaniline was efficiently reduced upon irradiation in MeCN in the presence of NaBH<sub>4</sub>.<sup>15</sup>



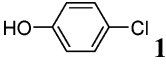
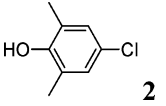
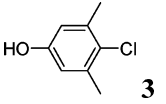
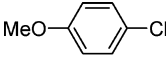
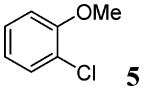
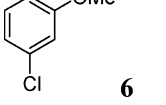
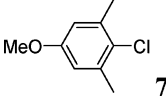
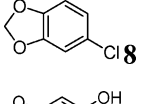
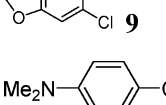
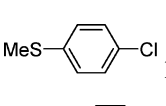
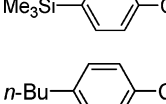
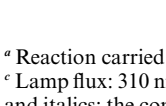
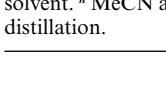
Scheme 1 Photohydrodehalogenation via phenyl cation.

We thus decided to explore whether a non nucleophilic reducing agent was effective. Reduction by hydrogen donor solvents (e.g. methanol)<sup>16</sup> has been observed as one of the reactions from phenyl cations; accordingly, we chose a better donor *i*-PrOH. Hypophosphorous acid was also used as a mild (and scarcely toxic)<sup>17</sup> hydrogen donor. Thus, a series of aryl chlorides and fluorides were irradiated ( $\lambda_{\text{exc}} = 254$  or 310 nm) in the presence of these reagents. Indeed, hydrodehalogenation occurred effectively affording the corresponding reduction products (ArH) in good to excellent yields, mostly exceeding 80%, as shown in Tables 1 and 2. In the H<sub>3</sub>PO<sub>2</sub> experiments, a 0.5 M solution of the acid in a polar medium such as MeCN, MeOH or a H<sub>2</sub>O/MeCN 1 : 5 mixture was used, while *i*-PrOH was used neat. Furthermore, Et<sub>3</sub>SiH that has been used as a diagnostic cation scavenger<sup>18</sup> was tested with halides **4**, **7**, **8**, **10**, **12** and **17**. Hydrodehalogenation occurred also in this case, but the yields (not reported) were somewhat lower than those obtained with the two other reagents.

Department of Organic Chemistry, University of Pavia, V. Taramelli 10, 27100, Pavia, Italy. E-mail: fagnoni@unipv.it; Fax: +39-0382-987323; Tel: +39-0382-987316

† Electronic supplementary information (ESI) available: Experimental details and <sup>1</sup>H and <sup>13</sup>C NMR spectra of compound **8**. See DOI: 10.1039/b904897a

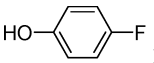
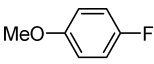
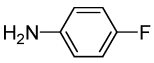
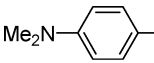
**Table 1** Photodehalogenation of aryl chlorides

ArCl (0.05 M) <sup>b</sup>	$\lambda^c$ /nm	H <sub>3</sub> PO <sub>2</sub> (0.5 M) <sup>a</sup>		neat <i>i</i> -PrOH	
		ArH (% yield) <sup>d</sup>	<i>t</i> /h	ArH (% yield) <sup>d</sup>	<i>t</i> /h
 <b>1</b>	254	100	15	86	15
 <b>2</b>	254	74, 82 <sup>e</sup>	15, 7 <sup>e</sup>	92	15
 <b>3</b>	254	86, 58 <sup>f</sup>	15	100	15
 <b>4</b>	254	80 <sup>g</sup> , 62 <sup>f,g</sup>	20	73	20
 <b>5</b>	254	81 <sup>g</sup> (73)	30	90	16
 <b>6</b>	310	56 (87)	30	100	16
 <b>7</b>	254	68 <sup>h</sup>	19	77, 86 <sup>i</sup>	19
 <b>8</b>	310	82	15	100	15
 <b>9</b>	310	82	15	78	15
 <b>10</b>	310	92 <sup>h</sup> , 97 <sup>e</sup>	6, 4 <sup>e</sup>	87, 99 <sup>i</sup> , 77 <sup>j</sup>	4
 <b>11</b>	310	74	16	34 (68)	35
 <b>12</b>	254	47 (89)	20	50	22
 <b>13</b>	254	67	15	100	15

<sup>a</sup> Reaction carried out in H<sub>2</sub>O/MeCN 1 : 5, unless otherwise stated; 2.5 mmol of acid used. <sup>b</sup> 0.25 mmol of aryl halide used, unless otherwise stated. <sup>c</sup> Lamp flux: 310 nm,  $\sim 2 \times 10^{-6}$  Einstein min<sup>-1</sup> cm<sup>-2</sup>; 254 nm,  $\sim 6 \times 10^{-6}$  Einstein min<sup>-1</sup> cm<sup>-2</sup>. <sup>d</sup> GC Yields based on consumed aryl halides. In parentheses and italics: the consumption of the aryl halide when different from 100%. <sup>e</sup> Reaction carried out in H<sub>2</sub>O/Me<sub>2</sub>CO 1 : 5. <sup>f</sup> H<sub>3</sub>PO<sub>2</sub> 0.2 M. <sup>g</sup> MeOH as the solvent. <sup>h</sup> MeCN as the solvent. <sup>i</sup> ArCl 0.1 M. <sup>j</sup> Reaction carried out on 15 mmol scale in an immersion-well reactor. Product isolated by bulb to bulb distillation.



**Table 2** Photodehalogenation of aryl fluorides

ArF (0.05 M) <sup>b</sup>	H <sub>3</sub> PO <sub>2</sub> (0.5 M) <sup>a</sup>		<i>i</i> -PrOH	
	ArH (% yield) <sup>c</sup>	<i>t</i> <sup>d</sup> /h	ArH (% yield) <sup>c</sup>	<i>t</i> <sup>d</sup> /h
 <b>14</b>	100 <sup>e</sup>	15	100	34
 <b>15</b>	98 <sup>e</sup> (81); 43 <sup>f</sup> (70)	30, 28 <sup>f</sup>	22 (45)	16
 <b>16</b>	87	16	100	16
 <b>17</b>	82 <sup>g</sup> , 71 <sup>g,h</sup>	15	97	6

<sup>a</sup> See Table 1. <sup>b</sup> See Table 1. <sup>c</sup> GC Yields based on consumed aryl halides. In parentheses and italic the consumption of the aryl halide when different from 100%. <sup>d</sup> Irradiation at 254 nm. Lamp flux:  $\sim 6 \times 10^{-6}$  Einstein min<sup>-1</sup> cm<sup>-2</sup>. <sup>e</sup> MeCN as the solvent. <sup>f</sup> Reaction carried out in H<sub>2</sub>O/Me<sub>2</sub>CO 1 : 5. <sup>g</sup> MeOH as the solvent. <sup>h</sup> H<sub>3</sub>PO<sub>2</sub> 0.2 M.

In detail, 4-chlorophenol (**1**), generally used as a model compound for chlorinated pollutants, was found to give phenol in 86% or 100% yield after 15 h irradiation in *i*-PrOH or with H<sub>3</sub>PO<sub>2</sub>, respectively. Methyl substituted chlorophenols **2** and **3** were likewise efficiently photoreduced despite the sterical hindering in the latter case. However, the yield of 3,5-dimethylphenol from **3** dropped from 86 to 58% when the amount of H<sub>3</sub>PO<sub>2</sub> was decreased to 0.2 M. As for isomeric chloroanisoles, irradiation in a methanol solution of hypophosphorous acid gave the best yields in the reduction of the *para* isomer (**4**, 80%), whereas isomers **5** and **6** were completely consumed only in *i*-PrOH and reduced in >90% yield. 3,5-Dimethyl-4-chloroanisole (**7**) was likewise transformed in 3,5-dimethylanisole in a good yield independently of the conditions used. Photoreduction, however, was less efficient (47% yield) when the reaction was carried out in *i*-PrOH/water 3 : 1. It is noteworthy that increasing the concentration of **7** to 0.1 M increased the yield of the anisole up to 86%. As for bis-ethers, H<sub>2</sub>O/MeCN 1 : 5 was the best solvent for the H<sub>3</sub>PO<sub>2</sub> mediated photoreduction of both 5-chloro[1,3]benzodioxole (**8**) and chlorosesamol (**9**) in yields similar to those obtained in neat *i*-PrOH. In the reduction of 4-chloro-*N,N*-dimethylaniline (**10**) the irradiation time required was shorter (4–6 h). *i*-PrOH was the best reducing agent and in this solvent *N,N*-dimethylaniline was formed quantitatively even using 0.1 M of **10**. The preparative value of the reaction was demonstrated in the photoreduction of **10** (15 mmol) where *N,N*-dimethylaniline was isolated in 77% yield after 2 h irradiation in an immersion-well apparatus followed by simple evaporation of the solvent and bulb to bulb distillation (see ESI).<sup>†</sup> This protocol was less efficient with S- or Si-bonded substituents, as shown in the case of 4-chlorothioanisole (**11**) and 1-chloro-4-(trimethylsilyl)benzene (**12**), which gave the corresponding dechlorinated derivatives in a medium yield and in some cases reached only a partial conversion. 1-*n*-Butyl-4-chlorobenzene, however, was quantitatively hydrodehalogenated in *i*-PrOH. As for the experiments in neat *i*-PrOH the quantum yield of reaction of compound **10** was high  $\Phi_r = 0.90$ ,<sup>19</sup> and

was satisfactory even in the irradiation of aryl halide **12**, ( $\Phi_r = 0.22$  at 254 nm) although it was not completely consumed after 20 h. In a couple of cases, when using H<sub>3</sub>PO<sub>2</sub> as the reductant, an acetone/water 5 : 1 mixture was tested as an alternative reaction medium. As a result, photoreduction of **2** and **10** occurred in a shorter irradiation time and in a comparable yield to those carried out in MeCN/water 5 : 1 (Table 1).

The extension to fluorides was successful; indeed the reduction yields were in most cases quantitative and higher than those observed with the corresponding aryl chlorides. In particular, 4-fluorophenol (**14**) was easily converted to phenol by irradiation either in an acetonitrile solution of hypophosphorous acid or in neat *i*-PrOH. 4-Fluoroanisole (**15**) was not completely consumed after 30 h irradiation but, at least in an acetonitrile solution of H<sub>3</sub>PO<sub>2</sub>, the reduction yield was good (98%). In this case, substituting MeCN with acetone was deleterious since both the consumption of **15** and the yield of formation of anisole were decreased (Table 2). The photoreduction by H<sub>3</sub>PO<sub>2</sub> was also effective with fluoroanilines **16** and **17** with a decrease of the yield when using a lower amount of H<sub>3</sub>PO<sub>2</sub> (0.2 M). However, with these compounds irradiation in *i*-PrOH was by far the best choice, with a yield of 100% and 97%, respectively.

The above data demonstrate a straightforward and environment-friendly procedure for the clean hydrodehalogenation of electron-rich aryl chlorides and fluorides *via* photoheterolysis and reduction of the thus generated triplet phenyl cation. Homolytic hydrogen abstraction from the solvent by this cation was supported by the formation of variable amounts of pinacol (from the dimerization of the dimethylketyl radical intermediate) in the experiments carried out in *i*-PrOH. It is noteworthy that the reduction is equally effective with both H<sub>3</sub>PO<sub>2</sub> (where it involves abstraction from a P–H bond) and *i*-PrOH (involving a C–H bond), as well as, though somewhat less efficiently, with Et<sub>3</sub>SiH (involving an Si–H bond). The smooth reaction in *i*-PrOH is due to the combined enhanced photocleavage yield in this polar solvent and to its good H-donating properties. The present protocol is advantageous with respect to thermal methods in that it avoids the use of neurotoxic organotin hydrides or aggressive metal hydrides as well as the use of expensive and labile metal catalysts. Moreover, contrary to some metal-catalyzed reductions<sup>6,20</sup> the present reaction took place at room temperature. A possible drawback of the method is the large consumption of energy for the UV lamps. The reactions in Tables 1 and 2 are referred to a small amount of aryl halide but the reaction can be scaled up to 15 mmol by using a 150 ml photochemical reactor with an internal lamp rather than a test tube with an external illumination. Furthermore, experiments in progress show that irradiation by solar light is also effective at least for derivatives absorbing in the UVA, such as anilines. Moreover, at least for aryl chlorides, an eco-friendly solvent such as acetone can be used in place of acetonitrile. At any rate, the simple experimental procedure does not require sophisticated operation, *e.g.* is not affected by moisture. Indeed, water, rarely used in reductions because of the chemical incompatibility with most reducing agents, is a convenient cosolvent in the reaction with hypophosphorous acid.

## Experimental

### General procedure for the photochemical reduction of aryl chlorides and fluorides

A solution of compound ArX (0.05 or 0.1 M, 0.25 or 0.5 mmol, respectively), the reducing agent (0.5 M H<sub>3</sub>PO<sub>2</sub> or 0.5 M Et<sub>3</sub>SiH, 2.5 mmol) in the chosen solvent (5 ml) was poured in quartz tubes, purged with nitrogen, serum capped and irradiated at 254 or 310 nm (see Tables 1 and 2). The end mixtures were analyzed by GC and the yields were determined by comparison with authentic samples of ArH. When hypophosphorous acid was used, the irradiated solutions were neutralized with solid potassium carbonate and filtered before analysis. In the experiments in neat *i*-PrOH, compounds ArX were dissolved in this solvent, treated as above and irradiated.

### Acknowledgements

Partial support of this work by Murst, Rome is gratefully acknowledged.

### References

- 1 F. Alonso, I. P. Beletskaya and M. Yus, *Chem. Rev.*, 2002, **102**, 4009–4091 and references therein.
- 2 F. Effenberger, *Angew. Chem., Int. Ed.*, 2002, **41**, 1699–1700.
- 3 V. V. Grushin, *Acc. Chem. Res.*, 1993, **26**, 279–286.
- 4 O. Navarro, N. Marion, Y. Oonishi, R. A. Kelly and S. P. Nolan, *J. Org. Chem.*, 2006, **71**, 685–692.
- 5 J. Chen, Y. Zhang, L. Yang, X. Zhang, J. Liu, L. Li and H. Zhang, *Tetrahedron*, 2007, **63**, 4266–4270.
- 6 V. Calò, A. Nacci, A. Monopoli, A. Damascelli, E. Ieva and N. Cioffi, *J. Organomet. Chem.*, 2007, **692**, 4397–4401.
- 7 F. Alonso, Y. Moglie, G. Radivoy, C. Vitale and M. Yusa, *Appl. Catal., A*, 2004, **271**, 171–176.
- 8 S. Kuhl, R. Schneider and Y. Fort, *Adv. Synth. Catal.*, 2003, **345**, 341–344.
- 9 R. J. Young and V. V. Grushin, *Organometallics*, 1999, **18**, 294–296.
- 10 L. Schutt and N. J. Bunce, Photodehalogenation of aryl halides, in *CRC Handbook of Organic Photochemistry and Photobiology*, ed. W. Horspool and F. Lenci, CRC Press, Boca Raton, 2nd edn, 2004, pp. 38/1–38/18.
- 11 A. L. J. Beckwith and S. H. Goh, *J. Chem. Soc., Chem. Commun.*, 1983, 907.
- 12 A. Ogawa, Y. Sumino, T. Nanke, S. Ohya, N. Sonoda and T. Hirao, *J. Am. Chem. Soc.*, 1997, **119**, 2745–2746.
- 13 V. Dichiarante and M. Fagnoni, *Synlett*, 2008, 787–800; M Fagnoni and A Albinì, *Acc. Chem. Res.*, 2005, **38**, 713–721.
- 14 S. Lazzaroni, D. Dondi, M. Fagnoni and A. Albinì, *J. Org. Chem.*, 2008, **73**, 206–211; M Winkler and W Sander, *Angew. Chem., Int. Ed.*, 2000, **39**, 2014–2016.
- 15 P. Coppo, M. Fagnoni and A. Albinì, *Tetrahedron Lett.*, 2001, **42**, 4271–4274.
- 16 S. Protti, M. Fagnoni, M. Mella and A. Albinì, *J. Org. Chem.*, 2004, **69**, 3465–3473.
- 17 Hypophosphorous acid was used to some extent in the reduction of aryl iodides and bromides. See: J. A. Murphy, *Pure Appl. Chem.*, 2000, **72**, 1327–1334.
- 18 J. Yang and M. Brookhart, *J. Am. Chem. Soc.*, 2007, **129**, 12656–12657.
- 19 The value was measured at 310 nm. See: B Guizzardi, M Mella, M Fagnoni, M Freccero and A Albinì, *J. Org. Chem.*, 2001, **66**, 6353–6363.
- 20 B. H. Lipshutz, T. Tomioka and K. Sato, *Synlett*, 2001, **SI**, 970–973.

# A dream combination for catalysis: highly reactive and recyclable scandium(III) triflate-catalyzed cyanosilylations of carbonyl compounds in an ionic liquid†

Boyoung Y. Park, Ka Yeon Ryu, Jung Hwan Park and Sang-gi Lee\*

Received 8th January 2009, Accepted 31st March 2009

First published as an Advance Article on the web 9th April 2009

DOI: 10.1039/b900254e

The catalytic activity of lanthanide triflates, particularly scandium triflate, increased dramatically in [bmim][SbF<sub>6</sub>], allowing the cyanosilylation of a variety of aldehydes and ketones with a turnover frequency up to 48 000 mol h<sup>-1</sup> and a total turnover number of 100 000.

The development of a recyclable catalytic system with high reactivity that enables economical and environmental sustainability is one of the most exciting challenges in chemistry. Emerging ionic liquids (ILs) have attracted increasing attention as novel vehicles for catalyst immobilization. Different types of metallic catalysts can be immobilized in ILs, allowing the recovery and reuse of both the catalyst and IL.<sup>1</sup> In addition to these advantages, unique reactivity and selectivity that cannot be achieved in conventional organic solvents are also observed in ILs.<sup>2</sup> As part of our continuing studies on catalysis in ionic liquids,<sup>3</sup> Song and ourselves collaboratively reported that metal triflate-catalyzed reactions, such as three-component reactions,<sup>3a</sup> Diels–Alder reactions,<sup>3b</sup> and Friedel–Crafts alkylation,<sup>3c</sup> were much faster in ionic liquids than in conventional organic solvents. In particular, hydrophobic ionic liquids with a non-coordinating anion, such as PF<sub>6</sub><sup>-</sup> and SbF<sub>6</sub><sup>-</sup>, exhibited positive ionic liquid effects that were attributed to *in situ* anion exchange between the catalyst and ionic liquid causing them to become a more electrophilic Lewis acid.<sup>3i</sup> With the aim of exploiting the synergic effects of lanthanide triflates in ionic liquids,<sup>4</sup> this study developed highly effective and environmentally benign catalytic cyanosilylation reactions of aldehydes and ketones in an ionic liquid with a turnover frequency (TOF) up to 48 000 mol h<sup>-1</sup> and a total turnover number (TON) of 100 000.

Cyanohydrines have demonstrated considerable synthetic potential as useful building blocks in organic synthesis. Hence, many catalytic methods, including asymmetric reactions, have been explored.<sup>5</sup> Among the various catalysts examined, Lewis acid-catalyzed cyanosilylations with trimethylsilyl cyanide (TMSCN) have been investigated most extensively.<sup>6</sup> Therefore, it is not surprising to expect that the Lewis acidic rare-earth triflates may be effective catalysts for cyanosilylation reactions. Lanthanide triflates, particularly scandium(III) triflate, are

ubiquitous in many Lewis acid-catalyzed reactions, mainly due to the pioneering work by Kobayashi.<sup>7</sup> However, only a few lanthanide triflates, such as Yb(OTf)<sub>3</sub><sup>8</sup> and Sc(OTf)<sub>3</sub>,<sup>9</sup> have been investigated for the cyanosilylation of carbonyl compounds, and their catalytic activities are lower or merely comparable to those of other active catalysts, such as Cu(OTf)<sub>2</sub>,<sup>10a</sup> ZnI<sub>2</sub>,<sup>10b</sup> LiClO<sub>4</sub>,<sup>10c</sup> and LiCl.<sup>10d</sup> Moreover, there are no reports on lanthanide triflate-catalyzed cyanosilylation of carbonyls in ionic liquids. Although, Loh *et al.* indicated that ionic liquids have their own catalytic activity for the cyanosilylation of aldehydes, their efficiencies were quite low.<sup>11</sup> Based on these observations, we hypothesized that a combination of lanthanide triflates with an ionic liquid would accelerate the cyanosilylation reaction with high recyclability.

The initial experiments on the reaction of benzaldehyde (**1a**) and TMSCN were carried out without a catalyst in 1-butyl-3-methylimidazolium (bmim)-based ionic liquids with different anions, such as BF<sub>4</sub><sup>-</sup>, SbF<sub>6</sub><sup>-</sup>, and PF<sub>6</sub><sup>-</sup>.<sup>‡</sup> Although the efficiency was relatively lower than that reported by Loh *et al.*,<sup>11</sup> only the ionic liquid with the SbF<sub>6</sub><sup>-</sup> anion, [bmim][SbF<sub>6</sub>], showed appreciable catalytic activity with 34% conversion (entry 1, Table 1). Accordingly, the cyanosilylation was carried out first with 0.5 mol% of Sc(OTf)<sub>3</sub> in [bmim][SbF<sub>6</sub>]. All the benzaldehyde was converted to the corresponding cyanosilyl ether **2a** within 5 min (entry 2, Table 1), even in the presence of 0.1 mol% catalyst (entry 3, Table 1). 40% conversion was achieved in 5 min when the Sc(OTf)<sub>3</sub> loading was decreased further to 0.01 mol%, indicating a TOF (defined as moles of product per mole of catalyst per hour) of 48 000 mol h<sup>-1</sup> (entry 4, Table 1). More than 99% conversion was achieved when the reaction time was extended to 30 min, thus indicating that the Sc(OTf)<sub>3</sub> in [bmim][SbF<sub>6</sub>] is one of the most reactive catalysts reported (entry 5, Table 1). In contrast, significantly decreased conversions were observed in other ionic liquids, [bmim][BF<sub>4</sub>] (entry 6, Table 1) and [bmim][PF<sub>6</sub>] (entry 7, Table 1) and in CH<sub>2</sub>Cl<sub>2</sub> (entry 8, Table 1). The catalytic activities of various lanthanide triflates and In(OTf)<sub>3</sub> were also investigated using a loading of 0.1 mol% in [bmim][SbF<sub>6</sub>]. As shown in Fig. 1, Gd(OTf)<sub>3</sub> (97%), Ho(OTf)<sub>3</sub> (97%), Er(OTf)<sub>3</sub> (97%), Tm(OTf)<sub>3</sub> (99%), Y(OTf)<sub>3</sub> (96%), and In(OTf)<sub>3</sub> (96%) also exhibited excellent activity. Other lanthanide triflates, such as Ce(OTf)<sub>3</sub> (87%), Sm(OTf)<sub>3</sub> (91%), Eu(OTf)<sub>3</sub> (86%), Tb(OTf)<sub>3</sub> (93%), Lu(OTf)<sub>3</sub> (94%), and La(OTf)<sub>3</sub> (93%), showed comparable activity with conversions ranging from 86 to 94%. On the other hand, Pr(OTf)<sub>3</sub> (<5%), Nd(OTf)<sub>3</sub> (<5%), and Dy(OTf)<sub>3</sub> (28%) showed extremely low catalytic activity. These results suggested that an appropriate choice of metal triflate and

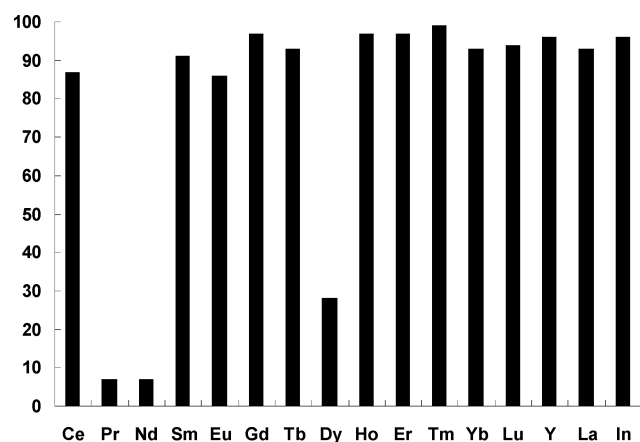
Department of Chemistry and Nano Science (BK 21), Ewha Womans University, Seoul, 120-750, Korea. E-mail: sanggi@ewha.ac.kr; Fax: +82 2 3277 3419; Tel: +82 2 3277 4505

† Electronic supplementary information (ESI) available: <sup>1</sup>H and <sup>13</sup>C NMR spectra for **2a–2t**, and **3a**, **3d**, **3i**, **3k**, **3m**. See DOI: 10.1039/b900254e

**Table 1** Sc(OTf)<sub>3</sub>-catalyzed cyanosilylation of benzaldehyde with TMSCN in an ionic liquid<sup>a</sup>

Entry	Sc(OTf) <sub>3</sub> (mol%)	Solvent	Time	Conv. (%) <sup>b</sup>
1	—	[bmim][SbF <sub>6</sub> ]	24 h	34
2	0.5	[bmim][SbF <sub>6</sub> ]	5 min	>99
3	0.1	[bmim][SbF <sub>6</sub> ]	5 min	>99 (98) <sup>c</sup>
4	0.01	[bmim][SbF <sub>6</sub> ]	5 min	40
5	0.01	[bmim][SbF <sub>6</sub> ]	30 min	>99
6	0.1	[bmim][BF <sub>4</sub> ]	5 min	11
7	0.1	[bmim][PF <sub>6</sub> ]	5 min	<5
8	0.1	CH <sub>2</sub> Cl <sub>2</sub>	5 min	7

<sup>a</sup> Reaction conditions: benzaldehyde (1.0 mmol), TMSCN (1.2 mmol) in [bmim][X] (1.0 mL) at room temperature. <sup>b</sup> Determined by <sup>1</sup>H NMR analysis with the average of three reactions. <sup>c</sup> Parentheses denote the isolated yield as cyanohydrine after acidic hydrolysis of the cyanosilyl ether with 1 N aqueous HCl solution for 2 h at room temperature.



**Fig. 1** Yields obtained with different lanthanide triflates. *Reaction conditions:* benzaldehyde (1.0 mmol), TMSCN (1.2 mmol), and Ln(OTf)<sub>3</sub> (0.1 mol%) in [bmim][SbF<sub>6</sub>] (1.0 mL) at room temperature for 5 min. The conversion was determined by <sup>1</sup>H NMR from the average three times reactions.

ionic liquid could generate a highly effective catalytic system for cyanosilylation of carbonyl compounds. The high catalytic activity of metal triflates in [bmim][SbF<sub>6</sub>] is ascribed to the anion exchange between Sc(OTf)<sub>3</sub> and [bmim][SbF<sub>6</sub>] resulted in a more Lewis acidic catalyst.<sup>31</sup>

The present catalytic system worked with a broad range of substrates. Various aldehydes were investigated in the presence of 0.1 mol% of Sc(OTf)<sub>3</sub> in [bmim][SbF<sub>6</sub>] for 5 min. As shown in Table 2 (entries 1–13, Table 2), all aromatic (**1b–1h**) and heteroaromatic aldehydes (**1i** and **1j**), α,β-unsaturated (**1k**) and aliphatic aldehydes (**1l–1n**) were uniformly transformed into the corresponding cyanohydrine trimethylsilyl ethers (**2b–2n**) in quantitative yields. Some of the selected cyanosilyl ethers (**2a**, **2d**, **2i**, **2k**, and **2m**) were hydrolyzed to the corresponding cyanohydrine with excellent yields (entry 3, Table 1 and entries 3, 8, 10, 12, Table 2). The reaction can also be extended to a variety of ketones. It has been reported that, compared to aldehydes, the lanthanide triflates are known to be less reactive

**Table 2** Sc(OTf)<sub>3</sub>-catalyzed cyanosilylation of various aldehydes and ketones in [bmim][SbF<sub>6</sub>]<sup>a</sup>

Entry	1	Product	Yield (%) <sup>b</sup>
1	2-CH <sub>3</sub> OC <sub>6</sub> H <sub>4</sub> CHO ( <b>1b</b> )	<b>2b</b>	>99
2	3-CH <sub>3</sub> OC <sub>6</sub> H <sub>4</sub> CHO ( <b>1c</b> )	<b>2c</b>	>99
3	4-CH <sub>3</sub> OC <sub>6</sub> H <sub>4</sub> CHO ( <b>1d</b> )	<b>2d (3d)</b>	>99 (94)
4	4-CH <sub>3</sub> C <sub>6</sub> H <sub>4</sub> CHO ( <b>1e</b> )	<b>2e</b>	>99
5	4-ClC <sub>6</sub> H <sub>4</sub> CHO ( <b>1f</b> )	<b>2f</b>	>99
6	4-PhOC <sub>6</sub> H <sub>4</sub> CHO ( <b>1g</b> )	<b>2g</b>	96
7	2-Naphthaldehyde ( <b>1h</b> )	<b>2h</b>	100
8	2-Furaldehyde ( <b>1i</b> )	<b>2i (3i)</b>	>99 (98)
9	2-Thiophenecarboxaldehyde ( <b>1j</b> )	<b>2j</b>	>99
10	<i>Trans</i> -C <sub>6</sub> H <sub>4</sub> CH=CHCHO ( <b>1k</b> )	<b>2k (3k)</b>	>99 (95)
11	PhCH <sub>2</sub> CH <sub>2</sub> CHO ( <b>1l</b> )	<b>2l</b>	>99
12	CH <sub>3</sub> CH <sub>2</sub> CH <sub>2</sub> CHO ( <b>1m</b> )	<b>2m (3m)</b>	>99 (95)
13	(CH <sub>3</sub> ) <sub>2</sub> CHCHO ( <b>1n</b> )	<b>2n</b>	>99
14	PhCOCH <sub>3</sub> ( <b>1o</b> )	<b>2o</b>	>99
15	PhCOCH <sub>2</sub> CH <sub>3</sub> ( <b>1p</b> )	<b>2p</b>	>99
16	PhCOPh ( <b>1q</b> )	<b>2q</b>	>99
17	1-Indanone ( <b>1r</b> )	<b>2r</b>	>99
18	α-Tetralone ( <b>1s</b> )	<b>2s</b>	>99
19	Cyclohexanone ( <b>1t</b> )	<b>2t</b>	>99

<sup>a</sup> Reaction conditions: carbonyl **1** (1.0 mmol), TMSCN (1.2 mmol), and Sc(OTf)<sub>3</sub> (0.1 mol%) in [bmim][SbF<sub>6</sub>] (1.0 mL) at room temperature for 5 min for aldehydes and 2 h for ketones. <sup>b</sup> Parentheses denote the isolated yield as cyanohydrine after acidic hydrolysis of the cyanosilyl ether with 1 N aqueous HCl solution for 2 h at room temperature.

toward cyanosilylation of ketones. For example, cyanosilylation of acetophenone with TMSCN using 5 mol% of Yb(OTf)<sub>3</sub> in CH<sub>2</sub>Cl<sub>2</sub> provided the corresponding cyanosilyl ether in 41% after 21 h reaction.<sup>10c</sup> To our delight, all aromatic and aliphatic ketones (**1o–1t**) reacted with TMSCN in the presence of 0.1 mol% of Sc(OTf)<sub>3</sub> for 2 h to yield the corresponding cyanohydrine silyl ethers (**2o–2t**) quantitatively (entries 14–19, Table 2).

The excellent recyclability of this catalytic system was examined with the reaction between benzaldehyde and TMSCN in the presence of 0.01 mol% of Sc(OTf)<sub>3</sub> in [bmim][SbF<sub>6</sub>] at room temperature for 30 min. After extracting the reaction mixture with *n*-hexane, the ionic liquid containing Sc(OTf)<sub>3</sub> was reused for the next run. No leaching of Sc into organic layer was observed. As shown in Table 3, the recovered Sc(OTf)<sub>3</sub> immobilized in [bmim][SbF<sub>6</sub>] could be reused 10 times without any loss of catalytic activity achieving a total turnover number of almost 100 000. These results clearly show that a combination of Sc(OTf)<sub>3</sub> with the ionic liquid increases both its catalytic activity and stability.

In summary, this study examined the catalytic activity of lanthanide triflates in the cyanosilylation of benzaldehyde with TMSCN in an ionic liquid. A highly reactive, recyclable and environmentally benign catalytic system consisting of Sc(OTf)<sub>3</sub> in [bmim][SbF<sub>6</sub>] was developed. With this catalytic system, various cyanohydrine silyl ethers were obtained from a wide range of aldehydes and ketones in quantitative yield. Anion exchange between Sc(OTf)<sub>3</sub> and [bmim][SbF<sub>6</sub>], which makes the catalyst more Lewis acidic, might be responsible for the excellent catalytic activity of Sc(OTf)<sub>3</sub> in [bmim][SbF<sub>6</sub>]. The ionic

**Table 3** Recycling of Sc(OTf)<sub>3</sub> and [bmim][SbF<sub>6</sub>] in the cyanosilylation of benzaldehyde with TMSCN<sup>a</sup>

Run <sup>b</sup>	1st	2nd	3rd	4th	5th	6th	7th	8th	9th	10th
Conv.(%)	>99	>99	98	96	>99	>99	97	97	>99	>99

<sup>a</sup> Reaction conditions: benzaldehyde (5.0 mmol), TMSCN (6.0 mmol) and Sc(OTf)<sub>3</sub> (0.01 mol%) in [bmim][SbF<sub>6</sub>] (5.0 mL) at room temperature for 30 min. <sup>b</sup> The product was extracted with *n*-hexane (50 mL × 3) and the ionic liquid containing Sc(OTf)<sub>3</sub> was reused for the next run.

liquid containing Sc(OTf)<sub>3</sub> could also be recovered and reused for several reaction cycles without any loss of catalytic activity. Studies aimed at applying this combination of lanthanide triflate with an ionic liquid to asymmetric cyanosilylations and to other catalytic reactions are currently under way.

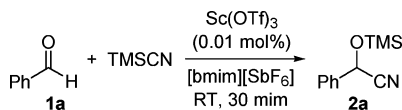
### Acknowledgements

This work was supported by the Korean Research Foundation (KRF-2006-312-C00587) and the Center for Intelligent Nano-Bio Materials at Ewha Womans University.

### Notes and references

‡ General procedure for the cyanosilylation of carbonyl compounds: a solution of Sc(OTf)<sub>3</sub> (0.1 mol%) in [bmim][SbF<sub>6</sub>] (1.0y) was stirred for 10 min at room temperature. A carbonyl compound (1.0 mmol) and TMSCN (1.2 mmol) were added successively, and the reaction mixture was stirred for 5 min for aldehydes (2 h for ketones) at room temperature under a nitrogen atmosphere. The reaction mixture was extracted with *n*-hexane (10 mL × 3), and the combined *n*-hexane layer was concentrated to give the corresponding cyanosilylated **2**. The results are shown in Tables 1 and 2. For catalyst recycling, the reaction was carried out in the presence of 0.01 mol% of Sc(OTf)<sub>3</sub>, and the recovered ionic liquid layer containing Sc(OTf)<sub>3</sub> was dried under a vacuum pump, and reused for the catalyst recycling test (Table 3). The hydrolysis of cyanohydrine trimethylsilyl ethers was carried out. The crude cyanosilyl ether obtained from the above reaction was treated with 1 N HCl (3.0 mL), and stirred for 2 h at room temperature. The reaction mixture was then extracted with CH<sub>2</sub>Cl<sub>2</sub> (5 mL × 5), and the combined organic layer was washed with a saturated aqueous NaHCO<sub>3</sub> solution, dried over anhydrous MgSO<sub>4</sub>, filtered, and concentrated to give the cyanohydrine.

- (a) P. Wasserscheid and W. Keim, *Angew. Chem., Int. Ed.*, 2000, **39**, 3772; (b) R. Sheldon, *Chem. Commun.*, 2001, 2399; (c) J. Dupont, R. F. de Souza and P. A. Z. Suarez, *Chem. Rev.*, 2002, **102**, 3667; (d) S.-g. Lee, *Chem. Commun.*, 2006, 1049; (e) P. Śledź, M. Mauduit and K. Grela, *Chem. Soc. Rev.*, 2008, **37**, 2433; (f) S.-g. Lee and T. J. Zhang, *Enantioselective Catalysis in Ionic Liquids and supercritical CO<sub>2</sub> in Handbook of Asymmetric Heterogeneous Catalysis*, ed. K. Ding, Y. Uozumi, Wiley-VCH, 2008, ch. 7, p. 233.
- Review, see: C. E. Song, M. Y. Yoon and D. S. Choi, *Bull. Korean Chem. Soc.*, 2005, **26**, 1321.
- (a) S.-g. Lee, J. H. Park, J. Kang and J. K. Lee, *Chem. Commun.*, 2001, 1698; (b) C. E. Song, W. H. Shim, E. J. Rho, S.-g. Lee and J. H. Choi, *Chem. Commun.*, 2001, 1122; (c) S.-g. Lee and J. H. Park, *Bull.*



*Korean Chem. Soc.*, 2002, **23**, 1367; (d) C. E. Song, D.-u. Jung, E. J. Rho, S.-g. Lee and D. Y. Chi, *Chem. Commun.*, 2002, 3038; (e) C. R. Oh, D. J. Choo, W. H. Shim, D. H. Lee, E. J. Rho, S.-g. Lee and C. E. Song, *Chem. Commun.*, 2003, 1100; (f) S.-g. Lee and J. H. Park, *J. Mol. Catal. A: Chem.*, 2003, **194**, 49; (g) S.-g. Lee, Y. J. Zhang, Z. Y. Piao, H. Yoon, C. E. Song, J. H. Choi and J. Hong, *Chem. Commun.*, 2003, 2624; (h) C. E. Song, D.-u. Jung, S. Y. Choung, E. J. Rho and S.-g. Lee, *Angew. Chem., Int. Ed.*, 2004, **43**, 6183; (i) J. H. Kim, J. W. Lee, U. S. Shin, J. Y. Lee, S.-g. Lee and C. E. Song, *Chem. Commun.*, 2007, 4683; (j) Y. S. Chun, J. Y. Shin, C. E. Song and S.-g. Lee, *Chem. Commun.*, 2008, 942.

- Ln(OTf)<sub>3</sub> catalyzed reactions in ionic liquids, see: K. Binnemans, *Chem. Rev.*, 2007, **107**, 2592.
- (a) R. J. H. Gregory, *Chem. Rev.*, 1999, **99**, 3649; (b) J.-M. Brunel and I. P. Holmes, *Angew. Chem., Int. Ed.*, 2004, **43**, 2752; (c) F.-X. Chen and X. Feng, *Synlett*, 2005, 892; (d) T. R. J. Achard, L. A. Clutterbuck and M. North, *Synlett*, 2005, 1828; (e) N. H. Khan, R. I. Kureshy, S. H. R. Abdi, S. Agrawal and R. V. Jasra, *Coord. Chem. Rev.*, 2008, **252**, 593.
- Selected recent papers, see: (a) J. B. King and F. P. Gabbaï, *Organometallics*, 2003, **22**, 1275; (b) R. Córdoba and J. Plumet, *Tetrahedron Lett.*, 2003, **44**, 6157; (c) C. Baleizão, B. Gigante, H. Garcia and A. Corma, *Tetrahedron Lett.*, 2003, **44**, 6813; (d) Y. N. Belokon', M. North and T. Parsons, *Org. Lett.*, 2000, **2**, 1617; (e) J. S. You, H.-M. Gau and M. C. K. Choi, *Chem. Commun.*, 2000, 1963; (f) A. Gama, L. Z. Flores-López, G. Aguirre, M. Parra-Hake, R. Somanathan and P. J. Waish, *Tetrahedron: Asymmetry*, 2002, **13**, 149; (g) S. Lundgren, S. Lutsenko, C. Jönsson and C. Moberg, *Org. Lett.*, 2003, **5**, 3663; (h) Y. Li, B. He, B. Qin, X. Feng and G. Zhang, *J. Org. Chem.*, 2004, **69**, 7910–7913.
- (a) S. Kobayashi, M. Sugiura, H. Kitagawa and W. W. L. Lam, *Chem. Rev.*, 2002, **102**, 2227; (b) S. Kobayashi, *Synlett*, 1994, **1994**, 689; (c) S. Kobayashi, *Eur. J. Org. Chem.*, 1999, **1999**, 15.
- (a) Y. Yang and D. Wang, *Synlett*, 1997, 861; (b) D. Wang and Y. Yang, *Synlett*, 1997, **1997**, 1379.
- (a) M. Bandini, P. G. Cozzi, A. Garelli, P. Melchiorre and A. Umani-Ronchi, *Eur. J. Org. Chem.*, 2002, **2002**, 3243; (b) M. Bandini, P. G. Cozzi, P. Melchiorre and A. Umani-Ronchi, *Tetrahedron Lett.*, 2001, **42**, 3041; (c) B. Karimi and L. Ma'Mani, *Org. Lett.*, 2004, **6**, 4813.
- (a) P. Saravanan, R. V. Anand and V. K. Singh, *Tetrahedron Lett.*, 1998, **39**, 3823; (b) P. G. Gassman and J. J. Talley, *Tetrahedron Lett.*, 1978, **19**, 3773; (c) G. Jenner, *Tetrahedron Lett.*, 1999, **40**, 491; (d) N. Kuroono, M. Yamaguchi, K. Suzuki and T. Ohkuma, *J. Org. Chem.*, 2005, **70**, 6530.
- Recently Loh and co-workers have reported that 1-methyl-3-octylimidazolium hexafluorophosphate showed catalytic activity in cyanosilylation of aldehydes, see: (a) Z.-L. Shen, S.-J. Ji and T.-P. Loh, *Tetrahedron Lett.*, 2005, **46**, 3137; (b) Z.-L. Shen, W.-J. Zhou, Y.-T. Liu, S.-J. Ji and T.-P. Loh, *Green Chem.*, 2008, **10**, 283.

# Gold nanoparticles promote the catalytic activity of ceria for the transalkylation of propylene carbonate to dimethyl carbonate†

Raquel Juárez, Avelino Corma\* and Hermenegildo García\*

Received 10th February 2009, Accepted 1st April 2009

First published as an Advance Article on the web 8th April 2009

DOI: 10.1039/b902850a

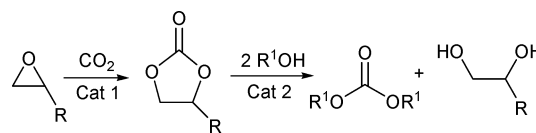
A series of metal oxide nanoparticles with acid or basic properties exhibit low to moderate activity towards the transalkylation of propylene carbonate with methanol; deposition of gold nanoparticles on nanoparticulated ceria significantly increases the activity of this metal oxide towards transalkylation.

Dimethyl carbonate (DMC) has been proposed as a green reagent to replace highly toxic phosgene.<sup>1</sup> Industrial application of DMC will require an efficient preparation procedure.

The direct synthesis of DMC by reaction of methanol and CO<sub>2</sub> is limited by an unfavourable equilibrium constant.<sup>2</sup> The current Enichem industrial process for DMC preparation is based on the oxidative reaction of methanol with CO.<sup>3</sup> Although this industrial process forms DMC in high yield, it has as drawback: the use as feedstock of CO obtained from steam reforming. Thus, the industrial process is based on the use of carbon, natural gas or hydrocarbons and therefore in the long-term contributes to increasing atmospheric CO<sub>2</sub> levels. Considering the negative impact of CO<sub>2</sub> emissions to the atmosphere, alternative processes that are based on CO<sub>2</sub> as feedstock will have the advantage of making the overall life cycle (DMC formation and use) CO<sub>2</sub>-neutral and, therefore, more favorable from the environmental point of view.<sup>5</sup>

An interesting possibility for DMC production from CO<sub>2</sub> will be a two-step route in which an intermediate cyclic carbonate obtained from the quantitative carboxylation of an epoxide undergoes transalkylation with methanol (Scheme 1). The stoichiometric amount of 1,2-propanediol resulting in the process can be used, as it is currently consumed, for the formation of polyurethanes. Actually, the hydrolytic ring opening of propylene oxide to 1,2-propanediol is currently a major industrial process that can be coupled with DMC synthesis, as shown in Scheme 1.

There are numerous reports describing efficient catalysts for CO<sub>2</sub> insertion into epoxides, particularly propylene oxide, to form cyclic carbonates.<sup>4,5</sup> However, there is still a need for developing more efficient heterogeneous catalysts for the transalkylation with methanol.<sup>4,6–9</sup> Current catalysts exhibit a maximum DMC yield of about 50%.<sup>7–9</sup> Herein, we describe that



**Scheme 1** Two-step route for the synthesis of dialkyl carbonates from epoxides.

gold nanoparticles significantly enhance the catalytic activity of nanoparticulated cerium oxide to promote the transalkylation of propylene carbonate (PC) with methanol to form DMC. Considering the current interest in exploiting the catalytic activity of supported gold nanoparticles for new reactions,<sup>10</sup> our finding may serve to develop a new generation of metal supported nanoparticles for the efficient formation of DMC from easily available cyclic carbonates.

In the first stage of our study, we screened the catalytic activity of a series of nanoparticulated metal oxides for the reaction of PC with methanol. The particle size of these metal oxides range from 5 nm (CeO<sub>2</sub>) to 30 nm (MgO). There are precedents in the literature reporting that some metal oxides, particularly with basic sites, promote transalkylation of organic carbonates.<sup>6–9,11</sup> The results obtained by us using five nanoparticulated metal oxides as catalysts are presented in Table 1. In this Table 1 we have indicated the disappearance percentage of PC (conversion%), the selectivity towards DMC (percentage of converted PC going to DMC) and the overall yield of DMC formation

**Table 1** Metal oxides and catalytic results for the transalkylation of PC by alcohols. Reaction conditions: PC (10 mmol), MeOH and other alcohol (100 mmol), metal oxide (115 mg), reaction time 6 h, reaction temperature 140 °C

Metal oxide	Conversion (%)	Selectivity (%)	Yield (%)
<b>Methanol</b>			
TiO <sub>2</sub>	22	15	33
Fe-promoted TiO <sub>2</sub>	0	—	—
MgO	55	15	9
ZrO <sub>2</sub>	14	50	7
CeO <sub>2</sub>	33	30	10
Au/CeO <sub>2</sub> (0.08 wt%)	40	73	30
Au/CeO <sub>2</sub> (0.5 wt%)	<b>63</b>	<b>55</b>	<b>35</b>
Au/CeO <sub>2</sub> (1.5 wt%)	68	41	28
Au/C (0.15 wt%)	17	35	6
<b>Ethanol</b>			
CeO <sub>2</sub>	12	10	2
Au/CeO <sub>2</sub> (1.5 wt%)	37	29	11
Au/CeO <sub>2</sub> (0.5 wt%)	<b>40</b>	<b>47</b>	<b>19</b>
<b>Propanol</b>			
Au/CeO <sub>2</sub> (0.5 wt%)	<b>39</b>	<b>13</b>	<b>5</b>
<b>Butanol</b>			
Au/CeO <sub>2</sub> (0.5 wt%)	<b>46</b>	<b>6</b>	<b>3</b>

Instituto de Tecnología Química CSIC-UPV, Universidad Politécnica de Valencia, Av. de los Naranjos s/n, 46022, Valencia, Spain. E-mail: acorma@itq.upv.es, hgarcia@qim.upv.es; Fax: (+ 34) 963 87 78 09

† Electronic supplementary information (ESI) available: TEM images of the catalysts and IR spectra of DMC adsorption on CeO<sub>2</sub>. See DOI: 10.1039/b902850a

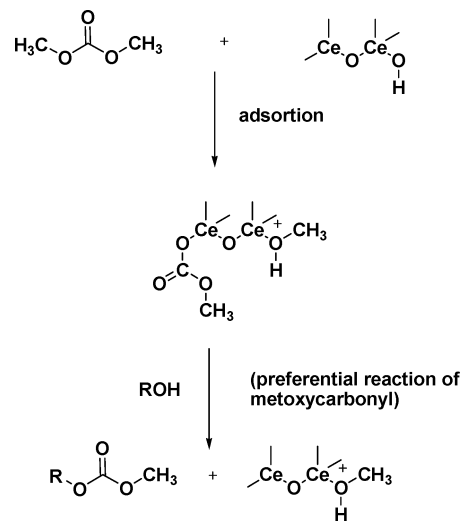
(mol of DMC formed divided by the initial PC mol, expressed as a percentage). It is worth commenting that besides transalkylation the decomposition of organic carbonates to  $\text{CO}_2$  and alcohol is an undesirable competing process.

As can be seen in Table 1, working at  $140^\circ\text{C}$  in the presence of an excess of methanol, most metal oxides were able to catalyze the formation of DMC with moderate to low selectivity at medium conversion.  $\text{TiO}_2$  in the anatase phase as nanoparticles (25 nm average size) exhibits low activity and selectivity towards transalkylation that even disappears upon doping with Fe. The strong basicity of the metal oxide nanoparticles, such as  $\text{MgO}$ , increases the conversion, but the major process was PC hydrolysis with very poor selectivity towards DMC. Typical acid metal oxides such as  $\text{ZrO}_2$  exhibit higher selectivity towards DMC, but low conversion. Nanoparticulated ceria oxide exhibits intermediate activity and selectivity towards DMC formation. Blank controls in the absence of any solid catalyst show very low PC conversion (<5%) when the reaction is carried out at  $140^\circ\text{C}$ . In contrast, PC undergoes substantial conversion when the reaction temperature increases to  $170^\circ\text{C}$  with only marginal formation of DMC (selectivity < 20%). For this reason no attempts were made to increase the reaction temperature beyond  $140^\circ\text{C}$ .

Recently, it has been reported that gold nanoparticles supported in ceria nanocrystals ( $\text{Au}/\text{CeO}_2$ ) are an extremely active catalyst for CO reactions.<sup>12</sup> This catalytic activity has been shown to arise from the creation of oxygen vacancies on the ceria support and the presence of positively charged gold species at the interphase with ceria.<sup>12</sup> It has been proposed that this catalyst interacts strongly with CO due the oxygen vacancies of the lattice. In addition, there is a large number of examples in the literature showing that gold nanoparticles supported on ceria are excellent catalysts for many other organic reactions.<sup>13</sup> We anticipated that the carbonyl group of PC could make this reagent also interact with  $\text{Au}/\text{CeO}_2$  similarly to CO. Based on this precedent, we prepared a series of catalysts, by the deposition-precipitation method, containing gold nanoparticles supported on nanocrystalline ceria ( $\text{Au}/\text{CeO}_2$ ). The gold loading was varied from 3 to 0.007 wt%. TEM microscopy of the catalyst revealed that the solids consist of small gold nanoparticles of average 5 nm size uniformly dispersed on the ceria nanocrystals (5 nm average dimension).<sup>†</sup> These materials are similar to those previously reported and a more exhaustive characterization can be found elsewhere.<sup>12,14</sup>

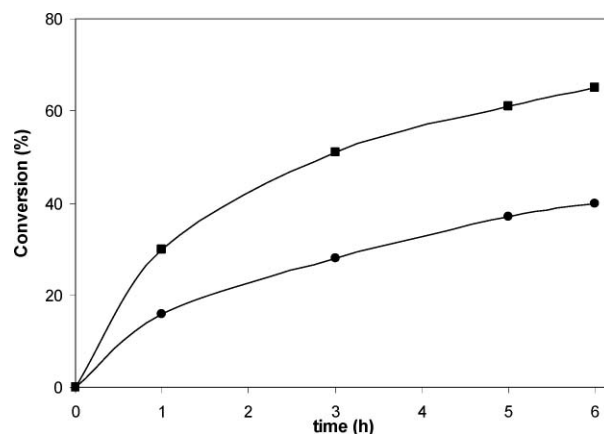
Before making catalytic tests we performed an IR study on the interaction of DMC with  $\text{CeO}_2$  and  $\text{Au}/\text{CeO}_2$  (1.5 wt%) to gain spectroscopic evidence of the interaction of these solids with organic carbonates. Upon absorption of DMC onto  $\text{CeO}_2$ , bands corresponding to methoxy (1104 and  $1044\text{ cm}^{-1}$ ) and metal carbonates ( $1588\text{ cm}^{-1}$ ) were observed (Figure S2 in the ESI).<sup>†15</sup> Thermal desorption by heating the  $\text{CeO}_2$  wafers containing adsorbed DMC shows that the bands of carbonate are lost (desorbed) at a lower temperature than the bands corresponding to methoxy groups. This IR spectroscopic data indicates that on the surface of  $\text{CeO}_2$ , organic carbonates can split resulting in alkylation and alkoxy-carbonylation and that the alkoxy groups are less reactive than alkoxy-carbonyl groups that desorb selectively at lower temperature. Therefore, the solid catalyst is more prone to transfer the alkoxy-carbonyl moiety

to the alcohol present in the medium. Scheme 2 illustrates our proposal based on the IR spectrum. For  $\text{Au}/\text{CeO}_2$  (1.5 wt%) a similar behaviour as that of observed for  $\text{CeO}_2$ , *i.e.*, splitting of DMC into methyl and methoxycarbonyl groups, takes place at a lower temperature than for  $\text{CeO}_2$  without gold. This shows that methoxycarbonyl transfer is facilitated by the presence of gold nanoparticles on the surface of  $\text{CeO}_2$ .<sup>15</sup> This suggests that reactivity towards transalkylation of  $\text{CeO}_2$  can be promoted by the presence of gold nanoparticles on the surface of  $\text{CeO}_2$ .



**Scheme 2** Proposal to rationalize the transalkylation mechanism on the surface of ceria based on IR spectroscopy, in which methoxy and carbonate groups are observed upon adsorption of DMC on  $\text{CeO}_2$  and  $\text{Au}/\text{CeO}_2$ .

To test this hypothesis we studied the reaction of PC with MeOH catalyzed by  $\text{Au}/\text{CeO}_2$ . The influence of gold promotion on the activity of ceria can be clearly seen in Fig. 1, which shows the time conversion plots for the transalkylation of PC in the presence of  $\text{CeO}_2$  and  $\text{Au}/\text{CeO}_2$  (0.5 wt%). We notice that longer reaction times lead to a decrease in DMC selectivity, indicating

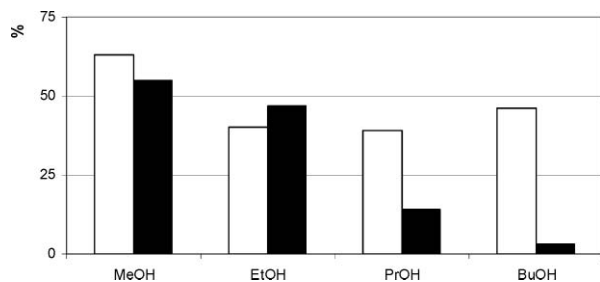


**Fig. 1** Time conversion plot of the reaction of methanol with PC in the presence of  $\text{CeO}_2$  (●) and  $\text{Au}/\text{CeO}_2$  (■) 0.5 wt%. Reaction conditions: Propylene carbonate (10 mmol), MeOH (100 mmol),  $\text{CeO}_2$  (115 mg) or  $\text{Au}/\text{CeO}_2$  (115 mg, 0.075 mol Au% respect PC),  $140^\circ\text{C}$ .

that this compound is not stable under the reaction conditions in the presence of Au/CeO<sub>2</sub> catalysts.

Although the kinetics of Fig. 1 clearly shows the promoting effect of gold, the overall yields shown in Table 1 do not surpass 35%. In this context, it should be mentioned that although in the chemical literature there are catalysts with similar performance, the temperature of the reported reactions is typically in the range 150–170 °C that is significantly higher than the reaction temperature employed in this work. We also note that some uncatalyzed reaction with low selectivity takes place at 170 °C.

After having found that gold promotes that catalytic activity of CeO<sub>2</sub> for transalkylation of PC by MeOH to form DMC, we also tested the applicability of Au/CeO<sub>2</sub> to catalyze PC transalkylation with other alcohols, in order to widen the scope of the reaction. As it can be seen in Table 1, the presence of gold in low weight percentages also increases the catalytic activity of CeO<sub>2</sub> for the formation of diethyl carbonate. Similarly, Au/CeO<sub>2</sub> also catalyzed the formation of propyl and butyl carbonates that are formed in lower yields. As can be seen in Fig. 2, the selectivity towards transalkylation significantly decreases with increasing alcohol chain length, suggesting that steric reasons make transalkylation more difficult and unfavorable as the number of carbons in the alcohol increases. Thus, PC decomposition seems to predominate as the number of alcohol carbons increases.



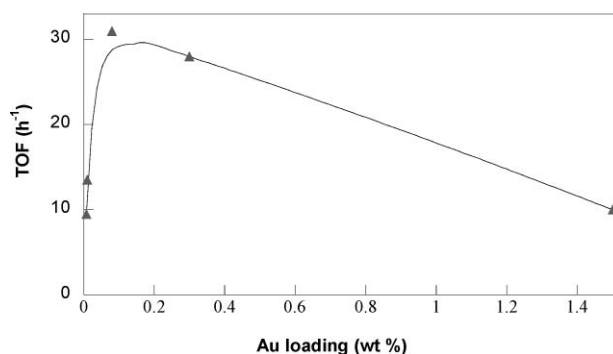
**Fig. 2** Conversion (white columns) and selectivity (black columns) data for the transalkylation reaction as a function of the alcohol number of carbons. *Reaction conditions:* alcohol (100 mmol), PC (10 mmol), Au/CeO<sub>2</sub> (0.5 wt%) (115 mg), reaction time 5 h, reaction temperature 140 °C.

Au/CeO<sub>2</sub> (0.5 wt%) acts as a heterogeneous catalyst. Thus, if the reaction was initiated under normal conditions in the presence of Au/CeO<sub>2</sub> (0.5 wt%) and then the solid hot filtered when the conversion was about 30% and the reaction continued in the absence of solid, no further conversion was observed in the supernatant solution. In addition, chemical analysis by inductively coupled plasma showed that no detectable amounts of gold were present in the liquid phase after the reaction.

After the reaction, the solid catalyst Au/CeO<sub>2</sub> (0.5 wt%) can be recovered from the liquid reaction mixture by filtration, washed with acetone and water (pH 10) and dried before reuse for consecutive runs. It was observed that the catalytic activity was maintained in four consecutive recycles. Chemical analysis of gold in the reused catalyst showed no leaching of gold from the solid.

When both the metal oxide support and the gold nanoparticles actively promote a reaction, it is often observed that there is an optimum amount of gold loading on the support. Comparing the performance of a series of Au/CeO<sub>2</sub> samples in which the loading of Au has been systematically increased from 0.007 to 1.5 wt%, it can be clearly demonstrated that the increased presence of gold nanoparticles gradually increases the reaction rate, with the samples containing gold giving higher conversion of PC compared to ceria.

The influence of the amount of gold on the catalytic activity of Au/CeO<sub>2</sub> catalyst for PC transalkylation to DMC was studied quantitatively by plotting the initial reaction rate at 140 °C vs. the amount of gold present, maintaining the total amount of CeO<sub>2</sub> constant. As can be seen in Fig. 3, concerning the initial reaction rate there is an optimum for the activity of Au/CeO<sub>2</sub> catalysts for a gold content at 0.08 wt%



**Fig. 3** Turnover frequencies (TOF) measured at low PC conversion vs. the amount of gold loaded on nanoparticulated ceria. *Reaction conditions:* PC 10 mmol, MeOH 100 mmol, weight of CeO<sub>2</sub> 115 mg, reaction temperature 140 °C.

Besides the initial PC reaction rate, the selectivity towards DMC is also strongly influenced by the gold loading. Thus, as can be seen in Table 1, DMC selectivity at 6 h reaction time increases substantially for very low gold loadings. Beyond a certain gold loading the selectivity towards DMC decreases. This DMC selectivity decrease with the gold loading beyond 0.5 wt% is due to the decomposition of PC and/or DMC to CO<sub>2</sub>. An optimum performance of the promotional influence of gold is achieved at about 0.5 wt%, at which the balance between increased PC conversion and high DMC selectivity results in the highest DMC yield at 6 h reaction time.

In conclusion, it has been shown that ceria nanocrystallites is a moderately active catalyst for the transalkylation of PC by methanol, exhibiting low selectivity. The presence of gold nanoparticles on ceria in appropriate loading significantly increases the activity and selectivity towards transalkylation.

## Notes and references

- 1 P. Tundo and M. Selva, *Acc. Chem. Res.*, 2002, **35**, 706.
- 2 M. Aresta and A. Dibenedetto, *Dalton Trans.*, 2007, 2975.
- 3 D. Delledonne, F. Rivettia and U. Romano, *Appl. Catal., A*, 2001, **221**, 241.
- 4 T. Sakakura, J. C. Choi and H. Yasuda, *Chem. Rev.*, 2007, **107**, 2365.
- 5 D. J. Darensbourg, *Chem. Rev.*, 2007, **107**, 2388.
- 6 H. Wang, M. H. Wang, N. Zhao, W. Wei and Y. H. Sun, *Catal. Lett.*, 2005, **105**, 253.



- 
- 7 T. Wang, M. W. Wei, Y. Sun and B. Zhong, *Green Chem.*, 2003, **5**, 343.
  - 8 T. Wei, M. H. Wang, W. Wei, Y. Sun and B. Zhong, *Fuel Process. Technol.*, 2003, **83**, 175.
  - 9 H. Wang, M. Wang, S. Liu, N. Zhao, W. Wei and Y. Sun, *J. Mol. Catal. A: Chem.*, 2006, **258**, 308.
  - 10 A. S. K. Hashmi and J. Hutchings Graham, *Angew. Chem., Int. Ed.*, 2006, **45**, 7896.
  - 11 H. Abimanyu, C. S. Kim, B. S. Ahn and K. S. Yoo, *Catal. Lett.*, 2007, **118**, 30.
  - 12 S. Carrettin, P. Concepcion, A. Corma, J. M. Lopez Nieto and V. F. Puentes, *Angew. Chem., Int. Ed.*, 2004, **43**, 2538.
  - 13 A. Corma and H. Garcia, *Chem. Soc. Rev.*, 2008, **37**, 2096.
  - 14 A. Abad, A. Corma and H. Garcia, *Chem.–Eur. J.*, 2008, **14**, 212.
  - 15 R. Juárez, P. Concepción, A. Corma, V. Fornés, H. Garcia, manuscript submitted.

# Solvent-free synthesis of thioglycosides by ball milling

Premanand Ramrao Patil and K. P. Ravindranathan Kartha\*

Received 4th March 2009, Accepted 9th April 2009

First published as an Advance Article on the web 24th April 2009

DOI: 10.1039/b904454j

Thioglycosides have been prepared in excellent yields by three different routes from a range of readily available glycosyl halides under solvent-free conditions employing a planetary ball mill.

## Introduction

Thioglycosides are amongst the most popular classes of glycosyl donor compounds used in oligosaccharide synthesis. The potential for their use as valuable glycosyl acceptor substrates, owing to their amenability to reactivity-tuning, has also been widely accepted.<sup>1</sup> Besides, they are also of great significance due to their applications in the area of enzyme inhibitors, ligands for affinity chromatography of carbohydrate-processing enzymes and proteins, *etc.*,<sup>2</sup> and therefore several reviews on their preparation and use have appeared over the past decade or so.<sup>3</sup> Recently, relatively large amounts of aryl thioglycosides were required in our laboratory for use as starting materials in the synthesis of building blocks for complex Agarinan C oligosaccharides for studies on their anticancer activity,<sup>4a</sup> as well as for the synthesis of biologically important galabiose<sup>4b</sup> and globotriose<sup>4c</sup> analogues. Although a number of methods are available in the literature for the synthesis of thioglycosides in general,<sup>1b,5</sup> aryl thioglycosides are best prepared by reacting a mixture of the desired per-*O*-acetylated glycosyl halide, the respective thiophenol and an alkali under phase transfer conditions.<sup>6</sup> The efficiency of the reaction (yield and by-product formation) has been found to be dependent upon the type of the phase transfer catalyst (PTC) and the organic solvent used, besides the nature of the glycosyl halide itself.<sup>6a,b</sup> This, along with

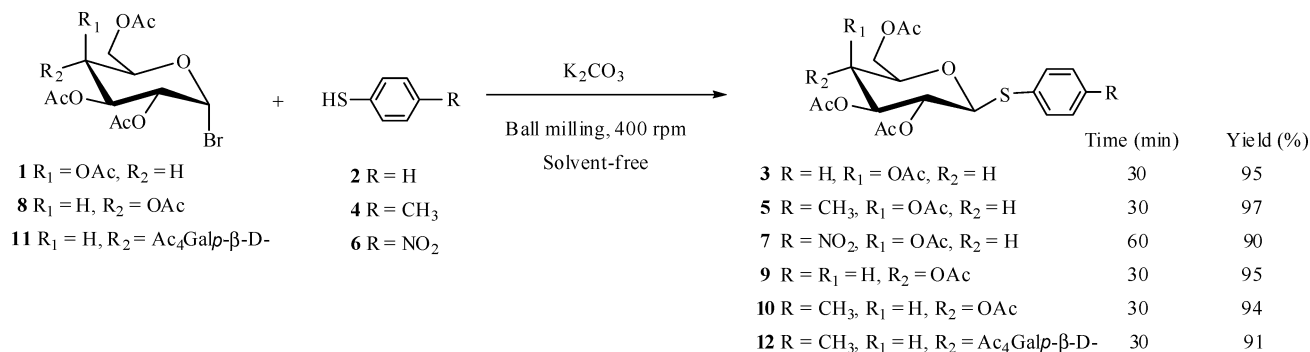
our recent success in the development of highly efficient methods for the synthesis of aryl glycosides by ball milling,<sup>7</sup> prompted us to look for solvent- and PTC-free, practical alternatives for aryl thioglycoside synthesis. The results are summarized below.

## Result and discussion

Homogenization of a mixture of 2,3,4,6-tetra-*O*-acetyl- $\alpha$ -D-galactopyranosyl bromide (**1**), thiophenol (**2**, 2 mol equiv) and  $K_2CO_3$  (2.2 mol equiv) in a planetary ball mill at 400 rpm for 30 min (Scheme 1) led to the complete disappearance of the bromide **1** with the resultant formation of a single product identical (TLC: eluent, EtOAc-*n*-Hex = 2 : 3) to the authentic phenyl thioglycoside **3**.<sup>8</sup> Most importantly, the isolation of the product was accomplished in a yield of 95% by simple aqueous work-up and crystallization. (recrystallization from  $Et_2O$ -*n*-Hex). The stereochemical outcome of the reaction was clearly evident from the <sup>1</sup>H-NMR spectrum of the product that showed the expected doublet for H-1 at  $\delta$  4.67 ( $J_{1,2} = 9.9$  Hz) along with the signal for H-2 at  $\delta$  5.22 (t,  $J_{2,3} = 9.9$  Hz) consistent with the desired 1,2-*trans*-configuration of **3**. No 1,2-*cis*-linked glycoside or any other by-product (orthoester/glycal/hemi-acetal/*etc.*) was detected (on TLC/NMR). The reaction worked extremely well and with the same efficiency even when the malodorous thiol was reduced to 1.5 mol equiv (as compared to 3–10 mol equiv as recommended<sup>5a,6</sup> in the phase transfer methodology) in multi-gram scale reactions (**1**, 25 g). Besides, it also totally eliminates the need for a PTC (being PTC-free) and the possibilities of unwanted side reactions involving solvent molecules as observed in the bi-phasic conditions<sup>6b</sup> (being solvent-free). Thus, the current method is more cost effective as well as simpler and greener, requiring no chromatographic purification step in the synthesis.

Reaction of the bromide **1** with a relatively more activated thiol **4** (a low melting solid) and a comparatively deactivated

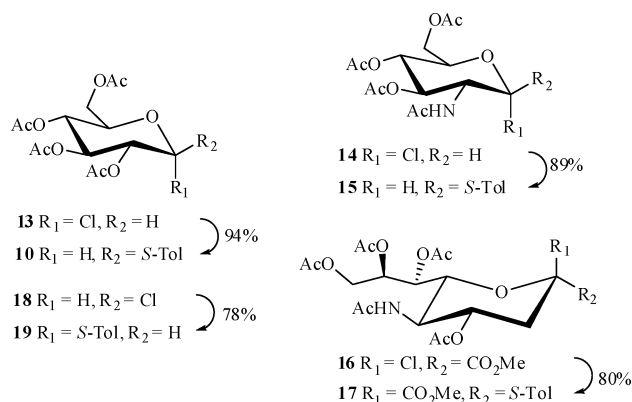
Department of Medicinal Chemistry, National Institute of Pharmaceutical Education and Research, Sector 67, S.A.S. Nagar, Punjab, 160 062, India. E-mail: rkartha@niper.ac.in; Fax: +91-172-2214692



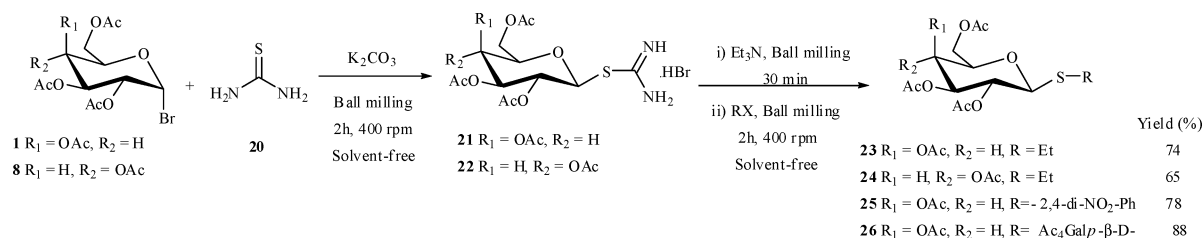
Scheme 1 Solvent-free, mechanochemical synthesis of aryl thioglycosides.

thiophenol **6** (a solid) also proceeded well (in 30 min and 1 h respectively) and the respective 1,2-*trans*-linked thiogalactosides **5<sup>o</sup>** and **7<sup>oc</sup>** were obtained in excellent yield (97% and 90% respectively, Scheme 1) in both cases. The work was then extended to the synthesis of the thioglucosides **9<sup>ob,10</sup>** and **10<sup>o</sup>** by grinding 2,3,4,6-tetra-*O*-acetyl- $\alpha$ -D-glucopyranosyl bromide (**8**) with **2** and **4** respectively for 30 min in the ball mill for which, again, yields in the range of 90–95% were obtained without having to resort to any chromatographic purification step. 1-Thio-lactoside **12<sup>9a</sup>** was also likewise prepared from the respective bromide **11** in 91% yield.

As the reaction of glycosyl chlorides such as **13** under the PTC conditions has been reported to lead to the orthoester formation,<sup>6a</sup> it was also used as a substrate for the reaction with thiol **4** under solvent-free conditions in the ball mill. It was observed that the reaction was complete in 1 h at 400 rpm providing **10** directly by crystallization in 94% yield (Scheme 2). Importantly, no orthoester was detected in the reaction mixture. The glucosamine-derived glycosyl chloride **14** also likewise gave the desired 1,2-*trans*-linked glucoside **15<sup>9a</sup>** in 89% yield without chromatography. The synthesis of sialo-oligosaccharides, that play a crucial role in biological processes such as cell growth, cell differentiation, cell adhesion and oncogenesis and also in their functions such as receptors for viruses and bacterial toxins, often require thiosialosides as glycosyl donors.<sup>11</sup> Therefore, the conversion of the sialosyl chloride **16** to the thiosialoside **17** was attempted by reacting **16** with thiol **4** for 1 h in the ball mill and the desired glycoside **17<sup>6c,9a</sup>** was obtained in 80% yield directly by crystallization. It is worthwhile to point out that the yield in the preceding examples can be further improved by recovering more of the product from the mother liquor. As the neighboring group participation can be excluded in the case of the formation of **17** (from **16**) as a possibility, the exclusive formation of the  $\alpha$ -thiosialoside **17** revealed that the reaction proceeded



Scheme 2



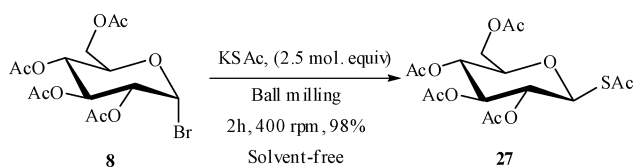
Scheme 3

through the S<sub>N</sub>2 pathway. However, the same could not be said about the products obtained from the bromides **1**, **8** and **11** owing to the fact that the products derived from a direct S<sub>N</sub>2 displacement as well as those obtained *via* the neighboring group participation of the C2-acetoxy group in them are expected to be the same (1,2-*trans*-linked thioglycosides). Therefore the reaction of tetra-*O*-acetyl- $\beta$ -D-glucopyranosyl chloride (**18**) with **5** was investigated in which the 1-thio- $\alpha$ -D-glucopyranoside (**19<sup>12</sup>**) could be isolated in 78% yield. Formation of the  $\beta$ -glycoside **10** was not observed in the reaction. The configuration of glucoside **19** was confirmed by <sup>1</sup>H-NMR spectrum which showed a doublet for H-1 characteristically at  $\delta$  5.82 ( $J_{1,2}$  = 5.8 Hz) and the H-2 double doublet at  $\delta$  5.11 ( $J_{1,2}$  = 5.8 Hz and  $J_{2,3}$  10.2 Hz). Moreover, in its <sup>13</sup>C-NMR spectrum the signal for C-1 characteristically appeared at 85.4 ppm (while the corresponding signal for the  $\beta$ -thioglycoside **10** was found at 86.4 ppm).

After realizing success in the above sets of reactions in which the need for the solvent as well as the phase transfer catalyst was eliminated completely, we turned our attention to alternative literature methods of thioglycoside synthesis for investigating them for possible ‘greening’. Among the available alternative routes, we have observed that accessing thioglycosides *via* the corresponding glycosylthiuronium salt is one that is also often employed.<sup>2,3a,13</sup> This method involves firstly the reaction of a glycosyl halide with thiourea to give the corresponding glycosylthiuronium derivative, usually under reflux in benzene<sup>13</sup>/acetone<sup>14</sup> (or more desirably, in acetonitrile<sup>2</sup>/2-propanol<sup>15</sup>) or in the melt.<sup>13</sup> The thiuronium halide thus obtained is then converted to the corresponding thioglycoside either directly or *via* the corresponding hemi-thioacetal in two steps by reacting it with the desired alkyl/sugar halide under basic conditions.<sup>2,3a,13</sup> For the direct conversion of the thiuronium salt to the thioglycoside a two-phase system consisting of benzene and water in the presence of a PTC has recently been recommended as well suited.<sup>13</sup> As benzene is a known carcinogen, eliminating the solvent in this reaction will be of particular value. Hence, a mixture of the galactopyranosyl bromide (**1**) and thiourea (**20**, 2.5 mol equiv) was allowed to mix in a planetary ball mill for 2 h at 400 rpm (Scheme 3), which resulted in the complete disappearance of the bromide **1** along with the formation of the isothiourethane derivative **21<sup>2,13</sup>** (TLC: eluent, EtOAc-*n*-Hex = 2 : 3). Et<sub>3</sub>N (10 mol equiv) was then added to the reaction mixture and was further mixed for 30 min at 400 rpm. Formation of the anomeric thiol was found to be complete at this stage. Thereafter, EtI (1.5 mol equiv) was added to the vessel and was further ground for 2 h under the same conditions. Aqueous work up followed by chromatographic purification (EtOAc-*n*-Hex = 1 : 4) yielded ethyl 2,3,4,6-tetra-*O*-acetyl- $\beta$ -D-galactopyranoside

(**23**, 74%; lit.<sup>2</sup> 72%), the structure of which was confirmed by <sup>1</sup>H and <sup>13</sup>C NMR spectroscopy. As would be expected, it was observed that the  $\alpha$ -analogue of **23**<sup>16</sup> (namely, ethyl 2,3,4,6-tetra-*O*-acetyl- $\alpha$ -D-galactopyranoside) was also formed in the reaction as a by-product (5–7% of isolated yield) resulting from the partial anomerization that occurred during the formation of the thiol intermediate. In the same manner, the glucopyranosyl bromide **8**, when subjected to the above grinding sequence, gave on reaction with EtI the respective thioglycoside **24**<sup>10b</sup> in 65% yield. Notably, preparation of the aryl thioglycoside **25**<sup>2,17</sup> from glucosyl bromide **8** via the isothioureia derivative **22** as above using 1-chloro-2,4-dinitrobenzene as the halide donor reagent was achieved without chromatographic purification (in 78% yield directly after aqueous work up (recrystallization from Et<sub>2</sub>O–*n*-Hex). The application of the current methodology was also demonstrated further by the preparation of the thiodisaccharide **26**,<sup>13</sup> in the same manner as above, from the galactosyl bromide **1** via the thiuronium bromide **21** in 88% yield after aqueous workup and recrystallization from Et<sub>2</sub>O–*n*-Hex. No chromatographic purification was, again, found to be necessary in this case as well. Other glycosyl halides such as **8** also reacted with the same efficiency.

Another important intermediate that gives access to a range of thioglycosides is the glycosyl thioacetate (*e.g.* **27**).<sup>1b,3a</sup> The thioacetate derivative is usually prepared by reacting the desired glycosyl halide with KSAc (4–5 mol equiv). The reaction can be carried out with or without the aid of a PTC. When carried out under heterogeneous conditions in CH<sub>2</sub>Cl<sub>2</sub> (DCM), it is very efficient but requires long reaction times (18 h or more depending upon the substrate). The reactions under homogeneous conditions in acetone on the other hand are faster but often are not as efficient as those carried out in DCM. And the use of a biphasic system (water and an immiscible organic solvent) requires use of a PTC. Therefore, the preparation of glycosyl thioacetates under solvent-free, PTC-free conditions by ball milling was subsequently addressed. Thus, when the glucopyranosyl bromide **8** and KSAc (2.5 mol equiv) were mixed at 400 rpm in the ball mill for 2 h (Scheme 4) 1,2,3,4,6-penta-*O*-acetyl-1-thio- $\beta$ -D-galactopyranose, **27**<sup>18</sup> was obtained in excellent yield (98%) after simple aqueous work-up (recrystallization from Et<sub>2</sub>O–*n*-Hex). No column chromatography was found to be necessary besides the significant savings (approximately 50%) achieved in the quantity of KSAc required for the reaction. Reactions with other glycosyl halides described above were also equally successful (results not shown).



Scheme 4

## Conclusion

A highly efficient practical route to aryl thioglycosides under solvent-free conditions, requiring neither chromatographic purification nor use of a PTC has been reported for the first time in

synthetic carbohydrate chemistry. Multi-step synthesis of alkyl, aryl and glycosyl thioglycosides via the glycosyl thiuronium salt intermediate, that eliminates the need for carcinogenic solvents such as benzene, toxic/malodorous thiols and/various PTCs, has been achieved in a planetary ball mill in one-pot. Solvent-free synthesis of per-acetylated-1-thio-glycoses that give access to various other thioglycosides by literature methods has also been achieved in excellent yields in the ball mill.

## Experimental

All reagents and chemicals were purchased from Aldrich Chemical Co (Milwaukee, WI, USA). TLC was performed on 0.2 mm Merck pre-coated silica gel 60 F254 aluminium sheets. Melting points were recorded on a capillary melting point apparatus and are uncorrected. Specific rotations were obtained on an AUTOPOL IV polarimeter at 20 °C. IR spectra were recorded on a Nicolet FT-IR Impact 410 instrument either as neat or KBr pellets. Mass spectra were obtained on an ultraflex TOF/TOF MALDI mass spectrometer, which is equipped with a reflector and controlled by Flexcontrol 1.4 software package. NMR spectra were recorded on 300/400 MHz Bruker FT-NMR (Avance<sup>DPX</sup>300/Avance<sup>III</sup>400) spectrometer at 300/400 MHz for <sup>1</sup>H and at 75.47/100.62 MHz for the <sup>13</sup>C nuclei. Chemical shifts are reported in ppm from TMS as the internal standard.

### General procedure for aryl thioglycoside synthesis by planetary ball mill

The glycosyl halide (**1/8/11/13/14/16/18**, 1 mmol), thiophenol (**2/4/6**, 2 mmol) and K<sub>2</sub>CO<sub>3</sub> (2.2 mmol) were allowed to mix in a stainless steel (SS) jar (capacity, 50 mL) containing 10 SS balls (10 mm o.d.) for 30/60 min (depending upon the glycosyl bromide/glycosyl chloride, respectively, as substrate) in a planetary ball mill (Retsch PM-100, Retsch GmbH & amp; Co. KG, Germany) at 400 rpm [for larger scale reactions (15 g or more of the glycosyl halide) 1.5 mol equiv of the thiol were mixed in presence of 2 mol equiv. K<sub>2</sub>CO<sub>3</sub> in the SS jar (125 ml capacity) using 6 SS balls (20 mm o.d.) for 30 min at 500 rpm]. DCM (or EtOAc, preferred as a greener alternative, is equally effective) followed by water was then added to the mixture, the organic layer was separated and washed successively with aq. Na<sub>2</sub>CO<sub>3</sub> solution (10%, w/v) and water, dried (Na<sub>2</sub>SO<sub>4</sub>), and concentrated under reduce pressure to afford the respective crude thioglycoside. It was crystallized from diethyl ether–*n*-Hex to obtain analytically pure product (**3**, **5**, **7**, **9**, **10**, **12**, **15**, **17** and **19**). The spectral data were in accordance with the expected structure and in agreement with the literature values (**3**,<sup>10a</sup> **5**,<sup>9</sup> **7**,<sup>6c</sup> **9**,<sup>10a</sup> **10**,<sup>10</sup> **12**,<sup>9a</sup> **15**,<sup>9a</sup> and **17**<sup>6c</sup>).

### Phenyl 2,3,4,6-tetra-*O*-acetyl-1-thio- $\beta$ -D-galactopyranoside (**3**)

Compound **3** was prepared by the general procedure described above in 94% yield as white solid; mp 64–65 °C (lit.<sup>10a</sup> 65–67 °C); [ $\alpha$ ]<sub>D</sub><sup>20</sup> +4.9 (lit.<sup>10a</sup> +4.2 1 in CHCl<sub>3</sub>);  $\nu_{\text{max}}$  (KBr)/cm<sup>-1</sup> 2928.8, 1750.4, 1369.9, 1222.9, 1082.9, 1054.4, 917.8 and 749.7;  $\delta_{\text{H}}$  (300 MHz; CDCl<sub>3</sub>) 7.49 (2H, m, ArH) 7.29 (3H, m, ArH), 5.40 (1H, d, *J*<sub>3,4</sub> 2.9 Hz, H-4), 5.22 (1H, t, *J*<sub>2,3</sub> 9.9 Hz, H-2), 5.01 (1H, dd, H-3), 4.67 (1H, d, *J*<sub>1,2</sub> 9.9 Hz, H-1), 4.12 (2H, m,

H-6a and H-6b), 3.71 (1H, t,  $J_{5,6}$  8.4 Hz, H-5), 2.10, 2.07, 2.02 and 1.95 (12H, 4 s, 4xCOCH<sub>3</sub>);  $\delta_C$  (75.47 MHz; CDCl<sub>3</sub>) 170.6, 133.0, 129.4, 128.7, 87.1, 74.9, 72.5, 67.7, 62.1, 21.4 and 21.1; MALDI-TOF MS C<sub>20</sub>H<sub>24</sub>O<sub>9</sub>S [M]<sup>+</sup> calcd.  $m/z$  440.464, found 479.590 (M + K<sup>+</sup>, 59%), 463.586 (M + Na<sup>+</sup>, 73%), 331.515 (M-SPH<sup>+</sup>, 100%).

#### 4-Methyl-phenyl 2,3,4,6-tetra-*O*-acetyl-1-thio- $\alpha$ -D-glucoopyranoside (19)

Compound **19** was prepared by the general procedure described above in 78% yield as white solid; mp 74–75 °C;  $[\alpha]_D^{20}$  +133.79 (0.5 in CHCl<sub>3</sub>);  $\nu_{\max}$  (KBr)/cm<sup>-1</sup> 2945.3, 1752.8, 1374.8, 1224.4, 1090.1, 1039.5, 913.7 and 809.4;  $\delta_H$  (300 MHz; CDCl<sub>3</sub>) 7.34 (2H, d,  $J$  10.6 Hz, ArH), 7.09 (2H, d,  $J$  10.6 Hz, ArH), 5.82 (1H, d,  $J_{1,2}$  5.8 Hz, H-1), 5.43 (1H, t,  $J_{3,4}$  9.8 Hz, H-3), 5.11–5.03 (2H, m, H-2 and H-4), 4.57 (1H, ddd, H-5), 4.28 (1H, dd,  $J_{5,6a}$  5.1 Hz and  $J_{6a,6b}$  12.3 Hz H-6a), 4.05 (1H, dd,  $J_{5,6b}$  2.7 Hz and  $J_{6a,6b}$  12.3 Hz H-6b), 2.32 (3H, 1 s, CH<sub>3</sub>) 2.10, 2.08, 2.05 and 2.03 (12H, 4 s, 4xCOCH<sub>3</sub>);  $\delta_C$  (75.47 MHz; CDCl<sub>3</sub>) 170.5, 169.9, 169.8, 169.6, 138.1, 132.5, 129.9, 128.6, 85.4, 70.8, 70.4, 68.6, 68.0, 62.0, 20.1, 20.7 and 20.6; MALDI-TOF MS C<sub>21</sub>H<sub>26</sub>O<sub>9</sub>S [M]<sup>+</sup> calcd.  $m/z$  454.491, found 493.156 (M + K<sup>+</sup>, 34%), 477.157 (M + Na<sup>+</sup>, 100%), 331.085 (M-SPH-4-CH<sub>3</sub><sup>+</sup>, 54%).

#### General procedure for thioglycoside synthesis via *S*-glycosyl isothiurea derivative using a planetary ball mill

The glycosyl halide (**1/8**, 1 mmol) and thiourea (**20**, 2.5 mmol) were allowed to mix in a SS jar (capacity, 50 mL) containing 10 SS balls (10 mm o.d.) for 2 h at 400 rpm in the ball mill. This led to the complete conversion of the glycosyl bromide to the corresponding glycosyl isothiurea derivative (**21/22**, TLC: eluent, EtOAc-*n*-Hex = 1 : 1). Et<sub>3</sub>N (10 mol equiv) was then added to the jar and was milled for 30 min followed by addition of the desired halide donor reagent (EtI/1-chloro 2,4-dinitrophenol/**1**, 1.5 mmol) and mixing was continued for 2 h. When the formation of the respective thioglycoside (**23/24/25/26**) was found to be complete. DCM (or EtOAc, preferred as a greener alternative, is equally effective) followed by water were then added to the mixture, the organic layer was separated and was washed successively with aq. Na<sub>2</sub>CO<sub>3</sub> solution (10%, w/v) and water, dried (Na<sub>2</sub>SO<sub>4</sub>), and was concentrated under reduce pressure to yield the respective analytically pure title product (**23**<sup>2</sup>/**24**<sup>10b</sup> after purification by column chromatography and **25**<sup>17</sup>/**26**<sup>13</sup> by recrystallization from Et<sub>2</sub>O-*n*-Hex). The spectral data were in accordance with the expected structure and in agreement with literature values.

#### General procedure for glycosyl *S*-acetate synthesis using a planetary ball mill

The glycosyl halide (**8**, 1 mmol) and KSAC (2.5 mmol) were allowed to mix in a SS jar (capacity, 50 mL) containing 10 SS balls (10 mm o.d.) for 2 h at 400 rpm in the ball mill. The reaction was found to be complete at this time (TLC: eluent, EtOAc-*n*-Hex = 1 : 1). Then, DCM or EtOAc (20 mL) was added and the mixture was washed in a separating funnel with water and was dried to afford the thioacetate as crystals (**27**,<sup>18</sup> 98%).

## Acknowledgements

Premanand R. Patil thanks NIPER for the research fellowship and Ravindranathan Kartha thanks the Department of Science and Technology, New Delhi for financial assistance.

## References

- (a) Reviewed in: J. D. C. Codée, R. E. J. N. Litjens, L. J. V. D. Bos, H. S. Overkleeft and G. A. V. D. Marel, *Chem. Soc. Rev.*, 2005, **34**, 769–782; (b) K. P. R. Kartha and R. A. Field, in *Best Synthetic Methods: Carbohydrates*, ed. H. M. I. Osborn, Elsevier science/Academic, Oxford, 2003, Ch.4, pp 121–145 and references cited therein. Also see, Z. Zhang, I. R. Ollamann, X.-S. Ye, R. Wischant, T. Baasov and C.-H. Wong, *J. Am. Chem. Soc.*, 1999, **121**, 734–753.
- F. M. Ibatullin, S. I. Selivanov and A. G. Shavva, *Synthesis*, 2001, 419–422 and references cited therein.
- (a) K. Pachamuthu and R. R. Schmidt, *Chem. Rev.*, 2006, **106**, 160–187 and references cited therein; (b) E. S. H. El Ashry, L. F. Awad and A. I. Atta, *Tetrahedron*, 2006, **62**, 2943–2998; (c) C. M. Taylor, *Tetrahedron*, 1998, **54**, 11317–11362; (d) P. H. Seeberger and W.-C. Haase, *Chem. Rev.*, 2000, **100**, 4349–4393; (e) See reference 1b cited above.
- (a) G. Chitra, K. K. Bhutani, I. P. Singh, and K. P. R. Kartha, Unpublished, results; (b) J. Ohlsson and G. Magnusson, *Carbohydr. Res.*, 2000, **329**, 49–55; (c) C. Wang, Q. Li, H. Wang, L.-H. Zang and X.-S. Ye, *Tetrahedron*, 2006, **62**, 11657–11662.
- (a) C. B. Purves, *J. Am. Chem. Soc.*, 1929, **51**, 3619–3627; (b) C.-C. Lin, L.-C. Huang, P.-H. Liang and C.-Y. Liu, *J. Carbohydr. Chem.*, 2006, **25**, 303–313 and the references cited therein.
- (a) J. Bogusiak and W. Szeja, *Pol. J. Chem.*, 1985, **59**, 293–298; J. Bogusiak and W. Szeja, *Chem. Abstr.*, 1986, **104**, 186748u; (b) F. D. Tropper, F. O. Andersson, C. Grand-Maitre and R. Roy, *Synthesis*, 1991, 734–736; (c) S. Cao, S. J. Meunier, F. O. Andersson, M. Letellier and R. Roy, *Tetrahedron: Asymmetry*, 1994, **5**, 2303–2312; (d) F. D. Tropper, F. O. Andersson, C. Grand-Maitre and R. Roy, *Carbohydr. Res.*, 1992, **229**, 149–154; (e) D. Carrière, S. J. Meunier, F. D. Tropper and R. Roy, *J. Mol. Catal. A: Chem.*, 2000, **154**, 9–22; (f) D. Giguere, S. Sato, C. St-Pierre, S. Sirois and R. Roy, *Bioorg. Med. Chem. Lett.*, 2006, **16**, 1668–1672.
- (a) P. R. Patil and K. P. R. Kartha, *J. Carbohydr. Chem.*, 2008, **27**, 411–419. For recent comments/reviews on the application of ball milling technology to various organic reactions see: G. Kaupp, *CrystEngComm*, 2009, **11**, 388–403; (b) B. Rodriguez, A. Bruckmann, T. Rantanen and C. Bolm, *Adv. Synth. Catal.*, 2007, **349**, 2213–2233; (c) A. Bruckmann, A. Krebs and C. Bolm, *Green Chem.*, 2008, **10**, 1131–1141.
- (a) G. Agnihotri, P. Tiwari and A. K. Misra, *Carbohydr. Res.*, 2005, **340**, 1393–1396; (b) N. Khair and M. Martin-Lomas, *J. Org. Chem.*, 1995, **60**, 7017–7021.
- (a) C.-S. Chao, M.-C. Chen, S.-C. Lin and K.-K. T. Mong, *Carbohydr. Res.*, 2008, **343**, 957–964; (b) C. Denekamp and Y. Sandler, *J. Mass Spectrom.*, 2005, **40**, 1055–1063.
- (a) S.-S. Weng, Y.-D. Lin and C.-T. Chen, *Org. Lett.*, 2006, **8**, 5633–5636; (b) B. Mukhopadhyay, K. P. R. Kartha, D. A. Russell and R. A. Field, *J. Org. Chem.*, 2004, **69**, 7758–7760.
- H. Ando, H. Ishida and M. Kiso, in *Best Synthetic Methods: Carbohydrates*, ed. H. M. I. Osborn, Elsevier science/Academic, Oxford, 2003, ch. 9, pp. 277–310 and references cited therein.
- M. A. Oturan, M. Médebille, S. A. Patil and R. S. Klein, *Turk. J. Chem.*, 2002, **26**, 317–322.
- T. Fujihira, T. Takido and M. Seno, *J. Mol. Catal. A: Chem.*, 1999, **137**, 65–75.
- R. J. Pearson, *Ph.D. Thesis*, University of St. Andrews, UK, 2001.
- W. A. Bonner and J. E. Kahn, *J. Am. Chem. Soc.*, 1951, **73**, 2241–2245.
- K. P. R. Kartha and R. A. Field, *J. Carbohydr. Chem.*, 1998, **17**, 693–702.
- H. Driguez and W. Szeja, *Synthesis*, 1994, 1413–1414.
- (a) G. J. L. Bernardes, D. P. Gamblin and B. G. Devis, *Angew. Chem., Int. Ed.*, 2006, **45**, 4007–4011; (b) C. A. Sanhueza, R. L. Dorta and J. T. Vázquez, *Tetrahedron: Asymmetry*, 2008, **19**, 258–264.

# Green Chemistry

Cutting-edge research for a greener sustainable future

[www.rsc.org/greenchem](http://www.rsc.org/greenchem)

Volume 11 | Number 7 | July 2009 | Pages 897–1068



ISSN 1463-9262

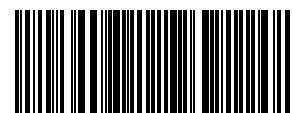
RSC Publishing

Schaak *et al.*  
Toward green metallurgy

Streit *et al.*  
Identifying ionic liquid stable cellulases

Zhang  
Fluorous techniques in green chemistry

Beckers *et al.*  
Marrying gas power and hydrogen energy



1463-9262(2009)11:7;1-7

# Applying metagenomics for the identification of bacterial cellulases that are stable in ionic liquids†

Julia Pottkämper,<sup>a</sup> Peter Barthen,<sup>a,b</sup> Nele Ilmberger,<sup>a</sup> Ulrich Schwaneberg,<sup>c</sup> Alexander Schenk,<sup>c</sup> Michael Schulte,<sup>b</sup> Nikolai Ignatiev<sup>b</sup> and Wolfgang R. Streit<sup>\*a</sup>

Received 12th November 2008, Accepted 31st March 2009

First published as an Advance Article on the web 15th April 2009

DOI: 10.1039/b820157a

Ionic liquids (ILs) are novel and chemically inert solvents for a wide range of reactions in organic synthesis and biocatalysis, and at least one of them is known to dissolve cellulose. ILs would provide novel options for cellulose degradation in homogenous catalysis if cellulases were sufficiently stable and active. By screening metagenomic libraries 24 novel cellulase clones were identified and tested for their performance in the presence of ILs. Most enzyme clones showed only very poor or no activities. Three enzyme clones (*i.e.* pCosJP10, pCosJP20 and pCosJP24) were moderately active and stable in the presence of 1-butyl-1-methyl-pyrrolidinium trifluoromethanesulfonate. The corresponding genes of these environment-derived cosmids were similar to known cellulases from *Cellvibrio japonicus* and a salt-tolerant cellulase from an uncultured microorganism, S. Voget, H. L. Steele and W. R. Streit, *J. Biotechnol.*, 2006, 126, 26–36.<sup>1</sup> The most active protein (CelA<sub>10</sub>) belonged to GH5 family cellulases and was active at IL concentrations of up to 30% (v/v). Recombinant CelA<sub>10</sub> was extremely tolerant to 4 M NaCl and KCl. Furthermore improved cellulase variants of CelA<sub>10</sub> were isolated in a directed evolution experiment employing SeSaM-technology. Analysis of these variants revealed that the N-terminal cellulose binding domain plays a pivotal role for IL resistance.

## Introduction

Inspired by the idea that many enzymes which are used in biotechnological applications should be able to function in the presence of high concentration of organic solvents we have initiated work to search for cellulose hydrolyzing enzymes that are stable in ionic liquids (ILs). ILs are so called *green solvents* that have recently become very attractive for biocatalysis.<sup>2–4</sup> However, the first reports on biocatalysis became public less than a decade ago.<sup>5,6</sup> Because cellulose is a valuable biopolymer for the production of biofuels (*i.e.* ethanol) and other bio-based products, much attraction has been paid to the solubilization of this polymer in ILs. Previous reports demonstrated cellulose solubilization in 1-butyl-3-methylimidazolium chloride<sup>7</sup> and 1-allyl-3-methylimidazolium chloride.<sup>8</sup> Furthermore Heinze *et al.* convincingly demonstrated that cellulose could be dissolved at relatively mild conditions and that the solvent was recyclable. In their study they demonstrated solubility of cellulose in the IL 3-methyl-*N*-butylpyridinium chloride.<sup>9</sup> A similar result

was obtained using 1-*N*-butyl-3-methylimidazolium chloride.<sup>10</sup> Furthermore it has also been demonstrated that wood chips can be dissolved in imidazolium based ILs.<sup>11</sup> Unfortunately, not much is known about the function of cellulose degrading enzymes in any of these ILs.<sup>2</sup> To further advance this field, we set out to identify novel metagenome-derived cellulases that are suitable for cellulose degradation in the presence of high concentrations of different ILs.

Metagenomics describes the investigation of the genetic potential of a specific habitat. Therefore total microbial DNA is extracted, ligated into suitable vectors and cloned into a host bacterium. The resulting library can be screened for enzymes or other characteristics. This technology has become a very powerful tool to search for novel enzymes that are useful for biotechnological applications. A number of reviews have summarized the technology.<sup>12–14</sup> Since its first publication and the description of the basic technology<sup>15</sup> a remarkable number of reports have been published that provide new enzymes with a high potential for industrial applications.<sup>16–19</sup> One of the earliest articles presenting metagenome-derived biocatalysts reported the detection of cellulases from a thermophilic, anaerobic digester fueled by lignocellulose<sup>20</sup> and a very recent study detected seven cellulases with novel features.<sup>21</sup> While most metagenomic surveys for novel cellulases concentrate on extreme environments, there is sufficient evidence that non extreme, and therefore highly genetically diverse, environments also contain a range of cellulases which are highly stable and suitable for industrial applications.<sup>1</sup> For instance functional screening of a soil metagenomic library revealed a total of eight

<sup>a</sup>Biozentrum Klein Flottbek, Abteilung für Mikrobiologie & Biotechnologie, Universität Hamburg, Ohnhorststrasse 18, 22609, Hamburg, Germany. E-mail: Wolfgang.streit@uni-hamburg.de; Fax: (49) 40-42816-459; Tel: (49) 40-42816-463

<sup>b</sup>Merk KGaA, PLS/R&D S&TS, Ionic Liquids Research Laboratory, 64293, Darmstadt, Germany

<sup>c</sup>Jacobs University Bremen, School for Engineering and Science, 28759, Bremen, Germany

† Electronic supplementary information (ESI) available: DNA isolation protocols and gene expression. See DOI: 10.1039/b820157a

cellulolytic clones, one of which was purified and characterized.<sup>1</sup> Metagenomic screening of extreme environments, *e.g.* soda-lakes, detected more than a dozen cellulases, some of which displayed habitat related halotolerant characteristics.<sup>22,23</sup> Thus the metagenome technology appears to be useful to quickly identify enzymes that are most suitable for use in ILs.

In this paper we have isolated 24 novel cellulase encoding cosmids from not yet cultured microbes. These cellulases were tested for their biocatalytic performance in different ILs. At least one of the identified bacterial enzymes (CelA<sub>10</sub>) showed moderate but significant activities at 30% (v/v) of 1-ethyl-3-methylimidazolium trifluoromethanesulfonate. This correlated with remarkable stability in the presence of high concentrations of sodium and potassium chloride. This enzyme was improved by a directed evolution experiment. The SeSaM technology randomizes a target sequence at every single nucleotide position. Therefore single stranded DNA libraries are generated for all four nucleotides by incorporation of a cleavable nucleotide during PCR followed by cleavage. These libraries are tailed with a universal base and subsequently elongated to full length. The universal base is changed to standard nucleotides by PCR.<sup>27</sup>

## Experimental

### Ionic liquids (ILs)

The ILs used in this study are indicated in Fig. 1 and were designated IL1: 1-butyl-3-methylimidazolium chloride ([bmim][cl]); IL2: 1-butyl-3-methylimidazolium trifluoromethanesulfonate ([bmim][otf]); IL4: 1-butyl-2,3-dimethylimidazolium

chloride ([bmmim][cl]); IL6: 1-ethyl-3-methylimidazolium trifluoroacetate ([emim][atf]); IL7: 1-butyl-1-methylpyrrolidinium trifluoromethanesulfonate ([bmp1][otf]); and IL8: 1-ethyl-3-methylimidazolium trifluoromethanesulfonate ([emim][otf]). The different ILs were supplied by Merck (Darmstadt, Germany) and were all liquid at room temperature, with the exception of IL1 and IL4. The melting points of these two ILs were lowered with the addition of 8.6% (v/w) H<sub>2</sub>O (IL1) and 13.6% (v/w) H<sub>2</sub>O (IL4), respectively, and therefore liquefied. The concentration of the six ILs used in this work in the stock solutions were at 1.72 M for IL1, 1.1 M for IL2, 1.6 M for IL4, 1.33 M for IL6, 1.0 M for IL7 and 1.15 M for IL8. The ILs did not affect the pH value in the test assay, the pH values in the assay-mixtures were around pH 8. In all the tested ILs carboxymethylcellulose (CMC) can be dissolved, when diluted with water or McIlvaine buffer (0.2 M Na<sub>2</sub>HPO<sub>4</sub>, adjusted with 0.1 M citric acid to pH 6.5). IL1 is known to solubilize crystalline cellulose as well.<sup>7,11</sup> But there is no information available about the solubilization of crystalline cellulose of the other ILs used in this study. Initially ten ILs were chosen to evaluate the cellulases' performance, but the assay used for measuring CMCase activity was not functional in four of the ILs, so that only six ILs were evaluated for their suitability as a reaction medium for cellulose degradation. The ILs were initially chosen to cover a wide range of ILs, as [cl] is very nucleophilic, [atf] is less so, and [otf] is the least nucleophilic. We did not choose PF<sub>6</sub> based ILs because of the hydrolysis of the anion resulting in HF, when these ILs are in contact with H<sub>2</sub>O. Imidazolium and pyrrolidinium based ILs were chosen because they are available in large scale commercially.

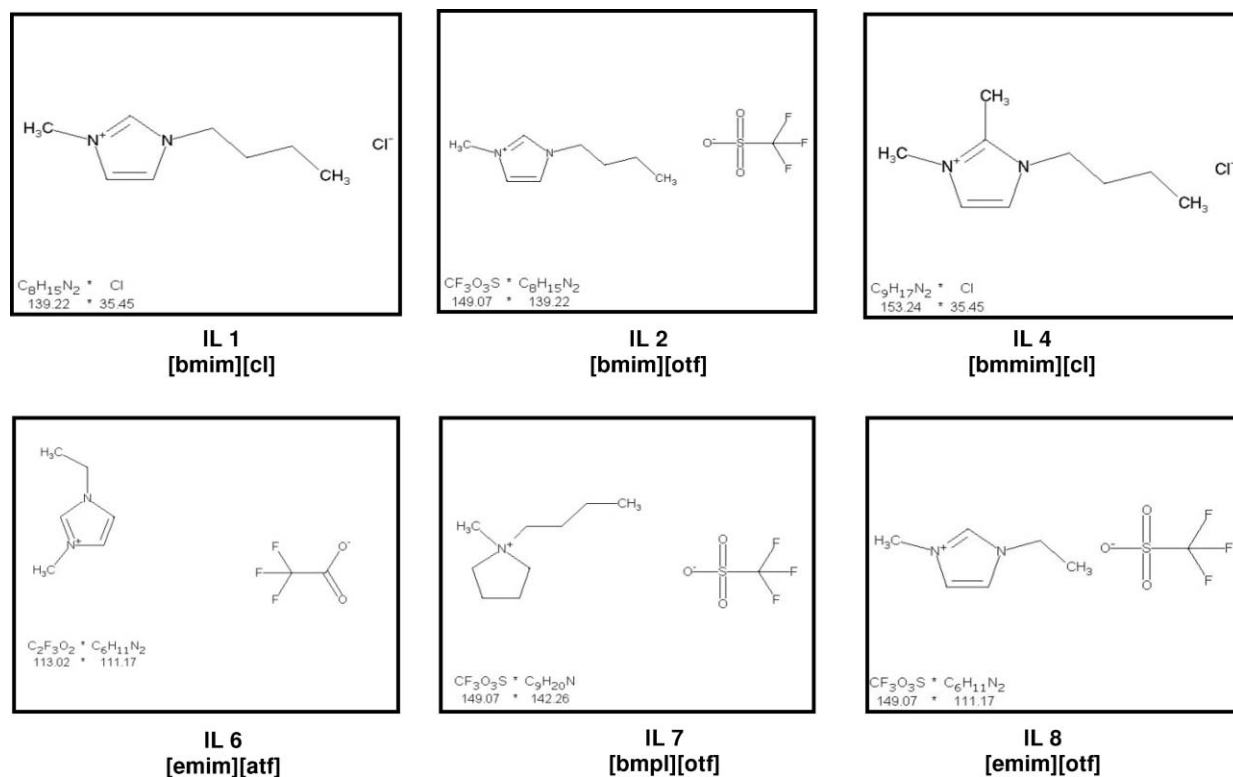


Fig. 1 Chemical structures and properties of the six ILs used in this work.



## Enzyme assays

The crude cell extract was used to examine the specific activity in McIlvaine buffer (0.2 M Na<sub>2</sub>HPO<sub>4</sub>, adjusted with 0.1 M citric acid to pH 6.5 at 65 °C) and in the different ILs (Fig. 1). The final concentration of McIlvaine buffer in the tests was 60 mM. Cellulase activity was assayed by measuring the amount of reducing sugar released from carboxymethylcellulose (CMC) (Sigma, Deisenhofen, Germany) using dinitrosalicylic acid reagent.<sup>24</sup> Units of enzyme activity (U) were expressed as micromoles of reducing sugar released per minute per milligram protein. Enzyme assays were carried out at least in duplicate or triplicate for each treatment. The standard assay mixture for measuring the cellulase activity contained 100 µl of the crude cell extract and 1% (w/v) CMC in a final volume of 0.5 ml. The concentration of ILs was 30% (v/v). These assays were incubated at 37 °C for 30 min. For the pre-incubation assays, 150 µl (60% (v/v)) IL or buffer and 100 µl crude cell extract were mixed and incubated at room temperature over night. Then, 1% (w/v) CMC was added to a total volume of 0.5 ml. Controls always include the same volume of McIlvaine buffer as IL in the assays with IL. The mixtures were incubated at 37 °C for 30 min. Protein concentrations were determined by the method of Bradford (1976) with the protein assay kit (Roth, Germany). Bovine serum albumin was used as a standard.

## Bacterial strains and molecular biology techniques

*Escherichia coli* was grown at 37 °C on complex Luria–Bertani (LB) medium supplemented with appropriate antibiotics.<sup>25</sup> The metagenomic cosmid libraries were generated from an aquatic community derived from the botanical garden of the city of Duisburg (Germany) and a soil metagenome sample (Hamburg, Germany).

All molecular cloning strategies starting with the isolation of environmental DNA and including the the protein expression are described in the supplementary material including all necessary information about primers, cloning and expression vectors and strains.

## Results

### Construction of metagenomic libraries and screening for clones encoding cellulase activity

To obtain a significant number of novel cellulases, two metagenomic libraries were generated using DNA isolated from two different locations (see material and methods). Altogether 3.744 clones were generated. Cosmid clones showing cellulolytic activity were identified by transfer to agar plates containing CMC. Positive clones were verified by repeated transfer on indicator plates<sup>26</sup> and then analyzed by DNA restriction digest to ensure that they differed from each other (data not shown). In this way 24 cellulase clones were identified that encoded for novel genes and that originated probably from a wide range of microbes.

### Testing of cellulase positive clones for activities in ILs

In order to estimate the activities of the isolated enzymes in different ILs, the metagenome-derived cellulases (*i.e.* crude

**Table 1** Screening of 17 metagenome-derived cellulase clones and their hydrolytic activities (mU mg<sup>-1</sup>) in six different ILs using cellulose as substrate without pre-incubation in the presence of 30% ILs (v/v)

Clone	Control	IL1	IL2	IL4	IL6	IL7	IL8
pCosJP#	mU mg <sup>-1</sup>						
7	7.1	0.9	0.7	—	1.3	0.5	0.9
8	3.3	0.7	0.5	—	1.2	0.3	0.7
9	4.9	0.8	0.8	—	1.7	0.4	0.7
10	10.2	2.4	2.1	0.9	3.9	3.4	3.8
11	0.2	0.6	0.5	—	0.8	0.2	0.4
12	1.7	0.8	0.9	—	1.3	0.6	0.9
13	0.2	0.5	0.4	—	0.9	0.2	0.5
14	0.3	0.4	0.4	—	0.8	—	0.5
15	0.2	0.8	0.8	—	1.0	0.3	0.6
16	0.2	0.7	0.8	—	1.1	0.2	0.7
17	0.2	0.7	0.8	—	1.0	—	0.7
18	30.3	1.0	0.6	—	0.8	0.3	0.5
19	1.7	0.5	0.5	—	0.9	0.2	0.5
20	0.5	0.8	0.7	—	0.5	0.4	0.4
21	3.0	1.1	0.9	—	0.5	0.2	0.8
22	24.5	0.9	0.9	—	1.3	0.3	0.8
23	3.5	0.7	0.7	—	1.0	0.2	0.6
24	6.8	0.7	0.8	—	1.0	0.3	0.7

“cosmid clone, derived from metagenome library; control, MIP McIlvaine buffer instead of IL; IL1–8 are depicted in Fig. 1 together with the respective cation; — represents ‘no activity detected’.

extracts of *E. coli* cosmid clones carrying the cellulases) were tested in six different ILs.

To identify the most active and stable cellulases from the metagenomic enzymes, we tested enzyme activities at relatively high concentrations of ILs (60% (v/v)). The ILs used are summarized in Fig. 1 together with their molecular weight. In general the activities of the cellulases decreased rapidly over time when incubated in ILs and only 17 of the initially identified 24 cosmid clones (clones 7–24) showed measurable activities at all (data not shown). Only these 17 are mentioned further in this manuscript. The highest activities without pre-incubation were observed for cosmid clone pCosJP10. It showed a residual activity of almost 40% in ILs 6–8 and had at least a 20% residual activity in IL1–2 (Table 1). Activity observed in IL4 was less than 10%. However, only pCosJP10 showed activity in IL4 ([bmmim] [cl]) (Table 1). These data indicated that pCosJP10 encoded for probably the most stable enzyme identified within the selected cellulase clones.

Furthermore, pre-incubation of the cellulase clones in the different ILs for 17 h resulted in a much more dramatic decrease of activities. The residual activities were in general less than 2% of the activities observed in the buffer control. For many of the cellulase-encoding clones no activity was observed after this extended incubation. However, the highest residual activities were detected in IL7 ([bmpl] [otf]). The clones pCosJP10 and 20 revealed residual activities that ranged from 2% for pCosJP10 to almost 15% for the clones pCosJP20 and pCosJP24 and were in general at least 50% higher than those of the other cellulase clones (data not shown). Altogether these data suggest, that most bacterial cellulases are not stable in ILs at concentrations of 60% (v/v) or higher. But the data also suggest that the cellulases encoded on cosmids 10, 20 and 24 were probably slightly more stable than all other enzymes.

**Table 2** Similarities observed for the metagenome-derived cellulases with moderate stability in ILs

Cosmid clone	Cellulase gene length (bp)	GenBank entry	Highest observed similarity, GenBank entry (similarity/identity%)
pCosJP10	<i>celA</i> <sub>10</sub> 3018/FJ422812		Endoglucanase cel5B, <i>C. japonicus</i> , YP_001983438 (83/74)
pCosJP20	<i>celA</i> <sub>20</sub> 2589/FJ422814		Endoglucanase cel9A, <i>C. japonicus</i> , YP_001982933 (83/73)
pCosJP24	<i>celA</i> <sub>24</sub> 1095/FJ422815		Cellulase, uncultured bacterium, ABA02176 (95/93)

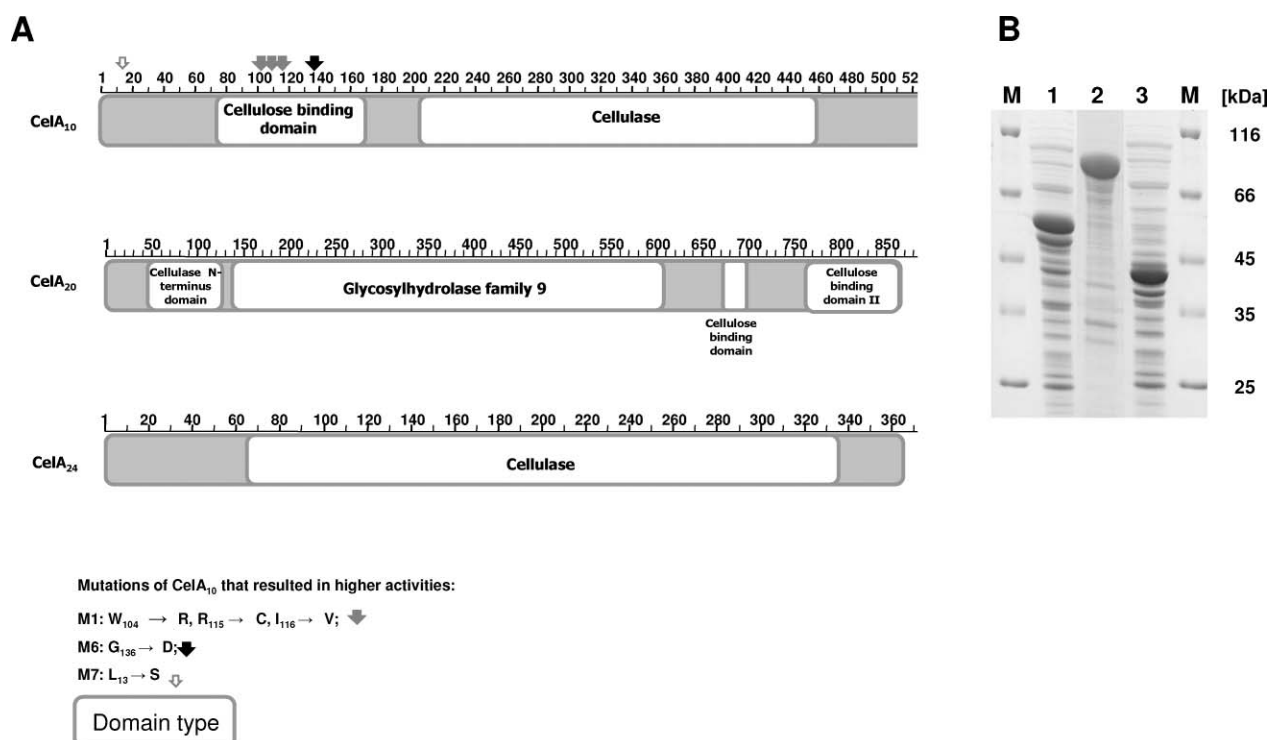
### Sequence analysis of the clones with highest activities in ILs

To identify the genes involved in cellulose degradation on pCosJP10, pCosJP20 and pCosJP24, subcloning and partial sequencing of the entire cosmid clones were initiated with a restriction analysis. For the clone pCosJP20 a 9 kb *EcoRI*-restriction fragment and for pCosJP24 a 2.5 kb *SmaI*-restriction fragment was identified carrying the respective cellulase genes. For the clone pCosJP10 the cellulolytic ORF was identified on two neighboring *EcoRI*-restriction fragments. The identified cellulase genes were designated *celA*<sub>10</sub>, *celA*<sub>20</sub> and *celA*<sub>24</sub>. A putative signal peptide was predicted at the N-terminus of each of the *CelA* proteins. BlastP searches with the deduced amino acid sequences identified significant similarities of 83% with known cellulase proteins from *Cellvibrio* (Table 2). Furthermore *CelA*<sub>24</sub> was similar to a previously identified metagenome-derived and halotolerant cellulase (Table 2). Motifs identified in the blastP searches suggested that *CelA*<sub>10</sub> and *CelA*<sub>24</sub> are members of the family 5 of the glycosyl hydrolases. *CelA*<sub>20</sub> most probably belongs to family 9 of the glycosyl hydrolases (Fig. 2).

### Biochemical characterization of *CelA*<sub>10</sub>, *CelA*<sub>20</sub> and *CelA*<sub>24</sub>

The estimated molecular masses of 60 kDa for *CelA*<sub>10</sub>, 96 kDa for *CelA*<sub>20</sub> and 41 kDa for *CelA*<sub>24</sub>, were in accordance with the theoretical molecular masses of 59.13 kDa (*CelA*<sub>10</sub>), 96.13 kDa (*CelA*<sub>20</sub>) and 40.52 kDa (*CelA*<sub>24</sub>), respectively (Fig. 2B). The ORF coding for *CelA*<sub>10</sub> had a size of 3018 bp and was initially cloned and overexpressed in this size. Interestingly we observed that the enzyme activity and stability were the same when only the first 1598 bp of this ORF were cloned. Analysis of *CelA*<sub>10</sub> indicated that the C-terminal part of this protein was probably not involved in cellulose degradation (Fig. 2A).

All three cellulases were tested for their activities on various substrates and showed the best activity on CMC (2.43 U mg<sup>-1</sup> for *CelA*<sub>10</sub>, 0.041 U mg<sup>-1</sup> for *CelA*<sub>20</sub> and 23.33 U mg<sup>-1</sup> for *CelA*<sub>24</sub>). *CelA*<sub>10</sub> was only active on CMC as a substrate, *CelA*<sub>20</sub> showed weak activity on laminarin and *CelA*<sub>24</sub> was also hydrolyzing β-1,3-glucan (0.0807 U mg<sup>-1</sup>). However, no activity in all three cellulases was found against Xylan (β-1,4-linked xylose) and crystalline forms of cellulose such as avicel.



**Fig. 2** Physical and genetic properties of the metagenome derived cellulases *CelA*<sub>10</sub>, *CelA*<sub>20</sub> and *CelA*<sub>24</sub>. (A) Conserved motifs identified in the different cellulase proteins; and (B) recombinant proteins. Lane M is the protein molecular weight marker; lane 1, the cell-free extract of *CelA*<sub>10</sub>; lane 2, the cell-free extract of *CelA*<sub>20</sub>; lane 3, the cell-free extract of *CelA*<sub>24</sub>.

## Temperature and pH optima

The maximum activity of all three cellulases was detected at 55 °C and the enzymes all displayed a broad temperature range of activity. CelA<sub>10</sub> was functioning at 95% of its maximal activity at 37 °C and 41% at 70 °C. In IL1, IL6 and IL7 the temperature optimum of CelA<sub>10</sub> was shifted to lower temperatures, in IL1 and IL7 to 20 °C and IL6 to 37 °C (data not shown). At 55 °C the activity of CelA<sub>10</sub> in 30% ILs was rather low, in IL1 at 9%, in IL6 18% and in IL7 11% of its maximal activity. CelA<sub>20</sub> had its temperature optimum in buffer as well as in IL6 at 55 °C. The activity in IL6 at lower temperatures was much higher compared to the activity observed in McIlvaine buffer without adding ILs. At 4 °C the activity of CelA<sub>20</sub> was 73% of its maximal activity in this IL (data not shown). CelA<sub>24</sub> was active in buffer at 20 °C with 65% of its maximal activity; but had at 70 °C only 13% of its maximal activity at 55 °C. In IL1, IL6 and IL7 the temperature optimum also shifted to lower temperatures, the optimum in IL6 was at 4 °C with 50% activity at 37 °C but no residual activity was observed at temperatures of 70 °C and higher. In IL1 and IL7 CelA<sub>24</sub> had its maximal activity at 20 °C but also 90% activity at 4 °C in IL1 and also no residual activity at 70 °C and higher temperatures. The activity at 4 °C in IL7 was still 83% of its maximum activity and at 37 °C 56%.

The optimal pH value of CelA<sub>10</sub>, CelA<sub>20</sub> and CelA<sub>24</sub> was tested in McIlvaine buffer with pH range from 2.5 to 8. The pH optimum of CelA<sub>10</sub> was pH 7.5, at pH 8 CelA<sub>10</sub> had residual activity of 89% and at pH 4, 14%. At pH lower than 4 no activity was left. CelA<sub>20</sub> had a pH optimum at pH 5 but at pH 4 only 10% and at pH 8 51% residual activity. There was no activity of CelA<sub>20</sub> below pH 4. CelA<sub>24</sub> had its pH optimum at pH 7, there was also 82% activity left at pH 8 and no more activity left below pH 5 (data not shown).

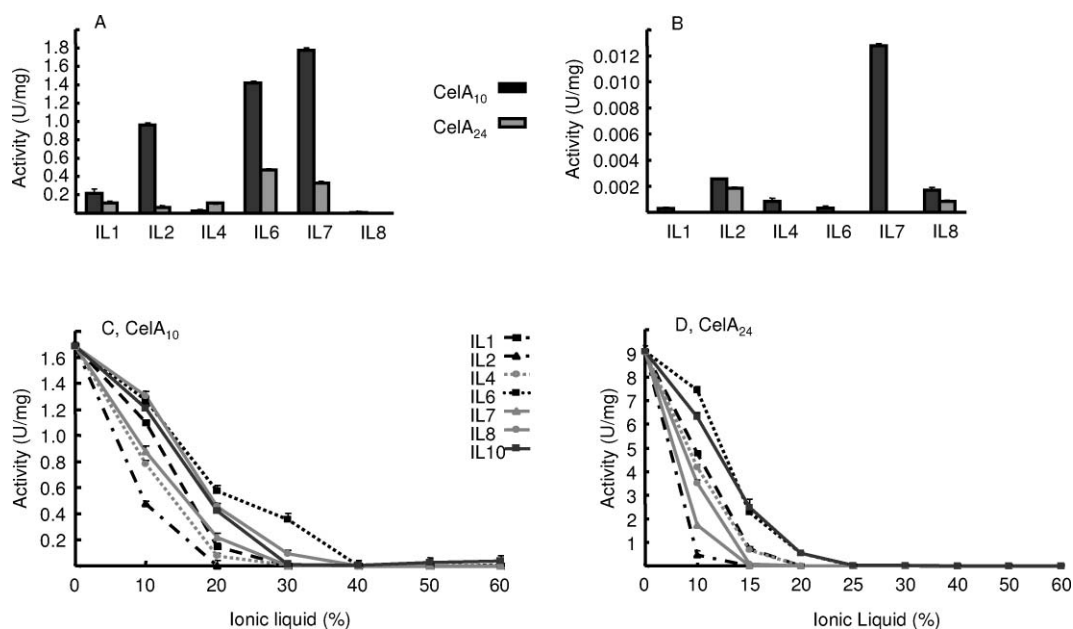
## Stability against solvents, detergents, metal ions and EDTA

CelA<sub>10</sub> was greatly inhibited by the presence of 2% (w/v) SDS to 50% activity compared to controls (see ESI† Supplementary Fig. 1A). The activity of CelA<sub>10</sub> was stimulated by addition of 5% (v/v) glycerin (119% of controls), 5% (v/v) TritonX (136% of control), 20% (v/v) Tween20 (140% of control) and 20% (v/v) Tween80 (128% of control). The addition of 10% (v/v) methanol, ethanol or acetonitrile had no influence of the activity of CelA<sub>10</sub> but in concentrations of 20% (v/v) it led to a decrease of activity to 88% residual activity for 20% (v/v) methanol, 74% activity for 20% (v/v) ethanol and 76% for 20% (v/v) acetonitrile. CelA<sub>20</sub> was inhibited most of all by the addition of 20% (v/v) methanol (78% residual activity), ethanol (56% residual activity) and acetonitrile (63% activity left). The addition of 10% (v/v) methanol, ethanol and acetonitrile led already to decrease of CelA<sub>20</sub> activity. The activity of CelA<sub>20</sub> was only weakly increased through the addition of 5% (v/v) TritonX (113% activity of controls) and 20% (v/v) Tween80 led to 104% activity in comparison to the controls. 2% (w/v) SDS had no influence of the activity of CelA<sub>20</sub>. CelA<sub>24</sub> had the best activity with the addition of 20% (v/v) Tween20 and Tween80, and was 120% and 117%, respectively, from the controls. With the addition of 2% (w/v) SDS and 20% (v/v) acetonitrile there

was no residual activity left. The addition of 5% (v/v) glycerin and 5% (v/v) DMSO had almost no effect on activity. In general we found that the addition of 5% (v/v) TritonX and 20% (v/v) Tween80 increased activity of all three cellulases in comparison to the controls. Similarly, the addition of 20% (v/v) ethanol, methanol or acetonitrile decreased cellulase activity. Additional tests were performed to assay the influence of cations and EDTA on CelA<sub>10</sub>, CelA<sub>20</sub> and CelA<sub>24</sub> by measuring residual activity (see ESI† Supplementary Fig. 1B). In these tests the enzyme activity of CelA<sub>10</sub> was only slightly reduced by up to 10 mM concentrations of most cations, a residual activity of at least 83% was left. The lowest activity was 42% residual activity in the presence of 10 mM Cu<sup>2+</sup> and 10 mM Ni<sup>2+</sup> with 61% activity and the best activities were reached with addition of 1 mM Co<sup>2+</sup> (140%) and Fe<sup>2+</sup> (117%). CelA<sub>20</sub> was stimulated in the presence of 1 mM Co<sup>2+</sup> (137%), 1 mM Cu<sup>2+</sup> (122%), 2 mM Ca<sup>2+</sup> (120%), 2 mM Mn<sup>2+</sup> (118%), 1 mM Fe<sup>3+</sup> (110%) and 2 mM Fe<sup>2+</sup> (124%). 10 mM concentrations of cations led to at least 89% residual activity except for Cu<sup>2+</sup> with only 8% residual activity. Besides CelA<sub>20</sub> indicates the best stability of the three cellulases in Cu<sup>2+</sup>. CelA<sub>24</sub> reveals the lowest stability of the three cellulases in the presence of different cations, mainly with 10 mM of Ni<sup>2+</sup> (24%), Cu<sup>2+</sup> (10%), Mn<sup>2+</sup> (52%), Fe<sup>3+</sup> (55%) and Cd<sup>2+</sup> (12% for 10 mM and 24% for 2 mM). In 2 mM Zn<sup>2+</sup> the residual activity averages 24%. CelA<sub>24</sub> shows higher activity than the control with 1 mM Co<sup>2+</sup> (114%) and Fe<sup>2+</sup> (113%). The addition of 50 mM EDTA resulted in residual activity of 67% for CelA<sub>10</sub> and 94% activity for CelA<sub>20</sub>. The addition of 50 mM EDTA to CelA<sub>24</sub> led to a residual activity of 8%. In general we found that CelA<sub>24</sub> had the worst and CelA<sub>20</sub> the best stability in the presence of most metal ions we tested. Higher activities than the controls were reached with the addition of Co<sup>2+</sup> and Cu<sup>2+</sup> up to 2 mM, the lowest residual activity was measured with the addition of 10 mM Cu<sup>2+</sup> and 10 mM Mn<sup>2+</sup>.

## Enzyme activities of CelA<sub>10</sub> and CelA<sub>24</sub> in different ILs

Highest activities were observed without pre-incubation in 30% ILs (v/v). CelA<sub>10</sub> was more active than CelA<sub>24</sub> (Fig. 3A). The highest activity was measured in IL7 [bmpl] [otf] for CelA<sub>10</sub> and almost no activity was observed in IL4 ([bmmim] [cl]). Pre-incubation overnight (17 h) in ILs resulted in an almost complete loss of activity for all the cellulases (Fig. 3B). Only very low activity—less than 1% residual activity—was observed for CelA<sub>10</sub> in IL7 ([bmpl] [otf]) (Fig. 3B). Altogether these data indicate that the bacterial cellulases were only poorly stable in the ILs used at relatively high concentrations. Because of the low performance of the metagenome-derived cellulases at high concentrations of IL (60%) (v/v), we decided to test the cellulases CelA<sub>10</sub> and CelA<sub>24</sub> at lower concentrations of ILs (Fig. 3C and D). CelA<sub>10</sub> showed relatively high activities at concentrations up to 10% IL (v/v) (Fig. 3C); the activities decreased quickly with increasing IL concentrations (Fig. 3C). At 30% IL (v/v) low residual activity was measured and at 40% IL (v/v) nearly no activity was determinable. CelA<sub>24</sub> was even less active at the different concentrations of ILs tested (Fig. 3D). At concentrations up to 10% IL (v/v), the activities of CelA<sub>24</sub> were relatively high but not comparable to the activities observed in the absence of ILs.



**Fig. 3** Specific residual activities of CelA<sub>10</sub> and CelA<sub>24</sub> after incubation in the indicated ILs. Activity was measured using the standard assay and tests were repeated at least two to three times. Error bars indicate the standard deviations. (A) Activities observed without pre-incubation with 30% ILs (v/v). Values for buffer control are: 2.43 U mg<sup>-1</sup> (CelA<sub>10</sub>) and 23.33 U mg<sup>-1</sup> (CelA<sub>24</sub>). (B) residual activities observed after 17 h pre-incubation in the indicated ILs. The ILs were added as a cosolvent at a 60% (v/v) concentration for pre-incubation. Values for buffer control are: 1.69 U mg<sup>-1</sup> (CelA<sub>10</sub>) and 9.09 U mg<sup>-1</sup> (CelA<sub>24</sub>). (C) Specific activities of two metagenome-derived enzymes in different ILs in the presence of increasing concentrations of the solvents from 0% to 60%. Enzyme tests performed with CelA<sub>10</sub> and (D) CelA<sub>24</sub>. Tests were done with cell extracts of the BL21 strains overexpressing the respective cellulases and as specified in the material and methods section.

### Halotolerance of CelA<sub>10</sub>

CelA<sub>10</sub> was still active in the presence of very high salt concentrations retaining 50% of its activity after 64 days of pre-incubation in the presence of 4 M NaCl (Fig. 4A) and 93% of its activity after pre-incubation in 1 M NaCl. Pre-incubation of 64 days in the presence of 4 M KCl resulted in 30% activity of CelA<sub>10</sub>, (Fig. 4B) whereas the enzyme retained 98% of the activity of the control after pre-incubation for 63 days in 1 M KCl. This is a remarkable salt stability for an enzyme derived from a non-halophilic soil microbial community.

### Sequence saturation mutagenesis (SeSaM) for a better stability of CelA<sub>10</sub> in ILs

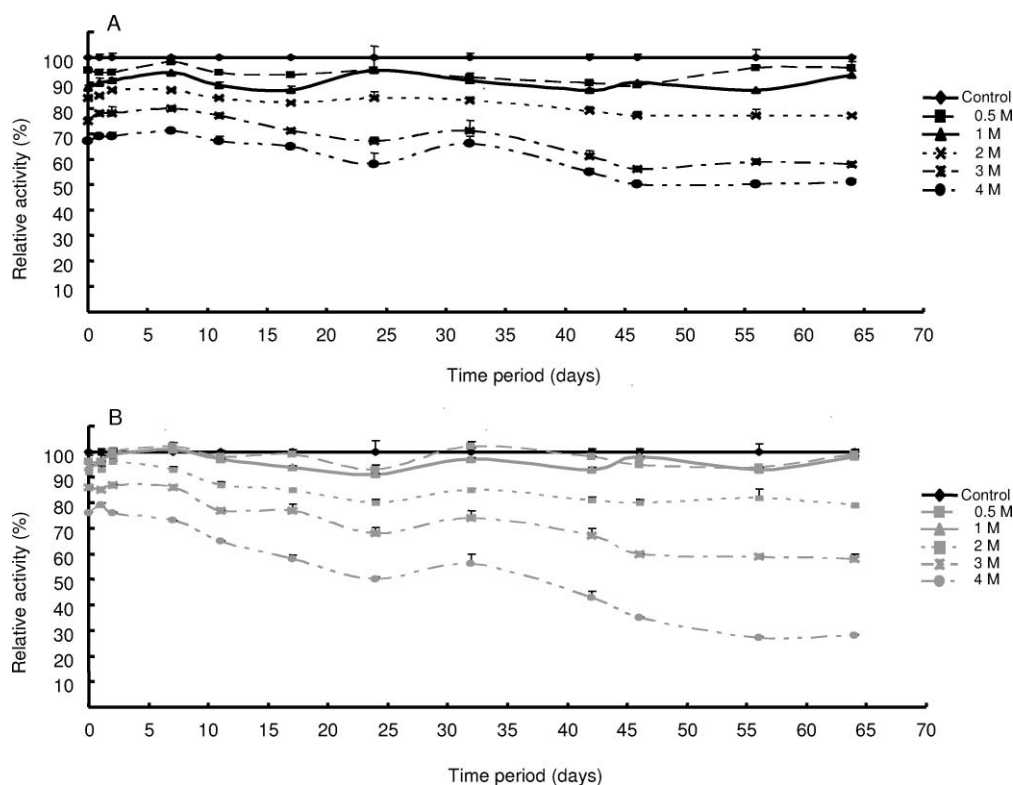
The SeSaM library containing 1700 clones was screened for a better activity after over night incubation in 30% IL6 (v/v) and we found 3 clones which showed significantly higher activity (CelA<sub>10M1</sub>, CelA<sub>10M6</sub> and CelA<sub>10M7</sub>) in IL6, IL7 and IL8 (Fig. 5). The observed increase of activity in the presence of the IL ranged from 1.3-fold to five-fold depending on the IL used and its concentration and the time of pre-incubation. For instance the enzyme variants M6 and M7 showed a five-fold higher activity compared to the wildtype after pre-incubation in IL7 (30% (v/v)); however, in 20% (v/v) IL6 and IL8 the observed increase activity was only 1.7 fold higher. The variants were also slightly more active in buffer, up to 1.3 fold for M6 and 1.02 fold for M7 and 1.11 fold for M1.

Sequence analysis revealed that the variant M1 carried an arginine at position 104 instead of tryptophan, and a cysteine instead of arginine at position 115; plus an isoleucine was

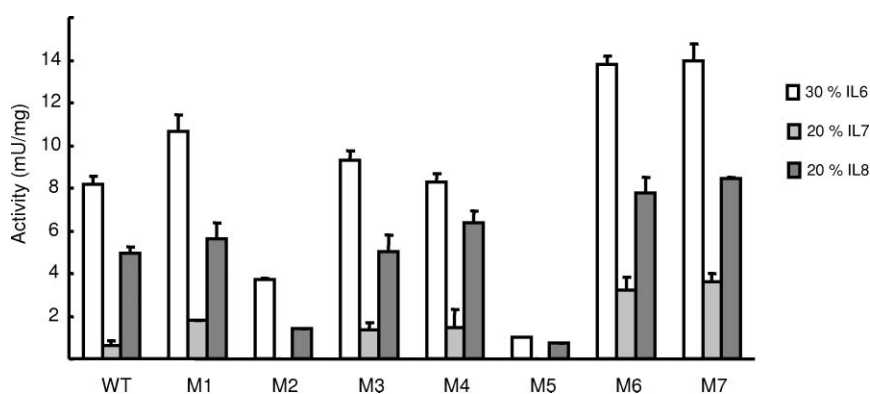
exchanged at position 116 for a valine. For M6 at aa position 136 the glycine residue was substituted by an aspartic acid residue; and in the variant M7 a leucine at aa position 13 was replaced by a serine. It is noteworthy, that all the mutations that increased the overall activity were located within the cellulose binding domain. Thus it is likely that these mutations might result in a better binding of the enzyme to its substrate. The majority of all other mutants analyzed were either neutral or resulted in a decreased activity and none of the mutants was more active at increased concentrations of the ILs. However, the observation that only mutations in the N-terminal part of the protein resulted in an increased activity suggest that the binding domain is of significance for the catalytic activities of the enzyme in the presence of ILs.

### Discussion

Cellulases have many industrial applications, among them the generation of bioethanol from wood.<sup>28,29</sup> Since cellulose is a water-insoluble substrate, different strategies are currently developed to dissolve cellulose in other solvents. Within this context, it has recently been reported that cellulose and wood can be dissolved in different ILs.<sup>7,11</sup> However, to hydrolyze the β-(1-4) glycosidic linkages of the dissolved cellulose the use of IL-tolerant cellulases would be most desirable. Furthermore, to achieve this ambitious goal, cellulases are needed that tolerate high IL concentrations. Unfortunately, with the exception of a few reports on *Trichoderma reesei* cellulases, not much is known about the general use of cellulases in ILs.<sup>30</sup> It is however well known, that cellulases derived from *T. reesei* are not or only



**Fig. 4** Halotolerance of recombinant CelA<sub>10</sub>. Enzyme activity was tested by assaying residual activity towards carboxymethylcellulose after pre-incubation in (A) 0.5 M NaCl, 1 M NaCl, 2 M NaCl, 3 M NaCl and 4 M NaCl; (B) 0.5 M KCl, 1 M KCl, 2 M KCl, 3 M KCl and 4 M KCl. Pre-incubation was performed at room temperature for up to 64 days. Activity was measured using the standard assay and tests were repeated at least two to three times. Error bars indicate the standard deviations.



**Fig. 5** Sequence saturation mutagenesis (SeSaM) for a better stability of CelA<sub>10</sub>. The activity of wildtype control (WT) and SeSaM-clones (M1–M7) was measured using the standard assay in IL6, IL7 or IL8 after pre-incubation over night in 20% (IL7 and IL8) or 30% (IL6) IL (v/v). Data are mean values of at least two different measurements in duplicate.

poorly active in ILs and are only active after colyophilization with polyethylene glycol.<sup>30</sup> In fact the *T. reesei* cellulase was already inactivated by very low concentrations (22 mM) of 1-butyl-3-methylimidazolium chloride. While the *T. reesei* enzyme has been derived from a fungus, almost no data are available on cellulases derived from bacteria. To advance our knowledge on bacterial cellulases and their performance in the presence of ILs, we set out to isolate a whole range of novel cellulases from diverse uncultured microbes. The 24 novel cellulases identified in this paper were tested in six different ILs in the presence of high concentrations of ILs. Thereby

enzymes were selected that are most stable at these elevated concentrations. As expected, most cellulases showed only weak activities after overnight incubation (Fig. 3B), and less than a handful of cellulase-encoding clones had significant activities. Since overall 24 enzymes were tested and which probably originated from a broad range of different microbes, we can speculate that bacterial cellulases are in general not suitable for use in the presence of high concentrations of ILs. Lower concentrations of ILs (<30% (v/v)) however, resulted in the observation of significant activities at least for one of the tested enzymes (CelA<sub>10</sub>) and in part for CelA<sub>24</sub> (Fig. 3C and D). Since

the microbial enzymes tested here were isolated from mesophilic and non-extreme communities it remains to be tested if cellulases derived from extremophilic (*i.e.* halophilic) microbes are more suitable for the use in ILs. It is noteworthy that CelA<sub>10</sub>, which does not derive from a halotolerant microbial community, is remarkably stable in the presence of high concentrations of NaCl and KCl. To our knowledge only very few cellulases have been identified that show such a remarkable high salt tolerance and long term stability. Among these one enzyme has been identified previously by our laboratory.<sup>1</sup> Within this framework it is noteworthy that cellulases are especially sensitive towards the presence of chloride ions in ILs.<sup>31</sup> Therefore it would be reasonable to speculate that halotolerant enzymes are more stable in ILs in comparison to non-halotolerant enzymes. Water may take part directly in the reaction or indirectly by providing a salvation medium for reactants, transition states and products, and it also has a profound influence on the flexibility of the enzyme.<sup>32,33</sup> Thus, if water is replaced by an inorganic ionic liquid this will have a strong influence on enzyme activities. This might partly be due to competition effects of the single components for the available water, though other factors will also effect enzyme activity.<sup>34</sup> This might be part of the explanation for the low activity of the cellulases in the IL/water mixtures and the negative effect of the highly polar chloride ions. In contradiction Tween and other solvents have previously been described as supporting additives.<sup>35</sup> However, at this point we can only speculate that the observed salt tolerance of CelA<sub>10</sub> is a general trait of cellulases that are stable in the presence of elevated concentrations of ILs.

Because CelA<sub>10</sub> and CelA<sub>24</sub> both showed considerable activities under our test conditions and are both members of the GH5 family we speculate that common structural motifs in the GH5 family allow the relative high resistance to ILs. The GH5 family enzymes are known to contain a wide variety of enzymes with different activities; *e.g.*  $\beta$ -mannosidase, endo-1,4- $\beta$ -glucosidase, endo-1,6- $\beta$ -glucosidase, exo-1,3- $\beta$ -glucosidase, cellobio-hydrolases and endo-1,4- $\beta$ -xylanases. Within this family more than 1200 bacterial enzymes have been identified and also 435 enzymes from Eukarya and 9 enzymes belonging to the Archaea (October 2008; <http://www.cazy.org/fam/GH5.html>). Furthermore data from our mutagenesis using the SeSaM technology suggested that decisive motifs are probably located within the N-terminal part of the protein and there within the CB-domain. The results of the SeSaM experiments suggest two different possibilities to further advance the biocatalytic activity in ionic liquids. The first opportunity is to perform a second and third SeSaM experiment with the same cellulase gene, which may lead to a up to ten-fold improvement of the desired characteristics of the enzyme. Another possibility might be the exploitation of knowledge that changes in the CB-domain leading to improvement of the cellulase's performance in ILs. Feasible would be the combination of this improved CB-domain with highly active catalytic domains.

## Conclusions

Despite the recent reports on dissolving cellulose in ILs it becomes evident that neither bacterial cellulases nor the

*T. reesei* cellulases<sup>30</sup> can be used easily for the quick degradation of cellulose in the presence of high concentrations of ILs. However, our work suggests that some bacterial cellulases can tolerate concentrations of approximately 30% of various ILs. Further work is needed to focus on the isolation of cellulases from a much broader spectrum of microbes. Also, it might be feasible to obtain in combination with evolutive technologies a smaller number of enzymes that are most stable in selected ILs.

## Acknowledgements

This work was supported in part by the BMBF-Kompetenznetzwerke Genomik-Plus, Fachagentur Nachwachsende Rohstoffe and Merck Company (Darmstadt, Germany).

## References

- 1 S. Voget, H. L. Steele and W. R. Streit, *J. Biotechnol.*, 2006, **126**, 26–36.
- 2 F. van Rantwijk and R. A. Sheldon, *Chem. Rev.*, 2007, **107**, 2757–2785.
- 3 S. Park and R. J. Kazlauskas, *Curr. Opin. Biotechnol.*, 2003, **14**, 432–437.
- 4 U. Kragl, M. Eckstein and N. Kaftzik, *Curr. Opin. Biotechnol.*, 2002, **13**, 565–571.
- 5 K. W. Kim, B. Song, M. Y. Choi and M. J. Kim, *Org. Lett.*, 2001, **3**, 1507–1509.
- 6 S. G. Cull, J. D. Holbrey, V. Vargas-Mora, K. R. Seddon and G. J. Lye, *Biotechnol. Bioeng.*, 2000, **69**, 227–233.
- 7 R. P. Swatloski, S. K. Spear, J. D. Holbrey and R. D. Rogers, *J. Am. Chem. Soc.*, 2002, **124**, 4974–4975.
- 8 J. Wu, J. Zhang, H. Zhang, J. He, Q. Ren and M. Guo, *Biomacromolecules*, 2004, **5**, 266–268.
- 9 T. Heinze, K. Schwikal and S. Barthel, *Macromol. Biosci.*, 2005, **5**, 520–525.
- 10 A. P. Dadi, S. Varanasi and C. A. Schall, *Biotechnol. Bioeng.*, 2006, **95**, 904–910.
- 11 I. Kilpeläinen, H. Xie, A. King, M. Granstrom, S. Heikkinen and D. S. Argyropoulos, *J. Agric. Food Chem.*, 2007, **55**, 9142–9148.
- 12 W. R. Streit, R. Daniel and K. E. Jaeger, *Curr. Opin. Biotechnol.*, 2004, **15**, 285–290.
- 13 R. Daniel, *Curr. Opin. Biotechnol.*, 2004, **15**, 199–204.
- 14 C. Schmeisser, H. Steele and W. R. Streit, *Appl. Microbiol. Biotechnol.*, 2007, **75**, 955–962.
- 15 T. M. Schmidt, E. F. DeLong and N. R. Pace, *J. Bacteriol.*, 1991, **173**, 4371–4378.
- 16 M. Ferrer, O. V. Golyshina, T. N. Chernikova, A. N. Khachane, D. Reyes-Duarte, V. A. Santos, C. Strompl, K. Elborough, G. Jarvis, A. Neef, M. M. Yakimov, K. N. Timmis and P. N. Golyshin, *Environ. Microbiol.*, 2005, **7**, 1996–2010.
- 17 M. Ferrer, O. V. Golyshina, T. N. Chernikova, A. N. Khachane, V. A. Martins Dos Santos, M. M. Yakimov, K. N. Timmis and P. N. Golyshin, *Chem. Biol.*, 2005, **12**, 895–904.
- 18 A. Beloqui, M. Pita, J. Polaina, A. Martinez-Arias, O. V. Golyshina, M. Zumarraga, M. M. Yakimov, H. Garcia-Arellano, M. Alcalde, V. M. Fernandez, K. Elborough, J. M. Andreu, A. Ballesteros, F. J. Plou, K. N. Timmis, M. Ferrer and P. N. Golyshin, *J. Biol. Chem.*, 2006, **281**, 22933–22942.
- 19 S. Voget, C. Leggewie, A. Uesbeck, C. Raasch, K. E. Jaeger and W. R. Streit, *Appl. Environ. Microbiol.*, 2003, **69**, 6235–6242.
- 20 F. G. Healy, R. M. Ray, H. C. Aldrich, A. C. Wilkie, L. O. Ingram and K. T. Shanmugam, *Appl. Microbiol. Biotechnol.*, 1995, **43**, 667–674.
- 21 Y. Feng, C. J. Duan, H. Pang, X. C. Mo, C. F. Wu, Y. Yu, Y. L. Hu, J. Wei, J. L. Tang and J. X. Feng, *Appl. Microbiol. Biotechnol.*, 2007, **75**, 319–328.
- 22 S. Grant, D. Y. Sorokin, W. D. Grant, B. E. Jones and S. Heaphy, *Extremophiles*, 2004, **8**, 421–429.
- 23 H. C. Rees, S. Grant, B. Jones, W. D. Grant and S. Heaphy, *Extremophiles*, 2003, **7**, 415–421.
- 24 G. Miller, *Anal. Chem.*, 1959, **31**, 426–428.
- 25 J. Sambrook, and D. W. Russell, *Molecular Cloning, A Laboratory Manual*, Cold Spring Harbor Laboratory Press, 2001.

- 
- 26 R. M. Teather and P. J. Wood, *Appl. Environ. Microbiol.*, 1982, **43**, 777–780.
- 27 T. S. Wong, D. Roccatano, D. Loakes, K. L. Tee, A. Schenk, B. Hauer and U. Schwaneberg, *Biotechnol. J.*, 2008, **3**, 74–82.
- 28 L. R. Lynd, P. J. Weimer, W. H. van Zyl and I. S. Pretorius, *Microbiol. Mol. Biol. Rev.*, 2002, **66**, 506–577, table of contents.
- 29 E. A. Bayer, R. Lamed and M. E. Himmel, *Curr. Opin. Biotechnol.*, 2007, **18**, 237–245.
- 30 M. B. Turner, S. K. Spear, J. G. Huddleston, J. D. Holbrey and R. D. Rogers, *Green Chem.*, 2003, **5**, 443–447.
- 31 S. H. Lee, S. H. Ha, S. B. Lee and Y.-M. Koo, *Biotechnol. Lett.*, 2006, **28**, 1335–1339.
- 32 L. Yang, J. S. Dordick and S. Garde, *Biophys. J.*, 2004, **87**, 812–821.
- 33 P. J. Halling, *Philos. Trans. R. Soc. London, Ser. B*, 2004, 359, 1287–1298.
- 34 P. J. Halling, *Enzyme Microb. Technol.*, 1994, **16**, 1178–1206.
- 35 S. B. Kim, H. J. Kim and C. J. Kim, *Appl. Biochem. Biotechnol.*, 2006, **129–132**, 486–95.

# Green Chemistry

Cutting-edge research for a greener sustainable future

[www.rsc.org/greenchem](http://www.rsc.org/greenchem)

Volume 11 | Number 7 | July 2009 | Pages 897–1068



Downloaded by City College of New York on 12 November 2010  
Published on 22 April 2009 on http://pubs.rsc.org | doi:10.1039/B814015D

ISSN 1463-9262

Varma *et al.*  
Synthesis of silver nanoparticles

Keller *et al.*  
Photocatalytic removal of  
monoterpenes

Ondruschka *et al.*  
Chemistry driven by suction

Dewulf *et al.*  
Preparative HPLC vs. preparative SFC

RSC Publishing



# Photocatalytic removal of monoterpenes in the gas phase. Activity and regeneration

Ibtissam Salem, Nicolas Keller and Valérie Keller\*

Received 7th November 2008, Accepted 9th April 2009

First published as an Advance Article on the web 22nd April 2009

DOI: 10.1039/b819022d

We show the photocatalytic removal of various monoterpenes such as  $\beta$ -pinene,  $\alpha$ -pinene, camphene and limonene in the gas phase as a function of the reaction temperature, from room temperature to 80 °C, taking also into account the thermal catalytic isomerization occurring on TiO<sub>2</sub> surfaces. The *on-stream* behaviour showed an initial plateau with total monoterpene removal followed by a progressive deactivation, associated to the surface poisoning by partially oxidized intermediates. Effective regenerative treatment could be performed under UV-A illumination with an oxidative humid air flow, for oxidizing the detrimental organic reaction intermediates into CO<sub>2</sub>. Deactivation phenomena were studied as well as the optimization of regeneration treatments, both depending on the surface density of the TiO<sub>2</sub> coating, and we proposed that non-illuminated TiO<sub>2</sub> layers could be involved for explaining the interesting activity/deactivation behaviour pattern observed. We tried to evidence that reaction–regeneration cycles could be put forward to hold a continuous high efficiency monoterpene removal.

## 1. Introduction

More than 22,000 individual terpenoids are known at present, making them the largest group of natural products. Monoterpenes in plants are known to have mainly ecological roles, by acting as deterrents against feeding by herbivores, as antifungal defenses and as attractants for pollinators.<sup>1</sup> Terpenes can also act in the prevention and the therapy of several diseases including cancer, as natural insecticides and antimicrobial agents, as sprouting inhibitor during agricultural produce storage and as building blocks for the synthesis of many high value compounds.<sup>2</sup> Terpene hydrocarbons are also the main component of natural resins. In addition, terpenes such as limonene are essential for the industrial production of thin films such as plasma TV and remain strategic molecules for device production.

However, in parallel to the above-mentioned positive influence of terpenes, terpenes negatively impact on many industrial fields using wood as a raw material, and eliminating terpenes takes on importance within such fields. This restriction results from the necessary control of irritant and odorous gas releases such as that of terpenes, and from environmental policy, with the actual and forthcoming environmental regulation towards industrial effluent releases. The regulation of Volatile Organic Compounds (VOCs, including the terpenoid class) emitted by industrial processes has indeed created a strong incentive for research in this area in the last few decades inside both industrial and academic communities involved in innovative sustainable environmental research.

Up to now, mainly liquid phase isomerization<sup>3–5</sup> and polymerization<sup>6</sup> processes have been reviewed for catalytically transforming pinene. Few papers concern the use of immobilised porphyrins as photosensitizers to promote singlet oxygen oxidation of mono-terpenes,<sup>7</sup> the use of ZnO or sensitizers for the photochemical hydroperoxidation of terpenes,<sup>8</sup> the photocatalytic oxygenation of  $\alpha$ -pinene using tetraphenylporphyrinatomolybdenum and niobium complexes and molecular oxygen for forming pinene epoxide and oxygenated products.<sup>9</sup> The disappearance of  $\alpha$ -pinene through an air purification photocatalytic system has been briefly mentioned by Kudo *et al.* within polluted indoor air containing 26 different VOCs,<sup>10</sup> whereas Salthammer and Furmann,<sup>11</sup> and Hodgson *et al.*<sup>12</sup> investigated, targeting some terpenoids among many VOCs, the cleaning of indoor air resulting from the use of photocatalytic wall paints and of a UV-A driven photocatalytic oxidation device, respectively. Over the past two decades, the gas-phase terpene oxidation reactions have been exclusively limited to non-catalytic tropospheric reactions involving reactive species present in the troposphere, like ozone (O<sub>3</sub>), hydroxyl (OH) and nitrate (NO<sub>3</sub>) radicals. Other studies have focused on the quantification of the aerosol formed during the simulated atmospheric oxidation of terpenes.<sup>13,14</sup>

Within the Advanced Oxidation Processes developed to meet the ever stricter anti-pollution legislation required by the environmental protection pressure, photocatalytic oxidation is very promising for purifying contaminated wastewater containing organic pollutants and removing contaminants as well as irritant and odorous gas from air.<sup>15–17</sup> Photocatalysis is advantageous because the energy required is supplied by the direct absorption of light at room temperature, which thus requires the use of semiconductor materials with adequate band gaps as photocatalysts. Amongst the used semiconductors, titanium dioxide (TiO<sub>2</sub>) is up to now the most attractive and efficient one, due to a high photocatalytic efficiency, its stability towards photocorrosion

Laboratoire des Matériaux, Surfaces et Procédés pour la Catalyse (LMSPC), European Laboratory for Catalysis and Surface Sciences (ELCASS), CNRS, Strasbourg University, 25 rue Becquerel, 67087, Strasbourg, France. E-mail: vkeller@chimie.u-strasbg.fr; Fax: +33 (0) 3 90 242 761; Tel: + 33 (0) 390 242 736

and chemicals, its insolubility in water, a low toxicity and low costs. Its band gap energy of 3.2 eV leads to photoexcitation requiring wavelengths less than *ca.* 385 nm corresponding to a near UV illumination.

This article reports on the use of UV-A photocatalysis for degrading  $\beta$ -pinene and its isomers  $\alpha$ -pinene, camphene and limonene. It evidences the possible setting of a continuous high efficiency monoterpene removal process by designing an optimized reaction/regeneration cycle procedure.

## 2. Experimental

### 2.1. Experimental set-up and procedures

The TiO<sub>2</sub> photocatalyst was commercially available Hombikat UV100 (Sachtleben), named UV100. It had a non-microporous BET specific surface area of 309 m<sup>2</sup>/g.

The photocatalytic activity measurements were carried out in an annular Pyrex reactor (300 mm length and 35 mm internal diameter), made of two coaxial tubes 4 mm apart, between which the reactant mixture was passing through. Details concerning both photocatalytic reactor and set-up can be found elsewhere.<sup>18</sup> The TiO<sub>2</sub> photocatalyst was evenly coated on the internal side of the external tube of the coaxial reactor by evaporating to dryness an aqueous slurry of TiO<sub>2</sub> and the coated reactor was further dried at 110 °C for 1 h in air. The annular reactor was thus classically working *on-stream* in a seep mode, with a direct illumination from the inner central lamp radially illuminating the photocatalytic coating.  $\beta$ -Pinene (Aldrich, > 99.5%) and water were fed at ambient temperature and atmospheric pressure by bubbling air through two saturators respectively, and mixed with additional air to obtain the required pinene–water–air ratios with a constant total air flow of 200 cm<sup>3</sup>/min. The relative humidity was set at 50%, whereas the pinene content was set at 200 ppm, corresponding to 1.22 g/m<sup>3</sup> of pinene per m<sup>3</sup> of flowing air. This high and unusual value for photocatalysis for carrying out the experiments resulted from *on-line* and *on-site* measurements performed at the outlet of an air effluent containing terpenes within a paper-maker factory. The surface density of the TiO<sub>2</sub> coating corresponds to the amount of TiO<sub>2</sub> deposited per cm<sup>2</sup> of glass reactor wall.

A cylindrical furnace surrounding the photoreactor 1 mm apart was used for performing the photocatalytic tests at temperatures up to 80 °C. Two procedures described in a further section were investigated using or not a pre-adsorption step prior to switching on the UV-A illumination. UV-A illumination was provided by commercial 8 W (for test), and 8 W or 15 W (for regeneration) black light tubes with a spectral peak centred around 380 nm, and located inside the inner tube of the reactor.

The reaction products were analyzed *on-line* on a micro-gas chromatography (M200H, HP) equipped with thermal conductivity detectors, and coupled when necessary to mass spectrometry. Pure  $\beta$ -pinene,  $\alpha$ -pinene, camphene and limonene were used for calibration.

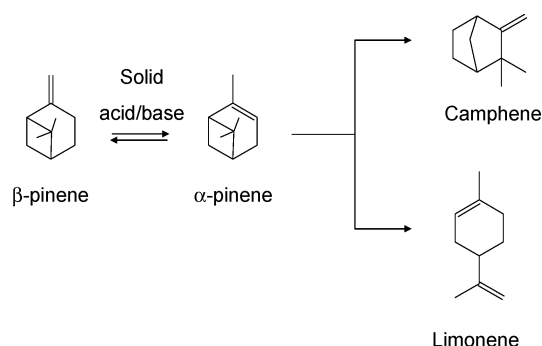
The regeneration phases were performed at 80 °C for a duration ranging from 2 h to 12 h under 8 W or 15 W UV-A illumination using humid air as oxidative flow at 200 cm<sup>3</sup>/min, *i.e.* in fully similar conditions than those of the tests, except the absence of any  $\beta$ -pinene flow.

Diffuse Reflectance Infrared Fourier Transform Spectroscopy (DRIFTS) was carried out with a Bruker IFS-66.

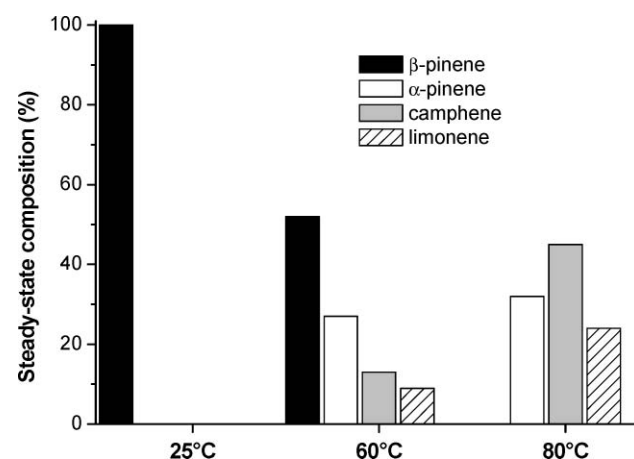
## 3. Results and discussion

### 3.1. Thermal catalytic activity

The catalytic isomerization of the  $\beta$ -pinene reactant is observed in the dark on UV100 TiO<sub>2</sub> powder, with the formation of  $\alpha$ -pinene, camphene and limonene at 60 °C and 80 °C, as represented in Scheme 1 (Fig. 1). Thermal isomerization reactions did not occur at room temperature, whereas the  $\beta$ -pinene/ $\alpha$ -pinene/camphene/limonene ratio was depending on the temperature. This seems to be related to the surface acidity of the oxide,<sup>4</sup> since basic MgO did not show any isomerization, whereas we observed it at different extents over  $\gamma$ -Al<sub>2</sub>O<sub>3</sub> and SiO<sub>2</sub> (not reported). Indeed, the selectivity of the terpene isomerization is known to vary with the catalyst acid strength, with weak acids favouring the formation of polycyclic camphene, and stronger acids resulting in monocyclic products such as limonene.<sup>19,20</sup> The rearrangement of  $\alpha$ -pinene is indeed selected to probe the effect of acid strength on catalytic performances.<sup>17</sup> It is known that the isomerization of  $\beta$ -pinene into  $\alpha$ -pinene occurs through thermally-activated acid/base solid catalysis. The acid-catalysed rearrangement of  $\alpha$ -pinene proceeds *via* two parallel pathways, one by ring expansion giving rise to polycyclic products such as camphene, and another yielding monocyclic



**Scheme 1** The most common isomers formed starting from  $\beta$ -pinene, adapted from ref. 4 evidencing both monocyclic and polycyclic pathways.



**Fig. 1** Distribution at steady-state of the isomers obtained from  $\beta$ -pinene on the UV100 TiO<sub>2</sub> samples at 25 °C, 60 °C and 80 °C.

products such as limonene.<sup>4,6,20–22</sup> It should be mentioned that at 60 °C–80 °C, the carbon balance was closed by the different isomerization products.

At high temperature, thermal catalytic isomerization thus happens together with the UV-A photocatalytic reaction, with formation of  $\alpha$ -pinene, camphene and limonene isomers. As a result, the observed removal performances are further expressed in terms of (total) terpene removal and not of  $\beta$ -pinene removal. Therefore, a terpene removal efficiency of 100% means that 100% of the terpene reactants (including the different isomers formed) have been removed. It was important to note that independently to the reactor temperature, the inlet total terpene concentration was 200 ppm. At room temperature, the terpene removal corresponded to the  $\beta$ -pinene removal due to the absence of any thermal reactions over  $\text{TiO}_2$ .

### 3.2. Photocatalytic oxidation/deactivation/regeneration

The photocatalytic behaviour shown by the commercially available UV100  $\text{TiO}_2$  was studied from room temperature up to 80 °C. The influence of the catalyst surface coverage, *i.e.* the  $\text{TiO}_2$  surface density, on the pinene removal and on the *on-stream* deactivation was only investigated at a temperature of 80 °C, because it appeared that increasing the reaction temperature was beneficial to the terpene removal efficiency. In addition to that, it must be noted that from an industrial application point of view, for which the removal of pinenes and most generally of terpenes from post-process tail-gas effluents is targeted (such as factories using wood as raw material), the temperature of such tail-gas effluents containing those VOC pollutants is usually close to 80 °C, as measured by *on-site* analysis. A reaction/regeneration cyclic procedure has also been optimized in order to maintain a total removal efficiency over a long period.

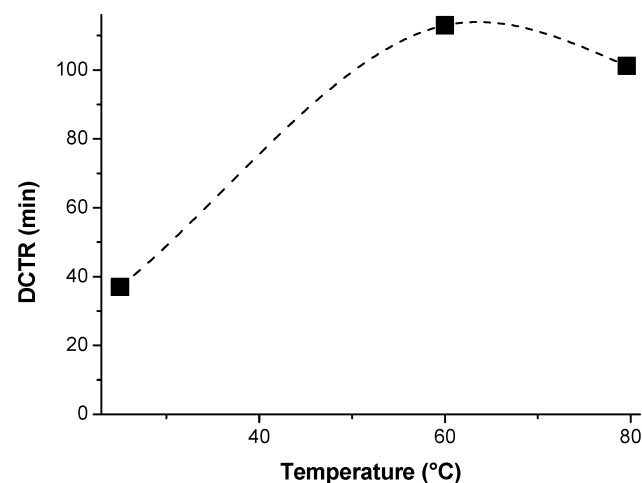
The temperature of the reactor was first increased to 80 °C before two different testing procedures were applied, consisting of: (i) a first dark adsorption step followed by the photocatalytic step when switching on the UV-A lamp and (ii) the direct photocatalytic step without waiting for any adsorption/desorption dark equilibrium. It could be noted that within the whole reaction temperature range, no photolysis phenomena occurred under UV-A illumination for both photocatalytic test procedures.

#### 3.2.1 Using a first dark adsorption step of $\beta$ -pinene followed by photooxidation.

**Activity.** As shown in the previous sub-section, mainly thermal isomerization reactions occurred in the dark, with the main formation of  $\alpha$ -pinene, limonene and camphene. Thus, proceeding with a first dark adsorption of  $\beta$ -pinene molecules at 60 °C and 80 °C (until reaching the adsorption equilibrium), led to performing the photocatalytic removal of a mixture of terpenes, instead of that of pure  $\beta$ -pinene, with an inlet flow containing a mixture of  $\beta$ -pinene,  $\alpha$ -pinene, camphene and limonene terpenes rather than pure  $\beta$ -pinene. It should be noted that removing a mixture of terpenes was in agreement with the problematic of some industrial fields, such as those using wood as raw material, which are concerned with polluted effluents containing terpene mixtures and not only  $\beta$ -pinene. As a result, the observed removal performances were expressed in term of (total) terpene removal and not of  $\beta$ -pinene removal. At room

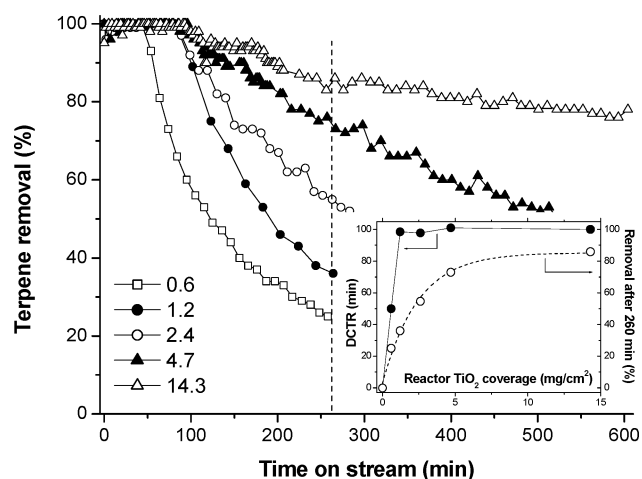
temperature, the terpene removal corresponds to the  $\beta$ -pinene removal due to the absence of any thermal reactions over  $\text{TiO}_2$ .

The  $\text{TiO}_2$  photocatalyst—independently of the reaction temperature and the testing procedure—displayed firstly a period with a total terpene removal, *i.e.* a 100% removal efficiency with no terpene release, before *on-stream* deactivation occurred. Therefore, the initial period during which 100% of terpene removal was observed (characterized by the Duration of Complete Terpene Removal, DCTR, and expressed in minutes) was an important parameter to take into account. Fig. 2 shows the DCTR as a function of the reaction temperature on the commercial UV100  $\text{TiO}_2$  photocatalyst, obtained with a first dark adsorption period and with a reactor surface coverage of 1.2  $\text{mg}/\text{cm}^2$ . The catalyst showed a DCTR of 40 min at 25 °C, whereas the DCTR increased to reach durations longer than 100–110 min at 60–80 °C. This was in agreement with the usual optimal operating range of photocatalysis, reported to be 20–80 °C with a slight increase in the photoactivity with the temperature within this range, due to the very small apparent activation energy in this medium range.<sup>23</sup> Since the terpene containing tail-gas effluents released in some industrial applications are generally at temperatures close to 80 °C, further investigations have been performed at this temperature.  $\text{CO}_2$  was the sole reaction product detected in the outlet stream, no gaseous intermediate by-products being observed, thus indicating that partially oxidized by-products remained adsorbed at the  $\text{TiO}_2$  surface, as shown later by DRIFT.



**Fig. 2** DCTR (in minutes) as a function of the reaction temperature on UV100  $\text{TiO}_2$  at 1.2  $\text{mg}/\text{cm}^2$  surface coverage, with a prior dark adsorption period, and an 8 W UV-A light.

The influence of the  $\text{TiO}_2$  surface density on the *on-stream* terpene removal is reported in Fig. 3. It could be observed that increasing the reactor surface coverage from 0.6 to 1.2  $\text{mg}/\text{cm}^2$  led to extending from 50 min to 100 min, the initial period during which complete terpene removal was observed, whereas this duration remained at about 100 min when increasing the  $\text{TiO}_2$  loading further up to 14.3  $\text{mg}/\text{cm}^2$ . This led to estimating the VOC conversion before deactivation occurred at 50  $\text{mg}_{\text{terpenes}}/\text{g}_{\text{TiO}_2}$ , 48  $\text{mg}_{\text{terpenes}}/\text{g}_{\text{TiO}_2}$ , 23  $\text{mg}_{\text{terpenes}}/\text{g}_{\text{TiO}_2}$ , 14  $\text{mg}_{\text{terpenes}}/\text{g}_{\text{TiO}_2}$  and 4  $\text{mg}_{\text{terpenes}}/\text{g}_{\text{TiO}_2}$  for  $\text{TiO}_2$  loadings of 0.6  $\text{mg}/\text{cm}^2$ , 1.2  $\text{mg}/\text{cm}^2$ , 2.4  $\text{mg}/\text{cm}^2$ , 4.7  $\text{mg}/\text{cm}^2$  and

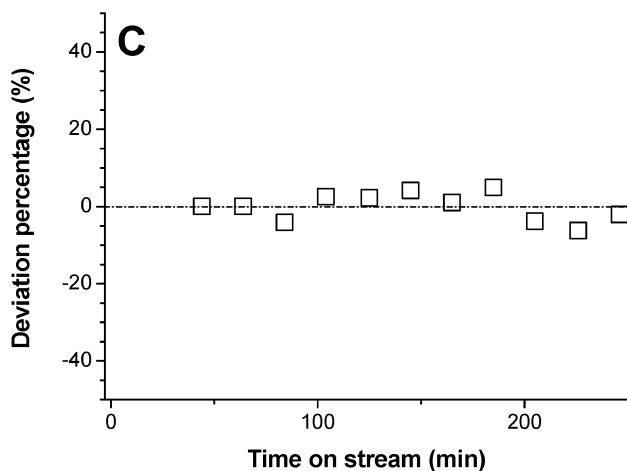
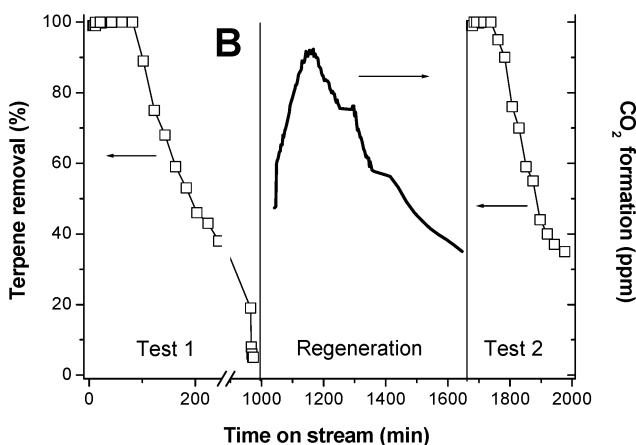
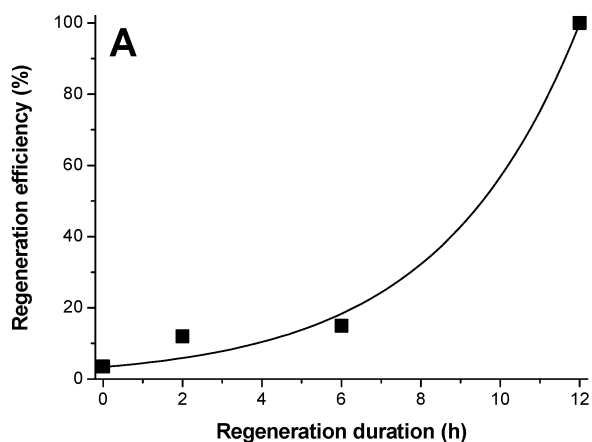


**Fig. 3** Terpene removal with time on stream at 80 °C as a function of the TiO<sub>2</sub> reactor surface coverage in mg/cm<sup>2</sup>, on UV100 TiO<sub>2</sub>, with prior dark adsorption period. Inset : DCTR (min) and removal efficiency at 260 min, as a function of the reactor TiO<sub>2</sub> coverage in mg/cm<sup>2</sup>.

14.3 mg/cm<sup>2</sup> respectively. Indeed, it is known that the photocatalytic activity first linearly increases with the surface covering ratio, due to the increase in the amount of TiO<sub>2</sub> in which all the particles, *i.e.* all the surfaces exposed—are totally illuminated.<sup>23</sup> For higher amounts of catalyst, a screening effect of excess particles occurs, which masks part of the photosensitive semiconductor surface, due to the limited penetration thickness of UV-A illumination. The value obtained, 1.2 mg/cm<sup>2</sup>, in agreement with that reported by Herrmann, was found equal to 1.3 mg TiO<sub>2</sub>/cm<sup>2</sup> for a fixed bed. However, whereas the DCTR remained around 100 min, increasing the TiO<sub>2</sub> surface density up to 14.3 mg/cm<sup>2</sup> allowed the catalyst deactivation to be strongly slowed down, the system loaded at 14.3 mg/cm<sup>2</sup> maintaining a terpene removal of 84% and 80% after 260 min and 600 min on stream respectively. By contrast, a lower surface density resulted in a quicker deactivation, a 1.2 mg/cm<sup>2</sup> coverage leading to a terpene removal around 35% after 260 min on stream.

This unusual behaviour led to putting forward the involvement of non-illuminated TiO<sub>2</sub> semi-conductor particles. As the thickness of the TiO<sub>2</sub> coatings used in this study was strongly larger than the UV-A penetration thickness, we assumed that non-illuminated TiO<sub>2</sub> particles could participate in the overall process. It was proposed that they could allow a possible storage of poisoning reaction intermediates at the surface of non-illuminated TiO<sub>2</sub> particles, and/or that they could artificially increase the residence time within the TiO<sub>2</sub> coating, thus increasing the contact probability with photocatalytic sites.

**Deactivation/regeneration.** Using a 1.2 mg/cm<sup>2</sup> surface coverage (considered as the reference coverage), continuous deactivation of the photocatalyst occurred till reaching a near-zero activity after 12 h on stream under UV-A illumination. Fig. 4A shows the influence on the photocatalyst efficiency, of the regeneration duration after complete deactivation. Recovering of the catalyst efficiency, *i.e.* recovery of an initial 100% terpene removal, could be obtained by performing a 8 W UV-A oxidative regeneration for 12 h under a 50% relative humidity air stream at 80 °C in the absence of any terpene reactant. Shorter regeneration periods led to the partial recovery of the terpene



**Fig. 4** (A) Regeneration efficiency (in %) as a function of the duration of the 8 W UV-A regeneration at 80 °C performed after complete deactivation of the catalyst (12 h of test). (B) Cycles of alternative photocatalysis and regeneration steps : test #1 with complete deactivation being obtained after 12 h of test, followed by a 8W-UVA regeneration at 80 °C for 12 h, and finally test #2 performed in similar conditions to test #1. (C) Deviation percentage between tests #1 and #2, evidencing the efficiency of the regenerative treatment. This deviation percentage corresponds to the difference in efficiency between both fresh and regenerated photocatalysts relatively to the efficiency of the first test.

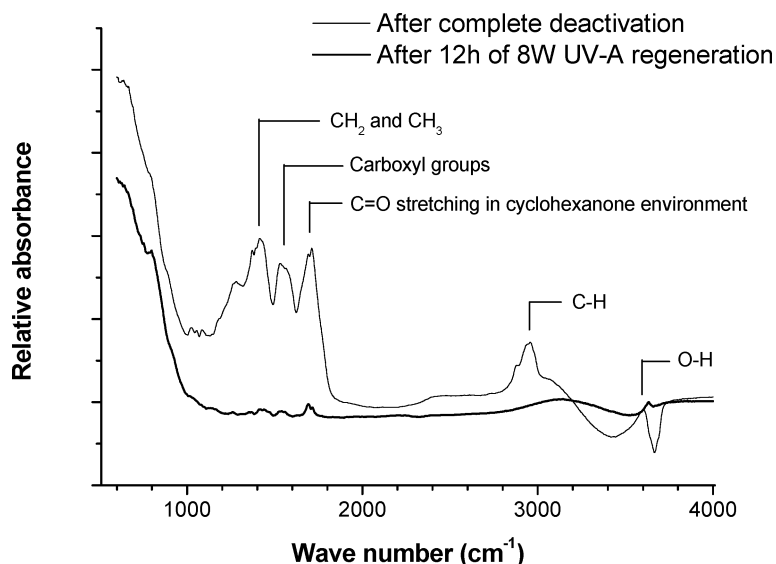


Fig. 5 DRIFT analyses of the TiO<sub>2</sub> photocatalyst after complete deactivation (overnight test) and after 12 h of 8 W UV-A regeneration.

removal efficiency, with regeneration efficiencies lower than 15% for regeneration durations shorter than 6 h. Regeneration conditions in terms of temperature, relative humidity and flow rate, were similar to those of the reaction step, in order to facilitate an efficient alternative switching between both test and regeneration periods. The recovery of the initial activity with a similar *on-stream* behaviour was confirmed by looking at Fig. 4A to 4C. No difference could be observed comparing the efficiency obtained on both fresh and regenerated photocatalysts. Indeed, by defining the deviation percentage as the difference in efficiency between both photocatalysts relatively to the efficiency of the initial test, this deviation percentage remained within a  $\pm 5\%$  relative range as a function of time on stream (Fig. 4C). Poisoning of the photocatalyst surface by reaction intermediates was reversible, as observed by comparing DRIFT analyses performed after complete deactivation of the catalyst (*i.e.* after 12 h of test) and after a regeneration procedure of 12 h (Fig. 5). These reaction intermediates resulting from a partial oxidation process and acting as surface poisons have mainly been identified as carbonyls, carboxylic acids and cyclic ketones. Investigating the different products issued from the oxidation of a series of terpenes with atmospheric constituents, Calogirou *et al.* have observed pina ketone (6,6-dimethyl-bicyclo[3.1.1]heptan-2-one), pinon aldehyde (*cis*-3-acetyl-2,2-dimethyl-cyclo-butyl-ethanal) and limona ketone (4-acetyl-1-methylcyclohexene) as the main reaction products resulting respectively from  $\beta$ -pinene/OH,  $\alpha$ -pinene/OH and limonene/OH oxidation.<sup>24</sup> The oxidative regeneration treatment with humid air and under UV-A illumination led to the photooxidation of the partially oxidized intermediates blocking the active sites of the TiO<sub>2</sub> surface, together with the corresponding formation of CO<sub>2</sub> (Fig. 4B). It should be noted that performing the photocatalytic tests and regenerating the deactivated TiO<sub>2</sub> did not result in any changes in the structural properties of the photocatalysts.

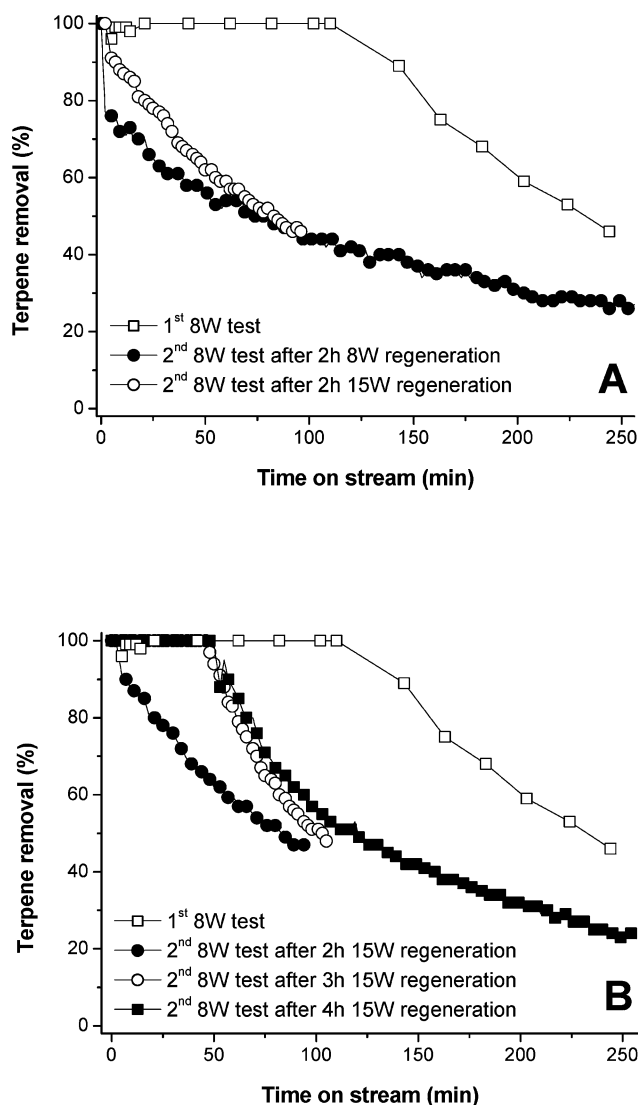
As the aim of the photooxidation of pinenes for industrial purposes is to maintain the longest duration at complete (100%) removal efficiency, the regeneration treatment has to be

performed directly at the terpene breakthrough, *i.e.* after 120 min of time on stream, when the terpene removal decreased with time on stream. The cyclic procedure alternating a 100% removal efficiency step and a consecutive regeneration treatment is reported in Fig. 6, with the reactor working at the reference covering ratio (1.2 mg/cm<sup>2</sup>). For this purpose and in order to shorten and optimize the regeneration duration, 8 W and 15 W-UVA regeneration procedures have been performed and compared, directly after 120 min of photocatalytic tests, corresponding to the beginning of the photocatalyst deactivation after total terpene removal.

It could be observed that increasing the UV-A lamp power from 8 to 15 W (Fig. 6A) yielded a more efficient regeneration procedure, because it allowed the full recovering of the terpene removal efficiency. However, 2 h of 15 W UV-A regeneration led to recover this total activity only for a few minutes, whereas increasing the regeneration duration to 3 h and 4 h resulted in maintaining this high efficiency for at least 60 minutes. Nevertheless, this procedure consisting of 120 minutes activity and 4 h 15 W UV-A regeneration is not valid for setting up activity/regeneration cycles using two photoreactors working alternatively for removing pinene and regenerating the photocatalyst: for this purpose, the regeneration duration should be similar to the duration at complete terpene removal. Targeting a high efficiency and continuous terpene elimination process would thus imply the use of three reactors with a 1/3 removal and 2/3 regeneration work-duration for each of them, the electrical power change being usually obtained by varying the lamp power input.

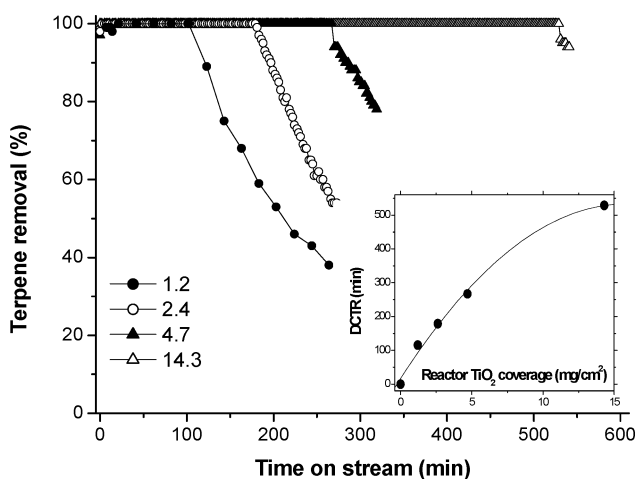
### 3.2.2. Direct photocatalytic experiment without any dark adsorption step.

*Activity.* In the absence of any dark pre-adsorption period, the reactant mixture was exclusively composed of  $\beta$ -pinene. The tests were performed at a temperature of 80 °C, under similar reaction conditions than when a first dark pre-adsorption period was observed (Fig. 7). At a 1.2 mg/cm<sup>2</sup> surface coverage, performing or not a dark adsorption step had no influence on



**Fig. 6** (A) Influence of the light power during the 2 h UV-A regeneration. (B) Influence of the duration of the 15 W UV-A regeneration. In all cases, the regeneration treatments were started after the total terpene removal period (around 120 min).

the duration of the initial 100% pinene removal plateau, with a similar *on-flow* behaviour being observed, *i.e.* a DCTR of 120 min followed by a similar deactivation step. The similar results obtained at the 1.2 mg/cm<sup>2</sup> surface coverage reference, with and without a dark pre-adsorption period, confirmed that the pinene removal did not occur just by physical adsorption, in agreement to the low *on-stream* adsorption capacity shown by TiO<sub>2</sub> towards pinenes. By contrast, increasing the TiO<sub>2</sub> surface coverage from 1.2 to 14.3 mg/cm<sup>2</sup> yielded a considerable increase in the duration of complete  $\beta$ -pinene removal. Indeed, the duration of the initial 100% removal plateau reached 5 h and 9 h when increasing the surface coverage to 4.7 mg/cm<sup>2</sup> and 14.3 mg/cm<sup>2</sup> respectively, before deactivation occurred. The longer DCTR obtained without any dark adsorption period, *i.e.* with no pre-isomerization of the  $\beta$ -pinene, could be attributed by assuming a higher photocatalytic reactivity of the inlet  $\beta$ -pinene molecule compared to that of the isomers such as limonene, camphene and  $\alpha$ -pinene formed on the non-illuminated particles.



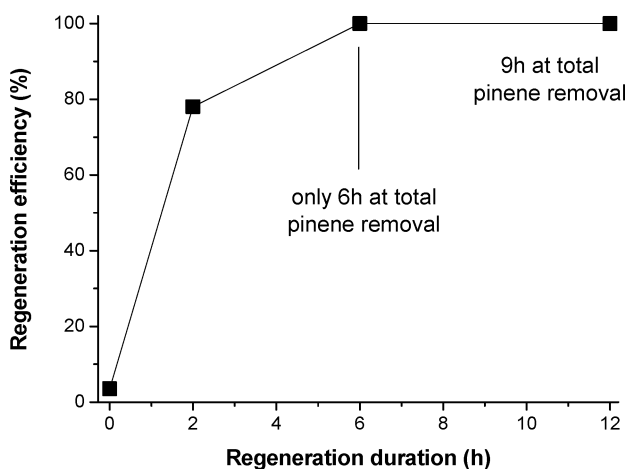
**Fig. 7** Terpene removal with time on stream at 80 °C as a function of the TiO<sub>2</sub> reactor surface coverage in mg/cm<sup>2</sup>, on UV100 TiO<sub>2</sub> without any prior dark adsorption. Inset: DCTR (in min) as a function of the reactor TiO<sub>2</sub> coverage in mg/cm<sup>2</sup>.

This led to estimate the VOC conversion before deactivation, at 48 mg<sub>terpenes</sub>/g<sub>TiO<sub>2</sub></sub>, 52 mg<sub>terpenes</sub>/g<sub>TiO<sub>2</sub></sub>, 40 mg<sub>terpenes</sub>/g<sub>TiO<sub>2</sub></sub> and 26 mg<sub>terpenes</sub>/g<sub>TiO<sub>2</sub></sub> for TiO<sub>2</sub> loadings of 1.2 mg/cm<sup>2</sup>, 2.4 mg/cm<sup>2</sup>, 4.7 mg/cm<sup>2</sup> and 14.3 mg/cm<sup>2</sup> respectively.

Compared to what was observed with a dark pre-adsorption period, similar surface functionalities were observed by DRIFT analyses on the used TiO<sub>2</sub> surface and selectivity into CO<sub>2</sub> close to 20% was obtained. Again, complete deactivation occurred for longer duration tests, although the duration necessary to reach a near-zero activity corresponding to a full deactivation of the catalyst, was strongly lengthened by increasing the TiO<sub>2</sub> amount. As previously suggested, the large amount of TiO<sub>2</sub> involved in the reactor wall coating and thus the too large thickness of the TiO<sub>2</sub> coating compared to the UV-A penetration depth, led to the consideration that the main part of the TiO<sub>2</sub> particles remained non-illuminated. The involvement of non-illuminated TiO<sub>2</sub> particles, located behind the UVA penetration depth, could also be put forward for possibly explaining such a great increase in efficiency with the increase in the TiO<sub>2</sub> coating depth. Further investigations are being conducted to provide more evidence on this point.

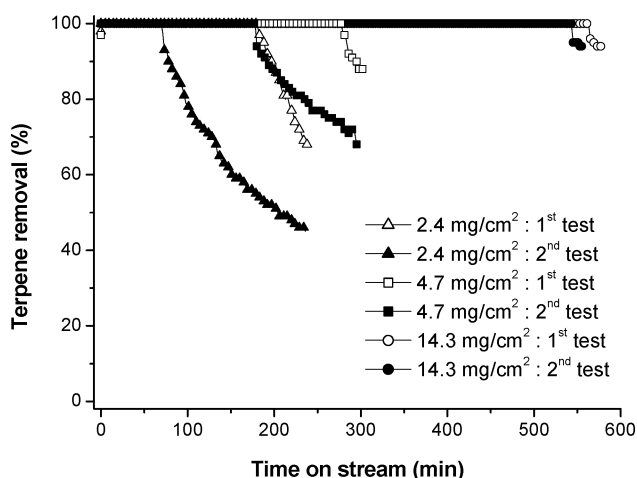
**Deactivation/regeneration.** Since the H<sub>2</sub>O/air regenerative treatment was more efficient using a 15 W illumination rather than an 8 W one (Fig. 6), the regeneration treatment has been performed in a similar way to the previous section, but with a 15 W UV-A light. Fig. 8 shows the efficiency of this regenerative treatment over a fully deactivated photocatalyst obtained after an 8 W test using a 14.3 mg/cm<sup>2</sup> reactor coverage. An *on-stream* regeneration of 2 h led to recover an initial terpene removal close to 80% before deactivation, whereas a regeneration of 6 h allowed a complete terpene removal to be recovered for 6 h, and a regeneration of 12 h led to recover the full activity of the photocatalyst, with a similar duration for the initial 100% removal efficiency period for both fresh and regenerated photocatalyst, *i.e.* a DCTR of 9 h.

The increase in the reactor surface coverage resulted in a considerable increase in complete  $\beta$ -pinene elimination duration, and therefore the influence of this surface coverage on the



**Fig. 8** Regeneration efficiency (in %) as a function of the duration of the 15 W UV-A regeneration at 80 °C performed after the complete deactivation of the photocatalyst during an 8 W test with a coverage of 14.3 mg/cm<sup>2</sup>.

regeneration procedure efficiency was studied. Only 15 W regeneration procedures were investigated as it has been shown previously that they are most efficient than 8 W UV-A regenerations. Fig. 9 shows the influence of the TiO<sub>2</sub> coverage on the efficiency of the regenerative treatments for similar alternative testing/regeneration durations. The 15 W UV-A regeneration treatments were performed on used catalysts at the beginning of the deactivation breakdown, *i.e.* when the catalyst did not show a total terpene removal under 8 W UV-A illumination (at 3 h, 5 h and 9 h for the 2.4 mg/cm<sup>2</sup>, 4.7 mg/cm<sup>2</sup> and 14.3 mg/cm<sup>2</sup> reactor coverage respectively). In order to investigate the possibility of designing an alternative activity/regeneration cyclic process, the regeneration treatments were performed for durations similar to



**Fig. 9** Influence of the TiO<sub>2</sub> reactor coverage on the efficiency of the 15 W UV-A regenerative treatments, performed after 8 W UV-A photocatalytic tests. Targeting the design of an alternative removal/regeneration procedure, the regeneration treatment was started exactly when the catalyst did not show a total terpene removal (after 3 h, 5 h and 9 h of testing for a reactor coverage of 2.4 mg/cm<sup>2</sup>, 4.7 mg/cm<sup>2</sup> and 14.3 mg/cm<sup>2</sup> respectively). The 15 W UV-A regeneration was then carried out for similar durations, *i.e.* 3 h, 5 h and 9 h for a reactor coverage of 2.4 mg/cm<sup>2</sup>, 4.7 mg/cm<sup>2</sup> and 14.3 mg/cm<sup>2</sup> respectively) and the 2nd 8 W UV-A photocatalytic test was further performed.

those of the corresponding photocatalytic removal tests. It was worth noting that performing the 15 W regeneration for a similar duration than that of the total removal plateau shown by the first test, did not allow the full activity to be recovered, independently of the TiO<sub>2</sub> coverage. Indeed, the duration of the complete pinene removal plateau obtained over the UV-A regenerated catalyst was shortened compared to that obtained over the fresh catalytic coating. However, the observed shortening was less pronounced when increasing the TiO<sub>2</sub> surface coverage from 2.4 mg/cm<sup>2</sup> to 14.3 mg/cm<sup>2</sup> coating, and thus increasing the depth of the TiO<sub>2</sub> coating. This was in agreement with the involvement of non-illuminated TiO<sub>2</sub> particles within the overall process, even if they could not be directly involved in the photocatalytic reactions. More characterization details on both used and regenerated photocatalyst will be presented elsewhere to provide more insight on the involvement of non-illuminated TiO<sub>2</sub> particles.

It should be noted that working with a surface coverage of 14.3 mg/cm<sup>2</sup> in a usual annular seep-flow photoreactor resulted in the low mechanical stability shown by the TiO<sub>2</sub> coatings inside the reactor, obviously not appropriate to design useful photoreactors. Therefore, there is the need for developing new photocatalytic substrates and/or new anchorage processes to further improve the mechanical stability of TiO<sub>2</sub> coatings at high loading.<sup>25</sup>

#### 4. Conclusion

This article reports on the first use of UV-A photocatalysis for removing terpenes from flowing air at temperatures ranging from 20 °C to 80 °C. Performing the photocatalytic tests at elevated temperatures required taking into account the thermal catalytic isomerization occurring on TiO<sub>2</sub> surfaces. The *on-stream* behaviour showed an initial plateau with total terpene removal, followed by a progressive deactivation, associated to the surface poisoning by partially oxidized intermediates. Effective UV-A mediated oxidative regenerative treatment was performed through humid air flow, with the photooxidation of the reaction intermediate organic poisons and the corresponding formation of CO<sub>2</sub>. We tried to evidence that reaction/regeneration cycles could be put forward to hold a continuous high efficiency pinene removal. The use of thick TiO<sub>2</sub> coating obtained by increasing the TiO<sub>2</sub> surface density from usual values (close to 1 mg/cm<sup>2</sup>) up to 14.3 mg/cm<sup>2</sup> resulted in an unexpected *on-flow* removal behaviour, notably by strongly limiting the *on-stream* deactivation. Depending on the way of testing, terpene removal before deactivation occurred was evaluated up to 52 mg of terpenes per g of TiO<sub>2</sub>. Due to the very high terpene concentration in the inlet flow, at a gram scale per m<sup>3</sup> of air, this weight percentage could not reach high values. The involvement in the terpene removal process, of non-illuminated TiO<sub>2</sub> particles located deep inside the TiO<sub>2</sub> coating has been advanced in order to explain both the large increase in the terpene removal efficiency and the reduced deactivation when increasing the thickness of the TiO<sub>2</sub> coating highly above the usual UV-A penetration depth. Further investigations are ongoing to explain in more detail the observed behaviour linked with the role of non-illuminated TiO<sub>2</sub> particles and the impact of the thermal isomerization, for alternatively pointing out the possible

dependence of the photocatalytic activity with the nature of the terpene isomers. However, using so large TiO<sub>2</sub> amounts led to seep-flow annular reactors with low mechanical stability, and therefore the design of new substrates and/or the use of new physico-chemical anchorage methods will be required for improving the mechanical stability of the TiO<sub>2</sub> coating.

## Acknowledgements

The authors are grateful to Dr. H. Haidara (ICSI, CNRS, Mulhouse) for the DRIFTS measurements.

## References

- 1 J. H. Langenheim, *J. Chem. Ecol.*, 1994, **20**, 1223.
- 2 C. C. R. Carvalho and M. M. R. Da Fonseca, *Biotechnol. Adv.*, 2006, **24**(2), 134.
- 3 K. A. Da Silva, I. Kozhevnikov and E. Gusevskoya, *Appl. Catal. A: Gen.*, 2005, **294**, 106.
- 4 M. A. Ecomier, K. Wilson and A. F. Lee, *J. Catal.*, 2003, **215**(1), 57.
- 5 M. Kr. Yadev, C. D. Chudarsama and R. V. Jasra, *J. Mol. Catal. A: Chem.*, 2004, **216**, 51.
- 6 C. Encarnação, A. Ramos, J. Vital and I. M. Fonseca, *Catal. Today*, 2003, **78**, 197.
- 7 S. M. Ribeiro, A. C. Serra and A. M. D'A. Rocha Gonsalves, *J. Catal.*, 2008, **256**(2), 331.
- 8 F. Chiron, J. C. Chalchat, R. P. Garry, J. F. Pilichowski and J. Lacoste, *J. Photochem. Photobiol. A*, 1997, **111**(1–3), 75.
- 9 L. Weber, G. Haufe, D. Rehorek and H. Hennig, *J. Mol. Catal.*, 1990, **60**(2), 267.
- 10 T. Kudo, Y. Kudo, A. Ruike, A. Hasegawa, M. Kitano and M. Anpo, *Catal. Today*, 2007, **122**(1–2), 14.
- 11 T. Salthammer and F. Fuhrmann, *Env. Sci. Technol.*, 2007, **41**(18), 6573.
- 12 A. I. Hodgson, H. Destailats, D. P. Sullivan and W. J. Fisk, *Indoor Air*, 2007, **17**(4), 305.
- 13 M. Lahaniati, C. Nacos, C. Konidari, B. Niccolin, G. A. Petrucci, D. Kotzias, in *The Oxidizing Capacity of the Troposphere, Proceedings of 7th European Symposium on Physico-Chemical Behaviour of Atmospheric Pollutants*, Venice, Italy, 2–4 October 1996, ed. B. Larsen, B. Versino and G. Angelletti, 1997.
- 14 T. Hoffmann, J. R. Odum, F. Bowman, D. Collins, D. Klockow, R. C. Flagan and J. H. Seinfeld, *J. Atmos. Chem.*, 1997, **26**, 189.
- 15 *Photocatalysis and Environment. Trends and Applications*, ed. M. Schiavello, Kluwer Academic Publishers, Dordrecht, 1988.
- 16 *Photocatalysis, Fundamentals and applications*, ed. E. Pelizzetti and N. Serpone, Wiley, New York, 1989.
- 17 D. F. Ollis, E. Pelizzetti and N. Serpone, *Environ. Sci. Technol.*, 1991, **25**, 1522.
- 18 V. Keller, P. Bernhardt and F. Garin, *J. Catal.*, 2003, **215**, 129.
- 19 A. Stanislaus and L. M. Yeddanapalli, *Canad. J. Chem.*, 1972, **50**, 61.
- 20 A. Severino, A. Esculcas, J. Roca, J. Vital and L. S. Lobo, *Appl. Catal. A-Gen.*, 1996, **142**, 255.
- 21 J. C. von der Waal, H. van Bekkum and J. M. Vital, *J. Mol. Catal.*, 1996, **105**, 185.
- 22 T. Yamamoto, T. Matsuyama, T. Tanaka, T. Funabiki and S. Yoshida, *Appl. Catal. A*, 2000, **155**, 43.
- 23 J. M. Herrmann, *Top. Catal.*, 2005, **34**(1–4), 49.
- 24 A. Calogirou, B. R. Larsen and D. Kotzias, *Atmosph. Environ.*, 1999, **31**(9), 1423.
- 25 S. Josset, S. Hajjesmaili, D. Begin, D. Edouard, C. Pham-Huu, M. C. Lett, N. Keller, V. Keller, *Catal. Today*, 2008, submitted.



# Toward green metallurgy: low-temperature solution synthesis of bulk-scale intermetallic compounds in edible plant and seed oils

Nathaniel L. Henderson, Matthew D. Straesser, Philip E. Sabato and Raymond E. Schaak\*

Received 4th September 2008, Accepted 24th March 2009

First published as an Advance Article on the web 7th April 2009

DOI: 10.1039/b815443k

Binary intermetallic compounds have been synthesized in edible plant and seed oils through the reaction of molten metal dispersions of low-melting p-block metals with late transition metal powders. Specifically, apricot kernel, almond, safflower, and canola oils have been used to synthesize FeSn<sub>2</sub>, Ni<sub>3</sub>Sn<sub>4</sub>, CoSn<sub>3</sub>, CoGa<sub>3</sub>, Cu<sub>6</sub>Sn<sub>5</sub>, and Bi<sub>3</sub>Ni. This low-temperature strategy yields bulk-scale products that are highly crystalline, and the solvents used to synthesize them can be re-used several times.

## Introduction

The principles of green chemistry have been established to promote environmentally-responsible and non-hazardous methods for the synthesis and utilization of chemicals.<sup>1</sup> Toward that goal, there is a significant focus on modifying the chemistry of organic transformations, with particular emphasis on industrially-relevant processes because of their scale and technological importance. There is also growing interest in green nanotechnology, which encompasses the use of nanoscale materials for catalysis and environmental remediation, as well as green methods for the synthesis and production of nanoscale solids.<sup>2</sup> For example, edible oils, which are both non-toxic and renewable, have been used as solvents for the synthesis of a variety of nanocrystalline materials.<sup>3</sup> A related area that has received less attention is the development of green methods for the synthesis of bulk-scale solids that are normally prepared by lengthy high-temperature “heat and beat” solid-state reactions. Examples of ways in which green chemistry principles have been integrated into bulk-scale solid state synthesis include the use of supercritical fluids and microwave heating.<sup>4–5</sup>

Metallurgical solids include alloys, which are crystalline solid solutions of two or more metals, and intermetallic compounds, which are a subset of alloys that tend to have stoichiometric compositions and atomically-ordered crystal structures. The most common methods for the synthesis of metallurgical solids include high-temperature arc melting of the constituent elements, as well as powder metallurgy techniques that involve heating physical mixtures of metal powders at high temperatures for long periods of time, typically several days. These methods are both energy- and thermally-intensive, which is a direct result of the long solid–solid diffusion distances that must be overcome for the reactions to occur. Lower-temperature and lower-energy alternatives to these traditional techniques include ball milling,<sup>6</sup> mechanochemical synthesis,<sup>7</sup> flux syntheses,<sup>8</sup> and some deposition techniques.<sup>9</sup>

During the past few years, solution chemistry techniques have been shown to be applicable to the synthesis of nanoscale intermetallic compounds and alloys. For example, modifications of the polyol process and related methods have generated a library of late transition metal intermetallics and alloys.<sup>10</sup> To accomplish this, metal salts are first dissolved in a high-boiling organic solvent such as ethylene glycol or tetraethylene glycol, then reduced to zero-valent metals by heating or, more commonly, by reduction with sodium borohydride prior to heating. We recently showed that a related strategy can be applied to the synthesis of bulk-scale intermetallic compounds. In this case, bulk elemental powders are added to tetraethylene glycol and, upon heating, the powders diffuse together and form intermetallic compounds.<sup>11</sup> This works for metals that have a melting point below the boiling point of the solvent, e.g. Sn, Bi, In, and Ga. Here, the solvent serves as a heat source to facilitate the melting of one of the metal components and as a dispersion medium so that the molten metal can attack the other higher-melting metals. Using this strategy, fourteen distinct bulk-scale intermetallic compounds were synthesized using simple “beaker chemistry” reactions at temperatures below 300 °C.

When the principles of green chemistry are superimposed on this inherently low-temperature “beaker chemistry” technique for the synthesis of bulk-scale metallurgical solids, a set of procedural modifications for generating a more environmentally-responsible process becomes apparent. Since the role of the solvent is primarily to serve as a heat source and dispersion medium (rather than supporting dissolution or redox chemistry), other non-toxic and renewable solvents become feasible alternatives. Accordingly, here we show that edible oils, which have been used previously to synthesize metal and semiconductor nanocrystals,<sup>3</sup> can serve as a reaction medium for the low-temperature synthesis of bulk-scale intermetallic compounds. Specifically, apricot kernel, almond, safflower, and canola oils have been used to synthesize FeSn<sub>2</sub>, Ni<sub>3</sub>Sn<sub>4</sub>, CoSn<sub>3</sub>, CoGa<sub>3</sub>, Cu<sub>6</sub>Sn<sub>5</sub>, and Bi<sub>3</sub>Ni, which have known applications as superconductors, battery electrodes, corrosion resistant coatings, and magnetic materials. From a green chemistry perspective, this alternative “green metallurgy” process represents increased energy efficiency, based

Department of Chemistry and Materials Research Institute, The Pennsylvania State University, University Park, PA 16802, USA.  
E-mail: [schaak@chem.psu.edu](mailto:schaak@chem.psu.edu)

on both lower temperatures and shorter reaction times, relative to traditional high-temperature synthetic methods such as arc melting and powder metallurgy. This process also involves the use of renewable feedstocks, non-hazardous solvents, and more environmentally-responsible reaction conditions relative to the most common reaction media, which utilize toxic glycol solvents.<sup>11</sup>

## Experimental

### Materials

The following chemicals were used as purchased without further purification: Bi (99.5%), Cu (99%), Sn (99.8%), Co (99.8%), and Fe (99%) powders (–325 mesh, Alfa Aesar); Ni powders (–325 mesh, 99.8%, Alfa Aesar; 2–3  $\mu\text{m}$ , 99%, Alfa Aesar); and Ga shot (6 mm shot broken into ~1 mm pieces, 99.9999%, Alfa Aesar). Apricot kernel, almond, safflower, and canola oils were obtained from Spectrum Organics and used as purchased.

### Synthesis

For a typical synthesis of the binary intermetallic phases, stoichiometric amounts of the two constituent metals (approximate total mass of 0.15 g) are added to a flask with 30–50 mL of oil. The system is purged with Ar, rapidly heated (~5–10  $^{\circ}\text{C min}^{-1}$ ) with vigorous, continuous stirring (800–1150 rpm), and then held at the reaction temperature (Table 1) until the precursors have fully reacted to form the desired intermetallic phase. The crystalline intermetallic powders are separated from the solvent through centrifugation and then rinsed twice with toluene and ethanol. Alternatively, all washing can be carried out using only ethanol with additional rinsing cycles, eliminating the need for toluene. Lower stirring speeds or higher solvent viscosity can lead to attraction between the magnetic transition metal powders and the magnetic stir bar, which can lead to non-ideal local stoichiometries. In this case, a slight excess (generally less than 5%) of molten metal remains, and it can be easily removed by briefly rinsing with ~2 M HCl prior to the final ethanol rinse. Larger sample sizes can also be produced using the same volume of oil, e.g. 1 g of  $\text{Cu}_6\text{Sn}_5$  was produced by scaling up only the amount of metals without increasing solvent volume or reaction time. The formation of intermetallic compounds is generally detectable by powder X-ray diffraction (XRD) within three hours of heating, though longer heating times (Table 1) are necessary for phase-pure formation of some of the phases, consistent with a diffusion-based process. Synthetic parameters for each phase are given in Table 1.  $\text{FeSn}_2$  and  $\text{Ni}_3\text{Sn}_4$  were

studied in-depth in order to investigate solvent recyclability and the general versatility of this synthetic method.  $\text{FeSn}_2$  was synthesized in safflower, almond, apricot kernel, and canola oils under identical reaction conditions.  $\text{Ni}_3\text{Sn}_4$  was synthesized repeatedly in safflower oil, with the recovered solvent used for subsequent reactions.

### Characterization

Powder XRD data were collected at room temperature using a Bruker D8 Advance Diffractometer with a LynxEye 1D-detector (Cu  $\text{K}\alpha$  radiation). Scanning electron microscopy (SEM), energy-dispersive X-ray spectroscopy (EDS), and elemental mapping data were collected using a JEOL JSM 5400 SEM operating at 20 kV.

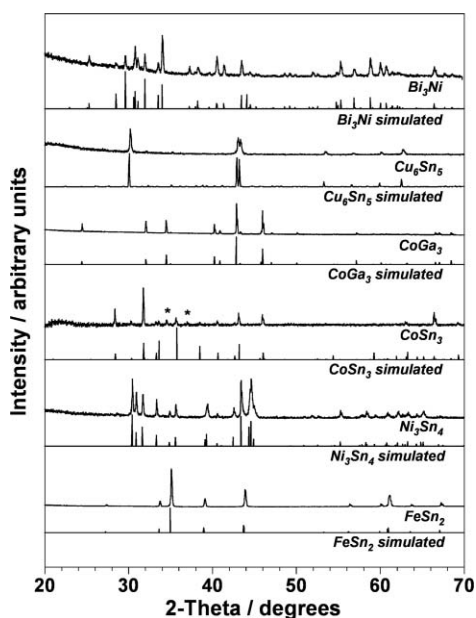
## Results and discussion

Commercially-available apricot kernel, almond, safflower, and canola oils have smoke points of 257  $^{\circ}\text{C}$ , 257  $^{\circ}\text{C}$ , 249  $^{\circ}\text{C}$ , and 242  $^{\circ}\text{C}$ , respectively. For comparison, the melting points of Bi, Sn, and Ga are 271  $^{\circ}\text{C}$ , 232  $^{\circ}\text{C}$ , and 30  $^{\circ}\text{C}$ , respectively. Accordingly, when Bi, Sn, or Ga are added to these edible oils and heated to an appropriate temperature, the elemental metals will be molten. (Though the melting point of Bi is higher than the smoke points of the oils, we observed that in an air-free environment, the oils can be heated to ~30  $^{\circ}\text{C}$  above their air-atmosphere decomposition temperatures, *i.e.* smoke points, without a noticeable increase in solvent degradation.) As we showed in a previous study,<sup>11</sup> dispersions of molten metals in high-boiling organic solvents readily attack higher-melting powders, forming intermetallic compounds *via* diffusion of the molten metal into the solid metal powders. Similar reactions occur in heated edible oils.

Fig. 1 shows representative XRD data for several intermetallics that are formed upon heating a low melting metal (Bi, Sn, Ga) with higher-melting metal powders (Fe, Co, Ni, Cu) in edible oils. Comparison of simulated and experimental powder XRD patterns unambiguously confirms the formation of the intermetallic phases. For example, phase pure  $\text{FeSn}_2$  forms when Fe powder reacts with molten Sn at 260  $^{\circ}\text{C}$  in safflower oil. Likewise,  $\text{Ni}_3\text{Sn}_4$  forms from the reaction of Ni and Sn powders in safflower oil at 270  $^{\circ}\text{C}$ .  $\text{CoSn}_3$ , formed from the reaction of Co and Sn metal powders at 260  $^{\circ}\text{C}$  in almond oil, shows evidence of preferred orientation, which is consistent with its layered crystal structure and its known preference to crystallize as anisotropic platelets.  $\text{CoGa}_3$  forms readily from reactions involving Co and Ga in almond oil at 260  $^{\circ}\text{C}$ , and the reaction of Cu and Sn in almond oil at 280  $^{\circ}\text{C}$  yields phase-pure  $\text{Cu}_6\text{Sn}_5$ . Finally,  $\text{Bi}_3\text{Ni}$  forms after heating the constituent elements at 280  $^{\circ}\text{C}$  in apricot kernel oil. The reaction times range from 6–48 h. These are equal to or longer than the times required using the more toxic glycol solvents.<sup>11</sup> The thermal stability of the chosen oils is partially attributable to a large concentration of unsaturated fatty acids, which are known to bind more strongly than glycols to metal and oxide surfaces and have been shown to slow diffusion rates *via* surface passivation.<sup>12</sup> In cases requiring longer reaction times, the energy efficiency relative to the glycol-based solvents is lower, but the non-toxic edible oil solvents help

**Table 1** Synthetic conditions for binary intermetallics in edible oils.

Intermetallic Compound	Oil	Reaction temperature/ $^{\circ}\text{C}$	Time at reaction temperature/h
$\text{Bi}_3\text{Ni}$	Apricot kernel oil	280	48
$\text{Cu}_6\text{Sn}_5$	Almond oil	280	6
$\text{CoGa}_3$	Almond oil	260	36
$\text{CoSn}_3$	Almond oil	260	36
$\text{Ni}_3\text{Sn}_4$	Safflower oil	270	6
$\text{FeSn}_2$	Safflower oil	260	6



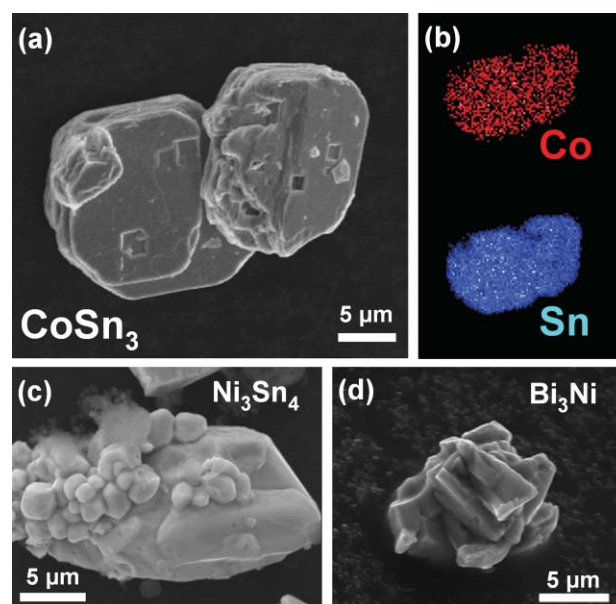
**Fig. 1** Powder XRD patterns of binary intermetallics obtained by reacting molten metal dispersions with late transition metal powders in hot plant and seed oils. The good agreement between simulated and observed patterns for each phase indicates phase purity, with the exception of  $\text{CoSn}_3$ . Two small reflections, indicated by asterisks, can be assigned to a slight impurity of  $\beta$ - $\text{CoSn}_3$  (minor phase), which is identical in stoichiometry to  $\alpha$ - $\text{CoSn}_3$  (main phase) but possesses a slightly different stacking sequence of Co-Sn layers.<sup>13</sup>

to mediate this concern. In all cases, the reactions occur at significantly lower temperatures than traditional high-temperature metallurgical reactions involving arc melting or dry powder processing.

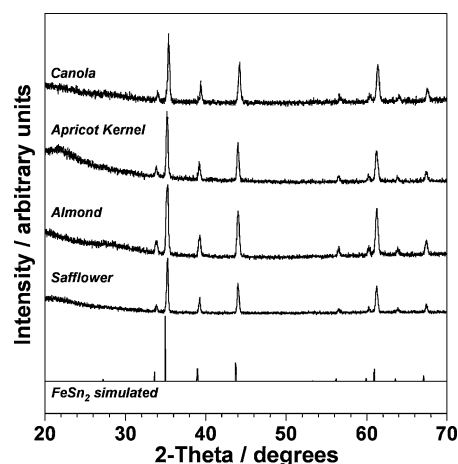
The products formed from the reaction of bulk metal powders in heated edible oils are highly crystalline, as evidenced from the sharp XRD peaks in Fig. 1, as well as the particle morphologies in Fig. 2. For example,  $\text{CoSn}_3$  (Fig. 2a) forms tabular particles with well-defined crystal facets. The platelet morphology is consistent with the preferred orientation observed in the XRD data in Fig. 1. EDS element mapping in Fig. 2b confirms that the particles contain homogeneously distributed Co and Sn in a ratio of approximately 20 : 80, which is within experimental error *via* EDS of the expected 1 : 3 ratio in  $\text{CoSn}_3$ . In addition to providing access to highly crystalline intermetallics, this approach is a viable means of rapidly synthesizing low-temperature phases (e.g.  $\alpha$ - $\text{CoSn}_3$  and  $\eta'$ - $\text{Cu}_6\text{Sn}_5$ ) that are typically obtained through metal flux methods or lengthy peritectic reactions with slow cooling rates.<sup>13,14</sup>

The  $\text{FeSn}_2$  system was chosen to demonstrate that multiple types of edible oils can be used to successfully synthesize a given intermetallic. Accordingly, Fig. 3 shows XRD data for phase-pure  $\text{FeSn}_2$  synthesized from Fe and Sn powders in safflower, almond, apricot kernel, and canola oils at 260 °C.

All of the chosen oils are largely composed of long chain unsaturated fatty acids (e.g. oleic and linoleic acids), which give rise to their high thermal stability.<sup>15</sup> Due to the similar composition of these high-smoke point oils, the choice of reaction medium can be determined based on other relevant

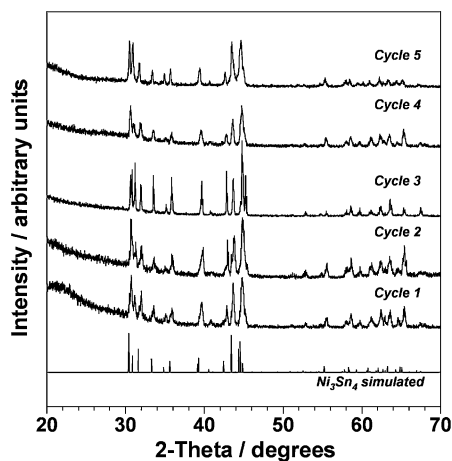


**Fig. 2** Representative SEM images of (a)  $\text{CoSn}_3$ , (c)  $\text{Ni}_3\text{Sn}_4$ , and (d)  $\text{Bi}_3\text{Ni}$  powders. EDS and elemental mapping data (b) for Co and Sn verify the composition and elemental distribution of  $\text{CoSn}_3$ .



**Fig. 3** Comparison between simulated and observed powder XRD patterns for  $\text{FeSn}_2$  synthesized in several different edible oils at 280 °C.

factors, such as solvent availability and cost of production. Likewise, the  $\text{Ni}_3\text{Sn}_4$  system in safflower oil was used to study the ability of the solvent to be recycled and re-used multiple times. Fig. 4 shows powder XRD data for  $\text{Ni}_3\text{Sn}_4$  synthesized from Ni and Sn powders in safflower oil at 250 °C for 48 h. The  $\text{Ni}_3\text{Sn}_4$  product was separated from the oil by centrifugation, and fresh Ni and Sn powders were added to the previously-used oil. After heating again to 250 °C for an additional 48 h, phase-pure  $\text{Ni}_3\text{Sn}_4$  was isolated. Three more cycles were performed, each successfully yielding  $\text{Ni}_3\text{Sn}_4$ . Although the solvent begins to degrade and change from a yellow to brown color from prolonged heating near the smoke point, it is still re-usable for at least five cycles, or approx. 240 h. The fact that intermetallics can still be formed using the degraded oils implies that waste oils could also be used as the reaction medium, providing an



**Fig. 4** Powder XRD patterns for  $\text{Ni}_3\text{Sn}_4$  formed at 250 °C in recycled safflower oil. The solvent was recovered by centrifugation after each reaction and reused for subsequent reactions.

additional opportunity for recyclability. The re-usability of the edible oil solvents after heating is significantly better than the glycols, which have been observed to degrade much faster at these reaction temperatures. Recyclability was tested in the  $\text{FeSn}_2$  system as well and was found to be reusable for several cycles, although Fe causes faster degradation of the solvent, presumably due to metal-catalyzed oxidation. This is consistent with studies showing that Fe increases the oxidation rate of linoleic and oleic acids, which are major components of safflower and other oils.<sup>16</sup>

## Conclusions

A method was developed for synthesizing metallurgical solids in edible plant and seed oils, providing a step toward “green metallurgy” using simple solution chemistry reactions. This low-temperature strategy yields bulk-scale products that are highly crystalline. The solvents used to synthesize them can be re-used several times, and the successful synthesis of intermetallics even in oils that have begun to degrade implies that waste oils could also be used as reaction media. Compared to traditional high-temperature metallurgical methods, such as arc melting and powder annealing, reaction times are generally either similar or shorter and reaction temperatures are significantly lower. Compared to other solution-mediated reactions, the edible oil solvents are a non-toxic alternative to most of the glycol-based systems that are typically used for such purposes. This study provides an intriguing look at replacing toxic glycol-based solvents with renewable edible oils for producing metallurgical solids, and opens the door to more in-depth analyses of the process. For example, it may be possible to further expand the recyclability by introducing additives that increase the oxidative stability of the oils.<sup>17</sup> Also, a complete assessment of the process that takes into account energy requirements for producing the edible oils relative to the petroleum-derived glycol solvents, as well as heat recovery during synthesis, would be interesting. Finally, preliminary scale-up studies involving larger gram-scale sample sizes appear promising and should support exploration of the physical properties of these materials for

comparison to analogous materials synthesized using traditional methods.

## Acknowledgements

This work was supported by the U.S. Department of Energy (DE-FG02-06ER46333), a Beckman Young Investigator Award, a Sloan Research Fellowship, a DuPont Young Professor Grant, and a Camille Dreyfus Teacher-Scholar Award. SEM imaging was performed at the Electron Microscopy Facility in the Huck Institutes of the Life Sciences at Penn State.

## Notes and references

- P. T. Anastas and J. C. Warner, *Green Chemistry; Theory and Practice*, Oxford University Press, Oxford, 1998, p. 30; M. Poliakoff and P. Licence, *Nature*, 2007, **450**, 810; R. Noyori, *Chem. Commun.*, 2005, 1807.
- Y. Mao, T.-J. Park, F. Zhang, H. Zhou and S. S. Wong, *Small*, 2007, **3**, 1122; C. J. Murphy, *J. Mater. Chem.*, 2008, **18**, 2173.
- P. Raveendran, J. Fu and S. L. Wallen, *Green Chem.*, 2006, **8**, 34; Y. Koltypin, N. Perkas and A. Gedanken, *J. Mater. Chem.*, 2004, **14**, 2975; S. K. Spear, S. T. Griffin, K. S. Granger, J. G. Huddleston and R. D. Rogers, *Green Chem.*, 2007, **9**, 1008.
- A. A. Galkin, B. G. Kostyuk, V. V. Lunin and M. Poliakoff, *Angew. Chem., Int. Ed.*, 2000, **39**, 2738; A. Cabañas, J. Li, P. Blood, T. Chudoba, W. Lojkowski, M. Poliakoff and E. Lester, *J. Supercrit. Fluids*, 2007, **40**, 284; C. Aymonier, A. Loppinet-Serani, H. Reverón, Y. Garrabos and F. Cansell, *J. Supercrit. Fluids*, 2006, **38**, 242; N. E. Fernandes, S. M. Fisher, J. C. Poshusta, D. G. Vlachos, M. Tsapatsis and J. J. Watkins, *Chem. Mater.*, 2001, **13**, 2023.
- C. Mastrovito, J. W. Lekse and J. A. Aitken, *J. Solid State Chem.*, 2007, **180**, 3262; J. W. Lekse, A. M. Pischera and J. A. Aitken, *Mater. Res. Bull.*, 2007, **42**, 395.
- C. C. Koch and J. D. Whittenberger, *Intermetallics*, 1996, **4**, 339; M. A. Meitl, T. M. Dellinger and P. V. Braun, *Adv. Funct. Mater.*, 2003, **13**, 795; H. Konrad, J. Weissmuller, R. Birringer, C. Karmonik and H. Gleiter, *Phys. Rev. B: Condens. Matter Mater. Phys.*, 1998, **58**, 2142.
- F. H. Froes, O. N. Senkov and E. G. Baburaj, *Mater. Sci. Eng., A*, 2001, **301**, 44; C. Ding, C. Zhang, C. Jianguo and C. Zhenhua, *J. Alloys Compd.*, 2008, **461**, L23; T. F. Grigorjeva, A. P. Barinova and N. Z. Lyakhov, *Russ. Chem. Rev.*, 2001, **70**, 45.
- M. G. Kanatzidis, R. Pottgen and W. Jeitschko, *Angew. Chem., Int. Ed.*, 2005, **44**, 6996; Z. Fisk and J. P. Remeika, *Handbook on the Physics and Chemistry of Rare Earths*, 1989, **12**, 55.
- M. Martín-González, A. L. Prieto, M. S. Knox, R. Gronsky, T. Sands and A. M. Stacy, *Chem. Mater.*, 2003, **15**, 1676; A. Onda, T. Komatsu and T. Yashima, *J. Catal.*, 2001, **201**, 13; T. Komatsu, K. Inaba, T. Uezono, A. Onda and T. Yashima, *Appl. Catal., A*, 2003, **251**, 315; S. Mathur, M. Veith, T. Ruegamer, E. Hemmer and H. Shen, *Chem. Mater.*, 2004, **16**, 1304; A. L. E. Smalley, M. L. Jepsersen and D. C. Johnson, *Inorg. Chem.*, 2004, **43**, 2486.
- C. Roychowdhury, F. Matsumoto, P. F. Mutolo, H. D. Abruña and F. J. DiSalvo, *Chem. Mater.*, 2005, **17**, 5871; A. J. Karkamkar and M. G. Kanatzidis, *J. Am. Chem. Soc.*, 2006, **128**, 6002; B. M. Leonard, N. S. P. Bhuvanesh and R. E. Schaak, *J. Am. Chem. Soc.*, 2005, **127**, 7326; R. E. Cable and R. E. Schaak, *Chem. Mater.*, 2007, **19**, 4098; R. E. Cable and R. E. Schaak, *J. Am. Chem. Soc.*, 2006, **128**, 9588; R. E. Cable and R. E. Schaak, *Chem. Mater.*, 2005, **17**, 6835; R. E. Schaak, A. K. Sra, B. M. Leonard, R. E. Cable, J. C. Bauer, Y.-F. Han, J. Means, W. Teizer, Y. Vasquez and E. S. Funck, *J. Am. Chem. Soc.*, 2005, **127**, 3506; N. H. Chou and R. E. Schaak, *Chem. Mater.*, 2008, **20**, 2081; N. H. Chou and R. E. Schaak, *J. Am. Chem. Soc.*, 2007, **129**, 7339; L. F. Alden, C. Roychowdhury, F. Matsumoto, D. K. Han, V. B. Zeldovich, H. D. Abruña and F. J. DiSalvo, *Langmuir*, 2006, **22**, 10465; C. Roychowdhury, F. Matsumoto, V. B. Zeldovich, S. C. Warren, P. F. Mutolo, M. J. Ballesteros, U. Wiesner, H. D. Abruña and F. J. DiSalvo, *Chem. Mater.*, 2006, **18**, 3365.
- N. L. Henderson and R. E. Schaak, *Chem. Mater.*, 2008, **20**, 3212.

- 
- 12 X. Lu, H.-Y. Tuan, J. Chen, Z.-Y. Li, B. A. Korgel and Y. Xia, *J. Am. Chem. Soc.*, 2007, **129**, 1733; A. L. Willis, N. J. Turro and S. O'Brien, *Chem. Mater.*, 2005, **17**, 5970.
- 13 A. Lang and W. Jeitschko, *Z. Metallkd.*, 1996, **87**, 759.
- 14 A.-K. Larsson, L. Stenberg and S. Lidin, *Acta Cryst.*, 1994, **B50**, 636.
- 15 G. Fuller, G. O. Kohler and T. H. Applewhite, *J. Am. Oil Chem. Soc.*, 1966, **43**, 477; E. N. Frankel, *J. Am. Oil Chem. Soc.*, 1993, **70**, 767.
- 16 K. U. Ingold, in *Lipids and Their Oxidation*, ed. H. W. Schultz, E. A. Day and R. O. Sinnhaber, AVIPublishing Co., Westport, CT, USA, 1962, pp. 93–121; D. H. Donovan and D. B. Menzel, *Cell. Mol. Life Sci.*, 1978, **34**, 775; S. U. Maheswari, C. S. Ramadoss and P. R. Krishnaswamy, *Mol. Cell Biol.*, 1997, **177**, 47.
- 17 B. Halliwell, M. A. Murcia, S. Chirico and O. I. Aruoma, *Crit. Rev. Food Sci. Nutr.*, 1995, **35**, 7; D. B. Min and J. Wen, *J. Food Sci.*, 1983, **48**, 1429.

# Selective hydrogenation of citral catalyzed with palladium nanoparticles in CO<sub>2</sub>-in-water emulsion

Ruixia Liu,<sup>a,b</sup> Chaoyong Wu,<sup>a,b</sup> Qiang Wang,<sup>a,b</sup> Jun Ming,<sup>a,b</sup> Yufen Hao,<sup>a,b</sup> Yancun Yu<sup>a</sup> and Fengyu Zhao<sup>\*a</sup>

Received 2nd December 2008, Accepted 7th April 2009

First published as an Advance Article on the web 22nd April 2009

DOI: 10.1039/b821601k

CO<sub>2</sub>-in-Water (C/W) emulsion was formed by using a nonionic surfactant of poly (ethylene oxide)-poly (propylene oxide)-poly (ethylene oxide) (P123), and palladium nanoparticles were synthesized *in situ* in the present work. The catalytic performance of Pd nanoparticles in the C/W emulsion has been discussed for a selective hydrogenation of citral. Much higher activity with a turnover frequency (TOF) of 6313 h<sup>-1</sup> has been obtained in this unique C/W emulsion compared to that in the W/C microemulsion (TOF, 23 h<sup>-1</sup>), since the reaction was taking place not only in the surfactant shell but also on the inner surface of the CO<sub>2</sub> core in the C/W emulsion. Moreover, citronellal was obtained with a higher selectivity for that it was extracted to a supercritical carbon dioxide (scCO<sub>2</sub>) phase as formed and thus its further hydrogenation was prohibited. The Pd nanoparticles could be recycled several times and still retain the same selectivity, but it showed a little aggregation leading to a slight decrease in conversion.

## Introduction

Emulsion systems have been an important research topic for years, and they are widely used in cleaning, materials science, chemical reactions, manufacturing, enhancing oil recovery and many other processes.<sup>1-8</sup> As is well known, emulsion is the heterogeneous system consisting of at least two immiscible liquids and amphiphile (surfactant). Water and carbon dioxide are the most abundant and green solvents on the earth, and the emulsions composed of water and carbon dioxide are nonflammable, essentially nontoxic and environmentally benign. However, the understanding of water-CO<sub>2</sub> emulsions is still in its infancy, relative to that of water-oil emulsions. Conventional surfactants used in water-oil emulsions often exhibit low solubilities in CO<sub>2</sub> due to the weak solvent strength of CO<sub>2</sub> limited by weak Van der Waals Forces.<sup>9</sup> To achieve satisfactory tail solvation in CO<sub>2</sub>, fluorinated polymers such as polyfluoroethers, polyfluoroacrylates, and polyfluoromethacrylates are usually used to stabilize the CO<sub>2</sub>-water emulsions.<sup>10-12</sup> However, these fluorinated compounds are more harmful and expensive compared with conventional surfactants. Therefore, much attention has been paid to the surfactants of CO<sub>2</sub>-philic groups of branched hydrocarbons. Da Rocha *et al.* reported that carbon dioxide-in-water (C/W) macroemulsions stabilized with inexpensive hydrocarbon surfactants of poly(ethylene oxide)-*b*-poly(butylene oxide)(EO<sub>15</sub>-*b*-BO<sub>12</sub>) were stable over 48 h against both flocculation and coalescence.<sup>13</sup> In addition, water-in-carbon dioxide

(W/C) microemulsions<sup>14,15</sup> and macroemulsions<sup>16</sup> have been prepared successfully with hydrocarbon surfactants.

The emulsion is the most often employed strategy to overcome the reagent incompatibility and increase the interfacial areas. It was reported that the organic reaction between a hydrophobe, benzyl chloride, and a hydrophile, KBr was performed smoothly in the CO<sub>2</sub>-water emulsions and in which the rate of the reaction increased dramatically compared with that in water-in-octane emulsions.<sup>17</sup> And the reaction rates of styrene hydrogenation in the CO<sub>2</sub>-water emulsions and/or microemulsions were reported to increase more than 38 and 5 times compared with those in toluene/water and CO<sub>2</sub>/water systems, respectively.<sup>18</sup> These results suggested that the CO<sub>2</sub>-water emulsions and microemulsions are efficient catalytic systems, especially for hydrogenation due to the improvements in hydrogen concentration, mass diffusion and interfacial area. Furthermore, the emulsions could be broken rapidly by decompressing.<sup>17,18</sup> Recently, the W/C microemulsion technology offers a new approach in the synthesis of metal nanoparticles such as Pd and Cu, and these nanoparticles formed *in situ* could catalyze chemical reactions efficiently.<sup>19-21</sup> Wai *et al.* have done thorough research into the preparation of metal nanoparticles in W/C microemulsions such as Pd nanoparticles, and these Pd nanoparticles presented high activity and stability in the hydrogenation of olefins in W/C microemulsions.<sup>22-25</sup>

In this work, Pd nanoparticles were prepared in the C/W emulsion through *in situ* reduction with H<sub>2</sub>. The catalytic performance of the Pd nanoparticles in C/W emulsion was investigated for a selective hydrogenation of unsaturated aldehyde of citral. Several important factors which affect the emulsion environments such as the surfactant concentration, temperature and CO<sub>2</sub> pressure have been discussed. In comparison to the catalytic systems reported, the present C/W emulsion is more suitable for the 'CO<sub>2</sub>-soluble reactants' reactions.

<sup>a</sup>State Key Laboratory of Electroanalytical Chemistry, Changchun Institute of Applied Chemistry, Chinese Academy of Sciences, Changchun, 130022, P. R. China. E-mail: zhaofy@ciac.jl.cn; Fax: +86 431-85262410; Tel: +86 431-85262410

<sup>b</sup>Graduate School of the Chinese Academy of Sciences, Beijing, 100049, P. R. China

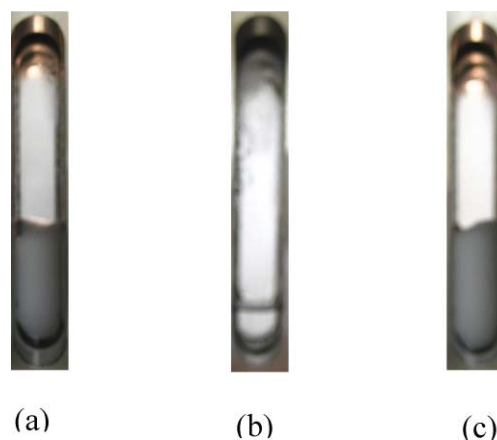
## Results and discussion

### Emulsion formation and stability

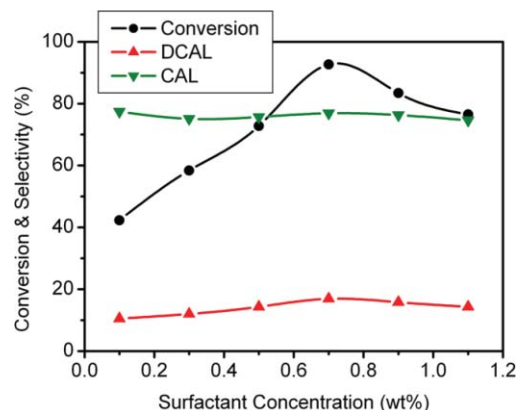
Emulsions are inherently thermodynamically unstable because of the large interfacial free energy compared with the microemulsions, but could be kinetically stable for long periods.<sup>26</sup> For the present C/W emulsion, block copolymer P123 was used as the surfactant to provide steric stabilization, the CO<sub>2</sub>-philic blocks are of poly (propylene oxide), and the CO<sub>2</sub>-phobic blocks are of poly (ethylene oxide), favored the formation of CO<sub>2</sub>-in-water (C/W) emulsion.<sup>27</sup> The stability of the C/W emulsion is highly dependent on the phase behavior.<sup>28</sup> Thus, the phase behavior was investigated by varying the surfactant concentration, temperature and CO<sub>2</sub> pressure. The concentration of surfactant was ranged from 0.1 wt% to 1.1 wt%, which is far beyond the critical micelle concentration of P123 (CMC 0.052 mM at 25 °C).<sup>29</sup> And the surface tension of the P123 aqueous solution has a negligible effect as the surfactant concentration changed during this range.<sup>30</sup> The emulsions could be stable for more than 15 min after ceasing stirrer at the lower temperatures from 35 °C to 65 °C, while a distinct phase separation was observed above 65 °C. Higher temperature caused the EO head groups to dehydrate, therefore its emulsification capacity and solubility in water decreased causing the surfactant to partition further towards CO<sub>2</sub>.<sup>13,31</sup> As the pressure increased, CO<sub>2</sub> was highly dispersed in water and the size of the foams became smaller. It was observed that the volume percentage of CO<sub>2</sub> is about 61% at 8.6 MPa and it increased to 72% when CO<sub>2</sub> pressure was increased up to 9.8 MPa under the ordinary conditions as illustrated in Fig. 1.

### Hydrogenation of citral in C/W emulsion

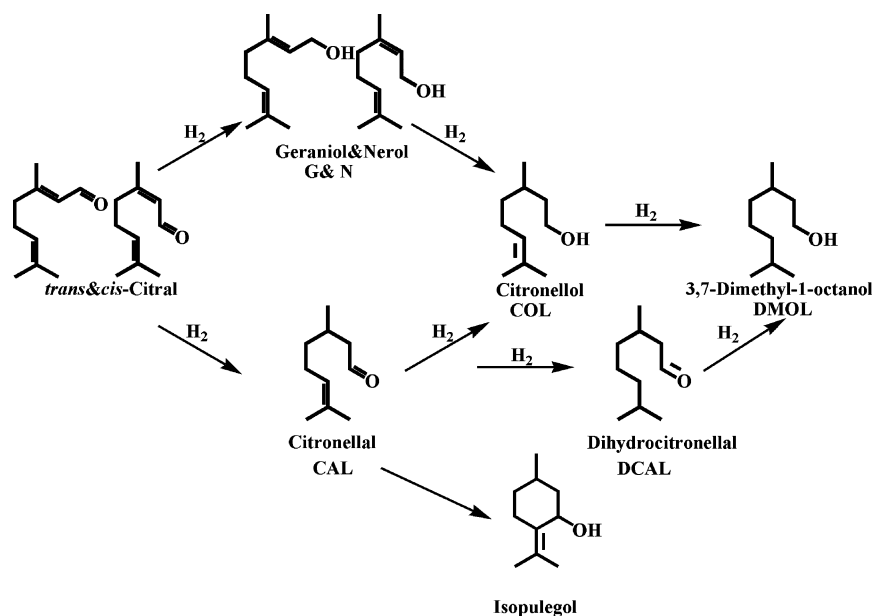
**Surfactant concentration.** Fig. 2 shows the results of citral hydrogenation (Scheme 1) catalyzed by Pd nanoparticles formed *in situ* in C/W emulsion at the different surfactant



**Fig. 1** Photographs of the phase behavior of the C/W emulsion at 0.5 wt% P123 concentration, 45 °C (a) C/W emulsion at 8.6 MPa (b) P123 aqueous solution without CO<sub>2</sub> (c) C/W emulsion at 9.8 MPa.



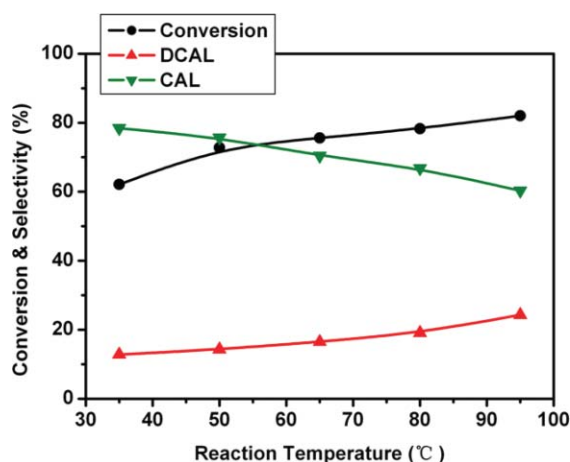
**Fig. 2** Influence of surfactant concentration on citral hydrogenation with Pd nanoparticles in C/W emulsion. Reaction conditions: Citral 5 mmol, H<sub>2</sub> 4 MPa, CO<sub>2</sub> 10 MPa, DI-H<sub>2</sub>O 5 ml, Pd(CH<sub>3</sub>COO)<sub>2</sub> 0.001 mmol, 50 °C, 45 min, wt % relative to the total weight of both water and surfactant.



**Scheme 1** Reaction pathways of citral hydrogenation.

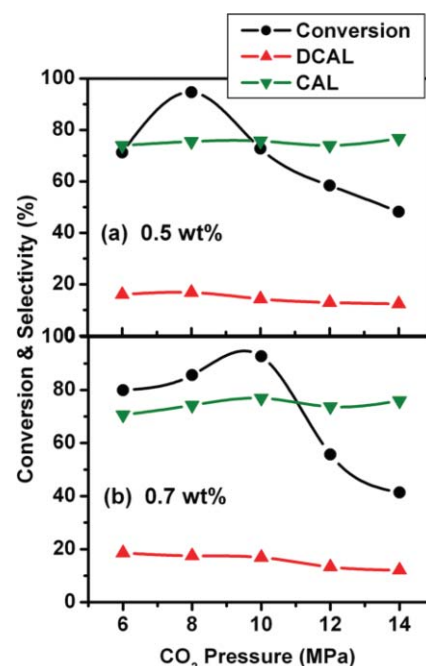
concentrations. As seen, with the surfactant concentration increased from 0.1 wt% to 1.1 wt%, the conversion increased sharply from ~42% to the maximal value of 93% at the concentration of 0.7 wt%, and then decreased as the concentration further increased to 1.1 wt%. However, the selectivity of the main products changed slightly, citronellal was produced with a selectivity above 75% and dihydrocitronellal, its further hydrogenated product, was about 15%, besides trace amounts of geraniol, nerol, isopulegol, as well as 3,7-dimethyl-1-octanol were also detected. The block copolymer, protected and combined with Pd nanoparticles, assembled at the interface of water and CO<sub>2</sub>, and so the emulsion droplets were formed, which act as microreactors (micelle aggregation) during the chemical reaction. And the increase in the surfactant concentration caused an increase of the microreactors, meanwhile the solubilization of the reactants in the micelle could increase, *i.e.* the concentration of citral was increased. Consequently, the conversion of citral increased sharply. But if the concentration of surfactant increases further after the reactants are solubilized almost completely in the micelle, the concentration of the reactants and the catalysts will decrease, causing the reaction rate decrease. Furthermore, as the surfactant concentration increases, the viscosity of the emulsion increases and thus the mass diffusion is hindered.

**Reaction temperature.** The conversion of citral increased linearly as temperature increased as shown in Fig. 3. While for the selectivity, dihydrocitronellal increased at the expense of citronellal. At a constant surfactant concentration of 0.5 wt%, as the temperature increased, the solubility of the surfactant in water decreased in that the EO-water interaction was weakened at a higher temperature causing the increase of microreactors,<sup>13,31,32</sup> which would condense the local concentration of the reactants, and accelerate the reaction rate, except for that the enhancement of temperature itself will accelerate the reaction rate.



**Fig. 3** Results for citral hydrogenation with Pd nanoparticles in C/W emulsion at different reaction temperatures. Reaction conditions: Citral 5 mmol, H<sub>2</sub> 4 MPa, CO<sub>2</sub> 10 MPa, 0.5 wt% P123 5 ml, Pd(CH<sub>3</sub>COO)<sub>2</sub> 0.001 mmol, 45 min.

**CO<sub>2</sub> pressure.** The influence of CO<sub>2</sub> pressure on catalytic activity and product distributions are presented in Fig. 4. The

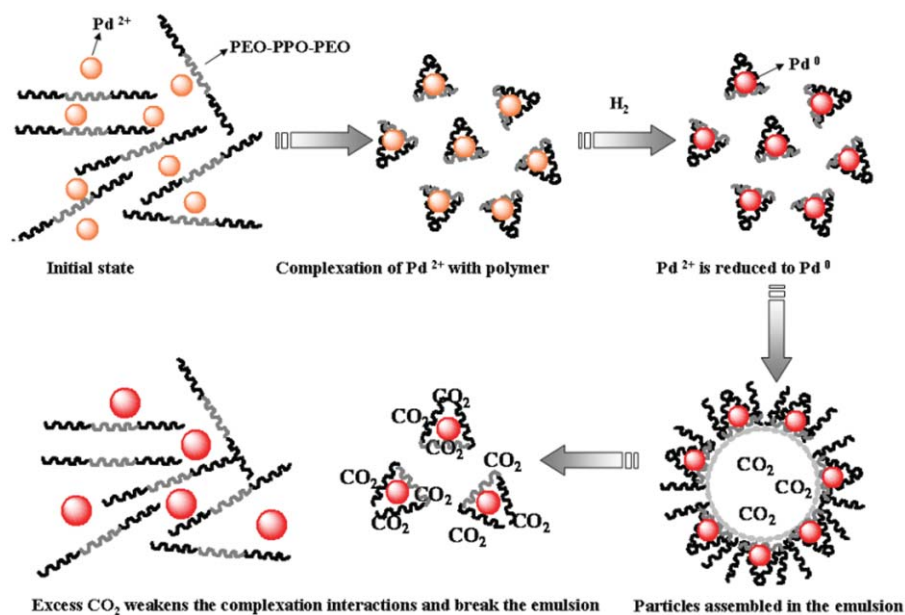


**Fig. 4** Influence of CO<sub>2</sub> pressure on citral hydrogenation with Pd nanoparticles in C/W emulsion with surfactant P123 concentration of (a) 0.5 wt% and (b) 0.7 wt%. Reaction conditions: Citral 5 mmol, H<sub>2</sub> 4 MPa, Pd(CH<sub>3</sub>COO)<sub>2</sub> 0.001 mmol, 50 °C, 45 min.

conversion showed a volcano-trend as CO<sub>2</sub> pressure increased and was irrespective to the concentration of surfactant. However, the maximum conversion was 94.7% at 8 MPa and 92.7% at 10 MPa with the surfactant concentration of 0.5 wt% and 0.7 wt%, respectively. While the product selectivity was almost independent of CO<sub>2</sub> pressure in the present C/W emulsions. But, it was reported that,<sup>33</sup> in W/C microemulsions, the product selectivity could be tuned by changing the pressure of CO<sub>2</sub>, which altered the balance between solvation of the citral molecule into the scCO<sub>2</sub> and its binding affinity to the metal surface.

At a constant temperature, increasing CO<sub>2</sub> pressure, the solubility of CO<sub>2</sub> in the micelle as well as citral in CO<sub>2</sub> increases.<sup>28</sup> In the present C/W emulsion system, CO<sub>2</sub> expanded the micelles and took the reactants (citral and H<sub>2</sub>) to approach the Pd nanoparticles in the micelles, accelerating the reaction rate. Most of the previous studies showed that excess CO<sub>2</sub> decreased the conversion due to the dilute effect.<sup>34,35</sup> It was reported that the stability of the C/W emulsions in the presence of the block copolymers depended strongly on CO<sub>2</sub> pressure.<sup>28</sup> First, the solvation of the stabilizing chains by CO<sub>2</sub> must be sufficient to mediate interactions between chain segments otherwise the solvent will expand away from the chains producing flocculation. Second, the surfactant chains must keep the particles far enough apart to prevent flocculation. So it was speculated that the block copolymer would be solvated properly at appropriate pressure, but at higher CO<sub>2</sub> pressure the emulsions might tend to break and become the solution of unimers of the block copolymer. Furthermore, excess CO<sub>2</sub> weakened the complex interaction between the polymer chains with the Pd nanoparticles. Consequently, the protecting capacity of block copolymer for the Pd nanoparticles would decrease and the schematic diagram was given in Scheme 2.





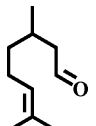
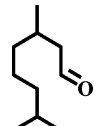
**Scheme 2** Schematic diagram of the formations of Pd nanoparticles and C/W emulsion.

It is well known that water becomes acidic (pH ~ 3) in the presence of CO<sub>2</sub>, due to the formation and dissociation of carbonic acid,<sup>36</sup> but the pH of the solution changed slightly with increasing the CO<sub>2</sub> pressure.<sup>37,38</sup> Acid can salt in non-ionic surfactants in aqueous solutions, because H<sup>+</sup> could form complexes with ether groups in the formation of oxonium compounds,<sup>39</sup> which disrupted the EO–water interactions and pushed the surfactant towards CO<sub>2</sub>, and decreased the capacity to form C/W emulsions.<sup>13</sup> However, the effect of H<sup>+</sup> at these conditions was small,<sup>13,40</sup> and could be ignored.

### Comparison with other catalytic systems

Table 1 gives the results of citral hydrogenation in different systems. When the hydrogenation was performed in neat water the conversion was 65%, while it increased sharply to 95% in the CO<sub>2</sub>/H<sub>2</sub>O system in the presence of 8.5 MPa CO<sub>2</sub>. However, in

**Table 1** Results of hydrogenation of citral in different systems with Pd nanoparticles protected by P123

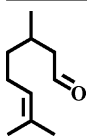
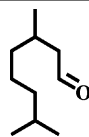
System	Conversion (%)	Selectivity (%)		TOF/h <sup>-1</sup>
				
H <sub>2</sub> O	65	65	22	4313
CO <sub>2</sub> /H <sub>2</sub> O	95	76	17	6333
N <sub>2</sub> /H <sub>2</sub> O	17	66	22	1147
Hexane/H <sub>2</sub> O	6	62	22	387

Reaction conditions: Citral 5 mmol, H<sub>2</sub> 4 MPa, CO<sub>2</sub> 8.5 MPa, 2 ml hexane, N<sub>2</sub> 9.4 MPa, DI-H<sub>2</sub>O 5 ml, Pd(CH<sub>3</sub>COO)<sub>2</sub> 0.001 mmol, 0.5 wt% P123 5 ml, 50 °C, 45 min. TOF (turnover frequency) was calculated as moles conversion of citral/moles of catalyst/time.

the case of using N<sub>2</sub> to replace CO<sub>2</sub>, the conversion decreased to 17%, and the lowest conversion was obtained in the hexane/H<sub>2</sub>O system. With respect to the product selectivity, citronellal was the main product and higher selectivity was obtained in the CO<sub>2</sub>/H<sub>2</sub>O emulsion system.

Furthermore, the hydrogenation of citral in the CO<sub>2</sub>/H<sub>2</sub>O system has been compared with literature as shown in Table 2. A high selectivity of 82% towards the fully hydrogenated aldehyde, dihydrocitronellal, was observed in the vapor phase, but it was 66% in the liquid phase. It was interesting to note that selectivity to dihydrocitronellal was very low (16%) in the present C/W emulsions, but citronellal, one of the most important products of hydrogenation of citral, was obtained as the main product with selectivity around 75% under complete conversion of citral. It was well documented that, for conventional metal catalysts,

**Table 2** Comparison with literature in other catalytic systems for hydrogenation of citral with Pd nanoparticles

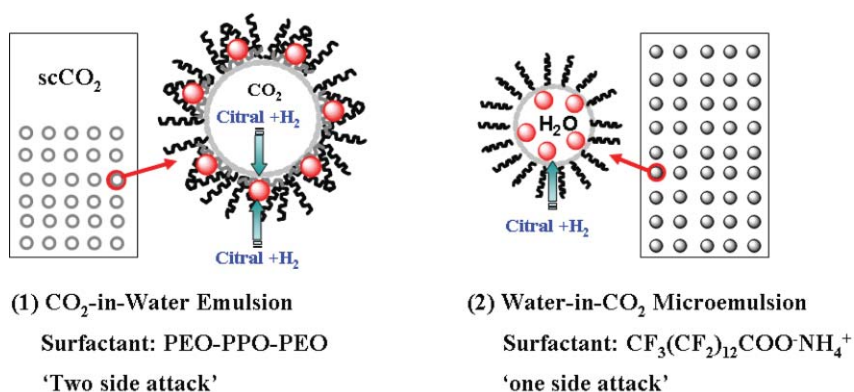
System	Surfactants	Yield (%)		TOF/h <sup>-1</sup>
				
<sup>a</sup> Vapor	—	1	82	—
<sup>a</sup> Cyclohexane	—	19	66	—
<sup>a</sup> W/C	CF <sub>3</sub> (CF <sub>2</sub> ) <sub>12</sub> COO <sup>-</sup> NH <sub>4</sub> <sup>+</sup>	68	12	23.2
Micromulsion	—	—	—	—
<sup>b</sup> C/W Emulsion	PEO-PPO-PEO	72	16	6313

TOF (turnover frequency) was calculated as moles conversion of citral/moles of catalyst/time under citral completely consumed. The product yield was calculated under 100% conversion of citral.<sup>a</sup> results in Ref. 42. <sup>b</sup> present work.

the subsequent hydrogenation of the unsaturated bonds of citral was very difficult to inhibit. Hence, a high selectivity to dihydrocitronellal was normally obtained over Pd catalysts, even for a short contact time.<sup>41</sup> It was reported that the micelle environment was responsible for the high selectivity to citronellal in the W/C microemulsions over Pd nanoparticles, and it was thought that the conjugated C=C bond preferred to be close to the metal particles in the W/C microemulsion.<sup>42</sup> In the present work, the higher selectivity of citronellal in C/W emulsions was also attributed to its higher solubility in scCO<sub>2</sub>, besides the presence of water would facilitate the adsorption of the conjugated C=C bond on the surface of the catalyst. It was observed that citral (5 mmol) is completely soluble in scCO<sub>2</sub> at 8.6 MPa and citronellal (5 mmol) soluble in scCO<sub>2</sub> at 7.9 MPa, 50 °C, *i.e.* the solubility of citronellal is 1.91% (molar fraction), which is higher than that of citral (1.75%). In the present system, the C/W emulsion and scCO<sub>2</sub> phases were observed through the view cell. Citronellal could be extracted into the scCO<sub>2</sub> phase as it formed during the reaction, and isolated from the catalytic C/W emulsion phase so its further hydrogenation to dihydrocitronellal was prohibited. With respect to the reaction activity, the current C/W emulsion system gave a much higher turnover frequency (TOF) (6313 h<sup>-1</sup>), which is 272 times higher than that in the W/C microemulsion (TOF, 23.2 h<sup>-1</sup>), although the area/volume is higher for a microemulsion droplet compared to emulsion one. These results could be well explained by the reaction mechanism as illustrated in Scheme 3, in present C/W emulsion formed with the nonionic surfactant P123, the reactants of citral and H<sub>2</sub> were dissolved in both the inner CO<sub>2</sub> core and outer surfactant shell, so the reactant molecules could attack the Pd nanoparticles from both the inter and outer surfaces of emulsion. While in the W/C microemulsion formed with ionic surfactant CF<sub>3</sub>(CF<sub>2</sub>)<sub>12</sub>COO<sup>-</sup>NH<sub>4</sub><sup>+</sup>, the reactants could only attack from the outer surfactant shell due to the reactants not being solubilized in the water core. So the present C/W emulsion is more efficient and suitable for the 'CO<sub>2</sub>-soluble reactants' reactions compared with W/C microemulsions.

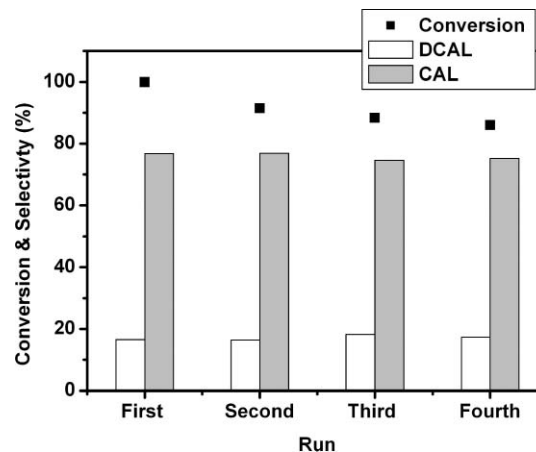
### Separation and recycling of the catalysts

It was also suggested that the Pd nanoparticles were more stable in the C/W emulsion stabilized with P123, because



**Scheme 3** Diagram of citral hydrogenation with Pd nanoparticles in (1) C/W emulsions (2) W/C microemulsions.

the PEO-PPO-PEO block copolymer could stabilize the Pd nanoparticles through the formation of a complexation bond between PEO and PPO with the metal particles. Moreover, the block copolymer could prohibit the agglomeration of Pd nanoparticles *via* the coverage of the block copolymer on the surface of Pd nanoparticles as reported in the literature.<sup>43</sup> The stability of Pd nanoparticles has been examined in the present work, the hydrogenated products were separated from the emulsion successfully by extraction with scCO<sub>2</sub>, and the Pd nanoparticles and surfactant left in the aqueous phase were reused several times. The recycling results are given in Fig. 5. The conversion decreased gradually in the recycling runs, but dropped to 86% from 99.9% after the fourth run due to the agglomeration of Pd nanoparticles. The TEM images of Pd nanoparticles in Fig. 6 show that the size of Pd nanoparticles was about 1 nm after the first run (Fig. 6a), but the size grew up to about 8 nm after the fourth runs (Fig. 6b). The agglomeration of Pd nanoparticles should be responsible for the activity decrease, which was also claimed in the hydrogenation of olefins in the W/C microemulsion stabilized with sodium bis(2-ethylexyl) sulfosuccinate (AOT).<sup>25</sup> In the recycling runs, the selectivity of the main products was almost unchanged,



**Fig. 5** Recycling results of Pd nanoparticles in citral hydrogenation in the C/W emulsion. Reaction conditions: Citral 5 mmol, H<sub>2</sub> 4 MPa, 8 MPa CO<sub>2</sub>, 0.5 wt% P123 5 ml, Pd(CH<sub>3</sub>COO)<sub>2</sub> 0.001 mmol, 60 min, 50 °C.

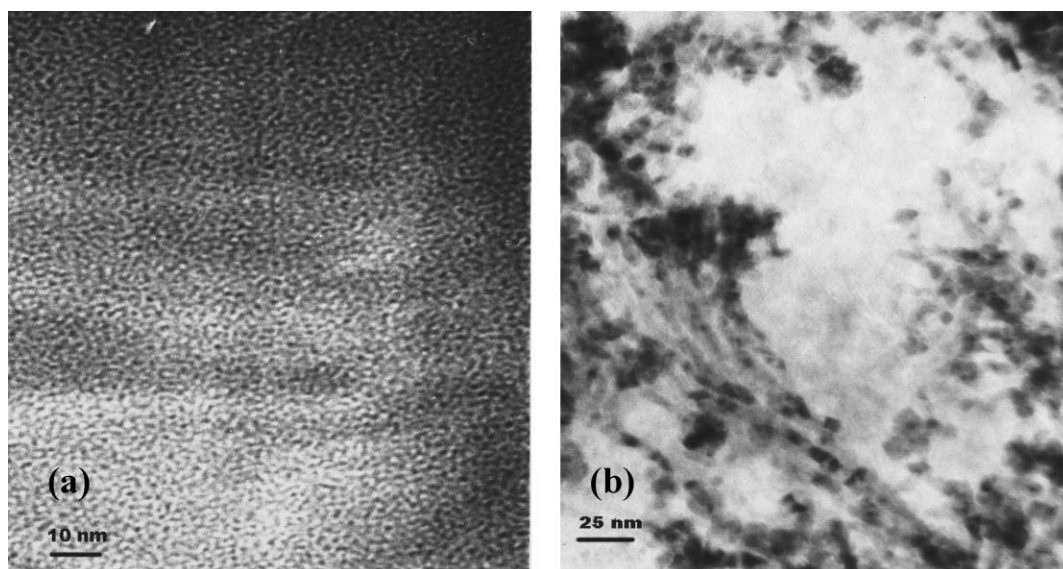


Fig. 6 TEM images of the Pd nanoparticles (a) After the first run; (b) After the fourth run.

suggesting that the product distribution does not depend on the Pd particle size under the conditions used, which is in agreement to the citral hydrogenation catalyzed with Ru catalyst.<sup>44</sup>

## Conclusion

The environmental benign CO<sub>2</sub>-in-water emulsion was formed by the assembly of the block copolymer P123 at the water–CO<sub>2</sub> interphase. Pd nanoparticles synthesized *in situ* by H<sub>2</sub> reduction was an efficient catalyst for citral hydrogenation in the emulsion. Higher TOF of 6313 h<sup>-1</sup> and higher selectivity to citronellal (>75 %) were obtained compared to other catalytic systems. The excellent performance is ascribed to the unique emulsion environment. The C/W emulsion formed with block copolymer P123 could make reactants of citral existing in CO<sub>2</sub> core as well as in the surfactant shell, so that the ‘two sides attack’ model resulted in the higher reaction rate compared with the W/C microemulsion. And the higher selectivity of citronellal obtained in the present system is due to citronellal being extracted to the scCO<sub>2</sub> phase and its further hydrogenation was prohibited. In addition, the Pd nanoparticles in C/W emulsion could be recycled several times and still retain the same selectivity, while the Pd nanoparticles aggregated slightly during recycling and led to a decrease in conversion.

## Experimental details

### Materials

Citral (*trans* and *cis*), Pd(CH<sub>3</sub>COO)<sub>2</sub>, and poly(ethylene oxide)-poly(propylene oxide)-poly(ethylene oxide) (EO)<sub>19</sub>(PO)<sub>70</sub>(EO)<sub>19</sub> block copolymer (P123) were purchased from Aldrich. Gases of CO<sub>2</sub> (99.9 %) and H<sub>2</sub> (99.999 %) (Changchun Xinxing Gas Company) were used as delivered. Double distilled water was used.

### Apparatus and phase behavior studies

The phase behavior of the CO<sub>2</sub>-in-water emulsions was observed in 80 ml view cell. In a typical experiment, appropriate amounts of citral, P123, de-ionized water and Pd(CH<sub>3</sub>COO)<sub>2</sub> were added into the reactor in order to create the same conditions as those in the 50 ml reactor, and then replaced the air in the view cell by CO<sub>2</sub>. After that, the contents were heated up to the desired temperature. After thermal equilibrium had been reached, the stirrer was started. H<sub>2</sub> firstly and then CO<sub>2</sub> were charged into the cell slowly and the solution was hazy and milky.

### Catalytic hydrogenation

The hydrogenation of citral was carried out in a stainless steel batch reactor (50 ml), and the Pd nanoparticles were synthesized *in situ* by H<sub>2</sub> reduction in the C/W emulsion. Typically, 5 ml of P123 aqueous solution, 0.001 mmol of Pd(CH<sub>3</sub>COO)<sub>2</sub> and 5 mmol of Citral (with a mole ratio of citral/Pd of 5000) were added into the reactor. The reactor was then sealed and flushed with 2 MPa CO<sub>2</sub> more than three times. H<sub>2</sub> firstly and then CO<sub>2</sub> were introduced into the reactor to the desired pressure with a high-pressure liquid pump after the reactor was heated up to the desired temperature. The mixture was stirred continuously during the reaction, and the speed of stirring kept constant for all the reactions. At the end of the reaction, the reactor was cooled to room temperature and the gases (H<sub>2</sub> and CO<sub>2</sub>) stream were vented to ambient pressure through the traps containing *n*-hexane. Then the reactor was opened, and the remaining residue was extracted with another portion of *n*-hexane. The resulting solutions were combined and analyzed with gas chromatography (GC-Shimadzu-14C, FID, Capillary column Rtx-Wax 30 m–0.53 mm–0.25 mm) and gas chromatography/mass spectrometry (GC/MS, Agilent 5890).

For the catalyst recycling, after one reaction was finished, the reaction mixture was extracted with 7.6 MPa CO<sub>2</sub> at a flowing rate of 2 ml min<sup>-1</sup> at 35 °C until no effusion came out, and

the reaction mixture were almost completely extracted within 30 min. Then the next run was carried out with recharging the fresh reactants.

## Acknowledgements

The authors gratefully acknowledge to the financial support from the NSFC 20573104 and the One Hundred Talent Program of CAS.

## References

- 1 Y. X. Liu, P. G. Jessop, M. Cunningham, C. A. Eckert and C. L. Liotta, *Science*, 2006, **313**, 958–960.
- 2 A. S. Utada, E. Lorenceau, D. R. Link, P. D. Kaplan, H. A. Stone and D. A. Weitz, *Science*, 2005, **308**, 537–541.
- 3 A. D. Dinsmore, M. F. Hsu, M. G. Nikolaidis, M. Marquez, A. R. Bausch and D. A. Weitz, *Science*, 2002, **298**, 1006–1009.
- 4 S. Partap, I. Rehman, J. R. Jones and J. A. Darr, *Adv. Mater.*, 2006, **18**, 501–504.
- 5 J. P. Hanrahan, K. J. Ziegler, J. P. Galvin and J. D. Holmes, *Langmuir*, 2004, **20**, 4386–4390.
- 6 R. Butler, I. Hopkinson and A. I. Cooper, *J. Am. Chem. Soc.*, 2003, **125**, 14473–14481.
- 7 K. P. Johnston, K. L. Harrison, M. J. Clarke, S. M. Howdle, M. P. Heitz, F. V. Bright, C. Carlier and T. W. Randolph, *Science*, 1996, **271**, 624–626.
- 8 J. Zhu, A. Robertson and S. C. Tsang, *Chem. Commun.*, 2002, **18**, 2044–2045.
- 9 K. E. O Shea, K. M. Kirmse, M. A. Fox and K. P. Johnston, *J. Phys. Chem.*, 1991, **95**, 7863–7867.
- 10 T. A. Hoefling, R. R. Beitle, R. M. Enick and E. J. Beckman, *Phase Equilibria*, 1993, **83**, 203–212.
- 11 J. B. McClain, D. E. Betts, D. A. Canelas, E. T. Samulski, J. M. DeSimone, J. D. Londono, H. D. Cochran, G. D. Wignall, D. C. Martino and R. Triolo, *Science*, 1996, **274**, 2049–2052.
- 12 S. R. P. da Rocha, J. Dickson, D. M. Cho, P. J. Rossky and K. P. Johnston, *Langmuir*, 2003, **19**, 3114–3120.
- 13 S. R. P. da Rocha, P. A. Psathas, E. Klein and K. P. Johnston, *J. Colloid Interface Sci.*, 2001, **239**, 241–253.
- 14 W. Ryoo, S. E. Webber and K. P. Johnston, *Ind. Eng. Chem. Res.*, 2003, **42**, 6348–6358.
- 15 J. C. Liu, B. X. Han, G. Z. Li, X. G. Zhang, Z. M. He and J. Liu, *Langmuir*, 2001, **17**, 8040–8043.
- 16 K. P. Johnston, D. M. Cho, S. R. P. da Rocha, P. A. Psathas, W. Ryoo, S. E. Webber, J. Eastoe, A. Dupont and D. C. Steytler, *Langmuir*, 2001, **17**, 7191–7193.
- 17 G. B. Jacobson, C. T. Lee, S. R. P. da Rocha and K. P. Johnston, *J. Org. Chem.*, 1999, **64**, 1207–1210.
- 18 G. B. Jacobson, C. T. Lee, K. P. Johnston and W. Tumas, *J. Am. Chem. Soc.*, 1999, **121**, 11902–11903.
- 19 M. Boutonnet, J. K. P. Stenius and G. Maire, *Colloids Surf.*, 1982, **5**, 209.
- 20 U. Nylen, S. Eriksson, S. Rojas and M. Boutonnet, *Appl. Catal. A.*, 2004, **265**, 207–219.
- 21 J. C. Liu, Y. Ikushima and Z. Shervani, *Curr. Opin. Solid. State. Mater. Sci.*, 2003, **7**, 255–261.
- 22 M. Ji, X. Y. Chen, C. M. Wai and J. L. Fulton, *J. Am. Chem. Soc.*, 1999, **121**, 2631–2632.
- 23 H. Ohde, C. M. Wai, H. Kim, J. Kim and M. Ohde, *J. Am. Chem. Soc.*, 2002, **124**, 4540–4541.
- 24 H. Ohde, F. Hunt and C. M. Wai, *Chem. Mater.*, 2001, **13**, 4130–4135.
- 25 M. Ohde, H. Ohde and C. M. Wai, *Langmuir*, 2005, **21**, 1738–1744.
- 26 C. T. Lee, P. A. Psathas, K. P. Johnston, J. de Grazia and T. W. Randolph, *Langmuir*, 1999, **15**, 6781–6791.
- 27 E. Ruckentein, *Langmuir*, 1996, **12**, 6351–6353.
- 28 K. P. Johnston, *Curr. Opin. Colloid Interface Sci.*, 2000, **5**, 351–356.
- 29 T. S. P. Alexandridis, *Langmuir*, 2004, **20**, 8426–8430.
- 30 Y. L. Su, C. Guo, X. F. Wei and H. Z. Liu, *Chin. J. Process. Eng.*, 2001, **1**, 214–217.
- 31 U. Olsson and H. Wennerstrom, *Adv. Colloid Interface Sci.*, 1994, **49**, 113.
- 32 M. L. O'Neill, Q. Cao, R. Fang, K. P. Johnston, S. P. Wilkinson, C. D. Smith, J. L. Kerschner and S. H. Jureller, *Ind. Eng. Chem. Res.*, 1998, **37**, 3067–3079.
- 33 P. Meric, K. M. K. Yu, A. T. S. Kong and S. C. Tsang, *J. Catal.*, 2006, **237**, 330–336.
- 34 R. X. Liu, F. Y. Zhao, S. Fujita and M. Arai, *Appl. Catal. A.*, 2007, **316**, 127–133.
- 35 M. Chatterjee, F. Y. Zhao and Y. Ikushima, *Adv. Syn. Catal.*, 2004, **346**, 459–466.
- 36 D. J. Holmes, K. J. Ziegler, M. Audriani, C. T. J. Lee, P. A. Bhargava, D. C. Steytler and K. P. Johnston, *J. Phys. Chem. B.*, 1999, **103**, 5703–5711.
- 37 L. Karen, R. M. S. Toews and C. M. Wai, *Anal. Chem.*, 1995, **67**, 4040–4043.
- 38 M. A. S. C. Roosen, M. Thomas, W. Leitner and L. Greiner, *Green Chem.*, 2007, **9**, 455–458.
- 39 H. Schott, *J. Colloid Interface Sci.*, 1973, **43**, 150.
- 40 R. Zhang, J. Liu, J. He, B. X. Han, X. G. Zhang, Z. M. Liu, T. Jiang and G. H. Hu, *Macromolecules*, 2002, **35**, 7869–7871.
- 41 R. L. Augustine, Marcel Dekker Inc., New York, 1996.
- 42 P. Meric, K. M. K. Yu and S. C. Tsang, *Langmuir*, 2004, **20**, 8537–8545.
- 43 T. Sakai and P. Alexandridis, *J. Phys. Chem. B*, 2005, **109**, 7766–7777.
- 44 C. M. S. Galvagno, A. Donato, G. Neri and R. Pietropaolo, *Catal. Lett.*, 1993, **18**, 349.

# Supercritical-fluid-assisted oxidation of oleic acid with ozone and potassium permanganate

Darrell L. Sparks, L. Antonio Estévez and Rafael Hernandez\*

Received 22nd September 2008, Accepted 23rd March 2009

First published as an Advance Article on the web 9th April 2009

DOI: 10.1039/b816515g

The goal of this research was to determine if any advantages could be realized by conducting the oxidation of oleic acid with ozone and potassium permanganate in supercritical carbon dioxide (SC-CO<sub>2</sub>). The ozonolysis of oleic acid without SC-CO<sub>2</sub> at 313.15 K and ambient pressure resulted in complete conversion of the oleic acid within 2 hrs. The reaction was zero-order, indicating the system was mass-transfer limited, and the rate of oleic acid disappearance was 0.077 mol s<sup>-1</sup> m<sup>-3</sup>. Due to experimental limitations, no reaction was observed in the case of ozone in SC-CO<sub>2</sub>. However, oxidation of oleic acid with potassium permanganate in SC-CO<sub>2</sub> at 12.2 MPa resulted in an increase in oleic acid conversion from 50.8% to 95.1% at 308.15 K and 51.7% to 95.6% at 318.15 K. Oleic acid oxidation with potassium permanganate in supercritical carbon dioxide was found to have a reaction order of 1.75 with rate constants of 5.33 × 10<sup>-5</sup> m<sup>2.25</sup> s<sup>-1</sup> mol<sup>-0.75</sup> and 1.43 × 10<sup>-4</sup> m<sup>2.25</sup> s<sup>-1</sup> mol<sup>-0.75</sup> at 308.15 K and 318.15 K, respectively. Also, increased yields of the target products, azelaic acid and pelargonic acid, were obtained when compared to the oxidation without SC-CO<sub>2</sub>. In terms of greenness, the addition of SC-CO<sub>2</sub> allows product separation to be combined with reaction, which reduces the need for other energy-intensive separations, such as distillation, which are traditionally used. In comparing the two oxidizers, ozone is more efficient, but the use of potassium permanganate would eliminate concerns associated with fugitive emissions of ozone into the environment.

## Introduction

With ever increasing demands for sustainability and stricter environmental controls, much research has gone into the area of alternative solvents. This is due to the use of large quantities of solvents in the chemical industry, especially in specialty-chemical and pharmaceutical production. Traditionally, organic solvents have been utilized in many chemical processes; however, they are often associated with having negative environmental and health impacts. Many pathways have been proposed to reduce the use of organic solvents, including:<sup>1-3</sup>

- Substitution of hazardous solvents with ones that show better environmental, health, and safety properties
- The use of solvents produced from renewable resources
- Substitution of organic solvents with solvents such as supercritical carbon dioxide that are environmentally harmless
- The use of ionic liquids that exhibit very low vapor pressures
- The use of water as a solvent
- Elimination of the need for a solvent
- The use of solid support reagents and catalysts

Supercritical fluids have been widely researched as alternative solvents and are useful in a variety of applications.<sup>4</sup> Worldwide, supercritical fluids have been incorporated into over 100 plants in the areas of production, environmental applications, and

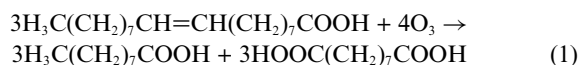
particle engineering.<sup>5</sup> Most of the research on supercritical fluids has dealt with mass-transfer applications such as extraction and chromatography because of the unique properties a fluid obtains in the supercritical state. Typically, the density of the supercritical fluid is closer to that of a liquid. However, when compared to its liquid state, a supercritical fluid has a lower viscosity and a higher diffusivity, which results in more efficient mass transfer. Supercritical fluids are often called *tunable* solvents because slight changes in temperature and pressure can have very pronounced effects on solvent properties. Since density is directly related to the solvating power of a fluid, the ability to finely control density results in facilitated separations.

Supercritical fluids can also be used in chemical reactions. For example, supercritical water has been found to be an effective oxidizer of organics such as pyridine, and supercritical propane can be used in the hydrogenation of fats and oils.<sup>6</sup> Carbon dioxide is one of the most researched supercritical fluids. Besides the inherent safety features (non-toxic, non-flammable) and low critical temperature of carbon dioxide, it is also very plentiful and inexpensive. Most carbon dioxide sold is isolated from existing processes such as production of ethanol, ammonia, and hydrogen. Compared to other commonly used supercritical fluids, particularly water, carbon dioxide has a low heat of vaporization, which can lead to lower energy costs.<sup>7</sup> These factors make supercritical carbon dioxide (SC-CO<sub>2</sub>) a very attractive reaction medium. For example, supercritical carbon dioxide has been heavily researched for use in the production of polymers such as polymethylmethacrylate, polystyrene, and fluoropolymers.<sup>8</sup> Supercritical carbon dioxide has been also

Dave C. Swalm School of Chemical Engineering, Mississippi State University, PO Box 9595, Mississippi State MS 39762-9595, USA.  
E-mail: rhernandez@che.msstate.edu; Fax: (662) 325-2482; Tel: (662) 325-0790

utilized for oxidation of organics such as cyclohexene and phenols.<sup>8</sup> Carbon dioxide is well-suited for oxidation reactions because it is already completely oxidized; hence, it does not form oxidation products. Also, gases such as oxygen are completely miscible with supercritical carbon dioxide, eliminating mass-transfer limitations. Depending upon the solubility of reaction products in supercritical carbon dioxide, the reaction can be coupled with extraction, reducing or even eliminating the need for typical separation processes such as distillation.

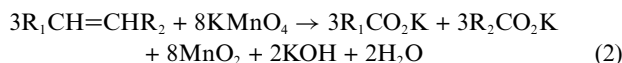
Currently, much research is being conducted on renewable sources for fuels and chemicals that have been traditionally supplied by petroleum processing. In particular, fatty acids that comprise lipids of plants, animals, and microorganisms can be used to generate a variety of chemical intermediates. One of the most common unsaturated fatty acids is oleic acid, and it can be oxidized to produce azelaic acid (a diacid) and pelargonic acid (a monoacid).<sup>9</sup> Azelaic acid is used in pharmaceuticals for treatment of skin conditions such as *acne rosacea* as well as in the formulation of polymers.<sup>10,11</sup> Pelargonic acid can be used to manufacture lacquers and plastics.<sup>12</sup> Due to the versatility of diacids such as azelaic acid, new sources and production pathways are being pursued.<sup>13</sup> Ozonolysis of oleic acid is currently the most economical method to generate azelaic and pelargonic acid. The overall reaction<sup>14–16</sup> of oleic acid with ozone can be shown as:



However, the efficiency of the process could be improved in terms of both the oxidation reaction and product separation. Since oleic acid is a liquid and ozone is a gas, the oxidation occurs in multiphase reactors initially at temperatures between 298.15 to 318.15 K. During the first phase of the oxidation, ozone produced from an oxygen-rich feed reacts with the oleic acid to form ozonide products. In the second step of the reaction, the ozonides are heated to between 348.15 and 393.15 K and contacted with oxygen (no ozone) to obtain the final products of carboxylic acids. To establish contact between the two reactants, countercurrent mixing is used. Since the reactants are in two separate phases, the ozone must diffuse into the liquid phase, which results in mass-transfer limitations. In terms of product separation, distillation is typically used to remove the pelargonic acid at conditions of 503.15 K and 3.33 kPa, and the remaining mixture is extracted with hot water. The azelaic acid is soluble in hot water, but as temperature is reduced, the solubility drops rapidly. Therefore, azelaic acid is removed from the aqueous extract *via* crystallization.<sup>17,18</sup> Both crystallization and distillation can be energy-intensive, resulting in high operating costs. If the reactants can be solubilized into a single phase, then mass-transfer limitations could be avoided. Gases such as oxygen and ozone are completely miscible with supercritical carbon dioxide.<sup>19</sup> Additionally, studies have shown that oleic acid has some degree of solubility in supercritical carbon dioxide.<sup>20–25</sup> Studies have also shown that azelaic acid and pelargonic acid significantly differ in terms of their solubility in supercritical carbon dioxide, indicating the possibility of product fractionation.<sup>26,27</sup> As previously mentioned, carbon dioxide is an ideal reaction medium for oxidation reactions because it is

already oxidized; hence, it will not react with ozone to form oxidation products.

Although no previous studies have reported on ozonolysis of lipids in supercritical carbon dioxide, a recent study by Mercangöz *et al.*<sup>28</sup> investigated the use of sub/supercritical carbon dioxide as a reaction medium for the oxidation of soybean oil with aqueous potassium permanganate.<sup>28</sup> Soybean oil is primarily composed of unsaturated fatty acids. To follow reaction progress, the authors monitored consumption of the double bonds with time. In a control reaction between oleic acid and aqueous potassium permanganate at conditions of 298.15 K and atmospheric pressure for 12 hours, no measurable reaction occurred. However, they observed 29% double bond consumption when using the supercritical fluid medium for a 12-hour batch reaction at 298.15 K and a pressure of 7 MPa. Mercangöz *et al.*<sup>28</sup> only considered aqueous solutions of potassium permanganate. However, Sam and Simmons<sup>29</sup> studied the oxidation of organic compounds with potassium permanganate without the use of water and proposed the following overall reaction:



with the oxidation being initiated by the electrocyclic addition of the permanganate ion to the olefinic  $\pi$  bond to form the corresponding manganate ester ion. Instead of water, a crown ether was used as a complexing agent to bring the solid potassium permanganate into an organic solvent (benzene) so that the oxidant could react with the compound of interest. Using this approach, reactions of olefins were found to occur very rapidly with complete conversion observed in many cases. The objective of this study was to evaluate the impact of supercritical carbon dioxide on the oxidation of oleic acid with ozone and potassium permanganate. The effects of the supercritical fluid on oleic acid conversion, reaction rate, and product yield were evaluated.

## Experimental

### Materials

The following lipids were purchased from Sigma-Aldrich: oleic acid (*cis*-9-octadecenoic acid;  $\approx$  99% purity), pelargonic acid (nonanoic acid; minimum 96% purity), methyl oleate (methyl *cis*-9-octadecenoate;  $\geq$  99% purity), methyl pelargonate (methyl nonanoate;  $\geq$  99.8% purity), azelaic acid (nonanedioic acid;  $\geq$  99% purity), dimethyl azelate (dimethyl nonanedioate; 80% purity), and pelargonaldehyde (nonanal;  $\geq$  95% purity). Potassium permanganate (99+% purity) and 1,3-dichlorobenzene ( $\geq$  99.0% purity) were also purchased from Sigma-Aldrich. Hexane (Optima grade), toluene (Optima grade), methanol (Optima grade), and sulfuric acid (technical grade) were purchased from Fisher Scientific. Ozone was generated *via* corona discharge from oxygen in a Model LC-1234 Ozone Generator from Ozonology, Inc. (Northbrook, IL). NexAir (Memphis, TN) provided carbon dioxide (Industrial grade,  $\geq$  99.8% purity), which was further purified by passing it through a 2- $\mu\text{m}$  filter (Valco Instrument Company, Inc., Houston, TX). All other chemicals were used without further purification.

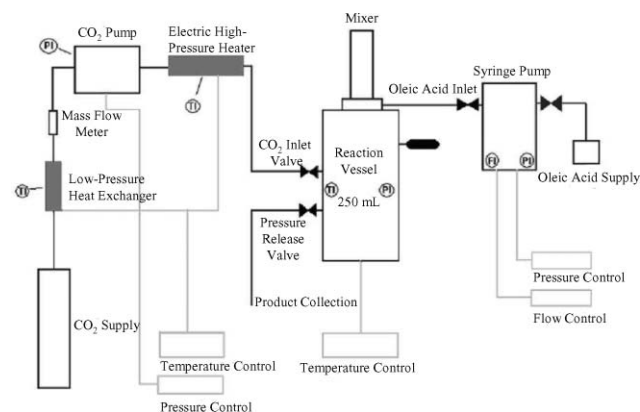
## Permanganate oxidation of oleic acid

**Ambient pressure permanganate oxidation.** For the experiments at ambient pressure, 8 g of potassium permanganate were placed into a 100-mL round bottom glass reactor (Chemglass Model CG 1514-01; Vineland, NJ), which was equipped with a thermometer to monitor temperature. The reactor was placed in an oil bath and heated to the desired temperature of the reaction. Then 1 mL (0.891 g) of oleic acid was added dropwise to the reactor over a period of 10 minutes using a pipette. Adding the oleic acid slowly to the potassium permanganate minimized the effect of the exothermic reaction on the bulk temperature. After addition of the oleic acid, magnetic stirring was initiated and the reaction time was started. The reactor was capped with a solid PTFE stopper to minimize oxidation of the oleic acid with atmospheric oxygen. Experiments were conducted for 12 hours at 308.15 K and 318.15 K.

At the end of the reaction time, the reactor was removed from the oil bath, and a solution of 2% by weight sulfuric acid in methanol was added to the reaction mixture in five 10-mL portions, which served to quench the reaction. The methanol with sulfuric acid reduced the potassium permanganate to manganese dioxide. Due to the large excess of methanol compared to potassium permanganate, the volume of methanol consumed in the quenching reaction was negligible. A 1-mL aliquot was filtered over a Whatman Type GF/B Filter (Fisher Scientific) with 3 mL of 2% by weight sulfuric acid in methanol to remove the manganese dioxide. The filtrate was collected in a 20 mL test tube. Then an additional 2 mL of the sulfuric acid in methanol solution was added to the test tube along with 1 mL of toluene, and the vial was incubated overnight at 323.15 K to convert the products to methyl esters for analysis.

**High pressure permanganate oxidation.** For the supercritical fluid experiments, 8 g of potassium permanganate were placed into a 250-mL stainless steel reaction vessel (Model R250; Thar Technologies; Pittsburgh, PA), and then the vessel was sealed with a Nitronic 60 stainless steel cap equipped with a magnetic stirrer. The reactor was heated while carbon dioxide was fed into the reactor using a dual-piston pump (Model P-50; Thar Technologies; Pittsburgh, PA) until the required pressure was reached. Then 1 mL (0.891 g) of oleic acid was added to the reactor over a period of 10 minutes using a syringe pump (Teledyne Isco Model 100DX; Lincoln, NE). Based upon data from the literature,<sup>20–25</sup> that amount of oleic acid was completely soluble in the supercritical carbon dioxide. After adding the oleic acid, stirring at 1000 RPM was initiated, and the reaction time was started. A schematic of the experimental apparatus can be seen in Fig. 1. Reactions were conducted at a pressure of 12.2 MPa and at temperatures of 308.15 K and 318.15 K for times ranging from 10 to 720 minutes.

At the end of the reaction period, agitation was stopped and heating was turned off. Then the reactor was depressurized by allowing the gas phase to exit through the pressure release valve shown in Fig. 1. An Erlenmeyer flask topped with glass wool trapped products entrained in the gas phase. Then five 10-mL portions of a 2% by weight sulfuric acid in methanol solution were added to both the contents of the Erlenmeyer flask and the stainless steel reactor. Then 1-mL aliquots from



**Fig. 1** Experimental apparatus used for permanganate reactions in SC-CO<sub>2</sub>.

the flask and the reactor were prepared for analysis as previously described.

**Analysis of permanganate oxidation products.** At the end of the derivatization period, the oxidation products were extracted with hexane. Then a solution of 1,3-dichlorobenzene was added as an internal standard prior to analysis with a Varian 3600 gas chromatograph (GC) coupled to a Saturn 2000 mass spectrometer (MS) detector (Varian; Palo Alto, CA). The chromatographic separation of reaction products from the potassium permanganate oxidation experiments was obtained using a Rtx-5MS column (30 m in length × 0.25 mm inner diameter × 0.25 μm film thickness) manufactured by Restek (Bellefonte, PA). The stationary phase of the column consisted of crosslinked 5% diphenyl/95% dimethyl polysiloxane. The injector was operated at 280 °C in splitless mode with 1 μL injection volume. The oven was programmed with an initial temperature of 50 °C, held for 3 minutes and was then ramped to 150 °C at 10 °C/min, then ramped to 190 °C at 1 °C/min, and finally ramped to 280 °C at 10°/min and held for 2 min. Helium served as the carrier gas, and the gas cylinders utilized a Built in Purifier (BIP®, AirGas; Radnor, PA). The chromatographic system utilized the NIST library to aid in compound identification. Prior to sample analysis, the GC-MS was calibrated in electron impact (EI) mode for methyl oleate, methyl pelargonate, and dimethyl azelate with 1,3-dichlorobenzene as an internal standard. All calibration curves generated had a minimum *r*<sup>2</sup> value of 0.995. The external standards were generated from fatty acid standards using the acid-catalyzed esterification technique previously mentioned. Chemical ionization (CI) mode with isobutane was used to determine molecular weight of unidentified species.

## Ozonolysis of oleic acid

**Traditional ozonolysis.** The goal of the traditional oxidation experiments was to provide benchmarks in terms of conversion, reaction rate, and products formed. A quantity of 75 g of oleic acid was combined with 310 g of pelargonic acid in a 500 mL jacketed reaction vessel (Chemglass Model CG-1928-01; Vineland, NJ) equipped with Morton indentations, which provided better mixing. The contents of the reactor were then mixed using a magnetic stir bar and heated to 313.15 K using an Isotemp Model 145D Dry-Bath Incubator (Fisher Scientific) to

circulate water through the reactor jacket. Then the reactor was capped with a lid (Chemglass Model CG-1944-01; Vineland, NJ) equipped with three 24/40 necks and one #7 Chem-Thread neck. Upon reaching 313.15 K, ozone was sparged into the reactor from the ozone generator at a mass fraction of 5.06% in oxygen (1.18 SLM) using a bubble stone. The ozone was delivered to the reactor using tubing inserted through a 0.635 cm wide hole drilled through a 24/40 PTFE stopper. Only 0.635 cm OD (outer diameter) PTFE tubing was used throughout these experiments. Unreacted ozone left the reactor through a separate neck equipped with another drilled PTFE stopper and traveled to a Model HC Ozone Monitor (PCI Ozone & Control Systems, Inc.; West Caldwell, NJ). Upon leaving the ozone monitor, the unreacted ozone was sent to a flask containing Carulite® 200 (manganese dioxide/copper oxide; Carus Chemical Company; Peru, IL), which served as a catalyst to decompose the oxidant. Ozone was supplied to the reactor for 2.5 hours. Then the stream of ozone in oxygen was turned off at the generator while the reaction mixture was heated to 353.15 K. Oxygen (no ozone) was then supplied to the reactor for an additional 3.5 hours for a total reaction time of 6 hours.

One of the 24/40 necks was outfitted with a sampling adapter equipped with a PTFE-silica-PTFE septum. Samples were collected using an 18-gauge needle (Popper Deflected Noncoring Septum Penetration Needle; Fisher Scientific) that was 30.5 cm in length connected to a 20-mL, Luer-lock syringe (Perfektum Micro-Mate Interchangeable Syringe; Fisher Scientific). Temperature was monitored *via* a thermometer placed through the Chem-Thread neck.

**Ozonolysis in supercritical carbon dioxide.** For the supercritical fluid experiments, 1 g of solid oleic acid was placed into a 250-mL stainless steel reaction vessel (Model R250; Thar Technologies; Pittsburgh, PA), and then the vessel was sealed with a Nitronic 60 stainless steel cap equipped with a magnetic stirrer. For these experiments, a batch configuration was used. Therefore, ozone was fed into the reactor at a mass fraction of 5.06% in oxygen until the pressure inside the reactor equaled the output pressure of the ozone generator, which was approximately 0.28 MPa. Then the reactor was heated while carbon dioxide was fed into the reactor using a dual-piston pump (Model P-50; Thar Technologies; Pittsburgh, PA) until the required pressure was reached. By the time the desired temperature and pressure were attained, oleic acid (melting point of  $\approx$  286.15 K) was a liquid. Achieving the reaction temperature and pressure required approximately 20 minutes. Then stirring at 1,000 RPM was initiated, and the reaction time was started. Reactions were conducted at pressures of 10 MPa to 35 MPa and temperatures of 313.15 K and 333.15 K for 12 hours. At the end of the reaction period, agitation was stopped and heating was turned off. The reactor was depressurized in a step-wise manner by sending the gas phase through a back-pressure regulator (Thar Technologies; Pittsburgh, PA). Upon leaving the back-pressure regulator, the stream went to a cyclone separator where the gas phase exited the system and passed through Carulite® 200 (Carus Corporation; Peru, Illinois) to destroy any unreacted ozone.

**Analysis of ozonation products.** The methyl ester derivatives of samples were used for product analysis. Samples (up to

100 mg) were placed in toluene and converted to methyl ester derivatives *via* acid-catalyzed esterification with 2% by weight sulfuric acid in methanol at 323.15 K overnight. At the end of the derivatization, the fatty acid methyl esters were extracted with hexane. This derivatization method was based upon the technique described by Christie.<sup>30</sup> Then a solution of 1,3-dichlorobenzene was added as an internal standard prior to analysis with gas chromatography with flame ionization detection (GC-FID). Separation was achieved using a fused-silica capillary column composed of stabilized poly(90% biscyanopropyl/10% cyanopropylphenyl siloxane) (SP-2380; Supelco, Bellefonte, PA). The dimensions of the column were 100 m in length  $\times$  0.25 mm inner diameter  $\times$  0.2  $\mu$ m film thickness. The method consisted of injecting 1  $\mu$ L of sample into the gas chromatograph with a split ratio of 100:1. The temperature program began at 110 °C and ended at 240 °C over a nonlinear temperature program totaling 99 min. Both the injector and detector were set to a temperature of 260 °C, and flow through the GC was maintained at a pressure of 0.27 MPa. Prior to sample analysis, the GC-FID (6890N; Agilent; Palo Alto, CA) was calibrated with external standards of methyl oleate, methyl pelargonate, and dimethyl azelate with 1,3-dichlorobenzene as an internal standard. All calibration curves generated had a minimum  $r^2$  value of 0.995 using a linear fit.

## Results and discussion

### Oxidation with potassium permanganate

Oxidation of oleic acid with potassium permanganate in supercritical carbon dioxide resulted in over 95% conversion within 12 hours at both 308.15 K and 318.15 K. The differential method of rate analysis described by Fogler<sup>31</sup> was used to determine the oleic acid oxidation rate law:

$$-r_{\text{OA}} = -\frac{dC_{\text{OA}}}{dt} = kC_{\text{OA}}^{\alpha} \quad (3)$$

where  $r_{\text{OA}}$  is the reaction rate,  $t$  is time,  $k$  is the reaction rate constant,  $C_{\text{OA}}$  is the concentration of oleic acid, and  $\alpha$  is the reaction order, which was found to be 1.75. The reaction rate constants are provided in Table 1, along with the corresponding 95% confidence interval (C.I.) and the coefficient of determination ( $r^2$ ) at each temperature when the reaction is treated as having  $\alpha = 1.75$ . Fig. 2 shows a plot of  $C_{\text{OA}}$  versus  $t$  with error bars representing standard deviations of triplicate measurements.

Once the reaction rate constants were determined, the activation energy could be evaluated. Since rate constants were determined for two temperatures, the activation energy can be expressed as follows:

**Table 1** Rate law modeling results for oxidation of oleic acid with potassium permanganate at 12.2 MPa

$T/\text{K}$	$k/\text{m}^{2.25} \text{ s}^{-1} \text{ mol}^{-0.75}$	95% C.I./ $\text{m}^{2.25} \text{ s}^{-1} \text{ mol}^{-0.75}$	$r^2$
308.15	$5.33 \times 10^{-5}$	$(4.56 \times 10^{-5}, 6.09 \times 10^{-5})$	0.98
318.15	$1.43 \times 10^{-4}$	$(1.41 \times 10^{-4}, 1.45 \times 10^{-4})$	0.99



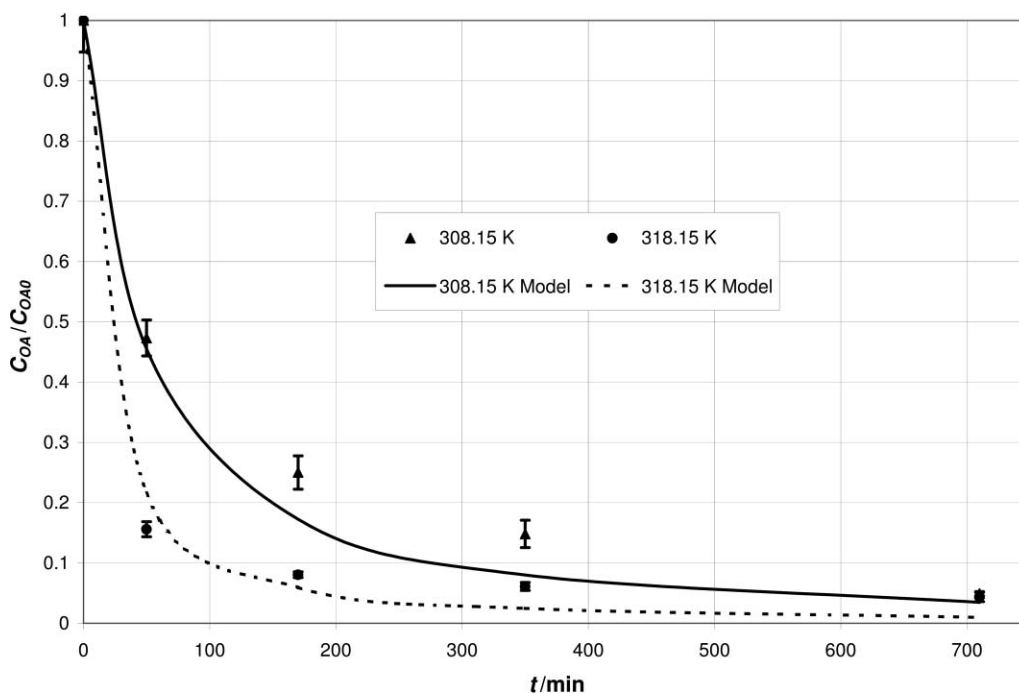


Fig. 2 Change of  $C_{OA}$  with time for oxidation of oleic acid with potassium permanganate in SC- $CO_2$  at 12.2 MPa.

$$E = \frac{-R \ln \left( \frac{k_1}{k_2} \right)}{\left( \frac{1}{T_1} - \frac{1}{T_2} \right)} \quad (4)$$

where  $k_1$  is the rate constant at temperature  $T_1$ ,  $k_2$  is the rate constant at temperature  $T_2$ ,  $E$  is the activation energy, and  $R$  is the gas constant. Based on the results from Table 1, the activation energy for this reaction was  $(80.31 \pm 2.81)$  kJ mol<sup>-1</sup>. As a comparison, the activation energy for the autoxidation of oleic acid (a second-order reaction) has been reported to be 134 kJ mol<sup>-1</sup>.<sup>32</sup> Therefore, the oxidation of oleic acid with potassium permanganate in supercritical carbon dioxide requires a lower activation energy and is therefore less sensitive to temperature.<sup>31</sup> Compared to oxygen, potassium permanganate has a higher oxidative potential; therefore the use of potassium permanganate should result in a lower activation energy.

A comparison of the 12-hour results between ambient reactions and high-pressure reactions is shown in Fig. 3. The error bars in Fig. 3 indicate standard deviation derived from triplicate measurements. The conversion of oleic acid in supercritical carbon dioxide reached 95.1% at 308.15 K and 95.6% at 318.15 K. In the absence of supercritical carbon dioxide, the oleic acid conversion after 12 hours was only 50.8% at 308.15 K and 51.7% at 318.15 K. Hence, conversion of oleic acid was improved greatly by incorporating the supercritical carbon dioxide. As Fig. 3 illustrates, target product yields were also affected by the presence of the supercritical fluid. The yields of azelaic acid and pelargonic acid were increased when supercritical carbon dioxide was used as a reaction medium. As previously mentioned, studies have shown that azelaic acid and

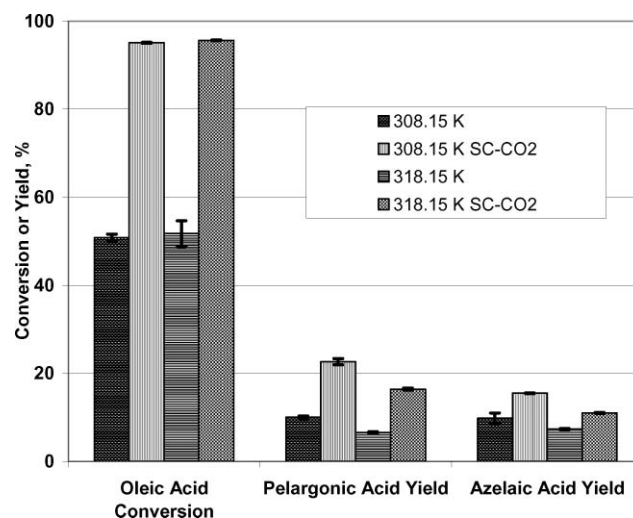


Fig. 3 Comparison of 12-hour oleic acid oxidation reactions with potassium permanganate conducted with and without supercritical carbon dioxide.

pelargonic acid significantly differ in terms of their solubility in supercritical carbon dioxide.<sup>26,27</sup> Therefore, in addition to being a medium for reaction, supercritical carbon dioxide can also be used to fractionate reaction products. This would reduce the need for downstream separations, resulting in a more energy-efficient and potentially cost-effective separation technique. However, the separation of azelaic acid (a solid under typical reaction conditions) from potassium permanganate (and manganese dioxide) with SC- $CO_2$  would need to be evaluated. However, this issue is avoided when ozone is used as the oxidizer because both ozone and its decomposition product (oxygen) are gases.

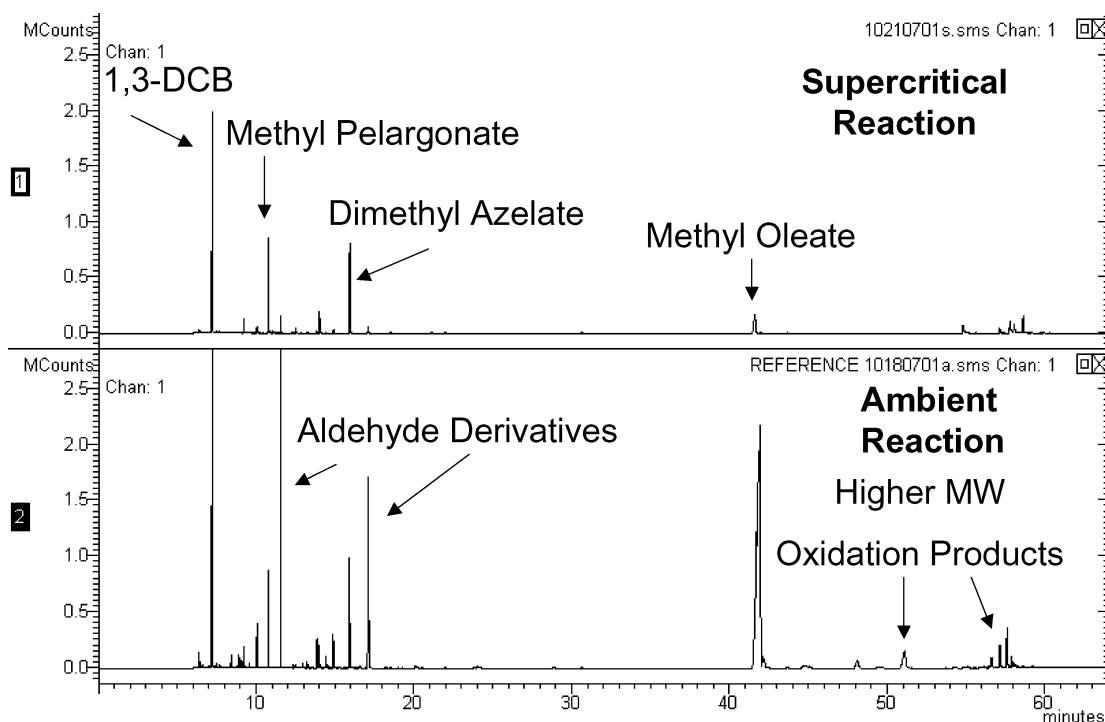


Fig. 4 Comparison of typical chromatograms for 12-hour reactions at 318.15 K.

Based upon GC-MS analysis, products other than azelaic acid and pelargonic were formed during the reaction. Fig. 4 provides a comparison of chromatograms for 12-hour reaction results at 318.15 K.

Based upon peak area, the major reaction products in the supercritical reaction were represented by dimethyl azelate and methyl pelargonate, which correspond to azelaic acid and pelargonic acid, respectively. However, in the case of the ambient pressure reaction, the major reaction products based on peak area were compounds eluting near the methyl pelargonate and dimethyl azelate. Based upon CI analysis with isobutane, these compounds were hypothesized to be derived from the aldehydes of pelargonic acid and azelaic acid. Aldehydes are oxidation precursors to carboxylic acids. The aldehyde precursor to azelaic acid would be 9-oxononanoic acid, while nonanal (pelargonaldehyde) would be the precursor to pelargonic acid. To aid in confirming this hypothesis, a pelargonaldehyde standard was put through the same derivatization process as a reaction sample and analyzed on the GC-MS. The resulting product (an acetal) had the same retention time, ion fragmentation pattern in EI mode, and molecular weight in CI mode as the unknown peak from the samples. Fig. 6 also shows that products were formed that had higher molecular weights than methyl oleate, which corresponds to oleic acid. Among the products identified using the NIST Mass Spectral Search Program 2.0 were derivatives of dihydroxystearic acid and epoxystearic acid; however, these products were not quantified. Both of these compounds are precursors to other oxidation products such as aldehydes. When supercritical carbon dioxide was not used as a reaction medium, more high-molecular-weight oxidation products were detected due to the slower progress of the reaction. These compounds are known to be intermediates to the formation of carboxylic acids.<sup>28</sup>

#### Oxidation with ozone

Oxidation of oleic acid using the traditional ozonolysis method resulted in complete conversion of oleic acid within 2 hours (120 minutes), which was before the end of the first phase of the reaction (2.5 hours). The second phase of the reaction was not needed because of the high concentration (5.06% by weight ozone in oxygen) of ozone used in the first phase. In the industrial process, the initial ozone stream is only about 1.75% ozone by weight in oxygen.<sup>17</sup> Fig. 5 shows a plot of how oleic acid concentration varied with time. The error bars correspond to standard deviations of duplicate measurements.

It is apparent that oleic acid concentration was a linear function of time. Hence, the reaction is zero-order, and the linear function can be expressed as the following:

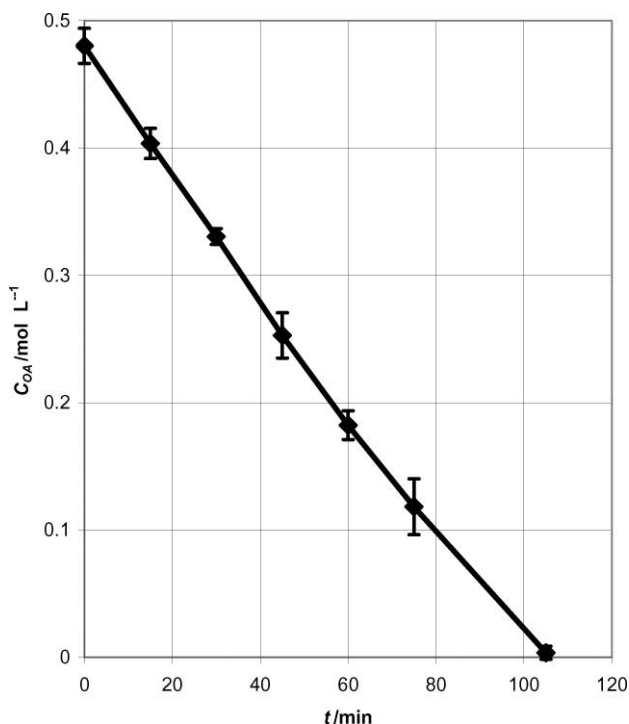
$$C_{\text{OA}} = C_{\text{OA}0} - kt \quad (5)$$

with

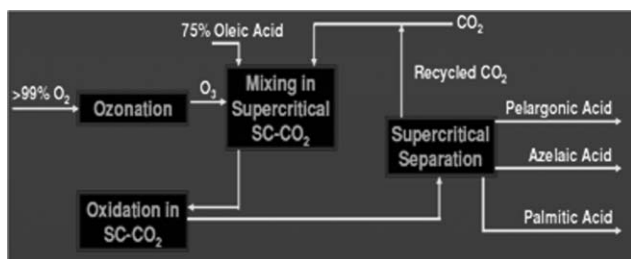
$$r_{\text{OA}} = -k \quad (6)$$

where  $C_{\text{OA}}$  is the concentration of oleic acid,  $C_{\text{OA}0}$  is the initial oleic acid concentration,  $t$  is time,  $k$  is the rate constant, and  $r_{\text{OA}}$  is the rate of reaction of oleic acid. Therefore, the slope of the line is  $-k$ . Based on Fig. 5, the rate of the disappearance of oleic acid is  $(0.077 \pm 0.002) \text{ mol s}^{-1} \text{ m}^{-3}$ . The zero-order reaction indicated that the rate of oleic acid ozonolysis was independent of oleic acid concentration. This is an indication of other processes controlling the rate of reaction, such as transport of ozone from the gas phase to the liquid phase. The reaction mixture was probably mass-transfer limited despite mixing and sparging.

The only products detected with GC-FID were pelargonic acid and azelaic acid. Based upon GC analysis, 73.15% of the



**Fig. 5** Change of oleic acid concentration over time at a temperature of 313.15 K and an ozone mass concentration of 5.06% in oxygen (1.18 SLM).



**Fig. 6** Ozonolysis of oleic acid in supercritical carbon dioxide.

initial mass (oleic acid + ozone) was accounted for by GC analysis. The unaccounted mass could be attributed to aldehydes that were formed as reaction intermediates between oleic acid consumption and formation of pelargonic acid and azelaic acid. Aldehydes such as pelargonaldehyde are known to be volatile, so they could have been carried out of the reaction mixture with the unreacted ozone + oxygen stream. Also, entrainment of compounds with the exiting gas stream could also have contributed to loss of mass.<sup>17</sup> Since only liquid-phase products were analyzed in this study, any volatile components carried off by unreacted ozone + oxygen would not be detected by GC-FID. Control experiments in which azelaic acid and pelargonic acid were subjected to ozonation for 12 hours at 313.15 K did not result in significant degradation of the target reaction products.

Unfortunately, no reaction of oleic acid with ozone was ever observed in the supercritical carbon dioxide. The main reason for this is likely the inability to get ozone into the reactor at a sufficient enough concentration for a measurable reaction to occur. Since the ozone was only 5.06% by weight in oxygen and could be delivered into the reactor at a maximum pressure of

0.28 MPa, the amount of ozone available for reaction with oleic acid was miniscule, especially considering the fact that ozone is not stable and decomposes. In the traditional process, ozone was continuously fed to the reactor; however, in the supercritical process, the oxidation occurred in a batch reactor. Therefore, only  $3.4 \times 10^{-5}$  moles of ozone were added to the reactor, which resulted in a theoretical maximum of  $7.2 \times 10^{-5}$  g (or 0.008% by weight) of the oleic acid consumed. This fraction of a change would not be detectable by the analytical equipment used in this study. As previously mentioned, the ozone was generated using a corona discharge. Modern corona units are now capable of generating upwards of 8% by weight ozone in oxygen. Newer models based on fuel-cell technology can produce up to 18% by weight ozone in oxygen. However, none of these units are capable of continuously generating and injecting ozone at high pressure, which is what would be desirable for this research. However, if sufficient ozone could be made available for the reaction and assuming that the major products are azelaic acid and pelargonic acid, then the reaction could be combined with supercritical fluid fractionation. A block-flow diagram of the proposed process is shown in Fig. 6. Although high purity oleic acid was used for this study, technical grade oleic acid is used industrially. Palmitic acid (a saturated fatty acid) is usually one of the major impurities in technical grade oleic acid.

In terms of comparing the use of ozone to potassium permanganate, ozone has a higher oxidative potential than potassium permanganate and less ozone is required per mole of oleic acid to achieve oxidation. However, ozone is a gas so fugitive emissions could be harmful to both the environment and personnel. Unlike potassium permanganate, ozone is unstable and must be generated on-site. Also, creation of ozone *via* corona discharge is an energy-intensive process. If the SC-CO<sub>2</sub> + potassium permanganate approach is utilized, an additional separation step may be required to recover the azelaic acid from any remaining permanganate (or its reduction product manganese dioxide). This extra separation step would probably either require the addition of a solvent or energy to create a second phase that would allow for recovery of the azelaic acid. Since the SC-CO<sub>2</sub> + ozone technique does not result in a solid by-product being formed, it would avoid the use of solvents or additional energy-intensive separations.

## Conclusions

The impact of incorporating a supercritical-fluid medium in the oxidation of oleic acid was evaluated. The oxidation of oleic acid with potassium permanganate was performed in supercritical carbon dioxide at 12.2 MPa. Conversions of over 95% were achieved in 12 hours at temperatures of 308.15 K and 318.15 K. Oxidation reactions in the absence of supercritical carbon dioxide only resulted in about 50% conversion of oleic acid. Incorporation of the supercritical fluid also resulted in higher yields of azelaic acid and pelargonic acid; moreover, in the absence of supercritical carbon dioxide, greater percentages of other oxidation products such as pelargonaldehyde and dihydroxystearic acid were observed.

The traditional method (no SC-CO<sub>2</sub>) of ozonolysis provided complete conversion of oleic acid in less than 2 hours. The two observed products were azelaic acid and pelargonic acid.

Based upon a mass balance of the oleic acid and ozone *versus* the observed products, 73.15% of mass was accounted for by pelargonic acid and azelaic acid. The unaccounted mass could be due to volatile aldehydes that were swept out of the reaction system by the exiting ozone + oxygen stream. The traditional ozonolysis reaction was zero-order with a reaction rate constant of  $(0.077 \pm 0.002) \text{ mol s}^{-1} \text{ m}^{-3}$ . Based upon the apparent order of the reaction, the ozonolysis of oleic acid was mass-transfer limited. No reaction was observed for the ozonolysis of oleic acid in supercritical carbon dioxide. This was due to the lack of sufficient ozone for reaction.

## Notation

$\alpha$	order of reaction in Eq. 3
$C_{\text{OA}}$	concentration of oleic acid in Eqs. 3 and 5 ( $\text{mol m}^{-3}$ )
$C_{\text{OA0}}$	initial concentration of oleic acid in Eq. 5 ( $\text{mol m}^{-3}$ )
$E$	activation energy in Eq. 4 ( $\text{kJ mol}^{-1}$ )
$k$	reaction rate constant in Eqs. 3 and 4 ( $\text{m}^{2.25} \text{ s}^{-1} \text{ mol}^{-0.75}$ ), 5 and 6 ( $\text{mol s}^{-1} \text{ m}^{-3}$ )
$R$	gas constant in Eq. 4 ( $\text{kJ mol}^{-1} \text{ K}^{-1}$ )
$r_{\text{OA}}$	reaction rate of oleic acid in Eqs. 3 and 6 ( $\text{mol s}^{-1} \text{ m}^{-3}$ )
$t$	time in Eqs. 3 and 5 (s)
$T$	temperature in Eq. 4 (K)

## Acknowledgements

This research was supported by the United States Department of Energy (Grant DE-FG36-04GO14251). The authors would like to thank Bill Holmes and Dr. Earl Alley of the Mississippi State Chemical Laboratory as well as John Slay and Jason McEwen of the Dave C. Swalm School of Chemical Engineering for their tremendous help with this project.

## References

- 1 A. S. Matlack, Chapter 8: Working Without Organic Solvents, in *Introduction to Green Chemistry*, Marcel Dekker, New York, NY, 2001, 201–239.
- 2 S. Srivastava and M. M. Srivastava, Green Chemistry: Innovations for a Cleaner World, in *Green Chemistry: Environment Friendly Alternatives*, ed. R. Sanghi and M. M. Srivastava, Narosa Publishing House, New Delhi, India, 2003, 18–27.
- 3 C. Capello, U. Fischer and K. Hungerbühler, What is a Green Solvent? A Comprehensive Framework for the Environmental Assessment of Solvents, *Green Chem.*, 2007, **9**, 927–934.
- 4 W. Leitner and M. Poliakoff, Supercritical Fluids in Green Chemistry, *Green Chem.*, 2008, **10**, 730.
- 5 G. Brunner, in *Supercritical Fluids as Solvents and Reaction Media*, Elsevier, Amsterdam, 2004, Preface.
- 6 A. Baiker, Supercritical Fluids in Heterogeneous Catalysis, *Chem. Rev.*, 1999, **99**, 453–473.
- 7 J. M. DeSimone, Practical Approaches to Green Solvents, *Science*, 2002, **297**, 799–803.
- 8 C. M. Rayner and R. S. Oakes, Chapter 4: Supercritical Carbon Dioxide, in *Green Reaction Media in Organic Synthesis*, ed. K. Mikami, John Wiley & Sons, Inc., Hoboken, NJ, 2005, 125–182.
- 9 Chemical Market Reporter, Cognis Expands Azelaic Acid, *Chemical Market Reporter*, 2001, **260**, p. 3.
- 10 M. S. Macsai, M. J. Mannis, and A. C. Huntley, Acne Rosacea, In *Eye and Skin Disease: Part X. Acneiform, Diseases, Dermatology Online Journal*, 1996, 1, no. 2, Chapter 41, <http://dermatology.cdlib.org/DOJvol1num2/review/rosacea.html>, last accessed 07/28/2008.
- 11 K. Hill, Fats and Oils as Oleochemical Raw Materials, *Pure Appl. Chem.*, 2000, **72**, 1255–1264.
- 12 Pelargonic Acid, 1996, *The Merck Index*, 12<sup>th</sup> Ed., Merck & Co., Inc., Whitehouse, NJ, 1214.
- 13 H. Kroha, Industrial Biotechnology Provides Opportunities for Commercial Production of New Long-Chain Dibasic Acids, *Inform.*, 2004, **15**, 568–571.
- 14 H. V. Smith, Oleochemicals in the Plastics Industry, *JAOCS*, 1985, **62**, 351–355.
- 15 J. O. Metzger and U. Bornscheuer, Lipids as Renewable Resources: Current State of Chemical and Biotechnological Conversion and Diversification, *Appl. Microbiol. Biotechnol.*, 2006, **71**, 13–22.
- 16 J. C. Reynolds, D. J. Last, M. McGillen, A. Nijis, A. B. Horn, C. Percival, L. J. Carpenter and A. C. Lewis, Structural Analysis of Oligomeric Molecules Formed from the Reaction Products of Oleic Acid Ozonolysis, *Environ. Sci. Technol.*, 2006, **40**, 6674–6681.
- 17 C. G. Goebel, A. C. Brown, H. F. Oehlschlaeger and R. P. Rolfes, Method of Making Azelaic Acid, *US Pat.*, 2 813 113, 1957.
- 18 S. G. Kadesch, Fat-Based Dibasic Acids, *JAOCS*, 1979, **56**, 845A–849A.
- 19 J. F. Brennecke, Chapter 16: Spectroscopic Investigations of Reactions in Supercritical Fluids, in *Supercritical Fluid Engineering Science: Fundamentals and Applications*, ed. E. Kiran and J. F. Brennecke, American Chemical Society, Washington, D. C., 1993, 201–219.
- 20 M. Zou, Z. R. Yu, P. Kashulines and S. S. H. Rizvi, Fluid-Liquid Phase Equilibria of Fatty Acid Methyl Esters in Supercritical Carbon Dioxide, *The Journal of Supercritical Fluids*, 1990, **3**, 23–28.
- 21 N. R. Foster, S. L. J. Yun and S. S. T. Ting, Solubility of Oleic Acid in Supercritical Carbon Dioxide, *The Journal of Supercritical Fluids*, 1991, **4**, 127–130.
- 22 W. B. Nilsson, E. J. Gauglitz and J. K. Hudson, Solubilities of Methyl Oleate, Oleic Acid, Oleyl Glycerols, and Oleyl Glycerol Mixtures in Supercritical Carbon Dioxide, *JAOCS*, 1991, **68**, 87–91.
- 23 P. Maheshwari, Z. L. Nikolov, T. M. White and R. Hartel, Solubility of Fatty Acids in Supercritical Carbon Dioxide, *JAOCS*, 1992, **69**, 1069–1076.
- 24 Z. Yu and S. S. H. Rizvi, Phase Equilibria of Oleic Acid, Methyl Oleate, and Anhydrous Milk Fat in Supercritical Carbon Dioxide, *The Journal of Supercritical Fluids*, 1992, **5**, 114–122.
- 25 M. Škerget, Ž. Knez and M. Habulin, Solubility of B-Carotene and Oleic Acid in Dense CO<sub>2</sub> and Data Correlation by a Density Based Model, *Fluid Phase Equilibria*, 1995, **109**, 131–138.
- 26 D. L. Sparks, R. Hernandez, L. A. Estévez, N. Meyer and T. French, Solubility of Azelaic Acid in Supercritical Carbon Dioxide, *J. Chem. Eng. Data*, 2007, **52**, 1246–1249.
- 27 D. L. Sparks, R. Hernandez, L. A. Estévez, K. Barlow and T. French, Solubility of Nonanoic (Pelargonic) Acid in Supercritical Carbon Dioxide, *J. Chem. Eng. Data*, 2008, **53**, 407–410.
- 28 M. Mercangöz, S. Küsefoğlu, U. Akman and Ö. Hortaçsu, Polymerization of Soybean Oil via Permanganate Oxidation with Sub/Supercritical CO<sub>2</sub>, *Chemical Engineering and Processing*, 2004, **43**, 1015–1027.
- 29 D. J. Sam and H. F. Simmons, Crown Polyether Chemistry: Potassium Permanganate Oxidations in Benzene, *Journal of the American Chemical Society*, 1972, **94**, 4024–4025.
- 30 W. W. Christie, Preparation of Derivatives of Fatty Acids, in *Lipid Analysis: Isolation, Separation, Identification and Structural Analysis of Lipids*, 3<sup>rd</sup> Ed., The Oily Press, Bridgwater, England, 2003, 208.
- 31 H. S. Fogler, *Elements of Chemical Reaction Engineering*, 3<sup>rd</sup> Ed., Prentice Hall, Upper Saddle River, NJ, 1999.
- 32 A. Takahashi, N. Kitakawa and T. Yonemoto, Kinetic Analysis for Oxidation of Oleic Acid, *Journal of Chemical Engineering of Japan*, 2000, **33**, 481–488.

# Baeyer–Villiger oxidation of ketones with a silica-supported peracid in supercritical carbon dioxide under flow conditions†

Rossella Mello,<sup>a,b</sup> Andrea Olmos,<sup>a</sup> Javier Parra-Carbonell,<sup>a</sup> María Elena González-Núñez<sup>\*a</sup> and Gregorio Asensio<sup>a</sup>

Received 4th December 2008, Accepted 25th March 2009

First published as an Advance Article on the web 15th April 2009

DOI: 10.1039/b821746g

[2-Pericarboxyethyl]-functionalized silica reacts with ketones in supercritical carbon dioxide at 250 bar and 40 °C under flow conditions to yield the corresponding esters and lactones. The solid reagent can be easily recycled through treatment with 70% hydrogen peroxide in the presence of an acid at 0 °C. This procedure not only simplifies the isolation of the reaction products, but has the advantage of using only water and carbon dioxide as solvents under mild conditions.

## Introduction

The Baeyer–Villiger oxidation of ketones **1** into esters and lactones **2** is an important transformation in organic synthesis,<sup>1</sup> particularly for ring-expansion in the synthesis of natural products and also for the preparation of monomers for polymerization. Organic peracids, such as *m*-chloroperbenzoic acid or trifluoroperacetic acid, are the most common reagents for performing this transformation.<sup>1</sup> However, these reagents are expensive and hazardous due to shock sensitivity. Moreover, their use results in the formation of one equivalent of the corresponding carboxylic acid, which must then be separated from the reaction products. Finally, the Baeyer–Villiger reaction is generally performed in organic solvents, typically dichloromethane or aromatics, which further enhance the environmental impact of the process. These disadvantages limit the commercial application of organic peracids in this reaction and have prompted the search for alternative approaches<sup>2</sup> to circumvent both the environmental and the safety issues associated with the classic Baeyer–Villiger procedure. Among other alternatives,<sup>2</sup> oxidations with supported peracids<sup>3,4</sup> have advantages because the immobilization of the peroxide minimizes the risk of uncontrolled decomposition and allows for a simple recovery and recycling of the reduced reagent.<sup>4</sup> Even further improvement of the Baeyer–Villiger reaction with supported peracids could be achieved by avoiding the use of chlorinated organic solvents.

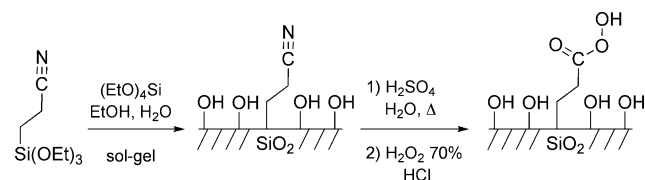
Supercritical carbon dioxide (*scCO*<sub>2</sub>), which has readily accessible critical conditions ( $T_c = 31.0$  °C,  $P_c = 73.8$  bar), a truly benign character, and a low cost, is a frequently discussed alternative reaction medium for chemical synthesis.<sup>5</sup> Indeed, the transport properties of *scCO*<sub>2</sub>, including its adjustable solvating power, low surface tension, low viscosity, and high diffusivity,<sup>5</sup> make this a convenient medium on which to perform reactions with supported reagents and catalysts under continuous flow

conditions.<sup>3a,6,7</sup> Furthermore, a technology platform for the use of *scCO*<sub>2</sub> in large-scale applications already exists in both the food and nutrition industries. These facts have prompted intense research into further development of the potential of *scCO*<sub>2</sub> as an alternative solvent for green chemistry.

Herein we report on the Baeyer–Villiger oxidation of ketones with a silica-supported peracid **3** in supercritical carbon dioxide under flow conditions. The reactions were carried out at 250 bar and 40 °C and gave excellent yields for the most reactive ketones. In addition, the solid reagent was easily recycled through treatment of the reduced acid with 70% hydrogen peroxide in the presence of an acid at 0 °C. The procedure simplifies the isolation of the reaction products and uses only water and carbon dioxide as solvents under mild conditions. Moreover, the results obtained with conventional solvents show that the hydrated silica-supported peracid **3** is even more efficient in these reactions than *meta*-chloroperbenzoic acid in solution, a fact that can be attributed to the acid catalysis promoted by the hydration layer on the silica surface.

## Results and discussion

The silica-supported peracid **3** was prepared following a previously reported procedure.<sup>4</sup> First, [2-cyanoethyl]-functionalized silica was prepared through co-condensation of tetraethoxysilane and 2-cyanoethyltriethoxysilane under sol–gel conditions. The compound was then treated with 0.05 M aqueous sulfuric acid under reflux for 48 h to yield the corresponding [2-carboxyethyl]-functionalized silica (Scheme 1). Treatment of this material with an excess of 70% hydrogen peroxide in the presence of hydrochloric acid followed by thorough washing with water and subsequent lyophilization yielded [2-pericarboxyethyl]-functionalized silica (**3**). Iodometric titration of this compound



Scheme 1 Preparation of the silica-supported peracid **3**.<sup>4</sup>

<sup>a</sup>Departamento de Química Orgánica, Universidad de Valencia, Avda. Vicente Andrés Estellés s.n., 46100, Burjassot, Valencia, Spain.

E-mail: elena.gonzalez@uv.es; Fax: +34 963544939; Tel: +34 963544939

<sup>b</sup>Fundación General de la Universidad de Valencia (FGUV), Valencia, Spain

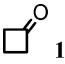
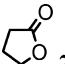
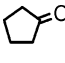
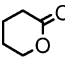
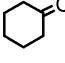
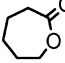
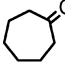
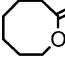

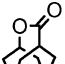


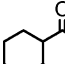
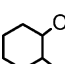
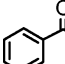
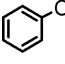
† Dedicated to Prof. Josep Font on the occasion of his 70th anniversary.

showed a load of 1.7–0.80 mmol of peracid g<sup>-1</sup>. The water content of this material was typically 22–26% w/w. The silica-supported peracid is safe to handle and it withstands contact with metals without decomposing. It can also be stored at –20 °C for weeks without a noticeable loss of peroxidic titer.

Baeyer–Villiger oxidations were carried out by flowing *sc*CO<sub>2</sub> (0.12–0.10 mL *sc*CO<sub>2</sub> min<sup>-1</sup>) at 250 bar and 40 °C for 3.5 h through a reservoir containing the substrate (0.8 mmol) and then through a column packed with the supported reagent (initial molar ratio of ketone : peracid = 1 : 3) (eqn 1). The system was depressurized through a micrometric valve and the reaction products were collected in a trap cooled with liquid nitrogen. Mass balance and substrate conversion were excellent under these conditions. The results are shown in Table 1.



**Table 1** Oxidation of ketones **1** with [SiO<sub>2</sub>]-CH<sub>2</sub>CH<sub>2</sub>COOOH (**3**) in *sc*CO<sub>2</sub>.<sup>a</sup>

Run	Substrate	Product <sup>b</sup>	Conv. <sup>c</sup> (%)
1			98
2			92
3			93
4			30
5			98
6			98
7			95
8			88

<sup>a</sup> Reactions in *sc*CO<sub>2</sub> at 250 bar, 40 °C and flow rate 0.11–0.12 mL *sc*CO<sub>2</sub> min<sup>-1</sup>; hydration of **3**: 22–26% w/w, load of peroxide: 1.7–0.8 mmol of peracid g<sup>-1</sup>; molar ratio ketone : peracid 1 : 3. <sup>b</sup> Esters or lactones were the only products (yield >99%). <sup>c</sup> Determined by GC analysis of the reaction mixtures; mass balance >98% in all the cases.

Cyclic ketones **1a–h** reacted efficiently with a three-fold excess of the silica-supported peracid **3** in *sc*CO<sub>2</sub> to yield the corresponding lactones **2a–h** exclusively, with total absence of products derived from competing hydrolysis of the lactones **2** or of acid-catalyzed aldol condensation reactions. The yields of the reactions depended on the ring size and the migratory ability of the substituents in the starting ketone **1**. Excellent conversions were achieved except for cycloheptanone (**1d**) (Table 1) and 2-octanone which gave 30% and 3% yields, respectively. Reactions carried out with an initial molar ratio of ketone : peracid = 1 : 2 led to lower substrate conversions, ranging between 10% for cyclohexanone (**1c**) and 81% for adamantanone (**1e**). It is worth noting that the contact between the substrate and the immobilized reagent in the reactions performed under flow conditions is limited to the residence time of the flowing substrate solution over the solid reagent. The contact time of the substrate solution in *sc*CO<sub>2</sub> with the supported peracid was estimated to be *ca.* 20 min, under our reaction conditions.

In order to compare the efficiencies of the flow and batch processes we also performed the oxidation of cyclohexanone (**1c**) with the supported peracid **3** in batch. Thus, a 100 mL stainless steel reactor charged with 0.23 mmol of cyclohexanone (**1c**) and 3 equivalents of the supported peracid **3** both placed in suitable separated containers, was pressurized with CO<sub>2</sub> to 250 bar at 40 °C and allowed to stand for 5 h. The reactor was depressurized through a micrometric valve and the products were collected in a trap cooled with liquid nitrogen. 25% of the organic material, which contained 71% of the starting ketone **1c** and 29% of the lactone **2c**, was recovered in the cold trap. An additional 74% of the organic material containing 23% of the cyclohexanone (**1c**) and 77% of the lactone **2c** was recovered by washing the solid phase with dichloromethane. These results indicate that the drop of pressure in the last stage of the batch procedure induces the condensation of the organic material onto the silica surface. At this instance, the recovery of the reaction products would require an additional *sc*CO<sub>2</sub> extraction process in order to avoid the use of organic solvents. This fact minimizes the improvement in the energy efficiency of the batch process with respect to the flow process associated to the suppression of a highly pressurized CO<sub>2</sub> flow.

The consumed reagent recovered from the column once the reactions in flow were complete was white in color and exhibited a loose appearance in all cases. Iodometric titration of the supported reagent used in the oxidation of cyclohexanone (**1c**) showed a peracid content of 0.1 mmol peracid g<sup>-1</sup>, which indicates a nearly complete conversion of the peroxide. This result contrasted with control experiments which showed that the silica-supported peracid **3** did not appreciably decompose upon standing under a flow of *sc*CO<sub>2</sub> at 250 bar and 40 °C for 5 h. These observations suggest the existence of a competing ketone-catalyzed decomposition of the peracid<sup>8</sup> under our reaction conditions which is more pronounced for the less reactive ketones. In fact, the use of an excess of the very reactive cyclobutanone (**1a**) with an initial molar ratio of ketone : peracid = 5 : 1 led to a nearly complete conversion of the supported peroxide and a 20% conversion of the ketone into the corresponding lactone **2a**. In addition, this result reveals that all the hydroperoxide groups at the active surface are available for reacting with the substrate. No attempts were made to further

investigate the decomposition of the silica-supported peracid **3** in these processes.

Hydration of the silica-supported peracid is an important parameter for the success of the reactions. Thus, the reaction of cyclohexanone (**1c**) with a sample of silica-supported peracid **3** that had previously been hydrated with 53% w/w of water, in *sc*CO<sub>2</sub> at 250 bar and 40 °C, with a flow rate 0.10 mL *sc*CO<sub>2</sub> min<sup>-1</sup> and with initial molar ratio ketone : peracid 1 : 3, enabled us to recover 68% of the organic material in the cold trap. The recovered material consisted of 94% of  $\epsilon$ -caprolactone (**2c**) and 6% of unreacted ketone. An additional 11% of organic material (79% mass balance) which contained 80% of the corresponding 6-hydroxy-hexanoic acid, was recovered from the solid phase. This result indicates that the reaction product undergoes acid-catalyzed hydrolysis on the silica surface. 6-Hydroxy-hexanoic acid was not eluted by the flow of *sc*CO<sub>2</sub> and remained retained onto the hydrophilic silica surface.

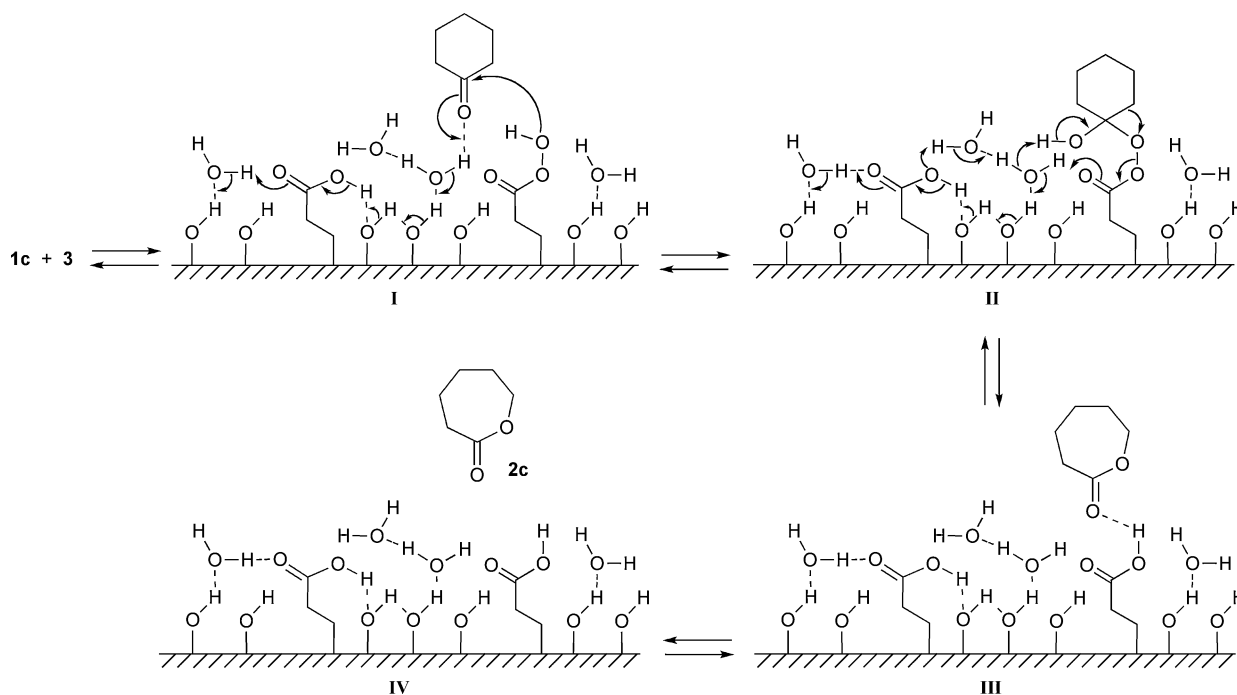
Conversely, anhydrous silica-supported peracid, which was prepared by drying solid **3** under vacuum at room temperature until it reached a constant weight, provoked a strong retention of the reaction products on the silica surface. For instance, the reaction of cyclohexanone (**1c**) with anhydrous **3** in *sc*CO<sub>2</sub> under our standard conditions led to the isolation of 84% of the organic material in the cold trap which contained  $\epsilon$ -caprolactone (76%) and unreacted ketone (24%). An additional 16% of  $\epsilon$ -caprolactone was recovered from the silica surface (>99% mass balance, 80% conversion).

The best results were obtained in the oxidation with silica-supported peracid **3** containing a 22–26% w/w of water. With this reagent both the retention and the hydrolysis of the reaction products on the silica surface are suppressed, probably because the interaction of the silanol group with the first hydration layer reduces both the nucleophilic character of the water

molecules and the hydrogen-bonding ability of the surface. Further hydration of the solid material provides water molecules less strongly bonded to the silica surface thus allowing the hydrolysis of the lactones **2** to take place. The experimental observations did not provide any evidence for the formation of carbonic acid on the silica surface under our reaction conditions.

The lower conversion of the substrate found for the reaction with anhydrous **3** with respect to that for the hydrated reagent can be attributed to the lower efficiency of the acid catalysis in the absence of the hydration layer. The Baeyer–Villiger reaction on the solid-supported peracid **3** requires the initial adsorption of the substrate onto the silica surface (**I**, Scheme 2) followed by the acid-catalyzed nucleophilic attack of a proximate hydroperoxide group to the carbonyl group (**II**, Scheme 2) to provide the tetrahedral intermediate which then undergoes the ring expansion step (**III**, Scheme 2). The acid catalysis can be attributed to either the [2-carboxyethyl]-ligands or the silanol groups present on the silica surface. The polar and protic layer on the reagent surface resulting from hydration extends the availability of acidic protons farther from the anchoring center of the [2-carboxyethyl]-ligands and silanol groups and enhances the efficiency of the acid catalysis in the hydrated reagent. In fact, the H-bonding interaction of [2-carboxyethyl]-ligands with the silanol groups of the silica surface has been recently evidenced by CP-MAS NMR.<sup>9</sup>

The importance of the silica surface in the course of these reactions is further evidenced by comparing the reaction of adamantanone **1e** with the silica-supported peracid **3** (0.7 mmol gr<sup>-1</sup>, 23% w/w hydrated) and *meta*-chloroperbenzoic acid (*m*CPBA) in dichloromethane. The reactions were carried out at room temperature with initial molar ratio **1e** : peracid 1 : 2 and initial concentration of **1e** 0.007 M. GC analysis of the reaction



**Scheme 2** Reaction mechanism at the reactive surface. The scheme shows the acid catalysis facilitated by the hydration layer on the silica surface.

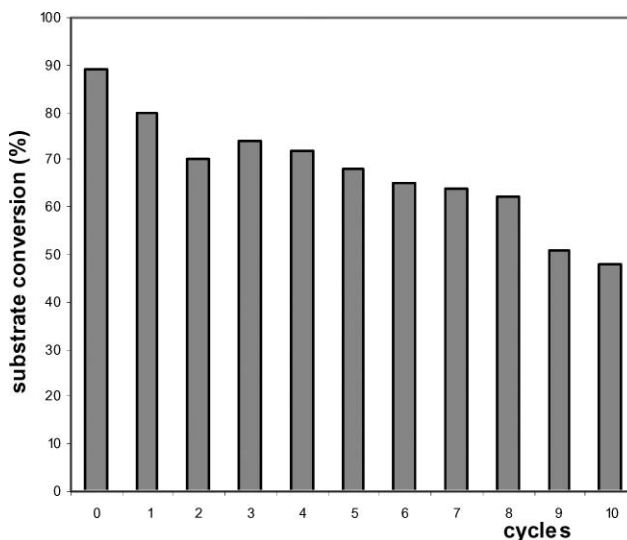
mixtures after 6 h showed 48% and 20% conversions of **1e** for **3** and *m*CPBA, respectively, to give the corresponding lactone **2e** as the only product in both cases. After 10 h the conversion rose to 78% for the silica-supported peracid **3** but remained 20% for *m*CPBA. The better efficiency of **3** compared to *m*CPBA can be attributed to the adsorption of the substrate on the silica surface, which facilitates the interaction between the substrate and the supported peroxidic ligands, and to the acid catalysis provided by the hydration layer of the supported reagent in the rate-determining migration step.

In order to compare the solvating properties of *sc*CO<sub>2</sub> with those of *n*-hexane and dichloromethane, we performed the Baeyer–Villiger reaction of cyclohexanone (**1c**) with the silica-supported peracid **3** in *n*-hexane and dichloromethane under flow conditions. We first established the average concentration of cyclohexanone (**1c**) in *sc*CO<sub>2</sub> under our standard reaction conditions by placing a weighted amount of the ketone in the substrate reservoir, flowing *sc*CO<sub>2</sub> at 250 bar, 40 °C, and 0.12 mL min<sup>-1</sup> for 90 min to subsequently determine the amount of ketone remaining in the reservoir after depressurization. The experiment was repeated four times with different amounts of cyclohexanone (**1c**); the result was an average concentration of cyclohexanone (**1c**) in *sc*CO<sub>2</sub> of 0.027 ± 0.002 M under our standard reaction conditions.

The reaction of cyclohexanone (**1c**) with the silica-supported peracid **3** containing 22% water in *n*-hexane or dichloromethane under flow conditions was carried out by flowing 12 mL of a 0.03 M solution of the ketone in the selected solvent at 0.106 mL min<sup>-1</sup> through a column containing the supported reagent at 40 °C. The initial molar ratio of ketone : peracid was 1 : 3 in all cases. The reaction mixture was then collected in an ice-cooled flask placed at the end of the column. Afterwards, an additional 15 mL of solvent were allowed to flow through the column. In the case of *n*-hexane, the reaction products did not elute from the column and had to be recovered after washing the solid support with dichloromethane. GC analysis of the mixture showed an 87% conversion of the substrate into the corresponding  $\epsilon$ -caprolactone. For the reaction in dichloromethane, 74% of the organic material was recovered from the collector and an additional 26% was obtained after washing the solid support with dichloromethane. GC analysis of the mixture showed a 78% conversion of the starting ketone into  $\epsilon$ -caprolactone. Iodometric titration of the recovered supported reagent showed complete absence of peroxide suggesting the existence of some competing reaction pathways different to the oxygen transfer to the ketone.

The results show that the oxidation is more efficient in *sc*CO<sub>2</sub> than in conventional solvents, a fact that might be attributed to the enhanced transport properties of *sc*CO<sub>2</sub>.<sup>5</sup> The high diffusivity, low viscosity, and low surface tension of *sc*CO<sub>2</sub> allows the substrate solution to penetrate the porous matrix more effectively, which in turn allows it to reach a more extensive active surface of the solid reagent. The results also show that the association of either the ketone or ester with the acidic sites on the supported reagent surface in *sc*CO<sub>2</sub> is weaker than in *n*-hexane. This is probably due to a better solvation of polar oxygenated molecules in the supercritical medium. These results indicate that *sc*CO<sub>2</sub> has peculiar solvating properties which cannot be directly compared to those of hydrocarbons.

The silica-supported peracid **3** could be easily regenerated upon treatment with 70% hydrogen peroxide in the presence of 1.5 equivalents of hydrochloric acid at 0 °C for 12 h, followed by centrifuging, washing with ultrapure water and lyophilizing the solid. The efficiency of the process was evaluated by monitoring the conversion of cyclohexanone (**1c**) under our standard reaction conditions in successive cycles (Fig. 1) without determining the peroxidic content of the reagent in each recycling step. After 10 cycles, the substrate conversion dropped from 90% to 50%, indicating the degradation of the organic ligands bonded to the silica surface in the oxidative treatment. A loss of 48% of the organic ligands was confirmed by analyses of the hybrid material with the aid of conventional <sup>1</sup>H and <sup>13</sup>C NMR techniques performed according to a previously reported procedure.<sup>10</sup>



**Fig. 1** Effect of recycling the silica-supported peracid **3** on the conversion of cyclohexanone (**1c**) in *sc*CO<sub>2</sub> at 250 bar and 40 °C under flow conditions (0.11–0.12 mL *sc*CO<sub>2</sub> min<sup>-1</sup>) with an initial ketone : peracid molar ratio of 1 : 3.

Regeneration of the silica-supported peracid **3** with sulfuric acid led to faster degradation of the reagent.<sup>10</sup> Thus, the treatment of a sample of [2-carboxyethyl]-functionalized silica containing 4.3 mmol of organic ligands g<sup>-1</sup> of material with 70% hydrogen peroxide in the presence of 1.5 equivalents of sulfuric acid for 12 h at 0 °C led to a 21% loss of the organic ligands bonded to the silica surface. After two recycling procedures, the loss of organic ligands reached 49%. These results can be attributed to the formation of the strong oxidant peroxomonosulfuric acid (Caro's acid) in the aqueous solution of hydrogen peroxide.

## Conclusions

[2-Pericarboxyethyl]-functionalized silica (**3**) allows the Baeyer–Villiger oxidation of ketones to be performed in supercritical carbon dioxide at 250 bar and 40 °C under flow conditions. Hydration of reagent **3** is an important parameter for the efficiency of the reaction. The solid reagent **3** can be easily recycled with 70% hydrogen peroxide in the presence of an acid at 0 °C. This procedure simplifies the isolation of the reaction



products and uses only water and carbon dioxide as solvents under mild conditions. The preparation of the supported peracid **3** requires only ethanol and water as solvents although the use of alkoxysilanes reduces the green features of the process. The process reported herein improves the Baeyer–Villiger oxidation with potassium peroxomonosulfate supported on silica in *scCO*<sub>2</sub> under flow conditions reported previously<sup>3a</sup> since it avoids the disposal of a strongly acidic reduced reagent.

## Experimental

Dichloromethane was purified in accordance with described procedures.<sup>11</sup> The glassware used in the reactions with 70% hydrogen peroxide was carefully cleaned and washed before use with a solution of EDTA in ultrapure water (0.25 g L<sup>-1</sup>) to remove any traces of metals. The peroxide content of the supported reagent was determined with the aid of standard iodometric titration. Hydration of the silica-supported peracid **3** was performed by placing in a closed 50 mL chamber two vials, one containing a weighted samples of anhydrous functionalized silica and the other the desired amount of ultrapure water, for 12 h at 4 °C. The high-pressure equipment consisted of a 250-mL AISI 316 stainless-steel jacketed autoclave, a diaphragm pump (Orlita MHS 30/8) with a maximum theoretical flow of 8.44 L h<sup>-1</sup> of liquid CO<sub>2</sub>, and a set of high-pressure valves, pressure and temperature probes, and security rupture-discs suitably placed to control the flow of CO<sub>2</sub> along the system.

### CAUTION!

*The experiments described in this paper involve the use of relatively high pressures and require equipment with the appropriate pressure rating.*

**[2-Cyanoethyl]-functionalized silica.** <sup>4</sup> To a stirred mixture of 91 mL of ethanol, 93 mL of ultrapure water, 25.6 mL of tetraethoxysilane (TEOS) (115 mmol), 13.4 mL of 2-cyanoethyltriethoxysilane (60.3 mmol), and 10% hydrochloric acid was added dropwise until the reaction mixture became transparent. An aqueous solution of 0.02 M in KH<sub>2</sub>PO<sub>4</sub> and 0.026 M in KH<sub>2</sub>PO<sub>4</sub> (pH 7,  $\mu$  0.1) was then added dropwise until pH 7 was reached, after which the solution was allowed to gel at room temperature without stirring. The gel was allowed to stand for 72 h covered with a 1 : 1 mixture of ethanol : water and then it was aged in ultrapure water for 5 days. The supernatant solvent was replaced daily throughout this period. The gel was decanted and lyophilized to obtain 11.3 g of hybrid silica; NMR analysis<sup>10</sup> of this material showed a load of 3.28 mmol of organic ligands g<sup>-1</sup>.

**[2-Carboxyethyl]-functionalized silica.** <sup>4</sup> A stirred suspension of 11.3 g of [2-cyanoethyl]-functionalized silica in a mixture of 500 mL of ultrapure water and 50 mL of concentrated sulfuric acid, was heated to reflux for 48 h. The solid was filtered and thoroughly washed with ultrapure water until the liquid phase reached pH 7. The solid was lyophilized to obtain 13.8 g of hybrid silica; NMR analysis<sup>10</sup> showed 3.85 mmol of organic ligands g<sup>-1</sup>.

**[2-Pericarboxyethyl]-functionalized silica.** <sup>4</sup> To a stirred suspension of 10.7 g of [2-carboxyethyl]-functionalized silica

(2.45 mmol g<sup>-1</sup>, 26.2 mmol) in 40 mL of 70% aqueous hydrogen peroxide (0.82 mol) cooled to 0 °C, 4 mL of a 37% aqueous solution of hydrogen chloride (1.5 equiv) were added dropwise. The mixture was stirred overnight. The suspension was centrifuged at 4200 rpm for 15 min and the solid was washed with cold ultrapure water and centrifuged until the decanted liquid phase showed pH 7 and no peroxidic titer. The solid was lyophilized and stored at -20 °C. Iodometric titration of the solid material showed 0.82 mmol of peracid g<sup>-1</sup>. Lyophilization renders a 22–26% w/w hydrated material under our ambient conditions.

### Oxidation of ketones with silica-supported peracid **3** in *scCO*<sub>2</sub>.

**General procedure.** Cyclohexanone (0.103 mL, 1 mmol) was placed in a U-shaped stainless-steel tube which was connected with suitable fittings to a stainless steel 8 mm ID column packed with 4.5 g of silica-supported peracid **3** (1.5 mmol gr<sup>-1</sup>, 3 equiv). Two filters placed at either end of the column prevented any displacement of the solid reagent throughout the experiment. The outlet of the column was connected to a high-pressure micrometric valve which was connected to a trap cooled with a liquid nitrogen or dry-ice bath run through a 1/8' Teflon-tube. The pressure in the trap was equilibrated with a flow of nitrogen. The inlet of the substrate reservoir was connected with a high-pressure valve to a 250 mL autoclave set at 40 °C. The autoclave was closed, charged with CO<sub>2</sub> and pressurized to 250 bar. Then, both the substrate reservoir and the column were placed into a water bath heated to 40 °C and the system was allowed to pressurize by carefully opening the inlet valve. The stroke volume of the pump and the aperture of the high-pressure micrometric outlet valve were regulated to achieve steady continuous flow conditions at 250 bar. The CO<sub>2</sub> flow at the outlet of the system was monitored with a bubble flow-meter. The system was left to operate for 3.5 h. The inlet valve was then closed and the system was allowed to depressurize. The trap was warmed to room temperature and the colorless residue was dissolved in deuterated chloroform and analyzed with the aid of GC, GC-MS, <sup>1</sup>H, and <sup>13</sup>C NMR techniques. The solid reagent recovered from the column was washed four times with 15 mL of dichloromethane in a round-bottomed flask under magnetic stirring. The filtered solution was analyzed by means of GC and then evaporated under vacuum at 0 °C.

### Oxidation of cyclohexanone (**1c**) with silica-supported peracid **3** in conventional solvents under flow conditions. General procedure.

A 5 mL Rezorian Luer-lock syringe-tip cartridge (Supelco) was charged with 2.1 g of silica-supported peracid **3** (1.3 mmol g<sup>-1</sup>, 2.7 mmol) and placed within a vertical jacketed-cylinder heated to 40 °C with the aid of a circulating bath. The cartridge outlet was connected to a 100 mL flask cooled to 0 °C through 1/8 inch Teflon tubing. A 50 mL polypropylene syringe was charged with 30 mL of a 0.03 M solution of cyclohexanone (**1c**) in *n*-hexane, placed in a syringe pump set at 0.106 mL min<sup>-1</sup>, and connected to the cartridge inlet through 1/8 inch Teflon tubing and suitable fittings. The assembly was run until the syringe was emptied. Then the cartridge was washed with an additional 30 mL of *n*-hexane. The solution in the collector was analyzed with the aid of GC and the solvent was removed under vacuum at 0 °C. The solid reagent recovered from the column was

washed four times with 15 mL of dichloromethane in a round-bottomed flask under magnetic stirring. The filtered solution was analyzed by means of GC and then evaporated under vacuum at 0 °C.

**Oxidation of adamantanone (1e) with silica-supported peracid 3 in dichloromethane.** To a suspension of 0.05 g of 3 (0.7 mmol g<sup>-1</sup>, 0.035 mmol) in 1.5 mL of dichloromethane, 1 mL of an equimolar 0.0175 M solution of adamantanone (1e) (with adamantane as an internal standard) in dichloromethane was added at once at room temperature under stirring. The reaction was monitored by means of GC and the substrate conversion was determined from the integrals of the peaks corresponding to the substrate 1e and the internal standard.

**Oxidation of adamantanone (1e) with m-CPBA.** To 1 mL of an equimolar 0.0175 M solution of adamantanone (1e) (adamantane as an internal standard) in dichloromethane, 1.5 mL of a 0.023 M solution of 98% m-CPBA were added at once at room temperature under stirring. The reaction was monitored through GC and the substrate conversion was determined from the integrals of the peaks corresponding to the substrate 1e and the internal standard.

## Acknowledgements

Financial support from the Spanish Dirección General de Investigación, CTQ2007-65251/BQU and Consolider Ingenio 2010 (CSD2007-00006), is gratefully acknowledged. AO thanks the Spanish Ministerio de Educación y Ciencia for a fellowship. We thank Solvay Química S.L. for a generous gift of 70% hydrogen peroxide. We also thank the SCSIE (Universidad de Valencia) for allowing us access to their instruments and facilities.

## Notes and references

- (a) C. Jiménez-Sanchidrián and J. R. Ruiz, *Tetrahedron*, 2008, **64**, 2011–2026; (b) M. Mihovilovic, F. Rudroff and B. Groetzel, *Curr. Org. Chem.*, 2004, **8**, 1057–1069; (c) Bolm C. Palazzi, and O. Beckmann, in *Transition Metals for Organic Synthesis*, ed. M. Beller, and C. Bolm, Wiley-VCH, Weinheim, 2004, p. 267–274; (d) M. Renz and B. Meunier, *Eur. J. Org. Chem.*, 1999, **4**, 737–750; (e) G. Strukul, *Angew. Chem., Int. Ed. Engl.*, 1998, **37**, 1199–1209; (f) G. R. Krow, *Org. React.*, 1993, **43**, 251–798.
- (a) M. Boronat, P. Concepción, A. Corma and M. Renz, *Catal. Today*, 2007, **121**, 39–44; (b) M. D. Mihovilovic, *Curr. Org. Chem.*, 2006, **10**, 1265–1287; (c) G.-J. Brink, I. W. C. E. Arends and R. A. Sheldon, *Chem. Rev.*, 2004, **104**, 4105–4123; (d) C. Bolm, C. Palazzi, G. Franzio and W. Leitner, *Chem. Commun.*, 2002, 1588–1589.
- (a) M. E. González-Núñez, R. Mello, A. Olmos and G. Asensio, *J. Org. Chem.*, 2006, **71**, 6432–6436; (b) M. E. González-Núñez, R. Mello, A. Olmos and G. Asensio, *J. Org. Chem.*, 2005, **70**, 10879–10882; (c) P. J. Kropp, G. W. Breton, J. D. Fields, J. C. Tung and B. R. Loornis, *J. Am. Chem. Soc.*, 2000, **122**, 4280–4285; (d) J. D. Fields and P. J. Kropp, *J. Org. Chem.*, 2000, **65**, 5937–5941.
- (a) A. Lambert, J. A. Elings, D. J. Macquarrie, G. Carr and J. H. Clark, *Synlett.*, 2000, **7**, 1052–1054; (b) J. A. Elings, R. Ait-Meddour, J. H. Clark and D. J. Macquarrie, *Chem. Commun.*, 1998, 2707–2708.
- (a) W. Leitner, *Acc. Chem. Res.*, 2002, **35**, 746–756; (b) *Chemical Synthesis Using Supercritical Fluids*, ed. P. Jessop, and W. Leitner, Wiley-VCH, Weinheim-New-York, 1999; (c) S. Wells and J. M. DeSimone, *Angew. Chem. Int. Ed. Engl.*, 2001, **40**, 519–527; (d) M. McHugh, and V. J. Krukoni, *Supercritical Fluid Extraction*, Butterworth-Heinemann, Boston, 1994.
- (a) R. T. Baker, S. Kobayashi and W. Leitner, *Adv. Synth. Catal.*, 2006, **348**, 1337–1340; (b) W. Leitner, *Pure Appl. Chem.*, 2004, **76**, 635–644; (c) J. R. Hyde, P. Licence, D. Carter and M. Poliakov, *Appl. Catal. A*, 2001, **222**, 119–121.
- (a) See for instance: Z. Hou, N. Theyssen, A. Brinkmann, K. V. Klementiev, W. Gruener, M. Buehl, W. Schmidt, B. Spliethoff, B. Tesche, C. Weidenthaler and W. Leitner, *J. Catal.*, 2008, **258**, 315–323; (b) F. Zayed, L. Greiner, P. S. Schulz, A. Lapkin and W. Leitner, *Chem. Commun.*, 2008, 79–81; (c) Z. Hou, N. Theyssen and W. Leitner, *Green Chem.*, 2007, **9**, 127–132; (d) M. I. Burguete, A. Cornejo, E. García-Verdugo, M. J. Gil, S. V. Luis, J. A. Mayoral, V. Martínez-Merino and M. Sokolova, *J. Org. Chem.*, 2007, **72**, 4344–4350; (e) P. Clark, M. Poliakov and A. Wells, *Adv. Synth. Catal.*, 2007, **349**, 2655–2659; (f) G. A. Leeke, R. C. D. Santos, B. Al-Duri, J. P. K. Seville, C. J. Smith, C. K. Y. Lee, A. B. Holmes and I. F. McConvey, *Org. Proc. Res. Dev.*, 2007, **11**, 144–148; (g) P. Stephenson, B. Kondor, P. Licence, K. Scovell, S. K. Ross and M. Poliakov, *Adv. Synth. Catal.*, 2006, **348**, 1605–1610; (h) M. E. González-Núñez, R. Mello, A. Olmos, R. Acerete and G. Asensio, *J. Org. Chem.*, 2006, **71**, 1039–1042; (i) J.-Q. Wang, D.-L. Kong, J.-Y. Chen, F. Cai and L.-N. He, *J. Mol. Catal. A*, 2006, **249**, 143–148; (j) Z. Hou, N. Theyssen, A. Brinkmann and W. Leitner, *Angew. Chem., Int. Ed. Engl.*, 2005, **44**, 1346–1349; (k) P. B. Webb, T. E. Kunene and D. J. Cole-Hamilton, *Green Chem.*, 2005, **7**, 373–379; (l) J. R. Hyde, B. Walsh, J. Singh and M. Poliakov, *Green Chem.*, 2005, **7**, 357–361; (m) J. R. Hyde, B. Walsh and M. Poliakov, *Angew. Chem., Int. Ed. Engl.*, 2005, **44**, 7588–7591; (n) Y. Kokubo, A. Hasegawa, S. Kuwata, K. Ishihara, H. Yamamoto and T. Ikariya, *Adv. Synth. Catal.*, 2005, **347**, 220–224; (o) C. K. Y. Lee, A. B. Holmes, S. V. Ley, I. F. McConvey, B. Al-Duri, G. A. Leeke, R. C. D. Santos and J. P. K. Seville, *Chem. Commun.*, 2005, 2175–2177; (p) P. Licence, W. K. Gray, M. Sokolova and I. F. McConvey, *J. Am. Chem. Soc.*, 2005, **127**, 293–298; (q) P. Stephenson, P. Licence, S. K. Ross and M. Poliakov, *Green Chem.*, 2004, **6**, 521–523; (r) M. T. Reetz and W. Wiesenhöfer, *Chem. Commun.*, 2004, 2750–2751; (s) M. T. Reetz, W. Wiesenhöfer, G. Francio and W. Leitner, *Adv. Synth. Catal.*, 2003, **345**, 1221–1228; (t) P. B. Webb, M. F. Sellin, T. E. Kunene, S. Williamson, A. M. Z. Slawin and D. J. Cole-Hamilton, *J. Am. Chem. Soc.*, 2003, **125**, 15577–15588; (u) J. DeSimone, M. Selva and P. Tundo, *J. Org. Chem.*, 2001, **66**, 4047–4049; (v) N. J. Meehan, M. Poliakov, A. J. Sandee, J. N. H. Joost, P. C. J. Kamer and P. W. N. M. vanLeeuwen, *Chem. Commun.*, 2000, 1497–1498; (w) W. K. Gray, F. R. Smail, M. G. Hitzler, S. K. Ross and Poliakov, *J. Am. Chem. Soc.*, 1999, **121**, 10711–10718; (x) M. G. Hitzler, F. R. Smail, S. K. Ross and M. Poliakov, *Chem. Commun.*, 1998, 359–360.
- (a) R. E. Montgomery, *J. Am. Chem. Soc.*, 1974, **96**, 7820–7821; (b) J. O. Edwards, R. H. Pater, R. Curci and F. Di Furia, *Photochem. Photobiol.*, 1979, **30**, 63–70; (c) R. Curci, M. Fiorentino, L. Troisi, J. O. Edwards and R. H. Pater, *J. Org. Chem.*, 1980, **45**, 4758–4760; (d) A. R. Gallopo and J. O. Edwards, *J. Org. Chem.*, 1981, **46**, 1684–1688.
- H.-H. G. Tsai, G.-L. Jheng and H.-M. Kao, *J. Am. Chem. Soc.*, 2008, **130**, 11566–11567.
- R. Mello, A. Olmos, T. Varea and M. E. González-Núñez, *Anal. Chem.*, 2008, **80**, 9355–9359.
- D. D. Perrin, W. L. F. Armarego, *Purification of Laboratory Chemicals*, 3rd edn, Pergamon, New York, 1988.

# Hydrogenolysis of glycerol catalyzed by Ru-Cu bimetallic catalysts supported on clay with the aid of ionic liquids

Tao Jiang,\* Yinxi Zhou, Shuguang Liang, Huizhen Liu and Buxing Han\*

Received 22nd January 2009, Accepted 25th March 2009

First published as an Advance Article on the web 9th April 2009

DOI: 10.1039/b901425j

Glycerol is a well-known renewable chemical, and its effective transformation to valuable chemicals accords well with the principles of green chemistry. In this work, a series of Ru-Cu bimetallic catalysts were prepared using cheap and abundant clay, bentonite, as the support. Bentonite was modified with a functional ionic liquid 1,1,3,3-tetramethylguanidinium lactate (TMGL) in an attempt to develop highly efficient catalysts. Hydrogenolysis of aqueous solution of glycerol was performed with the immobilized Ru-Cu catalyst under temperatures of 190–240 °C and pressures of 2.5–10 MPa. The bimetallic catalysts were very efficient for promoting the hydrogenolysis of glycerol. 100% of glycerol conversion and 85% yield of 1,2-propanediol could be achieved at 230 °C and 8 MPa. The conversion of glycerol and the selectivity to 1,2-propanediol did not decrease after the catalyst was used 5 times. TMGL played a crucial role in fabricating the new catalysts. The catalysts were characterized by FT-IR, XPS, SEM and TEM, and the reasons for the excellent performances of the catalyst were also discussed.

## Introduction

With the gradual depletion of fossil resources, an urgent task is to replace fossil resources with renewable materials. Commodity chemicals that are currently used to produce pharmaceuticals, plastics and transportation fuels are expected to be produced from renewable materials in future. This strategy is especially crucial for the sustainable development of the society and economy. Much effort, therefore, has been devoted to the conversion and utilization of renewable feedstocks and chemicals in recent years.<sup>1,2</sup> Glycerol is one of the top-12 building block chemicals identified by the U.S. Department of Energy.<sup>3</sup> As a biomass-derivate, glycerol can be commercially produced by the microbial fermentation of sugars such as glucose and fructose.<sup>4–6</sup> In addition, glycerol is a byproduct in a large amount from the production of biodiesel by transesterification of plant and animal oils with methanol.<sup>7</sup> 10 wt% of glycerol is produced in manufacturing biodiesel fuel. It is no doubt that development of chemical processes to convert low-cost glycerol to more valuable chemicals is of great importance. Recently, several excellent papers have given overviews on the recent development in the conversion of glycerol into value-added chemicals.<sup>8–11</sup>

It is known that glycerol can be catalytically converted into functionalized and value-added chemicals *via* a variety of reaction routes, such as oxidation, hydrogenolysis, dehydration, pyrolysis, steam reforming, etherification, esterification, oligomerization and polymerization, *etc.* The hydrogenolysis of glycerol produces oxygenated chemicals including ethylene glycol (EG) and propylene glycol. Propylene glycol is presently

produced through petroleum routes, such as the ethylene oxide route (Shell technology)<sup>12</sup> or acrolein (Degussa-DuPont technology)<sup>13</sup> for the production of 1,3-propanediol (1,3-PDO) and the hydrolysis of propylene oxide with water for manufacturing 1,2-propanediol (1,2-PDO). 1,3-PDO is mainly used as a starting material for producing polymers and 1,2-PDO is often used directly as intermediates or additives to produce antifreezing agent, lubricants, foods, cosmetics, and resins.<sup>9,14</sup> Increasing attention has consequently been paid to the hydrogenolysis of glycerol to produce 1,3-PDO and 1,2-PDO, and about 10 papers were published in 2008. Solid catalysts have exhibited unique advantages in separation and recovery of catalysts. Metals including Cu, Ni, Pd, Pt, Ru, Rh, Cr, and Au have been extensively used as the active components for hydrogenolysis of glycerol, and the reactions were conducted at temperatures of 453–513 K and hydrogen pressures of around 6–10 MPa.<sup>15–22</sup>

Among the metals used, ruthenium has shown a high activity for the hydrogenolysis of glycerol,<sup>23–26</sup> but C–C bond cleavage is often unavoidable<sup>27,28</sup> resulting in the high yields to products of small molecules, including methane, methanol, CO, and CO<sub>2</sub>, *etc.* The work by Davis *et al.* indicated that Ru favored the formation of EG over 1,2-PDO. C–C bond cleavage is thought to occur primarily *via* a metal-catalyzed reaction route over Ru.<sup>29,30</sup> Montassier *et al.*<sup>16</sup> carried out the hydrogenolysis of glycerol under 30 MPa H<sub>2</sub> at 533 K. Mainly methane was obtained in the presence of RANEY® Ni, Ru, Rh and Ir catalysts, while 1,2-PDO was the main product when RANEY® Cu was used as a catalyst. Cu also exhibited good performance for the hydrogenolysis of glycerol in other works.<sup>31,32</sup> Chaminand *et al.* reported the hydrogenolysis of glycerol over CuO/ZnO catalysts. At 180 °C and 80 bar hydrogen pressure 100% selectivity to 1,2-PDO can be obtained in water when the conversion of glycerol was 19%.<sup>23</sup> More recently, Xia and coworkers prepared

Beijing National Laboratory for Molecular Sciences (BNLMS), Centre for Molecular Science, Institute of Chemistry, Chinese Academy of Sciences, Beijing, 100190, China. E-mail: Jiangt@iccas.ac.cn, Hanbx@iccas.ac.cn; Fax: +86 10 62562821; Tel: +86 10 62562821

highly dispersed copper nanoparticles supported on silica by the precipitation–gel technique, which showed 94.3% selectivity toward 1,2-PDO with 73.4% glycerol conversion at 473 K and a total pressure of 9 MPa.<sup>33</sup>

Recently, the preparation of catalysts assisted by ionic liquids (ILs) has attracted much attention.<sup>34</sup> For example, Mehnert *et al.* dispersed 1-butyl-3-methylimidazolium hexafluorophosphate ([bmim][PF<sub>6</sub>]) and 1-butyl-3-methylimidazolium tetrafluoroborate ([bmim][BF<sub>4</sub>]) on silica gel to provide a solvent environment for the Rh complex. The as-prepared catalyst showed excellent catalytic activity and stability for hydrogenation.<sup>35</sup> More interestingly, some functional ILs exhibit a strong ability to stabilize nanoparticles. Different Pd or Ru nanoparticle catalysts have been prepared with the assistance of guanidinium-based IL, which also showed outstanding catalytic performance for the hydrogenation of benzene and olefins.<sup>36,37</sup> More recently, a series of very effective supported catalysts for different organic reactions have been prepared using different ILs and solid supports.<sup>38–40</sup>

Natural clay minerals are a type of environmentally benign material. Bentonite (BEN) is a clay consisting predominantly of montmorillonite. It has a layered structure, large surface areas, and cation exchange capacity. The special properties of bentonite make it a valuable material for a wide range of applications, such as pharmaceuticals, cosmetics, environment, agriculture, and catalysis, *etc.* Bentonite is potentially a good catalyst support. For example, an excellent catalyst has been prepared using ion-exchanged montmorillonite for the hydrogenation of benzene.<sup>41</sup> A montmorillonite-enwrapped scandium has been used as a heterogeneous catalyst for the Michael reaction.<sup>42</sup>

As discussed above, both Ru and Cu can catalyze the reaction, with certain advantages. A combination of them may produce a more efficient catalyst. In this work, a series of Ru-Cu bimetallic catalysts were prepared using bentonite as the support with the aid of 1,1,3,3-tetramethylguanidinium lactate (TMGL). Hydrogenolysis of glycerol was performed with the immobilized Ru-Cu catalyst (designated as Ru-Cu/TMG-BEN). The results demonstrated that the catalyst was highly active and selective for the hydrogenolysis of glycerol to produce 1,2-PDO. The IL played a crucial role in fabricating the new catalysts. As far as we know, this is the first work on the hydrogenolysis of glycerol carried out using Ru-Cu bimetallic catalysts.

## Experimental

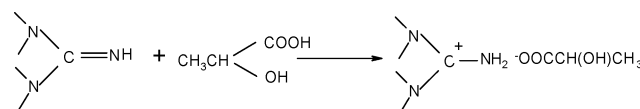
### Materials

The clay mineral used in this work is a smectite rich white bentonite provided by Zhejiang Sanding Scientific and Technology Co., Ltd., China. The composition of the clay was 58.98% SiO<sub>2</sub>, 19.82% Al<sub>2</sub>O<sub>3</sub>, 3.73% MgO, 5.18% Na<sub>2</sub>O, 0.42% K<sub>2</sub>O, 0.87% CaO, 1.31% Fe<sub>2</sub>O<sub>3</sub>, 0.10% TiO<sub>2</sub>, 0.74% P<sub>2</sub>O<sub>5</sub>, and 0.08% FeO. It was microporous and cation-rich. The cation exchange capacity (CEC) of the bentonite was 99 mmol/100 g. H<sub>2</sub> was purchased from Beijing Analytical Instrument Factory with a purity of 99.99%. Glycerol, 1,2-propanediol, ethylene glycol, n-butanol, and N,N-dimethylformamide (DMF) were purchased from Sinopharm Chemical Reagent Co., Ltd. NaBH<sub>4</sub>, Cu(NO<sub>3</sub>)<sub>2</sub>·3H<sub>2</sub>O, and RuCl<sub>3</sub>·3H<sub>2</sub>O were A.R. grade and

produced by Beijing Chemical Reagents Company. All chemicals were used as received.

### Catalyst preparation

In this work, bentonite was modified with ionic liquid 1,1,3,3-tetramethylguanidinium lactate (TMGL), which was prepared directly by neutralization of 1,1,3,3-tetramethylguanidine with lactic acid at room temperature (Scheme 1).<sup>43</sup> Before being used as the supports, bentonite was treated with TMGL to exchange the Na cations with the IL cations. The molar ratio of IL to the CEC of bentonite was 1.2:1. Bentonite was first dispersed in an aqueous solution of TMGL and stirred for 6 h at room temperature. After being separated from the solution by filtration, bentonite was treated for the second time with the same procedures. Then bentonite was washed three times with deionized water, and dried at 120 °C overnight, which was labeled as TMG-BEN.



**Scheme 1** The synthesis of TMGL.

The Ru or Cu catalysts supported on TMG-BEN were prepared by the following procedures: 1 g of TMG-BEN was dispersed in an aqueous solution of RuCl<sub>3</sub>·3H<sub>2</sub>O (0.0776 g, 0.297 mmol Ru; 20 mL of deionized water) or Cu(NO<sub>3</sub>)<sub>2</sub>·3H<sub>2</sub>O (0.0717 g, 0.297 mmol Cu; 20 mL of deionized water), and the mixture was stirred for 2 h at room temperature. Then water was removed under vacuum. The obtained catalyst was reduced in a flow of pure H<sub>2</sub> at 220 °C for 3 h. The as-obtained catalyst was designated as Ru/TMG-BEN and Cu/TMG-BEN, respectively.

The Ru-Cu bimetallic catalysts supported on TMG-BEN were prepared by the following procedures: 1 g of the modified bentonite was added to the aqueous solution of RuCl<sub>3</sub>·3H<sub>2</sub>O (0.0776 g, 0.297 mmol Ru; 20 mL of deionized water), and the mixture was stirred for 2 h at room temperature. Then NaBH<sub>4</sub> was used to reduce Ru. The solid was washed with deionized water and dried at 100 °C. Then the supported Ru catalyst was added to the aqueous solution of Cu(NO<sub>3</sub>)<sub>2</sub>·3H<sub>2</sub>O (0.0239 g, 0.1 mmol Cu; 20 mL of deionized water), and the mixture was stirred for 2 h at room temperature. After being reduced with NaBH<sub>4</sub> the solid was washed with deionized water and dried at 100 °C. Finally, the solid was reduced in a flow of pure H<sub>2</sub> at 220 °C for 3 h and then 300 °C for 3 h. The as-made catalysts were labeled as Ru-Cu/TMG-BEN. The content of Ru in this catalyst was 3 wt% of the support and the molar ratio of Ru to Cu was 3/1. The catalysts with other Ru/Cu ratios were prepared using the same procedures. For comparison, the Ru-Cu bimetallic catalyst supported on unmodified bentonite was also prepared using a similar method, which was referred to as Ru-Cu/BEN.

### Catalyst characterization

Fourier transform infrared spectroscopy (FT-IR) spectra were determined using a Bruker Tensor 27 spectrometer, and the samples were prepared by the KBr pellet method. The

morphology of the catalysts was observed with a transmission electron microscope (TEM, Tecnai 20, Philips). The X-ray photoelectron spectrum (XPS) data of the as-prepared samples were obtained with an ESCALab220i-XL electron spectrometer from VG Scientific using 300 W MgK $\alpha$  radiation. The base pressure was about  $3 \times 10^{-9}$  mbar. The binding energies were referenced to the C 1s line at 284.8 eV from adventitious carbon. X-ray Diffraction (XRD) was performed on a X'PERT SW X-ray diffractometer operated at 30 kV and 100 mA with CuK $\alpha$  radiation. Scanning electron microscope (SEM) examination was carried out on a scanning electron microscope (JEOL, JSM-4300) operated in a high-vacuum mode at 15 kV, which provided general textural information of the samples. Thermogravimetric analysis of TMG-BEN was performed on a TGA Q50 V20.7 Build 32 thermogravimetric analysis system in the atmosphere at a heating rate of 20 °C per min.

### Catalytic activity measurement

The hydrogenolysis of glycerol was carried out in a 7 mL autoclave reactor under stirring. Typically, the reactor was charged with glycerol (5 mmol, 0.46 g) and the catalyst (0.084 g, 0.3 mol% of Ru/glycerol) in 1.0 mL deionized water, and purged with 2.0 MPa hydrogen three times before the reaction. An air bath was used to heat the reactor and its temperature was controlled by a PID temperature controller (model SX/A-1, Beijing Tianchen Electronic Company). The temperature fluctuation of the constant temperature air bath was  $\pm 0.1$  °C. After the autoclave was heated to the reaction temperature, hydrogen was charged up to the desired pressure. After a required period, the autoclave was cooled and the gases were released and collected. The liquid products were analyzed using a GC (Agilent 6820) equipped with a PEG-20M (30 m) capillary column and a FID detector. n-Butanol was employed as the internal standard to calculate the product compositions and DMF was used as the solvent. The gas product was analyzed using a GC (Agilent 4890) equipped with a packed carbon molecular sieve column (2 m long, 3 mm o.d.) and a TCD detector.

### Recycling procedure of Ru-Cu/TMG-BEN

In the recycling experiment, the catalyst was separated by centrifugation and washed with deionized water three times.

Then the catalyst was dried at 60 °C under vacuum for 3 h and 100 °C for 2 h in air. The catalyst was reused in the next run directly. Reaction conditions were as follows: catalyst, Ru-Cu/TMG-BEN (Ru 3 wt%, Ru/Cu 3/1); catalyst amount, 0.3 mol% Ru/glycerol; reaction temperature, 225 °C; reaction time, 20 h; glycerol, 5 mmol (0.46 g); water, 1.0 mL; initial pressure, 10.0 MPa.

## Results and discussion

In the experiments, 1,2-PDO, 1,3-PDO, ethylene glycol (EG), 1-propanol (1-PO), 2-propanol (2-PO), C<sub>2</sub>H<sub>5</sub>OH, and CH<sub>3</sub>OH were detected in the liquid products. CH<sub>4</sub> and CO<sub>2</sub> were observed in the gas products. Conversion of glycerol is defined as the ratio of number of moles of glycerol consumed in the reaction to the total moles of glycerol initially added. Selectivity to liquid product is defined as the ratio of number of moles of glycerol consumed to produce liquid product to the number of moles of converted glycerol. Composition of liquid product was calculated based on C-based moles of each component in the liquid product.

### Effect of Ru/Cu molar ratio

A series of Ru/Cu bimetallic catalysts were prepared using TMGL modified BEN as the support by changing the molar ratio of Ru and Cu. In all of the catalysts, the content of Ru was 3 wt% of the support. Table 1 summarized the results of these catalysts in catalyzing the hydrogenolysis of aqueous glycerol. When Ru/TMG-BEN catalyst was used (Table 1, Entry 1), the conversion of glycerol could reach 90.7%. But obvious cleavage of C–C bonds was observed and the selectivity to liquid product was only 27.4%. A large amount of gas product (CH<sub>4</sub> and CO<sub>2</sub>) was detected. This is consistent with the results of other researchers.<sup>16,29,30</sup> In addition, the content of EG in the liquid product was more than 30%, which is also high compared with the results using other catalysts in Table 1. EG is formed *via* the cleavage of the C–C bond, further demonstrating that Ru is active for cleavage of the C–C bond. On the contrary, Cu/TMG-BEN exhibited low conversion of glycerol (26.5%), but high selectivity to liquid product, especially 1,2-PDO (Table 1, Entry 8), indicating Cu catalysts have poor activity towards C–C bond

**Table 1** Effect of molar ratio of Ru/Cu on the catalytic performance of Ru-Cu/TMG-BEN in the hydrogenolysis of glycerol

Entry	Molar ratio of Ru/Cu	Conversion of glycerol/%	Selectivity to liquid product/%	C-based composition of liquid products/mol%		
				1,2-PDO	EG	Others <sup>a</sup>
1	3/0	90.7	27.4	62.3	32.7	5.0
2	3/0.5	71.9	34.4	57.6	37.3	5.1
3	3/1	70.9	46.1	71.7	23.6	4.7
4	3/2	66.1	40.4	70.3	24.8	4.9
5	3/3	64.4	30.6	69.5	28.6	1.9
6	3/4	41.7	23.4	72.7	23.7	3.6
7	3/9	27.0	22.0	79.4	17.9	2.7
8	0/3	26.5	59.1	83.1	11.6	5.3

Reaction conditions: catalyst, Ru-Cu/TMG-BEN (Ru 3 wt%); temperature, 195 °C; reaction time, 18 h; catalyst amount, 0.6 mol% Ru/glycerol; glycerol, 5 mmol (0.46 g); water, 1.0 mL; Initial pressure at 195 °C, 10.0 MPa.<sup>a</sup> Including 1-propanol (1-PO), 2-propanol (2-PO), C<sub>2</sub>H<sub>5</sub>OH, and CH<sub>3</sub>OH.

**Table 2** Effect of H<sub>2</sub> pressure on the performance of Ru-Cu/TMG-BEN

T/°C	P/MPa	Conversion of glycerol/%	Selectivity to liquid product/%	C-based composition of liquid products/mol%		
				1,2-PDO	EG	Others <sup>a</sup>
210	10	71.4	65.0	83.3	14.7	2.0
	8	71.5	67.0	85.7	12.3	2.0
	6	77.4	66.3	84.6	12.9	2.5
	5	87.6	67.0	84.5	13.5	2.0
	2.5	81.6	31.3	87.3	7.3	5.4
230	10	100.0	98.5	86.4	9.4	4.2
	8	100.0	99.5	85.4	7.6	7.0
	6	100.0	79.1	83.4	3.3	13.3

Reaction conditions: catalyst, Ru-Cu/TMG-BEN (Ru 3 wt%, Ru/Cu 3/1); reaction time, 18 h; catalyst amount, 0.3 mol% Ru/glycerol; glycerol, 5 mmol (0.46 g); water, 1.0 mL.<sup>a</sup> Including 1-propanol (1-PO), 2-propanol (2-PO), C<sub>2</sub>H<sub>5</sub>OH, and CH<sub>3</sub>OH.

cleavage and good activity towards C–O bond hydrogenation. The results in Table 1 indicate that addition of Cu to Ru/TMG-BEN could restrain the catalyst from catalyzing the cleavage of the C–C bond and increase the selectivity to 1,2-PDO and other liquid products. With the decreased molar ratio of Ru to Cu, the conversion of glycerol gradually decreased and there were maxima in both of the selectivity to liquid product and the content of 1,2-PDO in the liquid product (Table 1, Entries 2–7). When the molar ratio of Ru/Cu was 3/1, Ru-Cu/TMG-BEN exhibited the best performance (Table 1, Entry 3).

### Effect of reaction conditions

In this work, the effects of reaction temperature, reaction time and H<sub>2</sub> pressure on the reaction were investigated systematically using the catalyst Ru-Cu/TMG-BEN with Ru/Cu molar ratio of 3/1 because it was the best catalyst, as can be seen from Table 1.

The effect of pressure was studied at 210 °C and 230 °C, and the results are given in Table 2. The data in the table indicate that the pressure did not affect the content of 1,2-PDO in the liquid product considerably. At 210 °C, the selectivity to liquid product was low when the pressure was low (2.5 MPa). At 230 °C, glycerol could be converted completely at the pressures studied. The

selectivity to liquid product also approached 100% under 8 MPa and 10 MPa, and the content of 1,2-PDO was 86%. Therefore, the yield of 1,2-PDO could be as high as 85.1% at the optimized reaction conditions.

Table 3 presents the results at 10 MPa and different temperatures. The conversion of glycerol increased with the rising temperature and reached 100% at 230 °C and 240 °C. The selectivity to liquid product also increased with increasing temperature. The content of 1,2-PDO in the liquid product reached a maximum at 230 °C. At 240 °C, the content of 1,2-PDO in the liquid product decreased to 76.1%, indicating that high temperature promoted the formation of small molecular products.

In order to investigate the effect of TMG on the properties of the as-prepared catalyst, the reaction was conducted using Ru-Cu/TMG-BEN and Ru-Cu/BEN at the same reaction conditions. As shown in Table 3, when the reaction was conducted for 18 h, the conversion of glycerol over the two catalysts was all 100% (Table 3, Entry 5 and Entry 8), and the content of 1,2-PDO in the liquid product was similar. The selectivity to liquid product over Ru-Cu/TMG-BEN was 98.5%, which was much higher than 78.1% catalyzed by Ru-Cu/BEN. When the reaction was conducted for a short time of 10 h, the conversion of glycerol over the two catalysts was all less than 100% (Table 3, Entry 6 and Entry 9). Although the content of 1,2-PDO in

**Table 3** Effect of reaction temperature on the performance of Ru-Cu/TMG-BEN

Entry	T/°C	Glycerol conversion/%	Selectivity to liquid product/%	C-based composition of liquid products/mol%		
				1,2-PDO	EG	Others <sup>a</sup>
1	190	48.8	34.0	60.7	32.9	6.4
2	200	59.2	59.6	74.3	22.1	3.6
3	210	71.4	65.0	83.3	14.7	2.0
4	220	90.0	75.7	84.4	13.1	2.5
5	230	100.0	98.5	86.4	9.4	4.2
6	230 <sup>b</sup>	86.9	97.3	87.1	9.8	3.1
7	240	100.0	98.9	76.1	9.3	14.6
8	230 <sup>c</sup>	100.0	78.1	87.1	9.5	3.4
9	230 <sup>d</sup>	80.1	72.1	85.9	11.2	2.9

Reaction conditions: catalyst, Ru-Cu/TMG-BEN (Ru 3 wt%, Ru/Cu 3/1); catalyst amount, 0.3 mol% Ru/glycerol; reaction time, 18 h; glycerol, 5 mmol (0.46 g); water, 1.0 mL; initial pressure, 10.0 MPa.<sup>a</sup> Including 1-propanol (1-PO), 2-propanol (2-PO), C<sub>2</sub>H<sub>5</sub>OH, and CH<sub>3</sub>OH. <sup>b</sup> Reaction time, 10 h. <sup>c</sup> Conducted using the catalyst unmodified with IL, Ru-Cu/BEN (Ru 3 wt%, Ru/Cu 3/1); reaction conditions were the same. <sup>d</sup> Conducted with Ru-Cu/BEN (Ru 3 wt%, Ru/Cu 3/1); reaction time, 10 h.

the liquid product over the two catalysts were similar, Ru-Cu/TMG-BEN showed higher activity and higher selectivity to liquid product than Ru-Cu/BEN. Therefore, Ru-Cu/TMG-BEN exhibited better performance than Ru-Cu/BEN.

### Catalyst characterization

Some typical catalysts were characterized by XPS. Fig. 1 displays the XPS spectra of Ru/TMG-BEN, Cu/TMG-BEN, and Ru-Cu/TMG-BEN (Ru/Cu, 3/1 in moles). The binding energy of Ru in Ru/TMG-BEN can be observed at 280.4 eV (Ru3d5, Fig. 1a), and the binding energy of Cu in Cu/TMG-BEN is 933.3 eV (Cu2p3, Fig. 1b). In catalyst Ru-Cu/TMG-BEN, the binding energy of Ru is shifted to 280.6 eV, and that of Cu to 934.0 eV. Therefore, there existed strong interaction between Ru and Cu and some electrons might be transferred from Ru to Cu in the Ru-Cu catalysts.

The morphology and microstructure of the support and catalysts were studied by SEM and TEM. Fig. 2 shows the SEM images of the pristine bentonite (a) and Ru-Cu/TMG-BEN (b). Clearly, the morphology of Ru-Cu/TMG-BEN was similar to that of bentonite. The TEM images of Ru-Cu/TMG-BEN and Ru-Cu/BEN are also shown in Fig. 2. In catalyst Ru-Cu/TMG-BEN, the diameters of the metal particles were in the range of 5–8 nm (Fig. 2c), and the particle size in Ru-Cu/BEN was similar (Fig. 2e). However, after these two catalysts were used separately once, the size of the nanoparticles on the surface of the two catalysts was quite different. For the former, most nanoparticles were still in the range of 5–8 nm (Fig. 2d). The metal particles in catalyst Ru-Cu/BEN aggregated and the size of the nanoparticles increased to about 50 nm (Fig. 2f). It can be deduced that the main reason for the better performance

of Ru-Cu/TMG-BEN is that the particle size was unchanged in the reaction process, while the metal particles in Ru-Cu/BEN became larger and larger during the reaction, and therefore, the performance of the catalyst was relatively poor. This indicates that TMG played an important role in dispersing and stabilizing the metallic particles in the catalyst because the only difference of the two catalysts was that ionic liquid TMGL was utilized when preparing Ru-Cu/TMG-BEN.

Bentonite has a layered structure and negative charge in the silicate layers. On the basis of these special characteristics, it can exchange cations with IL or other reagents to compensate the negative charge. There are successful examples which demonstrate that the interactions between nanoparticles and polymers or surfactants can be used to intercalate nanoparticles into the interlayer spaces of montmorillonite. For example, Dékány *et al.* proved rhodium particles can be stabilized by polymers and by the lamellae of layered silicates of montmorillonite.<sup>44</sup> Király *et al.* prepared ultrafine Palladium particles on ationic and nionic clays, mediated by oppositely charged surfactants.<sup>45</sup> In the as-prepared catalyst, TMG ions were fixed on the surface or interlayer of bentonite by electrostatic force after ion-exchange. On the other hand, TMG cations have the ability to stabilize nanoparticles, which stems from their electron-donor properties<sup>46,47</sup> and has been demonstrated in other work.<sup>36–38</sup> The metal particles combined with TMG ions on the surface of the bentonite with the assistance of coordination interaction. In this way, the nanoparticles were supported on the surface or interlayer of bentonite by combination of coordination and electrostatic force. The coordination interaction existed between metallic particles and TMG, and the electrostatic force between TMG and bentonite. Both the electrostatic and coordination forces are very strong, which prohibit aggregation

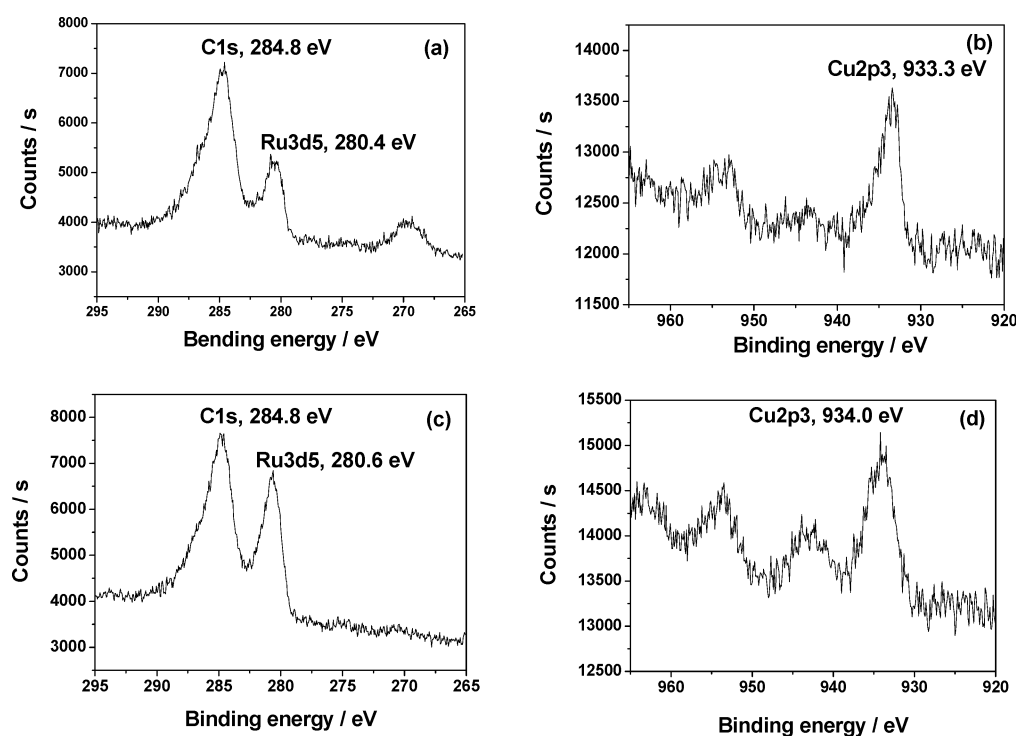
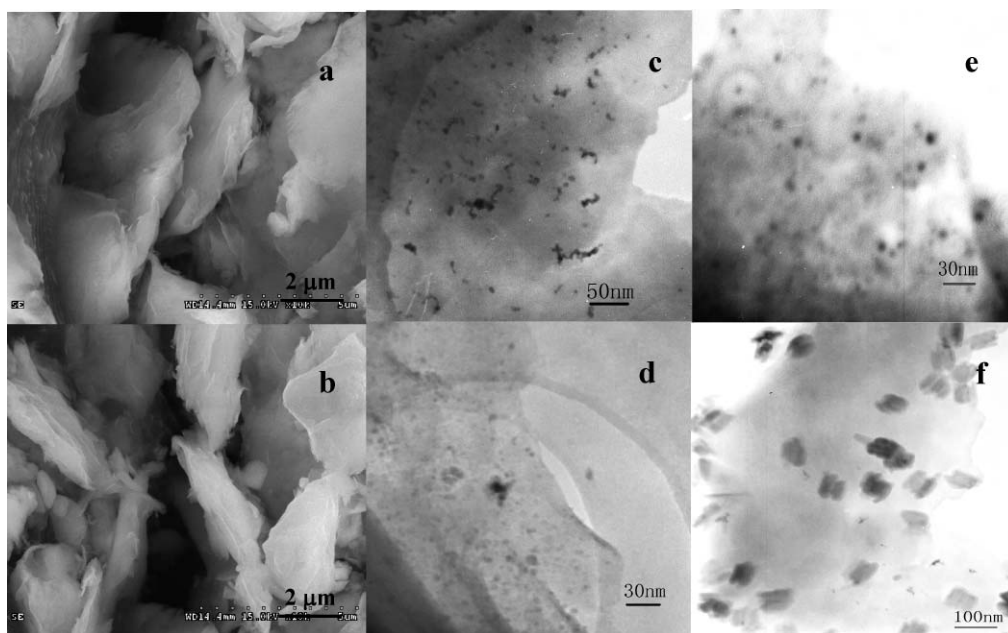
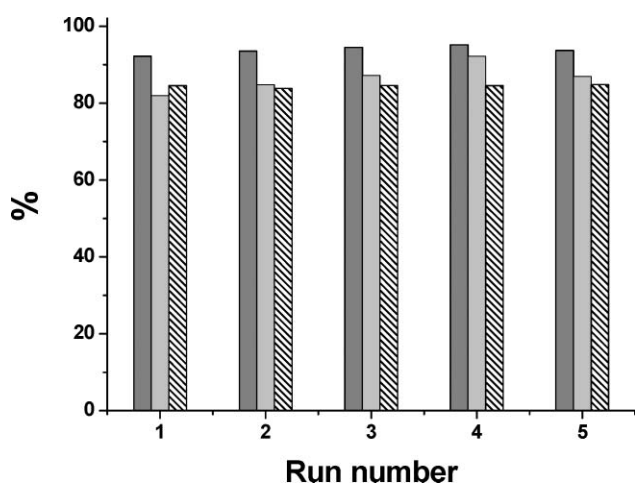


Fig. 1 XPS spectra of catalyst: (a) Ru/TMG-BEN, (b) Cu/TMG-BEN, (c) and (d) Ru-Cu/TMG-BEN (Ru/Cu, 3/1 in moles).



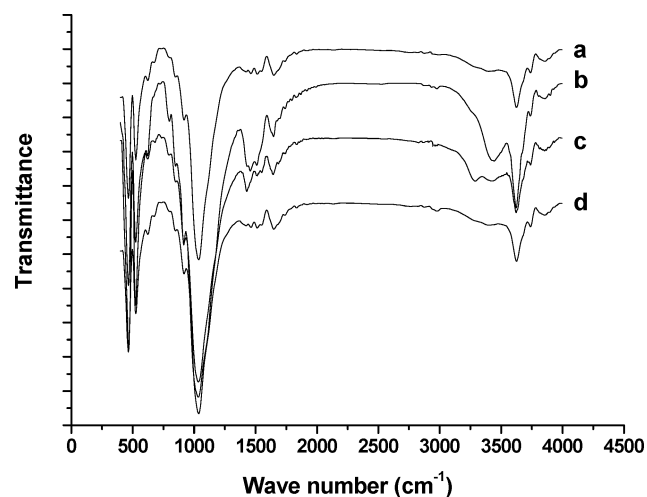
**Fig. 2** SEM images of (a) pristine bentonite; (b) Ru-Cu/TMG-BEN; (c) TEM images of fresh catalyst A (Ru-Cu/TMG-BEN); (d) Catalyst A after one run; (e) fresh catalyst B (Ru-Cu/BEN); and (f) catalyst B after one run.

of the nanoparticles effectively. Therefore, the catalyst was stable during the reaction. After reaction, the organic products were collected and analyzed by AAS (atomic absorption spectrum) analysis for Ru and Cu metals, and metal leaching was not detected. Results of recyclability of Ru-Cu/TMG-BEN also supported this from another aspect. It can be seen from Fig. 3 that the activity and selectivity of the catalyst did not change after recycling 4 times.



**Fig. 3** Results of the recycle of catalyst Ru-Cu/TMG-BEN. ■ Glycerol conversion; □ Selectivity to liquid product; ▨ 1,2-PDO content in liquid product.

Some characterizations were conducted to confirm the existence of TMG cations on the surface of the catalyst. The presence of the cation of the ionic liquid TMGL in this catalyst was supported by the fact that the catalyst contained 10 wt% organic compound, as determined by TGA. The existence of the TMG cations was also supported by the FT-IR spectra (Fig. 4).



**Fig. 4** FT-IR spectra of the pristine bentonite and the as-prepared catalysts: a) the pristine bentonite, b) TMG-bentonite, c) fresh catalyst A (Ru-Cu/TMG-bentonite), and d) catalyst A after one run.

The specific peaks of CH<sub>3</sub> group at 1414 cm<sup>-1</sup>, 1463 cm<sup>-1</sup>, and 2967 cm<sup>-1</sup>, and the peak of C=N bond at 1640 cm<sup>-1</sup> can be observed in the spectrum of Ru-Cu/TMG-BEN which accord well with the FT-IR spectrum of TMG-BEN (Fig. 4). In addition, Fig. 4d shows the FT-IR spectrum of Ru-Cu/TMG-BEN after one run. The specific peaks of the CH<sub>3</sub> group and C=N bond can also be observed clearly, indicating that TMG cations still existed on the surface of bentonite after the reaction. Therefore the metal particles in Ru-Cu/TMG-BEN did not aggregate.

## Conclusions

In conclusion, the Ru-Cu bimetal has been successfully supported on bentonite, a cheap and abundant clay, with the aid of ionic liquid TMGL. The cations of TMGL are necessary



for the excellent stability of the catalyst. Ru and Cu exhibits excellent combination for catalyzing the hydrogenolysis of aqueous glycerol to produce 1,2-PDO. The catalyst was most efficient with a molar ratio of Ru to Cu of 3/1. 100% conversion of glycerol and 85% yield of 1,2-PDO could be achieved at 230 °C and 8 MPa. The catalyst modified with IL showed excellent recyclability. We believe that more efficient catalysts can be prepared by combination of functional ionic liquids, clays and metals for different reactions.

## Acknowledgements

The authors wish to thank the National Natural Science Foundation of China (20733010) for financial support.

## References

- 1 T. Miyazawa, Y. Kusunoki, K. Kunimori and K. Tomishige, *J. Catal.*, 2006, **240**, 213–221.
- 2 G. W. Huber, J. N. Chhedha, C. J. Barrett and J. A. Dumesic, *Science*, 2005, **308**, 1446–1450.
- 3 S. Fernando, S. Adhikari, C. Chandrapal and N. Murali, *Energy Fuels*, 2006, **20**, 1727–1737.
- 4 T. Werpy and G. Petersen, Top Value Added Chemicals from Biomass, vol. 1, Results of Screening for Potential Candidates from Sugars and Synthesis Gas, US DOE Report, 2004.
- 5 C. S. Gong, J. X. Du, N. J. Cao and G. T. Tsao, *Appl. Biochem. Biotechnol.*, 2000, **84**, 543–560.
- 6 P. L. Rogers, Y. J. Jeon and C. J. Svenson, *Process Saf. Environ. Prot.*, 2005, **83**, 499–503.
- 7 G. W. Huber, S. Iborra and A. Corma, *Chem. Rev.*, 2006, **106**, 4044–4098.
- 8 M. Pagliaro, R. Ciriminna, H. Kimura, M. Rossi and C. D. Pina, *Angew. Chem. Int. Ed.*, 2007, **46**, 4434–4440.
- 9 A. Behr, J. Eilting, K. Irawadi, J. Leschinski and F. Lindner, *Green Chem.*, 2008, **10**, 13–30.
- 10 C. H. Zhou, J. N. Beltramini, Y. X. Fan and G. Q. Lu, *Chem. Soc. Rev.*, 2008, **37**, 527–549.
- 11 Y. G. Zheng, X. L. Chen and Y. C. Shen, *Chem. Rev.*, 2008, **108**, 5253–5277.
- 12 D. Zimmerman and R. B. Isaacson, US Pat., 3 814 725, 1974 (Shell).
- 13 P. N. Caley and R. C. Everett, US Pat., 3 350 871, 1967 (DuPont).
- 14 E. P. Maris and R. J. Davis, *J. Catal.*, 2007, **249**, 328–337.
- 15 S. Ludwig and E. Manfred, US Pat., 5,616,817, 1997.
- 16 C. Montassier, D. Giraud and J. Barbier, *Stud. Surf. Sci. Catal.*, 1988, 165–170.
- 17 M. A. Dasari, P.-P. Kiatsimkul, W. R. Sutterlin and G. J. Suppes, *Appl. Catal. A: Gen.*, 2005, **281**, 225–231.
- 18 L. Huang, Y. L. Zhu, H. Y. Zheng, Y. W. Li and Z. Y. Zeng, *J. Chem. Technol. Biotechnol.*, 2008, **83**, 1670–1675.
- 19 I. Furikado, T. Miyazawa, S. Koso, A. Shimao, K. Kunimori and K. Tomishige, *Green Chem.*, 2007, **9**, 582–588.
- 20 C.-W. Chiu, A. Tekeci, J. M. Ronco, M.-L. Banks and G. J. Suppes, *Ind. Eng. Chem. Res.*, 2008, **47**, 6878–6884.
- 21 T. Kurosaka, H. Maruyama, I. Naribayashi and Y. Sasaki, *Catal. Commun.*, 2008, **9**, 1360–1363.
- 22 J. Chaminand, L. Djakovitch, P. Gallezot, P. Marion, C. Pinel and C. Rosier, *Green Chem.*, 2004, **6**, 359–361.
- 23 L. Ma, D. H. He and Z. P. Li, *Catal. Commun.*, 2008, **9**, 2489–2495.
- 24 J. Feng, H. Y. Fu, J. B. Wang, R. X. Li, H. Chen and X. J. Li, *Catal. Commun.*, 2008, **9**, 1458–1464.
- 25 D. G. Lahr and B. H. Shanks, *Ind. Eng. Chem. Res.*, 2003, **42**, 5467–5472.
- 26 D. G. Lahr and B. H. Shanks, *J. Catal.*, 2005, **232**, 386–394.
- 27 C. Montassier, J. C. Menezes, L. C. Hoang, C. Renaud and J. Barbier, *J. Mol. Catal.*, 1991, **70**, 99–110.
- 28 B. Casale and A. M. Gomez, US Pat., 5 276 181, 1994.
- 29 E. P. Maris, W. C. Ketchie, M. Murayama and R. J. Davis, *J. Catal.*, 2007, **251**, 281–294.
- 30 E. P. Maris and R. J. Davis, *J. Catal.*, 2007, **249**, 328–337.
- 31 S. Wang and H. C. Liu, *Catal. Lett.*, 2007, **117**(1–2), 62–67.
- 32 M. Balaraju, V. Rekha, P. S. Sai Prasad, R. B. N. Prasad and N. Lingaiah, *Catal. Lett.*, 2008, **126**, 119–124.
- 33 Z. W. Huang, F. Cui, H. X. Kang, J. Chen, X. Z. Zhang and C. G. Xia, *Chem. Mater.*, 2008, **20**, 5090–5099.
- 34 A. P. Umpierre, G. Machado, G. H. Fecher, J. Morais and J. Dupont, *Adv. Synth. Catal.*, 2005, **347**, 1404–1412.
- 35 C. P. Mehnert, E. J. Mozeleski and R. A. Cook, *Chem. Commun.*, 2002, 3010–3011.
- 36 J. Huang, T. Jiang, H. X. Gao, B. X. Han, Z. M. Liu, W. Z. Wu, Y. H. Chang and G. Y. Zhao, *Angew. Chem. Int. Ed.*, 2004, **43**, 1397–1399.
- 37 J. Huang, T. Jiang, B. X. Han, W. Z. Wu, Z. M. Liu, Z. L. Xie and J. L. Zhang, *Catal. Lett.*, 2005, **103**, 59–62.
- 38 X. M. Ma, Y. X. Zhou, J. C. Zhang, A. L. Zhu, T. Jiang and B. X. Han, *Green Chem.*, 2008, **10**(1), 59–66.
- 39 Y. L. Gu, C. Ogawa, J. Kobayashi, Y. Mori and S. Kobayashi, *Angew. Chem. Int. Ed.*, 2006, **45**, 7217–7220.
- 40 M. R. Castillo, L. Fousse, J. M. Fraile, J. I. Garcia and J. A. Mayoral, *Chem.-Eur. J.*, 2006, **13**, 287–291.
- 41 S. D. Miao, Z. M. Liu, B. X. Han, J. Huang, Z. Y. Sun, J. L. Zhang and T. Jiang, *Angew. Chem. Int. Ed.*, 2006, **45**(2), 266–269.
- 42 T. Kawabata, T. Mizugaki, K. Ebitani and K. Kaneda, *J. Am. Chem. Soc.*, 2003, **125**, 10486–10487.
- 43 H. X. Gao, B. X. Han, J. C. Li, T. Jiang, Z. M. Liu, W. Z. Wu, Y. H. Chang and J. M. Zhang, *Synth. Commun.*, 2004, **34**, 3083–3089.
- 44 S. Papp, J. Szél, A. Oszkó and I. Dékány, *Chem. Mater.*, 2004, **16**(9), 1674–1685.
- 45 Z. Király, B. Veisz, Á. Mastalir and Gy. Köfaragó, *Langmuir*, 2001, **17**(17), 5381–5387.
- 46 S. Aoki, K. Iwaida, N. Hanamoto, M. Shiro and E. Kimura, *J. Am. Chem. Soc.*, 2002, **124**, 5256–5257.
- 47 P. J. Bailey and S. Pace, *Coordin. Chem. Rev.*, 2001, **214**, 91–141.

# Exergetic life cycle analysis for the selection of chromatographic separation processes in the pharmaceutical industry: preparative HPLC *versus* preparative SFC†

Geert Van der Vorst,<sup>a</sup> Herman Van Langenhove,<sup>a</sup> Frederik De Paep,<sup>a</sup> Wim Aelterman,<sup>b</sup> Jules Dingenen<sup>b</sup> and Jo Dewulf<sup>\*a</sup>

Received 20th January 2009, Accepted 31st March 2009

First published as an Advance Article on the web 16th April 2009

DOI: 10.1039/b901151j

Today, environmentally responsible chemistry is of huge importance in the wake of sustainable production. In the field of the fine chemical and pharmaceutical industry, preparative supercritical fluid chromatography (Prep-SFC) and preparative high performance liquid chromatography (Prep-HPLC) are widely used chiral separation techniques. Prep-SFC is often named as a green alternative for Prep-HPLC without having a thorough assessment of the greenness. However, if metrics are used for process selection with respect to green chemistry, they mainly show three shortcomings: (1) a narrow system boundary approach is used; (2) energy requirements are barely taken into account and (3) if energy requirements are considered, there is a differentiation in mass and energy inputs. Taking into account these shortcomings, Prep-HPLC and Prep-SFC are now compared and evaluated for their integral resource consumption. The evaluation is performed on a specific enantiomeric separation using exergetic life cycle analysis within enlarging system boundaries  $\alpha$ ,  $\beta$  and  $\gamma$ . Within the  $\alpha$  system boundary (process level), Prep-HPLC requires 26.3% more resources quantified in exergy than the Prep-SFC separation due to its inherent higher use of organic solvents. Within the  $\beta$  system boundary (plant level), Prep-HPLC requires 29.1% more resources quantified in exergy than Prep-SFC. However, the Cumulative Exergy Extracted from the Natural Environment (CEENE) to deliver all mass and energy flows to the  $\alpha$  and  $\beta$  system boundary *via* the overall industrial metabolism shows that Prep-SFC requires 34.3% more resources than Prep-HPLC. The poor score of Prep-SFC in the  $\gamma$  system boundary is attributed to the high CEENE value related to the production of liquid carbon dioxide and the use of electricity for heating and cooling. It can be concluded that for this case, the most sustainable process as for the integral resource consumption is Prep-HPLC, unlike the general perception that Prep-SFC outperforms Prep-HPLC.

## Introduction

To date, environmentally responsible chemistry is of huge importance. Next to the environmental benefits, economic profits can be made when aiming for a sustainable chemical production. Principles such as eco-efficiency and green chemistry, where green also refers to the color of money, were developed and served the bulk chemistry, the fine chemical and pharmaceutical industry well.<sup>1</sup> However, before being able to implement sustainable production technologies into industry, a lot of research has

to be done. Research towards a sustainable chemical production is twofold.

First, innovative chemical reactions and better performing unit operations have to be developed to make the green concepts happen. Research efforts are numerous, as well as their industrial implementations.<sup>2</sup> Preparative supercritical fluid chromatography (Prep-SFC) is such an implementation.<sup>3,4</sup> Pressurized CO<sub>2</sub> and a small amount of cosolvent are used as mobile phase instead of the huge amounts of organic solvents used in preparative high performance liquid chromatography (Prep-HPLC).<sup>5</sup>

Second, there is a need for an adequate assessment of the “greenness”. Researchers have to quantify the potential and impact of new technologies which requires the development of appropriate metrics and indicators.<sup>6</sup> Quantitative indicators can be used for unambiguous comparison of technologies. At the same time, indicators also allow better communication of the efforts, be it for stimulating involvement of personnel or for external communication. Different groups of indicators can be distinguished.<sup>7</sup> Not all indicator groups are however used by

<sup>a</sup>Research Group ENVOC, Ghent University, Coupure Links 653, Ghent, B-9000, Belgium. E-mail: jo.dewulf@ugent.be; Fax: +32 9 264 62 43; Tel: ++32 9 264 59 49

<sup>b</sup>Johnson & Johnson PRD, Janssen Pharmaceutica nv, Turnhoutseweg 30, Beerse, 2340, Belgium

† Electronic supplementary information (ESI) available: P&ID of the Prep-HPLC separation (Fig. S1) and the Prep-SFC separation (Fig. S2) in the  $\alpha$  system boundary; mass and energy balance in the  $\alpha$  system boundary for the Prep-HPLC separation (Table S1) and the Prep-SFC separation (Table S2) of 500 g racemic mixture. See DOI: 10.1039/b901151j

chemical manufacturers. The tools used by Johnson & Johnson, AstraZeneca<sup>8</sup>, GlaxoSmithKline<sup>9</sup>, Pfizer<sup>10</sup> and BASF<sup>11</sup> are mainly dealing with emission and toxicity type indicators and indicators dealing with mass efficiency. The metrics and indicators used in specialty chemicals and pharmaceutical industry today mainly show three shortcomings. First, the energy resource requirements are not taken into account to determine the efficiency of specific production processes. Production processes take place in multipurpose plants and energy requirements are only evaluated at the overall plant level. A second limitation is splitting up resource and energy inputs: kg vs. kJ. When looking to the overall production chain, numerous natural resources can fulfill both functions. For the evaluation of two alternative processes A and B, it is possible that based on mass requirements, A scores better, while for energy requirements, B is favorable. How can a good conclusion be drawn here? Third, there is the frequently too narrow system boundary approach. For example, in indicators for resource efficiency, it is common practice to use the gate-to-gate system boundary, resulting in the omission of the overall resource intake upstream of their own facility.

The first and second limitations can be overcome by taking into account the energy requirement of specific production technologies and by making use of exergy analysis for the evaluation of alternative processes or technologies. Exergy analysis provides a powerful tool for assessing the quality and quantity of resources and stands for the maximal amount of work that can be retrieved from a resource when bringing it into equilibrium with the natural environment.<sup>12</sup> Exergy analysis of production processes indicates how efficient resources are employed towards products and not towards waste and lost work, *i.e.* the irreversibilities. When evaluating the resource consumption, the emissions are also indirectly evaluated. The more resources are required to produce a product, the more emissions are produced *e.g.* CO<sub>2</sub> from fossils. More information and applications of exergy analysis in industry can be found in two reviews.<sup>13,14</sup> Within the pharmaceutical industry the applications are however limited.<sup>7,15,16</sup>

The third limitation of currently used environmental sustainability metrics and indicators in specialty chemicals and pharmaceutical industry, *i.e.* the narrow system boundaries, can be overcome through the life cycle approach. Life cycle assessment (LCA) is well known in the academic world and is already used in industry to evaluate the overall impact on the environment of the whole life cycle of processes and products.<sup>17</sup> The emphasis of life cycle impact assessment methods is however mostly on emissions and not on resource requirements. Combining exergy analysis with the LCA methodology enables one to overcome all three previous mentioned limitations and results in a good indicator: Exergetic Life Cycle Assessment (ELCA) for the evaluation of resource requirements of processes in the specialty and pharmaceutical industry.<sup>14</sup>

The scope of this paper is to evaluate the resource requirements for two preparative chromatographic separation processes, covering the integral energy and material resource requirements simultaneously. The evaluation is performed on a specific enantiomeric separation that can be performed by Prep-SFC or by Prep-HPLC. Most of the preparative separations are still carried out using organic solvents as mobile phase. These organic solvents can often be replaced by supercritical

fluids, *e.g.* supercritical CO<sub>2</sub>, which offers many advantages.<sup>18</sup> Supercritical CO<sub>2</sub> has gas-like viscosities enabling high flow rates with moderate pressure drop. Supercritical CO<sub>2</sub> also has a higher diffusion coefficient compared with organic solvents which improves the efficiency of separation. Additionally, the physical properties of the fluid can easily be changed by varying pressure and/or temperature.<sup>19–22</sup>

To date, no detailed analysis has been made of the integral resource requirement of both chromatographic separation techniques. In this article both techniques will be evaluated and compared on a thermodynamically quantitative method. For this, the exergetic life cycle assessment method is used. The exergy approach and the cumulative exergy extracted from the natural environment (CEENE) are envisaged in order to evaluate the overall resource intake at three different levels. First, resource consumption evaluation is carried out at the process level itself. This evaluation level is called the  $\alpha$  system boundary. In this narrow system boundary, both separation techniques are split up in three parts which is visualized in Fig. S1 and S2, available as ESI.† These three parts are: (1) the batch preparation including mixing, filtering and storage of the solution and solvents; (2) the separation step including pumps, the column, an UV spectrometer, a gas cleaner and cyclones; (3) the evaporators for removal of solvents from the separated compounds. Second, resource requirements are evaluated at the facility level which is the  $\beta$  system boundary. In this system boundary all resources bought by the pharmaceutical company to perform the separation are evaluated including resources required for the production of cooling and heating media, for storage, etc. Third, the overall resource intake from the environment into the industrial metabolism to feed and fuel both chromatographic separations is evaluated. This evaluation is performed in the  $\gamma$  system boundary.<sup>7</sup>

## Results and discussion

### Process level ( $\alpha$ system boundary)

The process and instrumentation diagrams (P&ID's) of both separation techniques Prep-HPLC and Prep-SFC are presented in Fig. S1 and S2† respectively in which three parts inside the  $\alpha$  system boundary can be distinguished. After defining the system boundaries  $\alpha$  (presented in Fig. S1 and S2†) and  $\beta$  and  $\gamma$  (presented in Fig. 3), the functional unit (FU) was set at “450 g isolated enantiomers” (225 g enantiomer 1 and 225 g enantiomer 2). Both techniques have the same separation efficiency of 90% and thus have to start with 500 g of the racemic mixture. After separation, 50 g goes to the waste stream and two times 225 g are isolated and are used in following production steps.

The resource requirements related to both separation techniques in the  $\alpha$  system boundary are presented in Fig. 1. The exergy consumption related to the Prep-HPLC technique is 26.3% higher than for the Prep-SFC technique. The exergy consumption is divided into 6 groups; chemicals, electromechanical, thermal, inert gas, liquid CO<sub>2</sub> and cleaning solvents. It is clear that exergy consumption related to the use of chemicals is important (70% for Prep-HPLC and 43% for Prep-SFC), especially in Prep-HPLC where a lot of organic solvents are required. The impact of the nitrogen gas is negligible for both

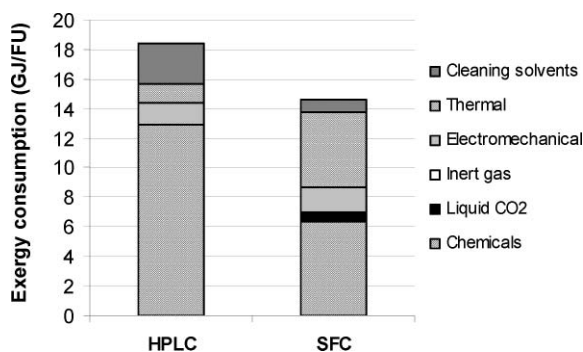


Fig. 1 Exergy consumption of Prep-HPLC and Prep-SFC in the  $\alpha$  system boundary divided over 6 categories.

techniques (0.01%). For the Prep-SFC technique, it is clear that the thermal exergy consumption is large (35%) compared with the Prep-HPLC alternative (7%). This is mainly due to the heating and cooling of liquid CO<sub>2</sub> in the separation installation. In Fig. 2, the exergy requirements are divided over the three parts; batch preparation, separation installation and solvent evaporation. The exergy requirements for the Prep-HPLC alternative are higher in the evaporator part because the huge amount of used organic solvents that have to be evaporated. The largest exergy consumption for the Prep-SFC technique occurs in the separation installation due the excessive requirements for heating and cooling of CO<sub>2</sub>.

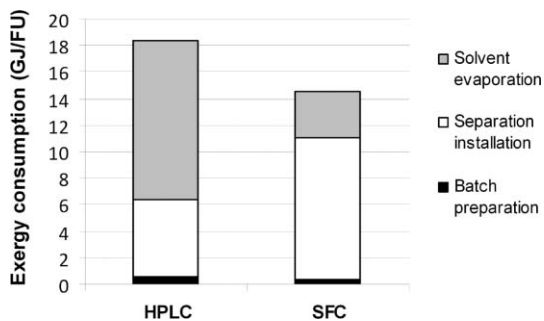


Fig. 2 Exergy consumption of Prep-HPLC and Prep-SFC in the  $\alpha$  system boundary divided over 3 parts.

### Plant level ( $\beta$ system boundary)

Enlarging the system boundary from the  $\alpha$  level to the  $\beta$  level will result in more resources that are required to perform both separation alternatives. The  $\beta$  system boundary equals the physical boundary of the production site and the resources passing this boundary are equal to the resources that have to be bought by the pharmaceutical company to perform the separation. In this case (Prep-HPLC vs. Prep-SFC), the supporting utilities within the plant are given in Fig. 3. The exergy requirements in the  $\beta$  system boundary are negligible when compared with those in the  $\alpha$  system boundary. For the Prep-HPLC only 3% extra exergy is required to the  $\alpha$  system boundary. For the Prep-SFC method, this is only limited to 1%.

These extra exergy requirements occur in the production of cooling and heating media, production of steam and cooling water, storage and the production of industrial water. In this case,

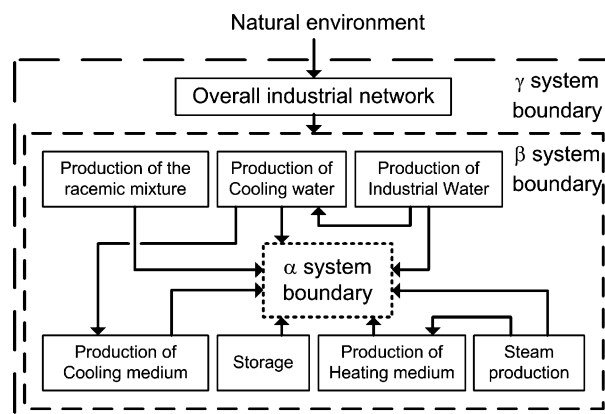


Fig. 3  $\beta$  and  $\gamma$  system boundaries for Prep-HPLC and Prep-SFC.

resource requirements for waste treatment and the production of the racemic mixture are not taken into account for the evaluation.

Normally the exergy consumption related to the previous production steps in a synthesis route is not negligible. However, in this case, the efficiency of both alternative separation processes is equal (90%). Including the resource requirements of previous production steps will not influence the difference between both alternatives in absolute numbers. In the  $\beta$  system boundary it can again be concluded that the Prep-HPLC alternative is the most favorable because less exergy input is required when separating 500 g of racemic mixture. The comparison of both separation techniques in the  $\beta$  system boundary is presented in Fig. 4.

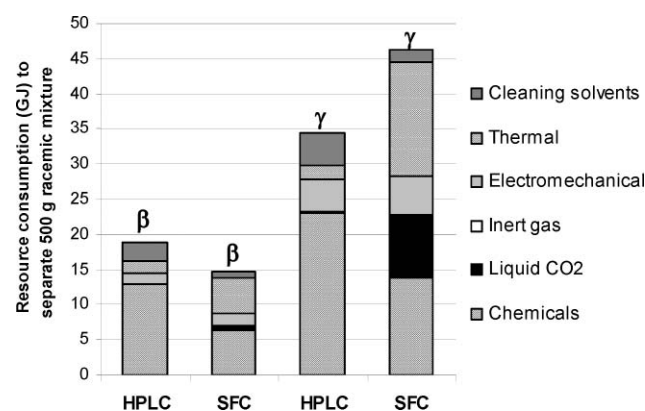


Fig. 4 Exergy consumption in the  $\beta$  system boundary and the CEENE in the  $\gamma$  system boundary for the Prep-HPLC and Prep-SFC separation techniques.

### Industry level ( $\gamma$ system boundary)

At last, both separation techniques are evaluated and compared in the  $\gamma$  system boundary, based on the CEENE value. In this level, the cumulative resources extracted from the natural environment to perform a separation of 500 g racemic mixture with Prep-HPLC or with Prep-SFC are quantified. In Fig. 4 the CEENE values of both techniques are presented and are compared with the exergy consumption in the  $\beta$  system boundary. It is remarkable that in the  $\gamma$  system boundary Prep-SFC is less favorable compared with the results from the previous

**Table 1** Resource fingerprint: CEENE values (MJ) over 8 categories for the Prep-HPLC and Prep-SFC separation techniques (FU = 500 g racemic mixture to be separated)

Category	HPLC		SFC	
	(MJ/FU)	(%)	(MJ/FU)	(%)
Renewable resource	220	0.6%	424	0.9%
Fossil fuels	29594	85.7%	27349	59.0%
Nuclear energy	2995	8.7%	15307	33.0%
Metal ores	6	0.0%	8	0.0%
Minerals	4	0.0%	6	0.0%
Water use	1229	3.6%	1905	4.1%
Land use	468	1.4%	1359	2.9%
Atmospheric resources	0	0.0%	0	0.0%
<b>CEENE</b>	<b>34516</b>	<b>100%</b>	<b>46358</b>	<b>100%</b>

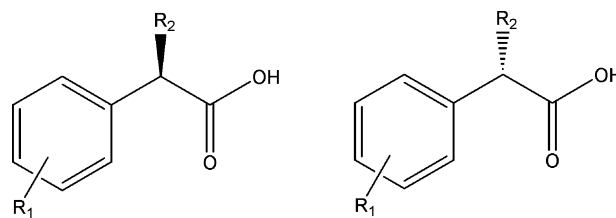
two system boundaries. This is due to the low cumulative degree of perfection (CDP) value related to the production of liquid CO<sub>2</sub>. The CDP is the ratio of the exergy content of a product over the CEENE value of this product. The closer the ratio to one, the more efficient the resource consumption of the production process is. For liquid CO<sub>2</sub>, the CDP is 0.071. The CDP of organic solvents is around 0.5, which is approximately 7 times higher than the CDP of liquid CO<sub>2</sub>. The impact of this difference in CDP is visualized in Fig. 4 by the large expansion of the black bar (Liquid CO<sub>2</sub>) when going from the β to the γ system boundary. The expansion is much less impressive for the chemicals group. A second reason why Prep-SFC is less favorable than Prep-HPLC in the γ system boundary can be found in the difference between the thermal exergy consumption in the β system boundary and the CEENE values related to the thermal group in the γ system boundary. The Prep-HPLC technique uses mostly steam and hot shellsol oil as heating medium; both produced by natural gas combustion. The CDP of natural gas is 0.91. For the Prep-SFC alternative, heating in the separation installation is done electrically. The CDP value of electricity is 0.31 and thus much lower than the CDP of natural gas. This results in a higher CEENE value for the thermal group and eventually in total for a separation using the Prep-SFC alternative.

Another evaluation between both alternatives can be made when using the CEENE method. The CEENE values for both techniques can be divided into 8 categories representing the nature of the resources extracted from the natural environment. This is summarized in Table 1. For both techniques, the share of the fossil fuels is remarkable (>59%). The largest difference in absolute numbers is made by the nuclear energy resources, which is related to the higher electricity consumption related to the Prep-SFC alternative.

## Materials and methods

### Data inventory

The investigated process concerns the separation of 500 g of a pharmaceutical racemic mixture into two enantiomers of a phenyl acetic acid derivative (Fig. 5). For this separation, two techniques, *i.e.* Prep-HPLC and Prep-SFC, are considered. Because both separation techniques have an equal efficiency of 90%, the functional unit can be defined as “the separation of 500 g enantiomeric mixture”. The complete data inventory for



**Fig. 5** Both enantiomers of the racemic mixture of phenyl acetic acid derivatives.

both separations in the three described stages; batch preparation, separation installation and solvent evaporation are listed in Table S1 and S2, available as ESI.†

Both processes, situated within the α system boundary, are embedded in a network of related processes in the plant (β system boundary); such as supporting processes for energy exchange (hot and cold media delivery, electricity delivery), and supporting processes for mass exchange (storage and water production). Similar process analyses as in Table S1 and S2† have been made for all the extra production steps in the β system boundary which deliver the utilities to the α system boundary. The previous production steps of the racemic mixture are not taken into account for the calculations in the β system boundary. The focus is on the resource consumption of the separation process and the supporting processes and not on the efficiency of the previous production steps. The treatment of the waste solvent, wastewater and waste gas are also not taken into account in this study. The waste gas and wastewater treatment are performed on-site (in the β system boundary) but the resource consumption is negligible. The waste solvent treatment occurs in an off-site incineration plant with heat recuperation. In this incineration installation, the waste solvents are used as a resource to replace fresh fossil fuels. These fossil fuels are required to obtain the optimal calorific value of waste streams to be incinerated. For this, the resource requirements to “treat” the waste solvents are not included in this study.

Data for both separation techniques for the α and β system boundary were collected from Janssen Pharmaceutica Belgium, part of Johnson & Johnson. Data concerning the resource requirements in the γ system boundary were inventoried from theecoinvent database.<sup>23,24</sup> Using this life cycle inventory database makes it possible to calculate the cumulative exergy extracted from the natural environment.<sup>25</sup> Also for the production of liquid CO<sub>2</sub>, data was retrieved fromecoinvent. Due to high uncertainties concerning this liquid CO<sub>2</sub> data, only the data with the least uncertainty were taken into account, being the electricity and heat consumption for the purification and liquefaction of 1 kg liquid CO<sub>2</sub>.<sup>26</sup> Transport, chemicals usage, plant installation, water consumption etc. are thus not included in the CEENE value of liquid CO<sub>2</sub>. In reality the CEENE value of liquid CO<sub>2</sub> should thus even be much higher than calculated for this case which will result in an even less favorable situation for Prep-SFC in the γ system boundary.

### Exergy and cumulative exergy extracted from the natural environment (CEENE)

All energy and material inputs and outputs related to both Prep-HPLC, Prep-SFC and the supporting processes have

been quantified in exergy terms. For these calculations, data available in the literature, data obtained by means of the group contribution method, and data obtained from Gibbs formation energy data have been employed. The method for the calculation of the cumulative exergy extracted from the natural environment is retrieved from Dewulf *et al.*<sup>25</sup> These CEENE calculations require the use of the ecoinvent database.<sup>24</sup>

## Conclusion

This study illustrates the possibility and advantages of quantifying both energy and material resource intake for industrial processes. Exergy analysis is here the unique scientifically sound tool that enables one to quantify all kinds of resources and products on the same scale. However, exergy analysis can only be performed if detailed data inventory are available, which is not common practice today, particularly with energy resource intake. Next to data acquisition it is proven that setting appropriate system boundaries is critical. It is important to see to what extent the particular processes require supporting processes for energy and materials not only within the facility itself, but also outside the facility in the overall industrial metabolism. Considering the traditional material resource efficiency in a narrow system boundary ( $\alpha$ ) would lead erroneously towards selecting Prep-SFC chromatography which is 26.3% better than Prep-HPLC. This is however without taking into account the integral amount of resources extracted from the natural environment to perform both processes. The use of electricity for heating and cooling and the production of liquid CO<sub>2</sub> disfavors Prep-SFC when it is evaluated on its cumulative amount of exergy extracted from the natural environment. When evaluated on this integral resource consumption, Prep-HPLC is the most sustainable requiring 34.3% less exergy than Prep-SFC. Furthermore, the study shows where efficiency gains can be made by identifying and quantifying the exergy requirements and the CDP of the resources used for both alternatives.

Although an evaluation was made for a representative case for the pharmaceutical industry, it can be concluded that a similar resource requirement evaluation of Prep-SFC and Prep-HPLC should be examined in every individual case. The way how such an analysis can be made properly is presented in this article. Further research can be performed on the uncertainty analysis of such comparisons. Characteristics such as separation efficiency, solvent recycling potential and heating requirements will be different in other cases which can favor Prep-HPLC or Prep-SFC as for their integral resource consumption. The solubility of the components can change for the different solvents used. The solvent recycling can be improved which, especially for the liquid CO<sub>2</sub>, can have a major impact on the evaluation in the  $\gamma$  system boundary. Taking into account the waste solvent incineration, this will in its turn result in an extra benefit in the  $\gamma$  system boundary for the Prep-HPLC alternative.

For this particular case, we have proven that Prep-SFC is not “greener” from a resource point of view when compared to Prep-HPLC. In our view both techniques have to exist next to

one another knowing that for other cases the one can outperform the other.

## Nomenclature

$\alpha$	System boundary at process level
$\beta$	System boundary at production site level
$\gamma$	System boundary at industrial network level
CEENE	Cumulative exergy extracted from the natural environment
CDP	Cumulative degree of perfection
C1	Column of the first method: HPLC
Cy1	Cyclone 1
ELCA	Exergetic life cycle assessment
F1–2	Filter 2 of the first method: HPLC
FU	Functional unit
LCA	Life cycle assessment
P & ID	Process and instrumentation diagram
Prep-HPLC	Preparative high performance liquid chromatography
Prep-SFC	Preparative supercritical fluid chromatography
R1–2	Reactor 2 of the first method: HPLC
T1–2	Tank 2 of the first method: HPLC

## Acknowledgements

The authors acknowledge the financial support of the Institute for the Promotion of Innovation through Science and Technology in Flanders (IWT-Vlaanderen).

## References

- J. Garcia-Serna, L. Perez-Barrigon and M. J. Cocero, *Chem. Eng. J.*, 2007, **133**, 7–30.
- A. M. Rouhi, *Chemical & Engineering News*, 2002, **80**, 30–33.
- C. J. Welch, F. Fleitz, F. Antia, P. Yehl, R. Waters, N. Ikemoto, J. D. Armstrong and D. J. Mathre, *Organic Process Research and Development*, 2004, **8**, 186–191.
- W. R. Leonard, D. W. Henderson, R. A. Miller, G. A. Spencer, O. S. Sudah and M. Biba, *Chirality*, 2007, **19**, 693–700.
- S. K. Ritter, *Chemical & Engineering News*, 2002, **80**, 19–23.
- A. Lapkin, in *Renewables-based Technology: Sustainability Assessment*, eds. J. Dewulf and H. Van Langenhove, Wiley, New York, 2006, pp. 39–53.
- J. Dewulf, G. Van der Vorst, W. Aelterman, B. De Witte, H. Vanbaelen and H. Van Langenhove, *Green Chemistry*, 2007, **9**, 785–791.
- C. Hairgreaves, in *AIChE 2008 annual meeting*, Philadelphia, 2008.
- A. D. Curzons, D. J. C. Constable, V. L. Cunningham and D. N. Mortimer, *Green Chemistry*, 2001, **3**, 1–6.
- K. Alfonsi, J. Colberg, P. J. Dunn, T. Fevig, S. Jennings, T. A. Johnson, H. P. Kleine, C. Knight, M. A. Nagy, D. A. Perry and M. Stefaniak, *Green Chemistry*, 2008, **10**, 31–36.
- P. Saling and A. Kicherer, in *Renewables-based Technology: Sustainability Assessment*, eds. J. Dewulf and H. Van Langenhove, Wiley, New York, 2006, pp. 299–313.
- J. Szargut, *Exergy method technical and ecological applications*, Witpress, Southampton, 2005.
- E. Sciubba and G. Wall, *International Journal of Thermodynamics*, 2007, **10**, 1–26.
- J. Dewulf, H. Van Langenhove, B. Muys, S. Bruers, R. Bakshi, G. Grubb, R. A. Gaggioli, D. M. Paulus and E. Sciubba, *Environ. Sci. Technol.*, 2008, **42**, 2221–2232.
- M. Lampret, V. Bukovec, A. Paternost, S. Krizman, V. Lojk and I. Golobic, *Applied Energy*, 2007, **84**, 781–794.

- 
- 16 A. I. Liapis and R. Bruttini, *Int. J. Heat Mass Transf.*, 2008, **51**, 3854–3868.
- 17 A. Azapagic, *Chem. Eng. J.*, 1999, **73**, 1–21.
- 18 S. Peper, M. Johannsen and G. Brunner, *Journal of Chromatography A*, 2007, **1176**, 246–253.
- 19 D. Berger, *LC GC Eur.*, 2007, **20**, 164.
- 20 G. Terfloth, *Journal of Chromatography A*, 2001, **906**, 301–307.
- 21 C. J. Welch, W. R. Leonard, J. O. DaSilva, M. Biba, J. Albaneze-Walker, D. W. Henderson, B. Laing and D. J. Mathre, *LC GC Eur.*, 2005, **18**, 264.
- 22 Y. Zhang, D. R. Wu, D. B. Wang-Iverson and A. A. Tymiak, *Drug Discovery Today*, 2005, **10**, 571–577.
- 23 Ecoinvent, Swiss Centre for Life Cycle Inventories, Düsseldorf, 2007, retrieved from: [www.ecoinvent.ch](http://www.ecoinvent.ch), 2007.
- 24 R. Frischknecht and G. Rebitzer, *Journal of Cleaner Production*, 2005, **13**, 1337–1343.
- 25 J. Dewulf, M. E. Bösch, B. De Meester, G. Van, der Vorst, H. Van Langenhove, S. Hellweg and M. A. J. Huijbregts, *Environ. Sci. Technol.*, 2007, **41**, 8477–8483.
- 26 R. Frischknecht, Bundesamt für Energie (BfE), Bern, 1999.

# Polyethylene glycol radical-initiated oxidation of benzylic alcohols in compressed carbon dioxide†

Jin-Quan Wang, Liang-Nian He\* and Cheng-Xia Miao

Received 6th January 2009, Accepted 31st March 2009

First published as an Advance Article on the web 16th April 2009

DOI: 10.1039/b900128j

The PEG radical from oxidative degradation of polyethylene glycol was first used to initiate the oxidation of benzylic alcohols to carbonyl compounds without the need of a catalyst and/or additive in a viable synthetic, cost-effective and environmentally benign way, in which PEG/O<sub>2</sub>/CO<sub>2</sub> acts as initiator, oxidant and solvent. Compressed CO<sub>2</sub> in this study not only provides a safe environment to conduct the oxidation employing molecular oxygen as an oxidant, but also could improve the reaction and adjust the selectivity of the target product by altering CO<sub>2</sub> pressure. Moreover, this methodology could be used to oxidize a set of benzyl alcohols. The findings introduced here provide useful examples for developing free-radical chemistry from PEG thermal oxidative degradation.

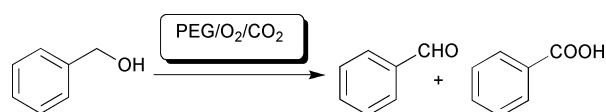
## Introduction

The oxidation of primary and secondary alcohols to aldehydes or acids and ketones, respectively, is of significant importance in organic chemistry, both for fundamental research and industrial manufacturing.<sup>1</sup> Traditionally, such transformation has been performed with stoichiometric inorganic oxidants, notably chromium reagents.<sup>2</sup> However, with the increasing environmental and economical concerns in recent years, much attention has been directed towards the development of environmentally benign methods for oxidation of alcohols, using molecular oxygen as a primary oxidant, which is readily available and produces water as the sole by-product. Recently, efficient systems using molecular oxygen have been developed for the catalytic oxidation of alcohols.<sup>3–6</sup>

Compressed CO<sub>2</sub> has been touted as a suitable solvent for organic synthesis, offering economical and environmental benefits due to its favorable properties and readily tunable solvent parameters,<sup>7</sup> particularly, compressed CO<sub>2</sub> appears to be an ideal solvent for use in oxidation. Unlike almost any organic solvent, CO<sub>2</sub> will not be oxidized further, and hence the use of CO<sub>2</sub> as a reaction medium eliminates by-products originating from solvents. At the same time, compressed CO<sub>2</sub> provides a safe reaction environment with excellent mass and heat transfer for aerobic oxidations. As a consequence, novel chemistry relevant to enhancing selectivity towards desired products, improving reactivity and ease of product separation could be created when utilizing compressed CO<sub>2</sub> as a reaction medium.

Polyethylene glycol (PEG) and its derivatives are commonly known to be inexpensive, thermally stable, environmentally

benign media for chemical reactions and phase transfer catalysts as well as having an almost negligible vapor pressure.<sup>8</sup> On the other hand, the oxidative thermal degradation of PEG<sup>9</sup> was also encountered because PEG is susceptible to free radical oxidative attack in the presence of oxygen at an elevated temperature over 70 °C. In this respect, PEG and oxygen can react to form PEG peroxide in excess air through a so-called random chain scission process.<sup>9</sup> We reasoned that the PEG radicals *in situ* generated from oxidative degradation could be used to induce organic reactions, specifically oxygenation of alcohols. To the best of our knowledge, this methodology has not yet been reported in the literature so far. In this work, we found that the PEG radical from oxidative degradation of polyethylene glycol could be used to initiate the oxidation of benzylic alcohols to produce carbonyl compounds without the need for a catalyst and/or additive, in which PEG/O<sub>2</sub>/CO<sub>2</sub> acts as initiator, oxidant and solvent, as shown in Scheme 1. Compressed CO<sub>2</sub> in this study not only could improve the oxidation but adjust the selectivity of the target product by altering CO<sub>2</sub> pressure.



**Scheme 1** Oxidation of benzyl alcohol by the PEG radical in compressed CO<sub>2</sub>.

## Results and discussion

### Optimization

To validate our hypothesis, we initially examined oxygenation of benzyl alcohol and the reaction was carried out in the presence of PEG and 2.5 MPa O<sub>2</sub> at 100 °C for 12 h. Under these conditions, the benzyl alcohol furnished the benzaldehyde (19%) and benzoic acid (13%) concomitant with 3% benzyl formate (Table 1, entry 2). The conversion was further improved by

State Key Laboratory and Institute of Elemento-Organic Chemistry Nankai University, Tianjin, 30071, P.R. China. E-mail: heln@nankai.edu.cn; Fax: +86 22-2350 4216; Tel: +86 22-2350 4216

† Electronic supplementary information (ESI) available: General information, EPR spectrum, GC chart, ESI-MS spectrum and NMR charts. See DOI: 10.1039/b900128j



**Table 1** Oxidation of benzyl alcohol initiated by PEG radical arising from oxidative/thermal degradation of PEG. Screening<sup>a</sup>

Entry	T/°C	Conv.(%) <sup>b</sup>	Yield of aldehyde (%) <sup>b</sup>	Yield of acid (%) <sup>b</sup>
1	100	77	22	50
2 <sup>c</sup>	100	36	19	13
3 <sup>d</sup>	100	0	0	0
4 <sup>e</sup>	100	0	0	0
5	80	8	7	0
6	120	97	1	89
7 <sup>f</sup>	100	98	6	84
8 <sup>g</sup>	100	88	8	61
9 <sup>h</sup>	100	0	0	0

<sup>a</sup> All the experiments were carried out with 1.93 mmol of benzyl alcohol, 0.7 mmol of PEG-1000, 2.5 MPa O<sub>2</sub> and 13.5 MPa CO<sub>2</sub> at 12 h, unless otherwise stated. <sup>b</sup> Determined by GC. <sup>c</sup> Without CO<sub>2</sub>. <sup>d</sup> In the absence of PEG. <sup>e</sup> Without O<sub>2</sub>. <sup>f</sup> 24 h. <sup>g</sup> 77.2 mmol of benzyl alcohol, 2.1 mmol of PEG-1000, 2 MPa O<sub>2</sub>, 100 °C, 18 h. <sup>h</sup> TEMPO (0.193 mmol) was added.

introducing 13.5 MPa CO<sub>2</sub> (entry 1), and reached up to 98% with benzoic acid as a main product when elongating reaction time to 24 h (entry 7). Furthermore, the reaction temperature had great influence on this transformation. The reaction gave only with 8% conversion at 80 °C (entry 5), suggesting that an elevated temperature (over 80 °C)<sup>9</sup> is required to induce thermal oxidative degradation of PEG; whereas, higher temperatures (120 °C) preferentially afforded benzoic acid with 97% conversion (entry 6). More importantly, the reaction could be scaled up (entry 8), making this method more synthetically viable in organic synthesis. Notably, the reaction could not take place without PEG or O<sub>2</sub> (entries 3 and 4). In other words, both PEG and molecule oxygen are prerequisites to performing those reactions smoothly. In addition, the oxygenation was completely suppressed by the presence of TEMPO (2, 2, 6, 6-tetramethylpiperidine-1-oxyl) (entry 9). In short, those results imply that PEG oxidative/thermal degradation<sup>9</sup> plays a critical role in this reaction and the “PEG/O<sub>2</sub>/CO<sub>2</sub>” possibly serves as a radical initiator, oxidant and solvent.

### Influence of PEG molecular weight

We next investigated what influence PEGs of different molecular weights had on the reaction. The conversion was gradually decreasing with the PEG molecular weight increasing from 300 to 20 000 (Table 2), being presumably ascribed to the increasing mass transport limitation of gaseous oxygen in highly viscous PEG with a long chain.<sup>10</sup> Interestingly, the product distribution between aldehyde and acid was also correlative with the PEG molecular weight (Table 2, entries 1–5). The reaction preferentially furnished the corresponding acid with PEG-300 (entry 1), and exclusively afforded the targeted aldehyde with PEG-6000 although the lower conversion was achieved (entry 4). In addition, the PEG with protected hydroxyl group also proved effective (entry 6).

### Influence of PEG amount

Furthermore, the effect of PEG amount on this oxygenation were also studied as shown in Table 3. The conversion was enhanced by increasing the quantity of PEG, the suitable molar

**Table 2** The influence of the PEG molecular weight on the oxidation of benzyl alcohol<sup>a</sup>

Entry	PEG	Conv. (%)	Yield of aldehyde (%) <sup>b</sup>	Yield of acid (%) <sup>b</sup>
1	300	95	7	83
2	1000	77	22	50
3	2000	73	28	43
4	6000	9	8	0
5	20 000	1	1	0
6	PEG-dimethyl ether (MW = 1000)	8	12	69

<sup>a</sup> All the reactions were conducted with 0.2 g (1.93 mmol) benzyl alcohol, 0.7 g PEG, 2.5 MPa O<sub>2</sub>, 13.5 MPa CO<sub>2</sub> at 100 °C for 12 h. <sup>b</sup> Determined by GC.

**Table 3** The influence of PEG-1000 amount on the oxidation of benzyl alcohol<sup>a</sup>

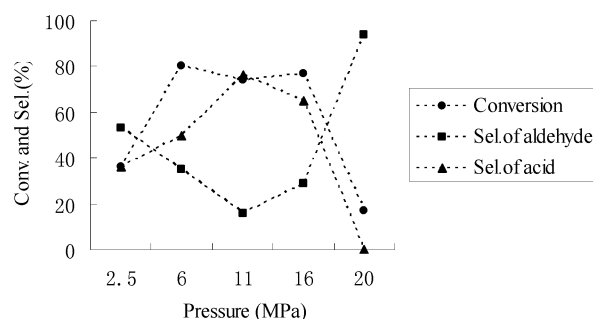
Entry	Substrate/PEG (molar ratio)	Conv. (%)	Yield of aldehyde (%) <sup>b</sup>	Yield of acid (%) <sup>b</sup>
1	11	1	1	0
2	5.5	3	0.2	0.4
3	2.8	77	22	50
4	1.4	82	21	55

<sup>a</sup> All the reactions were conducted with 1.93 mmol benzyl alcohol, 2.5 MPa O<sub>2</sub>, 13.5 MPa CO<sub>2</sub> at 100 °C for 12 h. <sup>b</sup> Determined by GC.

ratio of the substrate and PEG-1000 was around 1.4 under the otherwise identical reaction conditions.

### Effect of CO<sub>2</sub> pressure

Fig. 1 shows the effect of CO<sub>2</sub> pressure on the reaction. In the present study, an appropriate CO<sub>2</sub> pressure could significantly enhance the reaction rate probably due to the “CO<sub>2</sub>-expanded effect of PEG” in PEG/compressed CO<sub>2</sub> systems, thus resulting in changes in the physical properties of the PEG, including lowered melting points, lowered viscosity, increased gas/liquid diffusion rates.<sup>11</sup> Indeed, as judged by visual inspection through a window-equipped high-pressure reactor, we found that PEG and its derivatives are expandible with CO<sub>2</sub>, which possibly improves the solubility of O<sub>2</sub> and CO<sub>2</sub> in PEG reported in the literature.<sup>8,12</sup> Interestingly, the selectivity noticeably depended on the pressure of CO<sub>2</sub>. Lower pressure favored the formation of benzoic acid, and higher pressure preferentially afforded benzaldehyde.



**Fig. 1** CO<sub>2</sub> pressure effect on oxidation of benzyl alcohol. Reaction conditions: 1.93 mmol benzyl alcohol, 0.7 g PEG-1000, 2.5 MPa O<sub>2</sub> at 100 °C for 12 h.

**Table 4** The influence of O<sub>2</sub> pressure on the oxidation of benzyl alcohol<sup>a</sup>

Entry	O <sub>2</sub> /MPa	Conv. (%)	Yield of aldehyde (%) <sup>b</sup>	Yield of acid (%) <sup>b</sup>
1	1.5	9	8	0
2	2.5	77	22	50
3 <sup>c</sup>	2.5	36	19	13
4	3	97	4	88
5 <sup>e</sup>	0.1	0	0	0

<sup>a</sup> All the reactions were conducted with 1.93 mmol benzyl alcohol, 13.5 MPa CO<sub>2</sub> at 100 °C for 12 h, unless otherwise stated. <sup>b</sup> Determined by GC. <sup>c</sup> Without CO<sub>2</sub>.

### Influence of O<sub>2</sub> pressure

The influence of the pressure of O<sub>2</sub> on oxidation of benzyl alcohol was also examined. As shown in Table 4, the higher O<sub>2</sub> pressure was beneficial for the formation of the acid and the lower pressure preferentially afforded aldehyde although with the low conversion (entry 1 vs. entry 2). This is understandable because higher oxygen concentration favors further oxidation of aldehyde to carboxylic acid. It is worth mentioning that the oxidation reaction did not occur under 1 atm O<sub>2</sub> in the absence of CO<sub>2</sub> under the otherwise identical reaction conditions (entry 5), whereas 2.5 MPa O<sub>2</sub> gave 36% conversion (entry 3), hinting that enough pressure of O<sub>2</sub> is required for this transformation (entries 1–4).

### Substrate scope

The generality of this methodology was also evaluated. As shown in Table 5, primary and secondary alcohols can be oxygenized into the corresponding carbonyl compounds in fair to high yields (entries 1–4). In general, substrates with an electron donating group generally showed higher activity than those having an electron withdrawing group. The 4-methoxyphenyl methanol afforded the aldehyde in high selectivity at low temperature (entry 4). The 4-nitrophenyl methanol showed relatively poor activity (entry 5). In addition, the 2-nitrophenyl methanol only recovered starting material (entry 6), possibly due to the steric hindrance effect besides the electron effect. With regards to selectivity, secondary benzylic alcohols showed higher selectivity towards ketone (entries 1 and 2), while primary ones afforded carboxylic acid as a dominant product. On the other hand, the substrate with an electron-withdrawing group on the benzene ring predominantly gave a carboxylic acid (entry 5). Moreover, β-phenylethanol (entry 7) gave predominantly the formylated ester rather than the oxidized product, further supporting the proposed radical mechanism for PEG degradation.<sup>9</sup> This is reasonable because the main product was produced *via* formylation of alcohol with formic acid *in situ* generated during the degradation of PEG as previously reported.<sup>9</sup>

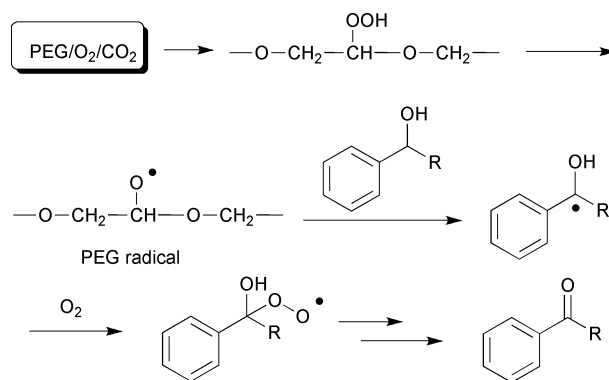
### Possible mechanism

Based on aforementioned findings, a plausible mechanism of this protocol may be considered to involve PEG radical *in situ* formed during PEG thermal degradation.<sup>13</sup> A mechanistic scheme was proposed as delineated in Scheme 2. The reaction

**Table 5** Oxidation of primary and secondary alcohols using PEG/O<sub>2</sub>/CO<sub>2</sub> system<sup>a</sup>

Entry	Substrate	Product	Conv. (%)	Yield (%) <sup>b</sup>
1			100	93
2			100	90
3			97	89
4 <sup>c</sup>			60	53
5 <sup>d</sup>			50	30
6 <sup>d</sup>		—	0	0
7 <sup>e</sup>			83	73

<sup>a</sup> All the experiments were carried out with 1.93 mmol substrate, 0.7 mmol PEG, 2.5 MPa O<sub>2</sub> and 13.5 MPa CO<sub>2</sub> at 120 °C for 12 h, unless otherwise stated. <sup>b</sup> Isolated yields. <sup>c</sup> 100 °C. <sup>d</sup> 24 h.



**Scheme 2** The proposed mechanism of oxidation of benzyl alcohols by the PEG radical from oxidative degradation of PEG.

of PEG with oxygen is prone to generating PEG radicals, which induces the hydrogen at the benzylic position, then goes through a free radical process. In our study, the free radical signals from EPR (electron paramagnetic resonance) experiments (Fig. S1, ESI<sup>†</sup>) and the formylated product from PEG oxidative degradation using β-phenylethanol as a substrate (Table 5, entry 7) presumably supports the proposed radical mechanism.

The proposed mechanism was also supported as evidenced by the following facts. Those include producing trace amounts of formylated products from degradation of PEG (Fig. S2, ESI<sup>†</sup>),

broadening PEG molecule weight distribution (Fig. S3, ESI<sup>†</sup>), generating a peroxide intermediate as detected by a KI/starch test, and the suppressing effect of TEMPO on this reaction (Table 1, entry 9).

## Conclusions

We have herein disclosed that the PEG radical presumably from oxidative degradation of PEG could be utilized to trigger oxygenation of benzylic alcohols without the need of a catalyst and additive under metal-free conditions in efficient, cost-effective and environmentally benign fashion. Compressed CO<sub>2</sub> could improve the oxidation and also adjust the selectivity of target product by altering CO<sub>2</sub> pressure. Those findings introduced here provide a useful example for developing free-radical chemistry from PEG thermal oxidative degradation. Further broadening this protocol to a wide set of organic reactions with enormous synthetic potentials requiring radical chemistry is in progress. Given more time for in-depth investigation, we believe that free-radical chemistry of PEG thermal degradation will become an even more powerful tool in organic synthesis.

## Experimental

### Safety warning

Experiments using large amounts of compressed gases, especially molecular oxygen and supercritical fluids, are potentially hazardous and must only be carried out by using the appropriate equipment and under rigorous safety precautions. In particular, oxygen is introduced into the substrate-loaded reactor after CO<sub>2</sub>. To avoid an explosive regime the following order should be used: substrate > CO<sub>2</sub> > oxygen. Moreover, the oxygen content should not exceed 14 vol% when CO<sub>2</sub> is used as a reaction medium.

### Materials

The alcohols were purchased from J & K CHEMICAL. Carbon dioxide with a purity of 99.99% was commercially available. The other organic compounds from Tianjin Guangfu Fine Chemical Research Institute were used without further purification except for the solvents, which were distilled by the known method prior to use.

### Oxidation reaction

A mixture of substrate (1.93 mmol) and PEG-1000 (0.7 g, 0.7 mmol) was placed in a 25 mL autoclave equipped with an inner glass tube. 3 MPa CO<sub>2</sub> and 2.5 MPa O<sub>2</sub> were sequentially introduced into the autoclave and heated to the reaction temperature. Then the final pressure was adjusted to the desired pressure at the reaction temperature by introducing the amount of CO<sub>2</sub>. The mixture was stirred continuously for the designed reaction time, then the reactor was placed into ice water and CO<sub>2</sub> was released slowly passing through a cold trap containing diethyl ether to absorb the trace amount of reactant and product entrained by CO<sub>2</sub>. After depressurization, diethyl ether and triphenylphosphine (1.01 g, 3.86 mmol) were added into the reactor. Products were then extracted by diethyl ether, and analyzed by a gas chromatograph (SHIMADZU-

2014) equipped with a capillary column (HP-5 30 m × 0.25 μm) using a flame ionization detector. The structure and the purity of the products were further identified using NMR (BRUKER-300 MHz, VARIAN-400 MHz), GC-MS (HP G1800A), HPLC-MS (LCQ Advantage) and GC, HPLC by comparing retention times and fragmentation patterns with those of authentic samples. The EPR (Bruker EMX-6) experiments were carried out with 5.7 mmol benzyl alcohol and 2.1 mmol PEG-300 at 100 °C in presence of 1 atm O<sub>2</sub> after 4 h. NMR spectral characterizations of the products are as follows:

**Benzaldehyde.** <sup>1</sup>H NMR (CDCl<sub>3</sub>, 400 MHz): δ = 7.50 (t, <sup>3</sup>J (H, H) = 7.7 Hz, 2H; PhH), 7.60 (t, <sup>3</sup>J (H, H) = 7.4 Hz, 1H; PhH), 7.84 (d, <sup>3</sup>J (H, H) = 7.9 Hz, 2H; PhH), 9.98 (s, 1H, CHO); <sup>13</sup>C {<sup>1</sup>H} NMR (CDCl<sub>3</sub>, 100.6 MHz): δ = 128.85, 129.58, 134.33, 136.19, 192.28.

**Acetophenone.** <sup>1</sup>H NMR (400 MHz, CDCl<sub>3</sub>): δ = 2.60 (s, 3H, CH<sub>3</sub>), 7.46 (t, <sup>3</sup>J (H, H) = 7.7 Hz, 2H; PhH), 7.56 (t, <sup>3</sup>J (H, H) = 7.5 Hz, 1H; PhH), 7.96 (d, <sup>3</sup>J (H, H) = 7.8 Hz, 2H; PhH); <sup>13</sup>C {<sup>1</sup>H} NMR (CDCl<sub>3</sub>, 100.6 MHz): δ = 26.54, 128.25, 128.51, 133.04, 137.10, 198.06.

**4-Methoxy-benzaldehyde.** <sup>1</sup>H NMR (300 MHz, CDCl<sub>3</sub>): δ = 3.87 (s, 3H, CH<sub>3</sub>), 7.00 (d, <sup>3</sup>J (H, H) = 8.72 Hz, 2H; PhH), 7.82 (d, <sup>3</sup>J (H, H) = 8.78 Hz, 2H; PhH), 9.87 (s, 1H, CHO); <sup>13</sup>C {<sup>1</sup>H} NMR (75 MHz, CDCl<sub>3</sub>): δ = 55.5, 114.3, 130.0, 131.9, 164.6, 190.7.

**Diphenyl-methanone.** <sup>1</sup>H NMR (300 MHz, CDCl<sub>3</sub>): δ = 7.48 (t, <sup>3</sup>J (H, H) = 7.9 Hz, 4H; PhH), 7.58 (t, <sup>3</sup>J (H, H) = 7.9 Hz, 2H; PhH), 7.81 (t, <sup>3</sup>J (H, H) = 5.7 Hz, 4H; PhH); <sup>13</sup>C {<sup>1</sup>H} NMR (75 MHz, CDCl<sub>3</sub>): δ = 128.3, 130.1, 132.4, 137.6, 196.7.

**Formic acid phenethyl ester.** <sup>1</sup>H NMR (300 MHz, CDCl<sub>3</sub>): δ = 2.97 (t, <sup>3</sup>J (H, H) = 7.01 Hz, 2H; CH<sub>2</sub>), 4.39 (t, <sup>3</sup>J (H, H) = 7.03 Hz, 2H; CH<sub>2</sub>), 7.21–7.32 (m, 5H, PhH), 8.03 (s, 1H, OCH); <sup>13</sup>C {<sup>1</sup>H} NMR (75 MHz, CDCl<sub>3</sub>): δ = 34.9, 64.3, 126.7, 128.5, 128.8, 137.4, 160.8.

## Acknowledgements

Financial support from National Science Foundation (Grant no. 20421202, 20672054 and 20872073), and the 111 project (B06005) and Tianjin Natural Science Foundation is gratefully acknowledged.

## Notes and references

- 1 R. C. Larock, *Comprehensive organic transformation*, VCH, New York, 1999, 1234-1250B. M. Trost, I. Fleming and S. V. Ley, *Comprehensive organic synthesis*, Pergamon, Oxford, 1991, Vol. 7; D. Lenoir, *Angew. Chem., Int. Ed.*, 2006, **45**, 3206; R. A. Sheldon, I. W. C. E. Arends, G.-J. T. Brink and A. Dijkstra, *Acc. Chem. Res.*, 2002, **35**, 774; B. Z. Zhan and A. Thompson, *Tetrahedron*, 2004, **60**, 2917.
- 2 G. Cainelli and G. Cardillo, *Chromium oxidation in organic chemistry*, Springer, Berlin, 1984.
- 3 Copper catalyzed aerobic oxidation of alcohol: T. Punniyamurthy and L. Rout, *Coord. Chem. Rev.*, 2008, **252**, 134; I. E. Marko, P. R. Giles, M. Tsukazaki, S. M. Brown and C. J. Urch, *Science*, 1996, **274**, 2044; I. E. Marko, P. R. Giles, M. Tsukazaki, I. Chelle-Regnaut, A. Gautier, S. M. Brown and C. J. Urch, *J. Org. Chem.*, 1999, **64**, 2433.
- 4 Palladium catalyzed aerobic oxidation of alcohol: S. Stahl, *Angew. Chem., Int. Ed.*, 2004, **43**, 3400; K. P. Peterson and R. S. Larock,

- J. Org. Chem.*, 1999, **64**, 2433; G.-J. ten Brink, I. W. C. E. Arends and R. A. Sheldon, *Science*, 2000, **287**, 1636; S. S. Stahl, J. L. Thorman, R. C. Nelson and M. A. Kozee, *J. Am. Chem. Soc.*, 2001, **123**, 7188; G.-J. ten Brink, I. W. C. E. Arends and R. A. Sheldon, *Adv. Synth. Catal.*, 2002, **344**, 355; B. A. Steinhoff, S. R. Fix and S. S. Stahl, *J. Am. Chem. Soc.*, 2002, **124**, 766; M. J. Schultz, C. C. Park and M. S. Singman, *Chem. Commun.*, 2002, 3034; Y. Uozumi and R. Nakao, *Angew. Chem., Int. Ed.*, 2003, **42**, 194; D. R. Jensen, M. J. Schultz, J. A. Mueller and M. S. Sigman, *Angew. Chem., Int. Ed.*, 2003, **42**, 3810.
- 5 For ruthenium catalyzed aerobic oxidation of alcohol, see: I. E. Marko, P. R. Giles, M. Tsukazaki, I. Chelle-Regnaut, C. H. Urch and S. M. Brown, *J. Am. Chem. Soc.*, 1997, **119**, 12661; M. Musawir, P. N. Davey, G. Kelly and I. V. I. Kozhevnikov, *Chem. Commun.*, 2003, 1414; K. Yamaguchi and N. Mizuno, *Angew. Chem., Int. Ed.*, 2002, **41**, 4538; B.-Z. Zhan, M. A. White, T.-K. Sham, J. A. Pincock, R. J. Doucet, K. V. Ramama Rao, K. N. Ronertson and T. S. Cameron, *J. Am. Chem. Soc.*, 2003, **125**, 2195; G. Csajenyik, A. H. Ell, L. Fadini, B. Pugin and J.-E. Backvall, *J. Org. Chem.*, 2002, **67**, 1657.
- 6 TEMPO-catalyzed aerobic oxidation of alcohol: Y. Ishii, S. Sakaguchi and T. Iwahama, *Adv. Synth. Catal.*, 2001, **343**, 395; F. Recupero and C. Punta, *Chem. Rev.*, 2007, **107**, 3800; R. A. Sheldon and I. W. C. E. Arends, *Adv. Synth. Catal.*, 2004, **346**, 1051; M. F. Semmelhack, C. R. Schmid, D. A. Cortes and C. S. Chou, *J. Am. Chem. Soc.*, 1984, **106**, 3374; A. Cecchetto, A. Marino-Gonzalez, A. Mairata, i Payeras, I. W. C. E. Arends and R. A. Sheldon, *J. Am. Chem. Soc.*, 2001, **42**, 6826; B. Betzemeier, M. Cavazzini, S. Quici and P. Knochel, *Tetrahedron Lett.*, 2000, **41**, 4343; R. Ben-Daniel, P. Alsters and R. Neumann, *J. Org. Chem.*, 2001, **123**, 6826; A. Ansari and R. Gree, *Org. Lett.*, 2002, **4**, 1507; P. Gamez and I. W. C. E. Arends, *Chem. Commun.*, 2003, 2414; J. Reedijk, R. A. Sheldon, R. Liu, X. Liang, C. Dong and X. Hu, *J. Am. Chem. Soc.*, 2004, **126**, 4112; R. Ciriminna, J. Blum, D. Avnir and M. Pagliaro, *Chem. Commun.*, 2000, 1441; J. Luo, C. Pardin, W. D. Lubell and X. X. Zhu, *Chem. Commun.*, 2007, 2136; B. Karimi, A. Biglari, J. H. Clark and V. Budarin, *Angew. Chem., Int. Ed.*, 2007, **46**, 7210; J. Piera and J.-E. Backvall, *Angew. Chem., Int. Ed.*, 2008, **47**, 3506; X. L. Wang, R. H. Liu, Y. Jin and X. M. Laing, *Chem.-Eur. J.*, 2008, **14**, 2679; Z.-Q. Liu, X. J. Shang, L. Z. Chai and Q. J. Sheng, *Catal. Lett.*, 2008, **123**, 317; P. Ferreira, W. Hayes, E. Phillips, D. Rippon and S. C. Tsang, *Green Chem.*, 2004, **6**, 310; J. Y. Huang, S. J. Li and Y. G. Wang, *Tetrahedron Lett.*, 2006, **47**, 5637; Y. Xie, W. M. Mo, D. Xu, Z. L. Shen, N. Sun, B. X. Hu and X. Q. Hu, *J. Org. Chem.*, 2007, **72**, 4288; Z. L. Lu, J. S. Costa, O. Roubeau, I. Mutikainen, U. Turpeinen, S. J. Teat, P. Gamez and J. Reedijk, *Dalton Trans.*, 2008, 3567.
- 7 For reviews and representative examples, see: P. G. Jessop, W. Leitner, *Chemical Synthesis Using Supercritical Fluids*, Wiley-VCH, Weinheim, 1999; E. J. Beckman, *J. Supercrit. fluids.*, 2004, **28**, 121; A. Baiker, *Chem. Rev.*, 1999, **99**, 453; G. Musie, M. Wei, B. Subramaniam and D. H. Busch, *Coord. Chem. Rev.*, 2001, **219–221**, 789; T. Sakakura, J. C. Choi and H. Yasuda, *Chem. Rev.*, 2007, **107**, 2365; J.-S. Tian, C.-X. Miao, J.-Q. Wang, F. Cai, Y. Du, Y. Zhao and L.-N. He, *Green Chem.*, 2007, **9**, 566; Y. Du, F. Cai, D. L. Kong and L.-N. He, *Green Chem.*, 2005, **7**, 518.
- 8 J. Chen, S. K. Spear, J. G. Huddleston and R. D. Rogers, *Green Chem.*, 2005, **7**, 64; Z. S. Hou, N. Theyssen, A. Brindmann and W. Leitner, *Angew. Chem., Int. Ed.*, 2005, **44**, 1346; Y. Du, Y. Wu, A.-H. Liu and L.-N. He, *J. Org. Chem.*, 2008, **73**, 4709; J.-Q. Wang, F. Cai, E. Wang and L.-N. He, *Green Chem.*, 2007, **9**, 882; Y. Du, J. Q. Wang, J. Y. Chen, F. Cai and L. N. He, *Tetrahedron Lett.*, 2006, **47**, 1271; X.-Y. Dou, J.-Q. Wang, Y. Du, E. Wang and L.-N. He, *Synlett*, 2007, **19**, 3058.
- 9 For typical examples on thermal/oxidative degradation of PEG, see: E. Bortel, S. Hodorowicz and R. Lamot, *Makromol. Chem.*, 1979, **180**, 2491; A. Riecke, *Angew. Chem.*, 1958, **709**, 251; J. Glastrup, *Polym. Degrad. Stab.*, 1996, **52**, 217; J. R. Conder, N. A. Fruitwala and M. K. Shingari, *J. Chromatogr.*, 1983, **269**, 171; E. A. Altwicker, *Chem. Rev.*, 1967, **67**, 475.
- 10 T. Seki, J.-D. Grunwaldt and A. Baiker, *Chem. Commun.*, 2007, 3562.
- 11 D. J. Heldebrant and P. G. Jessop, *J. Am. Chem. Soc.*, 2003, **125**, 5600.
- 12 M. Daneshvar, S. Kim and E. Gulari, *J. Phys. Chem.*, 1990, **94**, 2124; S. G. Kazarian and K. L. Andrew Chan, *Macromolecules*, 2004, **37**, 579.
- 13 S. Han, C. Kim and D. Kwon, *Polymer*, 1997, **38**, 317.

# Rosin-based acid anhydrides as alternatives to petrochemical curing agents

Xiaoqing Liu, Wenbo Xin and Jinwen Zhang\*

Received 25th February 2009, Accepted 7th April 2009

First published as an Advance Article on the web 17th April 2009

DOI: 10.1039/b903955d

In this paper, two bio-based epoxy curing agents were synthesized using rosin acids. The chemical structures of the rosin derivatives were confirmed in detail by  $^1\text{H}$  NMR,  $^{13}\text{C}$  NMR, FT-IR and ESI-MS. The synthesis methods of the rosin-based curing agents, curing behaviors and properties of the cured epoxy resins were studied. Two commercial curing agents, which have similar functionality and structural resemblance to the rosin-based curing agents, were also used in the study for comparison. Compared with the synthesis of petrochemical curing agents, the synthesis of rosin-based curing agents was simpler and more environmentally friendly, and has less strict requirements on reactors and catalysts. Non-isothermal curing of a commercial liquid epoxy was studied using differential scanning calorimetry (DSC). The thermal mechanical properties and thermal stability of the cured epoxy resins were evaluated using dynamic mechanical analysis (DMA) and thermogravimetric analysis (TGA), respectively. Results showed that the curing behaviors of the rosin-based curing agents were similar to those of the commercial curing agents. The epoxies cured by rosin-based curing agents also demonstrated similar thermal mechanical properties and thermal stability to the epoxies cured by commercial curing agent analogs.

## Introduction

Rosin is abundantly available as exudates of pines and conifers. It is also obtained by distillation of tall oil—a byproduct of the Kraft pulp process. Rosin is a mixture of acidic (*ca.* 90%) and neutral (*ca.* 10%) compounds. The acidic components, generally named rosin acids, are also a mixture consisting mainly of isomeric abietic-type acids (40–60%) and pimaric-type acids (9–27%) on the basis of total rosin weight.<sup>1</sup> Rosin and its derivatives are mainly used as adhesive tackifiers, printing inks, varnishes, paints, sealing wax, some soap, paper sizing, soldering, plasters, *etc.*<sup>2</sup>

Due to their large hydrogenated phenanthrene ring structure, rosin acids are similar in rigidity to petroleum-based cycloaliphatic or aromatic compounds. Therefore, in recent years rosin has received increasing attention as a renewable feedstock in polymer synthesis. For example, the Diels–Alder adduct of rosin with maleic anhydride, maleopimaric acid, has been used as a rigid building block in the main chains of aliphatic polyesters for modified mechanical properties and crystallization behavior.<sup>3–5</sup> Maleopimaric acid has also been used as a monomer for polycondensation reactions, such as the synthesis of polyamides,<sup>6–8</sup> polyamideimide,<sup>9,10</sup> saturated<sup>11</sup> polyesterimide,<sup>12–14</sup> and unsaturated polyesters.<sup>15,16</sup> There are only a few studies concerning the use of rosin in epoxy resins in the literature. Matynia<sup>17</sup> synthesized glycidyl esters from the reaction of epichlorohydrin with the Diels–Alder adducts of terpene and maleic anhydride, and cured the epoxides with 1,2-cyclohexanedicarboxylic anhydride. Recently, Atta *et al.*<sup>18–19</sup>

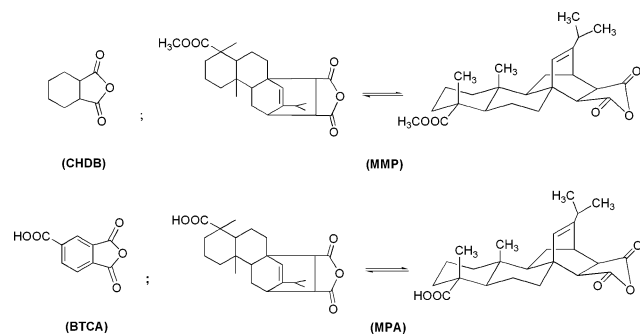
investigated the applications of rosin for epoxy resins. One epoxy was prepared by reacting hydroxymethylated rosin acid with epichlorohydrin, and the resulting epoxy contained a glycidyl ether group and a glycidyl ester group. Another epoxy was prepared by reacting dihydroxyethylamine with the adduct of diabietyl ketone/maleic anhydride or acrylic acid, and the resulting intermediate was reacted with epichlorohydrin. Poly(amide-imide) type hardeners derived from rosin were also prepared. However, these studies provided no information on the mechanical and thermal mechanical properties of the cured resins. Because the above epoxies and hardeners all had soft linear aliphatic segments, they were not intended for high performance engineering epoxy applications but for general coating applications. In our previous study,<sup>20</sup> glycidyl abietyl ether and methyl maleopimarate were synthesized and used as model rosin-based epoxy and anhydride curing agent, respectively, in the study of cure reactions. The results indicated that rosin could be used as a major feedstock for epoxy resins and curing agents.

The chemical structure of a curing agent has significant influence on the cure reactions and performance of the cured epoxy resin. So far, various types of curing agents, such as amines, polyamides,<sup>21</sup> mercaptans,<sup>22</sup> anhydrides have been developed. However, these hardeners are all petroleum-based and generally require complicated chemical processes in end-product syntheses or feedstock preparations. For example, 1,2-cyclohexanedicarboxylic anhydride (CHDB) and 1,2,4-benzenetricarboxylic anhydride (BTCA) are both important epoxy curing agents in encapsulation packaging of electronic products and are widely used in syntheses of other chemicals and polymers. The production of CHDB involves two complicated chemical processes: the Diels–Alder reaction of *cis*-1,3-butadiene and succinic anhydride to obtain

Wood Materials and Engineering Laboratory, Washington State University, Pullman, Washington State, 99164, USA.  
E-mail: jwzhang@wsu.edu; Tel: +1-509-335-8723

*cis*-4-cyclohexene-1,2-dicarboxylic anhydride, and the catalytic hydrogenation of the intermediate. The former reaction requires strict conditions to prevent the homopolymerization of the diene and the copolymerization between diene and succinic anhydride; while the latter reaction requires a highly selective catalyst to avoid the side reactions on the anhydride groups such as condensation, hydrogenation and crosslinking. BTCA is prepared by the liquid-phase air-oxidation of pseudocumene to form trimellitic acid, which is subsequently dehydrated by heating crude trimellitic acid with vanadium pentoxide. The oxidation is conducted in acetic acid with  $\text{Co}(\text{OAc})_2$  and  $\text{Mn}(\text{OAc})_3$  as major catalysts and tetrabromoethane as co-catalyst. The recovery of acetic acid is problematic in this process, and the trace amount of bromine anions in the product lead to the reduction of the dielectric constant of the cured epoxies. In view of the unique chemical structures of rosin acids, they can be converted to the analogues of CHDB and BTCA by simple reaction processes under mild reaction conditions.

In this study, two rosin derivatives, maleopimaric acid (MPA) and methyl maleopimarate (MMP) which resemble BTCA and CHDB in structure and functionality, respectively, were synthesized (Scheme 1) and studied as curing agents for the curing of a commercial epoxy resin. In comparison, BTCA and CHDB were also studied for the curing of the same epoxy. The major objectives of this study are to identify simple and effective synthesis methods for MPA and MMP, investigate the curing characteristics of the novel bio-based curing agents and determine the positive effects of the bulky hydrogenated phenanthrene ring structure of rosin acid on the properties of the cured epoxies. Furthermore, the results from this study could provide important information for the evaluation of potential scale-up of the laboratory synthesis in industrial process and for the feasibility of replacing some existing petrochemical curing agents with rosin-based compounds.



**Scheme 1** The chemical structures of curing agents used in this study.

## Experimental

### General

Abietic acid (75% by HPLC) was obtained from Aldrich and used as received. It was actually a mixture of abietic acid and other rosin acids with most neutral compounds removed. A liquid epoxy (2,2-bis[4-(glycidyloxy)phenyl]propane), with an epoxide equivalent weight of 171–175  $\text{g eq}^{-1}$  (DER 332), was obtained from Dow Chemical Company. Maleic anhydride (powder, 95%), iodomethane (99.5%), *p*-toluene sulfonic acid

(98.5%), 1,2-cyclohexanedicarboxylic anhydride (97%, CHDB), 1,2,4-benzenetricarboxylic anhydride (97%, BTCA) and 2-ethyl-4-methylimidazole (95%), were also obtained from Aldrich. Potassium carbonate (99%, anhydrous, granular) was obtained from B. T. Baker. Magnesium sulfate (anhydrous, reagent grade) was obtained from Fisher. Solvents of reagent grade for synthesis (acetic acid, dimethylformamide, ethyl ether, chloroform) were used as received.

### Synthesis of curing agents

**Synthesis of methyl abietate<sup>20</sup>.** To a 100 mL flask was charged 5.8 g of powdered  $\text{K}_2\text{CO}_3$  (42 mmol) and 90 mL of anhydrous DMF. The mixture was stirred for 30 min at room temperature, and then 5.0 g of abietic acid (12 mmol) and 5.7 g of iodomethane (30 mmol) were added. After the reaction was continued for 12 h at room temperature, another 5.7 g iodomethane (30 mmol) was added and the reaction was continued for another 12 h at room temperature. The salt precipitate was removed *via* filtration, and the filtrate was diluted with 300 mL of ethyl ether and washed with water three times. The ethyl ether layer was then dried with anhydrous  $\text{MgSO}_4$  and concentrated in vacuum. A white product weighing 3.16 g was obtained (yield 81%).  $^1\text{H NMR}$  ( $\text{CD}_3\text{Cl}$ ,  $\delta$  ppm) 5.77 (s, 1H), 5.37 (s, 1H), 3.61 (s, 3H), 2.23–1.56 (m, 11H), 1.25–1.18 (m, 6H), 1.02–1.00 (m, 7H), 0.82 (s, 3H).  $^{13}\text{C NMR}$  ( $\text{CD}_3\text{Cl}$ ,  $\delta$  ppm) 178.81, 145.39, 135.71, 122.62, 120.81, 51.99, 51.17, 46.79, 45.32, 38.56, 37.34, 35.10, 34.75, 27.68, 25.88, 22.69, 21.64, 21.08, 18.36, 17.24, 14.26. FT-IR ( $\text{cm}^{-1}$ ) 897, 1182, 1230, 1242, 1390, 1452, 1721, 2950. ESI-MS  $m/z$  317.6,  $[\text{M} + \text{H}^+]$ .

**Synthesis of MMP.** In a 100 mL three-necked round flask equipped with a heating bath, a magnetic stirrer and a reflux condenser, 15 g of methyl abietate (45 mmol) was slowly heated to 180 °C and then maintained at this temperature for 3 h to complete the isomerization from the abietic structure to the pimaric structure under an Ar atmosphere. The reaction was cooled to 120 °C before 50 mL of acetic acid was added. To this solution were added 4.4 g of maleic anhydride (45 mmol) and 0.85 g of *p*-toluene sulfonic acid (PTS) (4.5 mmol). The reaction mixture was refluxed for 12 h and then cooled to room temperature to receive the crude methyl maleopimarate. The crude product was recrystallized from acetic acid twice to obtain 17.0 g white crystals (yield 90%).  $^1\text{H NMR}$  ( $\text{CD}_3\text{Cl}$ ,  $\delta$  ppm) 5.52 (s, 1H), 3.66 (s, 3H), 3.11 (m, 2H), 2.70–2.74 (d, 1H), 2.47–2.52 (m, 1H), 2.25 (m, 1H), 1.78–1.24 (m, 13H), 1.15 (s, 3H), 1.00–0.98 (d, 6H), 0.59 (s, 3H).  $^{13}\text{C NMR}$  ( $\text{CD}_3\text{Cl}$ ,  $\delta$  ppm) 179.29, 173.13, 171.26, 148.22, 125.36, 53.51, 53.47, 52.39, 49.51, 47.21, 45.97, 40.58, 38.21, 37.89, 36.62, 35.58, 35.00, 32.69, 27.09, 21.85, 20.79, 20.17, 17.20, 16.95, 15.76. FT-IR ( $\text{cm}^{-1}$ ) 795, 850, 922, 947, 1000, 1080, 1140, 1246, 1388, 1458, 1718, 1776, 1843, 2860, 2960. Acid value: theoretical: 258  $\text{mg KOH g}^{-1}$ ; found: 270  $\text{mg KOH g}^{-1}$ . ESI-MS  $m/z$  415.4,  $[\text{M} + \text{H}^+]$ .

**Synthesis of MPA<sup>23</sup>.** In a 100 mL three-necked round flask equipped with a magnetic stirrer and a reflux condenser, 10 g of abietic acid (75% purity, 24 mmol) was heated to 180 °C and maintained at this temperature for 3 h to complete the isomerization from the abietic structure to the pimaric structure under an Ar atmosphere. The reaction was cooled to 120 °C,

and then 30 mL of acetic acid was added. To this mixture were added 2.35 g of maleic anhydride (24 mmol) and 0.46 g of *p*-toluene sulfonic acid (PTS) (0.24 mmol) and the reaction mixture was refluxed for 12 h. After the reaction was cooled to room temperature, a yellow solid was obtained. The crude product was recrystallized twice from acetic acid to obtain 9.6 g white crystals of MPA (yield: 92%). <sup>1</sup>H NMR (CD<sub>3</sub>Cl, δ ppm) 5.53 (s, 1H), 3.11–3.08 (m, 2H), 2.70–2.74 (d, 1H), 2.47–2.52 (m, 1H), 2.18–2.3 (m, 1H), 1.78–1.24 (m, 13H), 1.15 (s, 3H), 1.00–0.98 (d, 6H), 0.59 (s, 3H). <sup>13</sup>C NMR (CD<sub>3</sub>Cl, δ ppm) 184.67, 173.13, 171.26, 148.22, 125.36, 53.51, 53.47, 52.39, 49.51, 47.21, 45.97, 40.58, 38.21, 37.89, 36.62, 35.58, 35.00, 32.69, 27.09, 21.85, 20.79, 20.17, 17.20, 16.95, 15.76. FT-IR (cm<sup>-1</sup>) 795, 850, 926, 944, 1010, 1086, 1140, 1279, 1234, 1388, 1465, 1690, 1780, 1844, 2860, 2942, 3500–3100. Acid value: theoretical: 420 mg KOH g<sup>-1</sup>; found: 420 mg KOH g<sup>-1</sup>. ESI-MS *m/z* 401.3, [M + H<sup>+</sup>].

### Curing procedure

Liquid epoxy resin (DER 332), curing agent (CHDB, BTCA, MMP or MPA) in a 1 : 1 equivalent ratio, together with 2-ethyl-4-methylimidazole (1 wt% on the basis of the total weight of curing agent and epoxy) were charged into a small beaker. In order to achieve a good mixing of the reactants, a small amount of chloroform was added and stirred for 30 min at room temperature to dissolve them. The solvent was removed in a vacuum oven at 50 °C for 3 h and the mixture was transferred into a mold with cavity dimensions of 50 mm × 5 mm × 5 mm. The curing was performed at 100 °C for 2 h, 160 °C for 2 h and 180 °C for 1 h. The cured samples were carefully removed from the mold and used for dynamic mechanical analysis and thermal property tests.

### Characterizations

<sup>1</sup>H NMR and <sup>13</sup>C NMR spectra were recorded with a Bruker 300 MHz spectrometer at room temperature in deuterated chloroform (CDCl<sub>3</sub>). Chemical shifts were reported relative to chloroform (δ 7.26) for <sup>1</sup>H NMR. Fourier transform infrared spectra were recorded with NEXUS 670 FT-IR. The wavelength range was from 4000 to 400 cm<sup>-1</sup>. The samples were prepared by dissolving a small amount of compound in CHCl<sub>3</sub>, followed by smearing the solution onto a KBr crystal plate and evaporating the solvent completely. Mass spectra were recorded with a LCQ Advantage ESI mass spectrometer. The acid value of the curing agent was determined by the acid–base titration method using 0.05 N NaOH in methanol solution. Phenolphthalein was used as indicator.

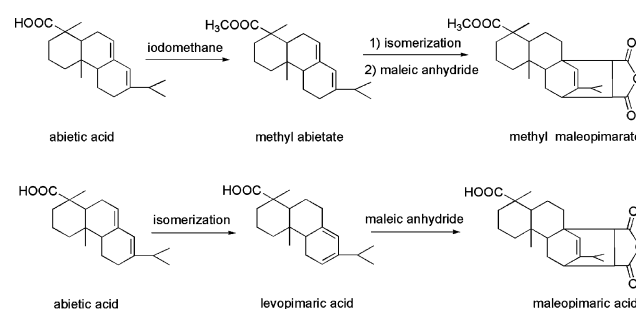
Non-isothermal curing of the epoxy was performed on a Mettler–Toledo 822e DSC under a nitrogen atmosphere. A heat scan ranging from 20 to 280 °C was performed at heating rates of 2, 5, 8, and 10 °C min<sup>-1</sup>, respectively. The samples for differential scanning calorimetry (DSC) analysis were the same ones used above for preparation of the dynamic mechanical analysis (DMA) test specimens. Approximately 8 mg of each sample was weighed and sealed in 40 μL aluminium crucibles and the curing progress was conducted immediately. The exothermic curves were recorded to determine the curing kinetic parameters. DSC analysis for each sample was repeated twice.

Dynamic mechanical analysis was carried out on Perkin-Elmer DMA-7 (Norwalk, CT, USA) using a three points bending fixture. All samples were tested from 30 °C to 250 °C at a heating rate of 2 °C min<sup>-1</sup> and at a frequency of 1 Hz. DMA analysis for each sample was repeated twice. Thermogravimetric analysis (TGA) was performed on a Rheometric Scientific STA Thermogravimetric Analyzer. Each sample was scanned from 50 to 600 °C under a N<sub>2</sub> atmosphere at a heating rate of 20 °C min<sup>-1</sup>.

## Results and discussion

### Synthesis of MMP and MPA

The synthesis route of MMP is shown in Scheme 2. Esterification of the carboxyl group using methanol/KOH or methanol/*p*-toluene sulfonic acid resulted in very low yields. By employing CH<sub>3</sub>I and K<sub>2</sub>CO<sub>3</sub>, the reaction took place at room temperature and gave a good yield (81%). Furthermore, the resulting methyl abietate was easily purified by extraction with ethyl ether.



**Scheme 2** The synthetic route of MMP and MPA.

Fig. 1(a) and 1(b) show the <sup>1</sup>H NMR spectra of abietic acid and methyl abietate, respectively. The signals from 0.6 to 2.2 ppm were all attributed to the protons attached on the six-member fused rings, and the peaks at 5.77 and 5.37 ppm were assigned to the protons on the unsaturated carbons. The peak at 3.61 ppm originated from the CH<sub>3</sub> group (Fig. 1(b), proton 3) of the methyl ester formed. The <sup>13</sup>C NMR spectrum further supported the esterification of the carboxyl group, which exhibited the appearance of the characteristic peak for ester at 178.8 ppm and the disappearance of the characteristic peak for the COOH group at 184.6 ppm.

Rosin acids exist in various isomers. Levopimaric acid is the only isomer that can undergo the Diels–Alder cycloaddition reaction. However, other isomeric rosin acids can assume the structure of levopimaric acid through isomerization at elevated temperatures without using any solvents and catalyst.<sup>2</sup> In this case, prior to the Diels–Alder reaction, methyl abietate was first heated at 180 °C for 3 h to complete the isomerization. Several types of reagents, such as H<sub>3</sub>PO<sub>4</sub>, hydroquinone and *p*-toluene sulfonic acid, work well as catalyst for the Diels–Alder reaction. In this study, *p*-toluene sulfonic acid was selected and a higher yield (92%) of MMP was obtained, which was better than our previous result when hydroquinone was employed as a catalyst for this reaction.<sup>20</sup> It is apparent that the whole synthesis process was fairly friendly without using harmful gas, hazardous solvents or special catalysts. In contrast, the synthesis of CHDB involves the high pressure catalytic hydrogenation of

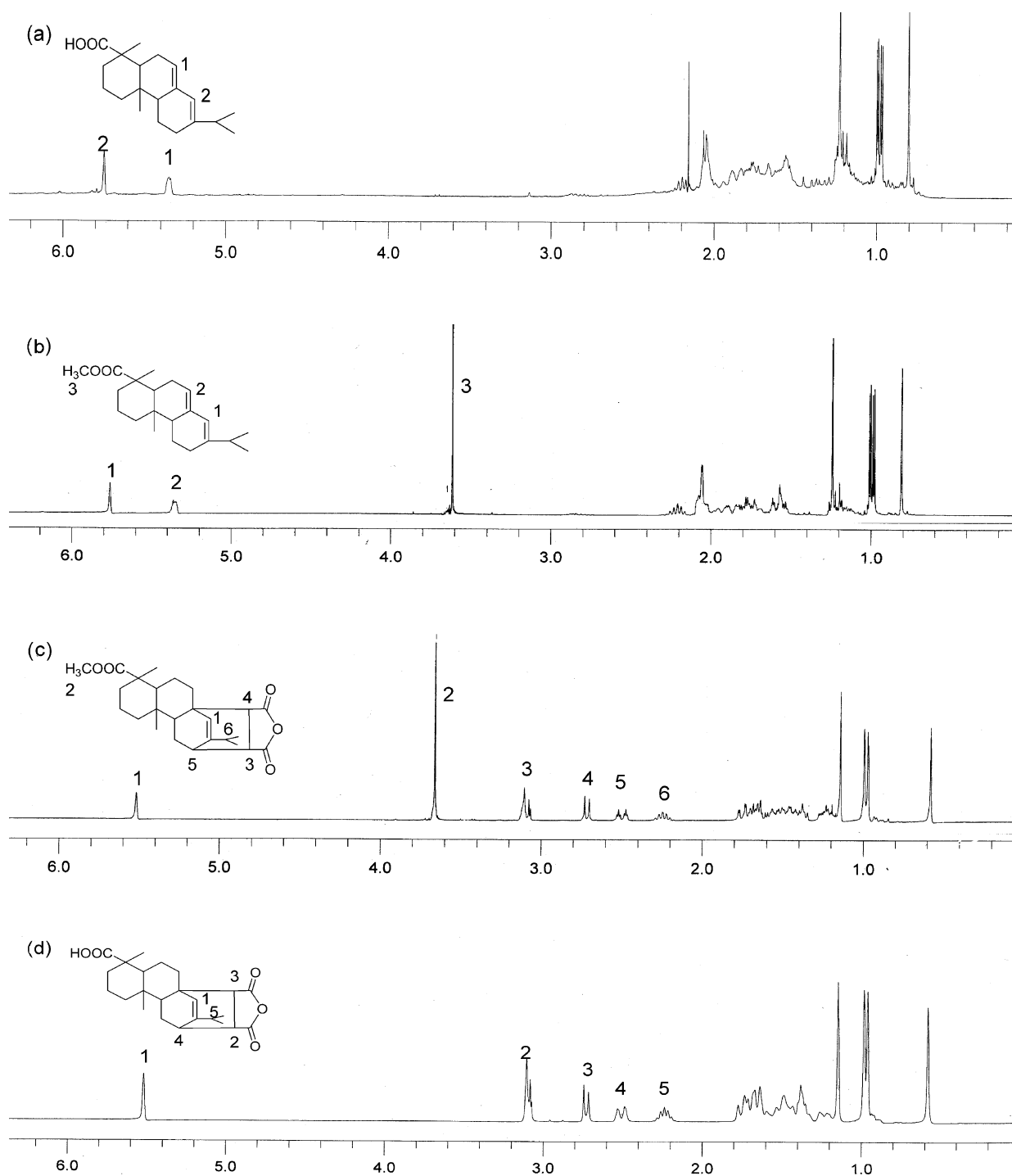


Fig. 1  $^1\text{H}$  NMR spectra of (a) abietic acid, (b) methyl abietate, (c) MMP and (d) MPA.

*cis*-4-cyclohexene-1,2-dicarboxylic anhydride which is produced by the Diels–Alder reaction of maleic anhydride and butadiene. Because of the side reactions and the risk of explosion, special catalyst and reactors are required for the production of CHDB. The chemical structure of MMP was confirmed by  $^1\text{H}$  NMR,  $^{13}\text{C}$  NMR and FT-IR. In Fig. 1(c), the peak at 5.36 ppm was attributed to proton 1 on the unsaturated carbon formed after the Diels–Alder cycloaddition reactions. Other specific peaks at 3.11 ppm (proton 3), 2.70–2.74 ppm

(proton 4), 2.47–2.52 ppm (proton 5) and 2.25 ppm (proton 6) were also identified. In Fig. 2(c), the two new peaks at 173.1 ppm and 171.2 ppm belonged to the carbonyl carbons of the grafted anhydride group. In addition, the strong absorption peaks for the asymmetrical and symmetrical stretching of carbonyl groups in anhydride could be observed at  $1844\text{ cm}^{-1}$  and  $1778\text{ cm}^{-1}$ , respectively (Fig. 3).

The synthesis of MPA actually required only the Diels–Alder reaction of levopimaric acid and maleic anhydride. The



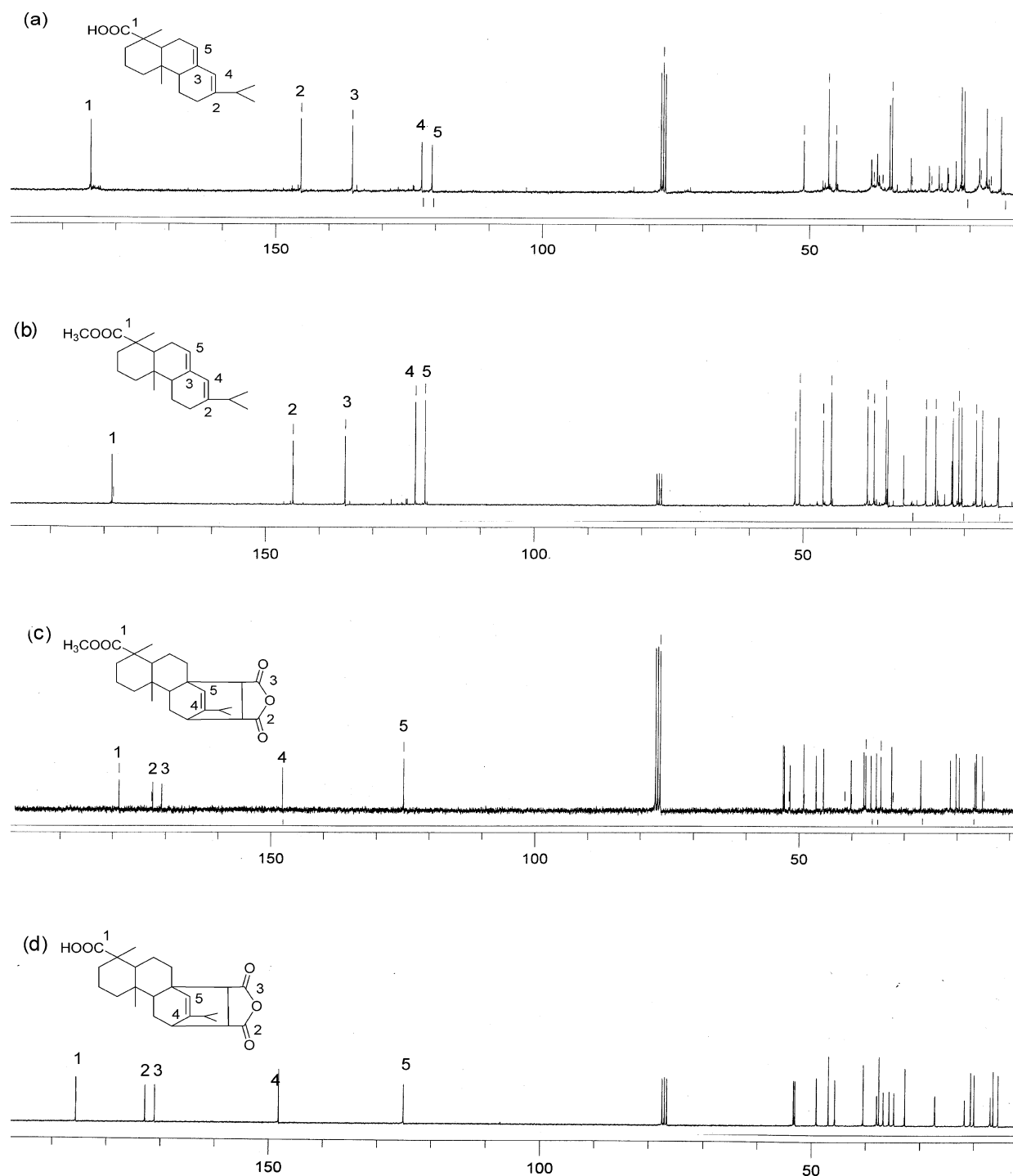


Fig. 2  $^{13}\text{C}$  NMR spectra of (a) abietic acid, (b) methyl abietate, (c) MMP and (d) MPA.

procedure and conditions of the Diels–Alder reaction in the synthesis of MPA were the same as those in the synthesis of MMP. The chemical structure of MPA was identified by  $^1\text{H}$  NMR (Fig. 1(d)),  $^{13}\text{C}$  NMR (Fig. 2(d)) and FT-IR (Fig. 3), respectively. In Fig. 3, the broad absorption peak of COOH from 3000 to 3500  $\text{cm}^{-1}$  for MPA almost disappeared after esterification in MMP. In contrast, the synthesis of BTCA involves two reaction processes: the liquid-phase air-oxidation of pseudocumene to form trimellitic acid and subsequent

dehydration by heating crude trimellitic acid. The oxidation has a strict requirement on catalysts and the purification of product is troubled by the trace amount of bromine anions resulting from the tetrabromoethane co-catalyst. In addition, toxic pseudocumene is used.

#### Curing and cure reactions

Non-isothermal (dynamic) curing behaviors of the liquid epoxy (DER 332) with CHDB, BTCA, MMP and MPA, were studied

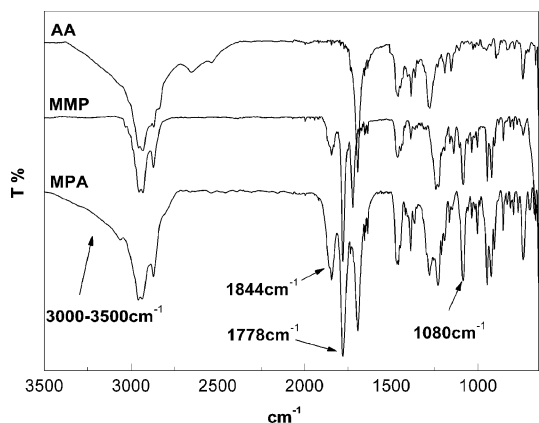


Fig. 3 FT-IR spectra of AA (abietic acid), MPA and MMP.

by DSC. Fig. 4 shows the DSC curing thermograms of these systems. As shown, the heat flow for the curing of CHDB/DER332, BTCA/DER332 or MMP/DER332 each displayed a single exothermic peak. For the curing of MPA/DER332, double peaks appeared. The peak at lower temperature was caused by the cure reaction of carboxyl groups with epoxy, whereas the peak at higher temperature was attributed to the cure reaction of anhydride groups. Unlike MPA, the carboxylic and anhydride groups in BTCA have similar reactivity in the curing of the epoxy due to the electronic effect of the phenyl ring and, therefore, only one wide peak was noted in the DSC curing thermogram. Usually, under the same curing conditions, the temperature of the exothermic peak can be taken as an indicator of reactivity of the compound in cure reactions. The lower the temperature of the peak, the higher the reactivity. BTCA and MMP seemed to be slightly more active than MPA and CHDB, respectively.

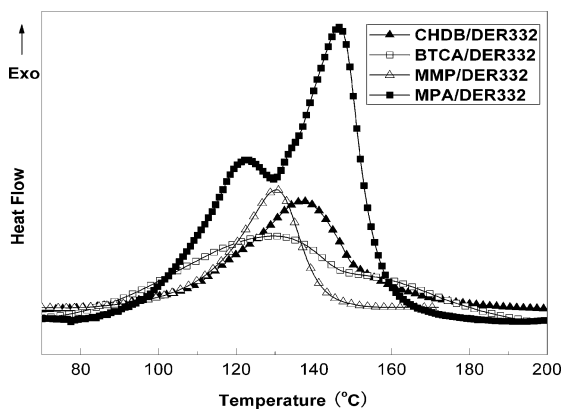


Fig. 4 DSC thermograms of non-isothermal curing of CHDB, BTCA, MMP and MPA with DER332. (Heating rate is  $5\text{ }^{\circ}\text{C min}^{-1}$ .)

The activation energy of the cure reaction was determined by both Kissinger's<sup>24</sup> and Ozawa's methods<sup>25</sup> for accuracy of results. Based on Kissinger's theory, the activation energy can be obtained from the peak temperatures at different heating rates. The equation is expressed as:

$$-\ln(q/T_p^2) = E_a/RT_p - \ln(AR/E)$$

where  $q$  is the heating rate,  $T_p$  is the exothermic peak temperature,  $E_a$  is the activation energy,  $R$  is the gas constant and  $A$  is the pre-exponential factor. A plot of  $-\ln(q/T_p^2)$  versus

$E_a/RT_p$  should be linear and the apparent activation energy can be obtained from the slope of the straight line. As for Ozawa's method, it can be expressed by the following equation:

$$\ln q = -1.052 \times E_a/RT_p + \ln(AE_a/R) - \ln F(x) - 5.331$$

where  $F(x)$  is a conversion dependent term. Therefore,  $E_a$  could be calculated from the slope of the plot of  $\ln q$  versus  $1/T_p$ .

Fig. 5 shows the linear plots of  $-\ln(q/T_p^2)$  versus  $1/T_p$  based on Kissinger's equation (a) and  $\ln q$  versus  $1/T_p$  based on Ozawa's theory (b) for the CHDB/DER332, BTCA/DER332, MMP/DER332 and MPA/DER332 systems. Although there were two exothermic peaks representing two different curing reactions for the MPA/DER332 system (Fig. 4), they could be applied to Kissinger's and Ozawa's equations separately, and this method has been widely used in other thermosetting systems.<sup>26</sup> In Fig. 5, MPA/DER332-L and MPA/DER332-H denoted the exothermic peaks at the lower and higher temperatures, respectively. Table 1 lists all the curing activation energies for these systems. As it can be seen, all epoxies cured with different curing agents showed quite similar activation energy values, indicating that the rosin curing agents, MMP and MPA, had a very similar reactivity and energy consumption in curing to the commercial curing agents, CHDB and BTCA.

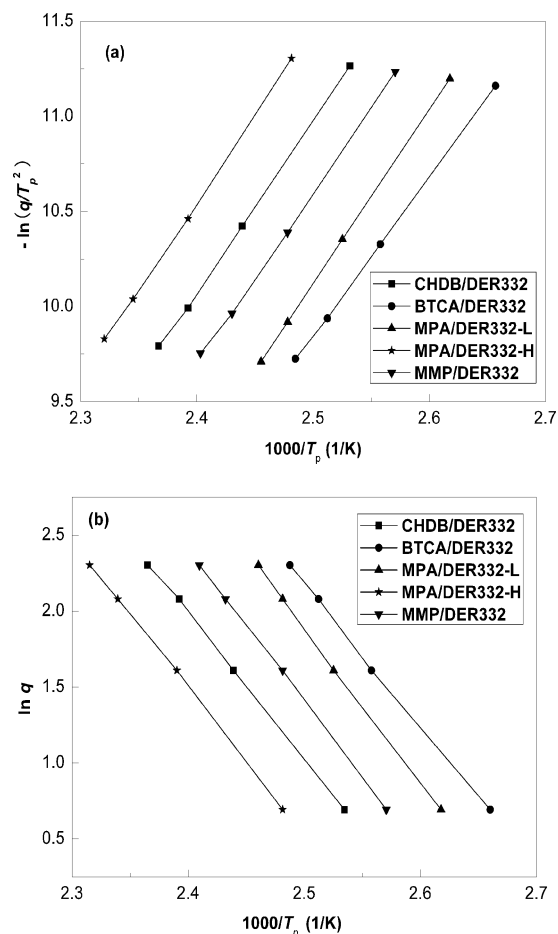


Fig. 5 Linear plot of  $-\ln(q/T_p^2)$  versus  $1/T_p$  based on Kissinger's equation (a) and  $\ln q$  versus  $1/T_p$  based on Ozawa's theory (b).

**Table 1** The thermal parameters of cured epoxy resin

System	$E_a/\text{kJ mol}^{-1}$		DMA/ $^{\circ}\text{C}$	TGA/ $^{\circ}\text{C}^a$	
	Kissinger	Ozawa	$T_g$	$T_{5\%}$	$T_{10\%}$
CHDB/DER332	74.8	75.6	113.7	330.3	351.2
MMP/DER332	73.3	76.9	123.6	312.1	334.9
BTCA/DER332	67.5	69.8	178.0	339.8	356.4
MPA/DER332 <sup>b</sup>	76.3-H 72.9-L	78.6-H 74.2-L	186.1	319.5	340.7

<sup>a</sup>  $T_{5\%}$  and  $T_{10\%}$ : temperatures of 5% degradation and 10% degradation.

<sup>b</sup> H and L represent the activation energy of the reactions occurring at the lower and higher temperatures, respectively, during DSC scanning.

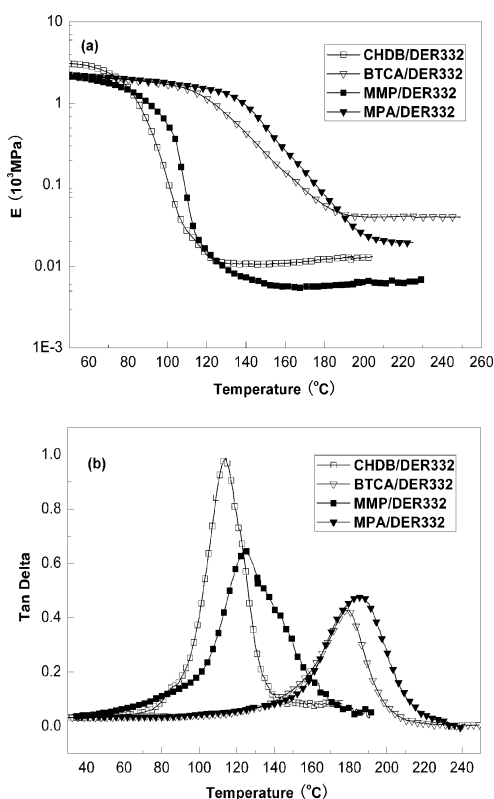
### Dynamic mechanical analysis

Although it is argued that rubbery elasticity is only valid for lightly crosslinked materials,<sup>27</sup> the following equation for rubbery elasticity is often employed to describe the relationship between  $M_c$  (crosslink density, expressed as the average molecular weight of the segment between two adjacent links) and Young's modulus ( $E$ ) of a thermoset above the  $T_g$ :

$$E = 3pRT/M_c$$

Because the storage modulus ( $E'$ ) obtained from DMA is similar in value to the elastic modulus ( $E$ ) at temperatures well above  $T_g$ ,  $E'$  is frequently used in the above equation for the evaluation of  $M_c$ .<sup>28</sup>

Fig. 6(a) demonstrates the effects of functionality and molecular structure of the curing agents on modulus. It is noted that epoxies cured with rosin-based curing agents exhibited



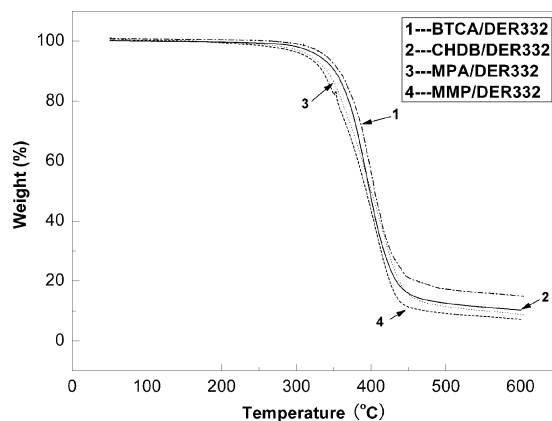
**Fig. 6** Storage modulus versus temperature (a) and  $\tan \delta$  versus temperature (b) for DER332 cured with different curing agents.

lower moduli in rubbery state than epoxies cured with their corresponding monocyclic curing agent analogues. This result might be attributed to the bulky hydrogenated phenanthrene ring in MMP and MPA, which decreased the crosslink density of the system.

The  $T_g$  of the cured samples were determined by the peak temperatures of the  $\alpha$ -transition detected in the  $\tan \delta$  versus temperature graph (Fig. 6b) of the DMA experiment, and the results are summarized in Table 1. Apparently, the resin cured with MPA had the highest  $T_g$ , which was followed by the resin cured with BTCA, MMP and CHDB. The difference in  $T_g$  values of the cured resins corresponded to the differences in chemical structure and functionality of the curing agents. Because the functionality of BTCA or MPA ( $f = 3$ ) was higher than that of CHDB or MMP ( $f = 2$ ), the epoxy resins cured with BTCA or MPA possessed higher crosslink density than the resins cured with the CHDB or MMP, displaying high  $T_g$ . It is also noted that the resins cured with rosin-based curing agents exhibited higher  $T_g$  (ca.  $10^{\circ}\text{C}$ ) than the resins cured with their corresponding commercial counterparts. The bulky fused ring structure of rosin probably imposed considerable restriction on the segmental mobility between crosslinks, hence resulting in higher  $T_g$ .

### Thermogravimetric analysis (TGA)

The thermal stability of an epoxy is one of the important factors in determining its end use. TGA is a convenient and most often used method to evaluate the thermal stability and degradation behaviors of polymers. Fig. 7 shows the TGA graphs for the DER332 resins cured with CHDB, BTCA, MMP and MPA, respectively. The temperatures at which 5 and 10% weight losses were incurred,  $T_{5\%}$  and  $T_{10\%}$ , are given in Table 1. It is noted that  $T_{5\%}$  for the epoxy resins cured with CHDB and BTCA were ca. 330 and 340  $^{\circ}\text{C}$ , respectively. For the MMP/DER332 and MPA/DER332 systems,  $T_{5\%}$  were ca. 312 and 320  $^{\circ}\text{C}$ , respectively. These results indicate that the epoxy cured with rosin-based curing agent exhibited slightly lower thermal degradation temperature compared to that of the epoxies cured with commercial petroleum curing agents.



**Fig. 7** TGA plots for the cured epoxy resin under nitrogen.

## Conclusions

Two potential bio-based epoxy curing agents, maleopimaric acid and methyl maleopimarate acid, were synthesized from rosin acids, and the synthesis methods were studied. Compared with hydroquinone, *p*-toluene sulfonic acid was proven to be a more efficient catalyst in the Diels–Alder reaction between methyl abietate and maleic anhydride. The chemical structures of the rosin-based curing agents were confirmed by  $^1\text{H}$  NMR,  $^{13}\text{C}$  NMR and FT-IR. The non-isothermal curing study showed that the temperature and activation energy of cure reactions of rosin-based curing agents were very similar to that of their commercial monocyclic (aliphatic or aromatic) analogs. The rosin curing agent cured epoxies displayed similar moduli to their commercial monocyclic analogs, but yielded a higher  $T_g$ . On the other hand, rosin-based curing agent exhibited slightly lower degradation temperature. Compared with petrochemical curing agents, rosin-based curing agents can be prepared by much simpler and more environmentally friendly synthesis routes. These results suggest that rosin acids have a great potential to replace some of the current aromatic or cycloaliphatic compounds in the synthesis of epoxy curing agents.

## Acknowledgements

This activity was funded, in part, with an Emerging Research Issues Internal Competitive Grant from the Washington State University, College of Agricultural, Human and Natural Resource Sciences, Agricultural Research Center.

## References

- J. W. Copen and G. A. Hone, *Gum naval stores: Turpentine and rosin from pine resin*, Food and Agriculture Organization of the United Nations, 1995, ch. 1.
- S. Maiti, S. S. Ray and A. K. Kundu, *Prog. Polym. Sci.*, 1989, **14**, 297–338.
- X. Q. Liu, C. C. Li, D. Zhang, Y. N. Xiao and G. H. Guan, *Polym. Int.*, 2006, **55**, 545–551.
- X. Q. Liu, C. C. Li, D. Zhang and Y. N. Xiao, *J. Polym. Sci., Part B: Polym. Phys.*, 2006, **44**, 900–913.
- X. Q. Liu, C. C. Li, G. H. Guan, X. P. Yuan, Y. N. Xiao and D. Zhang, *J. Polym. Sci., Part B: Polym. Phys.*, 2005, **43**, 2694–2704.
- S. S. Ray, A. K. Kundu, M. Ghosh and S. Maiti, *Eur. Polym. J.*, 1985, **21**, 131–133.
- B. Ioan and M. Fanica, *Angew. Makromol. Chem.*, 1999, **264**, 21–29.
- B. Ioan and M. Fanica, *Angew. Makromol. Chem.*, 2000, **281**, 47–53.
- S. S. Ray, A. K. Kundu and S. Maiti, *J. Appl. Polym. Sci.*, 1988, **36**, 1283–1293.
- S. S. Ray, A. K. Kundu and S. Maiti, *Eur. Polym. J.*, 1990, **26**, 471–474.
- U. V. Barabde, S. V. Fulzele, P. M. Satturwar, A. K. Dorle and S. B. Joshi, *React. Funct. Polym.*, 2005, **62**, 241–248.
- S. Das and S. Maiti, *J. Macromol. Sci. Chem.*, 1982, **A17**, 1177–1192.
- B. Ioan and M. Fanica, *J. Appl. Polym. Sci.*, 2004, **92**, 2240–2252.
- B. Ioan and M. Fanica, *Angew. Makromol. Chem.*, 1996, **234**, 91–102.
- L. Hoa, J. P. Pascault, L. T. My and C. Son, *Eur. Polym. J.*, 1993, **29**, 491–495.
- B. Ioan and M. Fanica, *Angew. Makromol. Chem.*, 1997, **246**, 11–22.
- T. Matynia, *J. Appl. Polym. Sci.*, 1980, **25**, 1–13.
- A. M. Atta, R. Mansour, M. I. Abdou and A. M. Sayed, *Polym. Adv. Technol.*, 2004, **15**, 514–522.
- A. M. Atta, R. Mansour, M. I. Abdou and A. M. Sayed, *J. Polym. Res.*, 2005, **12**, 127–138.
- H. H. Wang, B. Liu, X. Q. Liu, J. Zhang and M. Xian, *Green Chem.*, 2008, **10**, 1190–1196.
- E. M. Petrie, *Epoxy Adhesive Formulations*, McGraw-Hill, New York, 2006, pp. 95–96.
- T. Raju, D. Sebastien, S. Christophe, O. Tolid, G. Sara, G. Gabriel, M. Paula and T. Sabu, *Polymer*, 2007, **48**, 1695–1710.
- J. S. Lee and S. I. Hong, *Eur. Polym. J.*, 2002, **38**, 387–392.
- H. E. Kissinger, *J. Ind. Natl. Bur. Stand.*, 1956, **57**, 217–221.
- T. Ozawa, *J. Therm. Anal.*, 1976, **9**, 369–373.
- J. W. Wang, G. Laborie and M. P. Wolcott, *J. Appl. Polym. Sci.*, 2007, **105**, 1289–1296.
- A. V. Tobolsky, D. W. Carlson and N. J. Indictor, *J. Polym. Sci.*, 1961, **54**, 175–183.
- L. W. Hill, *Paint and Coating Testing Manual*, American Society for Testing and Materials, Philadelphia, PA, 1995, ch. 46, 534–546.

# Chemistry driven by suction

Zhilin Wu,<sup>a,b</sup> Bernd Ondruschka,<sup>\*a</sup> Yongchun Zhang,<sup>b</sup> David H. Bremner,<sup>c</sup> Haifeng Shen<sup>b</sup> and Marcus Franke<sup>a</sup>

Received 3rd February 2009, Accepted 14th April 2009

First published as an Advance Article on the web 27th April 2009

DOI: 10.1039/b902224d

The use of suction rather than positive pressure hydrodynamic cavitation is suggested as an energy efficient green technology. The restriction orifice for creating hydrodynamic cavitation is fixed on the suction side of the pump, and the upstream and downstream pressures are kept low, at atmospheric pressure and partial vacuum, respectively. Energy efficiency is much better by suction than by extrusion with the same pump. As an indicator of cavitation intensity, the conductivity of the aqueous solution increases linearly with the decomposition of chloroform driven by suction. The concentration of Cl<sup>-</sup> was found to synchronously rise with the increase of conductivity. The observed rates vary polynomially with the suction pressure and the solution temperature. Suction also facilitates the two-phase mixing, and promotes the ozonation of phenol, due to high-speed jetting of liquid along with the associated shock waves induced by collapsing cavitation. These results indicate that hydrodynamic cavitation induced by suction as a green tool is particularly promising especially for heterogeneous reactions, such as biodiesel synthesis, oxidation of organics, extraction and emulsification.

## Introduction

Hydrodynamic cavitation (HC) is produced by large pressure differentials within a flowing liquid,<sup>1,2</sup> and is well known for its destructive capabilities such as material damage and generation of intense noise. For these reasons, except for some special applications, it is to be avoided or controlled at all costs.<sup>3</sup> With the development of sonochemistry increasing importance has been attached to the chemical effects induced by hydrodynamic cavitation (*i.e.*, hydrolysis, preparation of nanocatalysts, oxidation and decomposition of organic compounds, and esterification) due to higher energy efficiency and easier scale up for hydrodynamic cavitation reactors compared with the acoustic counterparts.<sup>4–10</sup>

However, hydrodynamic cavitation and the resulting chemical reactions are usually driven by extrusion under positive pressure (push) but little is known about the chemical consequences of hydrodynamic cavitation created by suction (“pull”). Suction is the flow of a fluid into a partial vacuum, or region of low pressure. The pressure gradient between this region and the ambient pressure will propel matter towards the low pressure area.

A pump is the core component of any setup for creating hydrodynamic cavitation and typically has an inlet and an outlet, which are said to be at the suction side and at the discharge

side of the pump, respectively. In all previous cases,<sup>11–15</sup> the restriction components (*e.g.* orifice plate or venturi) for creating hydrodynamic cavitation are placed at the discharge side and the upstream pressures adopted were generally high (3–10 bar) or very high (150–1500 bar).<sup>15,16</sup> In contrast, the restriction counterpart is fixed on the suction side in this investigation, and the upstream and downstream pressures are atmospheric pressure and partial vacuum, respectively.

Sonochemistry arises from acoustic cavitation: the formation, growth, and implosive collapse of bubbles in a liquid generating transient hot spots (about 5000 K) responsible for high-energy chemistry and emission of light.<sup>17,18</sup> These extreme conditions lead to the thermal decomposition of water molecules and the formation of reactive species such as HO<sup>•</sup> and H<sub>2</sub>O<sub>2</sub>, which can oxidize substrates.<sup>19</sup> Meanwhile, the thermal decomposition of volatile substrates, *e.g.* chlorocarbons in or around the cavitation bubbles occurs, and produces Cl<sub>2</sub>, Cl<sup>-</sup>, ClO<sup>-</sup> and organic dimers.<sup>7</sup> Cavity collapse also induces high-speed jets of liquid which, along with the associated shock waves, can facilitate the two-phase mixing and modification of the highly heated solid surface.<sup>20,21</sup>

As a standard dosimeter, the Weissler reaction in which iodide is oxidized to triiodide has been widely used for measurement of the intensity of ultrasonic and hydrodynamic cavitation.<sup>1,22,23</sup> However, triiodide is also consumed at a rapid rate leading to an equilibrium concentration under hydrodynamic conditions, therefore the Weissler reaction was not a good model reaction for the assessment of the effectiveness of hydrodynamic cavitation.<sup>24</sup> As an alternative to the oxidation of KI, the species Cl<sub>2</sub>, Cl<sup>-</sup> and ClO<sup>-</sup> are released and result in an increase of the conductivity of aqueous solutions during the HC-induced degradation of chlorocarbons. This can be monitored in real time using conductivity measurements.<sup>7</sup>

<sup>a</sup>Institute of Technical Chemistry and Environmental Chemistry, Friedrich-Schiller-University Jena, Lessingstr. 12, D-07743, Jena, Germany. E-mail: bernd.ondruschka@uni-jena.de; Fax: +49 3641-948402; Tel: +49 3641-948400

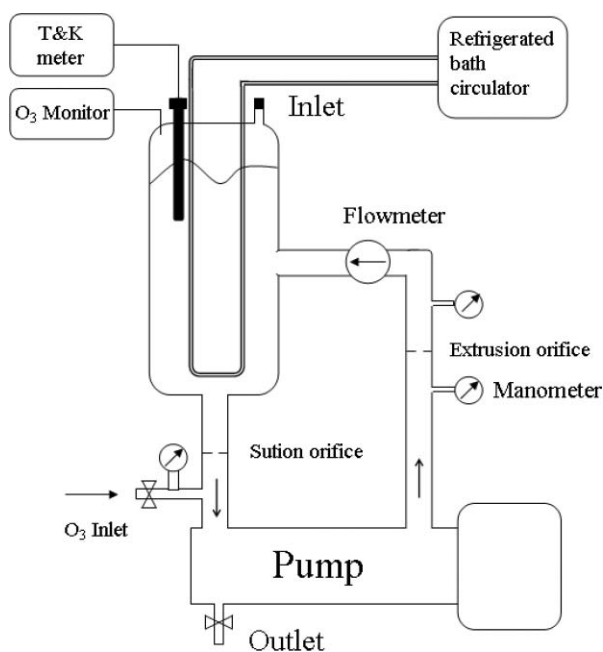
<sup>b</sup>Nanjing Institute of Environmental Sciences, MEP of China, Jiangwangmiaostr. 8, 210042, Nanjing, China

<sup>c</sup>School of Contemporary Sciences, University of Abertay Dundee, 40 Bell Street, Dundee, United Kingdom DD1 1HG

## Experimental

Chloroform ( $\text{CHCl}_3$ , Riedel-de Haen, 99.0%), carbon tetrachloride ( $\text{CCl}_4$ , Fluka, 99.5%), and other reagent grade chemicals were used as received. Water used for sample preparation was purified with a Millipore Milli-Q system ( $R = 18.2 \text{ M}\Omega \text{ cm}^{-1}$ ).

The studies on the decomposition behaviour of chlorocarbons in aqueous solutions induced by suction were performed with a lab-scale loop-device, as shown in Fig. 1, consisting of a pump (GY-028,  $2750 \text{ min}^{-1}$ ,  $0.1\text{--}0.7 \text{ MPa}$ ,  $200\text{--}1700 \text{ L h}^{-1}$ , Speck Pumps, Roth, Germany), 3 sets of manometers (Swagelok, Germany), a flowmeter and a water-reservoir with an online meter for conductivity and temperature (GMH 3430) and a heat exchanger. High-velocity pumping is also accompanied by bulk heating of the flowing liquid so a heat exchanger is therefore immersed in the reservoir and the bulk liquid is maintained at a constant temperature by a refrigerated/heating circulator (FP50, Julabo, Seelbach, Germany).



**Fig. 1** Schematic diagram of the lab-scale suction loop-device for creating hydrodynamic cavitation (T & K meter: Temperature and conductivity meter).

In addition, ozone (or other gases) can be introduced into the loop device through the ozone inlet at the suction side of pump. Ozone was generated and monitored by Fischer Ozon-generator 500 and Ozone Monitor EG-2001 (Meckenheim/Bonn, Germany), respectively.

In a typical run an aqueous solution ( $800 \text{ mL}$ ) containing chloroform ( $1.0 \text{ mmol L}^{-1}$ ) was introduced into the reservoir of the setup. The reaction solution, which by design was only exposed to stainless steel or glass, was sucked by the pump through the restriction hole at the suction side (namely the suction orifice) with velocities of  $7.5\text{--}10.2 \text{ m s}^{-1}$  controlled by the diameter of the suction orifices. The pressures at the suction side ( $P_s$ ) of the pump vary from  $12\text{--}100 \text{ kPa}$  by altering the diameter of the suction orifice. The reaction solution

temperature increased from  $17$  to  $20 \text{ }^\circ\text{C}$  within  $90 \text{ s}$  and stabilized at the temperatures reported herein.

Aliquots ( $5 \text{ mL}$ ) of the processed solution were periodically extracted from the reaction system by airtight syringes and analyzed using Headspace-GC/FID; or aliquots ( $50 \text{ mL}$ ) were taken by pipettes for the monitoring of  $\text{Cl}^-$  by using a Mettler DL67 Titrator. The rates of conductivity and degradation of chlorocarbons were measured and calculated as a function of reaction time.

Aliquots ( $1 \text{ mL}$ ) of the processed phenol solution were periodically extracted from the reaction system and analysed quantitatively and qualitatively by HPLC.

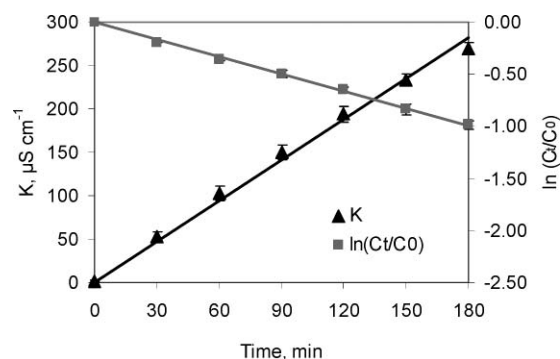
## Results and discussion

Organic products from the decomposition of chloroform and carbon tetrachloride using hydrodynamic cavitation have been reported in our previous study and demonstrated the formation and recombination of free radicals,<sup>7</sup> e.g.,  $\text{CCl}_4$ ,  $\text{C}_2\text{Cl}_4$ , and  $\text{C}_2\text{Cl}_6$  are produced from the degradation of  $\text{CHCl}_3$ , and  $\text{CHCl}_3$  and  $\text{C}_2\text{Cl}_6$  are produced from the degradation of  $\text{CCl}_4$ . Due to the cleavage of C–Cl bonds,  $\text{Cl}_2$ ,  $\text{Cl}^\cdot$ ,  $\text{Cl}^-$  and other ions released increased the conductivity and enhance the oxidation of KI in aqueous solutions. The products and chemical mechanisms of the degradation of chlorocarbons induced by hydrodynamic cavitation in aqueous solutions are consistent with those obtained from acoustic cavitation.

Chakinala, *et al.* demonstrated similar chemical mechanisms during hydrodynamic cavitation induced by a very high pressure as determined by the extent of oxidation of aqueous  $\text{I}^-$  to  $\text{I}_3^-$ , due to the generation of additional free radicals/oxidants in the presence of chloroalkanes in a liquid whistle reactor (LWR).<sup>16</sup> which, surprisingly, did not show any oxidation in the absence of additives.

### Indicator for cavitation intensity: increase in conductivity with decomposition of chlorocarbons in aqueous solutions

Fig. 2 shows that the conductivity of the aqueous solution increases linearly with the decomposition of  $\text{CHCl}_3$  driven by suction. The concentration of  $\text{Cl}^-$  was found to synchronously rise with the increase of conductivity from  $0$  to  $0.274 \text{ mmol L}^{-1}$  in  $1 \text{ h}$  and  $0.520 \text{ mmol L}^{-1}$  after  $2 \text{ h}$ .



**Fig. 2** Decomposition of chloroform driven by suction and increasing conductivity of solutions. Conditions:  $800 \text{ mL}$  of  $1.0 \text{ mM CHCl}_3$  solutions,  $20 \text{ }^\circ\text{C}$ .  $13.3 \text{ kPa}$  suction pressure,  $460 \text{ L h}^{-1}$  flow with  $4 \text{ mm}$  suction orifice.

Similar behaviour was also demonstrated during the degradation of  $\text{CCl}_4$  induced by suction. The linear relationships of the solution conductivity ( $K$ ) to the degradation of volatile chlorocarbons ( $\ln(C_t/C_0)$ ) are given for  $\text{CHCl}_3$  and  $\text{CCl}_4$  by eqn (1) and (2), respectively:

$$K_{\text{CHCl}_3} = -283.11 \ln(C_t/C_0), R^2 = 0.9944 \quad (1)$$

$$K_{\text{CCl}_4} = -103.79 \ln(C_t/C_0), R^2 = 0.9859 \quad (2)$$

$C_t$  and  $C_0$  are the concentrations at a given reaction time and the initial concentration of reactant, respectively.

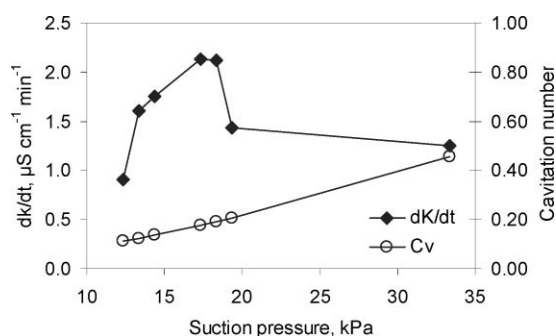
As seen from Fig. 2, there is a direct inverse relationship between reactant concentration and the increasing rate of conductivity so the latter can be used as an indicator to investigate the degradation of chlorocarbons induced by hydrodynamic cavitation and optimize the hydrodynamic system.

### Role of suction pressure

The effect of the pressure at the suction side (suction pressure or partial vacuum) was investigated over the range 12–100 kPa. The decomposition rate increases linearly with the pressure at the suction side when the hydrostatic pressure is below 17.3 kPa but decreases sharply when the hydrostatic pressure is over 17.3 kPa (Fig. 3). Theoretically, the shear and cavitation forces, and the number of cavitation events are a function of the cavitation numbers<sup>1,25</sup> as defined in eqn (3):

$$C_v = \frac{p_d - p_v}{p_u - p_d} = \frac{p_d - 2.34}{101.33 - p_d} \quad (3)$$

where  $p_d$ ,  $p_u$ , and  $p_v$  are the downstream, upstream and vapour pressures, respectively. Herein,  $p_v$  of water at 20 °C is 2.34 kPa;  $p_u$  is the atmospheric pressure (101.33 kPa) and  $p_d$  is the pressure at the suction side. Based on the calculation, it can be seen that the cavitation number increases with the pressure at the suction side (Fig. 3).



**Fig. 3** The conductivity rate and the cavitation number related to the pressure at the suction side. Conditions: 800 mL of solution containing  $\text{CHCl}_3$  (1.0 mM), 20 °C, 1 h processing time.

The number of cavitation events and therefore the reaction rate, increase with decreasing  $C_v$ ,<sup>1,11</sup> especially with  $C_v < 1$ . A larger flow area of the suction orifice produces a lower partial vacuum or, so it seems, higher pressure at the suction side. An increase in downstream pressure (pressure at suction side) should decrease the pressure differential and the velocity of the liquid at the throat of the constriction with the constant

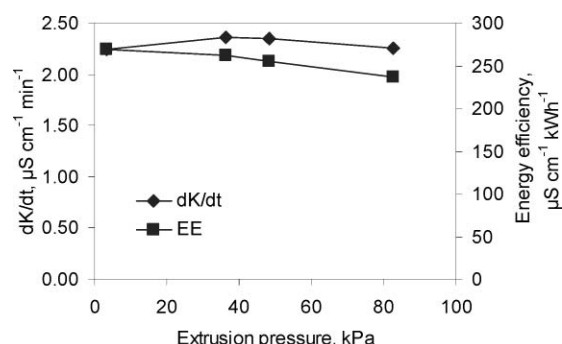
upstream pressure (atmosphere pressure) and consequently decreases the cavitation intensity and the number of cavitation events per cycle. This should decrease the decomposition rate of  $\text{CHCl}_3$  and the solution conductivity, if the chemistry is cavitation driven. This is consistent with the theory of cavitation number while  $C_v > 0.18$ , that is, the pressure at the suction side is higher than 17.3 kPa. However, when  $C_v < 0.18$ , the number of cycles (time  $\times$  flow-rate/processing volume) dominate the reaction rate since more flow causes more effective cavitation events in a given time over the cavitation threshold, although the cavitation forces are increased with the higher flow velocity and pressure differential.

### Effects of extrusion orifice and pump

The decomposition of chloroform by the extrusion-driven hydrodynamic cavitation has been previously demonstrated.<sup>7</sup> Under the optimal conditions (172 kPa extrusion pressure with orifice plate 16  $\times$  0.9 mm), the normalized rate of conductivity for a solution containing 1 mM chloroform was measured to be 2.17  $\mu\text{S cm}^{-1} \text{min}^{-1}$ , and the corresponding degradation rate of chloroform was 37% in 60 min. The energy efficiency (degradation rate per kilowatt hour of electrical energy) for the decomposition of chloroform was estimated to be 352  $\mu\text{mol kWh}^{-1}$ .

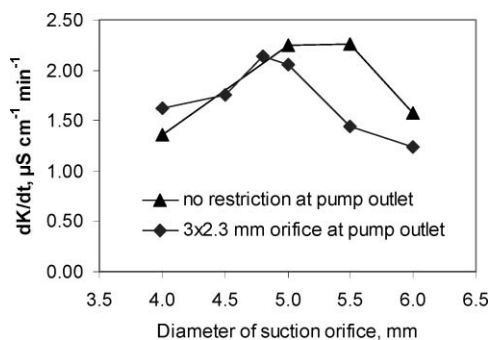
In this investigation, better efficiencies were achieved by using a suction orifice with the same pump. Under the optimal conditions (23 kPa suction pressure with 5 mm orifice), the normalized rate of conductivity was found to be 2.25  $\mu\text{S cm}^{-1} \text{min}^{-1}$ , and the corresponding degradation rate of chloroform was calculated to be 38% in 60 min. Due to the lower operating power at suction (500 W at suction vs. 840 W at extrusion), the energy efficiency for the decomposition of chloroform was estimated to be 608  $\mu\text{mol kWh}^{-1}$ , indicating that suction is more efficient than extrusion.

The orifice plate at the discharge side influences the reaction rate driven by suction slightly but it does weaken the energy efficiency significantly, as shown in Fig. 4. The highest energy efficiency is seen when the discharge side of the pump is fully opened (without an extrusion orifice), since the increasing pressure at the pump outlet generally depresses the contribution



**Fig. 4** The effects of an extrusion orifice on the rate of conductivity and energy efficiency (EE). Conditions: 800 mL of 1.0 mM  $\text{CHCl}_3$  solutions, 20 °C. Extrusion orifice configuration: fully open ( $p_u$  3.4 kPa), 5  $\times$  2.3 mm ( $p_u$  36.2 kPa), 4  $\times$  2.3 mm ( $p_u$  48.3 kPa), 3  $\times$  2.3 mm ( $p_u$  82.7 kPa). Extrusion pressure changes on altering the extrusion orifice, but the flow is kept constant (720 L h<sup>-1</sup>) with a 5 mm suction orifice.

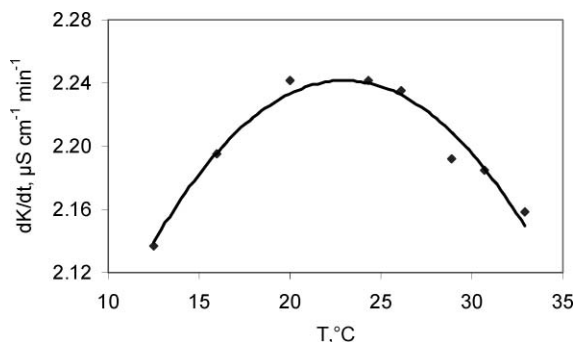
of the pump creating cavitation. Without a restriction orifice at the pump outlet, the extrusion pressure of the pump remains low, thus the total cavitation efficiency includes the contribution of a pump. With extrusion orifices, the pressure at the pump outlet rises with the increasing diameter of the suction orifice. The effect of the pump is significantly depressed at over 89.6 kPa by the 5.5 mm suction orifice, as shown in Fig. 5. Without an extrusion orifice at the discharge side, the contribution of the pump is 36.5% of the total effect.



**Fig. 5** Comparison of conductivity rates with and without extrusion orifice. Conditions: 800 mL of 1.0 mM  $\text{CHCl}_3$  solutions, 20 °C.

### Effect of temperature

The temperature of the bulk solution influences, not only the vapour pressure of the solvent, but also the solubility and vapour pressure of the solute, which governs the mass transfer of volatile substrates from the aqueous solution to the cavitation bubble.<sup>26</sup> Fig. 6 demonstrates that the observed rates vary polynomially with solution temperature and shows that the vapour pressure of water dominates the reaction rate at temperatures greater than 20 °C. The reaction rates decrease sharply with increasing temperature, consistent with previous investigations<sup>1,18,27</sup> where it is attributed to the increase in polyatomic vapour inside the bubble before collapse, which decreases the polytropic ratio of the dissolved gas and depresses the collapse of the cavitating bubble.<sup>28,29</sup> However, the reaction rates increase with increasing temperature below 20 °C, due to the decreasing solubility and increasing vapour pressure of chloroform with increasing temperature, which accelerates mass transfer of chloroform from bulk liquid to the cavitation bubble.<sup>26</sup>

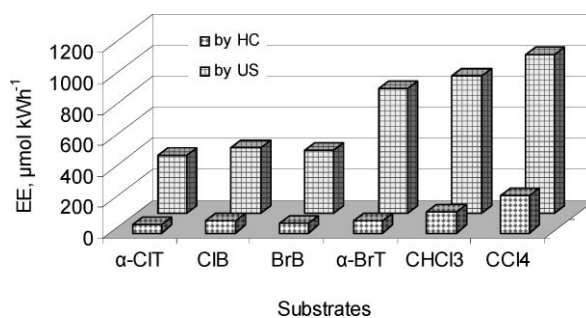


**Fig. 6** Dependence of the conductivity rate on the bulk temperature during hydrodynamic cavitation. Conditions: 800 mL of 1.0 mM  $\text{CHCl}_3$  solutions. Setup: 5 mm suction orifice, no restriction orifice at the discharge side, 23.3 kPa suction pressure.

### Comparison of energy efficiency between hydrodynamic and acoustic cavitation

Chakinala, *et al.* reported that the degree of intensification is directly proportional to the applied pressure and maximum rates of  $\text{I}_3^-$  production were obtained with a LWR at 1500 psi (10 342 kPa). When compared to LWR, the ultrasonic reactor was 2.5 times more efficient in the oxidation of  $\text{I}^-$  to  $\text{I}_3^-$  considering the relative energy consumption and scale of operation.<sup>16</sup> As mentioned above, the energy efficiency for the decomposition of chloroform appears to be superior by suction than by extrusion with the same pump, due to the lower operating power for suction.

In this study, under the optimal conditions and with the same processing volume and identical initial concentration of substrates, the energy efficiencies for degradation of halogen compounds ( $\alpha$ -chlorotoluene,  $\alpha$ -bromotoluene, chlorobenzene, bromobenzene, chloroform, and carbon tetrachloride) in aqueous solutions by hydrodynamic and acoustic cavitation have been compared. The energy efficiency of the degradation of volatile halocarbons in aqueous solutions by suction (negative pressure) is still lower than those by 850 kHz ultrasonic treatment, as shown in Fig. 7.



**Fig. 7** Comparison of the energy efficiency of hydrodynamic and ultrasonic cavitation. Hydrodynamic conditions: 800 mL of 0.2 mM halogen-compounds in aqueous solutions, 20 °C, 1 h. 5 mm suction orifice without an orifice plate at the discharge side, 23.3 kPa suction pressure, 500 W electrical power. Ultrasonic conditions: 800 mL of 0.2 mM halogen-compounds solutions, 20 °C, 1 h. 850 kHz, 120 W electrical power, 40 W acoustic power (EE: energy efficiency, HC: hydrodynamic cavitation, US: ultrasonic cavitation,  $\alpha$ -CIT:  $\alpha$ -chlorotoluene, CIB: chlorobenzene, BrB: bromobenzene,  $\alpha$ -BrT:  $\alpha$ -bromotoluene,  $\text{CHCl}_3$ : chloroform,  $\text{CCl}_4$ : tetrachlorocarbons).

The results of the investigation on energy efficiencies when using the suction process are similar to those of the high-pressure liquid whistle reactor (LWR), but the suction process is operated more expediently and safely. In future, more efforts should be put into the improvement of the energy efficiency by optimising the restriction orifice and using other chemical reactions, such as oxidation, esterification, *etc.*

### Enhanced effect of suction on the ozonation of phenol

As mentioned above, hydrodynamic cavitation induced by extrusion has been investigated and applied in hydrolysis, preparation of nanocatalysts, oxidation and decomposition of organic compounds, and esterification,<sup>4-10</sup> since it is able to promote the mass transfer between phases.



The effect of hydrodynamic cavitation induced by suction on the ozonation kinetics of phenol was compared to the treatment by suction alone, ozonation in the 3-tandem gas wash-cylinders (GWC) with micro-filter (16–40  $\mu\text{m}$  pore) and ozonation in the suction device. Phenol can not be degraded in 30 min by using suction (5 mm orifice) alone, while the oxidative degradation of phenol by ozone in the GWC or with suction follows first-order kinetics. With an ozone flow rate of 3.2  $\text{mg min}^{-1}$  the rate constants for 800 mL of 1  $\text{mmol L}^{-1}$  aqueous phenol solutions are 0.025 in the GWC and 0.050  $\text{min}^{-1}$  with suction at 20 °C, respectively. It demonstrates that hydrodynamic cavitation induced by suction, considerably promotes the mass transfer of ozone and enhances the ozonation of phenol. Compared to ozonation in the 3-tandem GWC, no ozone was observed in the tail gas during the first 15 min ozonation with suction, and then the concentration of ozone in the tail gas slowly increased, also indicating that the utilization rate of ozone is significantly improved by suction.

Therefore, hydrodynamic cavitation induced by suction as a green tool has a bright future in heterogeneous reactions, such as biodiesel synthesis, oxidation of organics, extraction and emulsification.

## Conclusions

In summary, the chemical effects driven by suction and the use of conductivity as a measure of the degradation of chlorocarbons induced by hydrodynamic cavitation have been demonstrated. The observed rates vary polynomially with the pressure at the suction side and the solvent temperature. When the cavitation number is over 0.18 cavitation number dominates the reaction rate, but when it is below this value the number of cycles and, consequently, the greater number of cavitation events in a given time govern the kinetics of degradation. In particular, the rates decrease with increasing solution temperature when the temperature is over 20 °C, due to the increased water vapour pressure inside the bubble. Increasing water vapour pressure attenuates the efficacy of cavitation collapse, the maximum temperature reached during such collapse and, consequently, the rates of cavitation reactions. However, the reaction rates increase with increasing temperature below 20 °C, due to the decreasing solubility and increasing vapour pressure of volatile solutes with increasing temperature, which accelerates mass transfer of volatile solutes from solution to the cavitation bubble.

Hydrodynamic cavitation driven by suction can be applied to the ozonation of phenol, and it considerably promotes the mass transfer of ozone in aqueous solution resulting in enhanced ozonation of phenol. In addition suction improved the utilization of ozone and contributed to operating cost savings.

The energy efficiency for the decomposition of chloroform appears to be superior by suction than by extrusion with the same pump, due to the lower operating power for suction. However, compared to 850 kHz ultrasonic treatment, more

efforts should be put into the improvement of the energy efficiency of suction by optimising the restriction orifice and using other chemical reactions, such as oxidation, esterification, etc.

## Acknowledgements

This work was supported by the Friedrich-Schiller-University of Jena, Germany, and the Nanjing Institute of Environmental, Chinese Ministry of Environmental Protection (G67001) and in part by the auspices of European Union COST Action D32 (WG 006/04). The device used in this study was made by Wolfgang Fährdrich, Jena, Germany.

## References

- 1 K. S. Suslick, M. M. Mdeleleni and J. T. Ries, *J. Am. Chem. Soc.*, 1997, **119**, 9303–9304.
- 2 P. R. Gogate and A. B. Pandit, *Rev. Chem. Eng.*, 2001, **17**, 1–85.
- 3 V. H. Arakeri and S. Chakraborty, *Curr. Sci.*, 1990, **59**, 1326–1333.
- 4 A. B. Pandit and J. B. Joshi, *Chem. Eng. Sci.*, 1993, **48**, 3440–3442.
- 5 J. E. Sunstrom, W. R. Moser and B. Marshik-Guerts, *Chem. Mat.*, 1996, **8**, 2061–2067.
- 6 K. M. Kalumuck and G. L. Chahine, *J. Fluids Eng.-Trans. ASME*, 2000, **122**, 465–470.
- 7 Z.-L. Wu, B. Ondruschka and P. Braeutigam, *Chem. Eng. Technol.*, 2007, **30**, 642–648.
- 8 M. A. Kelkar, P. R. Gogate and A. B. Pandit, *Ultrason. Sonochem.*, 2008, **15**, 188–194.
- 9 A. G. Chakinala, P. R. Gogate, R. Chand, D. H. Bremner, R. Molina and A. E. Burgess, *Ultrason. Sonochem.*, 2008, **15**, 164–170.
- 10 P. R. Gogate and A. B. Pandit, *Ultrason. Sonochem.*, 2005, **12**, 21–27.
- 11 S. Arrojo, C. Nerin and Y. Benito, *Ultrason. Sonochem.*, 2007, **14**, 343–349.
- 12 G. V. Ambulgekar, S. D. Samant and A. B. Pandit, *Ultrason. Sonochem.*, 2004, **11**, 191–196.
- 13 J. B. Ji, J. L. Wang, Y. C. Li, Y. L. Yu and Z. C. Xu, *Ultrasonics*, 2006, **44**, E411–E414.
- 14 A. G. Chakinala, D. H. Bremner, P. R. Gogate, K.-C. Namkung and A. E. Burgess, *Appl. Cat. B: Environ.*, 2008, **78**, 11–18.
- 15 X. Wang and Y. Zhang, *J. Hazard. Mater.*, 2009, **161**, 202–207.
- 16 D. H. Bremner, S. Di Carlo, A. G. Chakinala and G. Cravotto, *Ultrason. Sonochem.*, 2008, **15**, 416–419.
- 17 E. B. Flint and K. S. Suslick, *Science*, 1991, **253**, 1397–1399.
- 18 F. B. Peterson and T. P. Anderson, *Phys. Fluids*, 1967, **10**, 874–879.
- 19 K. S. Suslick, *Science*, 1990, **247**, 1439–1445.
- 20 S. J. Doktycz and K. S. Suslick, *Science*, 1990, **247**, 1067–1069.
- 21 K. S. Suslick, S. B. Choe, A. A. Cichowlas and M. W. Grinstaff, *Nature*, 1991, **353**, 414–416.
- 22 A. Weissler, H. W. Cooper and S. Snyder, *J. Am. Chem. Soc.*, 1950, **72**, 1769–1775.
- 23 P. R. Gogate, P. A. Tatake, P. M. Kanthale and A. B. Pandit, *AIChE J.*, 2002, **48**, 1542–1560.
- 24 K. R. Morison and C. A. Hutchinson, *Ultrason. Sonochem.*, 2009, **16**, 176–183.
- 25 J. Find, S. C. Emerson, I. M. Krausz and W. R. Moser, *J. Mater. Res.*, 2001, **16**, 3503–3513.
- 26 Z. L. Wu and B. Ondruschka, *J. Phys. Chem. A*, 2005, **109**, 6521–6526.
- 27 C. Sehgal, R. G. Sutherland and R. E. Verrall, *J. Phys. Chem.*, 1980, **84**, 525–528.
- 28 K. S. Suslick, J. J. Gawienowski, P. F. Schubert and H. H. Wang, *Ultrasonics*, 1984, **22**, 33–36.
- 29 Z. L. Wu, B. Ondruschka and A. Stark, *J. Phys. Chem. A*, 2005, **109**, 3762–3766.

# MOF-5/*n*-Bu<sub>4</sub>NBr: an efficient catalyst system for the synthesis of cyclic carbonates from epoxides and CO<sub>2</sub> under mild conditions†

Jinliang Song, Zhaofu Zhang, Suqin Hu, Tianbin Wu, Tao Jiang and Buxing Han\*

Received 6th February 2009, Accepted 7th April 2009

First published as an Advance Article on the web 20th April 2009

DOI: 10.1039/b902550b

The development of efficient heterogeneous catalysts for the cycloaddition of CO<sub>2</sub> with epoxides to produce five-membered cyclic carbonates under mild reaction conditions is of great importance. In this work, the coupling reaction of CO<sub>2</sub> with propylene oxide (PO) to produce propylene carbonate (PC) catalyzed by MOF-5 (metal-organic frameworks) in the presence of quaternary ammonium salts (Me<sub>4</sub>NCl, Me<sub>4</sub>NBr, Et<sub>4</sub>NBr, *n*-Pr<sub>4</sub>NBr, *n*-Bu<sub>4</sub>NBr) was studied in different conditions. It was discovered that MOF-5 and quaternary ammonium salts had excellent synergetic effect in promoting the reaction, and the MOF-5/*n*-Bu<sub>4</sub>NBr catalytic system was the most efficient among them. The optimal temperature for the reaction was around 50 °C. The reaction could be completed in 6 h at low CO<sub>2</sub> pressure with very high selectivity. A decrease of the yield of PC was not noticeable after MOF-5 was reused three times, indicating that the MOF-5 was stable. The MOF-5/*n*-Bu<sub>4</sub>NBr catalytic system was also very active and selective for the cycloaddition of CO<sub>2</sub> with other epoxides, such as glycidyl phenyl ether, epichlorohydrin and styrene oxide. The mechanism for the coupling reaction is also discussed.

## Introduction

Carbon dioxide (CO<sub>2</sub>) is the main greenhouse gas. On the other hand, as a cheap, nontoxic, nonflammable and abundant C1 building block, CO<sub>2</sub> can be converted into many useful chemicals,<sup>1</sup> such as dimethyl carbonate,<sup>2</sup> cyclic carbonates,<sup>3</sup> *N,N'*-disubstituted ureas,<sup>4</sup> urethanes,<sup>5</sup> formic acid,<sup>6</sup> and so on. In particular, five-membered cyclic carbonates derived from the coupling reactions of CO<sub>2</sub> with epoxides are promising target molecules. The cyclic carbonates can be widely used as precursors for producing polycarbonates and many fine chemicals.<sup>7</sup> Various catalysts, including homogeneous and heterogeneous catalysts, have been developed for the cycloaddition of CO<sub>2</sub> and epoxides. Homogeneous catalysts include quaternary ammonium<sup>8</sup> and phosphonium salts,<sup>9</sup> ionic liquids,<sup>10</sup> alkali metal salts,<sup>11</sup> Schiff bases,<sup>12</sup> salenCr(III) complexes,<sup>13</sup> salenCo(III)X complexes,<sup>14</sup> Cr(III) porphyrin complexes,<sup>15</sup> salenAl(III) complexes,<sup>16</sup> and so on. Generally, these homogeneous catalysts are effective, and some transition metal complexes are active<sup>13–16</sup> at mild temperatures in the presence of co-catalysts. But the separation of the catalysts from the products is difficult, which limits the wide application of these catalysts.

In order to overcome the separation problem, many heterogeneous catalysts have been developed for coupling reactions of CO<sub>2</sub> with epoxides, such as metal oxide,<sup>17</sup> gold

nanoparticles supported on resins,<sup>18</sup> functional polymers,<sup>19</sup> ion-exchange resins<sup>20</sup> and SiO<sub>2</sub> modified by quaternary ammonium or phosphonium salts.<sup>21</sup> Although heterogeneous catalysts solve the problem of catalyst separation, most of them are active only at high reaction temperatures (>100 °C), which increases the cost of the reaction processes. In addition, many of them need co-solvents.

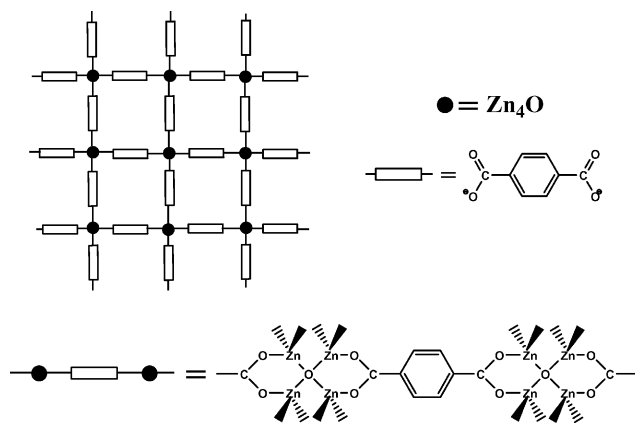
In recent years, metal-organic frameworks (MOFs), which are formed by copolymerization of organic molecules with metal ions or metal ion clusters, have received much attention<sup>22</sup> because of their zeolite-like properties, such as high internal surface area and microporosity, well-ordered porous structures and high absorption capacity. Various applications, including gas storage,<sup>23</sup> separation,<sup>24</sup> magnetism<sup>25</sup> and catalysis,<sup>26</sup> have been studied for the porous metal-organic frameworks. Among these applications, using MOFs as catalysts is very attractive. Some reactions using MOFs as catalysts have been conducted, such as the Knoevenagel condensation reaction,<sup>27</sup> Friedel–Crafts type reaction,<sup>28</sup> cyanosilylation of carbonyl compounds<sup>29</sup> and imines,<sup>30</sup> isomerization,<sup>31</sup> acetalization,<sup>32</sup> ZnEt<sub>2</sub> additions to aldehydes,<sup>33</sup> tetralin oxidation,<sup>34</sup> aldol reaction,<sup>35</sup> asymmetric olefin epoxidation,<sup>36</sup> oxidation of sulfides,<sup>37</sup> asymmetric hydrogenation of β-keto esters<sup>38</sup> and aromatic ketones,<sup>39</sup> transesterification<sup>40</sup> and photochemical reactions.<sup>41</sup> In addition, Pb supported on MOFs has been used as an effective hydrogenation catalyst.<sup>42</sup>

As discussed above, many catalysts have been developed for the coupling reaction of CO<sub>2</sub> and epoxides. However, it is still very interesting and challenging to develop heterogeneous catalysts that are efficient under mild reaction conditions. In this work, we conducted the reactions using MOF-5 [Zn<sub>4</sub>O(BDC)<sub>3</sub> (BDC = benzene-1,4-dicarboxylate)], which was copolymerized

Beijing National Laboratory for Molecular Sciences (BNLMS), Centre for Molecular Science, Institute of Chemistry, Chinese Academy of Sciences, Beijing, 100190, China. E-mail: hanbx@iccas.ac.cn; Fax: +86-10-62562821

† Electronic supplementary information (ESI) available: X-Ray diffraction pattern, thermogram and FTIR spectrum of MOF-5. See DOI: 10.1039/b902550b

by a  $\text{Zn}_4\text{O}$  cluster with BDC through octahedral arrays (Scheme 1),<sup>43</sup> as the heterogeneous catalyst in the presence of quaternary ammonium salts. It was found that the coupling reactions could be effectively carried out at mild temperature and low  $\text{CO}_2$  pressure. The catalyst was very active, selective, inexpensive, stable, and could be easily separated and reused. The possible catalytic mechanism is also discussed. As far as we know, this is the first work to conduct the coupling reactions using MOF-5 as a heterogeneous catalyst under mild conditions.



Scheme 1 The structure of the MOF-5 framework.

## Results and discussion

### Catalyst characterization

The X-ray diffraction pattern, thermogram and FTIR spectrum of the MOF-5 prepared in this work are given in the ESI† (Fig. S1–S3), which agree well with the results reported by other authors.<sup>44</sup>

### Reaction with different catalysts

The activity of various catalysts was tested at 50 °C and 6 MPa using the reaction of propylene oxide (PO) and  $\text{CO}_2$  to produce propylene carbonate (PC), and the results are summarized in Table 1. It can be seen from Table 1 that the activity of MOF-5 depends strongly on the ammonium salts used. Nearly no product was detected without ammonium salts (entry 1). The catalyst was active in the presence of quaternary ammonium salts, and the yield of PC increased with an increasing length of the alkyl chain of the ammonium salts (entries 2–6), and  $n\text{-Bu}_4\text{NBr}$  was the most effective. This could partially result from the structures of the quaternary ammonium ions, which probably affect the behavior of the anions.<sup>45</sup> The size of quaternary ammonium ions increases in the following order:  $\text{Me}_4\text{N}^+ < \text{Et}_4\text{N}^+ < n\text{-Pr}_4\text{N}^+ < n\text{-Bu}_4\text{N}^+$ . Indeed, the bulkiness of quaternary ammonium ions forces the bromide away from the cation. Therefore, the activity order of the quaternary ammonium salts was  $\text{Me}_4\text{NBr} < \text{Et}_4\text{NBr} < n\text{-Pr}_4\text{NBr} < n\text{-Bu}_4\text{NBr}$ . The solubility of quaternary ammonium salts in the PO phase may be another reason. Our experiments in this work showed that  $n\text{-Bu}_4\text{NBr}$  had the best solubility in PO. Some other catalysts were also tested in the presence of  $n\text{-Bu}_4\text{NBr}$  (entries 7–10). When the catalyst MOF-5 was not used or benzene-1,4-dicarboxylic acid (BDC) was used as catalyst,

Table 1 Coupling of  $\text{CO}_2$  and PO catalyzed by different catalysts<sup>a</sup>

Entry	Catalyst	Ammonium salts	Yield (%) <sup>c</sup>
1	MOF-5	None	0.1
2	MOF-5	$\text{Me}_4\text{NCl}$	0.1
3	MOF-5	$\text{Me}_4\text{NBr}$	0.25
4	MOF-5	$\text{Et}_4\text{NBr}$	27.1
5	MOF-5	$n\text{-Pr}_4\text{NBr}$	60.2
6	MOF-5	$n\text{-Bu}_4\text{NBr}$	97.6
7	$\text{ZnCl}_2$ <sup>b</sup>	$n\text{-Bu}_4\text{NBr}$	95.2
8	$\text{ZnO}$ <sup>b</sup>	$n\text{-Bu}_4\text{NBr}$	53.7
9	BDC <sup>b</sup>	$n\text{-Bu}_4\text{NBr}$	6.5
10	None	$n\text{-Bu}_4\text{NBr}$	7.2
11 <sup>d</sup>	MOF-5	$n\text{-Bu}_4\text{NBr}$	13.9
12 <sup>e</sup>	MOF-5	$n\text{-Bu}_4\text{NBr}$	77.6
13 <sup>f</sup>	MOF-5	$n\text{-Bu}_4\text{NBr}$	94.5
14	MOF-5 (2nd)	$n\text{-Bu}_4\text{NBr}$	96
15	MOF-5 (3rd)	$n\text{-Bu}_4\text{NBr}$	96

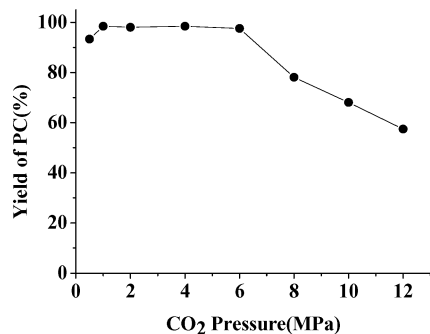
<sup>a</sup> Typical reaction conditions: a stainless reactor of 22 ml, 20 mmol PO with 2.5 mol% ammonium salts, 0.1 g MOF-5,  $\text{CO}_2$  pressure 6 MPa, reaction temperature 50 °C, reaction time 4 h. <sup>b</sup> The amount of  $\text{ZnCl}_2$ ,  $\text{ZnO}$  and BDC was 0.1 g. <sup>c</sup> The yields were determined by GC with an internal standard. <sup>d</sup> 0.63 mol%  $n\text{-Bu}_4\text{NBr}$  was used. <sup>e</sup> 1.25 mol%  $n\text{-Bu}_4\text{NBr}$  was used. <sup>f</sup> 1.88 mol%  $n\text{-Bu}_4\text{NBr}$  was used.

the yield of PC was very low (7.2% and 6.5%, respectively) (entries 9 and 10), indicating that MOF-5 was necessary for the reaction. Interestingly, the activity of MOF-5/ $n\text{-Bu}_4\text{NBr}$  was similar to that of  $\text{ZnCl}_2/n\text{-Bu}_4\text{NBr}$ , which is a homogeneous catalyst system for the reaction reported previously.<sup>46</sup> One of the reasons for the high catalytic activity of MOF-5 is that it is a porous material and has high surface area,<sup>44</sup> which is favorable for the access of reactants and ammonium salts to the active sites ( $\text{Zn}_4\text{O}$ ) of MOF-5. At the same time, we found that the amount of  $n\text{-Bu}_4\text{NBr}$  also had a great influence on the reaction. Increasing the amount of  $n\text{-Bu}_4\text{NBr}$  from 0.63 mol% to 2.5 mol% could enhance the yield of PC significantly (entries 6, 11–13).

The reusability of MOF-5 was also studied at the same experimental conditions of entry 6 and the results are also presented in Table 1 (entries 14, 15). It is obvious that a decrease of the activity of the catalyst was not noticeable after being used three times. It can be seen from the thermogram in Fig. S2 that MOF-5 began to decompose after 380 °C, which is much higher than the temperature used in this work. This provides partial support for the good stability of the catalyst.

### Effect of the $\text{CO}_2$ pressure on the PC yield

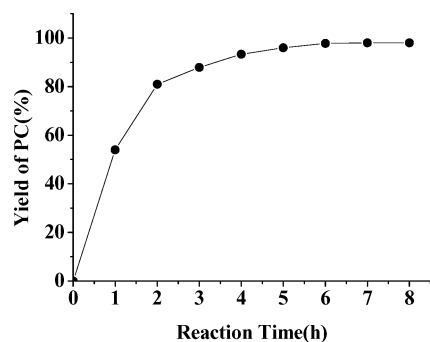
The partition behavior of the substrates between phases may affect the reaction rate of a biphasic reaction system.<sup>47</sup> The effect of the  $\text{CO}_2$  pressure on the catalytic activity of MOF-5 and  $n\text{-Bu}_4\text{NBr}$  was studied at 50 °C in a pressure range of 0.4–12 MPa (total pressure of PO and  $\text{CO}_2$ ), and the results are shown in Fig. 1. The PC yield increased with pressure in the range of 0.4–1.0 MPa, and remained nearly unchanged with pressure in the range of 1.0–6.0 MPa. However, the yield decreased as the pressure changed from 6 to 12 MPa. This can be explained qualitatively by the effect of the pressure on the concentrations of  $\text{CO}_2$  and epoxides in the two phases. In this work, it was observed that there were two phases in the reaction system by using a view cell reported previously.<sup>48</sup> The upper phase was the vapor phase and the bottom phase was



**Fig. 1** Effect of the CO<sub>2</sub> pressure on the PC yield. Reaction conditions: 20 mmol PO with 2.5 mol% *n*-Bu<sub>4</sub>NBr, 0.1 g MOF-5, reaction temperature 50 °C, reaction time 4 h.

the liquid phase. The reactions took place mainly in the liquid phase because the catalyst was dispersed in this phase. In our system, the pressure of CO<sub>2</sub> affects the reaction in two opposite ways. First, the solubility of CO<sub>2</sub> in PO increases with increasing pressure, which favoured the reaction considering that CO<sub>2</sub> was a reactant. Second, the solvent power of CO<sub>2</sub> to extract the reactant increases with increasing CO<sub>2</sub> pressure. In other words, the amount of PO in the vapor becomes larger as the pressure rises, which reduces the reaction rate. When the pressure was very low, the yield increased as the pressure rose, indicating that the first factor was dominant. The two factors compensated each other in the pressure range of 1.0–6.0 MPa and the effect of pressure on the yield was negligible. When the pressure was higher than 6.0 MPa, the second factor became dominant and the yield decreased with the increasing pressure.

The yield of PC at 0.4 MPa could reach 93% at a reaction time of 4 h, as shown in Fig. 1. The PC yield could reach 98% when the reaction time was prolonged to 6 h (Fig. 2). In addition, we also conducted the reaction at 0.2 MPa and a PC yield of 95% was obtained with a reaction time of 6.0 h, indicating that the reaction can be conducted effectively at mild conditions.



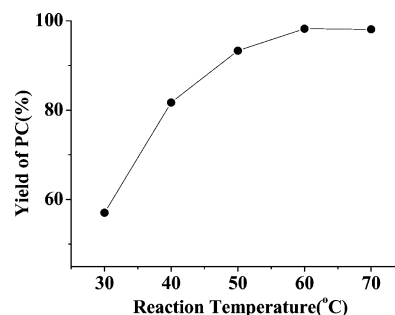
**Fig. 2** The influence of the reaction time on the PC yield. Reaction conditions: 20 mmol PO with 2.5 mol% *n*-Bu<sub>4</sub>NBr, 0.1 g MOF-5, total pressure 0.4 MPa, reaction temperature 50 °C.

### Influence of the reaction time

The influence of reaction time on the PC yield is shown in Fig. 2. The reaction was conducted at 50 °C and 0.4 MPa of total pressure. The yield of PC increased with increasing time at the beginning and approached 100% after a reaction time of 6 h.

### Effect of the reaction temperature

Fig. 3 shows the effect of the temperature on the cycloaddition reaction catalyzed by MOF-5 in the presence of *n*-Bu<sub>4</sub>NBr at 0.4 MPa in the temperature range of 30–70 °C, with a reaction time of 4 h. At a temperature higher than 60 °C, nearly all of the PO could be converted into PC. The yield of PC decreased with decreasing the temperature below 60 °C. The figure illustrates that the yield was 57% at 30 °C with a reaction time of 4 h. Our experiment also showed that the reaction could go to completion after 11 h at this temperature.



**Fig. 3** Effect of the reaction temperature on the PC yield. Reaction conditions: 20 mmol PO with 2.5 mol% *n*-Bu<sub>4</sub>NBr, 0.1 g MOF-5, total pressure 0.4 MPa, reaction time 4 h.

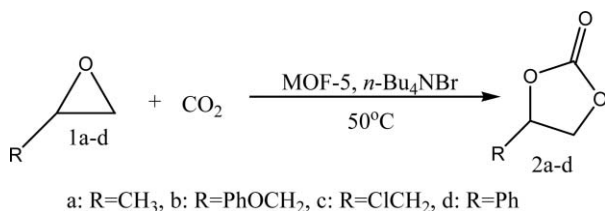
### Other substrates

The coupling reactions of CO<sub>2</sub> with different epoxides (Scheme 2) catalyzed by MOF-5/*n*-Bu<sub>4</sub>NBr were also studied, and the results are summarized in Table 2. The data in the table show that the catalytic system could convert all epoxides studied to the corresponding cyclic carbonates effectively under mild conditions. The reaction for **1b** was also conducted at 6 MPa because the reaction mixture became solid at 0.1 MPa after the

**Table 2** Various carbonates synthesis catalyzed by MOF-5 in the presence of *n*-Bu<sub>4</sub>NBr<sup>a</sup>

Entry	Epoxides	Products	Time/h	Yield (%)
1			3	56
2 <sup>b</sup>			4	97
3			12	93
4			15	92

<sup>a</sup> Reaction conditions: epoxide 20 mmol with 2.5 mol% *n*-Bu<sub>4</sub>NBr, 0.1 g MOF-5, CO<sub>2</sub> pressure 0.1 MPa, reaction temperature 50 °C. <sup>b</sup> CO<sub>2</sub> pressure 6 MPa.

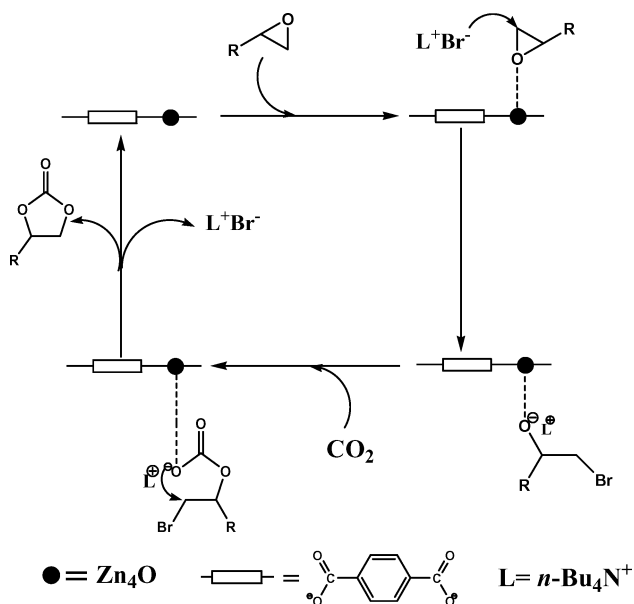


**Scheme 2** Coupling of CO<sub>2</sub> with different epoxides.

yield exceeded 56%. The reaction mixture was always liquid at 6 MPa because, as is well known, CO<sub>2</sub> can reduce the melting point of organic compounds.

### Reaction mechanism

We proposed a plausible mechanism for this chemical fixation reaction (Scheme 3), which is similar to that of the homogenous catalytic system with salenCo(III)X complexes as catalysts and quaternary ammonium salts as co-catalysts.<sup>14</sup> The coupling reaction is initiated by coordination of the Zn<sub>4</sub>O clusters in MOF-5 as a Lewis acidic site with the oxygen atom of the epoxide, and this step can activate the epoxy ring. Secondly, the Br<sup>-</sup> generated from *n*-Bu<sub>4</sub>NBr attacks the less-hindered carbon atom of the coordinated epoxides, followed by the ring opening step. Then, the oxygen anion of the opened epoxy ring interacts with the CO<sub>2</sub> and this can form an alkylcarbonate anion, which is converted into the corresponding cyclic carbonate through the ring closing step. Meanwhile, the catalyst is regenerated. The synergistic effect of MOF-5 and *n*-Bu<sub>4</sub>NBr is the main reason for the high catalytic activity of the catalyst system under mild conditions.



**Scheme 3** The plausible reaction mechanism for the cycloaddition of CO<sub>2</sub> with epoxides catalyzed by MOF-5 and *n*-Bu<sub>4</sub>NBr.

### Conclusions

We found that cyclic carbonates can be produced under mild conditions in high yield from the reaction of epoxides with

CO<sub>2</sub> in the presence of catalytic amounts of MOF-5 and *n*-Bu<sub>4</sub>NBr without using any organic solvent. In the MOF-5/*n*-Bu<sub>4</sub>NBr catalytic system, MOF-5 and *n*-Bu<sub>4</sub>NBr show excellent synergistic effect to catalyze the reactions. After easy separation, the MOF-5 can be reused and a decrease in activity and selectivity is not noticeable after being used three times. The greener, inexpensive, active, selective and stable catalytic system has potential applications for synthesizing cyclic carbonates from CO<sub>2</sub> and epoxides.

## Experimental

### Materials

CO<sub>2</sub> was supplied by Beijing Analytical Instrument Factory with a purity of 99.99%. Propylene oxide, epichlorohydrin, Zn(NO<sub>3</sub>)<sub>2</sub>·6H<sub>2</sub>O, *n*-Bu<sub>4</sub>NBr, Me<sub>4</sub>NCl and triethylamine were A. R. grade. Me<sub>4</sub>NBr, Et<sub>4</sub>NBr and benzene-1,4-dicarboxylic acid were C. P. grade. All the chemicals above were purchased from Beijing Chemical Reagents Company. *n*-Pr<sub>4</sub>NBr was A. R. grade and provided by Aldrich Chemical Company. Other epoxides were purchased from Acros Organics. All chemicals were used as received.

### Preparation and characterization of MOF-5

The procedure to prepare MOF-5 was similar to that reported previously.<sup>44</sup> Zn(NO<sub>3</sub>)<sub>2</sub>·6H<sub>2</sub>O (1.21 g, 4 mmol), benzene-1,4-dicarboxylic acid (0.32 g, 2 mmol) and 40 ml *N,N*-dimethylformamide were added into a 100 ml flask equipped with a magnetic stirrer. The flask was put into an oil bath at 60 °C. Then, triethylamine (1.6 g) was added into the mixture. The mixture was maintained at 60 °C for 4 h with stirring. The metal-organic frameworks (MOF-5) formed was collected by filtration and washed using *N,N*-dimethylformamide, and then was dried at 60 °C for 12 h under vacuum.

Thermogravimetric analysis of MOF-5 was performed on a NETZSCH STA 409 PC/PG thermogravimetric analysis system in N<sub>2</sub> atmosphere at a heating rate of 20 °C per min. The X-ray diffraction (XRD) patterns were collected on an X-ray diffractometer (D/MAX-RC) operated at 40 kV and 200 mA with Cu Kα radiation. FTIR spectra were obtained using a Bruker Tensor 27 spectrometer, and the sample was prepared by the KBr pellet method.

### Typical procedures for the cycloadditions

All the cycloaddition reactions were conducted in a 22 ml stainless steel reactor equipped with a magnetic stirrer. We describe the procedure for the cycloaddition of propylene oxide (PO) because the procedure for the reactions of other epoxides was similar. In the experiment, MOF-5 (0.1 g), PO (20 mmol) and desired amounts of quaternary ammonium salts were added into the reactor. After sealing, the reactor was put into a constant-temperature air bath at a desired temperature. CO<sub>2</sub> was then charged into the reactor until the desired pressure was reached, and the stirrer was started. After a certain time, the reactor was placed into ice water and CO<sub>2</sub> was released slowly passing through a cold trap containing ethyl acetate to absorb trace amounts of reactant and product entrained by CO<sub>2</sub>.

After depressurization, the ethyl acetate in the cold trap and the internal standard *n*-butanol were added into the reactor. The reaction mixture was analyzed by a GC spectrometer (Agilent 6820) equipped with a flame-ionized detector. The purity and structure of the product at some typical experimental conditions were also checked by <sup>1</sup>H NMR and GC-MS. The products of other epoxides were analyzed at room temperature on a Bruker 400 MHz <sup>1</sup>H NMR spectrometer using CDCl<sub>3</sub> as the solvent. In the experiments to test the reusability of MOF-5, the catalyst was recovered by centrifugation, washed using *N,N*-dimethylformamide and ethyl ether, respectively. After drying under vacuum for 12 h at 60 °C, the catalyst was reused for the next run with fresh *n*-Bu<sub>4</sub>NBr added into the system. Spectral characterizations of the products (**2b–d**) were obtained as follows:

**4-phenyloxymethyl-1,3-dioxolan-2-one (2b).** <sup>1</sup>H NMR (CDCl<sub>3</sub>, 400 MHz) δ (ppm) 4.16 (dd, *J* = 3.5, 10.5 Hz, 1H), 4.24 (dd, *J* = 4.4, 10.5 Hz, 1H), 4.54 (dd, *J* = 6.0, 8.4 Hz, 1H), 4.62 (t, *J* = 8.4 Hz, 1H), 5.00–5.05 (m, 1H), 6.91 (d, *J* = 8.4 Hz, 2H), 7.02 (t, *J* = 7.4 Hz, 1H), 7.31 (t, *J* = 8.2 Hz, 2H).

**4-chloromethyl-1,3-dioxolan-2-one (2c).** <sup>1</sup>H NMR (CDCl<sub>3</sub>, 400 MHz) δ (ppm) 3.75 (dd, *J* = 3.6, 12.3 Hz, 1H), 3.84 (dd, *J* = 4.9, 12.3 Hz, 1H), 4.42 (dd, *J* = 5.8, 8.8 Hz, 1H), 4.61 (t, *J* = 8.4 Hz, 1H), 5.00–5.06 (m, 1H).

**4-phenyl-1,3-dioxolan-2-one (2d).** <sup>1</sup>H NMR (CDCl<sub>3</sub>, 400 MHz) δ (ppm) 4.34 (t, *J* = 8.2 Hz, 1H), 4.80 (t, *J* = 8.4 Hz, 1H), 5.68 (t, *J* = 8.0 Hz, 1H), 7.35–7.45 (m, 5H).

## Acknowledgements

This work was supported by the National Key Basic Research Project of China (2006CB202504) and the Chinese Academy of Sciences (KJXC2.YWH16).

## Notes and references

- (a) T. Sakakura, J. C. Choi and H. Yasuda, *Chem. Rev.*, 2007, **107**, 2365; (b) K. M. K. Yu, C. M. Y. Yeung and S. C. Tsang, *J. Am. Chem. Soc.*, 2007, **129**, 6360; (c) P. G. Jessop, T. Ikariya and R. Noyori, *Chem. Rev.*, 1995, **95**, 259; (d) D. H. Gibson, *Chem. Rev.*, 1996, **96**, 2063; (e) T. Sakakura and K. Kohno, *Chem. Commun.*, 2009, 1312.
- (a) T. Sakakura, Y. Saito, M. Okano, J. C. Choi and T. Sako, *J. Org. Chem.*, 1998, **63**, 7095; (b) J. C. Choi, L. N. He, H. Yasuda and T. Sakakura, *Green Chem.*, 2002, **4**, 230; (c) J. S. Tian, C. X. Miao, J. Q. Wang, F. Cai, Y. Du, Y. Zhao and L. N. He, *Green Chem.*, 2007, **9**, 566.
- (a) M. Yoshida and M. Ihara, *Chem.–Eur. J.*, 2004, **10**, 2886; (b) T. Aida and S. Inoue, *J. Am. Chem. Soc.*, 1983, **105**, 1304; (c) H. S. Kim, J. J. Kim, B. G. Lee, O. S. Jung, H. G. Jang and S. O. Kang, *Angew. Chem., Int. Ed.*, 2000, **39**, 4096.
- (a) F. Shi, Y. Deng, T. SiMa, J. Peng, Y. Gu and B. Qiao, *Angew. Chem., Int. Ed.*, 2003, **42**, 3257; (b) T. Jiang, X. Ma, Y. Zhou, S. Liang, J. Zhang and B. Han, *Green Chem.*, 2008, **10**, 465.
- (a) M. Yoshida, N. Hara and S. Okuyama, *Chem. Commun.*, 2000, 151; (b) R. N. Salvatore, S. I. Shin, A. S. Nagle and K. W. Jung, *J. Org. Chem.*, 2001, **66**, 1035; (c) W. McGhee, D. Riley, K. Christ, Y. Pan and B. Parnas, *J. Org. Chem.*, 1995, **60**, 2820.
- (a) Z. Zhang, Y. Xie, W. Li, S. Hu, J. Song, T. Jiang and B. Han, *Angew. Chem., Int. Ed.*, 2008, **47**, 1127; (b) P. G. Jessop, T. Ikariya and R. Noyori, *Nature*, 1994, **368**, 231; (c) P. G. Jessop, Y. Hsiao, T. Ikariya and R. Noyori, *J. Am. Chem. Soc.*, 1996, **118**, 344; (d) Y. Himeda, N. Onozawa-Komatsuzaki, H. Sugihara and K. Kasuga, *J. Am. Chem. Soc.*, 2005, **127**, 13118.
- (a) S. Fukuoka, M. Kawamura, K. Komiya, M. Tojo, H. Hachiya, K. Hasegawa, M. Aminaka, H. Okamoto, I. Fukawa and S. Konno, *Green Chem.*, 2003, **5**, 497; (b) J. Bayardon, J. Holz, B. Schäffner, V. Andrushko, S. Verevkin, A. Preetz and A. Börner, *Angew. Chem., Int. Ed.*, 2007, **46**, 5971; (c) S. Fujita, B. M. Bhanage, H. Kanamaru and M. Arai, *J. Mol. Catal. A: Chem.*, 2005, **230**, 43.
- (a) V. Calò, A. Nacci, A. Monopoli and A. Fanizzi, *Org. Lett.*, 2002, **4**, 2561; (b) H. Yasuda, L. N. He, T. Sakakura and C. Hu, *J. Catal.*, 2005, **233**, 119.
- L. N. He, H. Yasuda and T. Sakakura, *Green Chem.*, 2003, **5**, 92.
- H. Kawanami, A. Sasaki, K. Matsui and Y. Ikushima, *Chem. Commun.*, 2003, 896.
- N. Kihara, N. Hara and T. Endo, *J. Org. Chem.*, 1993, **58**, 6198.
- Y. M. Shen, W.-L. Duan and M. Shi, *Eur. J. Org. Chem.*, 2004, 3080.
- R. L. Paddock and S. T. Nguyen, *J. Am. Chem. Soc.*, 2001, **123**, 11498.
- X. B. Lu, B. Liang, Y. J. Zhang, Y. Z. Tian, Y. M. Wang, C. X. Bai, H. Wang and R. Zhang, *J. Am. Chem. Soc.*, 2004, **126**, 3732.
- W. J. Kruper and D. V. Dellar, *J. Org. Chem.*, 1995, **60**, 725.
- (a) X. B. Lu, Y. J. Zhang, B. Liang, X. Li and H. Wang, *J. Mol. Catal. A: Chem.*, 2004, **210**, 31; (b) X. B. Lu, Y. J. Zhang, K. Jin, L. M. Luo and H. Wang, *J. Catal.*, 2004, **227**, 537.
- K. Yamaguchi, K. Ebitani, T. Yoshida, H. Yoshida and K. Kaneda, *J. Am. Chem. Soc.*, 1999, **121**, 4526.
- F. Shi, Q. Zhang, Y. Ma, Y. He and Y. Deng, *J. Am. Chem. Soc.*, 2005, **127**, 4182.
- Y. Xie, Z. Zhang, T. Jiang, J. He, B. Han, T. Wu and K. Ding, *Angew. Chem., Int. Ed.*, 2007, **46**, 7255.
- Y. Du, F. Cai, D. L. Kong and L. N. He, *Green Chem.*, 2005, **7**, 518.
- (a) J. Q. Wang, D. L. Kong, J. Y. Chen, F. Cai and L. N. He, *J. Mol. Catal. A: Chem.*, 2006, **249**, 143; (b) T. Takahashi, T. Watahiki, S. Kitazume, H. Yasuda and T. Sakakura, *Chem. Commun.*, 2006, 1664; (c) T. Sakai, Y. Tsutsumi and T. Ema, *Green Chem.*, 2008, **10**, 337.
- (a) B. Moulton and M. J. Zaworotko, *Chem. Rev.*, 2001, **101**, 1629; (b) S. Kitagawa, R. Kitaura and S. Noro, *Angew. Chem., Int. Ed.*, 2004, **43**, 2334; (c) Z. Wang and S. M. Cohen, *J. Am. Chem. Soc.*, 2007, **129**, 12368; (d) Y. F. Song and L. Cronin, *Angew. Chem., Int. Ed.*, 2008, **47**, 4635; (e) S. Natarajan and S. Mandal, *Angew. Chem., Int. Ed.*, 2008, **47**, 4798; (f) H. Li, M. Eddaoudi, M. O'Keefe and O. M. Yaghi, *Nature*, 1999, **402**, 276.
- (a) Y. Li and R. T. Yang, *Langmuir*, 2007, **23**, 12937; (b) R. E. Morris and P. S. Wheatley, *Angew. Chem., Int. Ed.*, 2008, **47**, 4966; (c) Y. Liu, J. F. Eubank, A. J. Cairns, J. Eckert, V. C. Kravtsov, R. Luebke and M. Eddaoudi, *Angew. Chem., Int. Ed.*, 2007, **46**, 3278; (d) C.-J. Li, Z.-J. Lin, M.-X. Peng, J.-D. Leng, M.-M. Yang and M.-L. Tong, *Chem. Commun.*, 2008, 6348.
- (a) B. Chen, C. Liang, J. Yang, D. S. Contreras, Y. L. Clancy, E. B. Lobkovsky, O. M. Yaghi and S. Dai, *Angew. Chem., Int. Ed.*, 2006, **45**, 1390; (b) P. K. Thallapally, J. Tian, M. R. Kishan, C. A. Fernandez, S. J. Dalgarno, P. B. McGrail, J. E. Warren and J. L. Atwood, *J. Am. Chem. Soc.*, 2008, **130**, 16842.
- O. Kahn, *Acc. Chem. Res.*, 2000, **33**, 647.
- B. Gómez-Lor, E. Gutiérrez-Puebla, M. Iglesias, M. A. Monge, C. Ruiz-Valero and N. Snejko, *Chem. Mater.*, 2005, **17**, 2568.
- S. Hasegawa, S. Horike, R. Matsuda, S. Furukawa, K. Mochizuki, Y. Kinoshita and S. Kitagawa, *J. Am. Chem. Soc.*, 2007, **129**, 2607.
- P. Horcajada, S. Surblé, C. Serre, D. Y. Hong, Y. K. Seo, J. S. Chang, J. M. Grenèche, I. Margiolaki and G. Férey, *Chem. Commun.*, 2007, 2820.
- S. Horike, M. Dincă, K. Tamaki and J. R. Long, *J. Am. Chem. Soc.*, 2008, **130**, 5854.
- O. Ohmori and M. Fujita, *Chem. Commun.*, 2004, 1586.
- L. Alaerts, E. Séguin, H. Poelman, F. Thibault-Starzyk, P. A. Jacobs and D. E. D. Vos, *Chem.–Eur. J.*, 2006, **12**, 7353.
- F. Gándara, B. Gomez-Lor, E. Gutiérrez-Puebla, M. Iglesias, M. A. Monge, D. M. Proserpio and N. Snejko, *Chem. Mater.*, 2008, **20**, 72.
- C. D. Wu, A. Hu, L. Zhang and W. Lin, *J. Am. Chem. Soc.*, 2005, **127**, 8940.
- F. X. L. i. Xamena, O. Casanova, R. G. Tailleux, H. Garcia and A. Corma, *J. Catal.*, 2008, **255**, 220.
- T. Dewa, T. Saiki and Y. Aoyama, *J. Am. Chem. Soc.*, 2001, **123**, 502.
- S. H. Cho, B. Ma, S. T. Nguyen, J. T. Hupp and T. E. Albrecht-Schmitt, *Chem. Commun.*, 2006, 2563.
- D. N. Dybtsev, A. L. Nuzhdin, H. Chun, K. P. Bryliakov, E. P. Talsi, V. P. Fedin and K. Kim, *Angew. Chem., Int. Ed.*, 2006, **45**, 916.

- 38 A. Hu, H. L. Ngo and W. Lin, *Angew. Chem., Int. Ed.*, 2003, **42**, 6000.
- 39 A. Hu, H. L. Ngo and W. Lin, *J. Am. Chem. Soc.*, 2003, **125**, 11490.
- 40 J. S. Seo, D. Whang, H. Lee, S. I. Jun, J. Oh, Y. J. Jeon and K. Kim, *Nature*, 2000, **404**, 982.
- 41 L. Pan, H. Liu, X. Lei, X. Huang, D. H. Olson, N. J. Turro and J. Li, *Angew. Chem., Int. Ed.*, 2003, **42**, 542.
- 42 M. Sabo, A. Henschel, H. Fröde, E. Klemm and S. Kaskel, *J. Mater. Chem.*, 2007, **17**, 3827.
- 43 M. Eddaoudi, J. Kim, N. Rosi, D. Vodak, J. Wachter, M. O'Keeffe and O. M. Yaghi, *Science*, 2002, **295**, 469.
- 44 L. Huang, H. Wang, J. Chen, Z. Wang, J. Sun, D. Zhao and Y. Yan, *Microporous Mesoporous Mater.*, 2003, **58**, 105.
- 45 L. F. Xiao, F. W. Li and C. G. Xia, *Appl. Catal., A*, 2005, **279**, 125.
- 46 J. Sun, S. I. Fujita, F. Zhao and M. Arai, *Appl. Catal., A*, 2005, **287**, 221.
- 47 P. B. Webb, M. F. Sellin, T. E. Kunene, S. Williamson, A. M. Z. Slawin and D. J. Cole-Hamilton, *J. Am. Chem. Soc.*, 2003, **125**, 15577.
- 48 H. F. Zhang, B. X. Han, Z. S. Hou and Z. M. Liu, *Fluid Phase Equilib.*, 2001, **179**, 131.

# Solvent-free selective epoxidation of cyclooctene using supported gold catalysts

Salem Bawaked,<sup>a</sup> Nicholas F. Dummer,<sup>a</sup> Nikolaos Dimitratos,<sup>a</sup> Donald Bethell,<sup>a</sup> Qian He,<sup>b</sup> Christopher J. Kiely<sup>b</sup> and Graham J. Hutchings<sup>\*a</sup>

Received 24th December 2008, Accepted 14th April 2009

First published as an Advance Article on the web 28th April 2009

DOI: 10.1039/b823286p

Oxidation is one of the major pathways for the synthesis of chemical intermediates. The epoxidation of alkenes by the electrophilic addition of oxygen to a carbon–carbon double bond remains one of the most significant challenges in oxidation. Of key importance is the use of oxygen as the oxidant, but in many cases more reactive, and less green, sources of oxygen are used. We report the solvent-free epoxidation of cyclooctene with air using supported gold catalysts with small amounts of a hydroperoxide. We identify the appropriate reaction conditions to maximize the selectivity of the epoxide. In the absence of a hydroperoxide initiator, using air at atmospheric pressure, no reaction is observed. Choice of the peroxide initiator is crucial and in the absence of a catalyst or a support the reaction of the alkene can be observed with di-*t*-butyl peroxide and *t*-butyl hydroperoxide (TBHP) only when high concentrations are used at high temperatures  $\geq 80$  °C, and TBHP was found to be the more selective to epoxide formation. In contrast, cumene hydroperoxide was highly reactive under all conditions evaluated. TBHP was selected for more detailed study. Use of graphite as a support was found to give the best combination of selectivity and conversion. In general the selectivity to the epoxide increased with reaction temperature from 60–80 °C and was highest at 80 °C. Other carbon supports, *e.g.* activated carbon, were found to be less effective. TiO<sub>2</sub>- and SiO<sub>2</sub>-supported Au catalysts were also selective for the epoxidation reaction and the general order of activity was: graphite > SiO<sub>2</sub> > TiO<sub>2</sub>. The major by-product is the allylic alcohol and the reaction pathways to the epoxides and the allylic alcohol are discussed. Preparation of catalysts using a sol-immobilisation method significantly enhanced catalyst activity with retention of selectivity to the epoxide.

## Introduction

The synthesis of chemical intermediates using selective oxidation includes reactions of major significance in the chemical processing industry. Invariably oxygen from the air is considered to be the oxidant of choice and represents the greenest choice. However, in many cases more active forms of oxygen have to be used, including non-green stoichiometric oxygen donors such as permanganate and chromates.<sup>1</sup> One of the greatest challenges in selective oxidation chemistry is the electrophilic addition of oxygen to an alkene to form an epoxide. For the simplest case, ethene, this is a reaction that can be carried out commercially on a very large scale and with very high specificity using oxygen with a supported silver catalyst.<sup>2</sup> However, even in this case non-green additives, *i.e.* chloro-compounds and NO<sub>x</sub> have to be added to limit non-selective oxidation. At present, the epoxidation of higher alkenes with oxygen has not proved to be successful on a commercial basis, and remains the subject

of great research interest. Propene can be efficiently epoxidised using hydrogen peroxide as an activated form of oxygen using the titanium silicalite TS-1 as catalyst.<sup>3</sup> Whilst hydrogen peroxide is considered to be a green oxidant, the use of oxygen in the form of air would be preferable.

Recently, Rossi *et al.*<sup>4</sup> have reviewed the key aspects concerning selective oxidation reactions, and, in particular, the recent advances that have been made using supported gold catalysts. Haruta *et al.* were the first to demonstrate the potential of supported gold catalysts for the epoxidation of propene with oxygen in the presence of H<sub>2</sub> as a sacrificial reductant that permits the activation of O<sub>2</sub> at relatively low temperatures.<sup>5,6</sup> Haruta *et al.* found that Au/TiO<sub>2</sub>, prepared using deposition precipitation, was selective for propene epoxidation and the catalysis was associated with an intimate contact between hemispherical gold nano-crystals (2–5 nm in diameter) and the TiO<sub>2</sub> support. Initial selectivities were low but promising and improvements were made by using different titanium-containing supports including TS-1, Ti-zeolite  $\beta$ , Ti-MCM-41 and Ti-MCM-48.<sup>7–20</sup> A key issue that remains with this experimental approach is the selectivity based on H<sub>2</sub>, which can be very low. Haruta *et al.* have tried to address the issue of poor H<sub>2</sub> utilisation and have shown that, using mesoporous titanosilicates as a support,<sup>21</sup> improved H<sub>2</sub> consumption was attained together

<sup>a</sup>Cardiff University, School of Chemistry, Main Building, Park Place, Cardiff, UK CF10 3AT. E-mail: hutch@cardiff.ac.uk; Fax: +44 29 2087 4059; Tel: +44 29 2087 4059

<sup>b</sup>Center for Advanced Materials and Nanotechnology, Lehigh University, 5 East Packer Avenue, Bethlehem, PA 18015-3195, USA



with high propene oxide yields ( $93 \text{ g h}^{-1} \text{ kg}_{\text{cat}}^{-1}$  at  $160 \text{ }^\circ\text{C}$ ). Propene oxide selectivities of  $>90\%$  were observed at propene conversions of *ca.*  $7\%$ , together with a hydrogen efficiency of  $40\%$ .<sup>17</sup> However, this  $\text{H}_2$  efficiency is far lower than currently achievable (*ca.*  $\geq 95\%$ ) with indirect  $\text{H}_2\text{O}_2$  synthesis<sup>22</sup> and so this approach cannot compete with the TS-1 catalysed epoxidation of propene using  $\text{H}_2\text{O}_2$ .<sup>3</sup>

Choudhary *et al.*,<sup>23–27</sup> and subsequently Yin *et al.*<sup>28</sup> have shown that gold nanoparticles supported on a range of oxides are active for the epoxidation of styrene using tertiary butylhydroperoxide (TBHP) in greater than stoichiometric amounts. Selectivities to styrene oxide of *ca.*  $50\%$  are readily achieved using this approach.

In our initial studies we showed that graphite-supported gold nanoparticles could selectively epoxidise a range of alkenes using oxygen as an oxidant if catalytic amounts of TBHP or  $\text{H}_2\text{O}_2$  were added.<sup>29</sup> We showed that for the oxidation of cyclooctene using mild solvent-free conditions selectivities of over  $80\%$  to the epoxide could be achieved. We also showed that the peroxy initiator was not required to achieve selective oxidation but that lower selectivities to the epoxides were observed in their absence. In addition we indicated that when the peroxy initiator was present in the absence of the catalyst, or in the presence of the graphite support some reactivity of the alkene was observed, but that it was not selective to the epoxide. This effect is presumably due to molecular oxygen being a di-radical in its ground state and so can participate in radical reactions without the need for activation at the catalyst surface. Subsequently, Caps *et al.*<sup>30–32</sup> have studied this experimental approach in detail for the oxidation of stilbene, for which they have proposed a radical mechanism. This mechanism is consistent with the initial observation that catalytic amounts of a peroxy species were required to observe selective epoxidation.<sup>29</sup> Deng and Friend<sup>33</sup> showed using model studies with a Au (111) surface that styrene could be directly epoxidised with oxygen giving  $53\%$  styrene oxide. Most recently, Lambert *et al.*<sup>34</sup> have shown that very small  $\text{Au}_{55}$  nanocrystals supported on carbon are active catalysts for styrene oxidation with oxygen but only minor selectivity to the epoxides was observed and the major product was benzaldehyde. In this paper we extend our initial studies<sup>29</sup> to determine the reaction conditions that are optimal for the selective epoxidation of cyclooctene using oxygen together with catalytic amounts of a peroxy initiator.

## Experimental

### Catalyst preparation

Unless otherwise stated, catalysts ( $1 \text{ wt}\%$  Au/support) were prepared using the following standard deposition precipitation method (denoted DP). A solution of  $\text{HAuCl}_4 \cdot 3\text{H}_2\text{O}$  ( $5 \text{ ml}$ ,  $2 \text{ g}$  in  $100 \text{ ml}$  distilled water) was diluted with water ( $45 \text{ ml}$ ). Aqueous sodium carbonate was added with stirring until  $\text{pH} = 10$  was attained. This solution was then added, with continuous stirring, to a slurry of the support in water ( $4.95 \text{ g}$  in water  $50 \text{ ml}$ ). The mixture was stirred for  $1 \text{ h}$  at  $20 \text{ }^\circ\text{C}$ , maintaining the  $\text{pH}$  at  $10$ . The mixture was heated to  $70 \text{ }^\circ\text{C}$  and formaldehyde was added as a reducing agent. The solid was recovered by filtration and washed with water ( $1 \text{ l}$ ) until the washings were found to be chloride free. The catalyst was dried ( $110 \text{ }^\circ\text{C}$ ,  $16 \text{ h}$ ) prior to use.

Two other preparation methods were also evaluated. For the impregnation method the support was suspended in distilled water ( $4.95 \text{ g}$  in  $100 \text{ ml}$ ) for  $15 \text{ min}$ . A solution of  $\text{HAuCl}_4 \cdot 3\text{H}_2\text{O}$  ( $5 \text{ ml}$ ,  $2 \text{ g}$  in  $100 \text{ ml}$  distilled water) was added to the slurry slowly dropwise over  $30 \text{ min}$ . The mixture was stirred under reflux for  $30 \text{ min}$ ; after cooling, formaldehyde was added as a reducing agent. The solid was recovered by filtration and washed with water ( $1 \text{ l}$ ) until the washings were found to be chloride free. The catalyst was dried ( $110 \text{ }^\circ\text{C}$ ,  $16 \text{ h}$ ) prior to use.

For the sol-immobilization method an aqueous solution of  $\text{HAuCl}_4 \cdot 3\text{H}_2\text{O}$  was prepared. Polyvinylalcohol (PVA) ( $1 \text{ wt}\%$  solution, Aldrich,  $\text{MW} = 10\,000$ ,  $80\%$  hydrolyzed) was added (PVA/Au (by wt) =  $0.65$ ); a freshly prepared solution of  $\text{NaBH}_4$  ( $0.1 \text{ M}$ , Aldrich,  $\text{NaBH}_4/\text{Au}$  (mol/mol) =  $5$ ) was then added to form a dark-brown sol. After  $30 \text{ min}$ , the colloid that had been generated was immobilized by adding the support (acidified at  $\text{pH} 1$  by sulfuric acid) with stirring. The amount of support material required was calculated so as to have a total final metal loading of  $1 \text{ wt}\%$ . After  $2 \text{ h}$  the slurry was filtered, the catalyst washed thoroughly with distilled water ( $1 \text{ l}$ ). The catalyst was dried ( $110 \text{ }^\circ\text{C}$ ,  $16 \text{ h}$ ) prior to use.

### Catalyst testing and characterisation

All reactions were performed in a stirred glass round bottom flask ( $50 \text{ ml}$ ) fitted with a reflux condenser and heated in an oil bath. Typically, *cis*-cyclooctene ( $10 \text{ ml}$ ) was stirred at the desired temperature. Then the radical initiator was added followed by the catalyst ( $0.12 \text{ g}$ ) and the reactions were typically carried out for  $24 \text{ h}$ . Analysis was carried out using a gas chromatography (Varian star 3400 CX) with DB-5 column and a flame ionization detector. As conversions were low and the reaction was carried out using solvent-free conditions, alkene conversion was determined on the basis of the concentrations of the observed products, and no  $\text{CO}_x$  was observed. Experiments were carried out in triplicate and the experimental variation was determined to be  $\leq 1\%$ , and mass balances were typically  $100\%$  within experimental error. Further experiments were conducted to determine the amount of cyclooctene hydroperoxides since these products are not detected by the standard gas chromatography analysis. Standard reactions ( $24 \text{ h}$  and  $72 \text{ h}$ ) using  $1\%$  Au/graphite prepared by deposition precipitation were carried out and after completion the reaction mixture was filtered and then divided into two aliquots; the first aliquot was stirred for  $1 \text{ h}$  with excess triphenylphosphine ( $\text{PPh}_3$ ) in air at room temperature, the second aliquot was not treated with  $\text{PPh}_3$ . All samples were analysed by GC (FID, DB-wax column, Varian 3400).  $^1\text{H}$  NMR spectroscopy (Bruker DPX 400 spectrometer) was used to confirm the presence of cyclooct-2-enyl hydroperoxide.

Samples for examination by transmission electron microscopy (TEM) were prepared by dispersing the catalyst powder in high purity ethanol, then allowing a drop of the suspension to evaporate on a holey carbon film supported by a lacey carbon TEM grid. Samples were then subjected to bright field diffraction contrast imaging experiments in order to determine particle size distributions. The instrument used for this analysis was a JEOL 2000FX TEM operating at  $200 \text{ kV}$ .

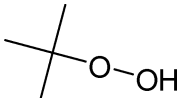
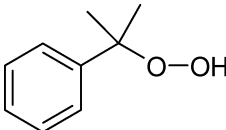
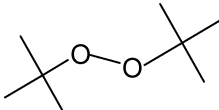
## Results and discussion

### Reaction in the absence of catalyst

Since we are seeking to oxidise cyclooctene with molecular oxygen it is important we determine the reactions that occur in the absence of catalyst. As we noted in our earlier research<sup>29</sup> we observed some non-selective conversion of cyclooctene in the absence of catalyst. Since molecular oxygen is a diradical in its ground state it can participate in radical reactions in the absence of a catalyst, especially in the presence of radical initiators. These non-catalysed reactions can often lead to lower selectivities being achieved and can, in the extreme cases, mask any catalytic reaction that may be occurring. Hence, we need to determine reaction conditions where no reaction occurs either in the absence of the catalyst or the undoped support. The reactivity of the supports will be considered alongside the data for the catalysts in subsequent sections. In the absence of a peroxy initiator and in the absence of a catalyst no reaction was observed over the temperature range we have studied in this paper. We then investigated the effect of the peroxy species. Three peroxy initiators were investigated at 80 °C with alkene/peroxy mol ratios between 74.6 and 748, and the results are shown in Table 1. Cumene hydroperoxide (CHP) is active

at all the concentrations evaluated and gave the epoxide with *ca.* 64–70% selectivity. TBHP and di-*t*-butyl peroxide (DTBP) were inactive at the lowest concentration evaluated, but were active at higher concentrations, but TBHP was more selective. Of the peroxides examined, CHP has the lowest reported<sup>35</sup> activation energy for homolysis of the O–O bond (126 kJ mol<sup>-1</sup> in benzene solvent) and is probably the most susceptible to radical-induced decomposition. DTBP is reported to have a shorter half-life at low concentrations, although it has a higher  $E_a = 162$  kJ mol<sup>-1</sup>. TBHP homolyses the least rapidly of the three ( $E_a = 134$  kJ mol<sup>-1</sup>). All three have 10 h half-lives at temperatures above that of the present experiments (TBHP 170 °C, CHP 135 °C, DTBP 125 °C), suggesting that, at least in part, the uncatalysed reaction may not require simple homolysis for initiation. TBHP was selected for more detailed evaluation (Table 2). At low concentrations of TBHP, even at 80 °C, no reaction is observed and consequently a concentration of  $1.03 \times 10^{-4}$  mol l<sup>-1</sup> TBHP was selected as the standard concentration for the subsequent studies. At higher concentrations a trace of reaction was observed at 60 °C, but no epoxide was formed, and the reactivity and selectivity to the epoxides increased with reaction temperature and with increasing initial peroxide concentration.

**Table 1** Reaction of cyclooctene using different peroxide initiators

Peroxy initiator/mol	Blank reaction <sup>a</sup>		1% Au/graphite <sup>b</sup>	
	Conversion (%)	Selectivity (%)	Conversion (%)	Selectivity (%)
	$0.1032 \times 10^{-2}$	0.68	66.8	8.5
	$0.0516 \times 10^{-2}$	0.12	36.9	6.6
	$0.0103 \times 10^{-2}$	0.02	0	4.0
	$0.1032 \times 10^{-2}$	7.0	68.9	8.1
	$0.0516 \times 10^{-2}$	3.92	69.8	5.8
	$0.0103 \times 10^{-2}$	1.3	64.1	2.9
	$0.1032 \times 10^{-2}$	0.91	36.9	0.53
	$0.0516 \times 10^{-2}$	0.27	8.0	0.26
	$0.0103 \times 10^{-2}$	0.04	0	0.04

<sup>a</sup> Reaction in the absence of catalyst: cyclooctene (10 ml, 0.077 mol), 80 °C, 24 h, atmospheric pressure. <sup>b</sup> Reaction using 1% Au/graphite: cyclooctene (10 ml, 0.077 mol), catalyst (0.12 g), 80 °C, 24 h, atmospheric pressure.

**Table 2** Effect of reaction of cyclooctene with TBHP in the absence of catalyst<sup>a</sup>

TBHP/Mol $\times 10^{-2}$	60 °C		70 °C		80 °C	
	Conversion (%)	Selectivity (%)	Conversion (%)	Selectivity (%)	Conversion (%)	Selectivity (%)
0.103	0.04	0	0.11	16.1	0.68	66.8
0.083	0.03	0	0.05	0	0.17	59.5
0.052	0.03	0	0.04	0	0.12	36.9
0.031	0.03	0	0.04	0	0.04	58.3
0.026	0.03	0	0.04	0	0.09	4.3
0.012	0	0	0.02	0	0.04	0
0.0103	0	0	0.02	0	0.04	0

<sup>a</sup> Reaction conditions: cyclooctene (10 ml, 0.077 mol), 24 h, atmospheric pressure.

**Table 3** Reaction using graphite as a support

TBHP/mol $\times 10^{-2}$	Temperature/ $^{\circ}\text{C}$	Graphite <sup>a</sup>		1% Au/graphite <sup>b</sup>	
		Conversion (%)	Selectivity (%)	Conversion (%)	Selectivity (%)
0.1032	60	0.40	58.4	1.9	68.3
0.0516		0.16	30.7	1.6	64.2
0.0103		0.01	0.01	0.6	63.9
0.1032	70	0.90	63.2	3.9	71.4
0.0516		0.36	64.5	2.6	72.3
0.0103		0.04	86.4	1.9	72.3
0.1032	80	4.46	74.2	8.5	78.7
0.0516		1.79	62.6	6.6	78.7
0.0103		0.1	42.6	4.0	78.2
0.1032	100	12.91	79.1	12.9	73.2
0.0516		9.91	78.8	11.1	76.1
0.0103		3.3	80.5	10.9	79.7
0.1032	120	16.41	77.1	13.4	71.4
0.0516		14.21	77.7	14.0	72.8
0.0103		13.88	77.3	14.6	73.6

<sup>a</sup> Reaction using graphite: cyclooctene (10 ml, 0.077 mol), catalyst (0.12 g), 80  $^{\circ}\text{C}$ , 24 h, atmospheric pressure. <sup>b</sup> Reaction using 1% Au/graphite: cyclooctene (10 ml, 0.077 mol), catalyst (0.12 g), 80  $^{\circ}\text{C}$ , 24 h, atmospheric pressure.

### Oxidation of cyclooctene using carbon-supported catalysts

**Graphite.** In our initial studies<sup>29</sup> we showed that 1 wt% Au/graphite was a very effective catalyst for the oxidation of cyclooctene at 80  $^{\circ}\text{C}$ . In addition, we showed that graphite also displayed some non-selective oxidation activity at this temperature. In view of this we now extend these studies to compare the catalytic and blank reactions to determine the optimal reaction conditions. We initially prepared the catalyst using an impregnation method coupled with a reduction step using formaldehyde. In this study we have used a modified technique designed by Prati and Rossi<sup>36</sup> to prepare the Au/graphite catalyst as they have shown the method to provide a robust recyclable catalyst for alcohol oxidation.

Our initial experiments were carried out to study the effect of different concentrations of TBHP using graphite and 1 wt% Au/graphite (Table 3). As noted by us previously,<sup>29</sup> the graphite support does show some catalytic activity, particularly at higher temperatures and higher concentrations of TBHP. Indeed at reaction temperatures  $\geq 100$   $^{\circ}\text{C}$  the support is as active as the gold catalyst (table 3) and shows the highest selectivity to the epoxide. However, at lower temperatures the 1 wt% Au/graphite is significantly more active and in the presence of gold the selectivity to the epoxides is greatly enhanced and, importantly, is independent of the TBHP concentration.

The effect of reaction time for the reactivity of 1 wt% Au/graphite is compared with the reactivity of the graphite support in Fig. 1 using the optimal conditions for epoxide formation that give a compromise between rate of reaction and selectivity ( $1.03 \times 10^{-4}$  mol TBHP, 80  $^{\circ}\text{C}$ ). Under these conditions the contribution to the reaction observed from the support or the non-catalysed reaction is minimized. The selectivity to the epoxide remains steady at *ca.* 80% throughout the reaction time and the major by-products are the allylic alcohol and cyclooctenone, which are formed throughout in approximately 2 : 1 molar ratio, which is consistent with our earlier study.<sup>29</sup> In addition traces of the dione are produced as we also observed in our earlier study.<sup>29</sup> Under these reaction conditions, after

24 h we observe a turnover frequency of 25 mol epoxide mol Au<sup>-1</sup> h<sup>-1</sup> which is comparable to that reported previously for the epoxidation of propene using Au/TiO<sub>2</sub> catalysts when H<sub>2</sub> is used as sacrificial reductant.<sup>7-20</sup> The turnover frequency for the TBHP is *ca.* 35. This is in contrast to earlier studies which used greater than stoichiometric amounts of TBHP which also gave lower epoxide selectivity.<sup>23-28</sup>

**Activated carbon.** We examined the reactivity of a range of different activated carbon supports manufactured from wood, coconut shell and coal. Activated carbons are widely used as supports and hence we contrasted their reactivity with that of graphite and the results are shown in Table 4 and 5. In general the activated carbons prepared from coal were the most selective for epoxide formation (Table 4). However, the addition of gold was not observed to enhance the catalytic activity under any conditions evaluated (Table 5) and in some cases the addition of gold led to a decreased activity (Table 4), although the presence of Au did lead to slightly higher epoxide selectivity. For the most active activated carbon support derived from wood (Aldrich G60) epoxidation of cyclooctene was observed at temperatures as low as 40  $^{\circ}\text{C}$  even with very low concentrations of TBHP. The heterogeneous nature of the functional groups present on the surface of the activated carbons provide a diverse set of sites that are capable of initiating the reaction with TBHP. Decoration of these sites by nanoparticles of gold can block this reactivity. Hence for the epoxidation of alkenes graphite is the preferred carbon support.

### Oxidation of cyclooctene using oxide-supported catalysts

The use of TiO<sub>2</sub> and SiO<sub>2</sub> as supports has also been investigated and the results for the effect of reaction temperature and concentration of TBHP are shown in Tables 6 and 7. Both oxide supports, in the absence of gold, show very limited activity with low concentrations of TBHP. The TiO<sub>2</sub>-supported gold catalysts display higher activity and epoxide selectivity than SiO<sub>2</sub>-supported catalysts which is consistent with earlier

**Table 4** Reaction using a range of activated carbon as a support

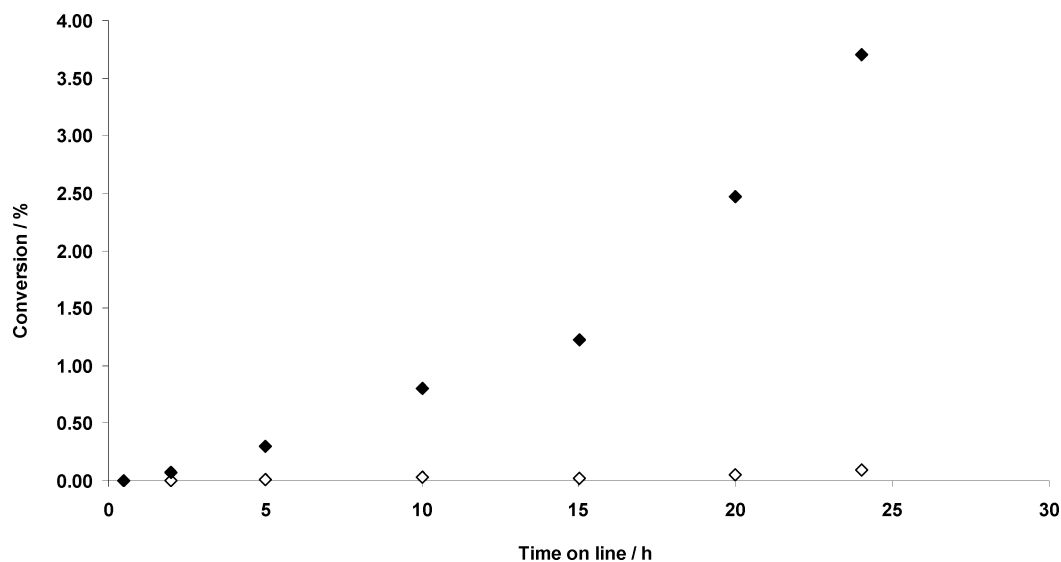
Carbon	Source	Conversion <sup>a</sup> (%)	Selectivity (%)
Aldrich G60	Wood	1.6	69.3
1 wt% Au/Aldrich G60	Wood	1.6	69.3
Norit Rox 0.8	Wood	0.1	59.4
1 wt% Au/Norit Rox 0.8	Wood	0.06	65.5
Norit GCN-3070	Coconut shell	0.01	—
1 wt% Au/Norit GCN-3070	Coconut shell	0.01	32.9
Norit PDKA 10 × 30	Coal	0.6	82.7
1 wt% Au/Norit PDKA 10 × 30	Coal	0.2	67.6

<sup>a</sup> Reaction conditions : cyclooctene (10 ml, 0.077 mol), catalyst/carbon (0.12 g), 80 °C, 24 h, atmospheric pressure, TBHP (0.1 mmol).

**Table 5** Reaction using activated carbon as a support

TBHP/mol × 10 <sup>-2</sup>	Temperature/°C	Activated carbon <sup>a</sup>		1% Au/activated carbon <sup>b</sup>	
		Conversion (%)	Selectivity (%)	Conversion (%)	Selectivity (%)
0.0103	50	0.4	62.4	0.4	58.7
0.0516	60	1.7	63.6	1.9	63.4
0.0258		1.5	63.2	1.5	66.4
0.0103		1.2	66.9	0.8	58.8
0.0516	70	2.9	63.5	2.9	70.5

<sup>a</sup> Reaction using activated carbon: cyclooctene (10 ml, 0.077 mol), carbon (0.12 g), 80 °C, 24 h, atmospheric pressure. <sup>b</sup> Reaction using 1% Au/activated carbon: cyclooctene (10 ml, 0.077 mol), catalyst (0.12 g), 80 °C, 24 h, atmospheric pressure.



**Fig. 1** Effect of reaction time for the conversion of cyclooctene using 1% Au/graphite (closed symbol) and graphite (open symbol). Reaction conditions: catalyst/graphite 0.12 g, cyclooctene (10 ml, 0.077 mol), TBHP 0.01 ml, temperature 80 °C, atmospheric pressure.

observations with propene epoxidation.<sup>7-23</sup> In a further set of experiments we investigated the use of Al<sub>2</sub>O<sub>3</sub> as a support which under standard reaction conditions (cyclooctene (0.077 mol), catalyst/support (0.12 g), 80 °C, 24 h, TBHP (0.1 mmol)) gave no conversion for the support, and with 1 wt% Au only gave 0.5% conversion, and the epoxide selectivity was >90%. However, in general, the oxide supports are less effective than graphite as a support for the epoxidation of cyclooctene.

#### Effect of the preparation method

In a final set of experiments we prepared 1 wt% Au graphite-catalysts using three different preparation methods (Table 8). In

our earlier studies we used a formaldehyde reduction method using an impregnation procedure (designated impregnation).<sup>29</sup> In this paper we have used a variant on this procedure in which the gold was deposited onto the support by precipitation with aqueous sodium carbonate prior to addition of the support<sup>35</sup> (designated DP). In addition, we have recently shown that a sol-immobilisation method<sup>37</sup> can be very effective for the preparation of active gold catalysts. We have now compared these three methods for the epoxidation of cyclooctene. The three 1 wt% Au/graphite catalysts have been characterized using transmission electron microscopy and the micrographs and particle size distributions are given in Fig. 2. The particle size

**Table 6** Reaction of cyclooctene with TiO<sub>2</sub> and TiO<sub>2</sub>-supported catalysts

TBHP/mol × 10 <sup>-2</sup>	Temperature/°C	TiO <sub>2</sub> <sup>a</sup>		1% Au/TiO <sub>2</sub> <sup>b</sup>	
		Conversion	Selectivity	Conversion	Selectivity
0.1032	60	1.1	65.7	1.8	67.7
0.0516		0.8	71.2	1.3	69.1
0.0103		0.3	85.6	0.9	71.6
0.1032	70	1.7	78.7	3.8	73.4
0.0516		1	77.0	3.0	64.9
0.0103		0.13	75.2	2.0	75.4
0.1032	80	4.96	80.4	8.8	77.7
0.0516		2.29	83.1	6.3	79.0
0.0103		0.07	78.8	0.3	78.3

<sup>a</sup> Reaction using TiO<sub>2</sub>: cyclooctene (10 ml, 0.077 mol), catalyst (0.12 g), 80 °C, 24 h, atmospheric pressure. <sup>b</sup> Reaction using 1% Au/TiO<sub>2</sub>: cyclooctene (10 ml, 0.077 mol), catalyst (0.12 g), 80 °C, 24 h, atmospheric pressure.

**Table 7** Reaction of cyclooctene with SiO<sub>2</sub> and SiO<sub>2</sub>-supported catalysts

TBHP/mol × 10 <sup>-2</sup>	Temperature/°C	SiO <sub>2</sub> <sup>a</sup>		1% Au/SiO <sub>2</sub> <sup>b</sup>	
		Conversion	Selectivity	Conversion	Selectivity
0.1032	60	0.4	64.5	0.9	64.8
0.0516		0.4	67.8	0.7	66.7
0.0103		0.1	0.1	0.4	67.8
0.1032	70	0.9	70.8	1.8	80.3
0.0516		0.3	74.5	1.3	81.1
0.0103		0.1	75.4	0.9	75.0
0.1032	80	4.5	74.5	6.0	80.2
0.0516		2.0	77.1	4.0	83.8
0.0103		0.1	0.1	2.7	79.7

<sup>a</sup> Reaction using SiO<sub>2</sub>: cyclooctene (10 ml, 0.077 mol), catalyst (0.12 g), 80 °C, 24 h, atmospheric pressure. <sup>b</sup> Reaction using 1% Au/SiO<sub>2</sub>: cyclooctene (10 ml, 0.077 mol), catalyst (0.12 g), 80 °C, 24 h, atmospheric pressure.

**Table 8** Reaction of cyclooctene with graphite- and TiO<sub>2</sub>-supported catalysts prepared using different methods

Preparation method	1% Au/graphite <sup>a</sup>	
	Conversion	Selectivity
Deposition precipitation	4.0	78.2
Sol-immobilization	7.7	81.5
Impregnation	4.2	71.3

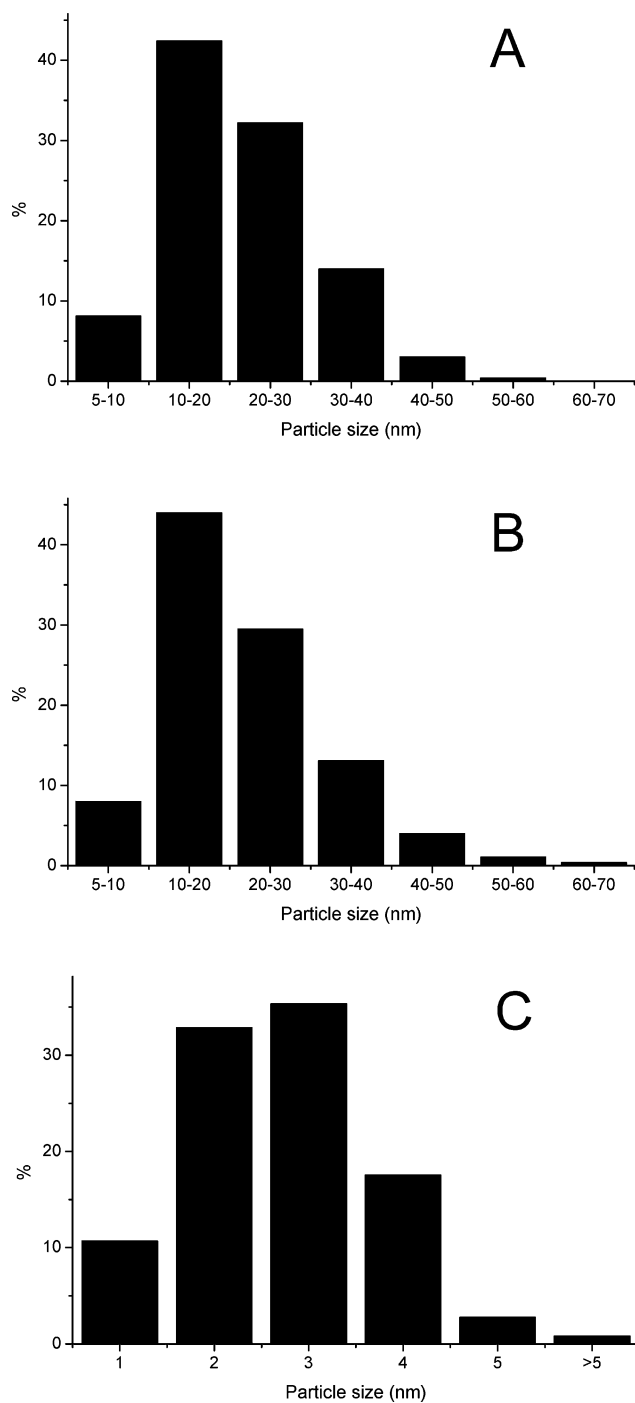
<sup>a</sup> Reaction condition: cyclooctene (10 ml, 0.077 mol), catalyst (0.12 g), 80 °C, 24 h, atmospheric pressure.

distributions for the impregnation and deposition precipitation methods are very similar, with most Au nanoparticles being in the 10–30 nm size range. This is in agreement with the activity of these two catalysts (Table 8) which are also very similar. In contrast, the particle size distribution of the 1 wt% Au/graphite catalyst prepared using the sol-immobilisation method shows this comprises much smaller particles, with most particles being 2–3 nm in diameter. This catalyst is more active for the epoxidation of cyclooctene (Table 8). With the 1 wt% Au/graphite catalyst prepared by sol-immobilisation, using our standard reaction conditions (1.03 × 10<sup>-4</sup> mol TBHP, 80 °C), after 24 h we observe a turnover frequency of 48 mol epoxide mol Au<sup>-1</sup> h<sup>-1</sup> which is higher than that reported previously for the epoxidation of propene<sup>7–23</sup> and the turnover frequency for the TBHP is enhanced to *ca.* 67. These results show that by careful

investigation of catalyst design further significant improvements in selectivity can be expected.

### Comments on the reaction mechanism

With respect to the peroxy initiators we have selected for study, TBHP is the only peroxide that shows strong enhancement in the presence of Au/graphite catalyst. CHP is susceptible to radical induced decomposition and its epoxidation performance is improved only slightly by the Au catalyst. DTBP shows no enhancement by the Au, suggesting that *t*-Bu-O radicals are not significant in the catalytic reaction pathway. We suggest that the uncatalysed epoxidation may not be a conventional radical chain reaction but seems to be a higher temperature analogue of epoxidation by peroxy-carboxylic acids. In particular, we observe that the selectivity to epoxide increases with TBHP concentration in the uncatalysed reaction but is constant in the catalysed process. If the uncatalysed peroxide were generating a reactive free radical species capable in part of O-transfer to the alkene, its partitioning between the various pathways should be roughly independent of peroxide concentration. In particular, the competition between epoxidation and allylic oxidation should be independent of TBHP concentration. This is not observed (Table 3) and we consider this to suggest that there is a direct O-transfer between the hydroperoxide and the alkene at temperatures below that necessary for homolysis of the O–O linkage.



**Fig. 2** Particle size distribution data, as determined from bright field TEM micrographs for the 1 wt% Au/graphite catalysts prepared by (A) impregnation, (B) deposition precipitation and (E) sol-immobilisation.

With Au, hydroperoxides seem necessary and that suggests to us that a surface O-species may be produced that is capable of O-transfer, either to an adsorbed alkene or an alkene in the liquid phase. With the Au-catalysed reaction we observe that the ratio between the epoxide and the byproducts remain constant as the conversion increases. This constant product ratio might come from parallel pathways but could equally arise by partitioning of an intermediate species on the catalyst surface that is partitioned between attacking cyclo-octene at its double bond or its two allylic positions. Abstraction of H from the allylic positions would allow formation of the allylic hydroperoxide, by incorporating O<sub>2</sub>, which could either eliminate water to give the enone or get involved in the catalytic cycle, in the same role as TBHP, to produce more of the O-transfer species. After O-transfer to the alkene, the surface species would have to be reconstituted either directly from gaseous O<sub>2</sub> or indirectly *via* formation of the intermediate allylic hydroperoxide.

Analyses have been carried out looking specifically for the presence of cyclo-oct-2-enyl hydroperoxide in reaction mixtures generated under standard conditions using 1% Au/graphite as a catalyst. Samples for analysis taken from the reaction mixture were divided into two; one half was analysed directly and the other was treated with triphenylphosphine, which is expected to convert any hydroperoxides quantitatively into the corresponding alcohol and triphenylphosphine oxide. After phosphine treatment, the glc results should thus show an increased level of cyclo-oct-2-enol. The amount of the related cyclo-oct-2-enone, the likeliest major decomposition product of the hydroperoxide when injected into the gas chromatograph, should show a comparable decrease. Representative results are shown in Table 9, where it can be seen that there is indeed a small increase in the selectivity to the allylic alcohol and decrease in the enone selectivity, suggesting the presence of fairly low levels of the allylic hydroperoxide, as expected if it is formed and then consumed in epoxidation. The results in Table 9 show that the increase in the allylic alcohol selectivity is greater than the decrease in the enone selectivity, a situation for which we have as yet no satisfactory explanation. Direct confirmation of the presence of the hydroperoxide was obtained using <sup>1</sup>H NMR spectroscopy. Examination of the spectrum of product samples, taken after 24 and 72 h reaction and not treated with triphenylphosphine, showed two multiplets (dt) centred at  $\delta$ 4.63 and 4.93, the former arising from the proton on the allylic carbon atom bearing the hydroxyl group in authentic cyclo-oct-2-enol and the other assigned to the corresponding proton in the hydroperoxide. After phosphine treatment, the signal at  $\delta$ 4.93 had disappeared.

Although we have demonstrated the presence of the allylic hydroperoxide in the reaction mixtures, it seems unlikely that it

**Table 9** Effect of the addition of triphenylphosphine (PPh<sub>3</sub>) on allylic alcohol selectivity in cyclooctene epoxidation

Reaction time/h	Conversion (%)	Selectivity Without PPh <sub>3</sub>			Selectivity With PPh <sub>3</sub> in air			Selectivity With PPh <sub>3</sub> in N <sub>2</sub>		
		Epoxide	Alcohol	Ketone	Epoxide	Alcohol	Ketone	Epoxide	Alcohol	Ketone
24	4.9	74.3	8.3	6.4	71.4	13.0	4.2	71.0	13.0	4.2
72	20.3	77.3	5.4	5.4	75.6	7.3	4.8	76.6	7.0	4.7

Reaction conditions: cyclooctene (10 ml), TBHP (0.01 ml), 80 °C, 1% Au/graphite (0.12 g) atmospheric pressure.

can play a major role in catalysis of epoxidation, since it seems likely that its role will be to transfer only one of its O-atoms, leaving a molecule of the allylic alcohol. The very high epoxide selectivities attainable in these systems would seem to preclude a catalytic cycle involving the hydroperoxide. On the basis of the present data, we can only speculate about the detailed course of the reaction. We plan further experimental studies to test these mechanistic proposals.

## Conclusions

We have shown that gold supported on graphite is a very promising catalyst for the epoxidation of cyclooctene using catalytic amounts of an added hydroperoxy species. The catalyst is effective under mild, solvent-free conditions using oxygen from air as the oxidant. Selectivities to the epoxide can be greater than 80% and we consider that with appropriate catalyst design further enhancements in activity and selectivity can be expected.

## Acknowledgements

This work formed part of an EPSRC funded project and we thank them for funding this research. We also thank King Abdul Aziz University (Saudi Arabia Government) for financial support. We thank a referee for helpful comments.

## References

- R. A. Sheldon, *Stud. Surf. Sci. Catal.*, 1991, **66**, 33.
- R. M. Lambert, F. J. Williams, R. L. Copley and A. Palermo, *J. Molec. Catal.*, 2005, **228**, 27.
- E. Klemm, E. Dietzsch, T. Schwarz, T. Kruppa, A. Lange de Oliveira, F. Becker, G. Markowz, S. Schirrmeister, R. Schütte, K. J. Caspary, F. Schüth and D. Hönicke, *Ind. Eng. Chem. Res.*, 2008, **47**, 2086.
- C. Della Pina, E. Falletta, L. Prati and M. Rossi, *Chem. Soc. Rev.*, 2008, **37**, 2077.
- T. Hayashi, K. Tanaka and M. Haruta, *J. Catal.*, 1998, **178**, 566.
- M. Haruta and M. Date, *Appl. Catal. A*, 2001, **222**, 427.
- T. A. Nijhuis, T. Visser and B. M. Weckhuysen, *J. Phys. Chem. B*, 2005, **109**, 19309.
- B. S. Uphade, S. Tsubota, T. Hayashi and M. Haruta, *Chem. Lett.*, 1998, 1277.
- T. A. Nijhuis, B. J. Huizinga, M. Makkee and J. A. Moulijn, *Ind. Eng. Chem. Res.*, 1999, **38**, 884.
- T. A. Nijhuis, T. Q. Gardner and B. M. Weckhuysen, *J. Catal.*, 2005, **236**, 153.
- T. A. Nijhuis, T. Visser and B. M. Weckhuysen, *Angew. Chem., Int. Ed.*, 2005, **44**, 1115.
- T. A. Nijhuis and B. M. Weckhuysen, *Chem. Commun.*, 2005, 6002.
- N. Yap, R. P. Andres and W. N. Delgass, *J. Catal.*, 2004, **226**, 156.
- A. Zwijnenburg, M. Makkee and J. A. Moulijn, *Appl. Catal. A*, 2004, **270**, 49.
- C. Qi, T. Akita, M. Okumura, K. Kuraoka and M. Haruta, *Appl. Catal. A*, 2003, **253**, 75.
- B. Taylor, J. Lauterbach and W. N. Delgass, *Appl. Catal. A*, 2005, **291**, 188.
- A. K. Sinha, S. Seelan, M. Okumura, T. Akita, S. Tsubota and M. Haruta, *J. Phys. Chem. B*, 2005, **109**, 3956.
- B. Chowdhury, J. J. Bravo-Suarez, M. Date, S. Tsubota and M. Haruta, *Angew. Chem., Int. Ed.*, 2006, **45**, 412.
- E. Sacaliuc, A. M. Beale, B. M. Weckhuysen and T. A. Nijhuis, *J. Catal.*, 2007, **248**, 235.
- J. Lu, X. Zhang, J. J. Bravo-Suarez, K. K. Bando, T. Fujitani and S. T. Oyama, *J. Catal.*, 2007, **250**, 350.
- A. K. Sinha, S. Seelan, S. Tsubota and M. Haruta, *Angew. Chem., Int. Ed.*, 2004, **43**, 1546.
- J. K. Edwards and G. J. Hutchings, *Angew. Chem., Int. Ed.*, 2008, **47**, 9192.
- N. S. Patil, B. S. Uphade, P. Jana, S. K. Bhargava and V. R. Choudhary, *Chem. Lett.*, 2004, **33**, 400.
- N. S. Patil, B. S. Uphade, D. G. McCulloh, S. K. Bhargava and V. R. Choudhary, *Catal. Commun.*, 2004, **5**, 681.
- N. S. Patil, B. S. Uphade, P. Jana, S. K. Bhargava and V. R. Choudhary, *J. Catal.*, 2004, **223**, 236.
- N. S. Patil, R. Jha, B. S. Uphade, S. K. Bhargava and V. R. Choudhary, *Appl. Catal. A*, 2004, **275**, 87.
- N. S. Patil, B. S. Uphade, P. Jana, R. S. Sonawane, S. K. Bhargava and V. R. Choudhary, *Catal. Lett.*, 2004, **94**, 89.
- D. Yin, L. Qin, J. Liu, C. L. and Y. Jin, *J. Molec. Catal. A*, 2005, **240**, 40.
- M. D. Hughes, Y.-J. Xu, P. Jenkins, P. McMorn, P. Landon, D. I. Enache, A. F. Carley, G. A. Attard, G. J. Hutchings, F. King, E. H. Stitt, P. Johnston, K. Griffin and C. J. Kiely, *Nature*, 2005, **437**, 1132.
- P. Lignier, F. Morfin, S. Mangematin, L. Massin, J.-L. Rousset and V. Caps, *Chem. Commun.*, 2007, 186.
- P. Lignier, S. Mangematin, F. Morfin, J.-L. Rousset and V. Caps, *Catal. Today*, 2008, **138**, 50.
- P. Lignier, F. Morfin, Laurent Piccolo, J.-L. Rousset and V. Caps, *Catal. Today*, 2007, **122**, 284.
- X. Deng and C. M. Friend, *J. Amer. Chem. Soc.*, 2005, **127**, 17178.
- M. Turner, V. B. Golovko, O. P. H. Vaughan, P. Abdulkina, A. Berenguer-Murcia, M. S. Tikhov, B. F. G. Johnson and R. M. Lambert, *Nature*, 2008, **454**, 981.
- J. Branderup, E. H. Immergut, and E. A. Grulke, *Polymer Handbook*, 4th Ed., John Wiley, New York, 1999, **11**, 2.
- L. Prati and M. Rossi, *J. Catal.*, 1998, **176**, 552.
- J. A. Lopez-Sanchez, N. Dimitratos, P. Miedziak, E. Ntainjua, J. K. Edwards, D. Morgan, A. F. Carley, R. Tiruvalam, C. J. Kiely and G. J. Hutchings, *Phys. Chem. Chem. Phys.*, 2008, **10**, 1921.

# Hydrosilylation of functionalised olefins catalysed by rhodium siloxide complexes in ionic liquids

Hieronim Maciejewski,<sup>a</sup> Karol Szubert,<sup>a</sup> Bogdan Marciniec<sup>\*a</sup> and Juliusz Pernak<sup>b</sup>

Received 3rd November 2008, Accepted 9th April 2009

First published as an Advance Article on the web 29th April 2009

DOI: 10.1039/b819310j

The use of ionic liquids for the immobilization of rhodium siloxide complexes has permitted development of highly effective catalysts for the hydrosilylation processes. Herein, we report the synthesis of organosilicon compounds in a biphasic reaction setup, allowing separation of the product, recovery and reuse of the catalyst, which is fundamental from the point of view of “green chemistry”.

## Introduction

Hydrosilylation is a fundamental and elegant method for the laboratory and industrial synthesis of organosilicon compounds.<sup>1–3</sup> Formation of silicon–carbon bonds is usually performed on small molecules. The products are used as silicone monomers and for organic synthesis. Some organosilane chemistry, however, is realised on a large scale, such as the commercially important crosslinking of silicone rubbers by hydrosilylation.<sup>4</sup> There is much more to be done to exploit organosilicon chemistry on polymeric backbones, particularly silicones, to make new materials. A lot of very interesting new materials, particularly polycarbosilanes, can be synthesised in the reaction of hydrosilylation polymerisation.<sup>5</sup> Moreover, hydrosilylation reactions are used for functionalisation of (poly)siloxanes with Si–H bonds. Modification of poly(dimethyl, hydromethyl)siloxanes with organic functional groups is intensively developed in order to obtain polymers of specific properties or to make them chemically active, which will increase the number of new potential applications.<sup>6</sup> It has been estimated that at present the share of organofunctional siloxanes in the world silicone market reaches about 15%.<sup>7</sup>

Hydrosilylation is a catalytic process that proceeds in the presence of precursors of free radicals or various catalysts, *e.g.* amines, Lewis acids (salts or metals), supported metals and transition metal complexes.<sup>1–3</sup> In most cases, the role of hydrosilylation catalysts is played by transition metal complexes, those of platinum in particular.<sup>8,9</sup> Platinum catalysts tolerate a variety of functional groups, however, some impurities may interact with them leading to catalyst poisoning.<sup>10</sup> That is why other metal complexes of comparably high catalytic activity are searched for. The catalysts that are characterised by a higher resistance to poisoning are rhodium complexes. Our contribution to this field was synthesis, isolation and full characterisation of several

new rhodium siloxide complexes, both dimeric and monomeric ones.<sup>11–13</sup> Their catalytic activity has been demonstrated for some reactions, *e.g.* hydrosilylation of alkenes<sup>14–16</sup> and allyl alkyl ethers or allyl polyethers,<sup>14,17–19</sup> both by hydrosilanes<sup>14,15,17,18</sup> and poly(dimethyl, hydromethyl)siloxanes<sup>15,16,19</sup> as well as for silylative coupling of vinylsilanes with alkenes.<sup>20,21</sup> In most of the above reactions, rhodium siloxide complexes have shown greater catalytic activity, even at room temperature, than that of the commonly used hydrosilylation catalysts, such as platinum complexes.

Rhodium siloxide complexes as representatives of homogeneous catalysts belong to the most efficient hydrosilylation catalysts. However, sometimes, the presence of metals in the reaction products, even in trace quantities, is unacceptable, but the separation of the catalyst from the reaction mixture, particularly in the case of polymer systems of high viscosity, is a serious problem. Therefore efforts have been made to apply heterogeneous catalysts or immobilised metal complexes in order to obtain high catalytic activity in many recycled runs and easy product isolation at the same time, which is fundamental from the point of view of “green chemistry”.

Biphasic catalysis in a liquid–liquid system seems to be an ideal solution allowing a combination of the advantages of both homogeneous and heterogeneous catalysis.<sup>22</sup> More recently, ionic liquids (IL) have been recognised as potential media for the immobilisation of catalysts and have been used with considerable success in a wide range of laboratory scale reactions.<sup>23,24</sup> Nowadays, many examples of biphasic reactions employing ionic liquids, *i.e.* hydroformylation, hydrogenation, oxidation, dimerisation are known, however, there are only a few examples of hydrosilylation with the use of ionic liquids.<sup>25–31</sup> Very recently, the first industrial application of hydrosilylation catalysis in ionic liquids for synthesis of organofunctional silanes was reported.<sup>31a</sup> Among all publications, only the papers by Weyershausen concern functionalisation of poly(dimethyl, hydromethyl)siloxanes, catalysed by platinum complexes in ionic liquid media, mainly imidazolium derivatives.<sup>29–31</sup> One of the most effective liquids in this system appeared to be trimethylimidazolium methylsulfate, [TriMIM][MeSO<sub>4</sub>]. We have made attempts at applying analogous liquids in association with a rhodium siloxide complex [{Rh(μ-O-SiMe<sub>3</sub>)(cod)}<sub>2</sub>]. The results confirmed high catalytic

<sup>a</sup>Adam Mickiewicz University, Faculty of Chemistry, Department of Organometallic Chemistry, Grunwaldzka 6, 60780, Poznań, Poland. E-mail: bogdan.marciniec@amu.edu.pl

<sup>b</sup>Poznan University of Technology, Faculty of Chemical Technology, 5 M. Skłodowskiej-Curie Sq., 60-965, Poznan, Poland, Email: Juliusz.Pernak@put.poznan.pl



activity of the rhodium siloxide complex for reactions carried out in the presence of ionic liquids.<sup>32–35</sup>

The present study was aimed at determining and comparing catalytic activity of different rhodium siloxide complexes immobilised in [TriMIM][MeSO<sub>4</sub>] and in various phosphonium ionic liquids for hydrosilylation reactions of functionalised olefins.

## Experimental section

### General methods and chemicals

All reagents were dried and purified before use by the usual procedures. Rhodium complexes  $[\{\text{Rh}(\mu\text{-OSiMe}_3)(\text{cod})\}_2]$ ,  $[\text{Rh}(\text{cod})(\text{PCy}_3)(\text{OSiMe}_3)]$  and  $[\{\text{Rh}(\mu\text{-Cl})(\text{tfb})\}_2]$  were prepared as described in Ref. 11, 13 and 36. Ionic liquids 1,2,3-trimethylimidazolium methylsulfate [TriMIM][MeSO<sub>4</sub>] (I) and CYPHOSIL (105 and 109) (II and III) were purchased from Aldrich and Strem, respectively. Other phosphonium IL were prepared as described in Ref. 37–39. All IL were dried prior to use under vacuum at 60 °C over 8 h. Heptamethyltrisiloxane and poly(dimethyl, hydromethyl) siloxane were purchased from Gelest, olefins and other reagents from Aldrich.

The NMR spectra (<sup>1</sup>H, <sup>13</sup>C, and <sup>29</sup>Si) were recorded on Varian Gemini 300 VT and Varian Mercury 300 VT spectrometers. C<sub>6</sub>D<sub>6</sub> or CDCl<sub>3</sub> were used as the solvents. GC analyses were carried out on a Varian 3800 chromatograph (equipped with a DB-1, 30 m capillary column and TCD detector, temperature program: 60 °C (3 min)–10 °C min<sup>-1</sup>–300 °C (10 min)).

FT-IR spectra were recorded on a Bruker Tensor 27 Fourier transform spectrometer equipped with a SPECAC Golden Gate diamond ATR unit. In all cases 16 scans at a resolution of 2 cm<sup>-1</sup> were used to record the spectra. Elemental analyses were made on an Elementar Analyser Vario EL III.

### Synthesis of $[\{\text{Rh}(\mu\text{-OSiMe}_3)(\text{tfb})\}_2]$

$[\{\text{Rh}(\mu\text{-Cl})(\text{tfb})\}_2]$  (0.4 g, 0.55 mmol) was dissolved in 4 ml of benzene and added to a suspension of NaOSiMe<sub>3</sub> (0.13 g, 1.12 mmol) in 4 ml of benzene and stirred for 24 h. Then benzene was carefully evaporated to dryness under vacuum and 5 ml of pentane was added. The mixture was stirred for 1 h and filtered from NaCl. Pentane solution was evaporated under reduced pressure and finally  $[\{\text{Rh}(\mu\text{-OSiMe}_3)(\text{tfb})\}_2]$  precipitated as yellow powder (yield 75%).

EA: Anal. Found: C, 43.24; H, 3.71. C<sub>30</sub>H<sub>30</sub>F<sub>8</sub>O<sub>2</sub>Rh<sub>2</sub>Si<sub>2</sub> Calc.: C, 43.07; H, 3.61%.

FT-IR: 2955; 1494; 1375, 1301, 1244, 1094–1039, 893, 822, 746, 680 cm<sup>-1</sup>

<sup>1</sup>H (C<sub>6</sub>D<sub>6</sub> δ(ppm)): 5,155 (br, 2H, –CH); 3,07 (br, 4H, =CH); 0,002 (s, 9H, OSiMe<sub>3</sub>)

<sup>13</sup>C (C<sub>6</sub>D<sub>6</sub> δ(ppm)): 138.43, 136.74 (C–F, tfb); 125.09 (C(sp<sup>2</sup>), tfb); 47.23, 46.07 (=CH–, tfb); 42.87, 38.96 (CH, tfb); 4.40 (SiMe<sub>3</sub>)

<sup>29</sup>Si (C<sub>6</sub>D<sub>6</sub> δ(ppm)): 10.14

### General procedure for catalytic test

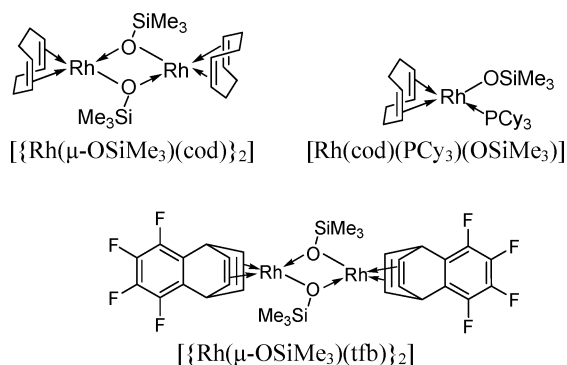
All manipulations were carried out under Ar using Schlenk techniques.

The appropriate amounts of the catalyst (in the ratio 10<sup>-5</sup> mol per mol Si–H) and the ionic liquid (1% based on the total weight of combined substrates) were placed into the reaction vessel and heated up to 120 °C for 0.5 h. The system was heated for 0.5 h to dissolve the catalyst in the ionic liquid, especially if the ionic liquid was solid at room temperature. Then the reaction system was cooled and the mixture of Si–H functional siloxane (or polysiloxane) and 1.2 equiv of the olefin (calculated to each Si–H group) were added and the reaction vessel was heated again up to 120 °C. After 1 h the reaction vessel was cooled to room temperature and then the reaction mixture was separated from the phase of the catalytic system by decantation. The mixture was analysed by GC method and the formation of desired products was verified by GC–MS and NMR analysis. All the obtained results are compatible in accordance with the characteristics of particular products, as described in the literature.<sup>33</sup> The recovered catalytic system (catalyst in ionic liquid) was reused in the next reaction cycle.

## Results and discussion

Our earlier studies have shown that the course of reactions in ionic liquids and the formation of biphasic systems are influenced by the kind of olefin and by the hydrosilylation product obtained from it.<sup>33</sup> More precisely speaking, it is associated with the hydrophobicity of these compounds. At the beginning of our study, we have compared catalytic activities of different rhodium siloxide complexes immobilised in ionic liquid for the reaction of hydrosilylation of allyl glycidyl ether.

Three different rhodium siloxide complexes, shown in Fig. 1, have been used in our studies.



**Fig. 1** Rhodium siloxide complexes used as catalysts in the reactions studied. The complexes were immobilised in [TriMIM][MeSO<sub>4</sub>] (see Fig. 2).

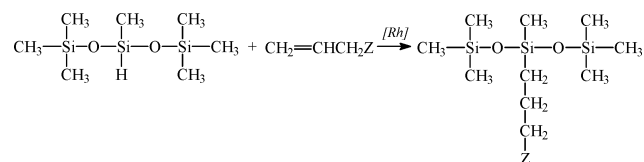
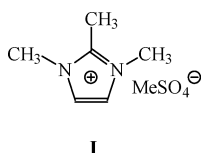
Such catalytic systems were applied as catalysts for hydrosilylation reactions. In order to establish basic conditions for hydrosilylation of olefins by polysiloxanes, some experiments were carried out using the model reaction between heptamethyltrisiloxane and olefins, according to Scheme 1:

Contrary to the polymeric system, these model reagents made the GC analysis of the reaction mixture possible. Catalytic activity of  $[\{\text{Rh}(\mu\text{-OSiMe}_3)(\text{cod})\}_2]$  in such a reaction has been reported previously,<sup>33</sup> and now we compare the results obtained with those for the other two complexes. In all the reactions, biphasic systems were obtained, which enabled easy separation

**Table 1** Catalyst recycling with Rh siloxide complexes in [TriMIM][MeSO<sub>4</sub>] in the reaction of heptamethyltrisiloxane with allyl glycidyl ether

Catalyst	Conversion of Si-H (%)	Yield of product (%)
<b>[[Rh(μ-OSiMe<sub>3</sub>)(cod)]<sub>2</sub>]</b>	85 (81, 82, 82, 83, 92)	80 (78, 78, 78, 79, 86)
<b>[Rh(cod)(PCy<sub>3</sub>)(OSiMe<sub>3</sub>)]</b>	87 (91, 89, 87, 83, 85)	80 (82, 82, 80, 76, 78)
<b>[[Rh(μ-OSiMe<sub>3</sub>)(tff)]<sub>2</sub>]</b>	82 (71, 73, 76, 65, 70)	74 (63, 68, 68, 54, 73)

[HSi≡]: [CH<sub>2</sub>=CH-]: [cat] = 1 : 1, 2 : 10<sup>-5</sup>; [IL] = 1% based on total weight of combined substrates; *T* = 120 °C; *t* = 1 h, value of the conversion and the yield in subsequent catalytic runs with the same recovered catalytic system given in parentheses.

**Scheme 1** Model reaction of hydrosilylation of olefins.**Fig. 2** 1,2,3-Trimethylimidazolium methylsulfate [TriMIM][MeSO<sub>4</sub>].

of the catalytic system after the reaction was completed, thus making it possible to reuse the catalyst. In addition to the desired product of hydrosilylation, small amounts of products of allyl glycidyl ether isomerisation and redistribution of hydrosiloxanes were obtained.

As shown in Table 1, six reaction runs were performed for each portion of the catalyst and no considerable reduction in catalytic activity was observed.

Relatively poor performance was found only for rhodium siloxide complex with tetrafluoroborene ligand **[[Rh(μ-OSiMe<sub>3</sub>)(tff)]<sub>2</sub>]**, whereas the other two complexes were very

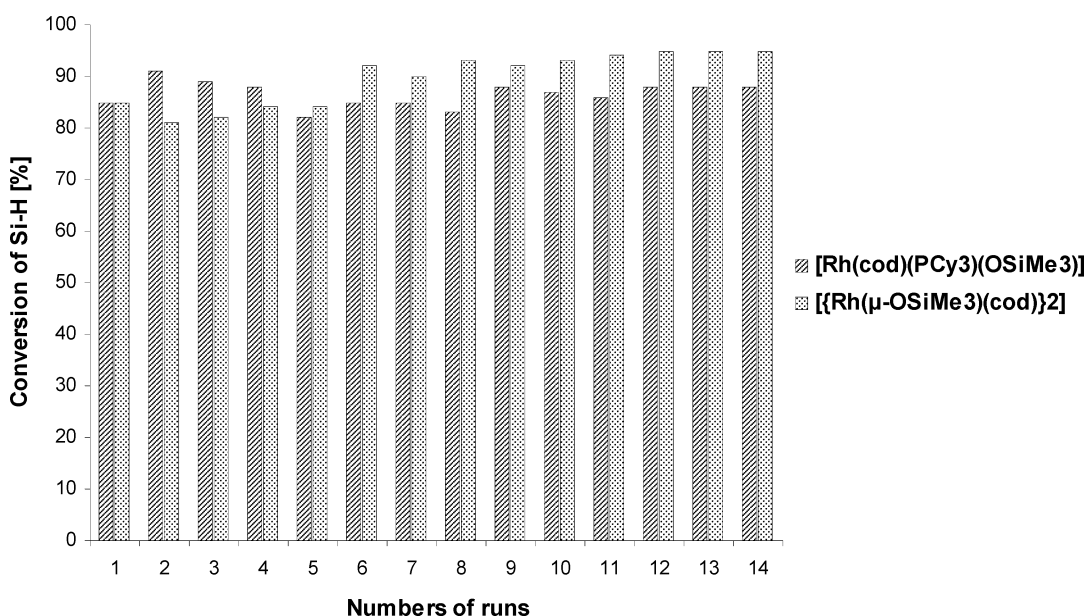
active. In order to determine the possibility of multiple use of the same portion of the catalyst in the hydrosilylation reactions studied, the subsequent reactions were conducted in the same conditions as above, using the first two complexes. The studies were discontinued after the 14th cycle, but it should be emphasised that both catalysts were still highly active as shown in Fig. 3.

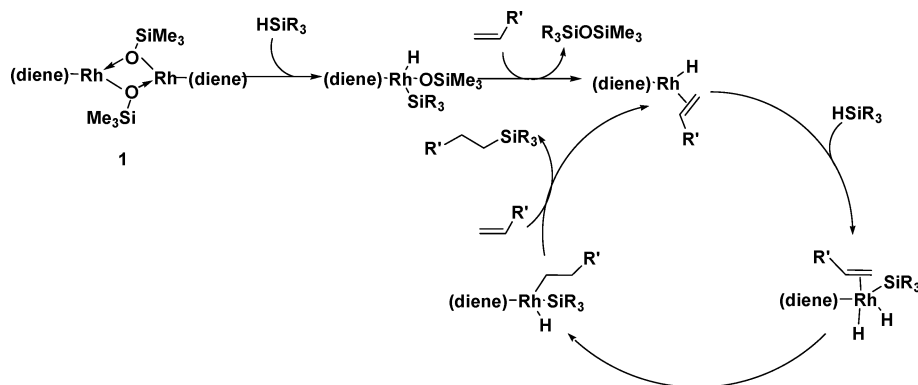
We also carried out hydrosilylation reactions of other allyl derivatives, namely allyl phenyl ether, allyl butyl ether and dimethoxyallylbenzene. The conversion of Si-H and the product yield in consecutive runs are given in parentheses (see Table 2).

It is well-known from the earlier study that in the presence of silicon hydride the soluble Rh-O-SiMe<sub>3</sub> complex undergoes the oxidative addition followed by elimination of disiloxane to generate a low-coordinated complex (16 e hydride complex with already coordinated alkene molecule) initiating the direct hydrosilylation process according to Scheme 2.

The increasing catalytic activity over the first runs, which was observed in some cases, can be easily interpreted in terms of activation of the dimeric rhodium siloxide complex in contact with subsequent portions of the substrate (particularly with the silicon-hydride bond),<sup>13,15</sup> (see scheme 2).

The differences in the activity of the catalytic system used in the reactions discussed, can be explained by the different hydrophilic-hydrophobic properties of the olefins employed. An increase in hydrophilic properties resulted to a greater extent

**Fig. 3** The conversion of heptamethyltrisiloxane in 14 subsequent runs with the same catalytic system recovered, in the reaction of allyl glycidyl ether with heptamethyltrisiloxane, catalysed by rhodium siloxide complexes in [TriMIM][MeSO<sub>4</sub>].



**Scheme 2** Mechanism of hydrosilylation catalyzed by soluble binuclear rhodium siloxide complex.

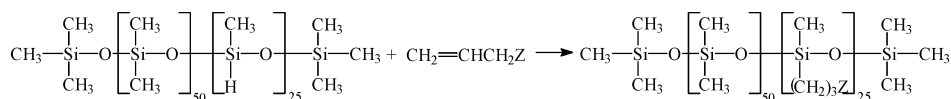
**Table 2** The conversion of  $[=SiH]$  and the yield of product obtained in the reaction between heptamethyltrisiloxane and  $CH_2=CHCH_2Z$  catalysed by  $[Rh(\mu-O-SiMe_3)(cod)]_2$  in  $[TriMIM][MeSO_4]$

Z	Conversion SiH (%)	Yield (%)
	85 (81, 82, 82, 84, 92, 90, 94, 92, 93)	80 (76, 76, 76, 79, 85, 83, 88, 88, 88)
$-O-C_4H_9$	85 (95, 92, 75, 43)	85 (92, 90, 72, 42)
	86 (98, 93, 87, 53)	84 (96, 92, 84, 52)

$[HSi\equiv][CH_2=CH-][cat] = 1 : 1, 2 : 10^{-5}$ ;  $[IL] = 1\%$  based on total weight of combined substrates;  $T = 120^\circ C$ ;  $t = 1$  h; value of the conversion and the yield in subsequent catalytic runs with the same recovered catalytic system given in parentheses.

in the catalyst leaching from the catalyst–ionic liquid system, therefore the amount of the catalyst in the subsequent cycles was smaller, which resulted in reduction in the yield. More precisely, the reaction mixtures were collected after each catalytic cycle and the rhodium content in such a total mixture was analyzed by ICP-OES. The results obtained showed that in the post-reaction mixture, from the reaction with allyl butyl ether, the content of rhodium equalled 30% of the starting rhodium concentration, so it was the highest in comparison with the reactions with dimethoxyallylbenzene and allyl phenyl ether, in which the content of rhodium equalled 22 and 7% respectively. Therefore, the leaching of the catalyst is the most probable reason for the decrease of the yield. Another possible cause of the decrease in the activity of the catalyst is its deactivation (resulting from the reaction with moisture and oxygen), however, taking into consideration that all the reagents were dried and purified before use and the reactions were conducted under argon, it seems rather improbable.

On the grounds of the model reaction results, we decided to carry out the reactions of olefin hydrosilylation with



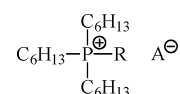
**Scheme 3** The hydrosilylation of olefins by poly(dimethyl, hydromethyl)siloxane.

poly(dimethyl, hydromethyl)siloxanes catalysed by a catalytic system based on the dimeric rhodium siloxide complex in  $[TriMIM][MeSO_4]$ , according to Scheme 3: the results shown in Table 3 confirmed high catalytic activity of the systems based on the dimeric rhodium siloxide complex in  $[TriMIM][MeSO_4]$ .

Moreover, in the case of polymeric systems, due to high viscosities of the products formed, the formation and separation of biphasic systems are considerably easier, which is reflected by higher product yields. As shown in Table 3, ten reaction runs were performed for each portion of the catalyst and no considerable reduction in catalytic activity was observed. Only for the reaction with allyl butyl ether, a decrease in conversion was observed (similarly to the reaction with heptamethyltrisiloxane).

Imidazolium derivatives make the majority of ionic liquids applied in catalysis, whereas a relatively small number of reports are available on phosphonium ionic liquids<sup>40,41</sup> however they unequivocally demonstrate that the application potential of these salts is just as high as that of more commonly studied imidazolium-, pyridinium-, and ammonium-based ILs. This fact prompted us to verify the activity of rhodium siloxide complexes in the above class of ionic liquids.

We used a number of different liquids of the general formula given in Fig. 4.



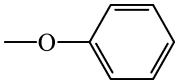
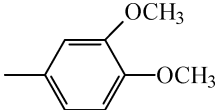
**II - IX**

**Fig. 4** The general formula of the phosphonium IL used.

Two of them, denoted as CYPHOSIL, are commercially available, whereas the remaining ones, were synthesised,<sup>37–39</sup> with the substituents R and anions listed in Table 4.

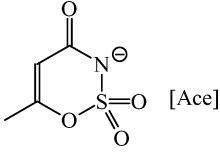
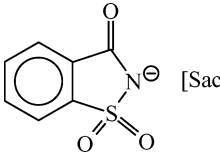
Then the liquids were applied to immobilise the dimeric rhodium siloxide complex and thus obtained systems were used as catalysts for the model reaction of hydrosilylation between heptamethyltrisiloxane and allyl glycidyl ether. In

**Table 3** The conversion of  $[\equiv\text{SiH}]$  obtained in the reaction between poly(dimethyl, hydromethyl)siloxane and  $\text{CH}_2=\text{CHCH}_2\text{Z}$  catalysed by rhodium siloxide complexes in  $[\text{TriMIM}][\text{MeSO}_4]$ 

Z	Complex	Conversion of Si-H (%)	Number of repetition experiments
$-\text{OCH}_2\text{CHCH}_2\text{O}$	$[\{\text{Rh}(\mu\text{-OSiMe}_3)(\text{cod})\}_2]$ $[\text{Rh}(\text{cod})(\text{PCy}_3)(\text{OSiMe}_3)]$	99 (99.....99) 99 (99.....99)	10 10
	$[\{\text{Rh}(\mu\text{-OSiMe}_3)(\text{cod})\}_2]$	99 (99.....99)	10
$-\text{O}-\text{C}_4\text{H}_9$	$[\{\text{Rh}(\mu\text{-OSiMe}_3)(\text{cod})\}_2]$	95 (95, 92, 85, 65)	5
	$[\{\text{Rh}(\mu\text{-OSiMe}_3)(\text{cod})\}_2]$	99 (99.....99)	10
$-\text{C}_{13}\text{H}_{27}$		99 (99.....99)	10

$[\text{HSi}\equiv][\text{CH}_2=\text{CHCH}_2\text{-}][\text{cat}] = 1 : 1, 2 : 10^{-5}$ ;  $[\text{IL}] = 1\%$  based on total weight of combined substrates;  $T = 120^\circ\text{C}$ ;  $t = 1\text{ h}$ ; value of the conversion in subsequent catalytic runs (mostly ten) with the same recovered catalytic system given in parentheses.

**Table 4** The phosphonium ionic liquids (II–IX)

Ionic Liquids	R	A
II (CYPHOSIL 105)	$\text{C}_{14}\text{H}_{29}$	$(\text{CN})_2\text{N}^\ominus$
III (CYPHOSIL 109)	$\text{C}_{14}\text{H}_{29}$	$(\text{CF}_3\text{SO}_2)_2\text{N}^\ominus$
IV	$\text{CH}_2\text{OC}_5\text{H}_{11}$	$\text{BF}_4^\ominus$
V	$\text{CH}_2\text{OC}_3\text{H}_7$	$\text{BF}_4^\ominus$
VI	$\text{CH}_2\text{OC}_5\text{H}_{11}$	 [Ace]
VII	$\text{CH}_2\text{OC}_5\text{H}_{11}$	 [Sac]
VIII	$\text{CH}_2\text{OC}_5\text{H}_{11}$	$\text{NO}_3^\ominus$
IX	$\text{CH}_2\text{OC}_8\text{H}_{17}$	$\text{CH}_3\text{OSO}_3^\ominus$

order to compare the effectiveness of different phosphonium ionic liquids, the reactions with the catalytic systems investigated were repeated three times using the same portion of the catalyst. The heptamethyltrisiloxane conversions are given in Fig. 5.

The results obtained enabled selection of the four most effective catalytic systems, which ensured high conversion of starting materials and high selectivity to the product formed. They are the catalytic systems based on the complex  $[\{\text{Rh}(\mu\text{-OSiMe}_3)(\text{cod})\}_2]$  immobilised in liquids **III**, **VI**, **VII** and **IX**. Moreover the results depict that liquids **IV** and **V** differ in the length of the alkoxy chain ( $-\text{CH}_2\text{OC}_5\text{H}_{11}$  and

**Table 5** Types of substituents R and anions A in other synthesised phosphonium IL

Ionic Liquid	R	A
X	$\text{CH}_2\text{OC}_3\text{H}_7$	$\text{MeSO}_4^-$
XI	$\text{CH}_2\text{OC}_3\text{H}_7$	$(\text{CF}_3\text{SO}_2)_2\text{N}^-$
XII	$\text{CH}_2\text{OC}_3\text{H}_7$	[Ace] <sup>-</sup>
XIII	$\text{CH}_2\text{OC}_3\text{H}_7$	[Sac] <sup>-</sup>

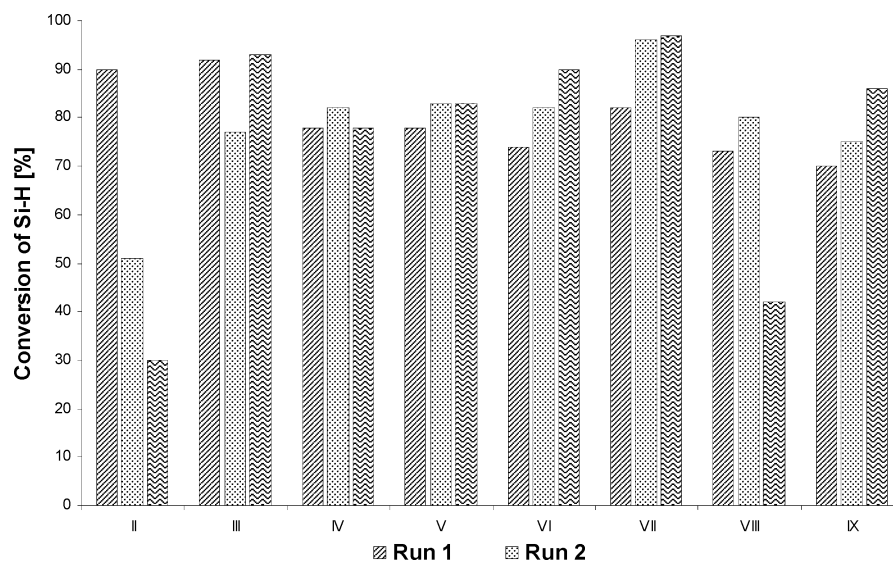
$-\text{CH}_2\text{OC}_3\text{H}_7$ , respectively), whereas the conversions recorded in the two liquids show that better results are obtained for shorter chains. That is why another set of ionic liquids being counterparts of the selected ones but with molecules of shorter chains  $-\text{CH}_2\text{OC}_3\text{H}_7$ , was prepared. The names of these ionic liquids are listed in Table 5.

The above liquids were used in the reactions of hydrosilylation of allyl glycidyl ether with heptamethyltrisiloxane. The results obtained for three runs carried out on the same portion of the catalyst are given in Fig. 6.

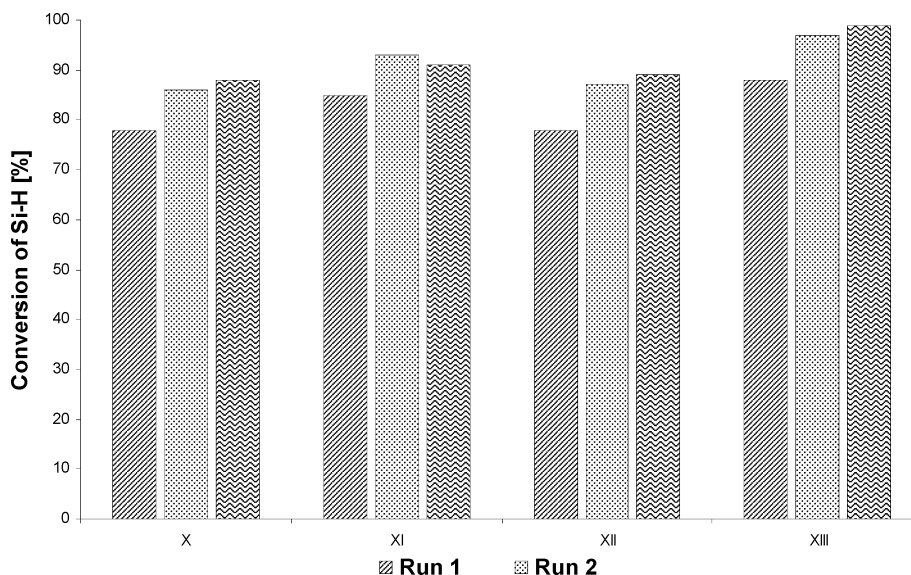
All the catalytic systems prepared have shown high activity, however, definitely the best appeared to be the one in which propoxymethyltrihexylphosphonium saccharinate was the ionic liquid. This system enables multiple recycling of the catalyst with no loss in activity. The above system is as effective as that based on the rhodium siloxide complex and imidazolium liquid. Both liquids immobilise rhodium siloxide complexes very well and protect them from leaching. Analysis of the reaction products by ICP technique was carried out to check for the possible presence of rhodium and proved none of it detectable. Because the liquids maintain the catalyst very well, no decrease in its activity is observed.

The four catalytic systems were applied as catalysts for hydrosilylation of functionalised olefins with poly(dimethyl,hydromethyl)siloxane, according to Scheme 3. The results obtained are shown in Table 6.

The results obtained confirm high catalytic activity of all the systems employed and point to the rhodium siloxide complex  $[\{\text{Rh}(\mu\text{-OSiMe}_3)(\text{cod})\}_2]$  immobilised in liquid **XIII** as the most efficient system, similarly as it was for the reaction with heptamethyltrisiloxane. They also confirm earlier observations



**Fig. 5** The conversion of heptamethyltrisiloxane in 3 subsequent runs using the same recovered catalytic system in hydrosilylation of allyl glycidyl ether catalysed by  $[\{\text{Rh}(\mu\text{-OSiMe}_3)(\text{cod})\}_2]$  in phosphonium IL (II–IX).



**Fig. 6** The conversion of heptamethyltrisiloxane in 3 subsequent runs with the same recovered catalytic system in the reaction of hydrosilylation of allyl glycidyl ether catalysed by  $[\{\text{Rh}(\mu\text{-OSiMe}_3)(\text{cod})\}_2]$  in phosphonium IL (X–XIII).

that the reactions in polymeric systems proceed with considerably higher yields and that hydrophilic–hydrophobic properties of the products also affect the yield. Alkylsilicones are highly hydrophobic, therefore they do not mix with the catalyst phase and are easily separable from it. In the case of olefins, such as glycidyl ethers and polyethers, their hydrophilicity increases, which can be the reason for a slow leaching of the catalysts from the catalytic system, thus resulting in a yield reduction.

From the ecological point of view, in homogeneous catalysis, the separation, immobilisation, and the reuse of the expensive metal catalyst in a subsequent reaction represent a serious problem. For example, the extraction of the catalyst or its adsorption at ion exchangers would enable separation of product and catalyst phase, however, in such processes a great amount of volatile solvents are very often used. Therefore, ionic liquids, which are shown to have a significant advantage over conven-

tional solvents for homogeneously catalyzed reactions, are a very good alternative for both homo- and heterogeneous catalytic systems.

## Conclusions

The studies performed have shown that immobilisation of rhodium siloxide complexes in ionic liquids permits the formation of biphasic systems which, when applied as catalysts for hydrosilylation of functionalised olefins, combine the advantages of homogeneous catalysts (high catalytic activity) and heterogeneous ones (easy separation and possibility of recycling).

In particular, two catalytic systems based on the  $[\{\text{Rh}(\mu\text{-OSiMe}_3)(\text{cod})\}_2]$  complex dissolved in  $[\text{TriMIM}][\text{MeSO}_4]$  (I) liquids and propoxymethyltriethylphosphonium saccharinate

**Table 6** The conversion of Si-H in 10 subsequent runs with the same recovered catalytic system in the reaction of the hydrosilylation of olefins  $\text{CH}_2=\text{CHCH}_2\text{Z}$  catalysed by  $[\{\text{Rh}(\mu\text{-OSiMe}_3)(\text{cod})\}_2]$  in phosphonium IL (X–XIII)

Z	IL	Conversion of Si-H (%)
–C <sub>13</sub> H <sub>27</sub>	X	98 (98, 98, . . . . ., 93)
	XI	100 (100, . . . . ., 100)
	XII	100 (100, . . . . ., 98)
	XIII	100 (100, . . . . ., 100)
–OCH <sub>2</sub> CHCH <sub>2</sub> O	X	98 (90, 90, 90, 83, 82, 80, 75, 70, 70)
	XI	99 (97, 97, 95, 95, 95, 90, 90, 85, 80)
	XII	97 (98, 98, 95, 94, 94, 90, 90, 85, 80)
	XIII	99 (99, 99, 99, 97, 95, 95, 92, 90, 85)
–(OCH <sub>2</sub> CH <sub>2</sub> ) <sub>7</sub> OCH <sub>3</sub>	X	92 (90, 90, 85, 84, 80, 80, 72, 68, 58)
	XI	95 (93, 93, 93, 90, 87, 83, 80, 75, 68)
	XII	95 (93, 93, 90, 85, 87, 86, 80, 78, 71)
	XIII	97 (95, 95, 95, 93, 92, 91, 85, 85, 75)

[HSi≡] [CH<sub>2</sub>=CHCH<sub>2</sub>–] [cat] = 1:1.2:10<sup>–5</sup>; [IL] = 1% based on total weight of combined substrates; T = 120 °C; t = 1 h; value of the conversion in subsequent catalytic runs with the same recovered catalytic system given in parentheses.

(XIII) make an alternative to all known effective catalysts for hydrosilylation processes.

## Acknowledgements

We are grateful to the Ministry of Science and Higher Education for financial support (project no. 204 162 32/4248).

## References

- 1 B. Marciniak, H. Maciejewski, C. Pietraszuk and P. Pawluc in *Hydrosilylation. A Comprehensive Review on Recent Advances*, ed. B. Marciniak, Springer, 2008.
- 2 A. K. Roy, *Adv. Organometal. Chem.*, 2008, **55**, 1.
- 3 I. Ojima, Z. Li and I. Zhu, in *The Chemistry of Organosilicon Compounds*, ed. S. Patai and Z. Rappoport, Wiley, New York, 1998.
- 4 M. A. Brook, H. A. Ketelson, F. J. La Ronde and R. Pelton, *Inorg. Chim. Acta*, 1997, **264**, 125.
- 5 M. Birot, J.-P. Pillot and J. Dunoques, *Chem. Rev.*, 1995, **95**, 1443.
- 6 B. Boutevin, F. Guida-Pietrasanta and A. Ratsimihety, in *Silicon-Containing Polymers*, ed. R.G. Jones, W. Ando and J. Chojnowski, Kluwer Academic Publishers, Dordrecht, 2000.
- 7 S. Stadtmuller, *Polymers and Polymers Composites*, 2002, **10**, 49.
- 8 B. Marciniak, in *Applied Homogeneous Catalysis with Organometallic Compounds*, ed. B. Cornils and W. A. Hermann, Wiley-VCH, Weinheim, 2002.
- 9 B. Marciniak, ed., *Comprehensive Handbook on Hydrosilylation*, Pergamon Press, Oxford, 1992.
- 10 M. A. Brook, *Silicon in Organic, Organometallic and Polymer Chemistry*, Wiley, New York, 2000.
- 11 B. Marciniak and P. Krzyżanowski, *J. Organometal. Chem.*, 1995, **493**, 261.
- 12 B. Marciniak, P. Krzyżanowski and M. Kubicki, *Polyhedron*, 1996, **15**, 4233.
- 13 B. Marciniak, P. Błażejewska-Chadyniak and M. Kubicki, *Can. J. Chem.*, 2003, **81**, 1292.
- 14 B. Marciniak, P. Krzyżanowski, E. Walczuk-Gusciora and W. Duczmal, *J. Mol. Catal.*, 1999, **144**, 263.
- 15 H. Maciejewski, B. Marciniak, P. Błażejewska-Chadyniak and I. Dąbek, in *Organosilicon Chemistry VI. From Molecules to Materials*, ed. N. Auner and J. Weis, Wiley-VCH, Weinheim, 2005.
- 16 B. Marciniak, D. Chadyniak, P. Pawluć, H. Maciejewski, P. Błażejewska-Chadyniak, Pol. Pat. Appl. P-351–451 (2001).
- 17 B. Marciniak, E. Walczuk, P. Błażejewska-Chadyniak, D. Chadyniak, M. Kujawa-Welten, S. Krompiec, in *Organosilicon Chemistry V. From Molecules to Materials*, (N. Auner, J. Weis, eds.) Wiley-VCH, Weinheim, 2003.
- 18 B. Marciniak, P. Błażejewska-Chadyniak, E. Walczuk-Gusciora and M. Kujawa-Welten, Pol. Pat. Appl., P-351–449 (2001).
- 19 B. Marciniak, D. Chadyniak, P. Pawluć, H. Maciejewski and P. Błażejewska-Chadyniak, Pol. Pat. Appl. P-351–450 (2001).
- 20 B. Marciniak, E. Walczuk-Gusciora and P. Błażejewska-Chadyniak, *J. Mol. Catal.*, 2000, **160**, 165.
- 21 B. Marciniak, E. Walczuk-Gusciora and C. Pietraszuk, *Organometallics*, 2001, **20**, 3423.
- 22 D. J. Adams, P. J. Dyson, S. J. Tavern, *Chemistry in Alternative Reaction Media*, Wiley, Hoboken, 2004.
- 23 P. J. Dyson, T. J. Geldbach, *Metal Catalysed Reactions in Ionic Liquids*, Springer, Dordrecht, 2005.
- 24 V. I. Parvulescu and Ch. Hardacre, *Chem. Rev.*, 2007, **107**, 2615.
- 25 S. Aubin, F. Le Floch, D. Carrie, J. P. Guegan and M. Vaultier, in *Ionic Liquids. Industrial Applications for Green Chemistry*, ed. R. D. Rogers and K. R. Seddon, ACS, Washington, 2002.
- 26 J. Van Den Broeke, F. Winter, B. J. Deelman and G. Van Koten, *Org. Lett.*, 2002, **4**, 3851.
- 27 J. Peng, J. Li, Y. Bai, W. Gao, H. Qiu, H. Wu, Y. Deng and G. Lai, *J. Mol. Catal. A.*, 2007, **278**, 97.
- 28 J. Peng, J. Li, Y. Bai, H. Qiu, K. Jiang, J. Jiang and G. Lai, *Catal. Commun.*, 2008, **9**, 2236.
- 29 B. Weyershausen, K. Hell and U. Hesse, *Green Chem.*, 2005, **7**, 283.
- 30 B. Weyershausen, K. Hell and U. Hesse, *ACS Symp. Ser.*, 2005, **902**, 133.
- 31 (a) T. J. Geldbach, D. Zhao, N. C. Castillo, G. Laurency, B. Weyershausen and P. J. Dyson, *J. Am. Chem. Soc.*, 2006, **128**, 9773; (b) N. Hofmann, A. Bauer, T. Frey, M. Auer, V. Stanjek, P. S. Schulz, N. Taccardi and P. Wasserscheid, *Adv. Synth. Catal.*, 2008, **350**, 2599.
- 32 H. Maciejewski, A. Wawrzynczak, M. Dutkiewicz and R. Fiedorow, *J. Mol. Catal. A*, 2006, **257**, 141.
- 33 B. Marciniak, H. Maciejewski, K. Szubert and M. Kurdykowska, *Monatshefte fur Chemie*, 2006, **137**, 605.
- 34 H. Maciejewski, B. Marciniak, J. Pernak and K. Szubert, Pol. Pat. Appl. P-380 735 (2006).
- 35 H. Maciejewski, B. Marciniak, J. Pernak and K. Szubert, Pol. Pat. Appl. P-380 734 (2006).
- 36 D. M. Roe and A. G. Massey, *J. Organomet. Chem.*, 1971, **28**, 273.
- 37 J. Pernak, B. Marciniak, H. Maciejewski and F. Stefański, Pol. Pat. Appl. P-379 059 (2006).
- 38 A. Cieniacka-Rosłonkiewicz, J. Pernak, J. Kubis-Feder, A. Ramani, A. J. Robertson and K. R. Seddon, *Green Chem.*, 2005, **7**, 855.
- 39 J. Pernak, F. Stefaniak and J. Węglewski, *Eur. J. Org. Chem.*, 2005, 650.
- 40 Ch. J. Bradaric, A. Downard, Ch. Kennedy, A. J. Robertson and Y. Zhou, *The Strem Chemiker*, 2003, **20**, 1.
- 41 C. J. Bradaric, A. Downard, C. Kennedy, A. J. Robertson and Y. Zhou, *Green Chem.*, 2003, **5**, 143.

# Chemo-enzymatic cascade oxidation in supercritical carbon dioxide/water biphasic media

Sanjib Kumar Karmee,<sup>a</sup> Christoph Roosen,<sup>a</sup> Christina Kohlmann,<sup>a,b</sup> Stephan Lütz,<sup>b</sup> Lasse Greiner<sup>\*a</sup> and Walter Leitner<sup>\*a,c</sup>

Received 19th November 2008, Accepted 16th April 2009

First published as an Advance Article on the web 30th April 2009

DOI: 10.1039/b820606f

Enantioselective sulfoxidation was carried out by cascade reaction of Pd(0) catalysed formation of H<sub>2</sub>O<sub>2</sub> and enzymatic oxidation using chloroperoxidase from *Caldariomyces fumago*. Supercritical carbon dioxide (scCO<sub>2</sub>) was used as medium for *in situ* generation of H<sub>2</sub>O<sub>2</sub> directly from H<sub>2</sub> and O<sub>2</sub> using Pd-catalysts. Subsequently, H<sub>2</sub>O<sub>2</sub> was utilised by the chloroperoxidase as an oxidant for the asymmetric sulfoxidation in the aqueous phase. This chemo-enzymatic cascade transformation exemplifies the potential of compartmentalisation of catalytic processes in multiphase systems.

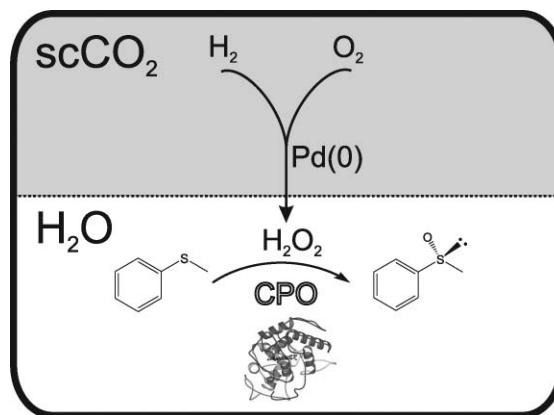
## Introduction

There is a steadily increasing demand for enantiomerically pure or enriched compounds especially in the life science industry. Therefore, the development of efficient catalytic methods for their production continues to be a major challenge for green chemistry. The cascading of reactions by integration of chemical and enzymatic catalysis is a promising approach in this context, as it combines advantages of both processes.<sup>1</sup> Cascade reactions offer the possibility to synthesise target compounds *via* subsequent transformations without isolation of reactive intermediates.<sup>2</sup> This becomes particularly relevant if a reagent for a given transformation is formed “on demand” in the first step and used immediately, avoiding unnecessary hold ups or potential substrate inhibition in the subsequent step. The development of such relay systems requires that all reagents and catalysts essential for a series of reactions in a single reaction vessel are compatible with each other. Multiphase reaction systems offer the potential to compartmentalise and, hence, effectively separate catalysts or reagents in such systems and may be particularly useful when biocatalysts and chemical catalysts are coupled in cascade reactions.

Hydrolytic enzymes (Enzyme Class 3) were proven to be robust enough for single phase cascade reactions in combination with chemical catalysts.<sup>2,3</sup> The most widely used applications are the racemisation and dynamic kinetic resolution of secondary alcohols and primary amines employing chemical catalysts and lipases.<sup>4</sup> Furthermore, a lipase-catalysed ring-opening polymerisation in combination with a chemo-catalytic atom transfer radical polymerisation has been reported in scCO<sub>2</sub>.<sup>5</sup> In contrast, only very few non-hydrolytic enzymes have been utilized successfully in cascade transformations involving chemical catalysts.<sup>6</sup>

Chloroperoxidase (CPO, Enzyme Class 1.11.1.10) from *Caldariomyces fumago* is recognised as a versatile and selective catalyst for various organic transformations.<sup>7,8</sup> Among these, asymmetric oxidations using H<sub>2</sub>O<sub>2</sub> to form sulfoxides or epoxides are of particular interest.<sup>8</sup> However, the main problem during CPO catalysed reactions is the irreversible deactivation of CPO in presence of excess H<sub>2</sub>O<sub>2</sub>. It has been shown that the poisoning can be circumvented to some extent by slow addition of H<sub>2</sub>O<sub>2</sub>.<sup>9</sup> Alternatively, deactivation of the enzyme can be prevented by *in situ* generation of H<sub>2</sub>O<sub>2</sub> followed by its immediate consumption in the oxidation step. This has been previously demonstrated for enzymatic<sup>10</sup> and electrochemical<sup>11</sup> generation of H<sub>2</sub>O<sub>2</sub>.

Herein, we report the synthesis of optically enriched sulfoxides by combination of enzyme and chemical catalysis in a scCO<sub>2</sub>/H<sub>2</sub>O biphasic reaction medium. The approach integrates the intrinsically safe generation of H<sub>2</sub>O<sub>2</sub> from H<sub>2</sub> and O<sub>2</sub> *via* palladium catalysis<sup>12–14</sup> and the successive enantioselective oxidation using CPO in a single reaction vessel (Fig. 1).



**Fig. 1** *In situ* generation of H<sub>2</sub>O<sub>2</sub> and its utilisation for enantioselective sulfoxidation by the chloroperoxidase (CPO) in scCO<sub>2</sub>/H<sub>2</sub>O (CPO structure representation taken from <http://metallo.scripps.edu/PROMISE/1CPO.html>).

<sup>a</sup>Institut für Technische und Makromolekulare Chemie, RWTH Aachen University, Worringerweg 1, D52056, Aachen, Germany.

E-mail: greiner@itmc.rwth-aachen.de, leitner@itmc.rwth-aachen.de

<sup>b</sup>Institute of Biotechnology 2, Forschungszentrum Jülich, Germany

<sup>c</sup>Max-Planck-Institut für Kohlenforschung, Kaiser-Wilhelm-Platz 1, D45470, Mülheim an der Ruhr, Germany

## Experimental

Pd/C (10 wt%), and Pd<sub>2</sub>(dba)<sub>3</sub> (tris(dibenzylideneacetone) dipalladium(0)) were purchased from Sigma-Aldrich. Thioanisole was obtained from Acros. CPO from *Caldariomyces fumago* (BioChemika, 25810) was obtained from Fluka (suspension in 0.1 M sodium phosphate pH 4.0 with activity > 10 000 U mL<sup>-1</sup> with 1 U corresponding to the amount of enzyme which converts 1 μmol of monochlorodimedone to dichlorodimedone per minute at pH 2.75 and 298 K in the presence of KCl and H<sub>2</sub>O<sub>2</sub>). Throughout, the activity is referred to as is determined spectrophotometrically for the oxidation of thioanisole with 26 μmol min<sup>-1</sup> μL<sup>-1</sup>.

All other solvents and chemicals were of at least p.a. grade. Sodium acetate was used as buffer (5 mmol L<sup>-1</sup>, pH 5.0) if not stated otherwise. All experiments were carried out three times and the results are given as the mean values. All results varied less than 5% of the mean value.

Conversion and enantiomeric ratio (er) or enantiomeric excess (ee), respectively, were determined by gas chromatography (GC) (Siemens, Germany) equipped with a Lipodex E column (Macherey & Nagel, Germany) (length 25 m; ID 0.25 mm; carrier gas H<sub>2</sub>; 120 °C 3 min, 15 °C min<sup>-1</sup> to 180 °C 10 min). Typical retention times of (*R*)- and (*S*)-sulfoxide were 9.0 and 10.1 min, respectively.

The CPO activity was determined spectrophotometrically by monitoring the decrease of absorbance of thioanisole at 284 nm (AvaSpec-2048TEC-FT-2, Avantes BV, The Netherlands).

A stock solution of CPO was prepared by diluting 50 μL of commercially obtained CPO in 10 mL of water. Stock solutions of thioanisole (2.0 mmol L<sup>-1</sup>), and H<sub>2</sub>O<sub>2</sub> (200 mmol L<sup>-1</sup>) were prepared in sodium acetate buffer (5 mmol L<sup>-1</sup>, pH 5 if not stated otherwise). Activity tests were conducted by mixing thioanisole (980 μL), H<sub>2</sub>O<sub>2</sub> (10 μL) and the reaction was started by adding CPO (10 μL). For the stability experiments 1 mL of the CPO stock solution was put into a glass tube and samples were analysed for residual activity. In a typical experiment, thioanisole (124 mg, 1.0 mmol), Pd/C (50 mg, 0.047 mmol Pd), CPO (200 μL, 5200 U, 0.43 kat L<sup>-1</sup>), and deionised H<sub>2</sub>O (5.0 mL) were placed into a glass tube together with a magnetic stirring bar. The tube was fitted as a liner into a stainless steel high pressure reactor (25 mL, mechanical workshop of the institute), which was further equipped with a thermocouple, a pressure sensor, and an inlet valve. The addition of gases was carried out using a dosing unit (mechanical workshop of the institute, Fig. 2) allowing pressurization without mixing of H<sub>2</sub> and O<sub>2</sub> in the absence of CO<sub>2</sub>. First, the reactor was heated to reaction temperature (typically 313 K) and then CO<sub>2</sub> was added up to 0.5 MPa, after which the required amount of O<sub>2</sub> was added; subsequently, the whole dosing unit was purged using CO<sub>2</sub>. Next, H<sub>2</sub> was added and the dosing unit was again flushed with CO<sub>2</sub>. Finally, the reactor was pressurized with CO<sub>2</sub> to 13.0 MPa.

After pressure and temperature equilibration (20 min), the agitation was started by stirring (~500 rpm). After a given reaction time (typically 6 h), the vessel was cooled using an ice bath and depressurised slowly. The water phase was extracted with ethyl acetate and conversion and ee were determined by GC. In the reactions with Pd<sub>2</sub>(dba)<sub>3</sub> as catalyst precursor (50 mg,

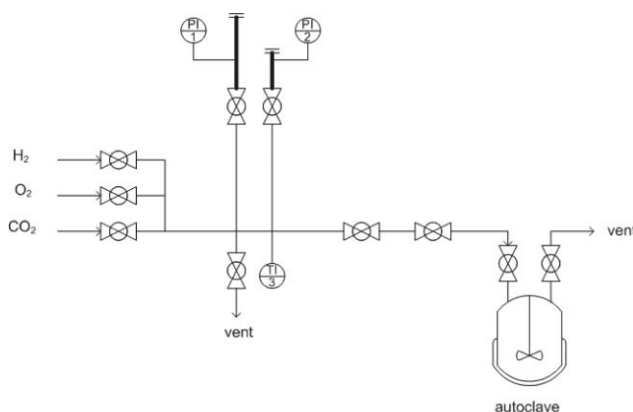


Fig. 2 Flow scheme of the reactor setup with gas manifold.

0.109 mmol Pd), and CHCl<sub>3</sub> (1.6 mL) were charged; otherwise, the same procedure as described above was followed.

## Results and discussion

Supercritical fluids (SCF), particularly scCO<sub>2</sub>, have been employed as environmentally benign solvents for chemical and enzymatic synthesis.<sup>15</sup> However, CPO has not been used under these conditions. Therefore, it was first necessary to verify that CPO is sufficiently active and stable in the presence of CO<sub>2</sub>.

A residual activity measurement showed that CPO retains 85% of its activity after incubation at pH 3.3 for 75 h at 293 K (half life estimated as 280 h, Fig. 3). At 313 K, however, the half life is significantly reduced to 21 h (Fig. 3). A similar half life of 29 h was observed after incubation with scCO<sub>2</sub>, which results also in a pH of 3.2 in the aqueous phase (Fig. 3).<sup>16</sup> This shows that CO<sub>2</sub> has no additional adverse effect on the stability at the given pH and temperature conditions. Surprisingly, the residual activity increases with increasing CO<sub>2</sub> pressure and only a 10% loss of activity was observed after 24 h of incubation at 30 MPa (Fig. 4). As sufficient stability of enzyme was found in the presence of scCO<sub>2</sub>,<sup>17</sup> the reactions were pursued by combining it with the chemo-catalytic process.

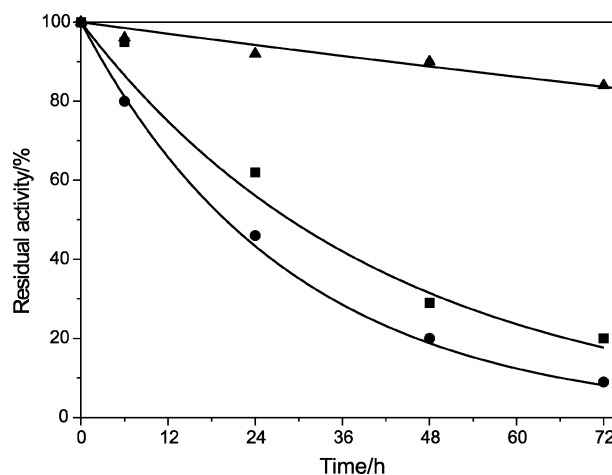


Fig. 3 Residual activity of CPO in scCO<sub>2</sub> at 13 MPa and 313 K (■); in pH 3.3 at 313 K (●) and in pH 3.3 at 293 K (▲), lines represent the first order exponential decay fitted to the data.

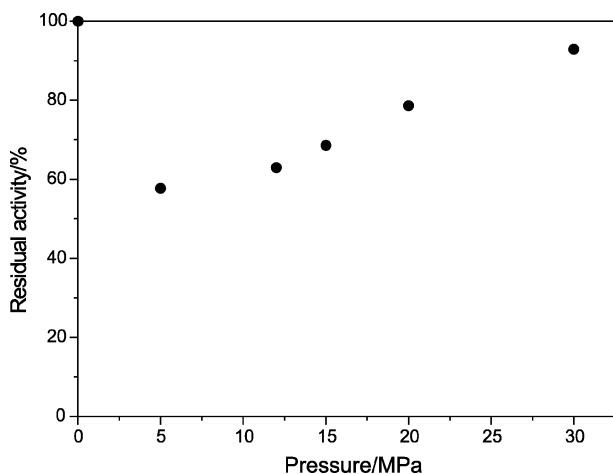


**Table 1** *In situ* generation of H<sub>2</sub>O<sub>2</sub> and its simultaneous utilisation by CPO towards sulfoxidation of thioanisole in scCO<sub>2</sub><sup>a</sup>

$$\text{H}_2 + \text{O}_2 + \text{C}_6\text{H}_5\text{S-CH}_3 \xrightarrow[\text{scCO}_2/\text{H}_2\text{O}]{\text{Pd(0), CPO}} \text{C}_6\text{H}_5\text{S(=O)-CH}_3 + \text{H}_2\text{O}$$

Entry	Thioanisole/mmol	CPO/kU	$p_{\text{H}_2}$ /MPa	$p_{\text{O}_2}$ /MPa	Pd(0) catalyst	Reaction time/h	er	Yield (%)
1	1.0	5.2	0.2	0.2	Pd/C	6	9.4	14
2	1.0	5.2	0.2	0.2	Pd/C	12	17.0	27
3	1.0	7.8	0.2	0.2	Pd/C	6	9.3	11
4	1.0	7.8	0.3	0.3	Pd/C	6	21.8	46
5	1.0	7.8	1.0	0.3	Pd/C	6	15.0	60
6	0.5	7.8	0.2	0.2	Pd/C	6	36.4	34
7	1.0	7.8	0.3	0.3	Pd <sub>2</sub> (dba) <sub>3</sub>	6	15.5	55

<sup>a</sup> All reactions were carried out at 313 K

**Fig. 4** Residual activity of CPO in H<sub>2</sub>O/scCO<sub>2</sub> after 24 h of incubation at different pressures and 313 K.

The combination of the enzymatic reaction with the chemo-catalytic H<sub>2</sub>O<sub>2</sub> formation was carried out using a standard high pressure autoclave with a gas manifold (Fig. 2). The enzyme solution together with the Pd-catalyst was placed inside the high pressure reactor. Subsequently, CO<sub>2</sub> and the reactive gases were added *via* a dosing unit following the procedure given in detail in the experimental section. This avoids mixing H<sub>2</sub> and O<sub>2</sub> in the absence of CO<sub>2</sub> as diluting gas. Control experiments with only H<sub>2</sub>/O<sub>2</sub> showed no conversion of the starting material, ruling out side reactions catalysed by stainless steel.<sup>18</sup>

First, experiments were carried out close to the reaction conditions reported by Beckman for the production of H<sub>2</sub>O<sub>2</sub>.<sup>13</sup> Using Pd/C as a catalyst along with CPO, fair ee at moderate yields showed that the cascading is possible in principle (Table 1, entries 1 and 2). When the amount of enzyme was increased, no apparent effect on ee and yield was observed, which implies that the production of H<sub>2</sub>O<sub>2</sub> is the limiting step (entry 3). The reactions were carried out for 6 h to minimise the inactivation of the enzyme by H<sub>2</sub>O<sub>2</sub>.

In line with this assumption, increasing the partial pressures of both H<sub>2</sub> ( $p_{\text{H}_2}$ ) and O<sub>2</sub> ( $p_{\text{O}_2}$ ), increases the yield and er (ee) up to 46% and 21.8 (91%), respectively (entry 4). When  $p_{\text{H}_2}$  was increased from 0.3 MPa to 1.0 MPa while keeping the  $p_{\text{O}_2}$  constant at 0.3 MPa, an increase in yield (60%) was observed with a slight decrease in ee (entry 5). Moreover, when the

concentration of substrate was halved, an increase in yield and in ee was observed giving the best result so far with an er (ee) of 36.4 (94%) and a 34% yield (entry 6).

Furthermore, Pd<sub>2</sub>(dba)<sub>3</sub> was used as a replacement for Pd/C for the H<sub>2</sub>O<sub>2</sub> production. This catalyst was chosen because it was found to be more efficient for the H<sub>2</sub>O<sub>2</sub> synthesis than Pd/C.<sup>14</sup> Also, Pd<sub>2</sub>(dba)<sub>3</sub> was soluble in CHCl<sub>3</sub>, which gave a homogenous phase with scCO<sub>2</sub>. The use of Pd<sub>2</sub>(dba)<sub>3</sub> increased the yield<sup>12d</sup> (entry 7). This observation is again consistent with the assumption (entry 3 and 4) that the overall reaction cascade is limited by production of H<sub>2</sub>O<sub>2</sub>.

## Conclusions

In summary, for the first time, CPO was found to be stable in scCO<sub>2</sub>/H<sub>2</sub>O biphasic media. This allows the cascading of chemical with enzymatic reactions for the synthesis of optically enriched (*R*)-sulfoxide. The presented chemo-enzymatic methodology opens up new opportunities for the efficient integration of non-hydrolytic enzymes together with chemical catalysts towards integrated cascade reactions.

## Acknowledgements

We are grateful to DFG (Deutsche Forschungsgemeinschaft) for funding *via* GRK 1166 BioNoCo. SKK thanks DFG for a postdoctoral fellowship. We thank Ralf Thelen, Hannelore Eschmann, Markus Kaever, and Bernd Niemeijer (all from RWTH Aachen University) and Lilia Härter (Forschungszentrum Jülich) for their skilful technical assistance and patience.

## References

- (a) H. C. Hailes, P. A. Dalby and J. M. Woodley, *J. Chem. Technol. Biotechnol.*, 2007, **82**, 1063–1066; (b) P. A. Dalby, G. J. Lye and J. M. Woodley, in *Handbook of Chiral Chemicals*, ed. D. J. Ager; CRC Press, Boca Raton, 2005, pp. 419–428.
- (a) C. Simons, U. Hanefeld, I. W. C. E. Arends, T. Maschmeyer and R. A. Sheldon, *Top. Catal.*, 2006, **40**, 35–44; (b) C. Simons, U. Hanefeld, I. W. C. E. Arends, T. Maschmeyer and R. A. Sheldon, *Adv. Synth. Catal.*, 2006, **348**, 471–475.
- (a) F. Gelman, J. Blum and D. Avnir, *J. Am. Chem. Soc.*, 2002, **124**, 14460–14463; (b) A. Kamal, M. Sandbhor and K. V. Ramana, *Tetrahedron: Asymmetry*, 2002, **13**, 815–820.
- (a) B. Martin-Matute and J. E. Bäckvall, *Curr. Opin. Chem. Biol.*, 2007, **11**, 226–232; (b) O. Pamies and J.-E. Bäckvall, *Trend.*

- Biotechnol.*, 2004, **22**, 130–135; (c) J. Paetzold and J. E. Bäckvall, *J. Am. Chem. Soc.*, 2005, **127**, 17620–17621.
- 5 C. J. Duxbury, W. Wang, M. de Geus, A. Heise and S. M. Howdle, *J. Am. Chem. Soc.*, 2005, **9**, 2385–2385.
- 6 (a) V. Berberian, C. C. R. Allen, N. D. Sharma, D. R. Boyd and C. A. Hardacre, *Adv. Synth. Catal.*, 2007, **349**, 727–739; (b) C. Paizs, A. Katona and J. Rétey, *Eur. J. Org. Chem.*, 2006, 1113–1116.
- 7 (a) V. M. Dembitsky, *Tetrahedron*, 2003, **59**, 4701–4720; (b) F. van Rantwijk and R. A. Sheldon, *Curr. Opin. Biotechnol.*, 2000, **11**, 554–564; (c) L. P. Hager, F. J. Lakner and A. Basavapathruni, *J. Mol. Catal. B: Enzym.*, 1998, **5**, 95–101; (d) A. Zaks and D. R. Dodds, *J. Am. Chem. Soc.*, 1995, **117**, 10419–10424; (e) R. L. Osborne, G. M. Raner, L. P. Hager and J. H. Dawson, *J. Am. Chem. Soc.*, 2006, **128**, 1036–1037.
- 8 (a) S. Colonna, N. Gaggero, A. Manfredi, L. Casella and M. Gullotti, *Chem. Commun.*, 1988, 1451–1452; (b) E. J. Allain, L. P. Hager, L. Deng and E. N. Jacobsen, *J. Am. Chem. Soc.*, 1993, **115**, 4415–4416; (c) S. Hu and L. P. Hager, *J. Am. Chem. Soc.*, 1999, **121**, 872–873; (d) V. Trevisan, M. Signoretto, S. Colonna, V. Pironti and G. Strukul, *Angew. Chem., Int. Ed.*, 2004, **43**, 4097–4099.
- 9 (a) S. Colonna, N. Gaggero, L. Casella, G. Carrea and P. Pasta, *Tetrahedron: Asymmetry*, 1992, **3**, 95–106; (b) K. Seelbach, M. P. J. van Deurzen, F. van Rantwijk, R. A. Sheldon and U. Kragl, *Biotechnol. Bioeng.*, 1997, **55**, 283–288.
- 10 (a) J. M. Campos-Martin, G. Blanco-Brieva and J. L. G. Fierro, *Angew. Chem., Int. Ed.*, 2006, **45**, 6962–6984; (b) J. H. Lunsford, *J. Catal.*, 2003, **216**, 455–460; (c) P. Landon, P. J. Collier, A. J. Papworth, C. J. Kiely and G. J. Hutchings, *Chem. Commun.*, 2002, **18**, 2058–2059; (d) B. E. Solsona, J. K. Edwards, P. Landon, A. F. Carley, A. Herzing, C. J. Kiely and G. J. Hutchings, *Chem. Mater.*, 2006, **18**, 2689–2695.
- 11 (a) C. Kohlmann and S. Lütz, *Eng. Life Sci.*, 2006, **6**, 170–174; (b) C. Kohlmann, W. Märkle and S. Lütz, *J. Mol. Catal. B: Enzym.*, 2008, **51**, 57–72; (c) K. Okrasa, E. Guibe-Jampel and M. Therisod, *Tetrahedron: Asymmetry*, 2003, **14**, 2487–2790; (d) F. van de Velde, N. D. Lourenco, M. Bakker, F. van Rantwijk and R. A. Sheldon, *Biotechnol. Bioeng.*, 2000, **69**, 286–291.
- 12 (a) D. I. Enache, J. K. Edwards, P. Landon, B. Solsona-Espriu, A. F. Carley, A. A. Herzing, M. Watanabe, C. J. Kiely, D. W. Knight and G. J. Hutchings, *Science*, 2006, **311**, 362–365; (b) J. K. Edwards, A. Thomas, A. F. Carley, A. A. Herzing, C. J. Kiely and G. J. Hutchings, *Green Chem.*, 2008, **10**, 388–394; (c) D. Hancu and E. J. Beckman, *Green Chem.*, 2001, **3**, 80–86; (d) G. Jenzer, T. Mallat, M. Maciejewski, F. Eigenmann and A. Baiker, *Appl. Catal., A*, 2001, **208**, 125–133.
- 13 E. J. Beckman, *Green Chem.*, 2003, **5**, 332–336.
- 14 D. Hancu, J. Green and E. J. Beckman, *Acc. Chem. Res.*, 2002, **35**, 757–764.
- 15 (a) P. G. Jessop and W. Leitner, in *Chemical Synthesis Using Supercritical Fluids*, ed. P. G. Jessop and W. Leitner, Wiley-VCH, Weinheim, 1999, pp. 1–36; (b) W. Leitner, *Acc. Chem. Res.*, 2002, **35**, 746–756; (c) W. Leitner, *Nature*, 2003, **423**, 930–931; (d) A. J. Mesiano, E. J. Beckman and A. J. Russel, *Chem. Rev.*, 1999, **99**, 623–634; (e) H. R. Hobbs and N. R. Thomas, *Chem. Rev.*, 2007, **107**, 2786–2820; (f) T. Matsuda, T. Harada and K. Nakamura, *Green Chem.*, 2004, **6**, 440–444; (g) T. Matsuda, T. Harada and K. Nakamura, *Tetrahedron: Asymmetry*, 2005, **16**, 909–915; (h) S. K. Karmee, L. Casiraghi and L. Greiner, *Biotechnol. J.*, 2008, **3**, 104–111.
- 16 C. Roosen, M. Ansoerge-Schumacher, T. Mang, W. Leitner and L. Greiner, *Green Chem.*, 2007, **9**, 455–458.
- 17 These findings are in line with the results obtained for a micellar system using compressed CO<sub>2</sub>: J. Chen, J. Zhang, B. Han, J. Li, Z. Li and X. Feng, *Phys. Chem. Chem. Phys.*, 2006, **8**, 877–881.
- 18 (a) F. Loeker and W. Leitner, *Chem.–Eur. J.*, 2000, **6**, 2011–2015; (b) N. Theyssen, Z. Hou and W. Leitner, *Chem.–Eur. J.*, 2006, **12**, 3401–3409.

# Effect of liophilicity of catalyst in cyclic carbonate formation by transesterification of polyhydric alcohols

Yogesh Patel,<sup>a</sup> Jimil George,<sup>b</sup> S. Muthukumar Pillai<sup>c</sup> and Pradip Munshi<sup>\*c</sup>

Received 19th February 2009, Accepted 22nd April 2009

First published as an Advance Article on the web 13th May 2009

DOI: 10.1039/b903529j

The effect of catalyst liophilicity is shown in cyclic carbonate formation by transesterification. 1,3-Dichlorodistannoxanes as liophilic transesterification catalysts facilitated cyclic carbonate formation from corresponding 1,2-diols and diethyl carbonate in continuous fashion without isolation of catalyst. Thus 0.5 mol% of catalyst could produce 1,2-glycerol carbonate quantitatively in 2 h with multiple recyclability. The product formed during the reaction was almost quantitative and did not require further purification. Isolation of catalyst at any stage showed retention of its activity and identity.

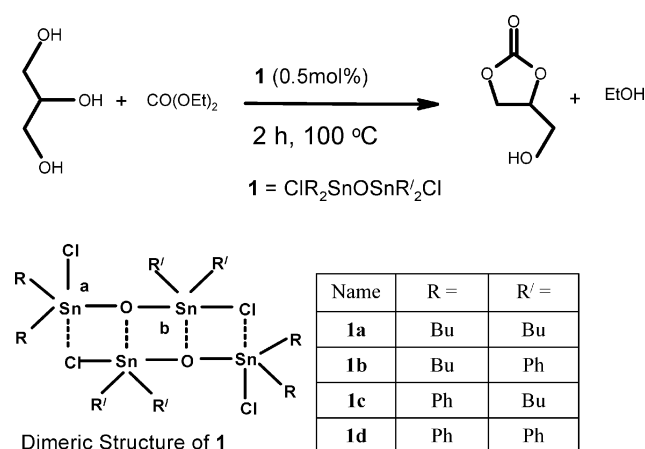
## Introduction

Cyclic carbonate has many applications *e.g.* as an inert solvent or as a reactive intermediate additive.<sup>1</sup> In recent years, production of glycerol (GL) has increased dramatically due to growing interests in biodiesel production. As glycerol has become an inexpensive chemical, there is a great opportunity and urgency to utilize glycerol to synthesize new commodity chemicals.<sup>2–5</sup> Such a pressing need for GL utilization inspired us to study its transformations into new commodity materials that substantially consume GL. Glycerol carbonate (GC), which can be synthesized from GL, offers an opportunity of a renewable synthon for further chemical synthesis.<sup>6</sup> GC has numerous applications as a bulk or fine chemical. Nonisocyanate polyurethane (NIPU) synthesis, developing polymer foams, solvents for cosmetics, and synthesizing biomaterials are a few recent advanced applications of GC.<sup>7</sup> But preparation of such a molecule has not been studied in depth and thus still offers a great challenge in making it on a commercial scale.

The use of toxic phosgene in making GC is certainly not a suitable process in terms of sustainable development. Aresta and co-workers recently reported a stoichiometric production of GC using carbon dioxide and glycerol.<sup>8</sup> We too have studied direct insertion of CO<sub>2</sub> into GL that produces GC with 35% yield catalytically.<sup>9</sup> However, these processes also do not seem to be commercially viable unless significant developments to increase yield are made. Transesterification of ethylene carbonate in scCO<sub>2</sub> to produce GC using a heterogeneous catalyst gives very poor yields along with several shortcomings associated with the process.<sup>10</sup> Diethyl carbonate (DEC), on the other hand, in presence of K<sub>2</sub>CO<sub>3</sub> as transesterification catalyst can produce

GC that shows commercial recognition.<sup>11</sup> In this method, almost quantitative yield is obtained using 3 mol% K<sub>2</sub>CO<sub>3</sub> in 4 h with a turn over frequency (TOF) of ~10 h<sup>-1</sup>. Nevertheless, undesired oligomers formation, formation of higher carbonated products and purification need extra care. Moreover, temperature and DEC to catalyst ratio are sensitive to making undesired products, and so purification by distillation is less preferred.<sup>12–13</sup>

We have found that 1,3-dichlorodistannoxanes (**1**), robustly recyclable and highly efficient (TOF, 100 h<sup>-1</sup>), and several recyclable transesterification catalysts can be used for making GC from DEC and GL without using any additional solvent (Scheme 1). Convenient separation of product and a cheap catalyst are the added benefit of the process. Other carbonates, ethylene carbonate (EC) and 1,2-propylene carbonate (PC) from respective polyols, ethylene glycol (EG) and 1,2-propylene glycol (PG), showed similar efficiencies. This finding will contribute significantly to GC synthesis research with great commercial promise.



**Scheme 1** Transesterification of glycerol with diethyl carbonate using 1,3-dichlorodistannoxane.

Previously, **1** as transesterification catalysts has been explored in various chemical transformations and found to be a highly

<sup>a</sup>M. B. Patel Science College, S. P. University, V. V. Nagar, Gujarat, 388120, India

<sup>b</sup>Department of Applied Chemistry, Cochin University of Science and Technology, Cochin, Kerala, 682022, India

<sup>c</sup>Reliance Technology Group, Research Centre, Reliance Industries Limited, Vadodara Manufacturing Division, Vadodara, Gujarat, 391346, India. E-mail: pradip.munshi@ril.com; Fax: +91 265 6693934; Tel: +91 265 6696049

efficient catalyst compared to other conventional transesterification catalysts.<sup>14–21</sup> Due to high lipophilicity,<sup>22</sup> structural rigidity and multi active catalytic centers (Sn<sup>a</sup>, Sn<sup>b</sup>, Scheme 1), **1** offer several advantages over alkali or other transesterification catalysts.<sup>23,24</sup> Fortunately, the study of **1** in cyclic carbonate synthesis has never been explored before and thus provides a great opportunity for us to explore further, especially for GC.

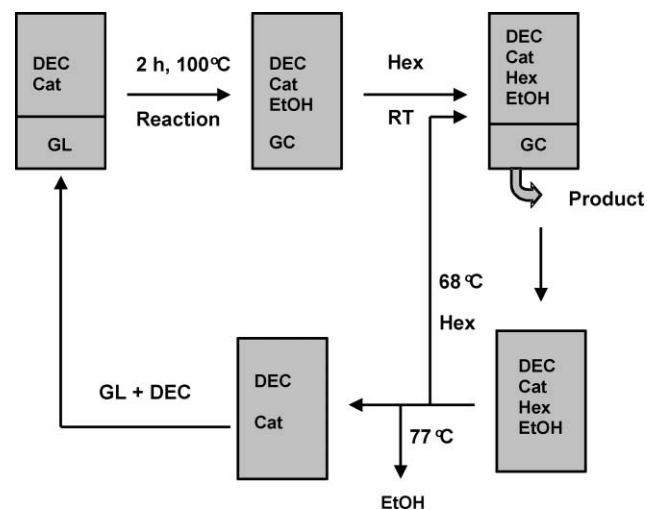
## Results and discussion

Results indicate that almost 100% yield is obtained within 2 h using 0.5 mol% catalyst (**1a**) while maintaining a concentration of DEC and GL of 5:1. The catalysts and product can be separated easily by simple solvent extraction, which offers great advantages. Interestingly, the reaction can be continued further in the same reaction vessel after separation of product that phases out at the bottom of the reaction mixture just by adding reactants again without isolating the catalyst. This indicates that the process can be modified to a continuous one which is highly economical. We have used a series of dichlorostannoxanes catalysts to show varying reactivity patterns. EG and PG also show similar efficiency (TOF 100 h<sup>-1</sup>) with **1a** (Table 1). However, separation of components from the mixture is different as described above for GL. There is no phase separation in the case of EG and PG upon addition of hexane.

All the catalysts, **1a**<sup>25</sup>, **1b**<sup>25</sup>, **1c**<sup>26</sup> and **1d**<sup>27</sup> are synthesized in a single reaction step from a cheap readily available source of materials according to previously reported literature procedures. <sup>1</sup>H-NMR, electrospray ionization mass analysis and elemental analysis data are in complete agreement with reported values.

Typically, DEC and GL forms two phases, is placed in a round bottom flask and 0.5 mol% catalyst (with respect to GL) is added

to the reaction mixture. The catalyst is completely miscible in the reaction mixture. The mixture becomes a single phase upon heating, which remains like that throughout the reaction and even after cooling. After completion, addition of hexane to the reaction mixture at room temperature forms two layers. The bottom layer is GC, which can be separated out easily. On the other hand, excess DEC, catalyst and hexane form the top layer. Evaporation of the top layer yields catalyst and excess DEC. 98% Hexane can be recovered from the top layer and further recycled. Ethanol forms during the reaction by the expense of DEC, mostly remaining in the upper phase. Addition of GL and DEC (to maintain the initial ratio) to the mixture of recovered catalysts and DEC can initiate the GC synthesis again. We have performed 5 such reaction cycles in this manner and found out that there is no depletion in productivity (Table 2). Therefore, it is possible to run the reaction in a continuous fashion as shown in Fig. 1.



**Fig. 1** Schematic representation of glycerol carbonate synthesis in a continuous manner. DEC = diethyl carbonate, Cat = Catalyst, GL = glycerol, Hex = hexane, RT = room temperature, EtOH = ethanol.

The catalyst can also be recovered by distilling off DEC after removal of hexane. We have recovered up to 98% of the catalyst and verified the recovery process by 5 independent studies. 2% loss is most likely due to manoeuvre error. The recovered catalyst

**Table 1** Reactivity of **1a** with different polyols

Reactants	Products	Time/h	Catalyst	Yield/%
GL	GC	2	<b>1a</b>	99.1
PG	PC	2	<b>1a</b>	99.4
EG	EC	2	<b>1a</b>	99.0

Reaction conditions: Substrate 0.87 mol, Cat 4.3 mmol, DEC 4.35 mol, 100 °C, yield by gas chromatography column DB-5 FID.

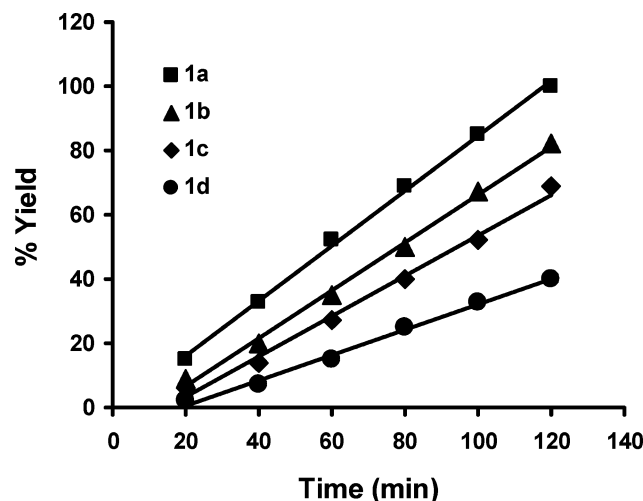
**Table 2** Recyclability test of catalyst **1a** for GC formation

Cycle		GL/g	DEC/g	<b>1a</b> /g	Hex <sup>d</sup> /mL	Isolated amount	
						<sup>e</sup> GC/g	<sup>f</sup> EtOH/g
1	U <sup>a</sup>	80	514	2.4	500		
	R <sup>b</sup>		411		480	102	70
2	U	+ 80	+ 103		+ 20		
	R		410		480	102	70
3	U	+ 80	+ 104		+ 20		
	R		411		480	102	70
4	U	+ 80	+ 103		+ 20		
	R		410.5		490	102	70
5	U	+ 80	+ 103		+ 0		
	R		410	2.35	490	101	70

<sup>a</sup> U = Used amount. <sup>b</sup> R = Recovered amount. <sup>c</sup> + indicates the amount added to the recovered component from the last cycle. <sup>d</sup> Hex = hexane. <sup>e</sup> Isolated amount. <sup>f</sup> Ethanol produced was measured from the hexane layer. Temp. 100 °C, reaction time in each cycle 2 h.

is found to be same as the starting one, which can be confirmed by identical elemental (C, H) analysis, mass spectrometer and  $^1\text{H}$  NMR. This is one of the biggest advantages of using chloro distannoxane over alkoxy distannoxane for transesterification reaction as the later transforms into a different composition after the reaction.<sup>28</sup> This gives a great opportunity to recycle **1**.

The progress of the reaction was monitored by gas chromatography using a DB5 column. The yield was estimated by an external standard method using authentic GC. GC formation using **1a** continues to completion within 2 h as revealed by gas chromatography studies (Fig. 2). Formation of GC was confirmed by the characteristics of a FTIR carbonyl signal ( $>\text{C}=\text{O}$ ) as an infra red peak<sup>11</sup> at  $1788\text{ cm}^{-1}$ ,  $^{13}\text{C}$  NMR peak at  $157.8\text{ ppm}$ <sup>29</sup> and molecular ion mass peak at  $m/z$  117.



**Fig. 2** Efficiencies of different catalysts on glycerol carbonate formation. Reaction conditions: GL 0.87 mol, Cat 4.3 mmol, DEC 4.35 mol,  $100\text{ }^\circ\text{C}$ , yield using a DB-5 FID gas chromatography column.

The observed high TOF of  $100\text{ h}^{-1}$  of **1a** can be attributed to the following reasons: a) a high degree of homogeneity arising due to the liophilic nature<sup>30–31</sup> of **1**, which makes the catalyst perform efficiently compared to the heterogeneous catalytic system and b) the dimeric nature of **1**<sup>32</sup> with two different Sn centers ( $\text{Sn}^{\text{a}}$ ,  $\text{Sn}^{\text{b}}$ , Scheme 1) which have a different Lewis acidity<sup>33</sup> and thus are able to activate both ester and alcohol simultaneously to form products making the catalysts more efficient than a conventional one.

The liophilic nature of the catalyst facilitates its dissolution in hexane and thereby separation from the product. Liophilicity increases upon esterification of alcohol<sup>34</sup> and thus the order for GL follows  $\text{GL} < \text{GC} < \text{DEC} < \mathbf{1a}$ . The significant difference in polarity due to the presence of  $-\text{OH}$  in GC from hexane and DEC facilitates the catalyst extraction through hexane leaving glycerol carbonate in a separate phase. This makes the process advantageous for GC compared to EC and PC, which remain in a single phase making separation difficult. Due to the smaller polarity difference of EC or PC with hexane or DEC no phase separation occurs. This is supported by the observation that **1d**, practically insoluble in hexane, sets at the bottom on addition of hexane.

We have studied ICP-OES and ion chromatography analyses for tin and chlorine respectively, of the product and found no

tin or chlorine (if leached from the catalyst) residues present in the product. It is apparent from Fig. 2 that introducing phenyl groups in the catalysts reduces activity significantly from its butyl analogue. The structural dissymmetry in **1b** and **1c** is also spectacularly reflected in the activity differences of the catalysts. However, it is of further interest to attempt to detail kinetic and mechanistic studies that will explain these observations.

## Conclusions

In conclusion, we have shown that catalyst liophilicity can accelerate reaction rate tremendously and provides the benefit of easy separation of components from the reaction mixture as well. **1** is found to act as a recyclable catalyst, which can form glycerol carbonate from diethyl carbonate and glycerol very efficiently with the additional benefits of easy product separation. Thus the procedure provides a completely continuous method of making glycerol carbonate without the requirement of separating catalyst and thus overall the process is highly economical and environmentally friendly.

## Experimental

### General

Chemicals were purchased from Aldrich chemical company, USA and used without further purifications unless otherwise mentioned. Solvents were purified using standard purification procedures before using in any reactions. Chloride was estimated using an Ion Chromatography (Metrohm) method. Tin was determined by Inductively Coupled Plasma Optical Emission Spectroscopy (ICP-OES) (Perkin Elmer, Optima 4300 DV) within the limit of 1 ppm. Reaction products were analyzed by Gas Chromatography (Shimadzu, GC 2010) using a DB-5 column (J & W Scientific).  $^1\text{H}$ -NMR spectra were obtained in a 300 MHz Varian FT spectrometer using deuterated solvent as the lock. The spectra were collected at  $25\text{ }^\circ\text{C}$  and chemical shifts ( $\delta$ , ppm) were referenced to residual solvent peak ( $\text{CDCl}_3$ ,  $\delta$ , 1H, 7.26 ppm). Electrospray ionization mass spectra (ESI-MS) were recorded using a Micromass Q-TOF mass spectrometer. Infra Red (IR) spectra were recorded using a Perkin Elmer, Spectrum 100 instrument. The elemental analyses (C, H) were carried out with a Perkin-Elmer 240 C elemental analyzer.

### Method of transesterification

513.86 g (4.35 mol) of DEC, 80.0 g (0.87 mol) GL and 2.40 g (0.0043 mol) catalyst **1a** were placed in a three necked round bottom flask and heated at  $100\text{ }^\circ\text{C}$  for 2 h. The initial biphasic solution containing GL at the bottom and catalyst dissolved in DEC on top became an homogeneous solution within 10 min. The progress of the reaction was monitored with a Shimadzu 2010 gas chromatograph using a DB 5 column comparing with authentic GC. After 2 h, the flask was cooled to room temperature. Hexane (500 mL) was added into the reaction mixture and stirred for a few mins. The bottom portion separated out as product, GC. The top layer contains **1a**, ethanol produced and excess DEC. DEC and **1a** were reused for the next reaction cycle after separation of hexane ( $68\text{ }^\circ\text{C}$ ) and ethanol ( $77\text{ }^\circ\text{C}$ ) by step wise distillation. 486 ml Hexane and 75 g ethanol were

recovered. 503.6 g of DEC and 2.27 gm catalyst were retained; adding 78.0 gm of DEC and 80.0 gm of GL, the catalyst mixture was recycled. Recovered hexane was reused for the next cycle. The same procedure was followed for other catalysts.

EG and PG was used in a similar manner and purification was carried out by distillation.

### Preparation of catalysts

**Preparation of 1,3-dichloride-1,1-3,3-tetrabutyl-distannoxane (1a).** **1a** was synthesized according to published procedures.<sup>25</sup> A mixture of Bu<sub>2</sub>SnO (1.0 g, 4.0 mmol) and Bu<sub>2</sub>SnCl<sub>2</sub> (1.22 g, 4.0 mmol) in toluene (50 mL) was refluxed for several hours. After 10 h reflux, the reaction mixture became a clear solution. The reaction was further refluxed for another 7 h. The hot mixture was filtered and concentrated in vacuum to get 1,3-dichlorotetra-*n*-butyl-distannoxane (**1a**). Pure product was obtained by recrystallizing from toluene. Yield 95%; Melting point, 110 °C (from ethanol) (lit.<sup>25</sup> 110 °C). Elemental analysis: Found C, 34.61; H, 6.52; Cl, 12.85; Sn, 43.01. Calculated for C<sub>32</sub>H<sub>72</sub>Sn<sub>2</sub>O<sub>2</sub>Cl<sub>2</sub>: C, 34.64; H, 6.54; Cl, 12.83; Sn, 42.95. ESI-TOF mass: *m/z* 1106.47. <sup>1</sup>H NMR: δ<sub>H</sub>(300 MHz; CDCl<sub>3</sub>; Me<sub>4</sub>Si) 0.87 (12H, t, Me), 1.4 (8H, m, Sn-CH<sub>2</sub>-), 1.8 (16H, m, CH<sub>2</sub>-CH<sub>2</sub>).

**1b** and **1c**. These catalysts were synthesized following a previously published literature method.<sup>26</sup>

**Preparation of 1,3-dichloride-1,1-dibutyl-3,3-diphenyl-distannoxane (1b).** Bu<sub>2</sub>SnO (0.720 g, 2.90 mmol) and Ph<sub>2</sub>SnCl<sub>2</sub> (1.0 g, 2.908 mmol) were dissolved in 25 mL acetone in a 100 mL round bottom flask and refluxed for 3 h while stirring the reaction mixture. Most of the solid dissolved within 3 h of the reaction. After filtration, the reaction mixture was cooled at room temperature and concentrated to obtain a solid product. Pure needle shaped crystals of **1b** were obtained after crystallizing the solid from hexane. Yield 90%; Mp, 148 °C. Elemental analysis: Found C, 40.58; H, 4.54; Cl, 12.03; Sn, 40.06. Calculated for C<sub>40</sub>H<sub>56</sub>Sn<sub>2</sub>O<sub>2</sub>Cl<sub>2</sub>: C, 40.52; H, 4.76; Cl, 11.96; Sn, 40.05. ESI-TOF mass: *m/z* × 2, 1185.76 (Calculated, 1185.46). <sup>1</sup>H NMR: δ<sub>H</sub>(300 MHz; CDCl<sub>3</sub>; Me<sub>4</sub>Si) 0.93 (6H, t, CH<sub>3</sub>), 1.65 (4H, m, Sn-CH<sub>2</sub>-), 2.37 (8H, m, -CH<sub>2</sub>-CH<sub>2</sub>-), 7.65 (6H, m, <sup>*o*</sup>Ph), 8.69 (6H, m, <sup>*m,p*</sup>Ph).

**Preparation of 1,3-dichloride-1,1-diphenyl-3,3-dibutyl-distannoxane (1c).** Ph<sub>2</sub>SnO (1.0 g, 3.46 mmol) and Bu<sub>2</sub>SnCl<sub>2</sub> (1.05 g, 3.45 mmol) were dissolved in 25 mL acetone in a 100 mL round bottom flask and refluxed for 5 h while stirring the reaction mixture. The reaction mixture was then cooled to room temperature and filtered to remove any insolubles. A solid product was obtained after concentrating the reaction mixture under vacuum (55 °C, 65 mmHg). Pure crystalline **1c** was obtained after crystallizing the solid from hexane. Yield 75%; Mp 152 °C (lit.<sup>26</sup> 149 °C). Elemental analysis: C, 40.54; H, 4.28; Cl, 12.01; Sn, 40.03. Calculated for C<sub>40</sub>H<sub>56</sub>Sn<sub>2</sub>O<sub>2</sub>Cl<sub>2</sub>: C, 40.52; H, 4.76; Cl, 11.96; Sn, 40.05. ESI-TOF mass: *m/z* × 2, 1185.813, (Calculated 1185.46). <sup>1</sup>H NMR: δ<sub>H</sub>(300 MHz; CDCl<sub>3</sub>; Me<sub>4</sub>Si): 1.22 (6H, t, CH<sub>3</sub>), 1.91 (4H, m, Sn-CH<sub>2</sub>-), 2.77 (8H, m, -CH<sub>2</sub>-CH<sub>2</sub>-), 7.41 (6H, m, <sup>*o*</sup>Ph), 8.18 (6H, m, <sup>*m,p*</sup>Ph).

**Preparation of 1,3-dichloride-1,1,3,3-tetraphenyl-distannoxane (1d).** **1d** was synthesized as per the literature reported procedure.<sup>27</sup> Ph<sub>2</sub>SnCl<sub>2</sub> (1.0 g, 2.9 mmol) and 2-amino-

benzthiazole (436 mg, 2.9 mmol) in 25 mL acetone were stirred for 3 h while a white precipitate appeared during the reaction. The solution was filtered to remove any insolubles and evaporated to dryness to yield a solid white product. Yield 25%; Mp, 198 °C (lit.<sup>16</sup> 195 °C). Elemental analysis: C, 45.67; H, 3.37; Cl, 11.24; Sn, 37.50. Calculated for C<sub>48</sub>H<sub>40</sub>Sn<sub>2</sub>O<sub>2</sub>Cl<sub>2</sub>: C, 45.56; H, 3.19; Cl, 11.21; Sn, 37.52. ESI-TOF mass: *m/z* × 2, 1265.441, (calculated 1265.42). <sup>1</sup>H NMR: δ<sub>H</sub>(300 MHz; CDCl<sub>3</sub>; Me<sub>4</sub>Si): 7.61 (8H, m, <sup>*o*</sup>Ph), 8.58 (12H, m, <sup>*m,p*</sup>Ph).

### Estimation of Cl<sup>-</sup> and Sn in the catalysts

A representative method for the estimation of % of Cl<sup>-</sup> and Sn of catalyst **1a** is described here. This was run similarly wherever required in order to obtain the % of Cl<sup>-</sup> and Sn: **1a** (110 mg, 0.1 mmol) was digested with an equivalent amount of concentrated HNO<sub>3</sub> (69%) in a porcelain crucible for 5 h. The resultant digested mass was then evaporated to dryness. The solid obtained after evaporation was dissolved in 10 mL water and acidified with dilute HNO<sub>3</sub> (6.9%) until the solution turned clear. After filtering the solution, the filtrate was transferred into a 100 mL volumetric flask and diluted with water. The solution was then analyzed to estimate Cl<sup>-</sup> by using a Metrohm column in an ion chromatography method. The same solution was used to determine Sn content by ICP-OES.

### Acknowledgements

We greatly acknowledge financial help from Reliance Industries Limited. We are very much thankful to Dr. A. J. Sophia, Dr. G. Kalpana, G. M. Desai and K. Solanki for analytical help.

### References

- J. H. Clements, *Ind. Eng. Chem. Res.*, 2003, **42**, 663.
- J. H. Clark, V. Budarin, F. E. I. Deswarte, J. J. E. Hardy, F. M. Kerton, A. J. Hunt, R. Luque, D. J. Macquarrie, K. Milkowski, A. Rodriguez, O. Samuel, S. J. Tavener, R. J. White and A. J. Wilson, *Green Chem.*, 2006, **8**, 853.
- M. Pagliaro, R. Ciriminna, H. Kimura, M. Rossi and C. D. Pina, *Angew. Chem. Int. Ed.*, 2007, **46**, 2.
- C. H. Zhou, J. N. Beltrami, Y. X. Fan and G. Q. Lu, *Chem. Soc. Rev.*, 2008, **37**, 527.
- Y. Zheng, X. Chen and Y. Shen, *Chem. Rev.*, 2008, **108**, 5253.
- C. Simao, B. L. Pukleviciene, C. Rousseau, A. Tatibouet, S. Cassel, A. Sackus, A. P. Rauter and P. Rollin, *Lett. Org. Chem.*, 2006, **3**, 744.
- O. L. Figovsky and L. D. Shapovalov, II International Scientific and Technical Conference Polymer, 2005, in "oniscyanate Polyurethane: Synthesis, Nano-structuring and Application.
- M. Aresta, A. Dibenedetto, F. Nocito and C. Pastore, *J. Mol. Catal. A*, 2006, **257**, 149.
- J. George, Y. Patel, M. Pillai and P. Munshi, *J. Mol. Catal. A*, 2009, **304**, 1.
- C. Vieville, J. W. Yoo, S. Pelet and Z. Mouloungui, *Catal. Lett.*, 1998, **56**, 245.
- G. Rokicki, P. Rakoczy, P. Parzuchowski and M. Sobiecki, *Green Chem.*, 2005, **7**, 529.
- L. C. Meher, D. Vidya Sagar and S. N. Naik, *Renewable and Sustainable Energy Reviews*, 2006, **10**, 248.
- T. Cerce, S. Peter and E. Weidner, *Ind. Eng. Chem. Res.*, 2005, **44**, 9535.
- G. Davies, in *Organotin Chemistry*, Wiley-VCH, Weinheim, 2004.
- I. Omae, *Organotin Chemistry*, Elsevier, Amsterdam, 1989.
- A. Nishio, A. Mochizuki, J. I. Sugiyama, K. Takeuchi, M. Asai, K. Yonetake and M. Ueda, *J. Polym. Sci., Part A*, 2001, **39**, 416.
- J. Otera, *J. Org. Chem.*, 1998, **63**, 2420.

- 18 R. P. Houghton and A. W. Mulvaney, *J. Organomet. Chem.*, 1996, **517**, 107.
- 19 K. Jarowicki and P. Kocienski, *J. Chem. Soc., Perkin Trans.*, 2000, **1**, 2495.
- 20 G. Pokicki, *Prog. Polym. Sci.*, 2005, **25**, 259.
- 21 J. Cai, K. J. Zhu and S. L. Yang, *Polymer*, 1998, **39**, 4009.
- 22 J. Otera, S. Ioka and H. Nozaki, *J. Org. Chem.*, 1989, **54**, 4013.
- 23 J. Otera, *Chem. Rev.*, 1993, **93**, 1449.
- 24 H. E. Hoydonckx, D. E. D. Vos, S. A. Chavan and P. A. Jacobs, *Topic Catal.*, 2004, **27**, 83.
- 25 J. Otera, N. Danoh and H. Nozaki, *J. Org. Chem.*, 1991, **56**, 5307.
- 26 Y. Lu, L. H. Weng, Z. L. Lan, J. Li and Q. L. Xie, *Chin. Chem. Lett.*, 2002, **13**, 185.
- 27 P. G. Harrison and K. Molloy, *J. Organomet. Chem.*, 1978, **152**, 63.
- 28 Jousseume, C. Laporte, M. C. Rasclé and T. Toupance, *Chem. Commun.*, 2003, 1428.
- 29 C. Copeland, R. J. Conway, J. J. Patroni and R. V. Stick, *Aust. J. Chem.*, 1981, **34**, 555.
- 30 M. Wada, M. Nishino and R. Okawara, *J. Organomet. Chem.*, 1965, **3**, 70.
- 31 J. Otera, N. Dah-oh and H. Nozaki, *J. Org. Chem.*, 1991, **56**, 5307.
- 32 P. G. Harison, M. J. Begley and K. C. Molloy, *J. Organomet. Chem.*, 1980, **186**, 213.
- 33 K. Wakamatsu, A. Orita and J. Otera, *Organometallics*, 2008, **27**, 1092.
- 34 Y. Chernyak, *J. Chem. Eng. Data*, 2006, **51**, 416.

# Enhancing the selectivity of the hydrogenation of naphthalene to tetralin by high temperature water†

Yan Cheng,<sup>a</sup> Honglei Fan,<sup>a</sup> Suxiang Wu,<sup>a</sup> Qian Wang,<sup>a</sup> Jin Guo,<sup>a,b</sup> Liang Gao,<sup>c</sup> Baoning Zong<sup>c</sup> and Buxing Han<sup>\*a</sup>

Received 13th March 2009, Accepted 23rd April 2009

First published as an Advance Article on the web 7th May 2009

DOI: 10.1039/b904305e

Enhancing selectivity and an efficient use of feedstocks in chemical reactions using greener methods is an important aspect of green chemistry. In this work, we conducted the hydrogenation of naphthalene to produce tetralin catalyzed by a cheap Fe–Mo based catalyst with and without high temperature water (HTW). The effects of various factors on the reaction, such as density of water, reaction temperature, reaction time and amounts of catalyst, were investigated. It was demonstrated that the addition of water could increase the yield of tetralin and suppress formation of coke effectively. The reaction in the presence of D<sub>2</sub>O indicated that H/D exchange occurred during the reaction process.

## Introduction

Investigations of high temperature water (HTW) as an environmentally benign medium for chemical reactions are attracting more and more attention in recent years. This is not only because it is cheap, naturally abundant and nontoxic but also because its physicochemical properties can be tuned with pressure and temperature. This means that the properties of the medium can be tuned without changing its composition.<sup>1–4</sup> HTW has been used in destruction of organic wastes,<sup>5,6</sup> preparation of synthetic natural gas from biomass,<sup>7</sup> crystalline-to-amorphous transformation of cellulose,<sup>8</sup> recovery of phenolic compounds through the decomposition of lignin,<sup>9</sup> hydrothermal synthesis of metal oxide nanoparticles,<sup>10–13</sup> etc. HTW-based organic chemistry is attractive because it is consistent with several goals of green chemistry and green engineering.<sup>2,14,15</sup> Up to now, some organic chemical reactions have been carried out in HTW, such as Beckmann rearrangements,<sup>16</sup> crossed aldol condensations,<sup>17</sup> ene reactions,<sup>18</sup> bisphenol A cleavage,<sup>19</sup> synthesis of terephthalic acid,<sup>20</sup> oxidation of methylaromatics,<sup>21</sup> oxidation of benzoic acid to phenol,<sup>22</sup> hydrogenation of different compounds,<sup>23,24</sup> synthesis of  $\epsilon$ -caprolactam from 6-aminocapronitrile,<sup>25</sup> catalytic selective partial oxidation using O<sub>2</sub> for the synthesis of carboxylic acids,<sup>26</sup> and chemical reactions of C-1 compounds.<sup>27</sup>

1,2,3,4-Tetrahydronaphthalene (tetralin) is a very useful high boiling point solvent which has been widely used in paint, coatings, inks, pharmaceuticals, paper, hydrogen donors and in other

fields.<sup>28–30</sup> Tetralin can be synthesized in a complicated Bergman cyclization or simply through the hydrogenation of naphthalene in the presence of noble metals or transition metals.<sup>31–35</sup> The reaction catalyzed by noble metals (*e.g.* platinum) usually shows high selectivity to tetralin because naphthalene interacts with surface metals strongly and prevents the hydrogenation of tetralin.<sup>36</sup> However, it is known that noble metals are much more expensive than transition metals. Transition metals are cheaper, but the selectivity to tetralin is low. How to enhance the selectivity of the reaction catalyzed by cheaper transition metal based catalysts is an interesting topic.

In the present work, the hydrogenation of naphthalene to produce tetralin using a Fe–Mo based catalyst was studied with and without HTW. It was demonstrated that water could enhance the selectivity of tetralin and suppress the formation of coke significantly under suitable conditions, *i.e.*, when water was used as a green solvent or additive, the feedstock can be used much more effectively and the selectivity of the desired product is much higher.

## Results and discussion

The main focus of this study is the impact of water on the hydrogenation of naphthalene to produce tetralin. The influence of different factors such as the density of the water, the reaction temperature, the reaction time and the loading of catalyst was studied. The thermal decomposition of formic acid has been studied and used as a source of H<sub>2</sub> for different hydrogenation reactions.<sup>24,37,38</sup> It was shown that on the laboratory scale, this approach is a simple, convenient, and safe method to carry out hydrogenation reactions. In this work, formic acid was also used as the source of H<sub>2</sub>. The conversion of naphthalene is defined as the weight percent of converted naphthalene, and the yield of a product is the weight percent of naphthalene converted into the corresponding product.

<sup>a</sup>Beijing National Laboratory for Molecular Sciences, Institute of Chemistry, Chinese Academy of Sciences, Beijing, 100190, China. E-mail: hanbx@iccas.ac.cn; Fax: +86 10-62559373; Tel: +86 10-62562821

<sup>b</sup>China University of Mining & Technology, Beijing, 100190, China

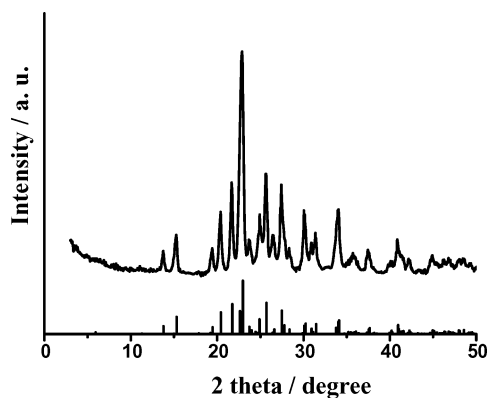
<sup>c</sup>Research Institute of Petroleum Processing, Sinopec, Beijing, 100083, China

† Electronic supplementary information (ESI) available: NMR data for the reaction product. See DOI: 10.1039/b904305e



### XRD pattern of the catalyst

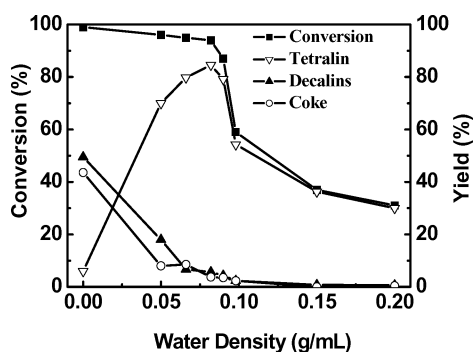
The catalyst was prepared following the procedures reported in the literature.<sup>39</sup> The XRD pattern of the prepared catalyst determined is presented in Fig. 1, together with the standard stick pattern of  $\text{Fe}_2(\text{MoO}_4)_3$ . Obviously, the pattern agreed well with the standard pattern, indicating that the catalyst was  $\text{Fe}_2(\text{MoO}_4)_3$ .



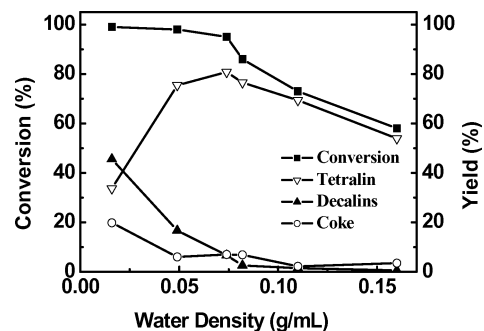
**Fig. 1** XRD pattern of the prepared catalyst (top) and the standard stick pattern of  $\text{Fe}_2(\text{MoO}_4)_3$  (bottom).

### Effect of water density

The influence of the water density on the reaction was studied at 606 K. The results with 12.8 mg and 100.0 mg of naphthalene in the reactor are given in Fig. 2 and 3, respectively. The density of the water was varied from 0 (without water) to 0.20  $\text{g mL}^{-1}$ . The density of the water was calculated from the mass of water charged divided by the volume of the reactor (6.1 mL). The figures show that in the absence of water the yield of the product tetralin was low. With an increase of the water density in the system, the yield of the product increased considerably. Our experiments showed that decalins, which were the fully hydrogenated product, were also produced. Other byproducts were mainly coke with a very small amount of other compounds, and we classified them as coke in the figures and in the following discussion for simplicity. Therefore, the amount of coke was easily calculated from the mass of the naphthalene charged, and the amounts of the naphthalene, tetralin and decalins after the reaction were determined by GC analysis. Fig. 2 and 3 show that



**Fig. 2** Effect of water density on naphthalene conversion and the yields of different compounds (12.8 mg naphthalene, 6.6 mg catalyst, 0.28 mL formic acid, 5 h, 606 K).



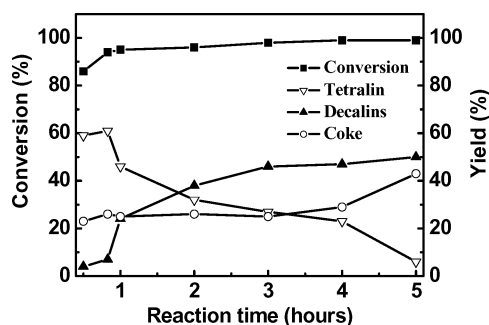
**Fig. 3** Effect of water density on naphthalene conversion and the yields of different compounds (100.0 mg naphthalene, 10.0 mg catalyst, 0.50 mL formic acid, 4 h, 606 K).

the amounts of decalins and coke decrease with an increase of the water density.

We can also see that with increasing water density, the conversion of naphthalene decreased slightly at the beginning and decreased quickly as the water density exceeded about 0.082  $\text{g mL}^{-1}$ . It can be known from the saturate vapour pressure of water and the density of steam,<sup>40</sup> that liquid water appeared as the density of water exceeded 0.082  $\text{g mL}^{-1}$  at this temperature. In other words, the water existed only in the vapour phase as the density of water was less than about 0.082  $\text{g mL}^{-1}$ , and some water began to liquefy as the density was larger than 0.082  $\text{g mL}^{-1}$ . Therefore, the main reason for the abrupt decrease in the conversion may be that liquid water covered the surface of the catalyst, which reduced the mass transfer of the reactants. It should be mentioned that water may affect the decomposition of formic acid and the amount of hydrogen produced under our experimental conditions.<sup>24</sup> Therefore, in order to keep a large amount of hydrogen in the reactor during the reaction, the amount of formic acid charged was in large excess in our experiments.

Fig. 2 and 3 show that the effect of water on the conversion and yield is less pronounced at a higher naphthalene concentration. The main reason for the difference may be that the amounts of naphthalene, catalyst, and formic acid at the different naphthalene concentrations were different. However, Fig. 2 and 3 show clearly that water can reduce the formation of coke effectively at different reactant concentrations, and the density of water affects the selectivity more significantly at the point around the phase separation.

In order to study the effect of water on the yield of the products at the same conversion of naphthalene, we determined the conversion and the yields at different reaction times in the absence of water, and the results are presented in Fig. 4. It can be seen by comparing Fig. 2 and 4 that the yield of tetralin in the presence of water was considerably higher than that without water at a similar conversion of naphthalene, and the amount of coke produced in the absence of water was much larger. The maximum yield of tetralin could reach 85% with water, while in the absence of water was only about 60%. The main reason was that the addition of water could effectively suppress the formation of coke. Therefore, the reactant can be used more effectively in the presence of water. The mechanism for producing coke is very complex even in the absence of water.<sup>41</sup>

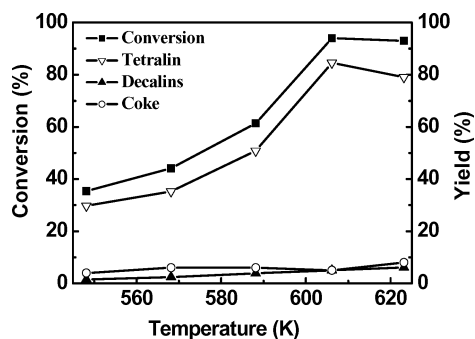


**Fig. 4** Effect of reaction time on naphthalene conversion and the yields of different compounds in the absence of water (12.8 mg naphthalene, 0.28 mL formic acid, 6.6 mg catalyst, 606 K).

The reasons for reducing the amount of coke after adding water need to be studied further.

### Effect of the reaction temperature

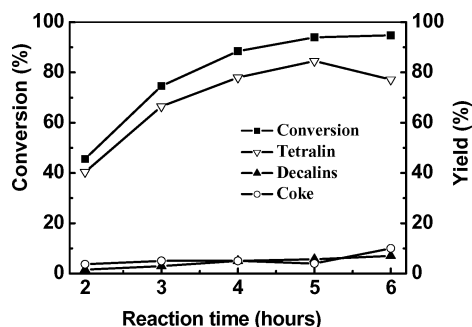
The effect of the reaction temperature was also evaluated at a water density of  $0.082 \text{ g mL}^{-1}$ , and the results are shown in Fig. 5. When the reaction temperature increased from 547 to 606 K, the conversion of naphthalene increased to a maximum and then decreased slightly with a further increase in temperature. The temperature affects the conversion in different ways. First, the reaction should be faster at higher temperatures due to the reduction of the activation energy. Second, the amount of liquid water decreased with an increase of temperature as the temperature was lower than 606 K, because liquid water existed in the reactor when the temperature was below 606 K. Both of the factors are favourable to enhance the reaction rate. Third, at 606 K, liquid water disappeared as discussed above and there was no liquid water at higher temperature. But a higher temperature is unfavourable for the thermodynamic equilibrium of naphthalene hydrogenation, since the hydrogenation is exothermic.<sup>42</sup> The competition of the above factors resulted in the maximum conversion at 606 K.



**Fig. 5** Effect of reaction temperature on naphthalene conversion and the yields of different compounds ( $0.082 \text{ g mL}^{-1}$  water, 12.8 mg naphthalene, 0.28 mL formic acid, 6.6 mg catalyst, 5 h).

### Effect of the reaction time

Fig. 6 shows the effect of reaction time on the conversion of naphthalene and the yield of tetralin with  $0.082 \text{ g mL}^{-1}$  water at 606 K. The figure shows that the yield of tetralin increased with the reaction time for 5 h. After that, extending the reaction time

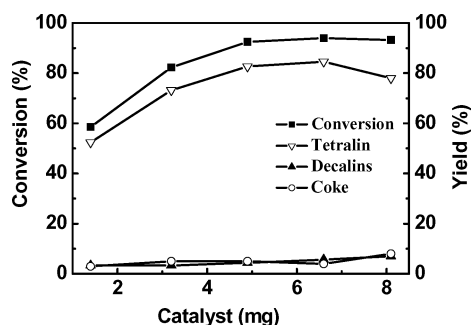


**Fig. 6** Effect of reaction time on naphthalene conversion and the yields of different compounds ( $0.082 \text{ g mL}^{-1}$  water, 12.8 mg naphthalene, 0.28 mL formic acid, 6.6 mg catalyst, 606 K).

resulted in a reduction in the yield of tetralin, and the amounts of coke and decalins increased as the reaction extended from 5 h to 6 h. Therefore, the obvious decrease in the yield of the tetralin was originated mainly from the deep hydrogenation of tetralin and the production of more coke. This is understandable considering the fact that most of the naphthalene could be converted within 5 h and, therefore, a further increasing in time resulted in more byproducts.

### Effect of the catalyst loading

Fig. 7 displays the dependence of naphthalene conversion and the yields of different compounds on the amount of the catalyst used. It can be seen that under the experimental conditions, the conversion increased with an increase of the amount of the catalyst up to 6.6 mg. The conversion did not change with the amount of the catalyst considerably when the amount of the catalyst exceeded 6.6 mg. However, the yield of tetralin was reduced slightly. The main reason for this was that 6.6 mg of catalyst was enough to convert the naphthalene under the experimental conditions. A further increase of the catalyst resulted in the production of more coke and the deep hydrogenated product decalins.



**Fig. 7** Effect of catalyst loading on naphthalene conversion and the yields of different compounds ( $0.082 \text{ g mL}^{-1}$  water, 12.8 mg naphthalene, 0.28 mL formic acid, 606 K, 5 h).

### H/D exchange between naphthalene and $\text{D}_2\text{O}$

H/D exchange of some compounds in supercritical or pressurized hot deuterium oxide has been confirmed in different reaction systems.<sup>43–46</sup> We also studied the naphthalene hydrogenation in the presence of  $\text{D}_2\text{O}$  with our catalyst. The  $^2\text{H}$  NMR

spectrum of the reaction mixture after the reaction is presented in the ESI (Fig. S1).† The peaks at 6.87, 2.58 and 1.63 ppm are assigned to deuterium atoms of the deuterated tetralin, and those at 7.31 and 7.67 ppm represent deuterium atoms of the deuterated naphthalene. This suggested that the hydrogen in water exchanged with the hydrogen in the naphthalene during the reaction. How this affected the reaction should be studied further.

## Conclusions

The effect of HTW on the hydrogenation reaction of naphthalene to produce tetralin was studied using  $\text{Fe}_2(\text{MoO}_4)_3$  as the catalyst. The results indicated that addition of water could enhance the yield of tetralin considerably. The maximum yield of tetralin could reach 85% in the presence of water, while in the absence of water was only about 60%. The main reason for this was that the addition of water could suppress the formation of coke effectively. In other words, the reactant can be used more effectively in the presence of water. We believe that using water as a greener additive to enhance the selectivity or yield of the product may also be applicable to more reactions.

## Experimental

Naphthalene was purchased from Shantou Xilong Chemical Factory (Guangdong, China). Formic acid was provided by Sinopharm Chemical Reagent Co., Ltd (Shanghai, China). *n*-Decane, sulfur (S) powders and *n*-hexane were obtained from Beijing Chemical Reagents Company. All the above chemicals were of analytical grade and used without further purification. Deuterium oxide was obtained in 99.9% isotopic purity from Cambridge Isotope Laboratories. Iron molybdenum oxide catalyst  $\text{Fe}_2(\text{MoO}_4)_3$  was prepared using the sol-gel method.<sup>37</sup> The X-ray diffraction (XRD) pattern was collected on a D/Max 2500 V/PC X-ray diffractometer with high-intensity Cu K $\alpha$  (40 kV, 200 mA) radiation. The  $^2\text{H}$  NMR spectrum was obtained on a BRUKER AVANCE (600 MHz) NMR spectrometer using  $\text{CCl}_4$  as the solvent.

All the reactions were carried out in a high pressure cylindrical-shaped 316 stainless steel reactor of 6.1 mL. In a typical experiment, a desired amount of naphthalene, catalyst, S powder (S was essential to activate the catalyst by maintaining it in the sulfided form; the mass ratio of S to catalyst was 6), water, and formic acid were added into the reactor, and then the reactor was purged with nitrogen. The loaded reactor was placed into a preheated isothermal furnace. The reaction time was recorded from the time when the reactor was placed in the furnace (about 12 min were required for the reactor to reach the reaction temperature). After the desired reaction time, the reactor was taken out of the furnace and cooled in a water bath to quickly quench the reaction. The cooled reactor was then opened and the reaction mixture was transferred into a 10 mL vial. The reactor was then triple-rinsed with *n*-hexane and the washings were added to the above vial. Then an internal standard, *n*-decane, was added into the vial for analysis. The amounts of tetralin and decalins were determined by an Agilent 4890D gas chromatograph equipped with a SUPELCOWAX-10 capillary column (30 m) and a FID detector. GC-MS analysis

of the compounds was performed on SHIMADZU-QP2010 equipment.

## Acknowledgements

This work was supported by the National Key Basic Research Project of China (2006CB202503, 2006CB202504) and the Chinese Academy of Sciences (KJCX2.YW.H16).

## Notes and references

- 1 P. E. Savage, *Chem. Rev.*, 1999, **99**, 603–621.
- 2 D. Bröll, C. Kaul, A. Krämer, P. Krammer, T. Richter, M. Jung, H. Vogel and P. Zehner, *Angew. Chem., Int. Ed.*, 1999, **38**, 2998–3014.
- 3 J. Fraga-Dubreuil and M. Poliakoff, *Pure Appl. Chem.*, 2006, **78**, 1971–1982.
- 4 J. P. Hallett, P. Pollet, C. L. Liotta and C. A. Eckert, *Acc. Chem. Res.*, 2008, **41**, 458–467.
- 5 K. Prikopský, B. Wellig and P. R. Rohr, *J. Supercrit. Fluids*, 2007, **40**, 246–257.
- 6 H. Erkonaka, O. Ö. Söğüta and M. Akgün, *J. Supercrit. Fluids*, 2008, **46**, 142–148.
- 7 F. Vogel, M. H. Waldner, A. A. Rouff and S. Rabe, *Green Chem.*, 2007, **9**, 616–619.
- 8 S. Deguchi, K. Tsujii and K. Horikoshi, *Green Chem.*, 2008, **10**, 191–196.
- 9 M. Sasaki Wahyudiono and M. Goto, *Chem. Eng. Process.*, 2008, **47**, 1609–1619.
- 10 A. A. Galkin, B. G. Kostyuk, V. V. Lunin and M. Poliakoff, *Angew. Chem., Int. Ed.*, 2000, **39**, 2738–2740.
- 11 T. Adschiri, Y. Hakuta and K. Arai, *Ind. Eng. Chem. Res.*, 2000, **39**, 4901–4907.
- 12 B. L. Cushing, V. L. Kolesnichenko and C. J. O'Connor, *Chem. Rev.*, 2004, **104**, 3893–3946.
- 13 S. Ohara, T. Mousavand, T. Sasaki, M. Umetsu, T. Naka and T. Adschiri, *J. Mater. Sci.*, 2008, **43**, 2393–2396.
- 14 M. Siskin and A. R. Katritzky, *Chem. Rev.*, 2001, **101**, 825–835.
- 15 A. R. Katritzky, D. A. Nichols, M. Siskin, R. Murugan and M. Balasubramanian, *Chem. Rev.*, 2001, **101**, 837–892.
- 16 Y. Ikushima, O. Sato, M. Sato, K. Hatakeda and M. Arai, *Chem. Eng. Sci.*, 2003, **58**, 935–941.
- 17 C. M. Comisar and P. E. Savage, *Green Chem.*, 2004, **6**, 227–231.
- 18 A. Laitinen, Y. Takebayashi, I. Kylänlahti, J. Yli-Kauhahuoma, T. Sugeta and K. Otake, *Green Chem.*, 2004, **6**, 49–52.
- 19 S. E. Hunter, C. A. Felczak and P. E. Savage, *Green Chem.*, 2004, **6**, 222–226.
- 20 J. B. Dunn and P. E. Savage, *Environ. Sci. Technol.*, 2005, **39**, 5427–5435.
- 21 E. Garcia-Verdugo, J. Fraga-Dubreuil, P. A. Hamley, W. B. Thomas, K. Whiston and M. Poliakoff, *Green Chem.*, 2005, **7**, 294–300.
- 22 J. Fraga-Dubreuil, J. Garcia-Serna, E. Garcia-Verdugo, L. M. Dudd, G. R. Aird, W. B. Thomas and M. Poliakoff, *J. Supercrit. Fluids*, 2006, **39**, 220–227.
- 23 T. Adschiri, R. Shibata, T. Sato, M. Watanabe and K. Arai, *Ind. Eng. Chem. Res.*, 1998, **37**, 2634–2638.
- 24 E. Garcia-Verdugo, Z. M. Liu, E. Ramirez, J. Garcia-Serna, J. Fraga-Dubreuil, J. R. Hyde, P. A. Hamley and M. Poliakoff, *Green Chem.*, 2006, **8**, 359–364.
- 25 C. Yan, J. Fraga-Dubreuil, E. Garcia-Verdugo, P. A. Hamley, M. Poliakoff, I. Pearson and A. S. Coote, *Green Chem.*, 2008, **10**, 98–103.
- 26 J. Fraga-Dubreuil, E. Garcia-Verdugo, P. A. Hamley, E. Vaquero, L. Dudd, I. Pearson, D. Housley, W. Partenheimer, W. B. Thomas, K. Whiston and M. Poliakoff, *Green Chem.*, 2007, **9**, 1238–1245.
- 27 M. Watanabe, T. Sato, H. Inomata, R. L. Smith, K. Arai, A. Kruse and E. Dinjus, *Chem. Rev.*, 2004, **104**, 5803–5822.
- 28 S. Hodoshima, H. Nagata and Y. Saito, *Appl. Catal., A*, 2005, **292**, 90–96.
- 29 M. Nuzzi and B. Marcandalli, *Fuel Process. Technol.*, 2003, **80**, 23–33.
- 30 Y. X. Zhao, M. R. Gray and F. Wei, *Catal. Lett.*, 2008, **125**, 69–75.

- 31 J. S. Yu, B. C. Ankianiec, M. T. Nguyen and I. P. Rothwell, *J. Am. Chem. Soc.*, 1992, **114**, 1927–1929.
- 32 T. Kotanigawa, M. Yamamoto and T. Yoshida, *Appl. Catal., A*, 1997, **164**, 323–332.
- 33 S. Albertazzi, G. Busca, E. Finocchio, R. Glöckler and A. Vaccari, *J. Catal.*, 2004, **223**, 372–381.
- 34 A. C. A. Monteiro-Gezork, A. Effendi and J. M. Winterbottom, *Catal. Today*, 2007, **128**, 63–73.
- 35 S. R. Kirumakki, B. G. Shpeizer, G. V. Sagar, K. V. R. Chary and A. Clearfield, *J. Catal.*, 2006, **242**, 319–331.
- 36 K. Ito, Y. Kogasaka, H. Kurokawa, M. Ohshima, K. Sugiyama and H. Miura, *Fuel Process. Technol.*, 2002, **79**, 77–80.
- 37 J. R. Hyde and M. Poliakoff, *Chem. Commun.*, 2004, 1482–1483.
- 38 J. R. Hyde, B. Walsh, J. Singh and M. Poliakoff, *Green Chem.*, 2005, **7**, 357–361.
- 39 W. Kuang, Y. Fan and Y. Chen, *J. Colloid Interface Sci.*, 1999, **215**, 364–369.
- 40 M. D. Koretsky, *Engineering and Chemical Thermodynamics*, John Wiley & Sons, Wiley-VCH, 1st edn., 2003, p. 509.
- 41 V. A. Munoz, S. V. Ghorpadkar and M. R. Gray, *Energy Fuels*, 1994, **8**, 426–434.
- 42 A. Corma, A. Martinez and V. Martines-Soria, *J. Catal.*, 1997, **169**, 480–489.
- 43 B. Kuhlmann, E. M. Arnett and M. Siskin, *J. Org. Chem.*, 1994, **59**, 5377–5380.
- 44 S. Bai, B. J. Palmer and C. R. Yonker, *J. Phys. Chem. A*, 2000, **104**, 53–58.
- 45 B. Kerler, J. Pól, K. Hartonen, M. T. Söderström, H. T. Koskela and M. Riekkola, *J. Supercrit. Fluids*, 2007, **39**, 381–388.
- 46 Z. Tian, L. Lis and S. R. Kass, *J. Am. Chem. Soc.*, 2008, **130**, 8–9.



## Realise the Value of Information – Turn to STN!

With STN® you can locate the high quality science and technology information your business needs to make important decisions easily, precisely and quickly.

### Using STN® you can:

- access more than 200 high quality databases, with a strong focus on chemistry and patents
- utilise outstanding tools for precise searching, analysing, visualising and reporting
- search CPlus<sup>SM</sup>, INPADOCDB, and Derwent WPI® on a single platform
- enjoy seamless access to the original journal and patent literature
- take advantage of a global system of expert customer support

When making business critical decisions turn to STN®!

**For local customer support in the UK and Ireland: The Royal Society of Chemistry (RSC)**  
 Phone: +44 1 223 432110 • Fax: +44 1 223 426017 • stnhlpuk@rsc.org • www.rsc.org/stn

**FIZ Karlsruhe**  
 STN Europe  
 Phone: +49 7247 808-555  
 helpdesk@fiz-karlsruhe.de  
 www.stn-international.de

**CAS**  
 STN North America  
 Phone: +8007534-227  
 help@cas.org  
 www.cas.org/supp.html

**Japan Association for International  
 Chemical Information (JAICI)**  
 STN Japan  
 Phone: +81-3-5978-3621  
 www.jaici.or.jp

**STN**

**FIZ Karlsruhe**



# Journal of Environmental Monitoring

## Focus on Medical Geology & Air- and Biomonitoring

*Journal of Environmental Monitoring (JEM)* issue 12, 2008, is focusing on the areas of Medical Geology & Air- and Biomonitoring.

**Medical Geology** has seen immense growth and maturation allowing biomedical/health professionals and geoscientists to take strong root in the international arena. The journal anticipates publishing many articles in this field. The first two reviews, included in this issue, are:

**The utility of mosquito-borne disease as an environmental monitoring tool in tropical ecosystems**

Andrew Jardine, Angus Cook and Philip Weinstein

**10th Anniversary Critical Review: Naturally occurring asbestos**

Martin Harper

**Air- and Biomonitoring** features six selected papers on exposure monitoring within the preventive framework of identifying and controlling health hazards within the workplace and in the environment presented at AIRMON 2008, held at Geilo, Norway, January 28-31, 2008.

**Highlighted papers:**

**Three dimensional modeling of air flow, aerosol distribution and aerosol samplers for unsteady conditions**

Albert Gilmutdinov and Ilya Zivliskii

**Experimental methods to determine inhalability and personal sampler performance for aerosols in ultra-low windspeed environments**

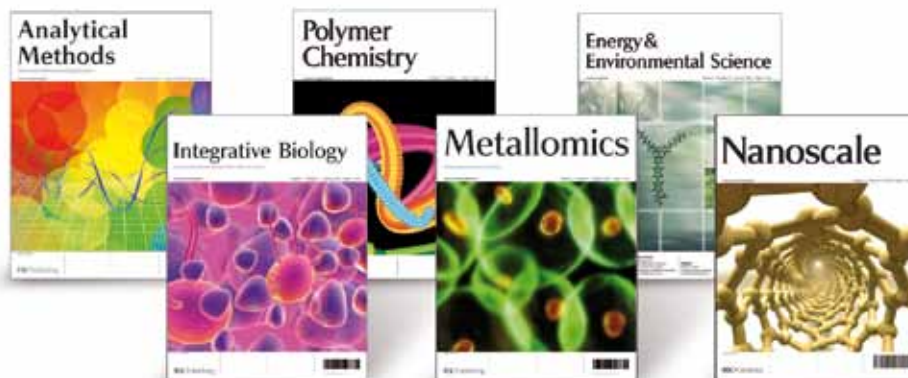
Darrah K. Schmees, Yi-Hsuan Wu and James H. Vincent

**A study of the bio-accessibility of welding fumes**

Balázs Berlinger, Dag G. Ellingsen, Miklós Náráy, Gyula Záráy and Yngvar Thomassen

110807

# Top science ...free institutional access



## New for 2010

**Polymer Chemistry** - publishing advances in polymer chemistry covering all aspects of synthetic and biological macromolecules, and related emerging areas. [www.rsc.org/polymers](http://www.rsc.org/polymers)

## New for 2009

**Analytical Methods** - highlights new and improved methods for the practical application of analytical science. This monthly journal will communicate research in the advancement of analytical techniques for use by the wider scientific community. [www.rsc.org/methods](http://www.rsc.org/methods)

**Integrative Biology** - focussing on quantitative multi-scale biology using enabling technologies and tools to exploit the convergence of biology with physics, chemistry, engineering, imaging and informatics. [www.rsc.org/ibiology](http://www.rsc.org/ibiology)

**Metallomics** - covering the research fields related to metals in biological, environmental and clinical systems. [www.rsc.org/metallomics](http://www.rsc.org/metallomics)

**Nanoscale** - publishing experimental and theoretical work across the breadth of nanoscience and nanotechnology. [www.rsc.org/nanoscale](http://www.rsc.org/nanoscale)

## New for 2008

**Energy & Environmental Science** - linking all aspects of the chemical sciences relating to energy conversion and storage alternative fuel technologies and environmental science.. [www.rsc.org/ees](http://www.rsc.org/ees)

Free institutional access, managed by IP address, is available on all these titles. For more details, and to register, visit [www.rsc.org/free\\_access\\_registration](http://www.rsc.org/free_access_registration)